# COMBINATORIAL APPROACHES FOR CANCER TREATMENT: FROM BASIC TO TRANSLATIONAL RESEARCH

EDITED BY: Daniela Spano, Aniello Cerrato and George Mattheolabakis
PUBLISHED IN: Frontiers in Oncology and Frontiers in Pharmacology

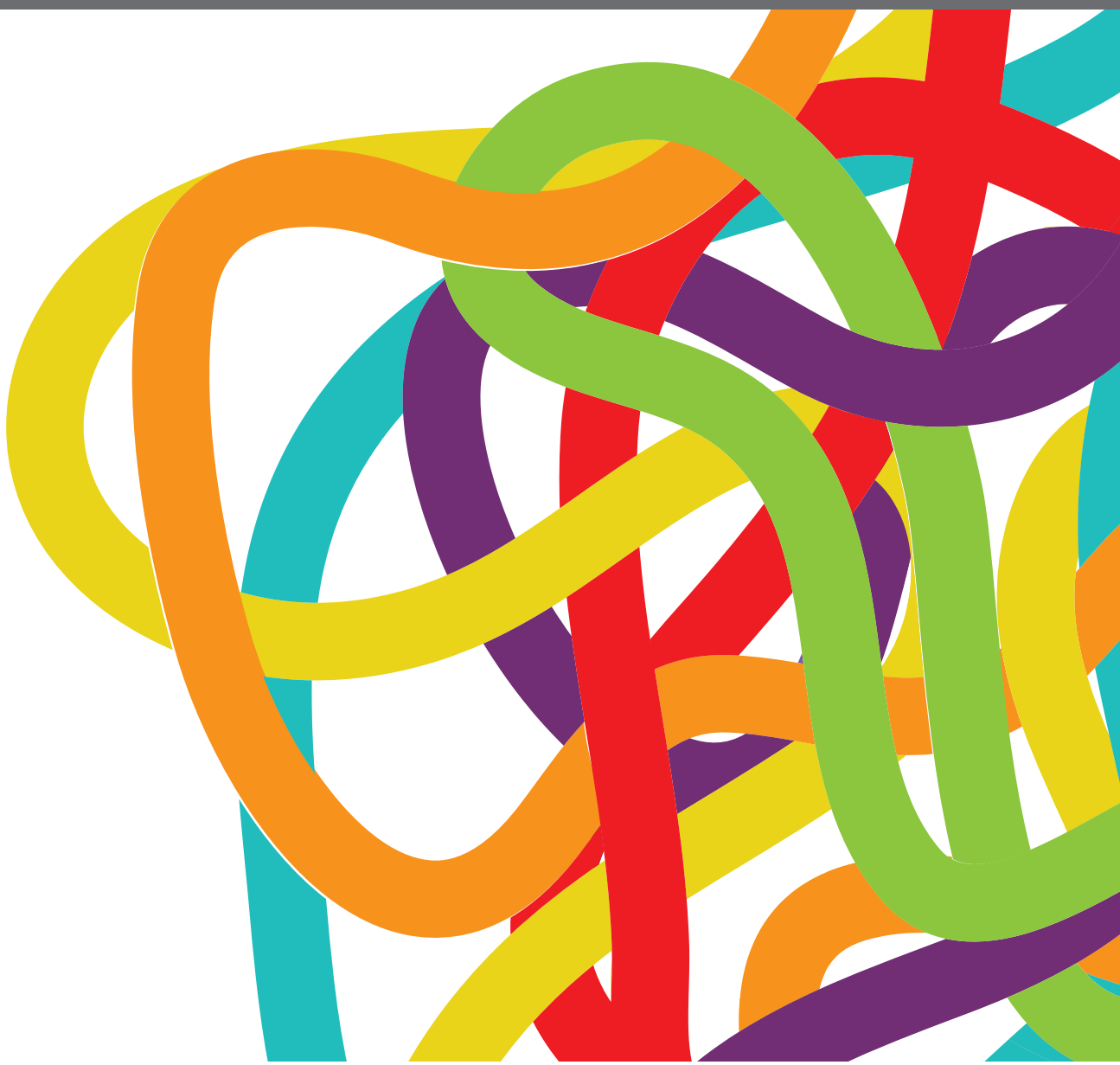

frontiers Research Topics

# frontiers



ISSN 1664-8714
ISBN 978-2-88974-570-8
DOI 10.3389/978-2-88974-570-8

## About Frontiers

Frontiers is more than just an open-access publisher of scholarly articles: it is a pioneering approach to the world of academia, radically improving the way scholarly research is managed. The grand vision of Frontiers is a world where all people have an equal opportunity to seek, share and generate knowledge. Frontiers provides immediate and permanent online open access to all its publications, but this alone is not enough to realize our grand goals.

## Frontiers Journal Series

The Frontiers Journal Series is a multi-tier and interdisciplinary set of open-access, online journals, promising a paradigm shift from the current review, selection and dissemination processes in academic publishing. All Frontiers journals are driven by researchers for researchers; therefore, they constitute a service to the scholarly community. At the same time, the Frontiers Journal Series operates on a revolutionary invention, the tiered publishing system, initially addressing specific communities of scholars, and gradually climbing up to broader public understanding, thus serving the interests of the lay society, too.

## Dedication to Quality

Each Frontiers article is a landmark of the highest quality, thanks to genuinely collaborative interactions between authors and review editors, who include some of the world's best academicians. Research must be certified by peers before entering a stream of knowledge that may eventually reach the public - and shape society; therefore, Frontiers only applies the most rigorous and unbiased reviews.
Frontiers revolutionizes research publishing by freely delivering the most outstanding research, evaluated with no bias from both the academic and social point of view. By applying the most advanced information technologies, Frontiers is catapulting scholarly publishing into a new generation.

## What are Frontiers Research Topics?

Frontiers Research Topics are very popular trademarks of the Frontiers Journals Series: they are collections of at least ten articles, all centered on a particular subject. With their unique mix of varied contributions from Original Research to Review Articles, Frontiers Research Topics unify the most influential researchers, the latest key findings and historical advances in a hot research area! Find out more on how to host your own Frontiers Research Topic or contribute to one as an author by contacting the Frontiers Editorial Office: frontiersin.org/about/contact

# COMBINATORIAL APPROACHES FOR CANCER TREATMENT: FROM BASIC TO TRANSLATIONAL RESEARCH

Topic Editors:
**Daniela Spano,** Institute of Biochemistry and Cell Biology, National Research Council (CNR), Italy
**Aniello Cerrato,** Istituto per l'Endocrinologia e l'oncologia "Gaetano Salvatore, Consiglio Nazionale Delle Ricerche (CNR), Italy
**George Mattheolabakis,** University of Louisiana at Monroe, United States

**Citation:** Spano, D., Cerrato, A., Mattheolabakis, G., eds. (2022). Combinatorial Approaches for Cancer Treatment: From Basic to Translational Research. Lausanne: Frontiers Media SA. doi: 10.3389/978-2-88974-570-8

# Table of Contents

frontiers in Oncology

EDITORIAL
published: 02 February 2022
doi: 10.3389/fonc.2022.842114

# Editorial: Combinatorial Approaches for Cancer Treatment: From Basic to Translational Research

*Aniello Cerrato*[1†], *George Mattheolabakis*[2†] *and Daniela Spano*[3*†]

[1] Institute Experimental Endocrinology and Oncology "Gaetano Salvatore", National Research Council, Naples, Italy, [2] School of Basic Pharmaceutical and Toxicological Sciences, College of Pharmacy, University of Louisiana Monroe, Monroe, LA, United States, [3] Institute of Biochemistry and Cell Biology, National Research Council, Naples, Italy

**Keywords: cancer resistance, molecular mechanisms, tumor cells heterogeneity, combinatorial therapy, treatment toxicity, computational studies, preclinical and clinical studies**

**Editorial on the Research Topic**

**Combinatorial Approaches for Cancer Treatment: From Basic to Translational Research**

OPEN ACCESS

***Edited and reviewed by:***
*Olivier Feron,*
*Université Catholique de Louvain, Belgium*

***Correspondence:**
*Daniela Spano*
*daniela.spano@ibbc.cnr.it*

*[†]These authors have contributed equally to this work*

***Specialty section:***
*This article was submitted to Pharmacology of Anti-Cancer Drugs, a section of the journal Frontiers in Oncology*

***Received:*** *23 December 2021*
***Accepted:*** *10 January 2022*
***Published:*** *02 February 2022*

***Citation:***
*Cerrato A, Mattheolabakis G and Spano D (2022) Editorial: Combinatorial Approaches for Cancer Treatment: From Basic to Translational Research. Front. Oncol. 12:842114. doi: 10.3389/fonc.2022.842114*

Cancer represents an important public health concern as the main leading cause of death worldwide. Current monotherapies, including radiotherapy, chemotherapy and molecular targeted therapy, show limited efficacy due to rapidly emerging resistance as a result either of target mutations, or engagement of parallel oncogenic pathways or onset of adaptive survival mechanisms. Moreover, the complexity of signaling networks and the activation of bypass pathway (s) render molecular targeted therapies ineffective. Therefore, combinatorial strategies could be more effective therapeutic approaches.

The most solid malignancies are characterized by hypoxia, which plays a relevant role in cancer resistance to conventional treatments (1). Therefore, therapies targeting tumor hypoxia have attracted considerable attention. Li et al. evaluate the development of prodrugs based on targeting hypoxia. They outline existing hypoxia-activated products and analyze their potential benefits in cancer treatment along with their effects in combination setting with traditional chemotherapeutics. In their second paper (Li et al.) go into detail for the hypoxia-activated prodrug TH-302 and its potential for combinatorial regime with other anti-cancer treatments, including radiotherapy, immunotherapies, anti-angiogenic agents and tissue oxygen modulators.

Oxidative stress also plays a relevant role in cancer cell sensitivity to drugs by promoting autophagy, apoptosis, or necrosis (2, 3). Zhu et al. report that metformin, an agent that exerts broad anti-cancer effects through activating AMPK and inhibiting mTOR, enhances the cytotoxicity of anlotinib, a multi-targeted tyrosine kinase inhibitor. Metformin enhances the effect of anlotinib on $NADP^+$/NADPH ratio, indicating that the combination regulates intracellular redox homeostasis and promotes switching to oxidative state. The molecular mechanisms underlying the anlotinib/metformin synergistic effect involve PARP1 and caspase-3 increased cleavage and Bax/Bcl-2 enhanced ratio, suggesting that the combinatorial treatment triggers apoptosis. ROS-mediated induction of p38/JNK MAPK and ERK signaling might explain the activation of Bcl-2/Bax-caspase signaling pathway and lead to apoptosis (4).

A typical approach exploited by cancer cells to escape apoptosis is the concomitant upregulation of anti-apoptotic BCL-2 family members, including BCL-2 and MCL-1 (5). BCL-2 targeting *via*

selective inhibitors ABT shows efficacy in several cancers (6, 7). However the concomitant expression of MCL-1 results in ABT-resistant cancer cells. Therefore, BCL-2/MCL-1 combined inhibition could represent a novel therapeutic approach to fight cancer. Following this hypothesis, Shi et al. investigate the therapeutic efficacy of the BCL-2 inhibitor ABT-199 combined with the MCL-1 inhibitor homoharringtonine in acute myeloid leukemia treatment. Their data suggest that the dual strategy is more effective in inducing apoptosis compared to monotherapies.

It is well known that genetic and epigenetic alterations, signaling pathways dysregulations, changes in cellular metabolism and tumor microenvironment are key players in cancer development and progression. Cancer cells metabolic reprogramming mainly consists in the activation of anaerobic glycolysis regardless of oxygen availability, which results in the higher production of glycolysis intermediates (8). Leone et al. review the dual role of Methylglyoxal, a glucose-derived reactive dicarbonyl, in cancer progression and the combined therapeutic strategies aimed to counteract tumor growth.

Lahooti et al. review the role of miRNAs in the angiogenesis. The authors present traditional anti-angiogenic chemotherapeutic agents and illustrate the potential that miRNAs have in the field. They attempt to critically evaluate how combinatorial analyses of miRNAs with traditional chemotherapeutics need to take into consideration the potential angiogenic activity of nucleic acids, an aspect frequently overlooked, even for miRNAs with known anti-angiogenic properties.

An interesting contribution is the review of Mancini et al. that raises awareness on the relevance of evaluating sex influence in preclinical and clinical trials to better comprehend sex/hormones in determining cancer development, progression, and sensitivity to therapy. Sex-related factors, mainly estrogenic hormones, affect the levels and/or function of p53 network both in hormone-dependent and -independent cancer. The review summarizes the studies reporting the relationship between sex and p53 circuitry, also focusing on preclinical studies and clinical trials to define sex effect on p53-targeted therapy. The review discusses the potential optimization of p53-targeted therapy given patients' sex and hormonal status. Gaining insights into the effects of sex on cancer therapy can help to identify more targeted and effective combinatorial treatments.

Despite advances in the development of molecular targeted therapies, tumor heterogeneity is a relevant aspect for tumor resistance to the treatments. The chemotherapy still represents the main therapeutic approach available for treatment of some cancer types, including triple negative breast cancer (TNBC), glioblastoma, pancreatic and colorectal cancer. However, the chemotherapeutic efficacy is often limited by the occurrence of resistance whose molecular bases are still poorly understood. In the effort to identify the molecular mechanisms of carboplatin resistance in TNBC, Abreu de Oliveira et al. demonstrate that Wnt signaling activation promotes cancer stem cells (CSCs) enrichment which underlies chemotherapy resistance. Wnt signaling inhibition reduces TNBC CSCs population and resensitizes carboplatin-resistant TNBC to the drug. CSCs are key players in cancer resistance to conventional protocols of radiotherapy, chemotherapy and molecular targeted therapy, thus causing the failure of cancer therapy and tumor relapse (9). The limited clinical efficacy of monotherapeutic regimes in CSCs eradication highlights the need for developing alternative combinatorial strategies. Catara et al. review the preclinical studies which provide the proof of concept that CSCs-centered combined therapies, based on the combination of two molecular targeted therapies and the combination of molecular targeted therapy with chemotherapy or radiotherapy, result in more effective CSCs targeting compared to single treatments.

The large number of anti-cancer drugs available implies a huge number of possible combinations to be assessed to identify the synergistic ones for cancer treatment. The computational methods could represent useful tools to screen drug combinations, thus restricting the prohibitive cost and intense labor required for the experiments. Li et al. construct transcriptomics- and network-based prediction models to screen the potential drug combinations for prostate cancer treatment and evaluate their accuracy by *in vitro* assays. Their approach identifies drugs combinations to be further investigated in preclinical and clinical trials. Gondal et al. present a novel computational framework using a literature-derived *in silico Drosophila Patient Model* for treating colorectal cancer (CRC) patients. The proposed model identifies synergistic combinations for treating different CRC patients and could be deployed in preclinical settings to evaluate potential combinations before an *in vivo* evaluation. The computational approaches might help to design specific and personalized interventions taking into account the inter-individual variations occurring on genomic, biochemical, behavioral and environmental levels. Gondal and Chaudhary present a review of existing computational resources that the scientific community can utilize for evaluating existing repositories of biomolecular cancer data, in conjunction with simulation software for the development of personalized cancer therapeutics. The authors present a critical review on existing methodologies and recognize limitations in them. Crook et al. profile advanced or refractory solid cancers by multi-analyte molecular and functional tumor interrogation [Encyclopedic Tumor Analysis (ETA)] to select personalized combination treatment regimens. The ETA-guided combined treatments of mTOR inhibitors with several anti-neoplastic agents, targeting different tumor-associated signaling pathways, improve significantly the Progression Free Survival of treated patients, thus providing clinical evidence of the therapeutic benefit achieved by personalized combinatorial strategies compared to mTOR inhibitors as monotherapies.

Among the combinatorial strategies, the local treatment based on photothermal therapy (PTT) might benefit of immunotherapy in combination setting. This strategy could enhance the efficacy with a limited toxicity of the treatment. Although the immunotherapy in combination setting is the subject of other Frontiers in Oncology Research Topics, the paper of Xia et al., which combine immunotherapy and PTT (10) for local cancer treatment of hepatocarcinoma, is included in this Research Topic as strategy to potentiate the local cancer

treatment. PTT induces the release of tumor-associated antigens by ablating tumor while Ganoderma Lucidum polysaccharides exert the anti-tumor action by stimulating the immune function without apparent toxicity.

In summary, this Research Topic is focused on the combinatorial treatment strategies to fight cancer which target cancer hallmarks, including signaling pathway dysregulation, hypoxia, oxidative stress, metabolic reprogramming, angiogenesis and stemness. The papers included in this Research Topic strengthen the relevance of combined approaches compared to single treatments in preclinical and in clinical setting.

## AUTHOR CONTRIBUTIONS

All authors listed have made a substantial, direct and intellectual contribution to the work, and approved it for publication.

## FUNDING

This work was supported for GM by the College of Pharmacy, University of Louisiana Monroe start-up funding and the National Institutes of Health (NIH) through the National Institute of General Medical Science Grants 5 P20 GM103424-15, 3 P20 GM103424-15S1.

## REFERENCES

1. Graham K, Unger E. Overcoming Tumor Hypoxia as a Barrier to Radiotherapy, Chemotherapy and Immunotherapy in Cancer Treatment. *Int J Nanomed* (2018) 13:6049–58. doi: 10.2147/IJN.S140462
2. Hayes JD, Dinkova-Kostova AT, Tew KD. Oxidative Stress in Cancer. *Cancer Cell* (2020) 38(2):167–97. doi: 10.1016/j.ccell.2020.06.001
3. Barrera G, Cucci MA, Grattarola M, Dianzani C, Muzio G, Pizzimenti S. Control of Oxidative Stress in Cancer Chemoresistance: Spotlight on Nrf2 Role. *Antioxidants (Basel)* (2021) 10(4):510–27. doi: 10.3390/antiox10040510
4. Wang X, Martindale JL, Holbrook NJ. Requirement for ERK Activation in Cisplatin-Induced Apoptosis. *J Biol Chem* (2000) 275(50):39435–43. doi: 10.1074/jbc.M004583200
5. Delbridge AR, Strasser A. The BCL-2 Protein Family, BH3-Mimetics and Cancer Therapy. *Cell Death Differ* (2015) 22:1071–80. doi: 10.1038/cdd.2015.50
6. Delbridge AR, Grabow S, Strasser A, Vaux DL. Thirty Years of BCL-2: Translating Cell Death Discoveries Into Novel Cancer Therapies. *Nat Rev Cancer* (2016) 16:99–109. doi: 10.1038/nrc.2015.17
7. Hata AN, Engelman JA, Faber AC. The BCL2 Family: Key Mediators of the Apoptotic Response to Targeted Anticancer Therapeutics. *Cancer Discov* (2015) 5:475–87. doi: 10.1158/2159-8290.CD-15-0011
8. DeBerardinis RJ, Chandel NS. We Need to Talk About the Warburg Effect. *Nat Metab* (2020) 2(2):127–9. doi: 10.1038/s42255-020-0172-2
9. Skvortsova I, Debbage P, Kumar V, Skvortsov S. Radiation Resistance: Cancer Stem Cells (Cscs) and Their Enigmatic Pro-Survival Signaling. *Semin Cancer Biol* (2015) 35:39–44. doi: 10.1016/j.semcancer.2015.09.009
10. Yata T, Takahashi Y, Tan M, Nakatsuji H, Ohtsuki S, Murakami T, et al. DNA Nanotechnology-Based Composite-Type Gold Nanoparticle-Immunostimulatory DNA Hydrogel for Tumor Photothermal Immunotherapy. *Biomaterials* (2017) 146:136–45. doi: 10.1016/j.biomaterials.2017.09.014

**Conflict of Interest:** The authors declare that the research was conducted in the absence of any commercial or financial relationships that could be construed as a potential conflict of interest.

**Publisher's Note:** All claims expressed in this article are solely those of the authors and do not necessarily represent those of their affiliated organizations, or those of the publisher, the editors and the reviewers. Any product that may be evaluated in this article, or claim that may be made by its manufacturer, is not guaranteed or endorsed by the publisher.

frontiers in Oncology

REVIEW
published: 22 March 2021
doi: 10.3389/fonc.2021.645686

# The Dual-Role of Methylglyoxal in Tumor Progression – Novel Therapeutic Approaches

*Alessia Leone*[1,2], *Cecilia Nigro*[1,2*], *Antonella Nicolò*[1,2], *Immacolata Prevenzano*[1,2], *Pietro Formisano*[1,2], *Francesco Beguinot*[1,2] *and Claudia Miele*[1,2*]

[1] URT Genomics of Diabetes, Institute of Experimental Endocrinology and Oncology, National Research Council, Naples, Italy, [2] Department of Translational Medicine, Federico II University of Naples, Naples, Italy

One of the hallmarks of cancer cells is their metabolic reprogramming, which includes the preference for the use of anaerobic glycolysis to produce energy, even in presence of normal oxygen levels. This phenomenon, known as "Warburg effect", leads to the increased production of reactive intermediates. Among these Methylglyoxal (MGO), a reactive dicarbonyl known as the major precursor of the advanced glycated end products (AGEs), is attracting great attention. It has been well established that endogenous MGO levels are increased in several types of cancer, however the MGO contribution in tumor progression is still debated. Although an anti-cancer role was initially attributed to MGO due to its cytotoxicity, emerging evidence has highlighted its pro-tumorigenic role in several types of cancer. These apparently conflicting results are explained by the hormetic potential of MGO, in which lower doses of MGO are able to establish an adaptive response in cancer cells while higher doses cause cellular apoptosis. Therefore, the extent of MGO accumulation and the tumor context are crucial to establish MGO contribution to cancer progression. Several therapeutic approaches have been proposed and are currently under investigation to inhibit the pro-tumorigenic action of MGO. In this review, we provide an overview of the early and latest evidence regarding the role of MGO in cancer, in order to define its contribution in tumor progression, and the therapeutic strategies aimed to counteract the tumor growth.

**Keywords: cancer therapy, glycolysis, glyoxalase, methylglyoxal, oncometabolites, tumor progression**

OPEN ACCESS

***Edited by:***
*Daniela Spano,*
*National Research Council (CNR), Italy*

***Reviewed by:***
*Cinzia Antognelli,*
*University of Perugia, Italy*
*Georg Wondrak,*
*University of Arizona, United States*

***Correspondence:**
*Claudia Miele*
*c.miele@ieos.cnr.it*
*Cecilia Nigro*
*c.nigro@ieos.cnr.it*

***Specialty section:***
*This article was submitted to Pharmacology of Anti-Cancer Drugs, a section of the journal Frontiers in Oncology*

***Received:*** *23 December 2020*
***Accepted:*** *01 March 2021*
***Published:*** *22 March 2021*

***Citation:***
*Leone A, Nigro C, Nicolò A, Prevenzano I, Formisano P, Beguinot F and Miele C (2021) The Dual-Role of Methylglyoxal in Tumor Progression – Novel Therapeutic Approaches. Front. Oncol. 11:645686. doi: 10.3389/fonc.2021.645686*

**Abbreviations:** AG, Aminoguanidine; AGEs, Advanced glycation end-products; ALDH, Aldehyde dehydrogenase 1; ATC, Anaplastic thyroid cancer; Bcl-2, B-cell lymphoma 2; BrBzGSHCp2, S-p-bromobenzylglutathione cyclopentyl diester; CRC, Colorectal cancer; ECM, Extracellular matrix; ER, Estrogen receptor; Glo1, Glyoxalase 1; GSH, Glutathione; HCC, Hepatocellular carcinoma; HL60, Leukaemia 60 cells; HSP, Heat shock proteins; iNOS, Inducible nitric oxide synthase; MAPK, Mitogen-activated protein kinase; MDR, Multidrug resistance; MGO-H1, Hydroimidazolone; MGO, Methylglyoxal; MGO-BSA-AGEs, MGO-derived bovine serum albumin AGEs; MMP-9, Matrix metalloproteinase 9; OPSCC, Oropharyngeal squamous cell carcinoma; PC3, Prostate cancer cells; RAGE, Receptor for advanced glycation end products; STAT, Signal transducer and activator of transcription; TCA, Tricarboxylic acid cycle; YAP, Yes-associated protein.

## INTRODUCTION

Cancer represents an important health problem being the leading cause of morbidity and mortality worldwide, with about 18 million new cases and 9.6 million cancer-induced deaths in 2018 (1). There are several risk factors contributing to carcinogenesis; lots of them can be classified as modifiable and include smoke, physical inactivity, obesity and unhealthy diet (2). However, cancer progression depends by changes in cancer cells resulting not only by activating mutations in oncogenes and inactivating mutations in suppressor genes, but also by alterations in cellular metabolism and tumor microenvironment (3).

In the last few years, cancer has emerged as a metabolic disease. In order to survive in adverse conditions, cancer cells develop metabolic adaption which allows their uncontrolled growth and proliferation (4).

One of the main changes in metabolism of cancer cells is represented by their preference for the use of anaerobic glycolysis to produce ATP, regardless of oxygen availability (5). This phenomenon known as "Warburg effect" has been described for the first time by Otto Warburg in the 1920s, when he showed that cultured tumor tissues have a high rate of glucose uptake, lactate secretion and oxygen availability (5). In normal tissue, with oxygen availability, cells use mitochondrial oxidative respiration to produce energy as this process guarantees a higher ATP generation compared to that produced by fermentation of glucose. The reason why cancer cells prefer fermentation of glucose to lactate, even in presence of oxygen-rich conditions and functional mitochondria, is because this process occurs 10-100 time faster than the complete oxidation of glucose in mitochondria (6, 7).

An important consequence of the increased glycolytic flux is the higher production of glycolysis intermediates. Among these, Methylglyoxal (MGO) is a glucose-derived highly reactive dicarbonyl and the major precursor of advanced glycation end-products (AGEs) (8). Compared to glucose, the glucose-derived glycolysis intermediates, especially MGO, form much more glycated proteins in a more rapid way (4). This leads to the AGEs accumulation and the related AGEs-receptor of AGEs (RAGE) pathway activation that contributes to the pathogenesis of many complications in age-related diseases, including cancer, by fostering tissue and cellular dysfunction (9, 10).

## METHYLGLYOXAL METABOLISM AND ITS MEDIATED CELLULAR DAMAGE

MGO is a α-oxoaldehyde metabolite, with a molecular weight of 72Da, mainly formed as byproduct of glycolysis starting from the spontaneous degradation of triose phosphate intermediates, glyceraldehyde-3-phosphate (G3P) and dihydroxyacetone phosphate (DHAP) (11). MGO can be produced also by other minor sources such as: i. the degradation of glycated proteins (8), ii. the threonine catabolism in which MGO is produced from aminoacetone oxidation (12) and iii. the ketone body metabolism where hydroxyacetone, derived from acetone hydroxylation, is further oxidized to form MGO (13, 14). MGO production by glycolysis has been estimated to be around 125 μmol/kg cell mass per day (15) and human plasmatic concentrations about 50-150 nM, while intracellular concentration are about 1-4 μM in human cells (16).

MGO action consists in the spontaneous chemical modification of nucleotides, lipids and proteins. It modifies DNA mainly reacting with deoxyguanosine (dG) to form imidazopurinone adduct 3-(2'-deoxyribosyl)-6,7-dihydro-6,7-dihydroxy-6/7-methylimidazo-[2,3-b]purine-9(8)one (MGdG) (17). MGO-derived DNA adducts can result in DNA strand breaks, nucleotide transversions, DNA-DNA crosslinks and DNA-protein crosslinks (4). In the steady state *in vivo*, approximately 9 adducts per 106 nucleotides are produced; anyway, this frequency increases and may be linked to mutagenesis in ageing, diabetes and other disorders, including cancer, characterized by high levels of dicarbonyls (14, 18).

MGO modifies from 1 to 5% of proteins irreversibly interacting with arginine residues to form hydroimidazolone (MGO-H1), the most frequent MGO-derived AGE, argypirimidine and tetrahydropyrimidine (THP). Since arginine residues are most frequently located in the functional sites of proteins (19), glycation in these sites results in protein inactivation and dysfunction (20). In a minor quantity, MGO also interacts with lysine residues to form $N_\varepsilon$-(1-carboxyethyl) lysine (CEL) and 1,3-di($N_\varepsilon$-lysino)-4-methyl-imidazolium (MOLD) (4). Increasing evidence indicates that an accumulation of MGO-modified proteins is associated to several type of cancers (21, 22).

To prevent the MGO harmful effect, mammalian cells have developed some detoxifying enzymatic mechanisms including glyoxalase (Glo), aldoketo reductases (AKRs) and aldehyde dehydrogenases (ALDHs) (23, 24). Among these, Glyoxalases 1 (Glo1) and 2 (Glo2) represent the most important system, committed to the detoxification of the majority of MGO produced. It is present in the cytosolic compartment of all cells (25) and includes: 1. a catalytic amount of reduced glutathione (GSH); 2. the Glo1, acting as the rate-limiting enzyme that catalyzes the conversion of hemithioacetal, formed by non-enzymatic reaction between MGO and GSH, in S-D-lactoylglutathione; 3. the Glo2 that hydrolyzes S-D-lactoylglutathione in D-lactate, thereby reforming GSH (26).

## THE HORMETIC ROLE OF METHYLGLYOXAL IN CANCER

Apparently conflicting data have been published in literature, sustaining both a pro-tumorigenic and an anti-cancer effect of MGO (**Figure 1**). The experimental evidence collected so far, suggests that the dual role of MGO depends on the metabolic adaptation ability of cells. If keeping tolerable, MGO stress results to be beneficial to cancer cells through apoptosis escape and enhanced cell growth. When the threshold of dicarbonyl stress is exceeded, MGO causes major toxic effects on cancer cells (**Figure 1**). This cellular response recalls the hormesis

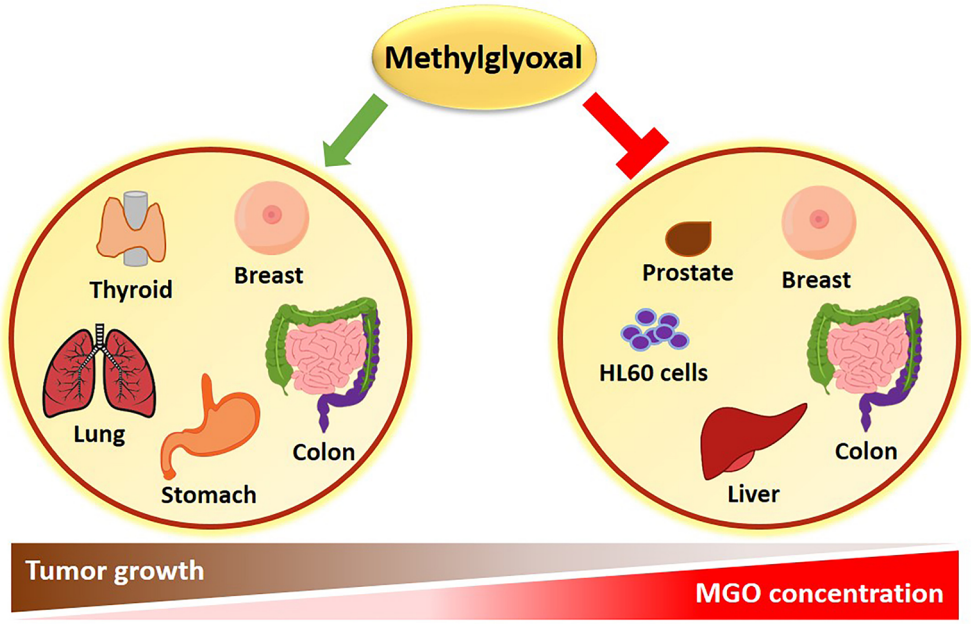


**FIGURE 1** | Role of MGO in cancer. An inverse correlation exists between MGO concentrations and tumor progression. High MGO levels cause growth arrest in several types of cancer. Conversely, a lower increase in MGO concentrations can promote cancer growth.

phenomenon, whereby a mild stress-induced stimulation increases cellular stress tolerance and results in beneficial biological effects, whereas cell death represents a final process where failure in adaptation or unhealthy adaptation occurs (27). Molecular effects of MGO on tumor progression are following described and summarized in **Table 1**.

## Methylglyoxal as an Anti-Cancer Metabolite

Pioneering investigations on the biological effects of MGO highlighted an anti-proliferative activity of this Glo substrate (47, 48). Its anti-proliferative activity is characterized by the inhibition of DNA synthesis, protein synthesis and cellular respiration (28). DNA modification by MGO is associated with increased mutation frequency, DNA strand breaks and cytotoxicity, which most likely explain the historically recognized anti-tumor activity of MGO (29–31, 48).

Studies on the mechanisms of MGO toxicity have exhibited marked selectivity for proliferating cells and some selectivity for malignant proliferating cells. Early investigations reported the inhibition of cell growth and toxicity induced by MGO exposure of human leukaemia 60 (HL60) cells *in vitro* (32). The accumulation of nucleic acids and protein adducts preceded the cellular apoptosis in these cells (33). Conversely, a no significant inhibition of cell growth was found in mature peripheral leucocytes (neutrophils and lymphocytes), demonstrating a selectivity of MGO toxicity for HL60 cells with a higher rate of cell growth than mature leucocytes (32, 33). Similarly, MGO treatment inhibited mitochondrial respiration of several types of malignant cells and tissues but it had no inhibitory effect on the respiration of any of the normal cells and tissues tested (34). In Ehrlich ascites cells, this tumoricidal effect of MGO was attributed to the potent inactivation of glyceraldehyde-3-phosphate dehydrogenase (GAPDH), which plays an important role in the high glycolytic capacity of the malignant cells (35).

Millimolar concentration of MGO induces apoptosis in various cancer cell types. Apoptosis was primary due to the block of cell cycle progression and glycolytic pathway in prostate cancer (PC3) cells (49). The activation of mitogen-activated protein kinase (MAPK) family (p-JNK, p-ERK and p-p38 levels) and the downregulation of B-cell lymphoma 2 (Bcl-2) and matrix metalloproteinase 9 (MMP-9) were demonstrated to impair cell viability, proliferation, migration, invasion, tubule formation and increase apoptosis in breast cancer cells (50). These effects were also associated to the impairment of c-Myc expression and glycolytic metabolism in human colon cancer cell lines (51). A study performed in liver cancer cells reported that much lower concentrations of MGO (1 μM) were able to decrease migration, invasion and adhesion of liver cancer cells, without impairing cell viability, in a p53-dependent manner (52). This implies that MGO could find a clinical benefit only in case of metastatic p53-expressing liver cancer. However, these preliminary data were obtained *in vitro* in cancer cell lines without considering the impact on the tumor microenvironment or the systemic effects.

The anti-tumor activity of MGO was also reported *in vivo* in rodents inoculated with tumor cells. The tumor growth was inhibited by single or continuous MGO administration (29–31,

**TABLE 1** | Effects of MGO and MGO-induced AGEs in different cancer types.

| Experimental condition | Model | Cancer type | Effect | Pathways involved | References |
|---|---|---|---|---|---|
| **Anti-cancer effects** | | | | | |
| MGO | HL60<br>EAT | Acute promyelocytic leukemia<br>Ehrlich ascites tumor | Inhibition tumor growth | ↓ proliferation<br>↓ DNA synthesis | (26, 28, 29) |
| MGO | EAT | Ehrlich ascites tumor | Inhibition tumor growth | ↓ mitochondrial respiration<br>↓ GAPDH activation | (30, 31) |
| MGO | PC3 | prostate | Induction of apoptosis<br>Inhibition of cell cycle<br>Inhibition of glycolytic pathway | Degradation of PARP<br>↓ cyclinD1, cdk2, cdk4, GAPDH, lactate<br>↓ RB phosphorylation | (32) |
| MGO<br>Glo1 inhibitor | MCF7<br>T47D<br>MDA-MB-231 | breast | ↓viability, migration, colony formation, tube formation<br>↑ apoptosis | ↑ p-JNK, p-ERK, p-p38<br>↓MMP-9, Bcl2 | (33) |
| MGO | DLD-1<br>SW480<br>BALB/c nude mice | colon | ↓viability, proliferation, migration, invasion<br>↑ apoptosis | ↓ glucose consumption<br>↓ lactate production<br>↓ ATP production<br>↓cMyc expression | (34) |
| MGO<br>3-deoxyglucosone | Huh-7<br>HepG2<br>Hep3B | liver | ↓ migration, invasion, adhesion | ↑ p53 nuclear translocation | (35) |
| **Pro-cancer effects** | | | | | |
| CML<br>Argpyrimidine | NCI-H23<br>SW1573<br>Human tissue | lung | Elusion of apoptosis | Hsp27 modification<br>↓ caspase-3 | (36, 37) |
| MGO | RGK1<br>HT29 | gastrointestinal | ↓ apoptosis | Hsp25/Hsp27 modification | (38) |
| MGO | MDA-MB-231 | breast | ↑ cell growth<br>↑ proliferation | Hsp90 modification<br>↑ nuclear YAP | (39) |
| Argpyrimidine | Human tissues | colorectal | ↑ tumor growth | | (40) |
| MGO | Mouse model | colorectal | ↑ glucose levels<br>↑ LDL/HDL ratio | ↑ IL6 | (41) |
| MGO-H1 | CAL62<br>850SC | thyroid | ↑ migration, invasion | ↑ TGF-β1, p-FAK, MMP1, IL1β | (42) |
| MGO<br>Glo1 silencing | MDA-MB-231<br>NOD-SCID mice | breast | ↑ metastatic phenotype<br>↑ ECM remodeling<br>↑ anchorage-independent growth ability<br>↑ migration | ↑ Tenascin C, CD24, TGF-β1, COL6A1, COL6A2, COL6A3, p-MEK, ERK, SMAD1<br>↓ Lumican, COL4A3, COL4A4, DUSP5 | (43) |
| MGO-BSA-AGE | MDA-MB-231 | breast | ↑ proliferation<br>↑ migration<br>↑ survival | ↑ MMP9, RAGE, p-ERK1/2, p70S6K1, STAT3, p38 | (44) |
| MGO-BSA-AGE<br>MGO-HSA-AGE | MCF-7 | breast | Dose-dependent effect of proliferation, migration, apoptosis | ↑ MMP9, p-ERK1/2, CREB1, RAGE<br>↑ caspase 3 cleavage | (45, 46) |

51, 53, 54). However, the potential efficacy of MGO as anti-cancer therapy was limited by the evidence of tumor regrowth once therapy was terminated. The small increase observed in median survival time may be due to a generalized MGO toxicity because of the use of doses close to the maximum tolerated dose (48). An open issue is on the side-effect of MGO in the context of chronic inflammatory conditions, like obesity and diabetes, which represent common risk factors for many tumors, e.g. hepatocellular carcinoma (HCC) and breast cancer.

## Glyoxalase 1 Expression: A Survival Mechanism of Cancer Cells

To compensate for high MGO levels, cancer cells may adopt survival mechanisms including Glo1 increased expression and activity. Indeed, higher levels of Glo1 have been described in several cancers (55–57) and have also been linked to multidrug resistance (MDR) in cancer chemotherapy (55).

The pro-tumorigenic role, initially attributed to Glo1, has been further validated in the last decade by studies sustaining its role as potential target in cancer therapies. The overexpression of Glo1 has been found in biopsies of pancreatic cancerous tissue (58) and HCC (59) but not in the adjacent non-cancerous tissue. In tumor cells of oropharyngeal squamous cell carcinoma (OPSCC), Glo1 expression is positively correlated to argypirimidine modification, and Glo1 protein levels are increased following exogenous MGO administration (60). This suggests that Glo1 expression represents an adaptive response to the accumulation of cytotoxic metabolites and an independent risk factor for unfavorable prognosis of OPSCC patients (60).

Amplification of Glo1 gene has been found to be a frequent genetic event in breast cancer, sarcoma, non-small-cell lung cancer (NSCLC) and, more recently, in HCC (61, 62). Interestingly, xenograft tumor growth is inhibited when Glo1 is silenced in HCC cells carrying genetic amplification but not in cells with normal copies (62), supporting the potential use of Glo1 as target in tailored therapies in patients with genetic Glo1 amplification.

In many tumors, it has been reported that the expression of Glo1 is higher in more aggressive and invasive cells than in less aggressive tumor cells, as described in: PC3 and LNCaP cell lines of prostate cancer, MDA and MCF-7 cell lines of breast cancer, skin carcinomas and skin benign neoplasms, respectively (63–65). Moreover, increased circulating levels of Glo1 have also been found in patients with metastatic compared to non-metastatic prostate cancer (66). These evidence suggest a prognostic role for Glo1 tumor expression (36), as further indicated in fibrosarcoma progression by a proteomic analysis (38). Furthermore, Glo1 emerged as an independent prognosticator of adverse significance in a colorectal cancer (CRC) patient cohort (37), later confirmed by the study showing that patients with low Glo1-expressing CRC had longer disease-free survival than the patients whose tumor expressed higher levels of Glo1 (39).

Some of these studies have described the pro-survival effect of Glo1 as a result of apoptosis elusion, rather than a direct regulation of cell proliferation (59, 62–64). In human CRC cells, Glo1 silencing inhibits colony formation, migration, invasion and induces apoptosis through the increase of the signal transducer and activator of transcription (STAT) 1, p53 and Bax and the decrease of c-Myc and Bcl-2 expression (39). The same pathways have been described in the apoptosis induced in tumor cells by high MGO levels (50–52), which are likely at least part of the effect obtained by Glo1 interfering.

The antitumor effect of Glo1 depletion underlines the potential role of Glo1 as therapeutic target. Beside the prognostic role described above for Glo1, its differential expression in malignant and less aggressive tumor cells may be useful for differential diagnosis.

## Methylglyoxal as a Pro-Cancer Metabolite

Besides the anti-tumor activity, in the last few years more and more evidence have shed light on the MGO ability to promote tumor progression (4).

Endogenous MGO-modified heat shock protein (Hsp) 27 has been found in several types of human cancer, including non-small cell lung (40) and gastrointestinal (41) cancer, where MGO protects cancer cells from apoptosis by increasing the anti-apoptotic activity of Hsp27 through the inhibition of caspase-3 and 9 activation (40–42). In breast cancer cells, MGO-induced post-translational glycation of Hsp90 affects its activity with a consequent decrease of the large tumor suppressor 1 (LATS1) expression, a key kinase for the regulation of the Hippo tumor suppressor pathway through Yes-associated protein (YAP) (43). This study demonstrated that, following MGO accumulation, YAP is retained in the nucleus where it promotes cell growth and proliferation by inducing the expression of genes involved in these processes (43).

More recently, novel molecular mechanisms related to the pro-oncogenic activity of MGO have been identified in different cancer tissues and cell lines.

In CRC human tissues, accumulation of MGO adducts (argypirimidine) are found to be positively correlated with primary tumor staging, indicating that the degree of dicarbonyl-induced stress is associated with CRC tumor aggressiveness (44). Consistent with this data, in experimental mouse models of colon cancer, MGO administration (50 mg/kg BW) causes low-grade carbonyl stress that can lead to inflammation and oxidative stress, responsible for chemically-induced colonic preneoplastic lesions deterioration. Moreover, MGO induces the growth of mouse CT26 colon cancer isografts by enhancing the expression or activation of proteins involved in cell survival, proliferation, migration and invasion (45).

*In vitro* experiments accomplished in anaplastic thyroid cancer (ATC) cell lines showed that MGO-H1 accumulation causes the increase of invasion/migration properties and a marked mesenchymal phenotype through a novel mechanism involving transforming growth factor β 1 (TGF-β1)/focal adhesion kinase (FAK) signaling (46). Similar effects are found in Glo1-depleted breast cancer cells where, the downregulation of the dual specificity phosphate 5 (DUSP5) phosphatase and the consequent over-activation of MEK/ERK/SMAD1 pathway promote the establishment of a metastatic phenotype characterized by increased cell migration and extracellular matrix (ECM) remodeling (67).

Treatment of estrogen receptor (ER)-negative MDA-MB-231 breast cancer cell line with different concentrations of MGO-derived bovine serum albumin AGEs (MGO-BSA-AGEs) causes an increase of the proliferation, migration and invasion capacity in a RAGE-dependent manner. This effect is mediated by a higher MMP-9 activity and phosphorylation of several proteins, including the ribosomal protein serine S6 kinase (p70S6K)-beta 1, STAT3, the p38 MAPK, the glycogen synthase-serine kinase (GSK)-3α and the MAPK/ERK protein-serine kinase 1/2 (MKK1/2), each of these belonging to the main signal pathways involved in tumor growth (68). Similar effects are also induced, in a dose-dependent way, in ER-positive MCF-7 human breast cancer cell line (69). In detail, MCF-7 treated with low doses (50-100 μg/ml) of MGO-BSA-AGEs show a significantly increase of cell proliferation and migration, without any alteration of cell invasion, due to the MAPK pathway activation and cAMP-response element binding protein (CREB1) 1 phosphorylation. Conversely, higher dose (200 μg/ml) of MGO-BSA-AGEs results in cytotoxicity through the activation of the apoptosis mediated by the caspase-3 cleavage (69). Probably, the inhibitory mitogenic effect observed following treatment with 200 μg/ml MGO-BSA-AGEs is due to an impediment to the correct RAGE oligomerization and consequent downstream pathways activation (69). Consistently, Khan M.S. et al. demonstrated that treatment of MCF-7 with MGO-derived human serum albumin AGEs (MGO-HSA-AGEs) (50 μg/ml) causes an increase in cell migration, likely through rearrangements of cytoskeleton (70).

These studies indicate that the conflicting literature available on the role of MGO in cancer progression could be explained by its "hormetic effect", by which exposure to low doses of MGO

causes an adaptive effect crucial for cancer cell survival. Indeed, following MGO treatment, cancer cells show a characteristic biphasic dose response growth curve (71). Moreover, difference in tumor cells response may depend on different ability of cells to face a stress condition. An increased formation of MGO in tumor cells that is not followed by a parallel increase in Glo1 activity or other detoxifying mechanisms results in toxicity (72). Thus, the correct balance between Glo1 activity and the increased MGO production, associated to the high glycolytic flux in cancer cells, is likely crucial for tumor growth response (72).

## METHYLGLYOXAL AND ITS DERIVED ADDUCTS AS NOVEL BIOMARKERS

A promising field of research is the use of MGO or MGO-derived adducts as novel biomarkers for cancer. In support of this, serum carboxymethyl lysine (CML) content has been detected at higher levels in a mouse model of lung cancer compared to controls (73). Consistently, a recent study by Irigaray and Belpomme has proved that free MGO blood levels increase in rats following subcutaneous administration of a tumorigenic cell clone of colon adenocarcinoma, compared to those measured in rats receiving non-growing tumor-associated clone. In addition, the increase of MGO levels correlates with the growth of implanted tumorigenic cell clone, indicating that MGO levels could also represent a useful marker in monitoring tumor progression (74).

Besides proteins, MGO modifies DNA thus enhancing its antigenicity. It has been demonstrated that, circulating autoantibodies against MGO-modified DNA are detectable in cancer patients and their use as markers could be relevant in certain types of cancer (75). Interestingly, a highly sensitive method has been later developed and validated for the simultaneous quantitation of 9 exocyclic DNA adducts derived from 8 aldehydes, including MGO, in human blood samples (76).

According to these data, in a pioneering study, Coluccio et al. have recently demonstrated a positive correlation between MGO-derived adducts and cancer staging by analyzing the secretome of blood-derived circulating cancer cells (BDCs) isolated from blood samples of cancer and healthy patients. This study provides a non-invasive method to detect dynamic changes of cancer in real time that may be used for alternative and personalized pharmacological strategies (77).

Together these studies spotlight the potential for a prognostic role of MGO and its derived adducts in cancer. Further clinical trials will be necessary to benefit from these early evidence and obtain a diagnostic application for MGO-derived adducts detection.

## THERAPEUTIC STRATEGIES

In this context, major efforts have been made to discover pharmacological approaches able to inhibit, or at least slow down, tumor growth (**Figure 2**). Possible strategies to this purpose have been initially focused on exploiting the cytotoxic effect of high MGO levels (9). Encouraging anti-cancer effects of a MGO-based formulation were early described in pre-clinical models and in a three-phase clinical study (78). Metronomic doses of MGO are able to sensitize breast cancer cells to doxorubicin and cisplatin, thus inducing cell death, without any additional deleterious effects (79). Given the association between Glo1 overexpression and the MDR in cancer chemotherapy, and the presence of Glo1 amplification in several human tumors, an anticancer strategy is further represented by the use of Glo1 inhibitory drugs (56, 80).

The GSH conjugate S-p-bromobenzylglutathione cyclopentyl diester (BrBzGSHCp2) exhibits a Glo1 inhibitor activity (81). The use of BrBzGSHCp2 has been proven to be effective both *in vitro* and *in vivo* models where Glo1 is expressed at high levels, as demonstrated in lung cancer cell line and mouse model (82), in drug resistant leukemia cells (83) and in Huh7 HCC cell line (84). Moreover, combination of BrBzGSHCp2 with sorafenib enhances susceptibility of HCC to the latter (84). Conversely, BrBzGSHCp2 treatment has been associated to a strengthening of aggressiveness in ATC and breast cancer (43, 46). This suggests that the efficacy of anti-tumor strategies involving the use of BrBzGSHCp2 can be ascribed to differences in cell lines and animal models used and, in general, is more efficient in a neoplastic context where Glo1 is expressed at high levels (4). Besides BrBzGSHCp2, troglitazone reduces the Glo1-induced MDR in doxorubicin-resistant K562 leukemia cells, in doxorubicin-resistant MCF7 cells and in astrocytoma cell line U-373 (85–87).

Several compounds are emerging as Glo1 inhibitor, namely curcumin, naringin, carmustine, myricetin, quercetin, delphinidine, γ-tocotrienol, lovastatin, piceatannol and TLSC702. Among these, curcumin is a polyphenol with anti-oxidant, antibacterial, anti-inflammatory, antidiabetic and anti-tumor activities (4, 88). It is known to hamper breast cancer, prostate cancer and brain astrocytoma cell growth (89, 90). By inhibiting Glo1 activity, naringin and carmustine induce apoptosis of human colon adenocarcinoma (Caco-2) cells and PC3 cells (91–93). While myricetin, quercetin, delphinidine, γ-tocotrienol, and lovastatin have been demonstrated to induce apoptosis in HL60 cells (94–98). Through their Glo1 inhibitor activity TLSC702 and piceatannol, a naturally occurring stilbene, reduce the proliferation of human non-small cell lung cancer cells expressing high Glo1 levels (99–101).

Following Glo1 inhibition, cancer cells switch from glycolysis to tricarboxylic acid (TCA) cycle to avoid apoptosis induced by MGO accumulation. Shimada et al. reported that the combination of TLSC702 with shikonin, a specific inhibitor of pyruvate kinase M2 that is a driver of TCA cycle, suppressed the metabolic shift from glycolysis to mitochondrial respiration (TCA cycle), leading to apoptosis of human non-small cell lung cancer (NCI-H522) cells (102). Moreover, TLSC702 decreases cell viability and suppresses tumor-sphere formation in ALDH1-positive cancer stem cells (CSCs) in breast cancer (103).

Metformin (N,N-dimethylbiguanide), a potent anti-diabetic molecule also used in cancer treatment for its anti-tumorigenic properties (104, 105), sensitizes endometrial cancer to progestin by targeting Tet methylcytosine dioxygenase 1 (TET1), which downregulates Glo1 expression (106). Through the inhibition of Glo1 expression, metformin overcomes resistance to chemotherapy. Indeed, combined treatment of metformin with chemotherapeutic

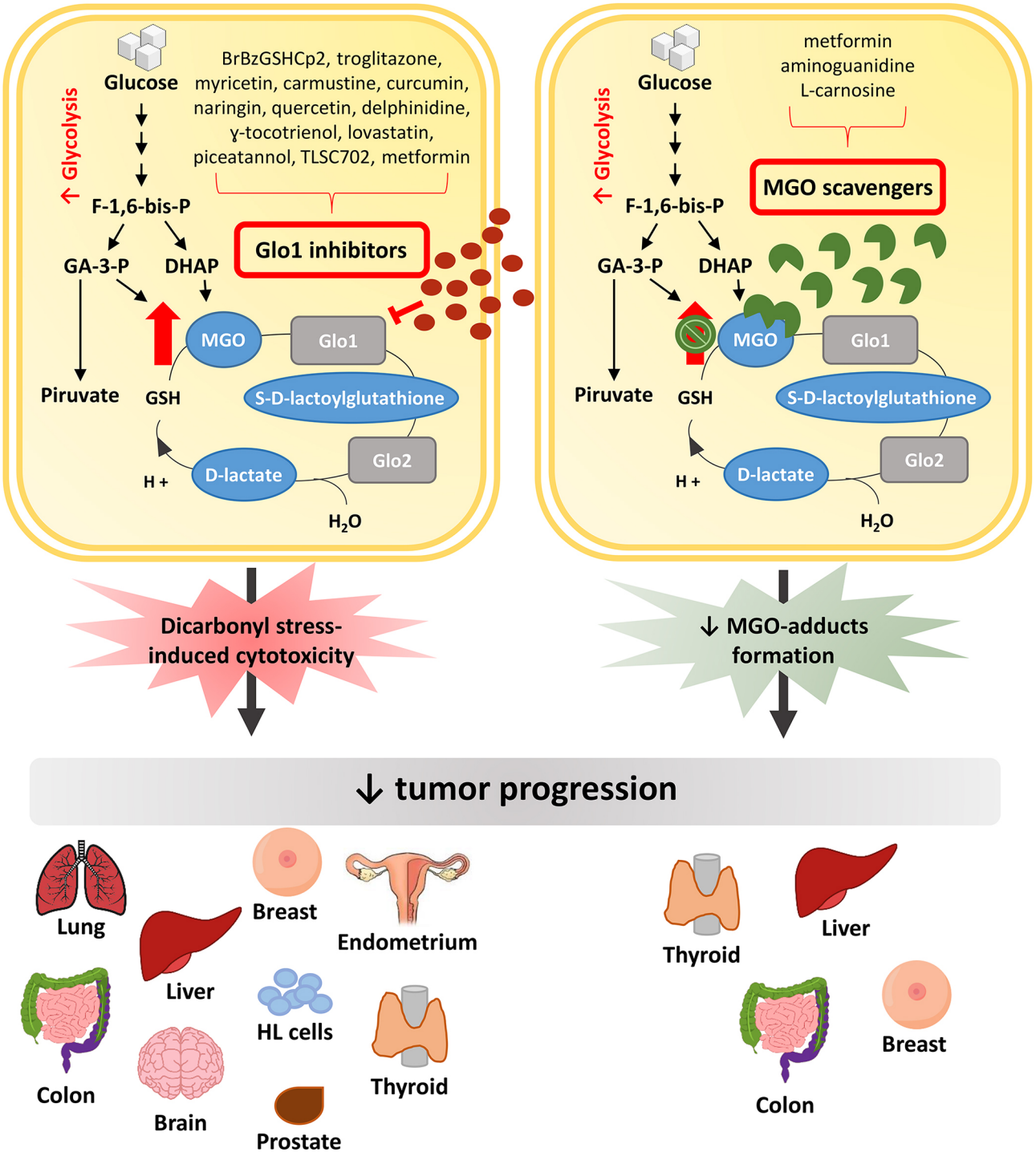


**FIGURE 2** | Anti-tumor pharmacological strategies. In cancer cells, the increased glycolytic flux causes a higher MGO production which can sustain tumor growth. Glo1 inhibitors block tumor progression by further increasing MGO intracellular levels and leading to dicarbonyl stress-induced cytotoxicity. Differently, MGO scavengers, by trapping MGO and reducing MGO-induced adducts formation, are able to block tumor progression preventing the cytotoxicity related to high MGO levels. MGO, methylglyoxal; Glo1, Glyoxalase 1; Glo2, Glyoxalase 2; F-1,6-bis-p, fructose-1,6-bis-phosphate; GA-3-P, glyceraldehyde 3-phosphate; DHAP, dihydroxyacetone phosphate; HL cells, Human Leukemia cells.

drugs, such as cisplatin and paclitaxel, reverses progestin resistance and enhances the sensitivity of endometrial cancer cells to chemotherapeutic drugs (104, 107). Moreover, Antognelli et al. demonstrated that metformin inhibits Glo1 thus hampering epithelial to mesenchymal transition (EMT), migration and invasion of metastatic PC3 cells (66). Besides its effect on Glo1 expression, metformin is emerging as MGO scavenger (108), anyway the knowledge about its action in this context is still limited.

A second and more promising anti-cancer strategy is represented by the use of MGO scavengers, in light of the pro-oncogenic effects of low doses of MGO. Indeed, the anti-cancer strategy based on Glo1 inhibition may result in potential toxic side effects related to the increasing MGO concentration, thus limiting their use in clinical practice.

Aminoguanidine (AG), a diamine oxidase with inhibitor activity on inducible nitric oxide synthase (iNOS), is a well known AGE inhibitor and MGO scavenger (9, 109). First evidence of the anti-cancer effect of AG were provided in thyroid follicular carcinoma, HCC and breast cancer progression, where AG had inhibitory effect on tumor growth by modulating iNOS (110–112). Anyway, there was no link between the AG anti-glycation action and its anticancer effect. Recently, the action of AG on the reversion of MGO pro-cancer effect has been demonstrated in breast cancer cells (67). Similarly, Antognelli et al. have demonstrated that AG treatment in ATC cell line is able to revert the pro-tumorigenic role of MGO and this effect is enhanced when AG is used in combination with resveratrol, a Glo1 activator (46).

L-Carnosine (β-alanyl-L-histidine), a naturally occurring dipeptide acting as MGO scavenger, has been shown to exert anti-proliferative effects in cancer cells (113, 114). It reverses MGO pro-tumorigenic action by decreasing migratory ability of breast cancer cells (43, 67) and inducing apoptosis in CRC cells, both *in vitro* and *in vivo* (44). Moreover, Bellier et al. demonstrated that the combined use of carnosine with cetuximab increases the apoptosis of KRAS-mutated CRC cells, unlike cetuximab treatment alone that has no effect. This effect has been also confirmed *in vivo* in mouse models (115).

Combination of natural compounds with chemotherapeutic drugs is attracting great attention for their low toxicity and potential efficacy against resistant tumors.

## CONCLUSIONS

The increasing number of cancer patients worldwide makes the search in this field more challenging. A hallmark of cancer is the altered cellular metabolism that leads to changes in the reactive metabolic intermediates levels, also called "oncometabolites", which influence cancer progression (116). The preferential use of anaerobic glycolysis implicates a higher formation of endogenous metabolites, such as MGO, in the highly proliferative and metabolically active cancer cells.

MGO contribution to tumor progression is still a debated topic, considering the apparently contrasting literature that attributes to this dicarbonyl both a pro- and anti-cancer effect. Indeed, the studies collected in this review indicate that, on one hand, MGO inhibits tumor growth by inducing cytotoxicity and impairing the expression or activity of factors having a pivotal role in invasiveness. On the other hand, recent studies demonstrate that MGO can support tumor growth essentially through the evasion from programmed cell death and the increased migration, invasion and ECM remodeling processes. This opposite action of MGO can be explained by several factors. First, the extent of MGO accumulation is essential to decide cancer cell destiny. Low levels of MGO are able to promote tumor growth as result of stress-responsive activation of survival mechanisms and apoptosis elusion, while high MGO accumulation induces cytotoxicity. Secondly, the different ability of cancer cells to face MGO-induced dicarbonyl stress is crucial for their survival. Indeed, overexpression of Glo1 is often present in more aggressive tumors and it is associated to MDR.

Many efforts have been made in the search of pharmacological strategies able to exploit the MGO cytotoxic action. Anyway, a promising strategy is represented by the use of natural compounds that can be used in association of chemotherapeutic drugs, with the advantage of showing minor risk of toxic side effects.

Given the complexity of carcinogenesis, further studies are needed to clarify the molecular pathways affected by MGO and involved in tumor progression. This will allow to identify and to optimize therapeutic strategies for personalized treatment of different types of cancer.

## AUTHOR CONTRIBUTIONS

AL, CN and CM conceived the idea and edited the manuscript. AL, CN, AN and IP wrote the paper. AL and CN prepared the figures. FB, PF and CM reviewed the manuscript. All authors contributed to the article and approved the submitted version.

## FUNDING

This study was funded, in part, by the Ministero dell'Istruzione, Università e della Ricerca Scientifica (grants PRIN 2017 and PON "RICERCA E INNOVAZIONE" 2014 - 2020 E FSC - progetto "Innovative Devices For SHAping the RIsk of Diabetes" (IDF SHARID) -ARS01_01270), by the Regione Campania (POR FESR 2014-2020 – Obiettivo specifico 1.2. - "Manifestazione di Interesse per la Realizzazione di Technology Platform nell'ambito della Lotta alle Patologie Oncologiche" - Projects COEPICA, RARE PLAT NET and SATIN), and by the European Foundation for the Study of Diabetes (EFSD)/Boehringer Ingelheim (2018-2020). The funders were not involved in the study design, collection, analysis, interpretation of data, the writing of this article or the decision to submit it for publication.

## ACKNOWLEDGMENTS

We thank Mr Antonio D'Andrea for his technical support.

## REFERENCES


1. Ferlay J, Colombet M, Soerjomataram I, Mathers C, Parkin DM. Estimating the global cancer incidence and mortality in 2018: GLOBOCAN sources and methods. *Int J Cancer* (2019) 144(8):1941–53. doi: 10.1002/ijc.31937
2. Wojciechowska J, Krajewski W, Bolanowski M, Krecicki T, Zatonski T. Diabetes and Cancer: a Review of Current Knowledge. *Exp Clin Endocrinol Diabetes* (2016) 124(5):263–75. doi: 10.1055/s-0042-100910
3. Charmsaz S, Collins DM, Perry AS, Prencipe M. Novel Strategies for Cancer Treatment: Highlights from the 55th IACR Annual Conference. *Cancers (Basel)* (2019) 11(8):1125. doi: 10.3390/cancers11081125
4. Bellahcene A, Nokin MJ, Castronovo V, Schalkwijk C. Methylglyoxal-derived stress: An emerging biological factor involved in the onset and progression of cancer. *Semin Cancer Biol* (2018) 49:64–74. doi: 10.1016/j.semcancer.2017.05.010
5. DeBerardinis RJ, Chandel NS. We need to talk about the Warburg effect. *Nat Metab* (2020) 2(2):127–9. doi: 10.1038/s42255-020-0172-2
6. Liberti MV, Locasale JW. The Warburg Effect: How Does it Benefit Cancer Cells? *Trends Biochem Sci* (2016) 41(3):211–8. doi: 10.1016/j.tibs.2015.12.001
7. Vazquez A, Liu J, Zhou Y, Oltvai ZN. Catabolic efficiency of aerobic glycolysis: the Warburg effect revisited. *BMC Syst Biol* (2010) 4:58. doi: 10.1186/1752-0509-4-58
8. Thornalley PJ, Langborg A, Minhas HS. Formation of glyoxal, methylglyoxal and 3-deoxyglucosone in the glycation of proteins by glucose. *Biochem J* (1999) 344 Pt 1:109–16. doi: 10.1042/bj3440109
9. Lin JA, Wu CH, Lu CC, Hsia SM, Yen GC. Glycative stress from advanced glycation end products (AGEs) and dicarbonyls: An emerging biological factor in cancer onset and progression. *Mol Nutr Food Res* (2016) 60 (8):1850–64. doi: 10.1002/mnfr.201500759
10. Chakraborty S, Karmakar K, Chakravortty D. Cells producing their own nemesis: understanding methylglyoxal metabolism. *IUBMB Life* (2014) 66 (10):667–78. doi: 10.1002/iub.1324
11. Sousa Silva M, Gomes RA, Ferreira AE, Ponces Freire A, Cordeiro C. The glyoxalase pathway: the first hundred years and beyond. *Biochem J* (2013) 453(1):1–15. doi: 10.1042/BJ20121743
12. Kazachkov M, Yu PH. A novel HPLC procedure for detection and quantification of aminoacetone, a precursor of methylglyoxal, in biological samples. *J Chromatogr B Analyt Technol BioMed Life Sci* (2005) 824(1-2):116–22. doi: 10.1016/j.jchromb.2005.07.006
13. Reichard GA, Jr., Skutches CL, Hoeldtke RD, Owen OE. Acetone metabolism in humans during diabetic ketoacidosis. *Diabetes* (1986) 35 (6):668–74. doi: 10.2337/diab.35.6.668
14. Nigro C, Leone A, Fiory F, Prevenzano I, Nicolo A, Mirra P, et al. Dicarbonyl Stress at the Crossroads of Healthy and Unhealthy Aging. *Cells* (2019) 8(7). doi: 10.3390/cells8070749
15. Thornalley PJ. Modification of the glyoxalase system in human red blood cells by glucose in vitro. *Biochem J* (1988) 254(3):751–5. doi: 10.1042/bj2540751
16. Rabbani N, Thornalley PJ. Dicarbonyl stress in cell and tissue dysfunction contributing to ageing and disease. *Biochem Biophys Res Commun* (2015) 458(2):221–6. doi: 10.1016/j.bbrc.2015.01.140
17. Rabbani N, Thornalley PJ. Dicarbonyl proteome and genome damage in metabolic and vascular disease. *Biochem Soc Trans* (2014) 42(2):425–32. doi: 10.1042/BST20140018
18. Thornalley PJ. Protecting the genome: defence against nucleotide glycation and emerging role of glyoxalase I overexpression in multidrug resistance in cancer chemotherapy. *Biochem Soc Trans* (2003) 31(Pt 6):1372–7. doi: 10.1042/bst0311372
19. Gallet X, Charloteaux B, Thomas A, Brasseur R. A fast method to predict protein interaction sites from sequences. *J Mol Biol* (2000) 302(4):917–26. doi: 10.1006/jmbi.2000.4092
20. Ahmed N, Dobler D, Dean M, Thornalley PJ. Peptide mapping identifies hotspot site of modification in human serum albumin by methylglyoxal involved in ligand binding and esterase activity. *J Biol Chem* (2005) 280 (7):5724–32. doi: 10.1074/jbc.M410973200
21. Bellier J, Nokin MJ, Larde E, Karoyan P, Peulen O, Castronovo V, et al. Methylglyoxal, a potent inducer of AGEs, connects between diabetes and cancer. *Diabetes Res Clin Pract* (2019) 148:200–11. doi: 10.1016/j.diabres.2019.01.002
22. Schalkwijk CG, Stehouwer CDA. Methylglyoxal, a Highly Reactive Dicarbonyl Compound, in Diabetes, Its Vascular Complications, and Other Age-Related Diseases. *Physiol Rev* (2020) 100(1):407–61. doi: 10.1152/physrev.00001.2019
23. Vander Jagt DL, Hunsaker LA. Methylglyoxal metabolism and diabetic complications: roles of aldose reductase, glyoxalase-I, betaine aldehyde dehydrogenase and 2-oxoaldehyde dehydrogenase. *Chem Biol Interact* (2003) 143-144:341–51. doi: 10.1016/s0009-2797(02)00212-0
24. Nigro C, Leone A, Raciti GA, Longo M, Mirra P, Formisano P, et al. Methylglyoxal-Glyoxalase 1 Balance: The Root of Vascular Damage. *Int J Mol Sci* (2017) 18(1):188. doi: 10.3390/ijms18010188
25. Thornalley PJ. The glyoxalase system in health and disease. *Mol Aspects Med* (1993) 14(4):287–371. doi: 10.1016/0098-2997(93)90002-U
26. Brandt RB, Waters MG, Muron DJ, Bloch MH. The glyoxalase system in rat blood. *Proc Soc Exp Biol Med* (1982) 169(4):463–9. doi: 10.3181/00379727-169-41376
27. Pennisi M, Crupi R, Di Paola R, Ontario ML, Bella R, Calabrese EJ, et al. Inflammasomes, hormesis, and antioxidants in neuroinflammation: Role of NRLP3 in Alzheimer disease. *J Neurosci Res* (2017) 95(7):1360–72. doi: 10.1002/jnr.23986
28. Reiffen KA, Schneider F. A comparative study on proliferation, macromolecular synthesis and energy metabolism of in vitro-grown Ehrlich ascites tumor cells in the presence of glucosone, galactosone and methylglyoxal. *J Cancer Res Clin Oncol* (1984) 107(3):206–10. doi: 10.1007/BF01032608
29. Conroy PJ. Carcinostatic activity of methylglyoxal and related substances in tumour-bearing mice. *Ciba Found Symp* (1978) 67):271–300. doi: 10.1002/9780470720493.ch17
30. Egyud LG, Szent-Gyorgyi A. Cancerostatic action of methylglyoxal. *Science* (1968) 160(3832):1140. doi: 10.1126/science.160.3832.1140
31. Jerzykowski T, Matuszewski W, Otrzonsek N, Winter R. Antineoplastic action of methylglyoxal. *Neoplasma* (1970) 17(1):25–35.
32. Ayoub FM, Allen RE, Thornalley PJ. Inhibition of proliferation of human leukaemia 60 cells by methylglyoxal in vitro. *Leuk Res* (1993) 17(5):397–401. doi: 10.1016/0145-2126(93)90094-2
33. Kang Y, Edwards LG, Thornalley PJ. Effect of methylglyoxal on human leukaemia 60 cell growth: modification of DNA G1 growth arrest and induction of apoptosis. *Leuk Res* (1996) 20(5):397–405. doi: 10.1016/0145-2126(95)00162-x
34. Ray M, Halder J, Dutta SK, Ray S. Inhibition of respiration of tumor cells by methylglyoxal and protection of inhibition by lactaldehyde. *Int J Cancer* (1991) 47(4):603–9. doi: 10.1002/ijc.2910470421
35. Halder J, Ray M, Ray S. Inhibition of glycolysis and mitochondrial respiration of Ehrlich ascites carcinoma cells by methylglyoxal. *Int J Cancer* (1993) 54(3):443–9. doi: 10.1002/ijc.2910540315
36. Peng HT, Chen J, Liu TY, Wu YQ, Lin XH, Lai YH, et al. Up-regulation of the tumor promoter Glyoxalase-1 indicates poor prognosis in breast cancer. *Int J Clin Exp Pathol* (2017) 10(11):10852–62.
37. Sakellariou S, Fragkou P, Levidou G, Gargalionis AN, Piperi C, Dalagiorgou G, et al. Clinical significance of AGE-RAGE axis in colorectal cancer: associations with glyoxalase-I, adiponectin receptor expression and prognosis. *BMC Cancer* (2016) 16:174. doi: 10.1186/s12885-016-2213-5
38. Wang Y, Kuramitsu Y, Tokuda K, Okada F, Baron B, Akada J, et al. Proteomic analysis indicates that overexpression and nuclear translocation of lactoylglutathione lyase (GLO1) is associated with tumor progression in murine fibrosarcoma. *Electrophoresis* (2014) 35(15):2195–202. doi: 10.1002/elps.201300497
39. Chen Y, Fang L, Zhang J, Li G, Ma M, Li C, et al. Blockage of Glyoxalase I Inhibits Colorectal Tumorigenesis and Tumor Growth via Upregulation of STAT1, p53, and Bax and Downregulation of c-Myc and Bcl-2. *Int J Mol Sci* (2017) 18(3):570. doi: 10.3390/ijms18030570
40. van Heijst JW, Niessen HW, Musters RJ, van Hinsbergh VW, Hoekman K, Schalkwijk CG. Argpyrimidine-modified Heat shock protein 27 in human non-small cell lung cancer: a possible mechanism for evasion of apoptosis. *Cancer Lett* (2006) 241(2):309–19. doi: 10.1016/j.canlet.2005.10.042
41. Oya-Ito T, Naito Y, Takagi T, Handa O, Matsui H, Yamada M, et al. Heat-shock protein 27 (Hsp27) as a target of methylglyoxal in gastrointestinal

cancer. *Biochim Biophys Acta* (2011) 1812(7):769–81. doi: 10.1016/j.bbadis.2011.03.017
42. Sakamoto H, Mashima T, Yamamoto K, Tsuruo T. Modulation of heat-shock protein 27 (Hsp27) anti-apoptotic activity by methylglyoxal modification. *J Biol Chem* (2002) 277(48):45770–5. doi: 10.1074/jbc.M207485200
43. Nokin MJ, Durieux F, Peixoto P, Chiavarina B, Peulen O, Blomme A, et al. Methylglyoxal, a glycolysis side-product, induces Hsp90 glycation and YAP-mediated tumor growth and metastasis. *Elife* (2016) 5:e19375. doi: 10.7554/eLife.19375
44. Chiavarina B, Nokin MJ, Bellier J, Durieux F, Bletard N, Sherer F, et al. Methylglyoxal-Mediated Stress Correlates with High Metabolic Activity and Promotes Tumor Growth in Colorectal Cancer. *Int J Mol Sci* (2017) 18 (1):213. doi: 10.3390/ijms18010213
45. Lin JA, Wu CH, Yen GC. Methylglyoxal displays colorectal cancer-promoting properties in the murine models of azoxymethane and CT26 isografts. *Free Radic Biol Med* (2018) 115:436–46. doi: 10.1016/j.freeradbiomed.2017.12.020
46. Antognelli C, Moretti S, Frosini R, Puxeddu E, Sidoni A, Talesa VN. Methylglyoxal Acts as a Tumor-Promoting Factor in Anaplastic Thyroid Cancer. *Cells* (2019) 8(6):547. doi: 10.3390/cells8060547
47. Egyud LG, Szent-Gyorgyi A. Cell division, SH, ketoaldehydes, and cancer. *Proc Natl Acad Sci USA* (1966) 55(2):388–93. doi: 10.1073/pnas.55.2.388
48. Apple MA, Greenberg DM. Arrest of cancer in mice by therapy with normal metabolites. II. Indefinite survirors among mice treated with mixtures of 2-oxopropanal (NSC-79019) and 2,3-dihydroxypropanal (NSC67934). *Cancer Chemother Rep* (1968) 52(7):687–96.
49. Milanesa DM, Choudhury MS, Mallouh C, Tazaki H, Konno S. Methylglyoxal-induced apoptosis in human prostate carcinoma: potential modality for prostate cancer treatment. *Eur Urol* (2000) 37(6):728–34. doi: 10.1159/000020226
50. Guo Y, Zhang Y, Yang X, Lu P, Yan X, Xiao F, et al. Effects of methylglyoxal and glyoxalase I inhibition on breast cancer cells proliferation, invasion, and apoptosis through modulation of MAPKs, MMP9, and Bcl-2. *Cancer Biol Ther* (2016) 17(2):169–80. doi: 10.1080/15384047.2015.1121346
51. He T, Zhou H, Li C, Chen Y, Chen X, Li C, et al. Methylglyoxal suppresses human colon cancer cell lines and tumor growth in a mouse model by impairing glycolytic metabolism of cancer cells associated with down-regulation of c-Myc expression. *Cancer Biol Ther* (2016) 17(9):955–65. doi: 10.1080/15384047.2016.1210736
52. Loarca L, Sassi-Gaha S, Artlett CM. Two alpha-dicarbonyls downregulate migration, invasion, and adhesion of liver cancer cells in a p53-dependent manner. *Dig Liver Dis* (2013) 45(11):938–46. doi: 10.1016/j.dld.2013.05.005
53. Tessitore L, Bonelli G, Costelli P, Matera L, Pileri A, Baccino FM, et al. Effect of two aliphatic aldehydes, methylglyoxal and 4-hydroxypentenal, on the growth of Yoshida ascites hepatoma AH-130. *Chem Biol Interact* (1989) 70 (3-4):227–40. doi: 10.1016/0009-2797(89)90046-x
54. Thornalley PJ. Advances in glyoxalase research. Glyoxalase expression in malignancy, anti-proliferative effects of methylglyoxal, glyoxalase I inhibitor diesters and S-D-lactoylglutathione, and methylglyoxal-modified protein binding and endocytosis by the advanced glycation endproduct receptor. *Crit Rev Oncol Hematol* (1995) 20(1-2):99–128. doi: 10.1016/1040-8428(94)00149-n
55. Thornalley PJ, Rabbani N. Glyoxalase in tumourigenesis and multidrug resistance. *Semin Cell Dev Biol* (2011) 22(3):318–25. doi: 10.1016/j.semcdb.2011.02.006
56. Geng X, Ma J, Zhang F, Xu C. Glyoxalase I in tumor cell proliferation and survival and as a potential target for anticancer therapy. *Oncol Res Treat* (2014) 37(10):570–4. doi: 10.1159/000367800
57. Cheng WL, Tsai MM, Tsai CY, Huang YH, Chen CY, Chi HC, et al. Glyoxalase-I is a novel prognosis factor associated with gastric cancer progression. *PloS One* (2012) 7(3):e34352. doi: 10.1371/journal.pone.0034352
58. Wang Y, Kuramitsu Y, Ueno T, Suzuki N, Yoshino S, Iizuka N, et al. (GLO1) is up-regulated in pancreatic cancerous tissues compared with related non-cancerous tissues. *Anticancer Res* (2012) 32(8):3219–22.
59. Hu X, Yang X, He Q, Chen Q, Yu L. Glyoxalase 1 is up-regulated in hepatocellular carcinoma and is essential for HCC cell proliferation. *Biotechnol Lett* (2014) 36(2):257–63. doi: 10.1007/s10529-013-1372-6
60. Kreycy N, Gotzian C, Fleming T, Flechtenmacher C, Grabe N, Plinkert P, et al. Glyoxalase 1 expression is associated with an unfavorable prognosis of oropharyngeal squamous cell carcinoma. *BMC Cancer* (2017) 17(1):382. doi: 10.1186/s12885-017-3367-5
61. Santarius T, Bignell GR, Greenman CD, Widaa S, Chen L, Mahoney CL, et al. GLO1-A novel amplified gene in human cancer. *Genes Chromosomes Cancer* (2010) 49(8):711–25. doi: 10.1002/gcc.20784
62. Zhang S, Liang X, Zheng X, Huang H, Chen X, Wu K, et al. Glo1 genetic amplification as a potential therapeutic target in hepatocellular carcinoma. *Int J Clin Exp Pathol* (2014) 7(5):2079–90.
63. Antognelli C, Mezzasoma L, Fettucciari K, Mearini E, Talesa VN. Role of glyoxalase I in the proliferation and apoptosis control of human LNCaP and PC3 prostate cancer cells. *Prostate* (2013) 73(2):121–32. doi: 10.1002/pros.22547
64. Chiavarina B, Nokin MJ, Durieux F, Bianchi E, Turtoi A, Peulen O, et al. Triple negative tumors accumulate significantly less methylglyoxal specific adducts than other human breast cancer subtypes. *Oncotarget* (2014) 5 (14):5472–82. doi: 10.18632/oncotarget.2121
65. Zou XY, Ding D, Zhan N, Liu XM, Pan C, Xia YM. Glyoxalase I is differentially expressed in cutaneous neoplasms and contributes to the progression of squamous cell carcinoma. *J Invest Dermatol* (2015) 135 (2):589–98. doi: 10.1038/jid.2014.377
66. Antognelli C, Cecchetti R, Riuzzi F, Peirce MJ, Talesa VN. Glyoxalase 1 sustains the metastatic phenotype of prostate cancer cells via EMT control. *J Cell Mol Med* (2018) 22(5):2865–83. doi: 10.1111/jcmm.13581
67. Nokin MJ, Bellier J, Durieux F, Peulen O, Rademaker G, Gabriel M, et al. Methylglyoxal, a glycolysis metabolite, triggers metastasis through MEK/ERK/SMAD1 pathway activation in breast cancer. *Breast Cancer Res* (2019) 21(1):11. doi: 10.1186/s13058-018-1095-7
68. Sharaf H, Matou-Nasri S, Wang Q, Rabhan Z, Al-Eidi H, Al Abdulrahman A, et al. Advanced glycation endproducts increase proliferation, migration and invasion of the breast cancer cell line MDA-MB-231. *Biochim Biophys Acta* (2015) 1852(3):429–41. doi: 10.1016/j.bbadis.2014.12.009
69. Matou-Nasri S, Sharaf H, Wang Q, Almobadel N, Rabhan Z, Al-Eidi H, et al. Biological impact of advanced glycation endproducts on estrogen receptor-positive MCF-7 breast cancer cells. *Biochim Biophys Acta Mol Basis Dis* (2017) 1863(11):2808–20. doi: 10.1016/j.bbadis.2017.07.011
70. Khan MS, Tabrez S, Al-Okail MS, Shaik GM, Bhat SA, Rehman TM, et al. Non-enzymatic glycation of protein induces cancer cell proliferation and its inhibition by quercetin: Spectroscopic, cytotoxicity and molecular docking studies. *J Biomol Struct Dyn* (2020) 39(3):777–86. doi: 10.1080/07391102.2020.1715838
71. Nokin MJ, Durieux F, Bellier J, Peulen O, Uchida K, Spiegel DA, et al. Hormetic potential of methylglyoxal, a side-product of glycolysis, in switching tumours from growth to death. *Sci Rep* (2017) 7(1):11722. doi: 10.1038/s41598-017-12119-7
72. Thornalley PJ, Waris S, Fleming T, Santarius T, Larkin SJ, Winklhofer-Roob BM, et al. Imidazopurinones are markers of physiological genomic damage linked to DNA instability and glyoxalase 1-associated tumour multidrug resistance. *Nucleic Acids Res* (2010) 38(16):5432–42. doi: 10.1093/nar/gkq306
73. Khan H, Khan MS, Ahmad S. The in vivo and in vitro approaches for establishing a link between advanced glycation end products and lung cancer. *J Cell Biochem* (2018) 119(11):9099–109. doi: 10.1002/jcb.27170
74. Irigaray P, Belpomme D. Circulating free methylglyoxal as a metabolic tumor biomarker in a rat colon adenocarcinoma model. *Mol Clin Oncol* (2020) 12(4):311–6. doi: 10.3892/mco.2020.2000
75. Ahmad MI, Ahmad S. Moinuddin. Preferential recognition of methylglyoxal-modified calf thymus DNA by circulating antibodies in cancer patients. *Indian J Biochem Biophys* (2011) 48(4):290–6.
76. Alamil H, Lechevrel M, Lagadu S, Galanti L, Dagher Z, Delepee R. A validated UHPLC-MS/MS method for simultaneous quantification of 9 exocyclic DNA adducts induced by 8 aldehydes. *J Pharm BioMed Anal* (2020) 179:113007. doi: 10.1016/j.jpba.2019.113007
77. Coluccio ML, Presta I, Greco M, Gervasi R, La Torre D, Renne M, et al. Microenvironment Molecular Profile Combining Glycation Adducts and Cytokines Patterns on Secretome of Short-term Blood-derived Cultures during Tumour Progression. *Int J Mol Sci* (2020) 21(13):4711. doi: 10.3390/ijms21134711

78. Talukdar D, Ray S, Ray M, Das S. A brief critical overview of the biological effects of methylglyoxal and further evaluation of a methylglyoxal-based anticancer formulation in treating cancer patients. *Drug Metabol Drug Interact* (2008) 23(1-2):175–210. doi: 10.1515/dmdi.2008.23.1-2.175
79. Roy A, Sarker S, Upadhyay P, Pal A, Adhikary A, Jana K, et al. Methylglyoxal at metronomic doses sensitizes breast cancer cells to doxorubicin and cisplatin causing synergistic induction of programmed cell death and inhibition of stemness. *Biochem Pharmacol* (2018) 156:322–39. doi: 10.1016/j.bcp.2018.08.041
80. Rabbani N, Xue M, Thornalley PJ. Dicarbonyls and glyoxalase in disease mechanisms and clinical therapeutics. *Glycoconj J* (2016) 33(4):513–25. doi: 10.1007/s10719-016-9705-z
81. Thornalley PJ, Edwards LG, Kang Y, Wyatt C, Davies N, Ladan MJ, et al. Antitumour activity of S-p-bromobenzylglutathione cyclopentyl diester in vitro and in vivo. Inhibition of glyoxalase I and induction of apoptosis. *Biochem Pharmacol* (1996) 51(10):1365–72. doi: 10.1016/0006-2952(96)00059-7
82. Sakamoto H, Mashima T, Sato S, Hashimoto Y, Yamori T, Tsuruo T. Selective activation of apoptosis program by S-p-bromobenzylglutathione cyclopentyl diester in glyoxalase I-overexpressing human lung cancer cells. *Clin Cancer Res* (2001) 7(8):2513–8.
83. Sakamoto H, Mashima T, Kizaki A, Dan S, Hashimoto Y, Naito M, et al. Glyoxalase I is involved in resistance of human leukemia cells to antitumor agent-induced apoptosis. *Blood* (2000) 95(10):3214–8. doi: 10.1182/blood.V95.10.3214
84. Michel M, Hollenbach M, Pohl S, Ripoll C, Zipprich A. Inhibition of Glyoxalase-I Leads to Reduced Proliferation, Migration and Colony Formation, and Enhanced Susceptibility to Sorafenib in Hepatocellular Carcinoma. *Front Oncol* (2019) 9:785. doi: 10.3389/fonc.2019.00785
85. Davies GF, Juurlink BH, Harkness TA. Troglitazone reverses the multiple drug resistance phenotype in cancer cells. *Drug Des Devel Ther* (2009) 3:79–88. doi: 10.2147/dddt.s3314
86. Helgager J, Li J, Lubensky IA, Lonser R, Zhuang Z. Troglitazone reduces glyoxalase I protein expression in glioma and potentiates the effects of chemotherapeutic agents. *J Oncol* (2010) 2010:373491. doi: 10.1155/2010/373491
87. Davies GF, Roesler WJ, Juurlink BH, Harkness TA. Troglitazone overcomes doxorubicin-resistance in resistant K562 leukemia cells. *Leuk Lymphoma* (2005) 46(8):1199–206. doi: 10.1080/10428190500102555
88. Ghosh S, Banerjee S, Sil PC. The beneficial role of curcumin on inflammation, diabetes and neurodegenerative disease: A recent update. *Food Chem Toxicol* (2015) 83:111–24. doi: 10.1016/j.fct.2015.05.022
89. Santel T, Pflug G, Hemdan NY, Schafer A, Hollenbach M, Buchold M, et al. Curcumin inhibits glyoxalase 1: a possible link to its anti-inflammatory and anti-tumor activity. *PloS One* (2008) 3(10):e3508. doi: 10.1371/journal.pone.0003508
90. Keating E, Martel F. Antimetabolic Effects of Polyphenols in Breast Cancer Cells: Focus on Glucose Uptake and Metabolism. *Front Nutr* (2018) 5:25:25. doi: 10.3389/fnut.2018.00025
91. Yadav A, Kumar R, Sunkaria A, Singhal N, Kumar M, Sandhir R. Evaluation of potential flavonoid inhibitors of glyoxalase-I based on virtual screening and in vitro studies. *J Biomol Struct Dyn* (2016) 34(5):993–1007. doi: 10.1080/07391102.2015.1064830
92. Finkelstein MP, Aynehchi S, Samadi AA, Drinis S, Choudhury MS, Tazaki H, et al. Chemosensitization of carmustine with maitake beta-glucan on androgen-independent prostatic cancer cells: involvement of glyoxalase I. *J Altern Complement Med* (2002) 8(5):573–80. doi: 10.1089/107555302320825084
93. Antognelli C, Talesa VN. Glyoxalases in Urological Malignancies. *Int J Mol Sci* (2018) 19(2):415. doi: 10.3390/ijms19020415
94. Takasawa R, Saeki K, Tao A, Yoshimori A, Uchiro H, Fujiwara M, et al. Delphinidin, a dietary anthocyanidin in berry fruits, inhibits human glyoxalase I. *Bioorg Med Chem* (2010) 18(19):7029–33. doi: 10.1016/j.bmc.2010.08.012
95. Chen CC, Liu TY, Huang SP, Ho CT, Huang TC. Differentiation and apoptosis induction by lovastatin and gamma-tocotrienol in HL-60 cells via Ras/ERK/NF-kappaB and Ras/Akt/NF-kappaB signaling dependent down-regulation of glyoxalase 1 and HMG-CoA reductase. *Cell Signal* (2015) 27(11):2182–90. doi: 10.1016/j.cellsig.2015.07.014
96. Xiong Z, Cao X, Wen Q, Chen Z, Cheng Z, Huang X, et al. An overview of the bioactivity of monacolin K / lovastatin. *Food Chem Toxicol* (2019) 131:110585. doi: 10.1016/j.fct.2019.110585
97. Takasawa R, Takahashi S, Saeki K, Sunaga S, Yoshimori A, Tanuma S. Structure-activity relationship of human GLO I inhibitory natural flavonoids and their growth inhibitory effects. *Bioorg Med Chem* (2008) 16(7):3969–75. doi: 10.1016/j.bmc.2008.01.031
98. Takasawa R, Tao A, Saeki K, Shionozaki N, Tanaka R, Uchiro H, et al. Discovery of a new type inhibitor of human glyoxalase I by myricetin-based 4-point pharmacophore. *Bioorg Med Chem Lett* (2011) 21(14):4337–42. doi: 10.1016/j.bmcl.2011.05.046
99. Takasawa R, Shimada N, Uchiro H, Takahashi S, Yoshimori A, Tanuma S. TLSC702, a Novel Inhibitor of Human Glyoxalase I, Induces Apoptosis in Tumor Cells. *Biol Pharm Bull* (2016) 39(5):869–73. doi: 10.1248/bpb.b15-00710
100. Yamamoto T, Sato A, Takai Y, Yoshimori A, Umehara M, Ogino Y, et al. Effect of piceatannol-rich passion fruit seed extract on human glyoxalase I-mediated cancer cell growth. *Biochem Biophys Rep* (2019) 20:100684. doi: 10.1016/j.bbrep.2019.100684
101. Takasawa R, Akahane H, Tanaka H, Shimada N, Yamamoto T, Uchida-Maruki H, et al. Piceatannol, a natural trans-stilbene compound, inhibits human glyoxalase I. *Bioorg Med Chem Lett* (2017) 27(5):1169–74. doi: 10.1016/j.bmcl.2017.01.070
102. Shimada N, Takasawa R, Tanuma SI. Interdependence of GLO I and PKM2 in the Metabolic shift to escape apoptosis in GLO I-dependent cancer cells. *Arch Biochem Biophys* (2018) 638:1–7. doi: 10.1016/j.abb.2017.12.008
103. Tamori S, Nozaki Y, Motomura H, Nakane H, Katayama R, Onaga C, et al. Glyoxalase 1 gene is highly expressed in basal-like human breast cancers and contributes to survival of ALDH1-positive breast cancer stem cells. *Oncotarget* (2018) 9(92):36515–29. doi: 10.18632/oncotarget.26369
104. Pernicova I, Korbonits M. Metformin–mode of action and clinical implications for diabetes and cancer. *Nat Rev Endocrinol* (2014) 10(3):143–56. doi: 10.1038/nrendo.2013.256
105. Vancura A, Bu P, Bhagwat M, Zeng J, Vancurova I. Metformin as an Anticancer Agent. *Trends Pharmacol Sci* (2018) 39(10):867–78. doi: 10.1016/j.tips.2018.07.006
106. Jiang Y, Chen X, Wei Y, Feng Y, Zheng W, Zhang Z. Metformin sensitizes endometrial cancer cells to progestin by targeting TET1 to downregulate glyoxalase I expression. *BioMed Pharmacother* (2019) 113:108712. doi: 10.1016/j.biopha.2019.108712
107. Dong L, Zhou Q, Zhang Z, Zhu Y, Duan T, Feng Y. Metformin sensitizes endometrial cancer cells to chemotherapy by repressing glyoxalase I expression. *J Obstet Gynaecol Res* (2012) 38(8):1077–85. doi: 10.1111/j.1447-0756.2011.01839.x
108. Kinsky OR, Hargraves TL, Anumol T, Jacobsen NE, Dai J, Snyder SA, et al. Metformin Scavenges Methylglyoxal To Form a Novel Imidazolinone Metabolite in Humans. *Chem Res Toxicol* (2016) 29(2):227–34. doi: 10.1021/acs.chemrestox.5b00497
109. Thornalley PJ. Use of aminoguanidine (Pimagedine) to prevent the formation of advanced glycation endproducts. *Arch Biochem Biophys* (2003) 419(1):31–40. doi: 10.1016/j.abb.2003.08.013
110. Imai T, Hasumura M, Cho YM, Ota Y, Takami S, Hirose M, et al. Inhibitory effects of aminoguanidine on thyroid follicular carcinoma development in inflamed capsular regions of rats treated with sulfadimethoxine after N-bis(2-hydroxypropyl)nitrosamine-initiation. *Cancer Sci* (2009) 100(10):1794–800. doi: 10.1111/j.1349-7006.2009.01250.x
111. Heinecke JL, Ridnour LA, Cheng RY, Switzer CH, Lizardo MM, Khanna C, et al. Tumor microenvironment-based feed-forward regulation of NOS2 in breast cancer progression. *Proc Natl Acad Sci USA* (2014) 111(17):6323–8. doi: 10.1073/pnas.1401799111
112. Calvisi DF, Pinna F, Ladu S, Pellegrino R, Muroni MR, Simile MM, et al. Aberrant iNOS signaling is under genetic control in rodent liver cancer and potentially prognostic for the human disease. *Carcinogenesis* (2008) 29(8):1639–47. doi: 10.1093/carcin/bgn155
113. Iovine B, Iannella ML, Nocella F, Pricolo MR, Bevilacqua MA. Carnosine inhibits KRAS-mediated HCT116 proliferation by affecting ATP and ROS production. *Cancer Lett* (2012) 315(2):122–8. doi: 10.1016/j.canlet.2011.07.021

114. Lee J, Park JR, Lee H, Jang S, Ryu SM, Kim H, et al. L-carnosine induces apoptosis/cell cycle arrest via suppression of NF-kappaB/STAT1 pathway in HCT116 colorectal cancer cells. *Vitro Cell Dev Biol Anim* (2018) 54(7):505–12. doi: 10.1007/s11626-018-0264-4
115. Bellier J, Nokin MJ, Caprasse M, Tiamiou A, Blomme A, Scheijen JL, et al. Methylglyoxal Scavengers Resensitize KRAS-Mutated Colorectal Tumors to Cetuximab. *Cell Rep* (2020) 30(5):1400–16.e6. doi: 10.1016/j.celrep.2020.01.012
116. Sullivan LB, Gui DY, Vander Heiden MG. Altered metabolite levels in cancer: implications for tumour biology and cancer therapy. *Nat Rev Cancer* (2016) 16(11):680–93. doi: 10.1038/nrc.2016.85

**Conflict of Interest:** The authors declare that the research was conducted in the absence of any commercial or financial relationships that could be construed as a potential conflict of interest.

frontiers in Pharmacology

ORIGINAL RESEARCH
published: 12 April 2021
doi: 10.3389/fphar.2021.634097

# Prediction of Synergistic Drug Combinations for Prostate Cancer by Transcriptomic and Network Characteristics

*Shiqi Li[1], Fuhui Zhang[1], Xiuchan Xiao[2], Yanzhi Guo[1], Zhining Wen[1], Menglong Li[1]* and Xuemei Pu[1]**

[1]College of Chemistry, Sichuan University, Chengdu, China, [2]School of Material Science and Environmental Engineering, Chengdu Technological University, Chengdu, China

OPEN ACCESS

**Edited by:**
Daniela Spano,
National Research Council, Italy

**Reviewed by:**
Gennaro Gambardella,
University of Naples Federico II, Italy
Wei-de Zhong,
Guangzhou First People's Hospital, China

***Correspondence:**
Menglong Li
liml@scu.edu.cn
Xuemei Pu
Puxmpuscu@scu.edu.cn

**Specialty section:**
This article was submitted to Pharmacology of Anti-Cancer Drugs, a section of the journal Frontiers in Pharmacology

**Received:** 27 November 2020
**Accepted:** 04 February 2021
**Published:** 12 April 2021

**Citation:**
Li S, Zhang F, Xiao X, Guo Y, Wen Z, Li M and Pu X (2021) Prediction of Synergistic Drug Combinations for Prostate Cancer by Transcriptomic and Network Characteristics. Front. Pharmacol. 12:634097. doi: 10.3389/fphar.2021.634097

Prostate cancer (PRAD) is a major cause of cancer-related deaths. Current monotherapies show limited efficacy due to often rapidly emerging resistance. Combination therapies could provide an alternative solution to address this problem with enhanced therapeutic effect, reduced cytotoxicity, and delayed the appearance of drug resistance. However, it is prohibitively cost and labor-intensive for the experimental approaches to pick out synergistic combinations from the millions of possibilities. Thus, it is highly desired to explore other efficient strategies to assist experimental researches. Inspired by the challenge, we construct the transcriptomics-based and network-based prediction models to quickly screen the potential drug combination for Prostate cancer, and further assess their performance by *in vitro* assays. The transcriptomics-based method screens nine possible combinations. However, the network-based method gives discrepancies for at least three drug pairs. Further experimental results indicate the dose-dependent effects of the three docetaxel-containing combinations, and confirm the synergistic effects of the other six combinations predicted by the transcriptomics-based model. For the network-based predictions, *in vitro* tests give opposite results to the two combinations (i.e. mitoxantrone-cyproheptadine and cabazitaxel-cyproheptadine). Namely, the transcriptomics-based method outperforms the network-based one for the specific disease like Prostate cancer, which provide guideline for selection of the computational methods in the drug combination screening. More importantly, six combinations (the three mitoxantrone-containing and the three cabazitaxel-containing combinations) are found to be promising candidates to synergistically conquer Prostate cancer.

**Keywords: prostate cancer, drug combinations, the transcriptomics-based prediction, the network-based prediction, computation**

## INTRODUCTION

In the past decades, the drug development has been dominated by one-target one-drug strategy. Although the targeted therapy has dramatically changed the treatment of cancer, confining the drug to a single target fails to consider the complexity of causative factors. Furthermore, cancer cells easily develop resistance to single-drugs through activating other pathways due to their heterogeneous mutation and functional redundancy (Al-Lazikani et al., 2012; Lavecchia and Cerchia, 2016; Liu et al., 2019). Conversely, combinatorial therapies exhibit significant advantages in overcoming drug resistance, reducing toxicity and improving curative effects, thus attracting considerable interests from researchers and drug companies (Bayat Mokhtari et al., 2017; Liu et al., 2019). Considering high attrition rates in the development of new drugs, one tempting option for exploring combinatorial therapies in tumor is to consider drugs already on the market, due to their well-documented safeties (Huang et al., 2019).

In spite of the successes of combinatorial therapies, most of them were derived from the clinical experience and serendipitous discovery, only covering a tiny fraction of the large-scale combinatorial space (Al-Lazikani et al., 2012). In fact, besides more than 200 currently approved cancer agents, there are several thousand drugs under investigation. Consequently, the number of combinations to be tested could reach millions (Ding et al., 2020). It is prohibitively cost and labor-intensive for the experimental approaches to pick out synergistic combinations from the millions of possibilities (Regan-Fendt et al., 2019). Thus, it is highly desired to introduce some effective and robust approaches to significantly narrow down the candidate space of drug combinations for wet-lab experimental validations, in turn facilitating the process of drug synergy prediction.

To mitigate these challenges, various computational methods are coming up recently to assist the combination therapies. Although the predictive ability of these methodologies is significantly better than random, some limitations should be mentioned. Firstly, many existing computational methods (Li et al., 2015; Chen et al., 2016; Regan-Fendt et al., 2019) are based on a similarity comparison between the query combinations and the known ones, thus needing a lot of known drug combinations. However, the number of synergistic combinations known is much less than that of the unknown ones. Secondly, most of the developed predictive models (Zhao et al., 2011; Li et al., 2015; Li et al., 2017; Celebi et al., 2019) require multiple kinds of features, such as physicochemical properties of drugs, interactions between biological entities. In fact, too many features as input would limit the applicability of the method, because the prediction of new drug combination will depend on the same descriptors for each component in the combination (Mason et al., 2018). However, some data may be non-existent or difficult to obtain, in particular for new agents (Chen et al., 2016). In addition, some features may not contribute much to elucidating the underlying mechanisms of drug synergy. As accepted, drug-induced gene expression profiles can be a snapshot of the biological effects induced by drug treatments, thereby benefiting in the recognition of mechanisms of drug action (Lamb et al., 2006; Bansal et al., 2014; Huang et al., 2019). Some studies indicated that gene expression profiles play a significant part in drug predictions (Sun et al., 2015; Celebi et al., 2019; Zhu et al., 2020). Furthermore, there is an growing number of databases which describe biological entities, chemical agents or genomic data and their relationships being produced and available to the public like the Cancer Genome Atlas (TCGA) (Chang et al., 2013) and the Library of Integrated Network-based Cellular Signatures (LINCS) (Subramanian et al., 2017; Keenan et al., 2018; Koleti et al., 2018). The predictive power of transcriptomics-based methods will gain further improvement owing to the availability of such databases. For example, Stathias et al. (Stathias et al., 2018) integrated gene expression data from Cancer Genome Atlas, Library of Integrated Network-based Cellular Signatures, and the Brain Tumor PDX national resource to build a computational platform named SynergySeq in order to identify synergistic combinations in glioblastoma multiforme (GBM). As a result, they identified compounds that synergize with BET inhibitors and further validated their synergistic effects in reducing glioblastoma multiforme cell expansion experimentally. In addition, in the last few years, network-based models were developed to enable researchers to screen synergistic pairs and examine the mechanisms of them, given that both physiological states and biological processes are modulated by a large interactive network with many signaling pathways (Jia et al., 2009; Barabási et al., 2011; Ryall and Tan, 2015; Wu et al., 2018; Cheng et al., 2019; Zhou et al., 2020). For example, according to the approved combinatorial therapies of hypertension and cancer, Cheng et al. (Cheng et al., 2019) quantified the distance between drug targets and disease proteins in the human protein-protein interaction network (PPI), and suggested that a drug combination is effective when meets the criteria of "Complementary Exposure" pattern: the target modules of each drug locates separately within or adjacent to different parts of the disease module. Using hypertension data as a validation set, this network-based predictor achieved 59% accuracy, outperforming traditional cheminformatics and bioinformatics approaches. The work exhibits the role of the network-based information in identifying efficacious combination therapies. However, most of the current models, including the network-based one (Cheng et al., 2019), were constructed using data from various diseases (Bansal et al., 2014; Sun et al., 2015). The models involved in multiple diseases do not take the context specificity into account, while synergy and antagonism have shown to be strongly context-dependent compound-pair properties (Bansal et al., 2014; Yin et al., 2014; Sun et al., 2015). Therefore, it is highly desired to study the context-specific therapies on drug combination prediction.

Prostate cancer (Prostate cancer) has remained an important public health concern since it is the most frequently diagnosed cancer and the second common reason for cancer death in men, which is predicted to have 191,930 new cases and 33,330 deaths in 2020 (Siegel et al., 2020). In 1941, Charles Huggins (Huggins and Hodges, 1941) reported androgen deprivation therapy (ADT) suppressing androgen receptor activity, which has played an

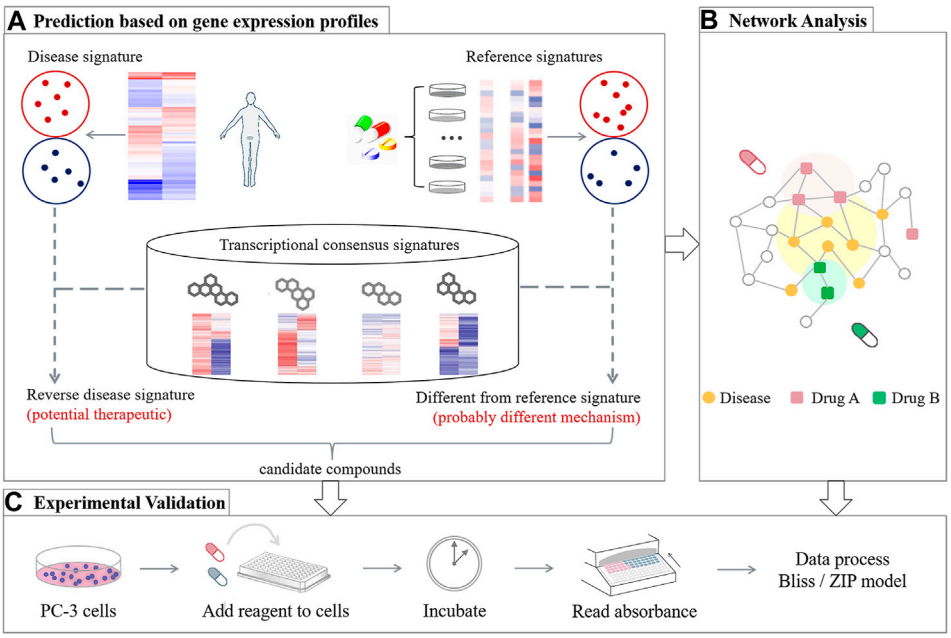


**FIGURE 1 |** Overview of the design strategy proposed for generating Prostate cancer-specific drug combinations, including three main frameworks: **(A)** Transcriptomics-based ranking, **(B)** network-based assessment, and **(C)** experimental validation.

important role in treating Prostate cancer. To date, ADT has been used as a standard treatment for Prostate cancer patients. Although ADT exerts certain remissions for 1–2 years for most patients, they still progress to castration-resistant Prostate cancer later, leading to the lethal condition in Prostate cancer. To overcome resistance to monotherapy, some clinical trials like the CHAARTED (Sweeney et al., 2015) and STAMPEDE (James et al., 2015), have shown a survival advantage when combining androgen deprivation therapy with chemotherapy, showing a promise of drug combination in the treatment of Prostate cancer. However, there are only a few approved and investigational drug combinations for Prostate cancer and the success of current Prostate cancer combination therapies are limited (Lee and Kantoff, 2019). Hence, the development of new combinations for Prostate cancer is of great importance.

Inspired by the challenge, we construct a computation-based strategy to screen potential drug combinations for Prostate cancer. Considering high attrition rates in the new drug development, herein, we focus on FDA approved drugs with potential to be repurposed with an existing Prostate cancer single-agent, due to their well-documented safeties. Our prediction framework mainly includes three parts (**Figure 1**): 1) Transcriptomics-based ranking: computing the synergistic potential for drug pairs by integrating disease transcriptional data with drug-perturbated transcription profiles; 2) Network-based assessment: quantifying the network-based relationship between drug targets of the top ranked pairs and Prostate cancer proteins, in order to assess the predicted drug pairs from a network perspective; and 3) Experimental validation: using cell viability assays to further evaluate the accuracy of the predicted results. The comparison of the two computational results also provides guidelines for selection of the computational methods when applied to a specific disease.

# MATERIALS AND METHODS

## Collection and Preprocessing of Gene Expression Datasets

In this study, we used two gene expression databases: 1) RNA-Seq data for Prostate cancer tumors and controls were downloaded from Cancer Genome Atlas database (Chang et al., 2013); and 2) the drug-perturbated profiles were downloaded from the Library of Integrated Network-based Cellular Signatures project (Subramanian et al., 2017; Koleti et al., 2018). Specifically, we downloaded the Level 4 panel standardized data from the Phase II L1000 dataset released from the Broad Institute Library of Integrated Network-based Cellular Signatures Data Generation Center through the GEO portal [https://www.ncbi.nlm.nih.gov/geo/query/acc.cgi?acc=GSE70138]. By reannotating all probe sets on different platforms, 12,299 genes shared between the two databases were retained.

## Computation of Disease Signature

Prostate cancer RNA datasets publicly available through Cancer Genome Atlas were downloaded using GenomicDataCommons download tool (Grossman et al., 2016). We obtained 52 prostate cancer and 52 matched normal controls. Then thresholds of $|\log_2 FC| > 1$ and FDR < 0.1 were used to select genes that differentially expressed between tumor and normal samples, leading to the Prostate cancer gene-expression signature.

## Collection and Preprocessing of Gene Expression Datasets

As described in the SynergySeq (Stathias et al., 2018), each compound will be assigned a transcriptional consensus signature (TCS) by utilizing the quantitative gene expression data measured before and after drug perturbation. Then the concordance ratio (CR) and the disease discordance ratio (DR) are calculated for each drug pair (Stathias et al., 2018). Herein, CR denotes the ratio of a compound's genes in the same direction as the reference signature to those in the opposite directions (**Eq. 1**). For DR, its definition is based on a comparison between the genes in TSC of a compound and the disease signature genes that are missing in the reference signature. Consequently, DR could be obtained as the ratio of differentially expressed genes induced by drug in an opposite direction to ones in the same direction (**Eq. 2**):

$$\mathrm{CR} = \frac{\sum_{i=1}^{\text{number of genes}} [a_i]}{\sum_{i=1}^{\text{number of genes}} [b_i]} \text{ with } a_i = \begin{cases} 1, \ if \ z_i \cdot r_i > 0 \\ 0, \ if \ z_i \cdot r_i < 0 \end{cases} \text{ and } b_i = \begin{cases} 1, \ if \ z_i \cdot r_i < 0 \\ 0, \ if \ z_i \cdot r_i > 0 \end{cases}, \tag{1}$$

$$\mathrm{DR} = \frac{\sum_{i=1}^{\text{number of genes}} [b_i \cdot c_i]}{\sum_{i=1}^{\text{number of genes}} [a_i \cdot c_i]} \text{ with } a_i = \begin{cases} 1, \ if \ z_i \cdot d_i > 0 \\ 0, \ if \ z_i \cdot d_i < 0 \end{cases}, \ b_i = \begin{cases} 1, \ if \ z_i \cdot d_i < 0 \\ 0, \ if \ z_i \cdot d_i > 0 \end{cases}, \text{ and } c_i = \begin{cases} 1, \ if \ r_i = 0 \\ 0, \ if \ r_i \neq 0 \end{cases}, \tag{2}$$

where z, d, and r denote the TCS vectors of the L1000 compound, the disease and the reference compound signature, respectively.

Combining CR with DR, the orthogonality of each compound to the transcriptional impact caused by the reference compound can be measured by a single value, Orthogonality Score (OS) (Stathias et al., 2018).

$$\mathrm{OS} = \sqrt{(1 - \mathrm{CR})^2 + \mathrm{DR}^2}. \tag{3}$$

## Construction of Human Protein-Protein Interaction Network

Here, we construct a comprehensive human PPI network by using high-quality protein-protein interaction data from different bioinformatics and systems biology databases (Cheng et al., 2019): 1) binary interactions from yeast two-hybrid high-throughputs; 2) binary, physical PPIs derived from protein 3D structures; 3) kinase-substrate pairs; 4) signaling interactions, and 5) literature-curated interactions. As a result, the final human PPI network consists of 217,109 edges and 15,911 nodes.

## Network Configurations of Drug–Drug–Disease Combinations

We assemble Prostate cancer-gene annotation data from eight different bioinformatics data sources: OMIM (Amberger et al., 2015), CTD (Davis et al., 2015), ClinVar (Landrum et al., 2014), GWAS Catalog (Welter et al., 2014), GWASdb (Li et al., 2016), PheWAS Catalog (Denny et al., 2013), HuGE Navigator (Yu et al., 2008), and DisGeNET (Piñero et al., 2015). In addition, we collect the target information of the approved drugs by searching in DrugBank (Law et al., 2014), and drug target interactions meeting three criteria were used (Cheng et al., 2019): 1) binding affinities ≤10 μM; 2) the manually verified target stored in the UniProt with unique identifiers.

In the human PPI network, when a drug targets the corresponding subnetwork of a disease or its adjacent communities, the drug is more likely to have therapeutic effects on the disease than other drugs with targets far from the disease subnetwork (Cheng et al., 2018; Cheng et al., 2019). Z-score is a reliable index to measure the network proximity between a drug (X) and a disease (Y), which is based on the shortest path lengths d(x, y) between drug targets (x) and disease proteins (y):

$$d(X, Y) = \frac{1}{\|Y\|} \sum_{y \in Y} \min_{x \in X} d(x, y), \ z = \frac{d - \mu}{\sigma}. \tag{4}$$

Select a random group of proteins each time, the size and degree distribution of which matches the ones of disease proteins and drug targets, repeat 100 times, and then the mean $\mu$ and standard deviation $\sigma$ were calculated. If the drug targets and the disease proteins separate from each other from a network-based perspective, their corresponding $z \geq 0$; otherwise, $z < 0$.

In addition, the isolated target protein modules between two drugs in the human PPI network indicating that they act in different ways, and the network-based separation is an effective measurement for this (Menche et al., 2015):

$$s_{AB} = \langle d_{AB} \rangle - \frac{\langle d_{AA} \rangle + \langle d_{BB} \rangle}{2}, \tag{5}$$

where <d> represents the shortest path between two nodes. If the two drug–target modules isolate from each other in the network, their corresponding $s_{AB} \geq 0$; otherwise, $s_{AB} < 0$.

## Cell Lines and Reagents

PC-3 cells were purchased from the Wuhan Bafeier Biological Co., Ltd. and grown in F12K mediums supplemented with 10% FBS and 1% penicillin-streptomycin at 37 under 5% $CO_2$. Docetaxel (D807092) was purchased from Macklin (Shanghai, China). Imatinib (I0906), cabazitaxel (C3390), and mitoxantrone (M3133) were purchased from Tokyo Chemical Industry (TCI, Shanghai, China). Indinavir sulfate (HY-B0689A) and cyproheptadine hydrochloride sesquihydrate (HY-B1165) were purchased from MedChemExpress (MCE, Shanghai, China). MTT (3580MG250) was purchased from BIOFROX (Guangzhou, China).

## MTT Assay

Cells were seeded into 96-well plate at a density of $4.0 \times 10^3$ cells/well in growth medium, cultured for 24 h, and then the indicated drugs were added and co-cultured for 72 h. For each concentration gradient, set three replicates, and a well without culture medium was set as control. Then 10 μl MTT solution was added to each well. After 4 h, the cell medium was removed and

150 μl/well of DMSO was added. Relative cell viability was obtained by measuring absorbance at 570 nm in a microplate reader (Flexstation® 3, Molecular Device, United States).

# RESULTS

## Transcriptomics-Based Ranking

In the area of recognizing the mechanisms of human diseases and drug actions, RNA-seq plays a significant role (Lamb et al., 2006; Rees et al., 2016; Wang et al., 2016). Advances in sequencing techniques have generated large-scale omics data, which provide opportunities for drug discovery. As aforementioned, Stathias et al. (Stathias et al., 2018) proposed a method termed SynergySeq to screen drug pairs acting in a synergistic way, in order to combat the resistance of BET inhibitors in glioblastoma multiforme. By assessing the expression of 978 representative landmark transcripts in glioblastoma multiforme and small molecule compounds, they screened some synergistic combinations with a reference compound (BET) from 285 L1000 compounds, and these combinations were further validated by both the external databases and various assays. Herein, we also applied SynergySeq to Prostate cancer. Different from (Stathias et al., 2018), we reannotated the probes on Cancer Genome Atlas and Library of Integrated Network-based Cellular Signatures platforms, resulting in 12,299 common genes, covering a more comprehensive gene space, and the compound library was expanded to 918 approved drugs, much more than 285 in the previous work (Stathias et al., 2018).

### Compound-Specific Transcriptional Consensus Signatures

In order to predict drug combinations for Prostate cancer, we first need to generate drug-perturbated transcription profiles of Prostate cancer cells from a large-scale database which collects gene expression data before and after drug perturbation across multiple cancer cell lines. For each compound, the Library of Integrated Network-based Cellular Signatures L1000 project provides data on gene expression measured at different time points and doses before and after treatment of multiple cells (Keenan et al., 2018). However, some compounds didn't treat any Prostate cancer cell lines, so there is a need to establish the respective transcriptional consensus signatures (TCS) for each compound. In the work of Stathias (Stathias et al., 2018), they introduced TCS to represent the transcription profiles of compounds in glioblastoma multiforme cells under the condition that most Library of Integrated Network-based Cellular Signatures L1000 compounds lack profiles from any glioblastoma multiforme cell, and demonstrated that TCSs could represent the compound used to perturb the cells, and be independent of the cell type. Following the work, we calculated TCS for each compound, based on the chemical perturbation experiments data across multiple cell lines. If a gene is observed to be consistently up or down regulated in multiple types of cancer cell lines after the compound disturbance, we deduce that the gene also produces the same transcriptional changes in the prostate cancer cells.

In order to confirm the assumption, correlation coefficients between all pairs of compounds were calculated using TCS and hierarchical clustering was then performed. As a result, various compound classes are aggregated respectively, as shown in **Figure 2** and **Supplementary Table S1**. **Figure 2** shows that compounds with highly correlated consensus signatures (Pearson Correlation > 0.7) could be incorporated into a subnetwork reflecting their mechanism of action, confirming that TCS could well characterize the transcriptomic changes induced by drugs. In addition, the observation further supports the idea that compounds with similar mechanisms produce similar gene expression changes (Lamb et al., 2006; Rees et al., 2016; Regan-Fendt et al., 2019).

### Reference Compounds

Herein, we need to identify available Prostate cancer drugs from the Library of Integrated Network-based Cellular Signatures L1000 dataset as reference candidates and then repositioned other marketed drugs to find the ones, which could produce synergistic effects with the reference compound selected. For Prostate cancer, only thirteen drugs are selected as preliminary reference candidates in the work, as they are approved drugs for Prostate cancer and also have experimental data for treating Prostate cancer cell lines in the Library of Integrated Network-based Cellular Signatures project. For the thirteen reference compounds, we only focused on genes that induce consistent transcriptional changes in at least half of the PC-3 cells to obtain robust reference signatures (Stathias et al., 2018). Because a high TCS gene score (max score = the number of the cell lines used) indicates that more genes over/under-expressed in different PC-3 cells, three compounds (mitoxantrone, cabazitaxel, and docetaxel), which exhibit significantly higher TCS scores than the other Prostate cancer drugs (vide **Supplementary Table S2**), are selected as final reference compounds.

In fact, mitoxantrone, cabazitaxel, and docetaxel are all conventional chemotherapeutics to treat Prostate cancer. Mitoxantrone was the only chemotherapeutic drug approved for the treatment of Prostate cancer before 2004. As a DNA intercalating agent and topoisomerase II inhibitor, it has been routinely used for the treatment Prostate cancer since its palliative benefit could enhance clinical remission of the Prostate cancer patients. However, it was also reported that the mitoxantrone failed to confer any survival advantage, and most patients frequently developed therapeutic resistance to the treatment (Song et al., 2018). In 2004, the docetaxel was approved by FDA, which brought certain improvements for the treatment of Prostate cancer patients. Thus, it became the standard chemotherapy treatment for castration-resistant prostate cancer (Song et al., 2018). Unfortunately, many patients did not respond to the therapy and all patients ultimately developed resistance to the docetaxel (Hwang, 2012; Song et al., 2018). Thus, many efforts have been devoted to overcome chemoresistance to docetaxel. Consequently, multiple novel anti-tumor agents were developed, including the cabazitaxel. The cabazitaxel, as the second taxane, could extend survival and is currently used as a single agent (Madan et al., 2011). Despite the antitumor activity of the cabazitaxel in

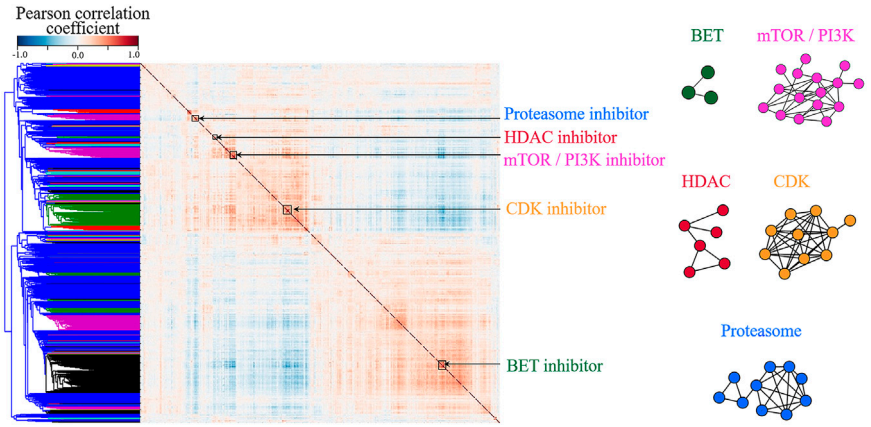


**FIGURE 2 |** The clustering of small molecules according to their L1000 consensus signatures. **(A)** Correlation matrix of the 918 consensus signatures. Blue to red denotes the correlation coefficient between the two compounds from −1 to 1, namely, from completely negative correlation and the completely positive one. The red clusters along the diagonal denote compounds with high transcriptional similarities (Pearson Correlation > 0.7). **(B)** Networks of highly correlated Library of Integrated Network-based Cellular Signatures compounds. The nodes in the network represent L1000 small molecules. If the correlation coefficient between two compounds is greater than 0.7, they are connected by a line. The color of the network is corresponding to the cluster annotation in **(A)**. For example, blue nodes in **(B)** are Proteasome inhibitors, corresponding to the blue cluster in **(A)**. Compound names and mechanisms of action are shown in **Supplementary Table S1**.

docetaxel-resistance models, cabazitaxel resistance was still proved both *in vitro* and *in vivo* and the resistance mechanisms are still unclear (Natsagdorj et al., 2019; Ylitalo et al., 2020). As known, the cabazitaxel is often administered as a last resort after patients develop resistance to docetaxel. Once the resistance to cabazitaxel is acquired, there are limited therapeutic options. Therefore, it is important to explore the combination therapy based on the three reference compounds to improve survival or clinical outcomes, in turn providing more options for the treatment of Prostate cancer.

### Prediction of Synergic Effects Based on Transcriptome-Based Data

As accepted, a drug might have the potential to treat a certain disease if its treatment could reverse the gene signature of the disease (Li et al., 2020). Thus, an ideal Prostate cancer drug should has a TCS, which could reverse all abnormally expressed genes in Prostate cancer (Stathias et al., 2018). In the other words, we hope to select the combination of drugs, which could to the largest extent reverse the abnormally expressed genes in Prostate cancer.

Using Cancer Genome Atlas RNA-Seq datasets for Prostate cancer tumors and controls, we identified 1283 differentially expressed genes to comprise the Prostate cancer disease signature. Then we prioritized the compounds based on how much they differ from the reference compounds and how much they reverse the disease signature. First, we calculated CR in terms of **Eq. 1**, which denotes the overlap between a reference small molecule and the Library of Integrated Network-based Cellular Signatures L1000 one. The higher the CR value is, the more similar the transcriptional responses induced by the two compounds. In other words, they are more likely to target the same disease pathway. Then, DR was estimated by **Eq. 2**, which gives the reversal degree of disease signature caused by a small molecule different from a reference drug (Stathias et al., 2018). These genes in DR are absent from the Prostate cancer reference signature. The compound has higher DR than the other, suggesting that it has more discordant genes with respect to the Prostate cancer differentially expressed genes. Finally, combining CR and DR, each compound can be scored by a single value (OS; **Eq. 3**) to quantify its orthogonality to the reference-induced transcriptional effect.

In order to select compounds with great potential, we did a scatterplot for each reference compound, as shown by **Figure 3**. According to the criteria that drug pairs with therapeutic effects tend to have high OS, three compounds located in the upper left corner, which have significantly higher OS scores than the others, were selected for each reference compound, leading to nine drug combination candidates. It can be seen from **Figure 3** that the top three combined objects are the same for each reference compound, which are indinavir, imatinib and cyproheptadine.

## Network-Based Assessment

It was indicated from the network analysis that a combinatorial therapy is efficacious only when it follows the "Complementary Exposure" pattern, namely, the target modules of each drug in the combination locates separately within or adjacent to different parts of the disease module (Cheng et al., 2019). Therefore, we further constructed the network-based model to assess the drug combinations predicted by the transcriptomics-based method. To achieve this goal, we quantified the network-based relationship between Prostate cancer disease module and two drug-target modules in order to observe if the nine drug combinations fall into the Complementary Exposure category. The results are shown as follows:

For indinavir, the network configuration between it and the three reference compounds are failed to be calculated because the target protein of the indinavir only has Pol polyprotein reported.

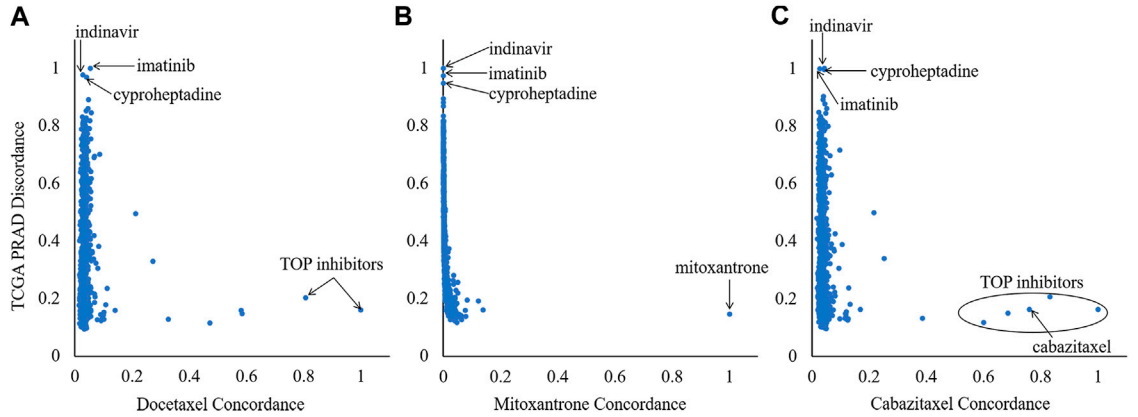


**FIGURE 3 |** Ranking of the 918 Library of Integrated Network-based Cellular Signatures compounds based on their orthogonality to the signatures of the three references (mitoxantrone, docetaxel and cabazitaxel). *X*-axis and *Y*-axis denote the CR and DR values, respectively.

**A**

| Imatinib-Reference Drug-PRAD | | | | |
|---|---|---|---|---|
| PRCA | mitoxantrone | cabazitaxel | docetaxel | imatinib |
| z-score | -1.4064 | -0.2169 | -0.2580 | -0.8325 |
| imatinib | mitoxantrone | cabazitaxel | docetaxel | |
| s-score | 0.1335 | 0.3312 | 0.3766 | |

**B**

| Cyproheptadine-Reference Drug-PRAD | | | | |
|---|---|---|---|---|
| PRCA | mitoxantrone | cabazitaxel | docetaxel | cyproheptadine |
| z-score | -1.4064 | -0.2169 | -0.2580 | 1.6975 |
| cyproheptadine | mitoxantrone | cabazitaxel | docetaxel | |
| s-score | 0.1500 | 0.2778 | 0.5556 | |

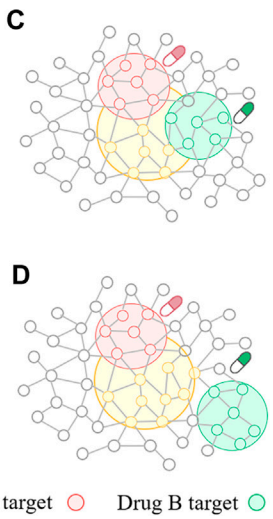


**FIGURE 4 |** Network configurations of drug–drug–disease combinations. **(A, B)** The network-based relationship between two drug–target modules and one disease module on imatinib-reference drug- Prostate cancer **(A)** and cyproheptadine-reference drug-Prostate cancer **(B)**. **(C, D)** The exposure mode of the Prostate cancer-associated protein module to the pairwise drug combinations: the three imatinib-containing combinations **(C)**, and the three cyproheptadine-containing combinations **(D)**. The z-scores measure the drug–disease separation. The s-scores denote the topological relationship between two drug target modules.

However, the pol polyprotein is marked as "unreviewed" in the UniProt database. In other words, there is lack of reliable data regarding the target protein for the indinavir so that the network relationship could not be calculated. This is a limitation for application of the network analysis in practice, which requires specific target proteins.

For the imatinib-containing combinations, our network analysis shows that imatinib and the three reference compounds all target different parts of the Prostate cancer-related subnetwork by "Complementary Exposure" pattern. Specifically, the relative proximity between the four drugs (imatinib and three reference compounds) and the Prostate cancer module is negative, $z < 0$, suggesting that the drug target modules in the combination overlap with the disease module. In addition, the network proximity between imatinib and the three reference compounds is positive ($s_{AB} \geq 0$), indicating that the two drug targets are topologically separated. Thus, the network analysis further supports that the imatinib-containing combinations may be potential for the treatment of Prostate cancer (**Figure 4A**), in line with the prediction of the transcriptomics-based analysis above.

For the cyproheptadine-containing combinations, although the cyproheptadine hits different targets from the reference compound ($s_{AB} \geq 0$), it failed to hit the disease module ($z > 0$). Cheng reported that the efficacy of the combinatorial therapy isn't better than the single-agent therapy if at least one agent locates far from the disease subnetwork (Cheng et al., 2019). Judged from the network-based result, the cyproheptadine-

**TABLE 1 |** Synergy scores for each drug combination according to Bliss model.

| Drug combination | Synergy score | Most synergistic area score | Model |
|---|---|---|---|
| docetaxel-indinavir | 2.49 | 3.11 | Bliss |
| docetaxel-imatinib | 1.55 | 2.66 | Bliss |
| docetaxel-cyproheptadine | 0.42 | 1.61 | Bliss |
| mitoxantrone-indinavir | 3.56 | 5.28 | Bliss |
| mitoxantrone-imatinib | 4.19 | 5.88 | Bliss |
| mitoxantrone-cyproheptadine | 3.91 | 5.63 | Bliss |
| cabazitaxel-cyproheptadine | 13.76 | 15.03 | Bliss |
| cabazitaxel-imatinib | 9.98 | 10.63 | Bliss |
| cabazitaxel-cyproheptadine | 11.34 | 13.66 | Bliss |

containing combinations should be ineffective for Prostate cancer, which is opposite to the transcriptomics-based prediction.

## Experimental Validation of the Predictions

As observed above, there are some discrepancies between the transcriptomics-based prediction and the network-based one. Thus, we further used the experimental method to validate the prediction results from the two methods. Herein, we used the MTT assay, which is a popular tool in measuring the metabolic activity of living cells, to estimate the cytostatic effects of a monotherapy or a combination of them on PC-3 cells (vide **Supplementary Table S3**). In order to assess the degree of synergy or antagonism, the combined effects of a drug pair are usually compared to the theoretically expected values using a reference mode, with the assumption that there is no interaction between the components of the combination. The reference models employed here are Bliss (Bliss, 1939) and ZIP (Yadav et al., 2015) models, which are implemented in SynergyFinder web-application (https://synergyfinder.fimm.fi; ref (Ianevski et al., 2017)).

Synergy scores are listed in **Table 1**, which are derived from the dose-matrix combinations. **Figure 5**, **Supplementary Figures S1, S2** show the 2D and 3D synergy heat maps for the Bliss and ZIP models of the interactions, through which the combined effects of the nine drug combinations against PC-3 cells (vide) could be obtained. The results shown in **Figure 5A** revealed that the docetaxel-containing combinations inhibit PC-3 cell proliferation in a dose-dependent manner. In other words, the combination could produce different effects on PC-3 cells due to the different concentration of its components, including antagonistic, addictive, or synergistic effects. Specifically, there is antagonism between the docetaxel and the indinavir when the concentration of the docetaxel is between 40 and 500 nM. The combination of the docetaxel and the imatinib also exhibits antagonism when the concentration of the docetaxel is higher than 100 nM. For the docetaxel-cyproheptadine, this pair presents antagonism when concentration of indinavir is lower than 50 nM, and cyproheptadine is greater than 50 nM. While at other range of drug doses pairs, the docetaxel-containing combination induces additive/synergistic effects. Different from the dose-dependent effects of the combinations containing docetaxel, the three combinations containing mitoxantrone all show overall synergistic effects within the experimental dose range, judged from **Figure 5B**). In addition, it can be observed from **Figure 5C** that the three combinations containing cabazitaxel show the strongest synergistic effects. In a whole, the experimental results almost support the transcriptomics-based predictions, but exhibit some discrepancies with the network-based predictions for the mitoxantrone-cyproheptadine and cabazitaxel-cyproheptadine.

# DISCUSSIONS

Drug combinations play a major part in combating various complex diseases due to increased therapeutic efficacy, decreased toxicity and counter drug resistance. And computational methods bypass the combinatorial explosion problem by greatly reducing the search space and prioritizing combinations. Among these approaches, the transcriptomics-based and the network-based methods have attracted much attention and achieved remarkable performance. In addition, most existing methods focused on multiple diseases. However, the drug synergy is a strongly context-dependent property. Thus, it is highly desired to explore disease-specific synergy combinations. Prostate cancer is a primary factor of male morbidity and mortality, and the inevitable drug resistance to exiting monotherapies highlights the need of new combination therapies. Therefore, we hope to establish a synergistic drug prediction model for Prostate cancer in the work. We firstly employ a transcriptomics-based approach to reposition 918 approved drugs in combination for Prostate cancer, through which the nine synergistic combinations are identified. To compare the performance of different computational methods to predict the drug pair of Prostate cancer, we further utilize the network-based method proposed by Cheng et al. (Cheng et al., 2019) to assess the synergistic potential of the six drug combinations from the transcriptomics-based prediction, excepting for the three indinavir-containing combinations, since the indinavir lacks reliable drug targets. The network-based results show that the three imatinib-containing combinations fall into the Complementary Exposure category with the Prostate cancer disease module. Thus, the network-based method show that they are effective combinations for Prostate cancer, in line with the transcriptomics-based prediction. However, the three cyproheptadine-containing combinations

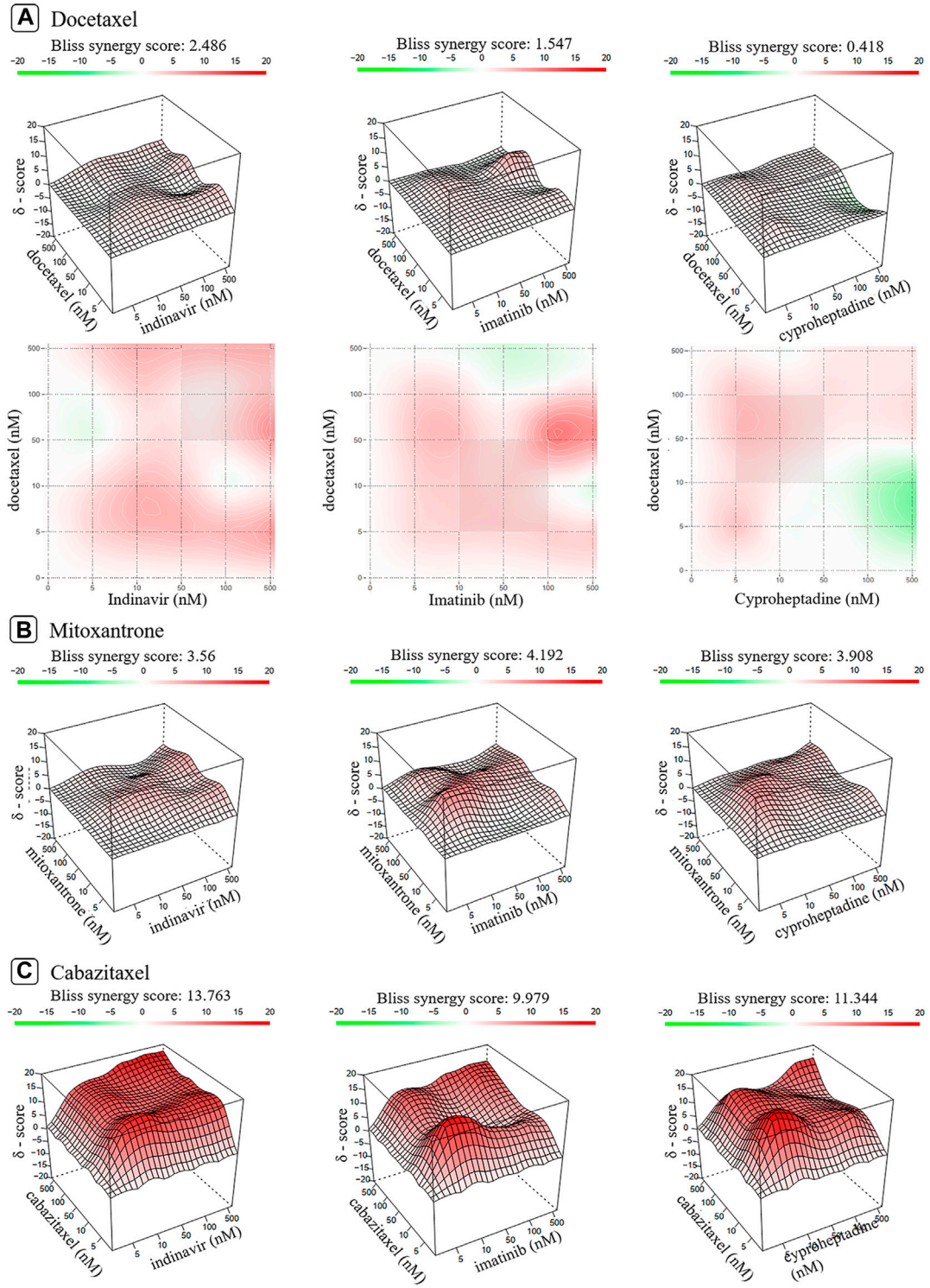


**FIGURE 5 |** The 2D and 3D heat maps of the combination responses for docetaxel-containing **(A)**, mitoxantrone-containing **(B)** and cabazitaxel-containing combinations **(C)** according to Bliss model. Red represents the synergistic interaction while green denotes the antagonistic interaction.

are predicted as nonsynergistic combinations, which conflicts with the transcriptomics-based results. To validate the computational results, we further conduct *in vitro* experiments. The *in-vitro* results show that the combined effects of the three docetaxel-containing combinations are in a dose-dependent manner while the other six combinations could

synergistically inhibit the growth of PC-3 cells, thus supporting the transcriptomics-based predictions. However, the two combinations (cyproheptadine-mitoxantrone and cyproheptadine-cabazitaxe), which are predicted to be nonsynergistic by the network-based method, present strongly synergistic in the *in-vitro* experiment instead. Only the network-based predictions of imatinib-mitoxantrone and imatinib-cabazitaxel are consistent with the *in-vitro* results.

Specifically, the two imatinib-containing combinations (mitoxantrone-imatinib and cabazitaxel-imatinib), which are consistently predicted as synergistic combinations in the transcriptomics-based and the network-based analysis, are further proved *in vitro* and exhibit highly potential for the combination therapy of Prostate cancer. In fact, it is revealed that imatinib could inhibit PDGFR, a potential therapeutic target in Prostate cancer (Pinto et al., 2012). Unfortunately, the efficacy of single-agent PDGFR inhibitors in patients with metastatic Prostate cancer appears limited. Interestingly, it was observed that combining imatinib with other anticancer drugs might increase the effectiveness of the single-agent PDGEF inhibitor (Kim et al., 2012). Moreover, the imatinib was found to decrease interstitial fluid pressure in solid tumors so that it could improve tumor delivery of anticancer drugs *in vivo* (Vlahovic et al., 2007). All the evidences also provide further support for the potential of the imatinib in combination therapy for Prostate cancer. The two cyproheptadine-containing combinations (mitoxantrone-cyproheptadine and cabazitaxel-cyproheptadine), which are predicted to be synergistic combinations in the transcriptomics-based prediction but nonsynergistic in the network-based analysis, show to inhibit the proliferation of PC-3 cells synergistically *in vitro*. Although the therapeutic effect of cyproheptadine in Prostate cancer has never been reported, the use of cyproheptadine in the treatment of multiple malignancies, such as myeloma, leukemia and hepatocellular carcinoma (Rosenberg and Mathew, 2013), to some extent suggest the effect of cyproheptadine in combating cancers. Therefore, it is reasonable for the two cyproheptadine-containing combinations to be potential for the Prostate cancer treatment. The two indinavir-containing combinations (mitoxantrone-indinavir and cabazitaxel-indinavir), which failed to conduct the network-based analysis, also were experimentally confirmed to be synergistic combinations. Indinavir is a human immunodeficiency virus protease inhibitor (HIV PIs), which was proved *in vitro* and *in vivo* to slow down the proliferation, promote the apoptosis and inhibit the growth of tumor cells (Toschi et al., 2011; Barillari et al., 2014; Maksimovic-Ivanic et al., 2017). The anti-tumor activity of HIV PIs has also reported in many studies on treating tumors like Kaposi's sarcoma, lymph-gland tumor, or Prostate cancer (Toschi et al., 2011; Barillari et al., 2014; Maksimovic-Ivanic et al., 2017). In addition, the CYP3A4 participates in the process of metabolism and the development of resistance (Ikezoe et al., 2004; Van Eijk et al., 2019), while indinavir as a potent inhibitor of CYP3A4 is thought to enhance the therapeutic effects of anticancer drugs in androgen-independent prostate cancer cells.

Judged from the experimental results, the transcriptomics-based predictor performs better than the network-based analysis, at least for Prostate cancer One reason may be that this network approach used in the work is based on the analysis of hypertension and pan-cancer data while the models built on data from a variety of diseases are more likely to miss some important features that being beneficial for capturing unique combinations with therapeutic effectiveness for a specific disease like Prostate cancer (Sun et al., 2015). As an attempt, we reconstructed a tissue specific Prostate interactome. Specifically, we first calculated the median expression of each gene in the tumor or normal samples from the prostate tissue, after downloading gene expression and phenotype data of Cancer Genome Atlas (Chang et al., 2013) and GTEx (Consortium, 2013). And then, proteins with median expression >1 Transcripts Per Million (TPM) (Sriram et al., 2019) were screened, which are considered to express in the prostate commonly. Finally, the full human PPI network is narrowed down to a subnetwork specific to the prostate, with 214,351 edges and 15,784 nodes. Then, we calculated the configurations of the six drug-drug- Prostate cancer combinations (vide **Supplementary Figure S3**) are the same as those obtained by the full network calculation (vide **Figure 4**). The result implies that it may be difficult for the network topology to capture the characteristic of the specific disease. In contrast, the information from the transcriptional level of the specific disease (Prostate cancer) could reflect individual characteristics. In addition, as proposed by Cheng (Cheng et al., 2019), some factors, the incompleteness of the human PPI network and the limited knowledge of proteins associated with the disease and drugs, may impose restrictions on the performance of the current network-based approaches used to develop therapeutic strategies. For example, some drugs have no target proteins available for the network calculation like the indinavir under study. Therefore, researchers should be more cautious when purely using network-based methods to predict drug combinations for a specific disease.

Also, it is noted that the reference signatures used in the transcriptomics-based model is derived from perturbational gene-expression data on PC-3 cell lines, which may not match the disease signature perfectly. But, only the PC-3 cell-line is disturbed by all the 13 approved prostate cancer drugs in the GSE70138 dataset while the LNCAP one is disturbed by one drug (mitoxantrone). For the DU-145 cell-line, there is no profiles induced by any of the 13 drugs. As known, the PC-3 cell-line is derived from metastatic prostate cancer and has been served as standard cell in the drug research on the prostate cancer. To maintain the consistency between the calculation and the experiment, we validated the predictive combinations by *in vitro* experiment only on the PC-3 cells. Additionally, we did a computational comparison. We used the gene expression profiles of LNCAP cells induced by the mitoxantrone to perform transcriptome-based predictions. As shown by **Supplementary Figure S4**, the three candidates (imatinib, indinavir and cyproheptadine) also rank the top, in line with the prediction from the PC-3 cell, implying to some extent consistency between the two cell-lines. In fact, many drug prediction models are also based on pan-cancer data without considering cancer types due to the limited data available for each cancer type, but they still achieved satisfactory performance when applied to specific cancer (Geeleher et al., 2014; Sun et al., 2015; Cheng et al., 2019), implying that there are some features shared across different cancers, which

contribut to drug predictions. In this study, we only studied one cancer type (i.e., Prostate cancer). Although the patient samples and cancer cells belong to different stage, it should be reasonable to assume that there are some characteristics shared between different stages of the prostate cancer. In addition, it is found from some previous literatures (Mao et al., 2008; Kim et al., 2012; Barillari et al., 2014; Hsieh et al., 2016; Sun et al., 2016; Takemoto et al., 2016; Maksimovic-Ivanic et al., 2017; Van Eijk et al., 2019) that the three drugs (i.e., indinavir, imatinib, and cyproheptadine) predicted as one component of the drug combination exhibited anticancer impact on various cancers, including prostate cancer, which also to some extent supports the rationality of using perturbational gene-expression data on PC-3 cell lines to predict drug combinations for the prostate cancer. However, more *in vitro* and *in vivo* experiments will be needed to further validate the therapeutic efficacy of our predictive drug combinations for the prostate cancer.

Despite fascinating advantages of combination therapies, there are still some limitations and challenges needed to be addressed. Firstly, using multiple drugs in the combination may precipitate undesired side effects, and make it difficult to identify which drug is responsible for the effects (Kavanagh et al., 2018). Secondly, the determination of drug dose and ratio in combination therapy is much more complicated than that of monotherapy, because the solubility, stability, pharmacodynamics, and pharmacokinetics of different drugs may vary greatly (Sun et al., 2016). In addition, most of the existing drug combination predictive models are based on omics and drug response data. There has been lack of sufficient data to model the unique characteristics of patients (Kening et al., 2020), which is a major limitation of current researches, including our study. Overcoming these limitations will further increase the value of combination therapies, which requires the joint efforts of researchers across various disciplines, such as biology, chemistry, medicine, and computer science.

## CONCLUSIONS

In summary, our results show that the transcriptomics-based strategy is more suitable for the specific disease than the network-based one, at least for Prostate cancer, which will assist in decision making for the usage of the computation methods in the drug combination prediction. More importantly, six drug combinations (i.e., the three mitoxantrone-containing and the three cabazitaxel-containing combinations) are found to be potential to synergistically conquer prostate cancer, which offer promising candidates for preclinical testing. Despite the encouraging results, our findings still require further preclinical testing and clinical trials.

## DATA AVAILABILITY STATEMENT

All datasets generated for this study are included in the article/ **Supplementary Material**. The source code used in this study is available at https://github.com/shiqili-17/drugpair_prediction.

## AUTHOR CONTRIBUTIONS

XP and ML engaged in study coordination and supervision. XX, XP, and ML provided material support for obtained funding. SL performed most of the literature search and analysis. FZ, XX, ZW, and YG contributed to the data curation and validation. XP and SL wrote and revised the manuscript. All authors reviewed and approved the final manuscript.

## FUNDING

This project was funded by Sichuan International Science and technology innovation cooperation project (Grant No. 2021YFH0140), NSAF (Grant No. U1730127), the National Science Foundation of China (Grant No. 21675114) and National Youth Foundation of China (Grant No. 21705011).

## SUPPLEMENTARY MATERIAL

The Supplementary Material for this article can be found online at: https://www.frontiersin.org/articles/10.3389/fphar.2021.634097/full#supplementary-material.

## REFERENCES

Al-Lazikani, B., Banerji, U., and Workman, P. (2012). Combinatorial drug therapy for cancer in the post-genomic era. *Nat. Biotechnol.* 30, 679–692. doi:10.1038/nbt.2284

Amberger, J. S., Bocchini, C. A., Schiettecatte, F., Scott, A. F., and Hamosh, A. (2015). OMIM.org: online mendelian inheritance in man (OMIM), an online catalog of human genes and genetic disorders. *Nucleic Acids Res.* 43, D789–D798. doi:10.1093/nar/gku1205

Bansal, M., Yang, J., Yang, J., Karan, C., Menden, M. P., et al. (2014). A community computational challenge to predict the activity of pairs of compounds. *Nat. Biotechnol.* 32, 1213–1222. doi:10.1038/nbt.3052

Barabási, A.-L., Gulbahce, N., and Loscalzo, J. (2011). Network medicine: a network-based approach to human disease. *Nat. Rev. Genet.* 12, 56–68. doi:10.1038/nrg2918

Barillari, G., Iovane, A., Bacigalupo, I., Labbaye, C., Chiozzini, C., Sernicola, L., et al. (2014). The HIV protease inhibitor indinavir down-regulates the expression of the pro-angiogenic MT1-MMP by human endothelial cells. *Angiogenesis* 17, 831–838. doi:10.1007/s10456-014-9430-9

Bayat Mokhtari, R., Homayouni, T. S., Baluch, N., Morgatskaya, E., Kumar, S., Das, B., et al. (2017). Combination therapy in combating cancer. *Oncotarget* 8, 38022–38043. doi:10.18632/oncotarget.16723

Bliss, C. I. (1939). The toxicity of poisons applied jointly. *Ann. Appl. Biol.* 26, 585–615. doi:10.1111/j.1744-7348.1939.tb06990.x

Celebi, R., Walk, O. B. D., Movva, R., Alpsoy, S., and Dumontier, M. (2019). In-silico prediction of synergistic anti-cancer drug combinations using multi-omics data. *Sci. Rep.* 9, 8949. doi:10.1038/s41598-019-45236-6

Chang, K., Creighton, C. J., Davis, C., Donehower, L., Drummond, J., Wheeler, D., et al. (2013). The cancer genome Atlas pan-cancer analysis project. *Nat. Genet.* 45, 1113–1120. doi:10.1038/ng.276410.1038/ng.2617

Chen, X., Ren, B., Chen, M., Wang, Q., Zhang, L., and Yan, G. (2016). NLLSS: predicting synergistic drug combinations based on semi-supervised learning. *Plos Comput. Biol.* 12, e1004975. doi:10.1371/journal.pcbi.1004975

Cheng, F., Desai, R. J., Handy, D. E., Wang, R., Schneeweiss, S., Barabási, A.-L., et al. (2018). Network-based approach to prediction and population-based validation of in silico drug repurposing. *Nat. Commun.* 9, 2691. doi:10.1038/s41467-018-05116-5

Cheng, F., Kovács, I. A., and Barabási, A.-L. (2019). Network-based prediction of drug combinations. *Nat. Commun.* 10, 1197. doi:10.1038/s41467-019-09186-x

Davis, A. P., Grondin, C. J., Lennon-Hopkins, K., Saraceni-Richards, C., Sciaky, D., King, B. L., et al. (2015). The comparative toxicogenomics database's 10th year anniversary: update 2015. *Nucleic Acids Res.* 43, D914–D920. doi:10.1093/nar/gku935

Denny, J. C., Bastarache, L., Ritchie, M. D., Carroll, R. J., Zink, R., Mosley, J. D., et al. (2013). Systematic comparison of phenome-wide association study of electronic medical record data and genome-wide association study data. *Nat. Biotechnol.* 31, 1102–1111. doi:10.1038/nbt.2749

Ding, P., Shen, C., Lai, Z., Liang, C., Li, G., and Luo, J. (2020). Incorporating multisource knowledge to predict drug synergy based on graph Co-regularization. *J. Chem. Inf. Model.* 60, 37–46. doi:10.1021/acs.jcim.9b00793

Geeleher, P., Cox, N. J., and Huang, R. (2014). Clinical drug response can be predicted using baseline gene expression levels and *in vitro* drug sensitivity in cell lines. *Genome Biol.* 15, R47. doi:10.1186/gb-2014-15-3-r47

Grossman, R. L., Heath, A. P., Ferretti, V., Varmus, H. E., Lowy, D. R., Kibbe, W. A., et al. (2016). Toward a shared vision for cancer genomic data. *N. Engl. J. Med.* 375, 1109–1112. doi:10.1056/NEJMp1607591

Hsieh, H.-Y., Shen, C.-H., Lin, R.-I., Feng, Y.-M., Huang, S.-Y., Wang, Y.-H., et al. (2016). Cyproheptadine exhibits antitumor activity in urothelial carcinoma cells by targeting GSK3β to suppress mTOR and β-catenin signaling pathways. *Cancer Lett.* 370, 56–65. doi:10.1016/j.canlet.2015.09.018

Huang, C.-T., Hsieh, C.-H., Chung, Y.-H., Oyang, Y.-J., Huang, H.-C., and Juan, H.-F. (2019). Perturbational gene-expression signatures for combinatorial drug discovery. *iScience* 15, 291–306. doi:10.1016/j.isci.2019.04.039

Huggins, C., and Hodges, C. V. (1941). Studies on prostatic cancer—I the effect of castration, of estrogen and of androgen injection on serum phosphatases in metastatic carcinoma of the prostate. *Cancer Res.* 1, 293–297.

Hwang, C. (2012). Overcoming docetaxel resistance in prostate cancer: a perspective review. *Ther. Adv. Med. Oncol.* 4, 329–340. doi:10.1177/1758834012449685

Ianevski, A., He, L., Aittokallio, T., and Tang, J. (2017). SynergyFinder: a web application for analyzing drug combination dose-response matrix data. *Bioinformatics* 33, 2413–2415. doi:10.1093/bioinformatics/btx162

Ikezoe, T., Hisatake, Y., Takeuchi, T., Ohtsuki, Y., Yang, Y., Said, J. W., et al. (2004). HIV-1 protease inhibitor, ritonavir. *Cancer Res.* 64, 7426–7431. doi:10.1158/0008-5472.can-03-2677

James, N. D., Spears, M. R., Clarke, N. W., Dearnaley, D. P., De Bono, J. S., Gale, J., et al. (2015). Survival with newly diagnosed metastatic prostate cancer in the "docetaxel era": data from 917 patients in the control arm of the STAMPEDE trial (MRC PR08, CRUK/06/019). *Eur. Urol.* 67, 1028–1038. doi:10.1016/j.eururo.2014.09.032

Jia, J., Zhu, F., Ma, X., Cao, Z. W., Li, Y. X., and Chen, Y. Z. (2009). Mechanisms of drug combinations: interaction and network perspectives. *Nat. Rev. Drug Discov.* 8, 111–128. doi:10.1038/nrd2683

Kavanagh, O. N., Albadarin, A. B., Croker, D. M., Healy, A. M., and Walker, G. M. (2018). Maximising success in multidrug formulation development: a review. *J. Controlled Release* 283, 1–19. doi:10.1016/j.jconrel.2018.05.024

Keenan, A. B., Jenkins, S. L., Jagodnik, K. M., Koplev, S., He, E., Torre, D., et al. (2018). The library of integrated network-based cellular signatures NIH program: system-level cataloging of human cells response to perturbations. *Cell Syst.* 6, 13–24. doi:10.1016/j.cels.2017.11.001

Kening, L., Yuxin, D., Lu, L., and Dong-Qing, W. (2020). Bioinformatics approaches for anti-cancer drug discovery. *Curr. Drug Targets* 21, 3–17. doi:10.2174/1389450120666190923162203

Kim, E., Matsuse, M., Saenko, V., Suzuki, K., Ohtsuru, A., Mitsutake, N., et al. (2012). Imatinib enhances docetaxel-induced apoptosis through inhibition of nuclear factor-κb activation in anaplastic thyroid carcinoma cells. *Thyroid* 22, 717–724. doi:10.1089/thy.2011.0380

Koleti, A., Terryn, R., Stathias, V., Chung, C., Cooper, D. J., Turner, J. P., et al. (2018). Data portal for the library of integrated network-based cellular signatures (LINCS) program: integrated access to diverse large-scale cellular perturbation response data. *Nucleic Acids Res.* 46, D558–D566. doi:10.1093/nar/gkx1063

Lamb, J., Crawford, E. D., Peck, D., Modell, J. W., Blat, I. C., Wrobel, M. J., et al. (2006). The connectivity map: using gene-expression signatures to connect small molecules, genes, and disease. *Science* 313, 1929–1935. doi:10.1126/science.1132939

Landrum, M. J., Lee, J. M., Riley, G. R., Jang, W., Rubinstein, W. S., Church, D. M., et al. (2014). ClinVar: public archive of relationships among sequence variation and human phenotype. *Nucl. Acids Res.* 42, D980–D985. doi:10.1093/nar/gkt1113

Lavecchia, A., and Cerchia, C. (2016). In silico methods to address polypharmacology: current status, applications and future perspectives. *Drug Discov. Today* 21, 288–298. doi:10.1016/j.drudis.2015.12.007

Law, V., Knox, C., Djoumbou, Y., Jewison, T., Guo, A. C., Liu, Y., et al. (2014). DrugBank 4.0: shedding new light on drug metabolism. *Nucl. Acids Res.* 42, D1091–D1097. doi:10.1093/nar/gkt1068

Lee, C.-H., and Kantoff, P. (2019). Treatment of metastatic prostate cancer in 2018. *JAMA Oncol.* 5, 263–264. doi:10.1001/jamaoncol.2018.5621

Li, L., Hu, M., Wang, T., Chen, H., and Xu, L. (2020). Repositioning aspirin to treat lung and breast cancers and overcome acquired resistance to targeted therapy. *Front. Oncol.* 9, 10. doi:10.3389/fonc.2019.01503

Li, M. J., Liu, Z., Wang, P., Wong, M. P., Nelson, M. R., Kocher, J.-P. A., et al. (2016). GWASdb v2: an update database for human genetic variants identified by genome-wide association studies. *Nucleic Acids Res.* 44, D869–D876. doi:10.1093/nar/gkv1317

Li, P., Huang, C., Fu, Y., Wang, J., Wu, Z., Ru, J., et al. (2015). Large-scale exploration and analysis of drug combinations. *Bioinformatics* 31, 2007–2016. doi:10.1093/bioinformatics/btv080

Li, X., Xu, Y., Cui, H., Huang, T., Wang, D., Lian, B., et al. (2017). Prediction of synergistic anti-cancer drug combinations based on drug target network and drug induced gene expression profiles. *Artif. Intell. Med.* 83, 35–43. doi:10.1016/j.artmed.2017.05.008

Liu, H., Zhang, W., Zou, B., Wang, J., Deng, Y., and Deng, L. (2019). DrugCombDB: a comprehensive database of drug combinations toward the discovery of combinatorial therapy. *Nucleic Acids Res.* 48, D871–D881. doi:10.1093/nar/gkz1007

Madan, R. A., Pal, S. K., Sartor, O., and Dahut, W. L. (2011). Overcoming chemotherapy resistance in prostate cancer. *Clin. Cancer Res.* 17, 3892. doi:10.1158/1078-0432.CCR-10-2654

Maksimovic-Ivanic, D., Fagone, P., Mccubrey, J., Bendtzen, K., Mijatovic, S., and Nicoletti, F. (2017). HIV-protease inhibitors for the treatment of cancer: repositioning HIV protease inhibitors while developing more potent NO-hybridized derivatives? *Int. J. Cancer* 140, 1713–1726. doi:10.1002/ijc.30529

Mao, X., Liang, S.-B., Hurren, R., Gronda, M., Chow, S., Xu, G. W., et al. (2008). Cyproheptadine displays preclinical activity in myeloma and leukemia. *Blood* 112, 760–769. doi:10.1182/blood-2008-02-142687

Mason, D. J., Eastman, R. T., Lewis, R. P. I., Stott, I. P., Guha, R., and Bender, A. (2018). Using machine learning to predict synergistic antimalarial compound combinations with novel structures. *Front. Pharmacol.* 9, 1096. doi:10.3389/fphar.2018.01096

Menche, J., Sharma, A., Kitsak, M., Ghiassian, S. D., Vidal, M., Loscalzo, J., et al. (2015). Uncovering disease-disease relationships through the incomplete interactome. *Science* 347, 1257601. doi:10.1126/science.1257601

Natsagdorj, A., Izumi, K., Hiratsuka, K., Machioka, K., Iwamoto, H., Naito, R., et al. (2019). CCL2 induces resistance to the antiproliferative effect of cabazitaxel in prostate cancer cells. *Cancer Sci.* 110, 279–288. doi:10.1111/cas.13876

Piñero, J., Queralt-Rosinach, N., Bravo, A., Deu-Pons, J., Bauer-Mehren, A., Baron, M., et al. (2015). DisGeNET: a discovery platform for the dynamical exploration of human diseases and their genes. *Database* 15, bav028. doi:10.1093/database/bav028

Pinto, A. C., Ângelo, S., Moreira, J. N., and Simões, S. (2012). Development, characterization and in vitro evaluation of single or Co-loaded imatinib mesylate liposomal formulations. *J. Nanosci. Nanotechnol.* 12, 2891–2900. doi:10.1166/jnn.2012.5703

Rees, M. G., Seashore-Ludlow, B., Cheah, J. H., Adams, D. J., Price, E. V., Gill, S., et al. (2016). Correlating chemical sensitivity and basal gene expression reveals mechanism of action. *Nat. Chem. Biol.* 12, 109. doi:10.1038/nchembio.1986

Regan-Fendt, K. E., Xu, J., Divincenzo, M., Duggan, M. C., Shakya, R., Na, R., et al. (2019). Synergy from gene expression and network mining (SynGeNet) method predicts synergistic drug combinations for diverse melanoma genomic subtypes. *Npj Syst. Biol. Appl.* 5, 15. doi:10.1038/s41540-019-0085-4

Rosenberg, A., and Mathew, P. (2013). Imatinib and prostate cancer: lessons learned from targeting the platelet-derived growth factor receptor. *Expert Opin. Investig. Drugs* 22, 787–794. doi:10.1517/13543784.2013.787409

Ryall, K. A., and Tan, A. C. (2015). Systems biology approaches for advancing the discovery of effective drug combinations. *J. Cheminform* 7, 7. doi:10.1186/s13321-015-0055-9

Siegel, R. L., Miller, K. D., and Jemal, A. (2020). Cancer statistics, 2020. *CA A. Cancer J. Clin.* 70, 7–30. doi:10.3322/caac.21590

Song, P., Huang, C., and Wang, Y. (2018). The efficacy and safety comparison of docetaxel, cabazitaxel, estramustine, and mitoxantrone for castration-resistant prostate cancer: a network meta-analysis. *Int. J. Surg.* 56, 133–140. doi:10.1016/j.ijsu.2018.06.010

Sriram, K., Moyung, K., Corriden, R., Carter, H., and Insel, P. A. (2019). GPCRs show widespread differential mRNA expression and frequent mutation and copy number variation in solid tumors. *PLOS Biol.* 17, e3000434. doi:10.1371/journal.pbio.3000434

Stathias, V., Jermakowicz, A. M., Maloof, M. E., Forlin, M., Walters, W., Suter, R. K., et al. (2018). Drug and disease signature integration identifies synergistic combinations in glioblastoma. *Nat. Commun.* 9, 5315. doi:10.1038/s41467-018-07659-z

Subramanian, A., Narayan, R., Corsello, S. M., Peck, D. D., Natoli, T. E., Lu, X., et al. (2017). A next generation connectivity map: L1000 platform and the first 1,000,000 profiles. *Cell* 171, 1437–1452. doi:10.1016/j.cell.2017.10.049

Sun, W., Sanderson, P. E., and Zheng, W. (2016). Drug combination therapy increases successful drug repositioning. *Drug Discov. Today* 21, 1189–1195. doi:10.1016/j.drudis.2016.05.015

Sun, Y., Sheng, Z., Ma, C., Tang, K., Zhu, R., Wu, Z., et al. (2015). Combining genomic and network characteristics for extended capability in predicting synergistic drugs for cancer. *Nat. Commun.* 6, 8481. doi:10.1038/ncomms9481

Sweeney, C. J., Chen, Y.-H., Carducci, M., Liu, G., Jarrard, D. F., Eisenberger, M., et al. (2015). Chemohormonal therapy in metastatic hormone-sensitive prostate cancer. *N. Engl. J. Med.* 373, 737–746. doi:10.1056/NEJMoa1503747

Takemoto, Y., Ito, A., Niwa, H., Okamura, M., Fujiwara, T., Hirano, T., et al. (2016). Identification of cyproheptadine as an inhibitor of SET domain containing lysine methyltransferase 7/9 (Set7/9) that regulates estrogen-dependent transcription. *J. Med. Chem.* 59, 3650–3660. doi:10.1021/acs.jmedchem.5b01732

Toschi, E., Sgadari, C., Malavasi, L., Bacigalupo, I., Chiozzini, C., Carlei, D., et al. (2011). Human immunodeficiency virus protease inhibitors reduce the growth of human tumors via a proteasome-independent block of angiogenesis and matrix metalloproteinases. *Int. J. Cancer* 128, 82–93. doi:10.1002/ijc.25550

Van Eijk, M., Boosman, R. J., Schinkel, A. H., Huitema, A. D. R., and Beijnen, J. H. (2019). Cytochrome P450 3A4, 3A5, and 2C8 expression in breast, prostate, lung, endometrial, and ovarian tumors: relevance for resistance to taxanes. *Cancer Chemother. Pharmacol.* 84, 487–499. doi:10.1007/s00280-019-03905-3

Vlahovic, G., Ponce, A. M., Rabbani, Z., Salahuddin, F. K., Zgonjanin, L., Spasojevic, I., et al. (2007). Treatment with imatinib improves drug delivery and efficacy in NSCLC xenografts. *Br. J. Cancer* 97, 735–740. doi:10.1038/sj.bjc.6603941

Wang, Z., Ravula, R., Shi, L., Song, Y., Yeung, S., Liu, M., et al. (2016). Overcoming chemoresistance in prostate cancer with Chinese medicine Tripterygium wilfordii via multiple mechanisms. *Oncotarget* 7, 38. doi:10.18632/oncotarget.10868

Welter, D., Macarthur, J., Morales, J., Burdett, T., Hall, P., Junkins, H., et al. (2014). The NHGRI GWAS Catalog, a curated resource of SNP-trait associations. *Nucl. Acids Res.* 42, D1001–D1006. doi:10.1093/nar/gkt1229

Wu, Z., Li, W., Liu, G., and Tang, Y. (2018). Network-based methods for prediction of drug-target interactions. *Front. Pharmacol.* 9, 1134. doi:10.3389/fphar.2018.01134

Yadav, B., Wennerberg, K., Aittokallio, T., and Tang, J. (2015). Searching for drug synergy in complex dose-response landscapes using an interaction potency model. *Comput. Struct. Biotechnol. J.* 13, 504–513. doi:10.1016/j.csbj.2015.09.001

Yin, N., Ma, W., Pei, J., Ouyang, Q., Tang, C., and Lai, L. (2014). Synergistic and antagonistic drug combinations depend on network topology. *PLoS One* 9, e93960. doi:10.1371/journal.pone.0093960

Ylitalo, E. B., Thysell, E., Thellenberg-Karlsson, C., Lundholm, M., Widmark, A., Bergh, A., et al. (2020). Marked response to cabazitaxel in prostate cancer xenografts expressing androgen receptor variant 7 and reversion of acquired resistance by anti-androgens. *Prostate* 80, 214–224. doi:10.1002/pros.23935

Yu, W., Gwinn, M., Clyne, M., Yesupriya, A., and Khoury, M. J. (2008). A navigator for human genome epidemiology. *Nat. Genet.* 40, 124–125. doi:10.1038/ng0208-124

Zhao, X.-M., Iskar, M., Zeller, G., Kuhn, M., Van Noort, V., and Bork, P. (2011). Prediction of drug combinations by integrating molecular and pharmacological data. *Plos Comput. Biol.* 7, e1002323. doi:10.1371/journal.pcbi.1002323

Zhou, Y., Hou, Y., Shen, J., Huang, Y., Martin, W., and Cheng, F. (2020). Network-based drug repurposing for novel coronavirus 2019-nCoV/SARS-CoV-2. *Cell Discov.* 6, 18. doi:10.1038/s41421-020-0153-3

Zhu, J., Muskhelishvili, L., Tong, W., Borlak, J., and Chen, M. (2020). Cancer genomics predicts disease relapse and therapeutic response to neoadjuvant chemotherapy of hormone sensitive breast cancers. *Sci. Rep.* 10, 8188. doi:10.1038/s41598-020-65055-4

**Conflict of Interest:** The authors declare that the research was conducted in the absence of any commercial or financial relationships that could be construed as a potential conflict of interest.

frontiers in Pharmacology

ORIGINAL RESEARCH
published: 16 April 2021
doi: 10.3389/fphar.2021.631135

# Improved Treatment Outcomes by Using Patient Specific Drug Combinations in Mammalian Target of Rapamycin Activated Advanced Metastatic Cancers

*Timothy Crook[1], Darshana Patil[2], Andrew Gaya[3], Nicholas Plowman[4], Sewanti Limaye[5], Anantbhushan Ranade[6], Amit Bhatt[6], Raymond Page[7] and Dadasaheb Akolkar[2]**

[1]Broomfield Hospital, Chelmsford, United Kingdom, [2]Datar Cancer Genetics, Nasik, India, [3]HCA Healthcare United Kingdom, London, United Kingdom, [4]St Bartholomew's Hospital, London, United Kingdom, [5]Kokilaben Dhirubhai Ambani Hospital, Mumbai, India, [6]Avinash Cancer Clinic, Pune, India, [7]Worcester Polytechnic Institute, Worcester, India

OPEN ACCESS

**Edited by:**
Daniela Spano,
National Research Council (CNR), Italy

**Reviewed by:**
Giovanni Grignani,
Institute for Cancer Research and Treatment (IRCC), Italy
Paola A. Marignani,
Dalhousie University, Canada

***Correspondence:**
Dadasaheb Akolkar
dadasaheb.akolkar@datarpgx.com

**Specialty section:**
This article was submitted to Pharmacology of Anti-Cancer Drugs, a section of the journal Frontiers in Pharmacology

**Received:** 19 November 2020
**Accepted:** 25 February 2021
**Published:** 16 April 2021

**Citation:**
Crook T, Patil D, Gaya A, Plowman N, Limaye S, Ranade A, Bhatt A, Page R and Akolkar D (2021) Improved Treatment Outcomes by Using Patient Specific Drug Combinations in Mammalian Target of Rapamycin Activated Advanced Metastatic Cancers. Front. Pharmacol. 12:631135. doi: 10.3389/fphar.2021.631135

**Background:** Activation of the mTOR signaling pathway is ubiquitous in cancers and a favourable therapeutic target. However, presently approved mTOR inhibitor monotherapies have modest benefits in labeled indications while poor outcomes have been reported for mTOR inhibitor monotherapy when administered in a label-agnostic setting based on univariate molecular indications. The present study aimed to determine whether patient-specific combination regimens with mTOR inhibitors and other anticancer agents selected based on multi-analyte molecular and functional tumor interrogation (ETA: Encyclopedic Tumor Analysis) yields significant treatment response and survival benefits in advanced or refractory solid organ cancers.

**Methods:** We evaluated treatment outcomes in 49 patients diagnosed with unresectable or metastatic solid organ cancers, of whom 3 were therapy naïve and 46 were pre-treated in whom the cancer had progressed on 2 or more prior systemic lines. All patients received mTOR inhibitor in combination with other targeted, endocrine or cytotoxic agents as guided by ETA. Patients were followed-up to determine Objective Response Rate (ORR), Progression Free Survival (PFS) and Overall Survival (OS).

**Results:** The Objective Response Rate (ORR) was 57.1%, the disease Control rate (DCR) was 91.8%, median Progression Free Survival (mPFS) was 4.9 months and median Overall Survival (mOS) was 9.4 months. There were no Grade IV treatment related adverse events (AEs) or any treatment related deaths.

**Conclusion:** Patient-specific combination regimens with mTOR inhibition and other anti-neoplastic agents, when selected based on multi-analyte molecular and functional profiling of the tumor can yield meaningful outcomes in advanced or refractory solid organ cancers.

**Trial Registration:** Details of all trials are available at WHO-ICTRP: https://apps.who.int/trialsearch/. RESILIENT ID CTRI/2018/02/011808. ACTPRO ID CTRI/2018/05/014178. LIQUID IMPACT ID CTRI/2019/02/017548.

**Keywords: encyclopedic tumor analysis, ETA, mTOR, PIK3CA, PI3K, Akt, mTOR inhibitor, rapalog**

## BACKGROUND

Mammalian Target of Rapamycin (mTOR) is a protein kinase which plays an important role in tumorigenesis by controlling protein synthesis, cell growth and proliferation and metastasis (Crespo et al., 2016). Since activation of the mTOR signaling pathway is ubiquitous in cancers, therapeutic inhibition of mTOR using analogs of Rapamycin ('Rapalogs') has been an attractive strategy for systemic management of cancer, albeit with modest benefits (Kwitkowski et al., 2010; Yao et al., 2011; Buti et al., 2016; Hua et al., 2019). Previous attempts to match alterations in mTOR pathway genes with label-agnostic mTOR blockade via monotherapy have reported inferior outcomes (Le Tourneau et al., 2015; Tsimberidou et al., 2019). The low efficacy of mTOR inhibitors has been attributed to the largely cytostatic rather than cytotoxic mechanisms of action (Meric-Bernstam and Gonzalez-Angulo, 2009), their limited inhibitory capacity as well as the activation of other resistance pathways (Faes et al., 2017). There is growing evidence that mTOR inhibitors in multi-drug combination regimens can overcome the largely cytostatic effect of mTOR inhibitor monotherapies thus leading to improved treatment outcomes especially in advanced cancers. Illustratively, the combination of Everolimus and Exemestane is superior to Everolimus alone in treatment of patients with non-steroidal aromatase-inhibitor refractory $ER^+/HER2^-$ metastatic breast cancer (Jerusalem et al., 2018). Likewise, the combination of Everolimus and lenvantinib has been approved for metastatic RCC (Leonetti et al., 2017) owing to higher efficacy over Everolimus monotherapy. Similarly, though Alpelisib monotherapy targeting mutant PIK3CA has shown limited efficacy (~6% ORR) in solid organ cancers, the combination of Alpelisib and Fulvestrant has yielded higher response rates (~26%) in ER+/HER2-metastatic breast cancers (Juric et al., 2018; André et al., 2019).

It is accepted that tandem therapeutic targeting of multiple signaling pathways can lead to improved outcomes in cancer (O'Reilly, 2002). The mTOR pathway cross-talks with multiple other signaling pathways such as MAKP/ERK (Mendoza et al., 2011; Liu et al., 2018), AR (Mulders, 2009) and VEGF (Crumbaker et al., 2017). Some crosstalk appears to be linked to resistance mechanisms, while a subset may present therapeutically relevant targets (Conciatori et al., 2018; Liu et al., 2018). Likewise, several other signaling pathways that are also known to be upregulated in cancers, offer additional opportunities for tandem therapeutic targeting (O'Reilly, 2002).

Although the potential benefits of Everolimus in combination with chemotherapy agents have been hypothesized in various cancers, the benefits of such regimens in a refractory setting has not yet been demonstrated. Further, selection of chemotherapy agents for such combination regimens have been largely derived from Randomized Clinical Trials (RCT) or Standard of Care (SoC) guidelines rather than via patient-specific evaluation of drug resistance or sensitivity in respective tumors. The benefits of the latter approach lie not only in identifying relevant drugs with higher antitumor activity (Jo et al., 2018) but also provide a repertoire of drugs that can be used in a label-agnostic setting.

The clinical utility of patient-specific multi-analyte tumor interrogation (called ETA for 'Encyclopedic Tumor Analysis') for identifying vulnerabilities in advanced refractory cancers (ARC) and their targeting with personalized *de novo* combination treatment regimens has been previously demonstrated (Nagarkar et al., 2019). Here, we report the efficacy of such personalized combination treatment regimens which achieve efficacious mTOR blockade as well as tandem targeting of other tumor vulnerabilities to yield meaningful outcomes in treatment of advanced refractory cancers.

## METHODS

### Study Design

This manuscript reports data from a subset of patients from three prospective interventional phase II/III trials, including RESILIENT (CTRI/2018/02/011808), ACTPRO (CTRI/2018/05/014178) and LIQUID IMPACT (CTRI/2019/02/017548) who received mTOR inhibitor-based treatments. The primary outcome data for the RESILIENT Trial has already been published (Nagarkar et al., 2019). The outcome data for the other two trials will be reported separately. The present manuscript only reports findings in a subset of patients from these trials where the therapy profile is relevant to the theme of this submission. Details of all trials are available at WHO-ICTRP. All trials were approved by institutional review boards and ethics committees of sponsor as well as clinical trial site. All trials were conducted in accordance with all applicable ethical guidelines and the Declaration of Helsinki. The present manuscript also retrospectively reports data from a curated subset of patients who availed of Encyclopedic Tumor Analysis (ETA) as a commercial service offered by the study sponsor for personalized treatments; outcomes are reported only for those patients who received mTOR-inhibitor based treatments.

### Patients

Between Jan 2018 and Jun 2019, 37 patients with advanced solid organ cancers received treatments with mTOR inhibitors in combination with other systemic anticancer agents as part of various prospective interventional clinical trials conducted by the study sponsor. All study participants were previously counseled regarding study objectives, potential benefits and potential risks and provided signed written informed consent for participation

in the trial and for publication of deidentified data. Between Jan 2018 and Dec 2018, 12 patients underwent ETA as a commercial service to inform precision systemic therapy options for advanced broadly refractory solid organ tumors and received treatments with mTOR inhibitors in combination with other systemic anticancer agents. Treatment outcomes were available in these patients and were hence considered for analysis. All patients consented for analysis and publication of deidentified data. Outcome data for these patients are reported.

## Encyclopedic Tumor Analysis

The process of ETA and generation of patient specific therapy recommendations have been described previously (Nagarkar et al., 2019) and is also provided as **Supplementary Material**. Briefly, ETA included molecular profiling of tumor tissue and blood samples by NGS, immunohistochemistry (IHC) on tumor tissue and *in vitro* chemoresponse profiling (CRP) of viable tumor tissue derived cells (TDCs) or Circulating Tumor Associated Cells (CTACs) from peripheral blood. Both cytotoxic anticancer agents as well as mTOR inhibitors were evaluated by CRP where viable TDCs/CTACs were treated *in vitro* with standardized concentrations of anti tumor agents and the proportion of cell death was measured. Next Generation Sequencing (NGS) analysis of tumor tissue DNA or peripheral blood circulating tumor DNA (ctDNA) using a targeted gene panel (452 or 411 genes) was performed to identify molecular alterations in the mTOR pathway genes that are known to be indicative for selection of mTOR inhibitor as well as molecular alterations to select appropriate targeted and endocrine agents. Finally, Immunohistochemistry (IHC) profiling of tumor tissue was used to determine expression of Estrogen Receptor (ER) and Androgen Receptor (AR) for selection of Endocrine agents. ETA findings were integrated to generate patient specific treatment recommendations which were shared with the treating oncologist.

## Treatments

All patients received individualized combination regimens with mTOR inhibitors and other targeted, endocrine or cytotoxic drugs which were informed by ETA findings. Among 39 patients where the combination regimen included ≥1 cytotoxic agents, the choice of single or multiple cytotoxic agents was based on reported safety information (AE profiles) of each individual cytotoxic agent (labeled toxicity), as well as phase I trial data of safety and toxicity of combinations. This safety information was used to anticipate/predict patient-wize expected AEs which was referred to while determining the appropriate starting dose as well as dose escalation in each patient. In all patients, the treatment agents were initially administered at lower (≤50%) doses, and were escalated based on an individualized dose escalation schedule. Other factors which guided patient-specific dosage and schedule included institutional guidelines and protocols as well as clinical assessment of the patients' health. As per the treatment plan in the trials, patients were to be administered treatments until progression or death or dose limiting toxicity. Patients who showed durable response were maintained with suitable dose reduction as decided by the treating clinician. For non-trial patients, schedule and duration were determined by the treating clinician based on clinical assessment of patients' health.

## Response Evaluation

Treatment response was assessed in all patients based on a baseline and follow-up radiological imaging (CT/PET-CT) as per RECIST 1.1 criteria (Eisenhauer et al., 2009) to determine Objective Response Rate (ORR), disease Control Rate (DCR), Progression Free Survival (PFS) and Overall Survival (OS). Patients in clinical trials underwent follow-up imaging scans after every two cycles of treatment or after every 8–12 weeks, whichever was longer. All radiological data were independently evaluated by an external expert radiologist who was blinded to the interpretation of the original radiologist. If the findings of the external expert radiologist concurred with the gross findings of the original radiologist, then the initially reported values were retained. In case of divergent findings, this was conveyed to the original radiologist for re-evaluation of the radiological scan data.

## Follow-Up

Patients were followed up until study termination or patient exclusion (death/loss to follow-up/withdrawal of consent) or until December 2020, to determine Progression Free Survival (PFS) as well as Overall Survival (OS). Post completion of study, patients were followed-up every 6 months for OS only. Patients who were not part of the clinical trials underwent follow-up imaging scans at intervals specified by the treating clinicians.

## Safety and Adverse Events

Treatment related AEs were prospectively obtained for trial patients during the trial. Treatment-related AEs for non-trial patients were obtained from patients' clinical records which were provided by the treating clinician. All AEs were graded according to NCI-CTCAE v5 (NCI, NIH, DHHS, 2017) and reported. For patients in the clinical trials, as well as commercial patients AEs were managed by standard procedures according to institutional protocols.

# RESULTS

## Study Cohort

The present manuscript reports outcomes in 49 patients (23 males, 26 females, median age 49 years) who received mTOR inhibitor-based treatment regimens informed by ETA (**Table 1**, **Supplementary Dataset**). This cohort includes prospective data of 37 cancer patients from clinical trials and retrospective data of 12 cancer patients who received ETA-guided treatment recommendation commercially from the sponsor. Among the 49 patients, three were therapy naïve (at presentation) whilst 46 had refractory cancers which had progressed following failure of multiple lines of prior systemic therapy.

## Treatments

All patients were administered mTOR inhibitors as part of multi-drug regimens where the combinations included either ≥1 cytotoxic agent ($n$ = 20), cytotoxic and other targeted/

**TABLE 1 |** Patient Demographics. The Study population includes 49 patients who received ETA guided combination treatments with mTOR inhibitors. Patient data was aggregated from three clinical trials conducted by the study sponsor as well as patients who availed of ETA as a commercial service from the sponsor.

| Parameter | mTOR_C | mTOR_CT | mTOR_T | Overall |
|---|---|---|---|---|
| **Gender** Male + female = total | 14 + 6 = 20 | 9 + 10 = 19 | 0 + 10 = 10 | 23 + 26 = 49 |
| **Age (years)** Median (range) | 45 (27–71) | 54 (8–68) | 50 (36–61) | 49 (8–71) |
| **Cancer type** | | | | |
| Bile duct | 1 | - | - | 1 |
| Breast | 1 | 6 | 8 | 15 |
| Colorectum | 1 | 1 | - | 2 |
| Endometrium | - | 1 | - | 1 |
| Esophagus | 1 | 1 | - | 2 |
| Head and neck | 4 | 3 | - | 7 |
| Kidney | - | 2 | - | 2 |
| Liver | 1 | - | - | 1 |
| Lung | 3 | 2 | - | 5 |
| Melanoma | 1 | - | - | 1 |
| Ovary | 1 | 1 | 2 | 4 |
| Pancreas | 2 | - | - | 2 |
| Hair follicle | 1 | - | - | 1 |
| Prostate | - | 1 | - | 1 |
| Sarcoma | 1 | - | - | 1 |
| Testes | 2 | - | - | 2 |
| Yolk sac tumor | - | 1 | - | 1 |

endocrine agents ($n$ = 19), or ≥1 targeted or endocrine agents ($n$ = 10). In this cohort, seven patients were AR+, three patients were ER+ and two patients were AR+, ER + by IHC. All anticancer drugs in the combination treatments were approved by the United States FDA for use as antineoplastic agents. Selection of all treatment agents (including mTOR inhibitors) was agnostic to the respective labeled indications. Patient-wize drugs and regimens are provided in **Supplementary Dataset**.

## Treatment Response

Among the 49 patients, 1 (2.0%) showed Complete Response (CR), 27 (55.1%) showed Partial Response (PR), 17 (34.7%) showed SD and 4 (8.1%) patients showed PD. The Objective Response Rate (ORR) in this sub-cohort was 57.1% and disease Control Rate (DCR) was 91.8%. Patient outcomes are summarized in **Table 2**. In three patients, failure of a prior line of Everolimus inhibitor monotherapy had led to a previous instance of PD; all three patients received ETA guided combination regimen in the present study and showed PR. Additional relevant or unique cases are discussed in the **Supplementary Material**. Patient-wize responses to treatment are provided in **Supplementary Dataset**. Findings of the original radiologist and the external expert radiologist were found to be concurrent with regards to determining gross treatment response (PR, SD and PD) in all cases and hence did not necessitate any re-evaluation.

Among 20 patients who received mTOR inhibitors in combination with cytotoxic agents (mTOR_C), PR was observed in 10 patients (50%). Among 29 patients, the combination regimen included an additional targeted or endocrine agent (mTOR_T, mTOR_CT) for tandem blockade of other signaling pathways; 18 of these patients (62.1%) showed PR. Within these 29 patients, PR was observed in 6/10 (60%) patients where AR/ER was targeted in tandem with mTOR, 5/9 (55.5%) patients where the VEGF signaling pathway was a tandem target and in 6/9 (66.7%) patients where the EGFR/ERBB2 pathway was targeted along with mTOR.

**TABLE 2 |** Gene variants indicative of mTOR activation. The table indicates the types of gene variants observed and the number of patients where the tumors harbored each type of gene variants. Indications in italicized text are probable indications.

| Gene | Reported indications |
|---|---|
| PIK3CA | p.E545 K (8), p.H1047 R (3), p.E542 K (3), p.M1043I (1), p.E1034G (1), p.E726 K (1), p.N345 K (1), p.C420 R (1), p.Y1021C (1). *CNV_ < 6 (3), c.*25T > C (1), p.Y343C (1), p.E110K (1), p.R693H (1)* |
| PTEN | p.D24 N (1), p.D92G (1), c.4932 A > G (1), p.R130* (1), p.V166 A (1), p.R159 S (1), p.R47G (1), p.D326G (1), p.Y68C (1), CNV_1 (3). *c.6354G > A (1)* |
| STK11 | CNV_1 (3), p.F354 L (1) |
| AKT1 | p.E17 K (2) |
| AKT2 | *CNV_3 (1)* |
| TSC2 | p.F1510del (2), p.F1510del (1), p.R1743Q (1). *p.S174L (1)* |
| MTOR | p.M2327I (1), p.R1709H (1) |
| NF1 | p.R1250Q (1), p.S340 F (1), p.Q1520* (1) |
| ARID1A | p.P1326_Q1327insQ (1), p.P1618 L (1), CNV_1 (1) |

**TABLE 3 |** Treatment Outcomes. Progression Free Survival and Overall Survival Data are censored at the last follow-up.

| | mTOR_C | mTOR_CT | mTOR_T | Overall |
|---|---|---|---|---|
| **Response** | | | | |
| CR / PR | 10 | 11 | 7 | 28 |
| SD | 8 | 6 | 3 | 17 |
| PD | 2 | 2 | - | 4 |
| **Response Rates (%)** | | | | |
| ORR | 50.0 | 57.9 | 70.0 | 57.1 |
| DCR | 90.0 | 89.5 | 100.0 | 91.8 |
| **Survival (months)** | | | | |
| mPFS* | 5.2 (3.8–6.6) | 4.9 (3.8–6.0) | 4.9 (2.0–10.0) | 4.9 (3.6–6.2) |
| mOS* | 7.2 (2.7–11.7) | 9.4 (4.6–14.2) | 12.1 (6.7–17.5) | 9.4 (6.6–12.2) |
| **Survival Rates (%)** | | | | |
| 12-month PFS | 40.0 | 85.0 | 65.0 | 60.0 |
| 12-month OS | 55.0 | 70.0 | 75.0 | 55.0 |
| 24-month OS | 40.0 | 35.0 | 20.0 | 35.0 |

*CR, Complete Response; PR, Partial Response, SD, Stable Disease; PD, Progressive Disease; ORR, Objective Response Rate; DCR, Disease Control Rate; PFS, Progression Free Survival; OS, Overall Survival; mPFS, median PFS, mOS: median OS. *values within parentheses indicate 95% Confidence Interval.*

## Progression Free Survival and Overall Survival

The study patients ($n$ = 49) reported median PFS (mPFS) and median OS (mOS) of 4.9 months (95% CI: 3.6–6.2) and 9.4 months (95% CI: 6.6–12.2) respectively. The PFS rate and OS rate at 12 and 24 months were ~60 and ~35% respectively. The mPFS, PFS rates, mOS and OS rates in the various regimen subtypes are summarized in **Table 3** along with the overall values. Kaplan Meier Plots of PFS and OS (overall as well as regimen subtypes are provided in **Figure 1**. In order to benchmark the benefits of ETA-guided therapy in the study cohort, we compared (**Figure 2**) the observed PFS of each patient on ETA-combination regimen (PFS2) against PFS on patient's last failed line of therapy (PFS1). PFS2 was delimited due to demise in seven patients, due to disease progression in four patients, due to censoring in 14 patients (6 withdrew consent for further follow-up, eight defaulted). At the last follow-up, among the 24 patients who remained Progression Free, the ongoing Progression Free duration was reported as interim PFS. Based on these cut-offs, the PFS2:PFS1 ratio was ≥2.5 in 20 patients, between 1.3–2.5 in 10 patients, and ~1 in six patients. The median PFS1 was 2.8 months, median PFS2 was 4.9 months and the overall PFS2:PFS1 ratio was 1.8, indicating that the median improvement was a significant extension of PFS over the last treatment. Patient-wize PFS and OS are provided in **Supplementary Dataset**.

## Molecular Alterations in the Mammalian Target of Rapamycin Pathway

The molecular landscape of mTOR pathway associated genes in the study cohort as determined by NGS is depicted in **Figure 3**. Variations in PIK3CA and PTEN were most common among all genes related to the mTOR pathway. In 27 patients, the tumor harbored gene variants which were previously reported to be indicative for mTOR activation. In five patients, the tumors harbored gene variants which were probably indicative for mTOR activation, in addition to known targetable variants. In four patients, the tumor harbored no known targetable variants and only probably indicative variants. The phenotypic consequence of the variations appeared to be aligned with the activity profile of other known variants, and hence deemed as probable indications for mTOR inhibitor selection. Finally, in 13 patients there were no known gene variants indicative of mTOR activation.

## Adverse Events

There were no grade IV treatment related Adverse Events (AEs) or any treatment related deaths. Grade III treatment related AEs were seen in 34 patients. The most common grade III treatment related AEs were Fatigue (27%), Anorexia (11%) and Oral Mucositis (8%) which were managed by administration of standard treatment modalities Hyperglycemia which has been previously reported in mTOR regimens was observed in one patient. Patient-wize AEs are provided in **Supplementary Dataset**.

# DISCUSSION

The study outcomes support the hypotheses of the study that ETA-guided combination regimens of mTOR inhibitors with other anti-neoplastic agents can achieve meaningful response in advanced refractory cancers especially when such combinations include other targeted/endocrine agents for tandem blockade of other tumor-associated signaling pathways. While PFS rates were higher in combination regimens that included another targeted agent (mTOR_T, mTOR_CT), the OS rates were similar across all therapy regimen subtypes indicating that mTOR inhibitors in combination regimens offer OS benefits while tandem targeting of additional tumor pathways yields PFS benefits as well apart from to OS benefits. It is generally accepted that subsequent lines of anticancer treatments are associated with decreasing probability of success. However. among patients who

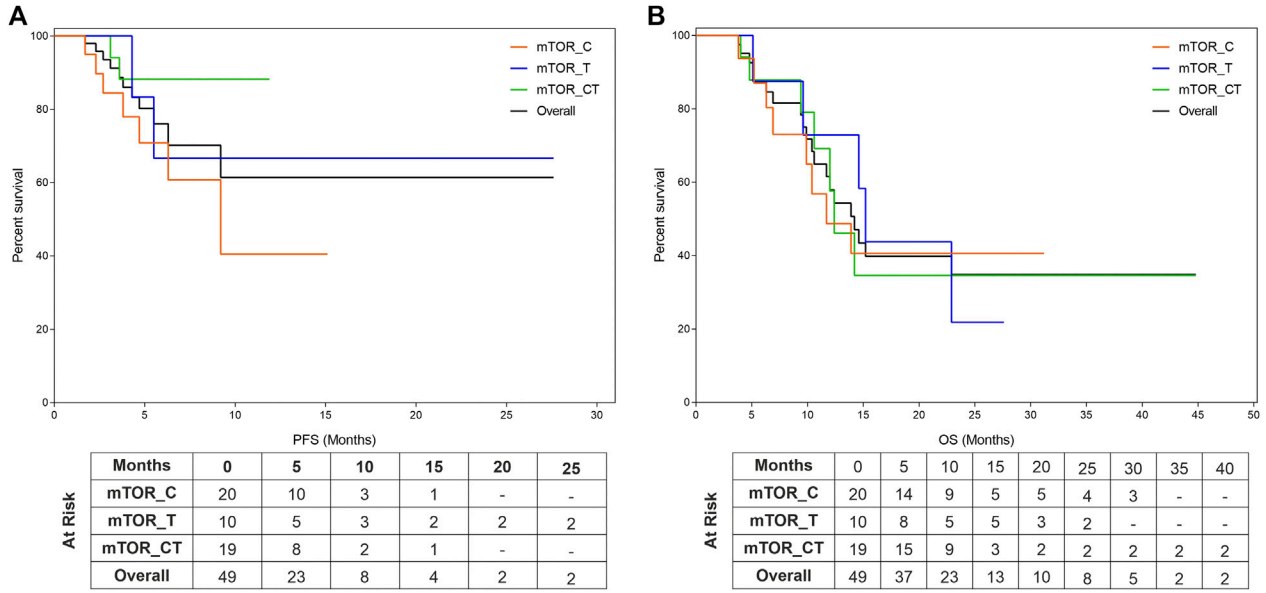


At Risk

| Months | 0 | 5 | 10 | 15 | 20 | 25 |
|---|---|---|---|---|---|---|
| mTOR_C | 20 | 10 | 3 | 1 | - | - |
| mTOR_T | 10 | 5 | 3 | 2 | 2 | 2 |
| mTOR_CT | 19 | 8 | 2 | 1 | - | - |
| Overall | 49 | 23 | 8 | 4 | 2 | 2 |

At Risk

| Months | 0 | 5 | 10 | 15 | 20 | 25 | 30 | 35 | 40 |
|---|---|---|---|---|---|---|---|---|---|
| mTOR_C | 20 | 14 | 9 | 5 | 5 | 4 | 3 | - | - |
| mTOR_T | 10 | 8 | 5 | 5 | 3 | 2 | - | - | - |
| mTOR_CT | 19 | 15 | 9 | 3 | 2 | 2 | 2 | 2 | 2 |
| Overall | 49 | 37 | 23 | 13 | 10 | 8 | 5 | 2 | 2 |

**FIGURE 1 |** Kaplan Meier Plots of Progression Free Survival and Overall Survival. Progression Free Survival (PFS, **(A)**) and Overall Survival (OS, **(B)**) were evaluated for the entire cohort as well as subgroups which include mTOR inhibitors in combination with either Cytotoxic Agents (mTOR_C), other targeted agents (mTOR_T) or with both cytotoxic and targeted agents (mTOR_CT).

received ETA-guided combination regimens, there was an almost doubling of the PFS (PFS2:PFS1 ratio) indicating significant therapeutic benefit to patients. The authors acknowledge that the instances of censored PFS may underrepresent the actual extent of benefit. However, the recorded data indicate a significant median advantage despite censored observations; since therapy was ongoing in several patients, eventual improvements to these ratios are anticipated. We hence conclude that ETA guided combination regimens can provide significant PFS improvements even in heavily pre-treated populations. The response and survival benefits indicate the ability of ETA guided combination treatments to exploit known targetable vulnerabilities as well as to overcome known resistance variants. The present outcomes are remarkable in context of the PFS and ORR reported for the mTOR arm in the SHIVA trial (Le Tourneau et al., 2015), as well as outcomes in the NCI Match arms where modest benefits were observed such as 23% ORR for Capivasertib (Kalinsky et al., 2018), 0% ORR and 27% 6-months PFS rate for Taselisib (Krop et al., 2018) and 4% ORR and 1.8 months median PFS for GSK2636771 (Janku et al., 2018).

Presently, apart from Alpelisib, selection of other mTOR inhibitors is not based on molecular indications. Prior attempts to match variations in mTOR pathway genes with label-agnostic mTOR blockade (such as the trials mentioned above) have reported largely discouraging outcomes. Several variations are associated with mTOR activation such as alterations in the AKT (1/2/3), PIK3CA and PTEN genes besides the mTOR gene itself (Grabiner et al., 2014). Among the 32 patients with known and probable mTOR activation, the most common gene variants associated with the mTOR pathway were SNVs in PIK3CA ($n$ = 24, 48.9%), loss of PTEN gene function via SNV or CNA ($n$ = 9, 18%). Deleterious SNV/CNA in multiple mTOR pathway genes were also observed in some patients ($n$ = 10, 20.4%). The present study does not aim to establish the predictive efficacy of these mTOR pathway variations for mTOR inhibitor selection or treatment response; the profile of (detected and undetectable) molecular variants in the known mTOR pathway genes suggests the role of additional hitherto unidentified genes and gene-variants linked to resistance or response toward mTOR inhibitors. Molecular alterations (SNV and CNV) of unknown significance in mTOR pathway genes were detected in 9 cases. These variations are speculated to be probable indications, which may be confirmed based on future insight into the phenotypic consequence (gain/loss of function) of these variations.

Prior attempts to identify potentially synergistic and safe anticancer drug combinations (Wang and Sorger, 2017; Sidorov et al., 2019; Zagidullin et al., 2019) as well as to predict drug efficacy via *in vitro* CRP of cell lines or primary tumor cellsy (Hurvitz et al., 2015; Mercatali et al., 2016; Kuo et al., 2019) reflect a consensus in favor of personalized combination regimens based on molecular and functional evidence. However, these prior reports do not have any correlation with clinical outcome data. In this regard, ours is the first report that provides clinical evidence demonstrating the utility and efficacy of a comprehensive, integrational multi-analyte-based approach (ETA) for informing personalized combination regimens. In ETA, targeted agents were selected based on NGS findings (SNV, CNA and Differential Gene Expression, DGE), endocrine agents were selected on the basis of hormone receptor (ER/AR) expression as determined by immunohistochemistry (IHC) on tumor tissue. mTOR inhibitors and cytotoxic agents

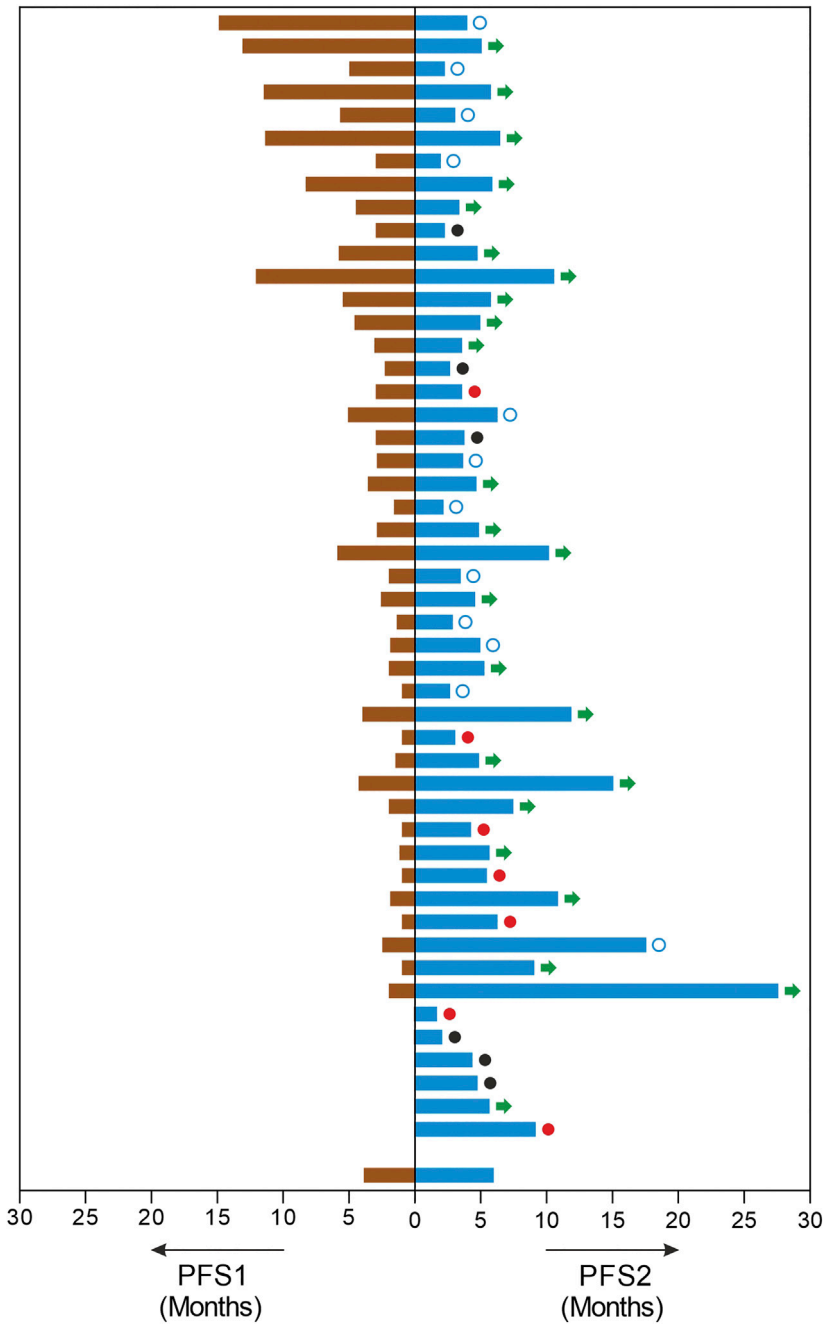


**FIGURE 2 |** Improvements in Progression Free Survival. The image depicts each patients PFS in months on the last line of treatment (PFS1, left) and the PFS in months observed on ETA guided mTOR combination therapy regimen (PFS, right). In this cohort, three patients were therapy naïve and three patients had undergone prior surgery or radiation only. □: censored. ●: demise; ●: progression; →: ongoing PFS.

were selected on the basis of *in vitro* CRP of viable TDCs or CTACs. It is pertinent to note that the observed drug efficacies by *in vitro* CRP is a summation of all known and latent resistance mechanisms including tumor-specific pathways as well as transiently dysregulated pathways. Since mTOR activation is associated with resistance to chemotherapy agents, *in vitro* CRP identified efficacious cytotoxic anticancer agents to which the tumor had not acquired resistance despite mTOR activation. Since the primary indication for mTOR inhibitor selection was *in vitro* CRP rather than molecular variations, ETA thus identified several patients ($n$ = 13) with *in vitro* and largely *in vivo* response to mTOR inhibition, but where the tumor harbored no known alterations indicative of mTOR activation.

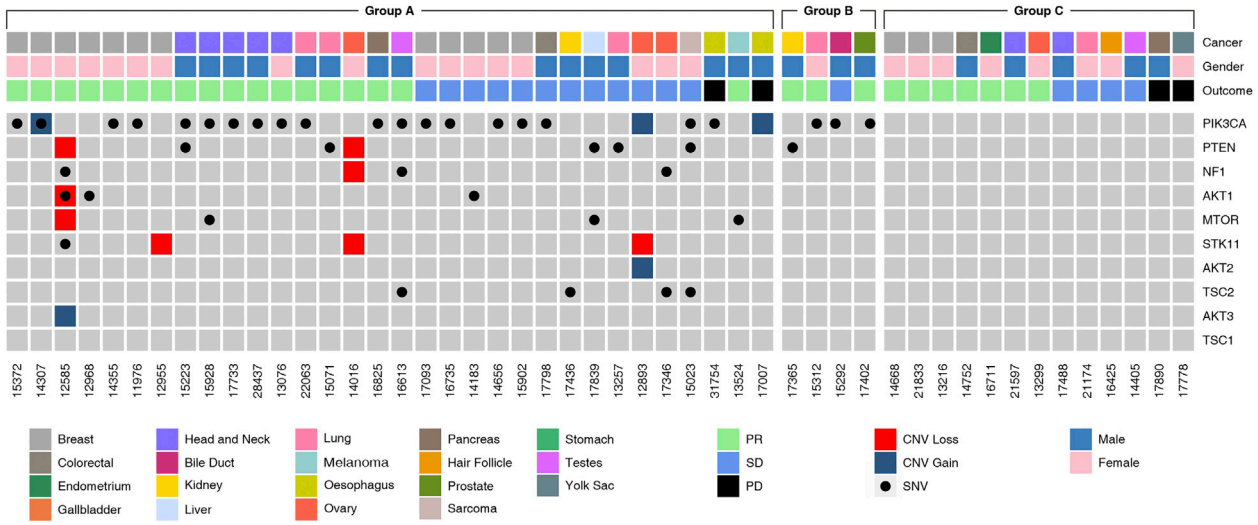


**FIGURE 3 |** Molecular Landscape of Study Cohort**.** Molecular alterations observed in genes in the mTOR pathway genes as determined by Next Generation Sequencing (NGS) analysis of tumor tissue DNA or cell free tumor DNA (ctDNA) are depicted. Five-digit numbers at the bottom of each column indicate individual patients in the study cohort. Cancer types (topmost row) and gender (second row from top) are color coded. SNV and CNV (gain or loss) are color coded. The Study Cohort consisted of 49 patients divided into various sub-groups:Group A ($n$ = 31, known ± probable mTOR activating variants), Group B ($n$ = 5, probable mTOR activating variants) and Group C ($n$ = 13, no known mTOR activating variants).

Having established the utility of ETA for selection of efficacious combination treatments with mTOR inhibitors and other antineoplastic agents, it is pertinent to review the safety of such *de novo* drug combinations. The safety profile of multi-drug anticancer regimens especially those with combinations of targeted and cytotoxic agents has been discussed at length in prior meta analyses (Liu et al., 2016; Nikanjam et al., 2016; Nikanjam et al., 2017). These studies observe that it is been possible to safely administer *de novo* (targeted and cytotoxic) drug combinations in most patients with manageable profiles of adverse events (AEs). It is generally agreed that although the actual profile of Adverse Events (AEs) in any given patient cannot be accurately predicted, the commonly occurring AEs associated with each drug or combinations can be anticipated. The profile of AEs shows that even though this heavily pretreated cohort was at an inherently higher risk of AEs due to cumulative toxicities from prior treatments, ETA guided therapies were generally well tolerated with a manageable toxicity profile (Li et al., 2015; Wilks, 2015).

The present study was largely based on a heavily pretreated cohort with minimal representation of therapy naïve patients. Hence, we are unable to demonstrate the benefits of ETA guided combination regimens as initial line therapy in treatment naïve patients at presentation.

To conclude, the present study is the first to demonstrate that ETA-guided combination regimens with mTOR inhibitor and other anticancer agents yield superior response rates and survival benefits as compared to mTOR inhibitor as monotherapy or in physician's choice of combination regimens, in a (mostly) heavily pretreated cohort of patients with acceptable toxicity profile.

## CONCLUSION

We demonstrate that patient-specific combination regimens which achieve mTOR blockade and tandem targeting of other tumor vulnerabilities not only lead to favourable outcomes in advanced refractory cancers but also had manageable toxicity profiles. While prior attempts to expand the scope of mTOR inhibitor monotherapy in an organ agnostic setting based on univariate molecular profiling have been largely successful, we show that personalized combination regimens based on multi-analyte tumor profiling can yield significant and meaningful treatment benefits in various solid organ cancers. This is a viable pan-cancer treatment strategy since it overcomes the limited efficacy of mTOR inhibitors as well as the drug-resistance associated with activation of mTOR.

## DATA AVAILABILITY STATEMENT

The original contributions presented in the study are included in the article/**Supplementary Material**, further inquiries can be directed to the corresponding author.

## ETHICS STATEMENT

The studies involving human participants were reviewed and approved by Institutional Ethics Committees of the Study Sponsor and the Study Site(s). The patients/participants provided their written informed consent to participate in this study. Written informed consent was

obtained from the individual(s) for the publication of any potentially identifiable images or data included in this article.

## AUTHOR CONTRIBUTIONS

DP and DA: Study Design, Supervision, Data Review, advised on results interpretation, Manuscript Writing; TC, AG, NP, SL and RP: Study Design, Manuscript Review; AR, AB: Study Design.

## FUNDING

No external funding was obtained for this study. The entire study was funded by the Study Sponsor (DCG).

## ACKNOWLEDGMENTS

The authors are grateful toward all study participants and their caregivers. The contributions of HCG Manavata Cancer Center, Avinash Cancer Center, and Datar Cancer Genetics toward managing various clinical, operational and laboratory aspects of the study are acknowledged with gratitude.

## SUPPLEMENTARY MATERIAL

The Supplementary Material for this article can be found online at: https://www.frontiersin.org/articles/10.3389/fphar.2021.631135/full#supplementary-material.

## REFERENCES

André, F., Ciruelos, E., Rubovszky, G., Campone, M., Loibl, S., Rugo, H. S., et al. (2019). Alpelisib for PIK3CA-mutated, hormone receptor-positive advanced breast cancer. *N. Engl. J. Med.* 380 (20), 1929–1940. doi:10.1056/nejmoa1813904

Buti, S., Leonetti, A., Dallatomasina, A., and Bersanelli, M. (2016). Everolimus in the management of metastatic renal cell carcinoma: an evidence-based review of its place in therapy. *Core Evid.* 11, 23–36. doi:10.2147/ce.s98687

Conciatori, F., Ciuffreda, L., Bazzichetto, C., Falcone, I., Pilotto, S., Bria, E., et al. (2018).mTOR cross-talk in cancer and potential for combination therapy, *Cancers (Basel)* 10, 23. doi:10.3390/cancers10010023

Crespo, S., Kind, M., and Arcaro, A. (2016). The role of the PI3K/AKT/mTOR pathway in brain tumor metastasis. *Jcmt* 2, 80–89. doi:10.20517/2394-4722.2015.72

Crumbaker, M., Khoja, L., and Joshua, A. M. (2017). AR signaling and the PI3K pathway in prostate cancer. *Cancers (Basel)* 9 (4), 34. doi:10.3390/cancers9040034

Eisenhauer, E. A., Therasse, P., Bogaerts, J., Schwartz, L. H., Sargent, D., Ford, R., et al. (2009). New response evaluation criteria in solid tumours: revised RECIST guideline (version 1.1). *Eur. J. Cancer* 45 (2), 228–247. doi:10.1016/j.ejca.2008.10.026

Faes, S., Demartines, N., and Dormond, O. (2017). Resistance to mTORC1 inhibitors in cancer therapy: from kinase mutations to intratumoral heterogeneity of kinase activity. *Oxid Med. Cel Longev* 2017, 1726078. doi:10.1155/2017/1726078

Grabiner, B. C., Nardi, V., Birsoy, K., Possemato, R., Shen, K., Sinha, S., et al. (2014). A diverse array of cancer-associated MTOR mutations are hyperactivating and can predict rapamycin sensitivity. *Cancer Discov.* 4 (5), 554–563. doi:10.1158/2159-8290.cd-13-0929

Hua, H., Kong, Q., Zhang, H., Luo, T., and Jiang, Y. (2019). Targeting mTOR for cancer therapy. *J. Hematol. Oncol.* 12 (1), 71. doi:10.1186/s13045-019-0754-1

Hurvitz, S. A., Kalous, O., Conklin, D., Desai, A. J., Dering, J., Anderson, L., et al. (2015). *In vitro* activity of the mTOR inhibitor everolimus, in a large panel of breast cancer cell lines and analysis for predictors of response. *Breast Cancer Res. Treat.* 149 (3), 669. doi:10.1007/s10549-015-3282-x

Janku, F., Jegede, O., and Puhalla, S. L. (2018). NCI-MATCH arms N & P: phase II study of PI3K beta inhibitor GSK2636771 in patients with cancers with PTEN mutation/deletion or PTEN protein loss. *Ann. Oncol.* 29 (Suppl. l_8), viii133–viii148. doi:10.1093/annonc/mdy279.406

Jerusalem, G., de Boer, R. H., Hurvitz, S., Yardley, D. A., Kovalenko, E., Ejlertsen, B., et al. (2018). Everolimus plus Exemestane vs everolimus or capecitabine monotherapy for estrogen receptor-positive, HER2-negative advanced breast cancer. *JAMA Oncol.* 4 (10), 1367. doi:10.1001/jamaoncol.2018.2262

Jo, Y., Choi, N., Kim, K., Koo, H.-J., Choi, J., and Kim, H. N. (2018). Chemoresistance of cancer cells: requirements of tumor microenvironment-mimicking in vitro models in anti-cancer drug development. *Theranostics* 8 (19), 5259. doi:10.7150/thno.29098

Juric, D., Rodon, J., Tabernero, J., Janku, F., Burris, H. A., Schellens, J. H. M., et al. (2018). Phosphatidylinositol 3-kinase α-selective inhibition with Alpelisib (BYL719) in PIK3CA-altered solid tumors: results from the first-in-human study. *J. Clin. Oncol.* 36 (13), 1291–1299. doi:10.1200/jco.2017.72.7107

Kalinsky, K., Hong, F., McCourt, C., Sachdev, J., Mitchell, E., Zwiebel, J., et al. (2018). AZD5363 in patients (pts) with tumors with AKT mutations: NCI-match subprotocol EAY131-Y, A trial of the ECOG-ACRIN cancer Research group (EAY131-Y). EORTC-NCI-AACR, Dublin, Ireland, November 13-16, 2018.

Krop, I. E., Jegede, O., Grilley-Olson, J. E., Lauring, J. D., Hamilton, S. R., Zwiebel, J. A., et al. (2018). Results from molecular analysis for therapy choice (MATCH) arm I: Taselisib for PIK3CA-mutated tumors. *Jco* 36 (15_Suppl. l), 101. doi:10.1200/jco.2018.36.15_suppl.101

Kuo, C. T., Chen, C. L., and Li, C. C. (2019). Immunofluorescence can assess the efficacy of mTOR pathway therapeutic agent Everolimus in breast cancer models. *Sci. Rep.* 9 (1), 10898. doi:10.1038/s41598-019-45319-4

Kwitkowski, V. E., Prowell, T. M., Ibrahim, A., Farrell, A. T., Justice, R., Mitchell, S. S., et al. (2010). FDA approval summary: temsirolimus as treatment for advanced renal cell carcinoma. *The Oncologist* 15 (4), 428–435. doi:10.1634/theoncologist.2009-0178

Le Tourneau, C., Delord, J.-P., Gonçalves, A., Gavoille, C., Dubot, C., Isambert, N., et al. (2015). Molecularly targeted therapy based on tumour molecular profiling versus conventional therapy for advanced cancer (SHIVA): a multicentre, open-label, proof-of-concept, randomised, controlled phase 2 trial. *Lancet Oncol.* 16 (13), 1324–1334. doi:10.1016/s1470-2045(15)00188-6

Leonetti, A., Leonardi, F., Bersanelli, M., and Buti, S. (2017). Clinical use of lenvatinib in combination with everolimus for the treatment of advanced renal cell carcinoma. *Tcrm* 13, 799–806. doi:10.2147/tcrm.s126910

Li, J. Y., Daniels, G., Wang, J., and Zhang, X. (2015). TBL1XR1 in physiological and pathological states. *Am. J. Clin. Exp. Urol.* 3 (1), 13–23.

Liu, F., Yang, X., Geng, M., and Huang, M. (2018). Targeting ERK, an Achilles' Heel of the MAPK pathway, in cancer therapy. *Acta Pharmaceutica Sinica B* 8 (4), 552–562. doi:10.1016/j.apsb.2018.01.008

Liu, S., Nikanjam, M., and Kurzrock, R. (2016). Dosing de novo combinations of two targeted drugs: towards a customized precision medicine approach to advanced cancers. *Oncotarget* 7, 11310–11320. doi:10.18632/oncotarget.7023

Mendoza, M. C., Er, E. E., and Blenis, J. (2011). The Ras-ERK and PI3K-mTOR pathways: cross-talk and compensation. *Trends Biochem. Sci.* 36 (6), 320–328. doi:10.1016/j.tibs.2011.03.006

Mercatali, L., Spadazzi, C., Miserocchi, G., Liverani, C., De Vita, A., Bongiovanni, A., et al. (2016). The effect of everolimus in an in vitro model of triple negative breast cancer and osteoclasts. *Ijms* 17 (11), 1827. doi:10.3390/ijms17111827

Meric-Bernstam, F., and Gonzalez-Angulo, A. M. (2009). Targeting the mTOR signaling network for cancer therapy. *Jco* 27 (13), 2278–2287. doi:10.1200/jco.2008.20.0766

Mulders, P. (2009). Vascular endothelial growth factor and mTOR pathways in renal cell carcinoma: differences and synergies of two targeted mechanisms. *BJU Int.* 104 (11), 1585–1589. doi:10.1111/j.1464-410x.2009.08987.x

Nagarkar, R., Patil, D., Crook, T., Datta, V., Bhalerao, S., Dhande, S., et al. (2019). Encyclopedic tumor analysis for guiding treatment of advanced, broadly

refractory cancers: results from the RESILIENT trial. *Oncotarget* 10 (54), 5605–5621. doi:10.18632/oncotarget.27188

NCI, NIH, DHHS (2017). *Common terminology criteria for adverse events v5.0*. Washington, D.C.: U.S. Department of Health and Human Services.

Nikanjam, M., Liu, S., and Kurzrock, R. (2016). Dosing targeted and cytotoxic two-drug combinations: lessons learned from analysis of 24,326 patients reported 2010 through 2013. *Int. J. Cancer* 139 (9), 2135–2141. doi:10.1002/ijc.30262

Nikanjam, M., Liu, S., Yang, J., and Kurzrock, R. (2017). Dosing three-drug combinations that include targeted anti-cancer agents: analysis of 37,763 patients. *Oncologist* 22 (5), 576–584. doi:10.1634/theoncologist.2016-0357

O'Reilly, M. S. (2002). Targeting multiple biological pathways as a strategy to improve the treatment of cancer. *Clin. Cancer Res.* 8 (11), 3309.

Sidorov, P., Naulaerts, S., Ariey-Bonnet, J., Pasquier, E., and Ballester, P. J. (2019). Predicting synergism of cancer drug combinations using NCI-almanac data. *Front. Chem.* 7, 509. doi:10.3389/fchem.2019.00509

Tsimberidou, A. M., Hong, D. S., and Wheler, J. J. (2019). Long-term overall survival and prognostic score predicting survival: the IMPACT study in precision medicine. *J. Hematol. Oncol.* 12 (1), 145. doi:10.1186/s13045-019-0835-1

Wang, A. C., and Sorger, P. K. (2017). Combination cancer therapy can confer benefit via patient-to-patient variability without drug additivity or synergy. *Cell* 171 (7), 1678–1691. doi:10.1016/j.cell.2017.11.009

Wilks, S. T. (2015). Potential of overcoming resistance to HER2-targeted therapies through the PI3K/Akt/mTOR pathway. *Breast* 24 (5), 548. doi:10.1016/j.breast.2015.06.002

Yao, J. C., Shah, M. H., Ito, T., Bohas, C. L., Wolin, E. M., Van Cutsem, E., et al. (2011). Everolimus for advanced pancreatic neuroendocrine tumors. *N. Engl. J. Med.* 364 (6), 514–523. doi:10.1056/NEJMoa1009290

Zagidullin, B., Aldahdooh, J., Zheng, S., Wang, W., Wang, Y., Saad, J., et al. (2019). DrugComb: an integrative cancer drug combination data portal. *Nucleic Acids Res.* 47 (W1), W43–W51. doi:10.1093/nar/gkz337

**Conflict of Interest:** DP and DA are in full time employment of the Study Sponsor (DCG).

All remaining authors declare that the research was conducted in the absence of any commercial or financial relationships that could be construed as a potential conflict of interest..

## GLOSSARY

**mTOR** mammalian target of rapamycin
**ETA** encyclopedic tumor analysis
**ORR** objective response rate
**DCR** disease control rate
**mPFS,** median progression free survival
**mOS** median overall survival
**ER** estrogen receptor
**HER2** human epidermal growth factor receptor 2
**MAKP** mitogen activated protein kinase
**ERK** extracellular signal-regulated kinase
**AR** androgen receptor
**VEGF** vascular endothelial growth factor
**RCT** randomized clinical trial
**SoC** standard of care
**ARC** advanced refractory cancers
**IHC** immunohistochemistry
**USFDA** united states food and drug administration
**CR** complete response
**PR** partial response
**SD** stable disease
**PD** progressive disease (disease progression)
**EGFR** epidermal growth factor receptor
**ERBB2** synonym of HER2
**PFS** progression free survival
**OS** overall survival
**AE** adverse event
**CRC** colorectal cancer
**ctDNA** circulating (cell-free) tumor DNA
**SNV** single nucleotide variations
**CNV** copy number variations
**CRP** chemoresponse profiling
**NGS** next generation sequencing
**DGE** differential gene expression
**TDCs** tumor tissue derived cells
**C-TACs** circulating tumor associated cells
**RECIST** response evaluation criteria in solid tumors
**CTCAE** common terminology criteria for adverse events

frontiers in Pharmacology

REVIEW
published: 19 April 2021
doi: 10.3389/fphar.2021.636892

# The Hypoxia-Activated Prodrug TH-302: Exploiting Hypoxia in Cancer Therapy

*Yue Li*[1,2,3], *Long Zhao*[1,3] *and Xiao-Feng Li*[1,3]*

[1]*Department of Nuclear Medicine, The Second Clinical Medical College, Jinan University (Shenzhen People's Hospital), Shenzhen, China,* [2]*The First Affiliated Hospital, Jinan University, Guangzhou, China,* [3]*Department of Nuclear Medicine, The First Affiliated Hospital of Southern University of Science and Technology, Shenzhen, China*

Hypoxia is an important feature of most solid tumors, conferring resistance to radiation and many forms of chemotherapy. However, it is possible to exploit the presence of tumor hypoxia with hypoxia-activated prodrugs (HAPs), agents that in low oxygen conditions undergo bioreduction to yield cytotoxic metabolites. Although many such agents have been developed, we will focus here on TH-302. TH-302 has been extensively studied, and we discuss its mechanism of action, as well as its efficacy in preclinical and clinical studies, with the aim of identifying future research directions.

**Keywords: Hypoxia, Hypoxia-activated prodrugs, TH-302, radiotherapy, Chemotherapy**

OPEN ACCESS

***Edited by:***
*George Mattheolabakis, University of Louisiana at Monroe, United States*

***Reviewed by:***
*Adam Patterson, The University of Auckland, New Zealand*
*Violaine SEE, University of Liverpool, United Kingdom*

***Correspondence:**
*Xiao-Feng Li*
*linucmed@hotmail.com*

***Specialty section:***
*This article was submitted to Pharmacology of Anti-Cancer Drugs, a section of the journal Frontiers in Pharmacology*

***Received:*** *02 December 2020*
***Accepted:*** *25 February 2021*
***Published:*** *19 April 2021*

***Citation:***
*Li Y, Zhao L and Li X-F (2021) The Hypoxia-Activated Prodrug TH-302: Exploiting Hypoxia in Cancer Therapy. Front. Pharmacol. 12:636892. doi: 10.3389/fphar.2021.636892*

## INTRODUCTION

Hypoxia is an important characteristic of tumors, and generally results in a poor response to radiation and chemotherapy. However, it also presents a therapeutic opportunity, as normal tissue is generally well oxygenated. There have been numerous candidate molecules with enhanced toxicity to hypoxic cells, and they all share a general mechanism: an inert compound is enzymatically reduced to a reactive species, which is easily re-oxidized in the presence of oxygen. Such agents are referred to as hypoxia-activated prodrugs, or HAPs.

The first studies on HAPs were conducted by Alan Sartorelli's group at Yale, who showed that mitomycin C was preferentially activated under hypoxic conditions, and was thus able to selectively kill hypoxic cells (Lin et al., 1972; Rockwell et al., 1982; Fracasso and Sartorelli, 1986; Pritsos and Sartorelli, 1986). Further HAPs included RSU-1069 and tirapazamine (SR4233) (Laderoute and Rauth, 1986; Whitmore and Gulyas, 1986; Zeman et al., 1986), though neither agent achieved clinical recognition. Recently, a second generation HAP, TH-302 (evofosfamide) has been the subject of extensive preclinical research, much of it supporting the belief that the agent would have a valuable future. However, these hopes were significantly undermined by the failure of phase III clinical trials. Nonetheless, research on TH-302 is still ongoing, and here we will summarize the state of the field.

## PHARMACOLOGICAL MECHANISMS

TH-302 was first described in 2008 (Duan et al., 2008). The prodrug consists of a 2-nitroimidazole moiety linked to bromo-iso-phosphoramide mustard (Br -IPM), a DNA cross-linking agent. TH-302 is a substrate for certain cellular reductases that generate a radical anion through 1-electron reduction. Under normoxic conditions, the free radical anions are quickly oxidized back to either the original prodrug or superoxides, and no cytotoxic product is released. However, in the absence of oxygen, the free radical anions are further reduced, leading to the release of Br-IPM or its

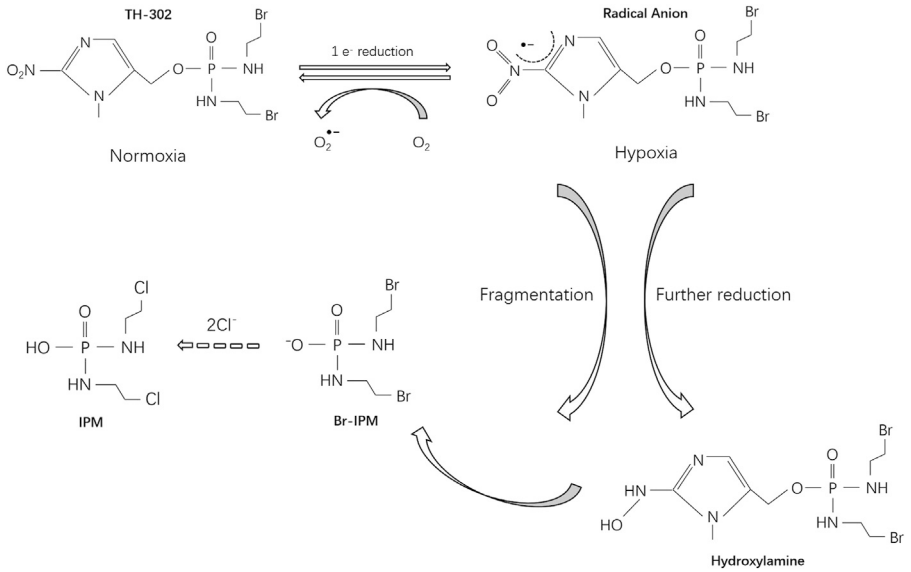


**FIGURE 1 |** Metabolism of TH-302.

stable downstream product, isophosphoramide mustard (IPM) (**Figure 1**). The reductase involved in this selective activation under hypoxia is not yet fully understood. However, Hunter et al. investigated potential modifiers of TH-302 metabolism by RNA sequencing, whole-genome CRISPR knockout, and reductase-focused short hairpin RNA screens, and found that the activation of TH-302 is related to genes involved in mitochondrial electron transfer, DNA damage-response factors and mitochondrial function regulators, such as *SLX4IP*, *C10orf90 (FATS)*, *SLFN11*, *YME1L1* (Hunter et al., 2019).

TH-302 shows obvious biliary excretion and/or gut secretion (Jung et al., 2012), with a short half-life of 12.3 min, a high clearance rate of 2.29 L/h/kg, and its volume of distribution is 0.627 L/kg.

# PRECLINICAL STUDIES

## *In vitro* Cytotoxicity

In a panel of 32 human cancer lines, Meng et al. found that all cells displayed enhanced sensitivity to TH-302 under severely hypoxic conditions (~0.1% $O_2$). Consistent with enhanced cell killing, TH-302/hypoxia also induced γH2AX phosphorylation, DNA cross-linking and cell cycle arrest. Additional studies with repair deficient CHO cells found that loss of homologous repair increased drug sensitivity; non-homologous end-joining, base and nucleotide excision played no role in processing the DNA/IPM lesions (Meng et al., 2012). Also consistent with a DNA damage response, TH-302/hypoxia can down-regulate levels of the three D cyclins, as well as CDK4/6, p21 (cip-1) p27 (kip-1), and phosphorylated Rb, and up-regulate the expression of caspases-3,8 and 9, and poly ADP-ribose polymerase to induce both G0/1 cell cycle arrest and trigger apoptosis in multiple myeloma (Hu et al., 2010). TH-302 decreased proliferation and HIF-1α expression in acute myeloid leukemia (AML) and nasopharyngeal carcinoma (NPC) cells and induced cell-cycle arrest, and enhanced double-stranded DNA breaks (Portwood et al., 2013; Huang et al., 2018). TH-302 was selectively toxic to hypoxic (1% $O_2$) osteosarcoma cells while normal osteoblasts were protected (Liapis et al., 2015). The combination of TH-302 with cisplatin (DDP) had a synergistic effect on cytotoxicity in nasopharyngeal cancer cell lines (Huang et al., 2018). Under hypoxic conditions (1% $O_2$), TH-302 significantly inhibited the survival of melanoma cells in two/three-dimensional (2D/3D) culture, and the combination with sunitinib further enhanced the effect (Liu et al., 2017).

In 3D tumor spheroids and multi-cellular layer models, TH-302 was more effective in tumor spheroids compared with monolayer cells, indicating that TH-302 had a significant "bystander effect" (Meng et al., 2012; Voissiere et al., 2017). Ham et al. showed that in a 3D breast cancer cell (MDA-MB-157) model, the combination treatment with doxorubicin and TH-302 could significantly reduce drug resistance (Ham et al., 2016).

## Response of Experimental Tumors

### Monotherapy

Single agent TH-302 has shown efficacy against multiple human xenografts, including hepatoma, multiple myeloma (MM), neuroblastoma, rhabdomyosarcoma, osteolytic breast cancer, non-small cell lung cancer (NSCLC), head and neck squamous cell carcinoma (HNSCC), and acute myeloid leukemia (Hu et al., 2010; Li et al., 2010; Portwood et al., 2013; Liapis et al., 2016; Sun et al., 2016; Zhang et al., 2016a; Harms et al., 2019). Using two high-grade glioma models (C6 glioblastoma and 9 L glioma) with different levels of hypoxia, Stokes et al. showed that the more hypoxic, less perfused C6 tumor model was more sensitive to TH-302 (Stokes et al., 2016).

A study by Sun et al. further supported the "bystander effect" of TH-302 in animal models. They found that the DNA damage

induced by TH-302 initially only appeared in hypoxic regions, but subsequently spread to the entire tumor (Sun et al., 2012). However, the bystander hypothesis was questioned by Hong et al. who found that the toxic metabolites Br-IPM and IPM were unable to pass across cell membranes. They proposed that any effect on oxygenated tumor cells was due to high concentrations of pro-drug leading to some residual Br-IPM formation even in the presence of oxygen. (Hong et al., 2018; Hong et al., 2019).

Nytko et al. demonstrated that the efficacy of TH-302 is highly dependent on tumor type, largely due to levels of cytochrome P450 oxidoreductase activity (POR) (Nytko et al., 2017). Through the study of 22 cases of papillomavirus-negative head and neck squamous cell carcinoma (HPV-negative HNSCC), Jamieson et al. confirmed that for hypoxic HPV-negative HNSCC cells, TH-302 exhibited stronger potency and selectivity than the previous generation HAP (PR- 104 A or SN30000), and the responsiveness was dependent on the sensitivity to DNA cross-linking and the activation rate of the prodrug. They also revealed the correlation between TH-302 sensitivity and proliferative rate/proliferation metagene (Jamieson et al., 2018). Recent evidence suggests that TH-302 can not only kill hypoxic pancreatic cancer cells, but also has the ability to improve the oxygenation status of residual tumor cells, so it can be used to enhance the effect of radiotherapy and chemotherapy (Kishimoto et al., 2020) (**Table 1**).

## Combination of TH-302 With Conventional Chemotherapy

TH-302 has been shown to enhance the anti-tumor effect of many conventional chemotherapy drugs, such as docetaxel, cisplatin, pemetrexed, irinotecan, doxorubicin, gemcitabine, temozolomide, and topotecan (Liu et al., 2012; Saggar and Tannock, 2014; Liapis et al., 2015; Sun et al., 2015b; Zhang et al., 2016b; Liapis et al., 2016; Huang et al., 2018). Saggar and Tannock demonstrated that TH-302 could inhibit tumor reoxygenation and as well as the proliferation of hypoxic tumor cells that survived chemotherapy (Saggar and Tannock, 2015).

For the treatment of osteosarcoma, TH-302 combined with proapoptotic receptor agonists (dulanermin or drozitumab) or doxorubicin could effectively reduce the tumor burden of bone as well as pulmonary metastases and could prevent bone destruction caused by osteosarcoma (Liapis et al., 2015; Liapis et al.,2017).

As cancer-initiating cells (C-ICs) are associated with hypoxic niches, Haynes et al. investigated and proposed that conventional treatments such as fluorouracil with or without radiotherapy, would enhance tumor hypoxia and thus expand the C-IC population, which could be counteracted by TH-302 treatment (Haynes et al., 2018). The PI3K pathway is involved in cell adaptation to hypoxia, via Akt mitochondrial translocation (Chae et al., 2016). However, in pancreatic ductal adenocarcinoma (PDAC) cells, resistance to the PI3K pathway inhibitor was associated with tumor hypoxia. Conway et al. combined TH-302 and AZD2014 for the treatment of tumor-bearing mice. The results showed that single use of AZD2014 improved survival and had additional anti-invasive effects, while TH-302 as a single agent exhibited higher efficacy under hypoxic conditions. As expected, the combination of TH-302 and AZD2014 enhanced the potency of each drug, ultimately leading to an overall improvement in anti-tumor effects (Conway et al., 2018).

## Combination of TH-302 With Radiotherapy

Since hypoxic cells are known to be extremely radioresistant, there is a powerful rationale for combing radiation and TH-302. Several investigators have demonstrated increased tumor growth delay and decreased hypoxic fraction in a variety of tumor types (NSCLC, rhabdomyosarcoma, squamous cell carcinoma, colorectal adenocarcinoma, pancreatic cancer) when using this combination (Peeters et al., 2015; Hajj et al., 2017; Nytko et al., 2017; Takakusagi et al., 2018). Lohse et al. studied 11 pancreatic cancer PDX models and found that the combination of TH-302 and ionizing radiation (IR) could significantly delay tumor growth, reduce tumor volume, and reduce the frequency of tumor initiating cells (TIC), especially in the more rapidly growing/hypoxic models (Lohse et al., 2016). Spiegelberg et al. confirmed that TH-302 could increase the sensitivity of esophageal carcinoma to radiotherapy, without any additional toxicity to the gastrointestinal tract (mucosal damage) and lung (fibrosis) (Spiegelberg et al., 2019b).

## Combination of TH-302 With Tissue Oxygen Modulators or Anti-Angiogenic Therapy

Any treatment that increases tumor hypoxia might be expected to enhance the response to TH-302. For example, pretreatment with pyruvate has been shown to increase TH-302 sensitivity, through increased mitochondrial oxygen consumption and concomitant transient tumor hypoxia (Takakusagi et al., 2014; Wojtkowiak et al., 2015). Hydralazine (a vasodilator) that is known to profoundly exacerbate hypoxia in murine tumors, enhanced the efficacy of TH-302 (Bailey et al., 2014).

However, the most obvious candidates for such an approach are anti-angiogenics. In two renal cell carcinoma models, the mTOR inhibitors everolimus and temsirolimus both reduced vessel density, with resultant increase in hypoxia and TH-302 response (Sun et al., 2015a). Yoon et al. combined TH-302 with the VEGF-A inhibitor DC101, a HIF-1α inhibitor (low-dose doxorubicin) and radiotherapy for the treatment of mouse models of sarcoma. The results showed that this multi-modal therapy could effectively block sarcoma growth. The mechanism involved the increase of DNA damage and apoptosis in endothelial cells, the reduction of HIF-1α activity, and the inhibition of cancer stem cell-like cells (Yoon et al., 2015; Yoon et al., 2016). Experiments conducted by Kumar et al. using a subcutaneous xenograft model of neuroblastoma showed that the combined use of TH-302 and sunitinib (an anti-angiogenic multikinase inhibitor) resulted in greater tumor growth delay, increased apoptosis and tumor hypoxia. They also found that the combination therapy significantly reduced the burden of liver metastases (Kumar et al., 2018). With genetically engineered melanoma mouse models, Liu et al. showed that while sunitinib alone would lead to greater hypoxia without tumor suppression, TH-302 in combination with sunitinib could significantly reduce tumor volume and prolong survival (Liu et al., 2017).

**TABLE 1 |** Pre-clinical studies of TH-302.

| Ref | Tumor type (Cell lines/tumor models) | Combined therapy | | | | | |
|---|---|---|---|---|---|---|---|
| | | Radioherapy | Chemotherapy | Anti-angiogenic agents | Molecular targeted agents | Immunoherapy | Other therapy |
| Li et al. (2010) | Hepatoma (H22) | — | — | — | — | — | — |
| Hu et al. (2010) | Multiple myeloma (5T33 MM model) | — | — | — | — | — | — |
| Sun et al. (2012) | 11 xenograft models | — | — | — | — | — | — |
| Meng et al. (2012) | Chinese hamster ovary cell, H460, H116 | — | — | — | — | — | — |
| Liu et al. (2012) | 11 human xenograft models | — | Docetaxel, cisplatin, pemetrexed, irinotecan, doxorubicin, gemcitabine, temozolomide | — | — | — | — |
| Portwood et al. (2013) | Acute myeloid leukemia (HEL, HL60) | — | — | — | — | — | — |
| Saggar and Tannock (2014) | Breast cancer (MCF-7)/ prostate caner (PC-3) | — | Docetaxel Doxorubicin | — | — | — | — |
| Takakusagi et al. (2014) | Squamous cell carcinoma (SCCVII)/ Adenocarcinoma (HT29) | — | Pyruvate | — | — | — | — |
| Bailey et al. (2014) | PDAC (MiaPaCa-2, SU.86.86) | — | Hydralazine | — | — | — | — |
| Wojtkowiak et al. (2015) | PDAC (Hs766t, MiaPaCa-2, SU.86.86) | — | Pyruvate | — | — | — | — |
| Liapis et al. (2015) | Osteosarcoma | — | Docetaxel | — | — | — | — |
| Saggar and Tannock (2015) | Breast cancer (MCF-7)/ prostate caner (PC-3) | | docetaxel, doxorubicin | — | — | — | — |
| Sun et al. (2015a) | Renal cell carcinoma (786-O, Caki-1) | — | Everolimus/Temsirolimus (mTOR inhibitor) | — | — | — | — |
| Yoon et al. (2015) | Sarcoma | RT | — | DC101(VEGF-A inhibitor) | | | |
| Peeters et al. (2015) | NSCLC and rhabdomyosarcoma | RT | — | — | — | — | — |
| Sun et al. (2015b) | PDAC (Hs766t, MIA PaCa-2, PANC-1, and BxPC-3) | — | gemcitabine,nab-paclitaxel | — | — | — | — |
| Liapis et al. (2016) | Osteolytic breast cancer (MDA- B- 31- XSA) | — | Paclitaxel | — | — | — | — |
| Sun et al. (2016) | NSCLC (H460) | — | Docetaxel | Sunitinib | — | — | — |
| Benito et al. (2016) | Leukemia (KBM-5, KG-1, OCI-AML3, MOLM-13, REH, Nalm-6) | — | — | — | Sorafenib | — | — |
| Lohse et al. (2016) | Pancreatic cancer (PDX model) | IR | — | — | — | — | — |
| Zhang et al. (2016a) | Neuroblastoma/ rhabdomyosarcoma | — | Topotecan | — | — | — | — |
| Yoon et al. (2016) | Undifferentiated pleomorphic sarcoma (KP mice model) | — | Low dose doxorubicin (HIF-1α inhibitor) | DC101(VEGF-A inhibitor) | — | — | — |
| Lindsay et al. (2016) | EGFR-mutant NSCLC | — | — | — | Erlotinib | — | — |
| Stokes et al. (2016) | Glioma (C6 glioblastoma/ 9 L gliosarcoma) | — | — | — | — | — | — |
| Ham et al. (2016) | Breast cancer (MDA-mb-157) | — | Doxorubicin | — | — | — | — |
| Duran et al. (2017) | Hepatocellular carcinoma (VX2) | — | — | — | — | — | cTACE (doxorubicin) |

(Continued on following page)

**TABLE 1 |** (*Continued*) Pre-clinical studies of TH-302.

| Ref | Tumor type (Cell lines/tumor models) | Combined therapy | | | | | |
|---|---|---|---|---|---|---|---|
| | | Radioherapy | Chemotherapy | Anti-angiogenic agents | Molecular targeted agents | Immunoherapy | Other therapy |
| Nytko et al. (2017) | Lung adenocarcinoma (A549)/HNSCC (UT-scc-14) | Fractionated IR | — | — | — | — | — |
| Voissiere et al. (2017) | Chondrosarcoma (HEMC-SS) | — | — | — | — | — | — |
| Liapis et al. (2017) | Osteosarcoma (BTK-143, K-OS) | — | Dulanermin/drozitumab | — | — | — | — |
| Hajj et al. (2017) | Pancreatic cancer (AsPC1) | RT | — | — | — | — | — |
| Liu et al. (2017) | Melanoma (WM35, WM793, 1205LU) | — | — | Sunitinib | — | — | — |
| Takakusagi et al. (2018) | Squamous cell carcinoma (SCCVII)/ Adenocarcinoma (HT29) | IR | — | — | — | — | — |
| Huang et al. (2018) | NPC (CNE-2, HONE-1, HNE-1) | — | Cisplatin (DDP) | — | — | — | — |
| Haynes et al. (2018) | Colorectal cancer (PDX model) | RT | 5-Fu | — | — | — | — |
| Conway et al. (2018) | PDAC (KPC primary PDAC cells) | — | AZD2014 | — | — | — | — |
| Jamieson et al. (2018) | HNSCC (SCC-4, SCC-7, SCC-9, FaDu, UT-SCC and PDX model) | — | — | — | — | CTLA-4 blockade | — |
| Kumar et al. (2018) | Neuroblastoma (SK-N-BE (2)) | — | — | Sunitinib | — | — | — |
| Hong et al. (2018) | Colon carcinoma (HCT116) | — | — | — | — | — | — |
| Jayaprakash et al. (2018) | Prostate cancer (TRAMP-C2) | — | — | — | — | αCTLA-4/αpd-1 | — |
| Hong et al. (2019) | NSCLC (H460) | — | — | — | — | — | — |
| Harms et al. (2019) | HNSCC (PDX model) | — | — | — | — | — | — |
| Spiegelberg et al. (2019) | Esophageal carcinomas (OE19/OE21) | RT | — | — | — | — | — |

### Combination of TH-302 With Molecular Targeted Therapy

Benito et al. found that the combination of TH-302 and sorafenib resulted in greater anti-leukemia efficacy than either alone (Benito et al., 2016). Lindsay et al. established a stochastic mathematical model, parameterized experimental and clinical data, and concluded that the combination therapy of TH-302 and erlotinib was better than single-agent therapy of either in EGFR-mutant NSCLC, which was mainly reflected in delayed drug resistance (Lindsay et al., 2016).

### Combination of TH-302 With Immunotherapy

A new and promising way to exploit TH-302 may be in combination with immunotherapy. Jayaprakash et al. demonstrated that the hypoxic regions in the prostate cancer models lacked T cell infiltration, potentially creating zones of immunotherapy resistance. To overcome this, they combined TH-302 with a maximal checkpoint blockade directed against both CTLA-4 and PD-1, dramatically enhancing the effect of the immunotherapy treatment (Jayaprakash et al., 2018). Likewise, Jamieson et al. also found that the combined therapy of TH-302 and CTLA-4 blockade can further improve the survival rate of the HNSCC model compared with single use either alone (Jamieson et al., 2018).

### Combination of Th-302 With Other Therapies

For the treatment of hepatocellular carcinoma, Duran et al. used hepatic hypoxia activated intra-arterial therapy (HAIAT) and found that the addition of TH-302 to conventional Trans Arterial ChemoEmbolization (cTACE) achieved promising anti-cancer effects, which mainly manifested as reduced tumor burden, decreased tumor growth rate and increased necrotic fraction (Duran et al., 2017).

## CLINICAL TRIALS

TH-302 entered clinical trials in 2007 and results were first reported in 2011 (**Table 2**). Weiss et al. enrolled 57 patients

**TABLE 2 |** Clinical trials of TH-302.

| Ref | Tumor type | Clinical trial | Number of patients | Combined therapy |
|---|---|---|---|---|
| Weiss et al. (2011a) | Solid tumors | Phase 1 | 57 | — |
| Ganjoo et al. (2011) | Soft tissue sarcoma | Phase 1 | 16 | Doxorubicin (chemotherapy) |
| Weiss et al. (2011b) | Melanoma | Phase 1 | 1 | — |
| Chawla et al. (2014) | Soft tissue sarcoma | Phase 2 | 91 | Doxorubicin (chemotherapy) |
| Borad et al. (2015) | Pancreatic cancer | Phase 2 | 214 | Gemcitabine (chemotherapy) |
| Van Cutsem et al. (2016) | Pancreatic cancer | Phase 3 | 660 | Gemcitabine (chemotherapy) |
| Badar et al. (2016) | Leukemia | Phase 1 | 49 | — |
| Riedel et al. (2017) | Advanced solid tumors | Phase 1 | 30 | Pazopanib (anti-angiogenic agents) |
| Conroy et al. (2017) | Ovarian serous carcinoma | Case report | 2 | — |
| Tap et al. (2017) | Soft-tissue sarcoma | Phase 3 | 640 | Doxorubicin (chemotherapy) |
| Brenner et al. (2018) | Glioblastoma | Phase 1 | 28 | Bevacizumab (anti-angiogenic agents) |
| Jamieson et al. (2018) | HNSCC | Phase 2 | 5 | — |
| Laubach et al. (2019) | Multiple myeloma | Phase 1/2 | 59 | Bortezomib (chemotherapy) |

with advanced solid tumors who were treated with TH-302 monotherapy (dose and scheme: TH-302 was administered i. v. over 30–60 min. Arm A: 7.5–670 mg/m$^2$, 3 times weekly dosing followed by 1 week off; Arm B: 670–940 mg/m$^2$, every 3 weeks dosing). They reported skin and/or mucosal toxicity with a maximum tolerated dose (MTD) of 670 mg/m$^2$. They observed two partial responses and 27 cases of stable disease. Additionally, TH-302 helped to resolve Cullen's sign in patients with metastatic melanoma (Weiss et al., 2011a, Weiss et al., 2011b). Riedel et al. conducted a phase one clinical trial on 30 patients with advanced solid tumors. Their results revealed the potential therapeutic value of co-targeting tumor angiogenesis and hypoxia (dose and scheme: pazopanib, orally dosed at 800 mg daily on days 1–28; TH-302, administered i. v. on days 1, 8, and 15 of a 28 days cycle at doses of 340 or 480 mg/m$^2$) (Riedel et al., 2017). Conroy et al. reported the efficacy of TH-302 as a monotherapy on two patients with advanced ovarian serous carcinoma with BRCA1 mutations. Both individuals responded well (dosed at either 300 mg/m$^2$ (9 cycles, 15 months) or 340 mg/m$^2$ (6 cycles, 3 months)) showing partial response or stable disease (Conroy et al., 2017). A phase one surgical study of TH-302 (dose range 240–670 mg/m$^2$, every 2 weeks) combined with bevacizumab (dose: 10 mg/kg) in the treatment of bevacizumab-refractory glioblastoma found that the therapy was well-tolerated at 670 mg/m$^2$, with an overall response rate of 17.4% and a disease control rate of 60.9% (Brenner et al., 2018). The phase 1/2 study of TH-302 (NCT01522872) conducted by Laubach et al. showed that for relapsed/refractory myeloma, TH-302 alone or in combination with bortezomib was well tolerated and could prolong survival (dose and scheme: Arm A: 340 mg/m$^2$ dose of TH-302 was administered i. v. over 30–60 min with a fixed oral 40 mg dose of dexamethasone on days 1, 4, 8 and 11 of a 21 days cycle; Arm B: 340 mg/m$^2$ dose of TH-302 was administered i. v. over 30–60 min with a fixed oral 40 mg dose of dexamethasone and a fixed i. v. or s. c. administration of 1.3 mg/m$^2$ dose of bortezomib on days 1, 4, 8, and 11 of a 21 days cycle) (Laubach et al., 2019). The anti-tumor effect of TH-302 (300 mg/m$^2$ administered i. v. on days 1 and 8 of each 21 days cycle, 6 cycles) combined with doxorubicin (75 mg/m$^2$ administered i. v. on day 1 of each 21 days cycle, 6 cycles) in the treatment of advanced soft tissue sarcoma (STS) has also been tested in phase two clinical trials, and complete and partial responses have been observed (Chawla et al., 2014). Borad et al. evaluated the therapeutic effect of TH-302 combined with gemcitabine on pancreatic cancer. Prolonged progression-free survival (PFS) and CA19–9 response were observed (dose and scheme: 240 or 340 mg/m$^2$ TH-302 administered i. v. over 30–60 min followed 2 h later by a 30 min i. v. infusion of gemcitabine 1,000 mg/m$^2$ on days 1, 8, and 15 of each 28 days cycle). Skin and mucosal toxicity and bone marrow suppression are the most common toxicities (Borad et al., 2015). Another phase two study enrolled five HNSCC patients receiving TH-302 monotherapy (480 mg/m$^2$ qw × 3 each month). Two of them achieved partial response, and the other three had stable disease (Jamieson et al., 2018).

TH-302 was successfully applied in the clinic but the outcomes were not sufficient to receive approval from requlatory authorities. Badar et al. revealed that TH-302 exhibited limited activity in leukemia patients (doses ranging between 120 and 550 mg/m$^2$) (Badar et al., 2016). In the phase three multicenter clinical trial (TH CR-406/SARC021), 640 patients with soft tissue sarcoma were enrolled. The results showed that the combination of TH-302 (300 mg/m$^2$ administered i. v. for 30–60 min on days 1 and 8 of every 21 days cycle, 6 cycles) and doxorubicin (75 mg/m$^2$ administered on day 1 of every 21 days cycle, six cycles) failed to improve overall survival compared with doxorubicin alone (Tap et al., 2017). But it should be noted that the historical survival benefit of doxorubicin monotherapy shows a trend for improvement over time, perhaps due to superior clinical management of associated toxicities. The initial phase two combination study (Dox + TH-302) was a single arm study that utilized historical doxorubicin single agent survival results (12–13 months) as reference. Ultimately this proved to be an invalid comparison. In addition, antagonistic effects between drugs (Anderson et al., 2017) and changes in drug formulations (Higgins et al., 2018) should also be considered as potential causes. TH-302 plus gemcitabine in the treatment of patients with pancreatic ductal adenocarcinoma (PDAC) also missed the end point of another phase three clinical trial (dose and scheme: TH-302 340 mg/m$^2$ and gemcitabine 1,000 mg/m$^2$ administered i. v. on days 1, 8, and 15 of a 28 days cycle)

(NCT01746979) (Van Cutsem et al., 2016). In this case, lack of patient screening based on tumor hypoxia may have been the most important cause of the trial's failure (Domenyuk et al., 2018; Spiegelberg et al., 2019a). In contrast to the prevalent belief that all PDAC are severely hypoxic, evidence showed that the levels of hypoxia observed in PDAC were highly heterogeneous (range from 0 to 26%) and were similar to those reported in other tumor types (Dhani et al., 2015). Patients with a low tumor hypoxic fraction are not expected to benefit from TH-302 treatment, and a more efficient approach to the clinical application of TH-302 may be to determine the tumor hypoxic status of tumor prior to patient selection.

## DISCUSSION AND DIRECTIONS FOR FUTURE APPLICATIONS

Hypoxia is an important feature of solid tumors and may also be an effective new target for tumor therapy. We are trying to put forward new suggestions on the clinical application of TH-302 or other HAPs. Hypoxia is not only a characteristic of macroscopic tumors. In 2007, our group reported that peritoneal disseminated micro-metastases (less than 1 mm in diameter) are severely hypoxic and poorly proliferative (Li et al., 2007; Li and O'Donoghue, 2008; Li et al., 2010b; Li et al., 2010a; Huang et al., 2013). Further, our data indicated that tumor cells in these hypoxic micro-metastases could survive for several weeks (data to be published). In view of this special state of early micro-metastases of tumors, TH-302 may have the potential to prevent them from developing into macroscopic tumors, thereby reducing the recurrence and metastasis rate of tumors. In this area, TH-302 may be superior to traditional radiotherapy and chemotherapy. Our group is conducting further research.

## AUTHOR CONTRIBUTIONS

YL performed the literature search and wrote the manuscript; LZ performed the literature search and figure editing; X-FL contributed to write and revise the manuscript; all authors had approved the final manuscript to be submitted.

## ACKNOWLEDGMENTS

We thank Dr. James Russell from Memorial Sloan-Kettering Cancer Center (New York, NY) for critically reading and editing the manuscript. The authors' research is supported in part by a grant from Shenzhen People's Hospital for "Climbing" Program (XFL), and a Shenzhen Science and Technology Project grant (JCYJ20190806151003583) (XFL).

## REFERENCES

Anderson, R. F., Li, D., and Hunter, F. W. (2017). Antagonism in effectiveness of evofosfamide and doxorubicin through intermolecular electron transfer. *Free Radic. Biol. Med.* 113, 564–570. doi:10.1016/j.freeradbiomed.2017.10.385

Badar, T., Handisides, D. R., Benito, J. M., Richie, M. A., Borthakur, G., Jabbour, E., et al. (2016). Phase I study of evofosfamide, an investigational hypoxia-activated prodrug, in patients with advanced leukemia. *Am. J. Hematol.* 91 (8), 800–805. doi:10.1002/ajh.24415

Bailey, K. M., Cornnell, H. H., Ibrahim-Hashim, A., Wojtkowiak, J. W., Hart, C. P., Zhang, X., et al. (2014). Evaluation of the "steal" phenomenon on the efficacy of hypoxia activated prodrug TH-302 in pancreatic cancer. *PLoS One.* 9 (12), e113586. doi:10.1371/journal.pone.0113586

Benito, J., Ramirez, M. S., Millward, N. Z., Velez, J., Harutyunyan, K. G., Lu, H., et al. (2016). Hypoxia-activated prodrug TH-302 targets hypoxic bone marrow niches in preclinical leukemia models. *Clin. Cancer Res.* 22 (7), 1687–1698. doi:10.1158/1078-0432.CCR-14-3378

Borad, M. J., Reddy, S. G., Bahary, N., Uronis, H. E., Sigal, D., Cohn, A. L., et al. (2015). Randomized phase II trial of gemcitabine plus TH-302 versus gemcitabine in patients with advanced pancreatic cancer. *J. Clin. Oncol.* 33 (13), 1475–1481. doi:10.1200/JCO.2014.55.7504

Brenner, A., Zuniga, R., Sun, J. D., Floyd, J., Hart, C. P., Kroll, S., et al. (2018). Hypoxia-activated evofosfamide for treatment of recurrent bevacizumab-refractory glioblastoma: a phase I surgical study. *Neuro Oncol.* 20 (9), 1231–1239. doi:10.1093/neuonc/noy015

Chae, Y. C., Vaira, V., Caino, M. C., Tang, H.-Y., Seo, J. H., Kossenkov, A. V., et al. (2016). Mitochondrial Akt regulation of hypoxic tumor reprogramming. *Cancer Cell.* 30 (2), 257–272. doi:10.1016/j.ccell.2016.07.004

Chawla, S. P., Cranmer, L. D., Van Tine, B. A., Reed, D. R., Okuno, S. H., Butrynski, J. E., et al. (2014). Phase II study of the safety and antitumor activity of the hypoxia-activated prodrug TH-302 in combination with doxorubicin in patients with advanced soft tissue sarcoma. *J. Clin. Oncol.* 32 (29), 3299–3306. doi:10.1200/JCO.2013.54.3660

Conroy, M., Borad, M. J., and Bryce, A. H. (2017). Hypoxia-activated alkylating agents in BRCA1-mutant ovarian serous carcinoma. *Cureus.* 9 (7), e1517. doi:10.7759/cureus.1517

Conway, J. R. W., Warren, S. C., Herrmann, D., Murphy, K. J., Cazet, A. S., Vennin, C., et al. (2018). Intravital imaging to monitor therapeutic response in moving hypoxic regions resistant to PI3K pathway targeting in pancreatic cancer. *Cell Rep.* 23 (11), 3312–3326. doi:10.1016/j.celrep.2018.05.038

Dhani, N. C., Serra, S., Pintilie, M., Schwock, J., Xu, J., Gallinger, S., et al. (2015). Analysis of the intra- and intertumoral heterogeneity of hypoxia in pancreatic cancer patients receiving the nitroimidazole tracer pimonidazole. *Br. J. Cancer* 113 (6), 864–871. doi:10.1038/bjc.2015.284

Domenyuk, V., Liu, X., Magee, D., Gatalica, Z., Stark, A., Kennedy, P., et al. (2018). Poly-ligand profiling differentiates pancreatic cancer patients according to treatment benefit from gemcitabine + placebo versus gemcitabine + evofosfamide and identifies candidate targets. *Ann. Oncol.* 29 (Suppl. l_5). v36. doi:10.1093/annonc/mdy151.131

Duan, J.-X., Jiao, H., Kaizerman, J., Stanton, T., Evans, J. W., Lan, L., et al. (2008). Potent and highly selective hypoxia-activated achiral phosphoramidate mustards as anticancer drugs. *J. Med. Chem.* 51 (8), 2412–2420. doi:10.1021/jm701028q

Duran, R., Mirpour, S., Pekurovsky, V., Ganapathy-Kanniappan, S., Brayton, C. F., Cornish, T. C., et al. (2017). Preclinical benefit of hypoxia-activated intra-arterial therapy with evofosfamide in liver cancer. *Clin. Cancer Res.* 23 (2), 536–548. doi:10.1158/1078-0432.CCR-16-0725

Fracasso, P. M., and Sartorelli, A. C. (1986). Cytotoxicity and DNA lesions produced by mitomycin C and porfiromycin in hypoxic and aerobic EMT6 and Chinese hamster ovary cells. *Cancer Res.* 46 (8), 3939–3944. doi:10.1016/0304-3835(86)90123-0

Ganjoo, K. N., Cranmer, L. D., Butrynski, J. E., Rushing, D., Adkins, D., Okuno, S. H., et al. (2011). A phase I study of the safety and pharmacokinetics of the hypoxia-activated prodrug TH-302 in combination with doxorubicin in patients with advanced soft tissue sarcoma. *Oncology* 80 (1-2), 50–56. doi:10.1159/000327739

Hajj, C., Russell, J., Hart, C. P., Goodman, K. A., Lowery, M. A., Haimovitz-Friedman, A., et al. (2017). A combination of radiation and the hypoxia-

activated prodrug evofosfamide (TH-302) is efficacious against a human orthotopic pancreatic tumor model. *Translational Oncol.* 10 (5), 760–765. doi:10.1016/j.tranon.2017.06.010

Ham, S. L., Joshi, R., Luker, G. D., and Tavana, H. (2016). Engineered breast cancer cell spheroids reproduce biologic properties of solid tumors. *Adv. Healthc. Mater.* 5 (21), 2788–2798. doi:10.1002/adhm.201600644

Harms, J. K., Lee, T.-W., Wang, T., Lai, A., Kee, D., Chaplin, J. M., et al. (2019). Impact of tumour hypoxia on evofosfamide sensitivity in head and neck squamous cell carcinoma patient-derived xenograft models. *Cells* 8 (7), 717. doi:10.3390/cells8070717

Haynes, J., McKee, T. D., Haller, A., Wang, Y., Leung, C., Gendoo, D. M. A., et al. (2018). Administration of hypoxia-activated prodrug evofosfamide after conventional adjuvant therapy enhances therapeutic outcome and targets cancer-initiating cells in preclinical models of colorectal cancer. *Clin. Cancer Res.* 24 (9), 2116–2127. doi:10.1158/1078-0432.CCR-17-1715

Higgins, J. P., Sarapa, N., Kim, J., and Poma, E. (2018). Unexpected pharmacokinetics of evofosfamide observed in phase III MAESTRO study. *J. Clin. Oncol.* 36 (15_Suppl. l), 2568. doi:10.1200/jco.2018.36.15_suppl.2568

Hong, C. R., Dickson, B. D., Jaiswal, J. K., Pruijn, F. B., Hunter, F. W., Hay, M. P., et al. (2018). Cellular pharmacology of evofosfamide (TH-302): a critical re-evaluation of its bystander effects. *Biochem. Pharmacol.* 156, 265–280. doi:10.1016/j.bcp.2018.08.027

Hong, C. R., Wilson, W. R., and Hicks, K. O. (2019). An intratumor pharmacokinetic/pharmacodynamic model for the hypoxia-activated prodrug evofosfamide (TH-302): monotherapy activity is not dependent on a bystander effect. *Neoplasia* 21 (2), 159–171. doi:10.1016/j.neo.2018.11.009

Hu, J., Handisides, D. R., Van Valckenborgh, E., De Raeve, H., Menu, E., Vande Broek, I., et al. (2010). Targeting the multiple myeloma hypoxic niche with TH-302, a hypoxia-activated prodrug. *Blood* 116 (9), 1524–1527. doi:10.1182/blood-2010-02-269126

Huang, T., Civelek, A. C., Zheng, H., Ng, C. K., Duan, X., Li, J., et al. (2013). (18)F-misonidazole PET imaging of hypoxia in micrometastases and macroscopic xenografts of human non-small cell lung cancer: a correlation with autoradiography and histological findingsF-misonidazole PET imaging of hypoxia in micrometastases and macroscopic xenografts of human non-small cell lung cancer: a correlation with autoradiography and histological findings. *Am. J. Nucl. Med. Mol. Imaging* 3 (2), 142–153.

Huang, Y., Tian, Y., Zhao, Y., Xue, C., Zhan, J., Liu, L., et al. (2018). Efficacy of the hypoxia-activated prodrug evofosfamide (TH-302) in nasopharyngeal carcinoma *in vitro* and *in vivo*. *Cancer Commun.* 38 (1), 1–9. doi:10.1186/s40880-018-0285-0

Hunter, F. W., Devaux, J. B. L., Meng, F., Hong, C. R., Khan, A., Tsai, P., et al. (2019). Functional CRISPR and shRNA screens identify involvement of mitochondrial electron transport in the activation of evofosfamide. *Mol. Pharmacol.* 95 (6), 638–651. doi:10.1124/mol.118.115196

Jamieson, S. M. F., Tsai, P., Kondratyev, M. K., Budhani, P., Liu, A., Senzer, N. N., et al. (2018). Evofosfamide for the treatment of human papillomavirus-negative head and neck squamous cell carcinoma. *JCI Insight* 3 (16). e122204. doi:10.1172/jci.insight.122204

Jayaprakash, P., Ai, M., Liu, A., Budhani, P., Bartkowiak, T., Sheng, J., et al. (2018). Targeted hypoxia reduction restores T cell infiltration and sensitizes prostate cancer to immunotherapy. *J. Clin. Invest.* 128 (11), 5137–5149. doi:10.1172/JCI96268

Jung, D., Jiao, H., Duan, J.-X., Matteucci, M., and Wang, R. (2012). Metabolism, pharmacokinetics and excretion of a novel hypoxia activated cytotoxic prodrug, TH-302, in rats. *Xenobiotica* 42 (4), 372–388. doi:10.3109/00498254.2011.622810

Kishimoto, S., Brender, J. R., Chandramouli, G. V. R., Saida, Y., Yamamoto, K., Mitchell, J. B., et al. (2020). Hypoxia-activated prodrug evofosfamide treatment in pancreatic ductal adenocarcinoma xenografts alters the tumor redox status to potentiate radiotherapy. *Antioxid. Redox Signaling* 15. doi:10.1089/ars.2020.8131

Kumar, S., Sun, J. D., Zhang, L., Mokhtari, R. B., Wu, B., Meng, F., et al. (2018). Hypoxia-targeting drug evofosfamide (TH-302) enhances sunitinib activity in neuroblastoma xenograft models. *Transl Oncol.* 11 (4), 911–919. doi:10.1016/j.tranon.2018.05.004

Laderoute, K. R., and Rauth, A. M. (1986). Identification of two major reduction products of the hypoxic cell toxin 3-amino-1,2,4-benzotriazine-1,4-dioxide. *Biochem. Pharmacol.* 35 (19), 3417–3420. doi:10.1016/0006-2952(86)90448-x

Laubach, J. P., Liu, C.-J., Raje, N. S., Yee, A. J., Armand, P., Schlossman, R. L., et al. (2019). A phase I/II study of evofosfamide, A hypoxia-activated prodrug with or without bortezomib in subjects with relapsed/refractory multiple myeloma. *Clin. Cancer Res.* 25 (2), 478–486. doi:10.1158/1078-0432.ccr-18-1325

Li, S., Zhang, J., Li, J., Chen, D., Matteucci, M., Curd, J., et al. (2010). Inhibition of both thioredoxin reductase and glutathione reductase may contribute to the anticancer mechanism of TH-302. *Biol. Trace Elem. Res.* 136 (3), 294–301. doi:10.1007/s12011-009-8544-1

Li, X.-F., Carlin, S., Urano, M., Russell, J., Ling, C. C., and O'Donoghue, J. A. (2007). Visualization of hypoxia in microscopic tumors by immunofluorescent microscopy. *Cancer Res.* 67(16), 7646–7653. doi:10.1158/0008-5472.CAN-06-4353

Li, X.-F., and O'Donoghue, J. A. (2008). Hypoxia in microscopic tumors. *Cancer Lett.* 264 (2), 172–180. doi:10.1016/j.canlet.2008.02.037

Li, X.-F., Sun, X., Ma, Y., Suehiro, M., Zhang, M., Russell, J., et al. (2010b). Detection of hypoxia in microscopic tumors using 131I-labeled iodo-azomycin galactopyranoside (131I-IAZGP) digital autoradiography. *Eur. J. Nucl. Med. Mol. Imaging* 37 (2), 339–348. doi:10.1007/s00259-009-1310-y

Li, X. F., Ma, Y., Sun, X., Humm, J. L., Ling, C. C., and O'Donoghue, J. A. (2010a). High 18F-FDG uptake in microscopic peritoneal tumors requires physiologic hypoxia. *J. Nucl. Med.* 51 (4), 632–638. doi:10.2967/jnumed.109.071233

Liapis, V., Labrinidis, A., Zinonos, I., Hay, S., Ponomarev, V., Panagopoulos, V., et al. (2015). Hypoxia-activated pro-drug TH-302 exhibits potent tumor suppressive activity and cooperates with chemotherapy against osteosarcoma. *Cancer Lett.* 357 (1), 160–169. doi:10.1016/j.canlet.2014.11.020

Liapis, V., Zinonos, I., Labrinidis, A., Hay, S., Ponomarev, V., Panagopoulos, V., et al. (2016). Anticancer efficacy of the hypoxia-activated prodrug evofosfamide (TH-302) in osteolytic breast cancer murine models. *Cancer Med.* 5 (3), 534–545. doi:10.1002/cam4.599

Liapis, V., Zysk, A., DeNichilo, M., Zinonos, I., Hay, S., Panagopoulos, V., et al. (2017). Anticancer efficacy of the hypoxia-activated prodrug evofosfamide is enhanced in combination with proapoptotic receptor agonists against osteosarcoma. *Cancer Med.* 6 (9), 2164–2176. doi:10.1002/cam4.1115

Lin, A. J., Cosby, L. A., Shansky, C. W., and Sartorelli, A. C. (1972). Potential bioreductive alkylating agents. 1. Benzoquinone derivatives. *J. Med. Chem.* 15 (12), 1247–1252. doi:10.1021/jm00282a011

Lindsay, D., Garvey, C. M., Mumenthaler, S. M., and Foo, J. (2016). Leveraging hypoxia-activated prodrugs to prevent drug resistance in solid tumors. *PLoS Comput. Biol.* 12 (8), e1005077. doi:10.1371/journal.pcbi.1005077

Liu, Q., Sun, J. D., Wang, J., Ahluwalia, D., Baker, A. F., Cranmer, L. D., et al. (2012). TH-302, a hypoxia-activated prodrug with broad *in Vivo* preclinical combination therapy efficacy: optimization of dosing regimens and schedules. *Cancer Chemother. Pharmacol.* 69 (6), 1487–1498. doi:10.1007/s00280-012-1852-8

Liu, S., Tetzlaff, M. T., Wang, T., Chen, X., Yang, R., Kumar, S. M., et al. (2017). Hypoxia-activated prodrug enhances therapeutic effect of sunitinib in melanoma. *Oncotarget* 8 (70), 115140–115152. doi:10.18632/oncotarget.22944

Lohse, I., Rasowski, J., Cao, P., Pintilie, M., Do, T., Tsao, M.-S., et al. (2016). Targeting hypoxic microenvironment of pancreatic xenografts with the hypoxia-activated prodrug TH-302. *Oncotarget* 7 (23), 33571–33580. doi:10.18632/oncotarget.9654

Meng, F., Evans, J. W., Bhupathi, D., Banica, M., Lan, L., Lorente, G., et al. (2012). Molecular and cellular pharmacology of the hypoxia-activated prodrug TH-302. *Mol. Cancer Ther.* 11 (3), 740–751. doi:10.1158/1535-7163.MCT-11-0634

Nytko, K. J., Grgic, I., Bender, S., Ott, J., Guckenberger, M., Riesterer, O., et al. (2017). The hypoxia-activated prodrug evofosfamide in combination with multiple regimens of radiotherapy. *Oncotarget* 8 (14), 23702–23712. doi:10.18632/oncotarget.15784

Peeters, S. G. J. A., Zegers, C. M. L., Biemans, R., Lieuwes, N. G., van Stiphout, R. G. P. M., Yaromina, A., et al. (2015). TH-302 in combination with radiotherapy enhances the therapeutic outcome and is associated with pretreatment [18F] HX4 hypoxia PET imaging. *Clin. Cancer Res.* 21 (13), 2984–2992. doi:10.1158/1078-0432.CCR-15-0018

Portwood, S., Lal, D., Hsu, Y.-C., Vargas, R., Johnson, M. K., Wetzler, M., et al. (2013). Activity of the hypoxia-activated prodrug, TH-302, in preclinical human acute myeloid leukemia models. *Clin. Cancer Res.* 19 (23), 6506–6519. doi:10.1158/1078-0432.CCR-13-0674

Pritsos, C. A., and Sartorelli, A. C. (1986). Generation of reactive oxygen radicals through bioactivation of mitomycin antibiotics. *Cancer Res.* 46 (7), 3528–3532.

Riedel, R. F., Meadows, K. L., Lee, P. H., Morse, M. A., Uronis, H. E., Blobe, G. C., et al. (2017). Phase I study of pazopanib plus TH-302 in advanced solid tumors. *Cancer Chemother. Pharmacol.* 79 (3), 611–619. doi:10.1007/s00280-017-3256-2

Rockwell, S., Kennedy, K. A., and Sartorelli, A. C. (1982). Mitomycin-C as a prototype bioreductive alkylating agent: *in vitro* studies of metabolism and cytotoxicity. *Int. J. Radiat. Oncol. Biol. Phys.* 8 (3-4), 753–755. doi:10.1016/0360-3016(82)90728-3

Saggar, J. K., and Tannock, I. F. (2014). Activity of the hypoxia-activated pro-drug TH-302 in hypoxic and perivascular regions of solid tumors and its potential to enhance therapeutic effects of chemotherapy. *Int. J. Cancer* 134 (11), 2726–2734. doi:10.1002/ijc.28595

Saggar, J. K., and Tannock, I. F. (2015). Chemotherapy rescues hypoxic tumor cells and induces their reoxygenation and repopulation-an effect that is inhibited by the hypoxia-activated prodrug TH-302. *Clin. Cancer Res.* 21 (9), 2107–2114. doi:10.1158/1078-0432.CCR-14-2298

Spiegelberg, L., Houben, R., Niemans, R., de Ruysscher, D., Yaromina, A., Theys, J., et al. (2019a). Hypoxia-activated prodrugs and (lack of) clinical progress: the need for hypoxia-based biomarker patient selection in phase III clinical trials. *Clin. Transl. Radiat. Oncol.* 15 (15), 62–69. doi:10.1016/j.ctro.2019.01.005

Spiegelberg, L., van Hoof, S. J., Biemans, R., Lieuwes, N. G., Marcus, D., Niemans, R., et al. (2019b). Evofosfamide sensitizes esophageal carcinomas to radiation without increasing normal tissue toxicity. *Radiother. Oncol.* 141, 247–255. doi:10.1016/j.radonc.2019.06.034

Stokes, A., Hart, C., and Quarles, C. C. (2016). Hypoxia imaging with PET correlates with antitumor activity of the hypoxia-activated prodrug evofosfamide (TH-302) in rodent glioma models. *Tomography* 2 (3), 229–237. doi:10.18383/j.tom.2016.00259

Sun, J. D., Ahluwalia, D., Liu, Q., Li, W., Wang, Y., Meng, F., et al. (2015a). Combination treatment with hypoxia-activated prodrug evofosfamide (TH-302) and mTOR inhibitors results in enhanced antitumor efficacy in preclinical renal cell carcinoma models. *Am. J. Cancer Res.* 5 (7), 2139–2155.

Sun, J. D., Liu, Q., Ahluwalia, D., Ferraro, D. J., Wang, Y., Jung, D., et al. (2016). Comparison of hypoxia-activated prodrug evofosfamide (TH-302) and ifosfamide in preclinical non-small cell lung cancer models. *Cancer Biol. Ther.* 17 (4), 371–380. doi:10.1080/15384047.2016.1139268

Sun, J. D., Liu, Q., Ahluwalia, D., Li, W., Meng, F., Wang, Y., et al. (2015b). Efficacy and safety of the hypoxia-activated prodrug TH-302 in combination with gemcitabine and nab-paclitaxel in human tumor xenograft models of pancreatic cancer. *Cancer Biol. Ther.* 16 (3), 438–449. doi:10.1080/15384047.2014.1003005

Sun, J. D., Liu, Q., Wang, J., Ahluwalia, D., Ferraro, D., Wang, Y., et al. (2012). Selective tumor hypoxia targeting by hypoxia-activated prodrug TH-302 inhibits tumor growth in preclinical models of cancer. *Clin. Cancer Res.* 18 (3), 758–770. doi:10.1158/1078-0432.CCR-11-1980

Takakusagi, Y., Kishimoto, S., Naz, S., Matsumoto, S., Saito, K., Hart, C. P., et al. (2018). Radiotherapy synergizes with the hypoxia-activated prodrug evofosfamide: in vitro and in vivo studies. *Antioxid. Redox Signaling* 28 (2), 131–140. doi:10.1089/ars.2017.7106

Takakusagi, Y., Matsumoto, S., Saito, K., Matsuo, M., Kishimoto, S., Wojtkowiak, J. W., et al. (2014). Pyruvate induces transient tumor hypoxia by enhancing mitochondrial oxygen consumption and potentiates the anti-tumor effect of a hypoxia-activated prodrug TH-302. *PLoS One* 9 (9), e107995. doi:10.1371/journal.pone.0107995

Tap, W. D., Papai, Z., Van Tine, B. A., Attia, S., Ganjoo, K. N., Jones, R. L., et al. (2017). Doxorubicin plus evofosfamide versus doxorubicin alone in locally advanced, unresectable or metastatic soft-tissue sarcoma (TH CR-406/SARC021): an international, multicentre, open-label, randomised phase 3 trial. *Lancet Oncol.* 18 (8), 1089–1103. doi:10.1016/S1470-2045(17)30381-9

Van Cutsem, E., Lenz, H.-J., Furuse, J., Tabernero, J., Heinemann, V., Ioka, T., et al. (2016). MAESTRO: a randomized, double-blind phase III study of evofosfamide (Evo) in combination with gemcitabine (Gem) in previously untreated patients (pts) with metastatic or locally advanced unresectable pancreatic ductal adenocarcinoma (PDAC). *J. Clin. Oncol.* 34 (15_Suppl. l), 4007. doi:10.1200/JCO.2016.34.15_suppl.4007

Voissiere, A., Jouberton, E., Maubert, E., Degoul, F., Peyrode, C., Chezal, J.-M., et al. (2017). Development and characterization of a human three-dimensional chondrosarcoma culture for *in vitro* drug testing. *PLoS One* 12 (7), e0181340. doi:10.1371/journal.pone.0181340

Weiss, G. J., Infante, J. R., Chiorean, E. G., Borad, M. J., Bendell, J. C., Molina, J. R., et al. (2011a). Phase 1 study of the safety, tolerability, and pharmacokinetics of TH-302, a hypoxia-activated prodrug, in patients with advanced solid malignancies. *Clin. Cancer Res.* 17 (9), 2997–3004. doi:10.1158/1078-0432.CCR-10-3425

Weiss, G. J., Lewandowski, K., Oneall, J., and Kroll, S. (2011b). Resolution of *Cullen*'s sign in patient with metastatic melanoma responding to hypoxia-activated prodrug TH-302. *Dermatol. Rep.* 3 (3), 56. doi:10.4081/dr.2011.e56

Whitmore, G. F., and Gulyas, S. (1986). Studies on the toxicity of RSU-1069. *Int. J. Radiat. Oncology*Biology*Physics* 12 (7), 1219–1222. doi:10.1016/0360-3016(86)90262-2

Wojtkowiak, J. W., Cornnell, H. C., Matsumoto, S., Saito, K., Takakusagi, Y., Dutta, P., et al. (2015). Pyruvate sensitizes pancreatic tumors to hypoxia-activated prodrug TH-302. *Cancer Metab.* 3 (1), 2. doi:10.1186/s40170-014-0026-z

Yoon, C., Chang, K. K., Lee, J. H., Tap, W. D., Hart, C. P., Simon, M. C., et al. (2016). Multimodal targeting of tumor vasculature and cancer stem-like cells in sarcomas with VEGF-A inhibition, HIF-1α inhibition, and hypoxia-activated chemotherapy. *Oncotarget* 7 (28), 42844–42858. doi:10.18632/oncotarget.10.18632/oncotarget.10212

Yoon, C., Lee, H.-J., Park, D. J., Lee, Y.-J., Tap, W. D., Eisinger-Mathason, T. S. K., et al. (2015). Hypoxia-activated chemotherapeutic TH-302 enhances the effects of VEGF-A inhibition and radiation on sarcomas. *Br. J. Cancer* 113 (1), 46–56. doi:10.1038/bjc.2015.186

Zeman, E. M., Brown, J. M., Lemmon, M. J., Hirst, V. K., and Lee, W. W. (1986). SR-4233: a new bioreductive agent with high selective toxicity for hypoxic mammalian cells. *Int. J. Radiat. Oncology*Biology*Physics* 12 (7), 1239–1242. doi:10.1016/0360-3016(86)90267-1

Zhang, L., Marrano, P., Wu, B., Kumar, S., Thorner, P., and Baruchel, S. (2016a). Combined antitumor therapy with metronomic topotecan and hypoxia-activated prodrug, evofosfamide, in neuroblastoma and rhabdomyosarcoma preclinical models. *Clin. Cancer Res.* 22 (11), 2697–2708. doi:10.1158/1078-0432.CCR-15-1853

Zhang, X., Wojtkowiak, J. W., Martinez, G. V., Cornnell, H. H., Hart, C. P., Baker, A. F., et al. (2016b). MR imaging biomarkers to monitor early response to hypoxia-activated prodrug TH-302 in pancreatic cancer xenografts. *PLoS One* 11 (5), e0155289. doi:10.1371/journal.pone.0155289

**Conflict of Interest:** The authors declare that the research was conducted in the absence of any commercial or financial relationships that could be construed as a potential conflict of interest.

frontiers in Pharmacology

ORIGINAL RESEARCH
published: 06 July 2021
doi: 10.3389/fphar.2021.648708

# Ganoderma Lucidum Polysaccharides Enhance the Abscopal Effect of Photothermal Therapy in Hepatoma-Bearing Mice Through Immunomodulatory, Anti-Proliferative, Pro-Apoptotic and Anti-Angiogenic

*Qing-Hai Xia, Cui-Tao Lu, Meng-Qi Tong, Meng Yue, Rui Chen, De-Li Zhuge, Qing Yao, He-Lin Xu and Ying-Zheng Zhao**

*Department of Pharmaceutics, School of Pharmaceutical Sciences, Wenzhou Medical University, Wenzhou City, China*

OPEN ACCESS

**Edited by:**
*Aniello Cerrato, Istituto per l'Endocrinologia e l'oncologia "Gaetano Salvatore (CNR), Italy*

**Reviewed by:**
*Bin Yang, Guangzhou Medical University, China*
*Pengfei Zhang, Shenzhen Institutes of Advanced Technology (CAS), China*

***Correspondence:**
*Ying-Zheng Zhao*
*zhaoyzwmu@163.com*

**Specialty section:**
*This article was submitted to Pharmacology of Anti-Cancer Drugs, a section of the journal Frontiers in Pharmacology*

**Received:** *01 January 2021*
**Accepted:** *15 June 2021*
**Published:** *06 July 2021*

**Citation:**
*Xia Q-H, Lu C-T, Tong M-Q, Yue M, Chen R, Zhuge D-L, Yao Q, Xu H-L and Zhao Y-Z (2021) Ganoderma Lucidum Polysaccharides Enhance the Abscopal Effect of Photothermal Therapy in Hepatoma-Bearing Mice Through Immunomodulatory, Anti-Proliferative, Pro-Apoptotic and Anti-Angiogenic. Front. Pharmacol. 12:648708. doi: 10.3389/fphar.2021.648708*

Hepatocellular carcinoma is a malignant tumor with high morbidity and mortality, a highly effective treatment with low side effects and tolerance is needed. Photothermal immunotherapy is a promising treatment combining photothermal therapy (PTT) and immunotherapy. PTT induces the release of tumor-associated antigens by ablating tumor and Ganoderma lucidum polysaccharides (GLP) enhance the antitumor immunity. Results showed that Indocyanine Green (ICG) was successfully encapsulated into SF-Gel. ICG could convert light to heat and SF-Gel accelerates the photothermal effect *in vitro* and *in vivo*. PTT based on ICG/ICG-SF-Gel inhibited the growth of primary and distal tumors, GLP enhanced the inhibitory efficacy. ICG/ICG-SF-Gel-based PTT and GLP immunotherapy improved the survival time. ICG/ICG-SF-Gel-based PTT induces tumor necrosis and GLP enhanced the photothermal efficacy. ICG/ICG-SF-Gel-based PTT inhibited cell proliferation and angiogenesis, induced cell apoptosis, enhanced cellular immunity, and GLP enhanced these effects. In conclusion, GLP could enhance the abscopal effect of PTT in Hepatoma-bearing mice.

**Keywords: ganoderma lucidum polysaccharides, photothermal immunotherapy, abscopal effect, hepatoma, immunomodulatory, anti-proliferative, pro-apoptotic, anti-angiogenic**

## INTRODUCTION

Primary liver cancer is one of the malignant tumors with high morbidity and mortality in the world. In 2018, Liver cancer ranks 6th in new incidence and 4th in mortality in the world, and the overall 5-years survival rate is only 18% (Bray et al., 2018). Hepatocellular carcinoma (HCC) is the main type of primary liver cancer (75–85%). In 2019, HCC ranks 4th in the incidence and 2nd in mortality among malignant tumors in China (Rongshou et al., 2019).

**Abbreviations:** CAR, Chimeric Antigen Receptor; GLP, Ganoderma lucidum polysaccharides; HCC, Hepatocellular carcinoma; H22, Hepatoma 22; HE, Haematoxylin-eosin; ICG, Indocycline green; ICG-SF-Gel, Indocyanine green and Silk fibroin Gel; IPP, Image-Pro plus; NIR, Near-infrared; PI3K, Phosphoinositide 3-kinase; PTT, Photothermal therapy; SF, Silk fibroin; UV, Ultraviolet-visible.

Surgical resection is the main radical treatment for HCC. Due to the late stage of the disease, poor liver function, poor general condition, only 20% of patients can be diagnosed with radical treatment. Radiofrequency ablation, hepatic arterial chemoembolization, systemic therapy and radiotherapy are available for patients who can't or refuse surgery. However, these treatments have problems such as high side effects and tolerance. The 5-years overall survival rate of surgical resection is only 50%, and the recurrence rate is 70% (Tabrizian et al., 2015). There is no effective treatment, resulting in few options for patients with recurrence and advanced stage. Therefore, highly effective cancer treatment is urgently needed.

In recent years, cancer immunotherapy that stimulates the immune system to attack tumors has gradually become a new strategy (Kun, 2015; Ribas and Wolchok, 2018). Immunotherapy is divided into Targeted antibodies (Sliwkowski and Mellman, 2013; Compte et al., 2018), adoptive cell therapies (Restifo et al., 2012; Maude et al., 2014), oncolytic viruses (Twumasi-Boateng et al., 2018), cancer vaccines (Carreno et al., 2015; Zhu et al., 2017), and immunomodulators (Gubin et al., 2014; Momin et al., 2019). However, most immunotherapies have limitations such as high cost (Ledford, 2013; Ledford, 2015), cytokine release syndrome (DeFrancesco, 2014), risk of serious autoimmune diseases (Montero et al., 2007), delayed effect of curative effect (Hoos, 2007), and poor Chimeric antigen receptor T Cell persistence or cancer cell resistance (Shah and Fry, 2019).

Among these immunotherapies, cancer vaccine therapy may have advantages (Fang et al., 2014; Palucka and Banchereau, 2014). Tumor antigens are introduced into the body and activate B and T cells to recognize and act on specific tumor cells, to inhibit the growth, metastasis, and recurrence of tumors. In recent years, tumor vaccines have been widely studied, and whole-cell or cell lysate vaccine shows a good application prospect (Ellebaek et al., 2012; Fang et al., 2014). However, the clinical efficacy of whole-cancer vaccines is poor, and there are problems such as the complex production process, the uncertainty of nature and dose (Cicchelero et al., 2014). Therefore, more effective tumor immunotherapy is urgently needed.

PTT utilize the heat generated by optical absorbing agents under near-infrared (NIR) light to dissolve tumor. PTT has the advantages of local treatment, high selectivity, low systemic toxicity, non-invasive and controllable temperature (Chen et al., 2014). Indocyanine green (ICG) is a safe, effective, and widely used clinical contrast agent, which was approved by the United States Food and Drug Administration in 1959. Because of its NIR optical properties, ICG absorbs light and generates heat for the ablation of the tumor (Deng et al., 2015). Hyperthermia can be effective for local cancer treatment due to the sensitivity of tumor cells to temperature elevation (Hynynen and Lulu, 1990). However, it's difficult to completely eradicate the tumor by PTT alone, heterogeneous heat distribution may lead to residual tumors (You et al., 2012). Therefore, successful cancer treatment requires the combination of PTT with other therapies, such as immune stimulation.

Photothermal immunotherapy is a promising treatment combining PTT and immunotherapy (Yata et al., 2017). PTT induces apoptosis or necrosis of tumor cells through hyperthermia (Zhang et al., 2014), releases tumor-associated antigens, triggers specific antitumor immunity, and clearing the residual tumor (Guo et al., 2014). However, weak immunogenicity affects the cancer immunotherapy effects (Zhou et al., 2012). Immunomodulators can activate the antitumor immune response and enhance immune function. Ganoderma lucidum polysaccharides (GLP) is one of the critical bioactive components of Ganoderma lucidum, which has been recognized as a promising natural source of immunomodulatory (Wang et al., 2018). Clinical studies have shown beneficial effects of GLP as an immunomodulatory in cancer patients without obvious toxicity and GLP exerts the antitumor action by stimulating the immune function (Sohretoglu and Huang, 2018). It was reported that GLP could activate bone marrow-derived macrophages to produce immunomodulatory substances, such as TNF-α, IL-1β and IL-6 (Wang et al., 1997; Zhang et al., 2010). The *in vitro* and *in vivo* studies have shown that GLP can promote the proliferation of splenocytes stimulated by Concanavalin A or lipopolysaccharide, enhance the phagocytosis of macrophages, increased cytotoxic T lymphocyte cytotoxicity and natural killer activity, increase the expression of IL-6 and TNF-α, and decrease the expression of VEGFA, which indicating that GLP possesses potential anticancer activity through immunomodulatory, anti-proliferative, pro-apoptotic and anti-angiogenic effects (Lin and Zhang, 2004; Gao et al., 2005; Chang et al., 2009; Weng and Yen, 2010).

Silk fibroin is an FDA-approved natural polymer extracted from Bombyx mori cocoons, has been extensively used because of its good biocompatibility, controllable biodegradability, remarkable biomechanical properties and self-assembling capacity (Yucel et al., 2014). Injectable SF hydrogel can be formed by physical and chemical methods through β-Sheet (Matsumoto et al., 2006). It can control drug release and widely used in local therapy (Rojas et al., 2019).

In this study, SF was extracted from the Bombyx mori cocoons, ICG-SF-Gel was formed by ultrasonic oscillation method, GLP was prepared by heating and dissolving. ICG was encapsulated into SF-Gel for phototherapy of Hepatic Tumor (As illustrated in **Figure 1**) (Chen et al., 2016). Then, the ultraviolet-visible (UV) absorbance of ICG and ICG-SF solution and photothermal effect were carefully characterized *in vitro*. Meanwhile, we established a subcutaneous bilateral hepatic tumor model. GLP was administered by intragastric administration daily, and photothermal treatment was performed. The photothermal effect of ICG/ICG-SF-Gel on tumors was recorded, the inhibitory effect on tumor growth was monitored, the body weight was measured and the mortality of mice was recorded. The morphological changes and pathological changes of tumors were detected by Haematoxylin-eosin (HE)-staining. Finally, immunohistochemical staining was used to detect the expressions of Ki-67, Caspase-3, BAX, bcl-2, PECAM-1, VEGFA, FGF-2, TNF-α, CD68, IL-1β, IL-6 and IL-13 (**Figure 4**). Our study indicated that GLP could enhance the abscopal effect of PTT in Hepatoma-bearing mice through immunomodulatory, anti-proliferative, pro-apoptotic and anti-angiogenic.

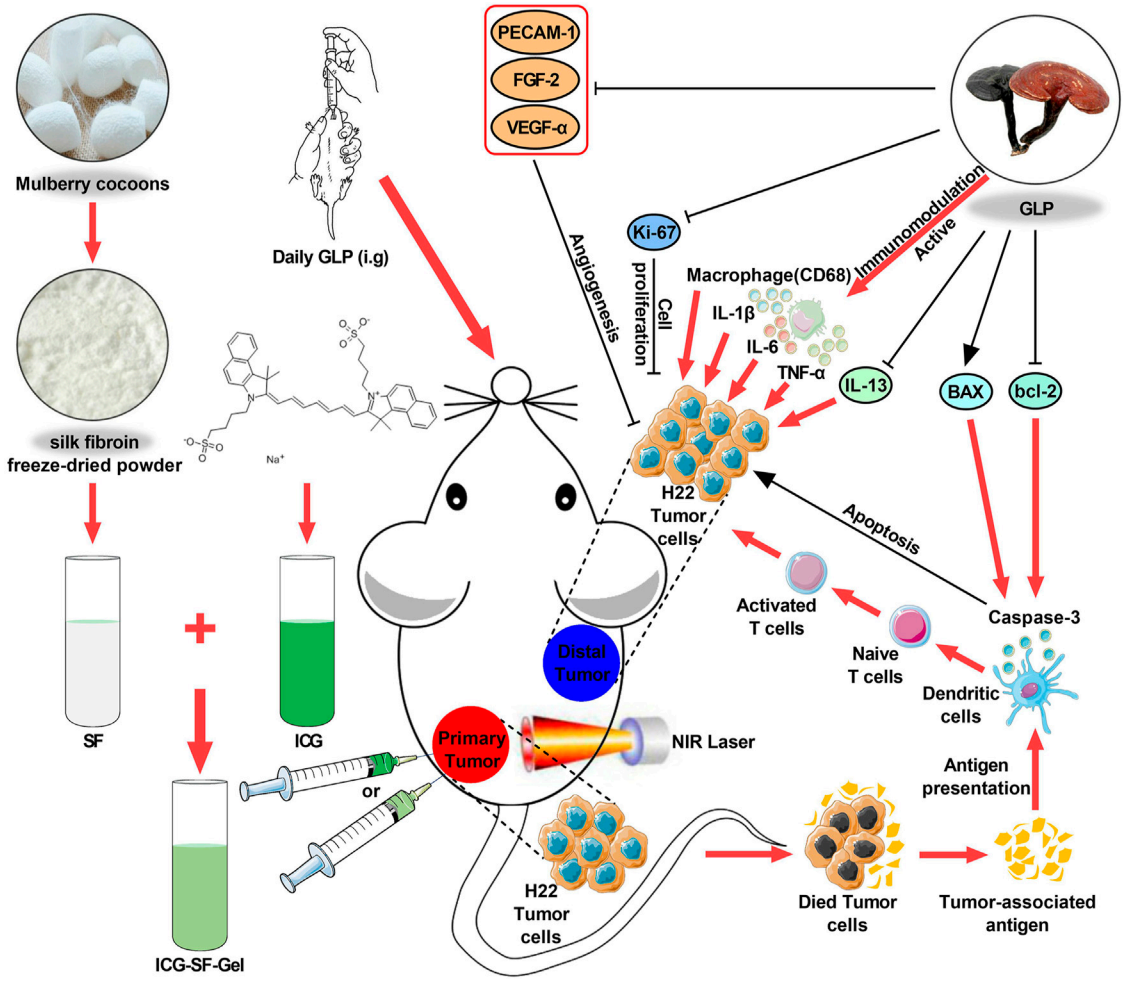


**FIGURE 1 |** Schematic design of ICG/ICG-SF-Gel and the distal antitumor mechanism of ICG/ICG-SF-Gel-based photothermal therapy and GLP immunotherapy in hepatoma-bearing mice.; Abbreviations: SF, Silk fibroin; GLP, Ganoderma lucidum polysaccharides; ICG, Indocycline green; ICG-SF-Gel, Indocyanine green and Silk fibroin Gel; NIR, near-infrared.

# MATERIALS AND METHODS

## Materials and Reagents

GLP was extracted from the fruiting body of Ganoderma lucidum (Leyss. ex Fr.) Karst by Hangzhou Johncan International, the content was about 30%. ICG was purchased from Dalian Meilun Biotech (Dalian, China). Bombyx mori Cocoons were purchased from Bozhou Naxi Pharmaceutical (Bozhou, China). Lithium Bromide was purchased from Sigma-Aldrich (St Louis, MO, United States). Dialysis bag (3,500 Da) and HE staining kit were purchased from Solarbio (Beijing, China).

## Preparation of Silk Fibroin, Indocyanine Green and Silk Fibroin Gel and Ganoderma Lucidum Polysaccharides

SF was prepared as the method previously described (Kim et al., 2017). Bombyx mori Cocoons were cut into pieces and soaked in 0.02 M $Na_2CO_3$ solution. Then boiled for 1 h to remove sericin while stirring constantly. Washed 3 times and dried at 65°C. After drying, cocoons were dissolved in a water bath with 9.3 M LiBr solution at 60°C for 3 h. Then, filtrated twice with filter paper. Finally, dialyzed with dialysis bag (MWCO 3500) against 2,000 ml ultra-pure water for 72 h to remove the LiBr. The SF solution was further purified by freeze-drying to obtain silk fibroin freeze-dried powder, sealed and stored in a drying box.

ICG-SF-Gel was prepared by ultrasonic oscillation. Briefly, ICG solution (2 mg/ml) and SF solution (60 mg/ml) were mixed in an equal proportion. Then, ultrasound (100 W) was performed until turbidity appeared. Finally, the ultrasound was stopped and standing for 30 min.

GLP was prepared by heating and dissolving. Briefly, 1 g of GLP powder was added to 6 ml of pure water, heated and dissolved in a constant temperature water bath at 60°C, centrifuged at 2,000 rpm for 5 min, then the precipitation was discarded to get about 6 ml of GLP solution.

## The Photothermal Effect of Indocyanine Green and Indocyanine Green and Silk Fibroin Gel *in vitro*

To investigate the photothermal effect of ICG and ICG-SF-Gel *in vitro*, 200 μl of ICG solution (1 mg/ml) and ICG-SF-Gel were added into a 48-well cell culture plate and irradiated with 808 nm NIR laser (1.0 W/cm$^2$) for 300 s. During the irradiation, the temperature was recorded. SF (30 mg/ml) and Ultra-pure water were used as control. To investigate the photothermal circle stability, the temperature changes of four groups were measured by light on/off (5 min/30 min) three times.

## Cell Culture

Mouse hepatoma 22 (H22) cells were purchased from Shanghai Zhong Qiao Xin Zhou Biotechnology (Zqxzbio, ZQ0109, China). The cells were cultured in RMPI Medium 1,640 (Gibco, C11875500BT, United States), supplemented with 10% fetal bovine serum (Gibco, 1600044, United States), 1% penicillin, and streptomycin (Solarbio, P1400, China) at 37°C under a circumstance containing 5% $CO_2$. Adjust H22 cell strains to $1 \times 10^7$ cells/ml, then injected 0.2 ml into the abdomen of male BALB/C mice for 6–8 days. The ascites cells were passaged three times for usage. The cell concentration was $1 \times 10^7$ cells/ml.

## Animal Experiments

### Animals

Male BALB/C mice (20–24 g) were supplied by the Laboratory Animals Center of Wenzhou Medical University. The mice were kept with regulated humidity (50 ± 10%) and temperature (22 ± 2°C) in a 12 h light/dark cycle, fed with forage and clean water ad libitum. All the experiments were performed under the approval and guidance of the Animal Experimentation Ethics Committee of Wenzhou Medical University, Wenzhou, China.

Mice were randomly divided into seven groups. In the H22, H22 + ICG + Laser, H22 + ICG-SF-Gel + Laser and H22 + Laser groups, mice received ultra-pure water intragastric administration daily, while in the H22 + GLP, H22 + ICG + GLP + Laser and H22 + ICG-SF-Gel + GLP + Laser groups, mice received GLP (50 mg/ml) intragastric administration daily.

### The Primary Tumor Inoculation

After 7 days of intragastric administration, 0.2 ml of the H22 cells ($1 \times 10^7$ cells/ml) were subcutaneously injected into the back of the left hindlimb of each mouse as primary tumors. The body weight and primary tumor volume were measured daily. Tumor volumes (V) were calculated using an ellipsoid approximation: $V = 0.5 \times L \times W^2$ (L = the maximum diameters of the tumor, W = a longest transverse diameter perpendicular to the maximum diameters of the tumor). Relative primary tumor volumes were calculated as $V/V_0$ ($V_0$ is the tumor volume when ICG/ICG-SF-Gel were injected). The mortality of mice was recorded daily, draw the curve of the survival time in mice by Kaplan-Meier method.

### The Distal Tumor Inoculation

Eight days after the primary tumor inoculation, 0.2 ml of the H22 cells ($1 \times 10^7$ cells/ml) were subcutaneously injected into the back of the right forelimb of each mouse as the distal tumors. The distal tumor volumes were measured daily. Tumor volumes (V) were calculated using an ellipsoid approximation: $V = 0.5 \times L \times W^2$. Relative distal tumor volumes were calculated as $V/V_0$ ($V_0$ is the tumor volume of the third day after distal tumor inoculation).

### The Photothermal Effect of Indocyanine Green and Indocyanine Green and Silk Fibroin Gel *in vivo*

When the primary tumors reached 60 mm$^3$, 0.1 ml ICG (1 mg/ml) was injected into the tumor site of H22 + ICG + Laser and H22 + ICG + GLP + Laser groups, 0.1 ml ICG-SF-Gel was injected into the tumor site of H22 + ICG-SF-Gel + Laser and H22 + ICG-SF-Gel + GLP + Laser groups. After injections, the tumor site of mice in the four groups was irradiated with an 808 nm NIR laser for 90 s. The maximum temperatures of the tumor area and thermo-graphic images were recorded at every 10 s intervals for 90 s. The irradiation and temperature thermal imaging were performed again each day for the next 2 days.

## The Distal Antitumor Mechanism of Photothermal Therapy and Ganoderma Lucidum Polysaccharides Immunotherapy

### Histopathological Examination

Four mice from each group were randomly sacrificed 7 days after the distal tumor inoculation and their primary and distal tumors were collected. Tumors were fixed in 4% paraformaldehyde and embedded in paraffin wax, cut into 5 μm thick slices. HE-stained slides were obtained for morphological and pathological analysis.

### Immunohistochemical Staining

Tumor slices were deparaffinized in a xylene series and hydrated in distilled water. Then, Incubating slides in 3% $H_2O_2$ in methanol for 10 min. Antigen retrieval was performed by heating slides in an autoclave with 10 mM pH 6.0 citrate buffer for 5 min after pressure gaining and washing with PBS. Nonspecific antibody binding was blocked with 5% BSA in PBS for 30 min at room temperature before incubation with primary antibodies at 4°C overnight. Then, incubated with secondary antibody for 1 h at 37°C. Finally, stained with DAB and counterstained with hematoxylin. Negative control slides were obtained by omitting the primary antibody. Cell nuclei were counterstained with reformative Gill's hematoxylin.

### Quantitation of Ki-67 Proliferation Index

The method has been described previously. Briefly, the tumors from different treatment groups were collected for immunohistochemical staining of Ki-67. Ki-67 positive cells were counted from at least five random microscopic fields (400 × original magnifications) per subject and quantified by optical density using Image-Pro Plus 6.0. The Ki-67 proliferation index (%) was calculated according to the following formula: the number of Ki-67 positive cells/the total cell count × 100%.

### Detection of Tumor Apoptosis, Tumor Vascularity, and Immune Index

The method has been described previously. Briefly, tumors from different treatment groups were collected for

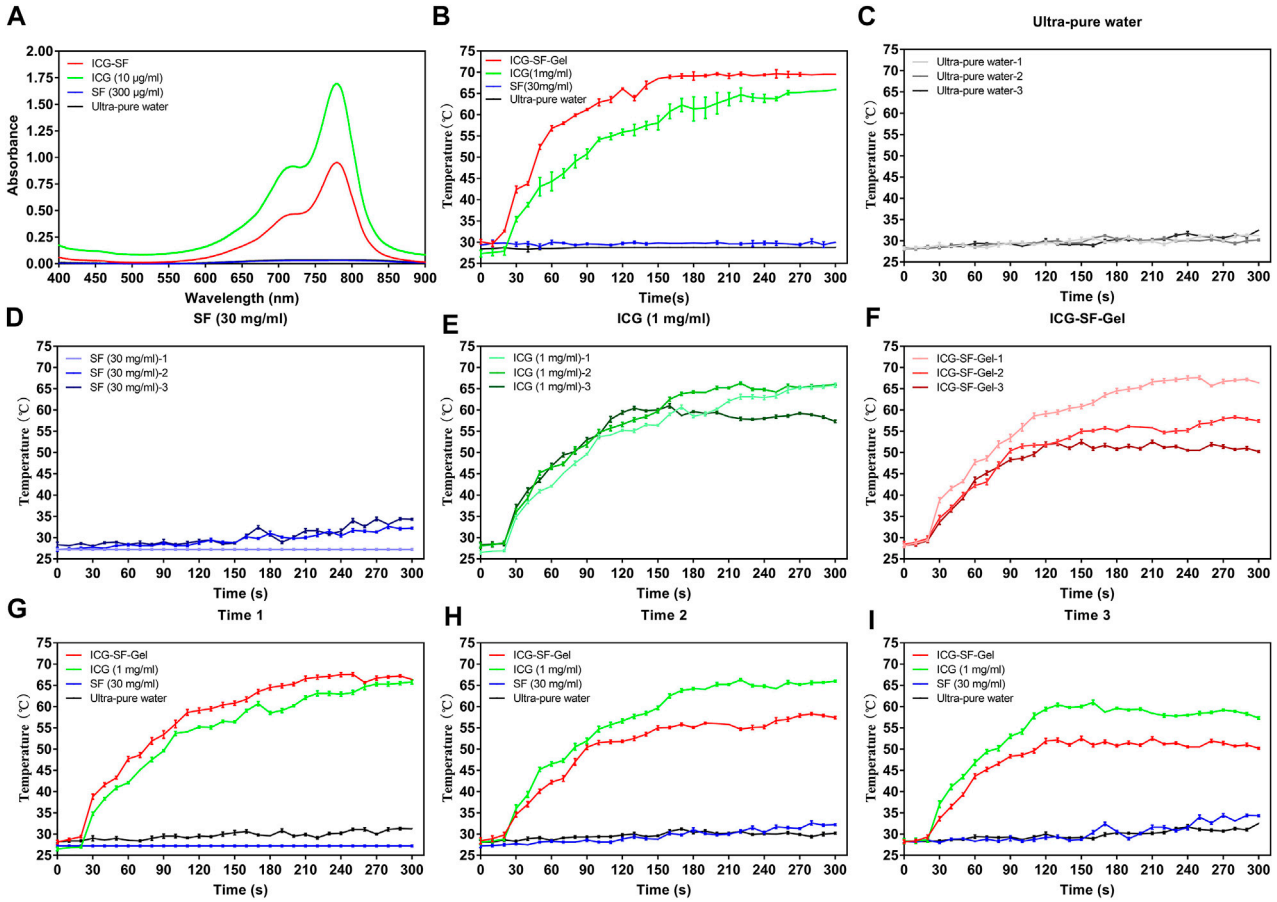


**FIGURE 2 |** The photothermal effect of ICG and ICG-SF-Gel *in vitro*. **(A)** The ultraviolet-visible spectrum of the ICG-SF, ICG, SF, and Ultra-pure water; **(B)** The temperature change of ICG-SF-Gel, ICG, SF and Ultra-pure water under continuous 808 nm NIR laser irradiation (1 W/cm$^2$) for 300 s; **(C–F)** Temperature change of Ultra-pure water **(C)**, SF **(D)**, ICG **(E)** and ICG-SF-Gel **(F)** under the discontinuous 808 nm NIR irradiation mode (ON = 5 min, OFF = 30 min, three cycles, 1 W/cm$^2$) for 300 s; **(G–I)** Three cycles temperature change of Ultra-pure water, SF, ICG and ICG-SF-Gel under the discontinuous 808 nm NIR irradiation mode (ON = 5 min, OFF = 30 min, 1 W/cm$^2$) for 300 s.

immunohistochemical staining of Caspase-3, BAX, bcl-2, PECAM-1, VEGFA, FGF-2, TNF-α, CD68, IL-1β, IL-6, and IL-13. Positive-staining cells were counted from at least five random microscopic fields (400 × original magnifications) per subject and quantified by optical density using Image-Pro Plus 6.0.

## Statistical Analysis

All the data were presented as mean ± SD. All statistical analysis was carried out using GraphPad Prism 7.04 for Windows. For all the immunohistochemical staining analysis, the Student's t-test was performed to determine the significance of differences between two groups, and one-way analysis of variance (ANOVA) was employed for multiple group comparison. Survival curves were plotted using the Kaplan-Meier method and compared between groups using the Log-rank (Mantel-Cox) test. Two-way ANOVA was used for time-temperature curves. The temperature curve, relative tumor growth curve and body weight curve were analyzed by two-way ANOVA. In all tests, $p < 0.05$ was considered statistically significant. Statistical significance was expressed by $^*p < 0.05$, $^{**}p < 0.01$, $^{***}p < 0.001$ and $^{****}p < 0.0001$.

# RESULTS AND DISCUSSION

## Preparation of Silk Fibroin and Indocyanine Green and Silk Fibroin Gel and Ganoderma Lucidum Polysaccharides

SF was prepared as the method previously described. The concentration of SF solution was approximately 3 wt%. ICG solution (2 mg/ml) and SF solution (60 mg/ml) were mixed in an equal proportion. Then, ultrasound (100 W) was performed until turbidity appeared. Finally, the ultrasound was stopped and standing for 30 min to obtain ICG-SF-Gel.

The UV spectrum of ICG (10 μg/ml) and ICG-SF solutions was investigated and results were displayed in **Figure 2A**. The Ultra-pure water and SF solution exhibited no absorption peaks at 400–900 nm. ICG and ICG-SF solutions exhibited a strong

characteristic absorption peak at 779 nm, indicating that the successful encapsulation of ICG in the SF solution and SF did not affect the UV absorbance of ICG.

In our previous study, we carried out the characterization experiments of ICG-SF-Gel, which proved the safety of ICG-SF-Gel (Xu et al., 2018; Yao et al., 2020).

GLP was extracted from the fruiting body of Ganoderma lucidum (Leyss. ex Fr.) Karst by Hangzhou Johncan International, the content was about 30%. It was prepared by heating and dissolving. Briefly, 1 g of GLP powder was added to 6 ml of pure water, heated and dissolved in a constant temperature water bath at 60°C, centrifuged at 2000 rpm for 5 min, then the precipitation was discarded to get about 6 ml of GLP solution.

## The Photothermal Effect of Indocyanine Green and Indocyanine Green and Silk Fibroin Gel *in vitro*

The photothermal effect of ICG-SF-Gel, ICG (1 mg/ml) *in vitro* was evaluated for 300 s and results were shown in **Figures 2B–I**.

To explore a more suitable concentration of ICG, we carried out experiments on the photothermal effect of ICG at different concentrations and 1 mg/ml was selected. (**Figure 2B**). The result showed that the photothermal effect of the continuous 808 nm NIR radiation on Ultra-pure water and SF (30 mg/ml) was negligible. By contrast, after radiation for 10 s, the temperature of ICG (1 mg/ml) began to rise rapidly, after 260 s the temperature was elevated up to 65°C. ICG-SF-Gel also showed a temperature rising after radiation. The temperature of ICG-SF-Gel began to rise rapidly after 10 s, then rose and remained at 69°C after 160 s. Compared with the ICG solution, ICG-SF-Gel has a higher temperature and faster heating rate (**Figure 2B**).

To investigate the photothermal circle stability *in vitro*, the temperature change of ICG (1 mg/ml) and ICG-SF-Gel under the discontinuous 808 nm NIR irradiation mode (ON = 5 min, OFF = 30 min, three cycles, 1 W/cm$^2$) was performed (**Figures 2C–I**) and the similar results were obtained (**Figure 2G**). The photothermal effect of the first radiation on the temperature of Ultra-pure water and SF (30 mg/ml) was negligible. By contrast, after radiation for 20 s, the temperature of ICG (1 mg/ml) began to rise rapidly, after 200 s the temperature was elevating up to 60°C. ICG-SF-Gel also exhibited a temperature rising after the first radiation, the temperature began to rise rapidly after 20 s, and after 140 s the temperature was elevated up to 60°C. Compared with the ICG solution, a higher temperature and faster heating rate were observed for ICG-SF-Gel (**Figure 2G**). As expected, the photothermal effect of discontinuous 808 nm NIR irradiation mode on the temperature of Ultra-pure water and SF (30 mg/ml) were negligible (**Figures 2C,D**). Compared with the ICG solution, the heating rate and maximum platform temperature of ICG-SF-Gel decreased more obviously (**Figures 2E,F**). In **Figure 2E**, the temperature rise of the three radiations was the same in the first 40 s, indicating that the photothermal stability of ICG is good. Besides, the first radiation also consumed ICG, but less than the ICG-SF-Gel group, which was still enough to support the ICG consumption of the second radiation, so the second photothermal curve did not decrease. However, in the third radiation, the content of ICG has been consumed too much, resulting in a decrease in the temperature in the third photothermal curve. In **Figure 2F**, SF-Gel could control the release of ICG and aggregate ICG, resulting in more ICG consumption, more temperature rise, and faster heating rate during the first radiation. Then, also due to the controlled release and aggregation effect of SF-Gel on ICG, the consumption of ICG was higher. Therefore, in the second and third laser irradiations, the content of ICG was lower, the heating rate and the maximum platform temperature of the ICG-SF-Gel group decreased more obviously. Therefore, in the follow-up animal experiments, we had an injection of ICG before every radiation to ensure the stability of the effect of PTT.

Overall, these results suggested that ICG could convert light to heat, and ICG-SF-Gel may converge and accelerate the photothermal effect so that ICG can achieve a faster and stronger photothermal effect.

## The Photothermal Effect of Indocyanine Green and Indocyanine Green and Silk Fibroin Gel *in vivo*

To confirm the photothermal transformation of ICG/ICG-SF-Gel *in vivo*, and to stimulate the immune response of the body, we treated the mice with 808 nm NIR laser (1 W/cm$^2$) every 24 h intervals for 3 days. The maximum temperatures of the tumor area and thermo-graphic images were recorded for 90 s (**Figure 3A** and **Supplementary Material**).

As shown in **Figures 3C–F**, on the first day, the tumor area temperature of H22 group mice increased slowly from 36.6 to 40.2°C. By contrast, the tumor area temperature of H22 + ICG group mice rapidly increased from 35.6 to 55.5°C after irradiation for 10 s, then kept increasing at a relatively fast rate. Finally, the temperature was elevated up to 75.5°C. In the ICG-SF-Gel group, the tumor area temperature rapidly increased from 35.6 to 56.8°C after 10 s, then kept increasing at a relatively fast rate. Finally, the temperature was elevated up to 81.4°C. Compared with the H22 + ICG group, the tumor area temperature of the ICG-SF-Gel group increased faster and higher, which may be due to the aggregation effect of SF-Gel on ICG, so that ICG can achieve a faster and stronger photothermal effect.

In the 3 days NIR irradiation experiment, the tumor area temperature of H22 group mice increased slowly from 36 to 40°C (**Figure 3C**). The heating rate of H22 + ICG group mice was faster and higher on day 2 than day 1, then decreased on day 3, but still faster and higher than day 1 (**Figure 3D**). The heating rate of ICG-SF-Gel group mice was faster and higher on day 2 than day 1, then decreased on day 3, but still slightly faster and higher than day 1 (**Figure 3E**). However, in the experiment of discontinuous NIR radiation *in vitro*, the heating rate of ICG and ICG-SF-Gel groups decreased slightly, and the maximum platform temperature kept decreasing. The reason for this difference may be the effect of skin color and tissue on NIR heat absorption. As shown in **Figure 3B**, after irradiation, the tumor areas of the mice were burned and the tissue moisture

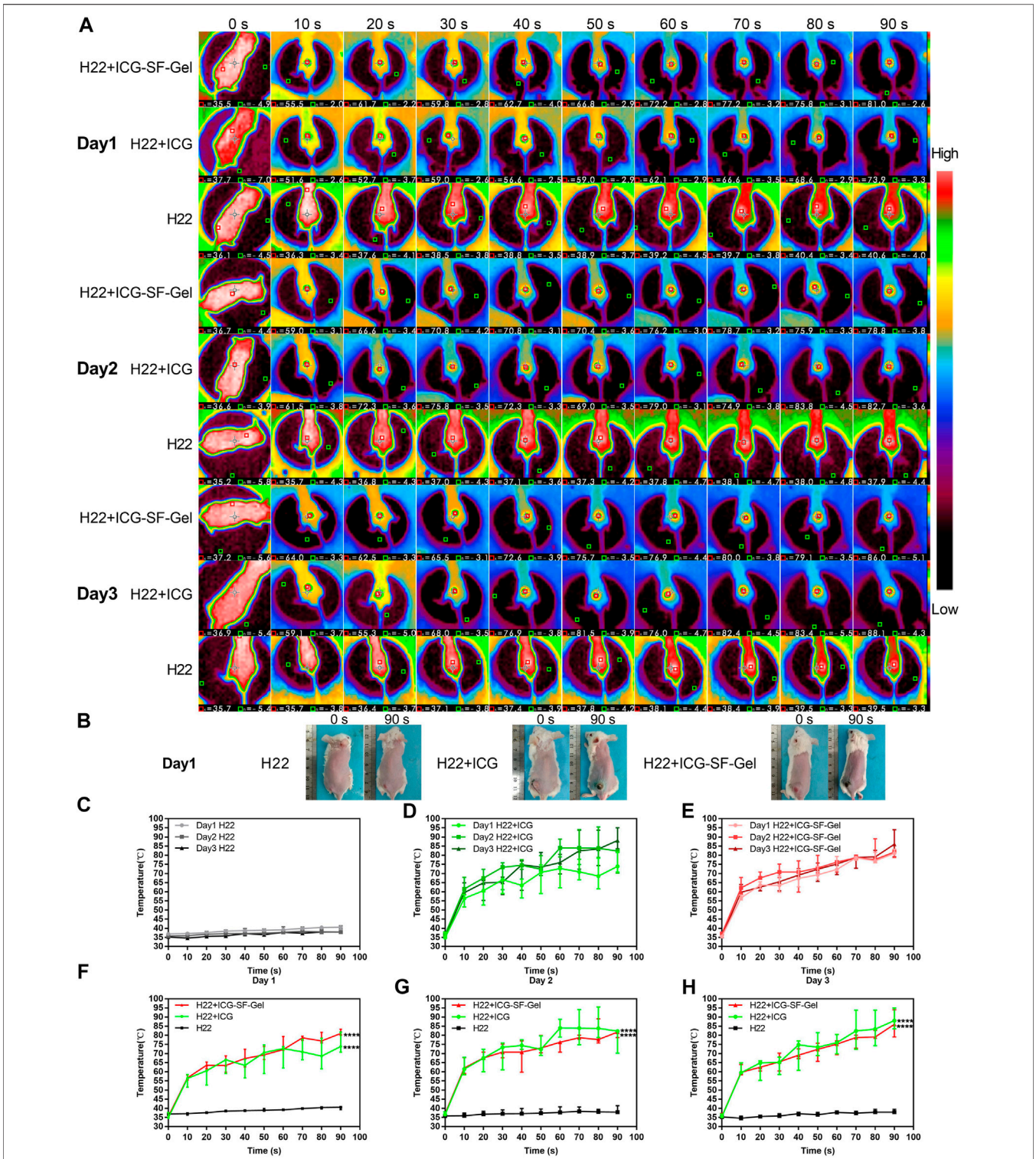


**FIGURE 3 |** The photothermal effect of ICG and ICG-SF-Gel *in vivo*. **(A)** The thermo-graphic images of H22 + ICG-SF-Gel, H22 + ICG, and H22 groups mice after NIR irradiation at every 10 s intervals for 90 s during the 3 days NIR irradiation; **(B)** The digital photograph of H22 + ICG-SF-Gel, H22 + ICG and H22 groups mice before and after NIR irradiation on Day 1; **(C–E)** The temperature changes of tumor area in H22 **(C)**, H22 + ICG **(D)** and H22 + ICG-SF-Gel **(E)** groups mice after NIR irradiation at every 10 s intervals for 90 s during the 3 days NIR irradiation; **(F–H)** The temperature changes of tumor area in H22, H22 + ICG and H22 + ICG-SF-Gel groups mice after NIR irradiation at every 10 s intervals for 90 s on Day 1 **(F)**, Day 2 **(G)** and Day 3 **(H)** ($n$ = 3 mice per group, data are presented as the mean ± SD. Statistical significance was expressed by $^{*}p < 0.05$, $^{**}p < 0.01$, $^{***}p < 0.001$ and $^{****}p < 0.0001$, comparing other groups with the H22 group).

content decreased, making it easier to heat up. Besides, the pigmentation in the tumor area increases the absorption of light energy, thus making the thermal effect of the laser more significant.

Compared with the H22 + ICG group, the tumor area temperature of the ICG-SF-Gel group increased faster and higher on day 1, but slightly slower and lower on day 2 and day 3 (**Figures 3F–H**). It is consistent with results of discontinuous NIR radiation *in vitro*, which may be due to the aggregation effect of SF-Gel on ICG. Due to the higher consumption of ICG in the ICG-SF-Gel group mice on day 1, the photothermal effect of ICG-SF-Gel group mice was slightly weaker than that of H22 + ICG group mice on day 2 and day 3.

All in all, the results of *in vivo* experiments also demonstrated that ICG could convert light to heat, and ICG-SF-Gel may converge and accelerate the photothermal effect of ICG so that ICG can achieve a faster and stronger photothermal effect.

## Indocyanine Green/Indocyanine Green and Silk Fibroin Gel-Based Photothermal Therapy and Ganoderma Lucidum Polysaccharides Immunotherapy to Inhibit the Tumor Growth

The Schematic illustration of ICG/ICG-SF-Gel-based PTT and GLP immunotherapy to inhibit distal tumor growth is shown in **Figure 4A**. After 7 days of ultra-pure water or GLP intragastric administration, 0.2 ml of the H22 cells ($1 \times 10^7$ cells/ml) were subcutaneously injected into the back of the left hindlimb of each mouse as the primary tumors. When the primary tumors reached 60 $mm^3$, H22 + ICG + Laser and H22 + ICG + GLP + Laser groups were intratumorally injected with 0.1 ml ICG (1 mg/ml), H22 + ICG-SF-Gel + Laser and H22 + ICG-SF-Gel + GLP + Laser groups were intratumorally injected with 0.1 ml ICG-SF-Gel. After injections, the tumor site of mice in five groups was irradiated for 90 s. The maximum temperatures of the tumor area and thermo-graphic images were recorded for 90 s. The irradiation and temperature thermal imaging were performed again each day for the next 2 days. In the 3 days experiment, the tumor area temperature of mice injected with ICG or ICG-SF-Gel under laser irradiation quickly rose to 55°C in 30 s, which was high enough to effectively ablate tumors. While in the H22 group, the tumor area temperatures of mice exhibited no significant increase during irradiation (**Figure 4B**).

To investigate the antitumor efficiency of ICG/ICG-SF-Gel-based PTT and GLP immunotherapy in hepatoma-bearing mice, the primary tumor size was measured daily. The relative primary tumor volumes were calculated as $V/V_0$ ($V_0$ is the tumor volume when ICG/ICG-SF-Gel were injected). As illustrated in **Figure 4C**, ICG/ICG-SF-Gel-based PTT and GLP immunotherapy significantly inhibited the growth of the primary tumors. Compared with the H22 group, the increase of relative primary tumor volume in H22 + ICG + Laser and H22 + ICG-SF-Gel + Laser groups were slowed down significantly, while that in H22 + ICG + GLP + Laser and H22 + ICG-SF-Gel + GLP + Laser groups slowed down more obviously, suggesting that ICG/ICG-SF-Gel-based PTT inhibited the growth of primary tumors and GLP could enhance the inhibitory effect.

Besides, GLP mainly plays the role of an immunomodulator to enhance the inhibition of tumors. GLP alone can't directly inhibit tumor growth, and GLP needs to be dissolved by heating during intragastric administration. In this process, GLP may be decomposed into glucose-based monosaccharides, which has been proved in the literature published in science that glucose can promote the growth of the primary tumor (Goncalves et al., 2019), which may lead to the relative primary tumor volume in the GLP + H22 group is higher than that in the H22 group alone. Laser alone can't kill the H22 tumor, but due to the mild temperature stimulation caused by the laser, it accelerates the blood circulation around the tumor and promotes the growth of the primary tumor, which may lead to the relative primary tumor volume in the GLP + Laser group is higher than that in the H22 group alone (**Figure 4C**).

Eight days after the primary tumor inoculation, 0.2 ml of the H22 cells ($1 \times 10^7$ cells/ml) were subcutaneously injected into the back of the right forelimb of each mouse as the distal tumors with no direct treatments. To further investigate the distal antitumor efficiency of ICG/ICG-SF-Gel-based PTT and GLP immunotherapy in hepatoma-bearing mice, the distal tumor size was measured daily. The relative distal tumor volumes were calculated as $V/V_0$ ($V_0$ is the tumor volume of the third day after distal tumor inoculation). As shown in **Figure 4D**, ICG/ICG-SF-Gel-based PTT and GLP immunotherapy significantly inhibited the growth of distal tumors. Compared with the H22 group, the increase of relative tumor volume in H22 + ICG + Laser and H22 + ICG-SF-Gel + Laser groups were slowed down significantly, while that in H22 + ICG + GLP + Laser and H22 + ICG-SF-Gel + GLP + Laser groups slowed down more obviously, suggesting that ICG/ICG-SF-Gel-based PTT inhibited the growth of distal tumors and GLP could enhance the inhibitory efficacy.

However, unlike primary tumors, there was no significant difference in distal tumors between the H22 + GLP and H22 + laser groups and the H22 group. This may be due to the different mechanisms of combined treatment of primary and distal tumors. The inhibitory effect of combination therapy on the primary tumor is mainly the direct killing effect on tumor cells, while the inhibitory effect on the distal tumor is achieved through the distal effect brought by immune function. In the H22 + GLP group, because the effect of combination therapy on the distal tumor is achieved through immune function, the promoting effect of sugar on tumor growth may be offset by strong immune function. In the H22 + Laser group, the laser did not directly stimulate the distal tumor, so it did not affect the growth of the distal tumor.

To evaluate the health status of mice, the body weight was measured daily. The relative body weight was calibrated by normalizing the initial body weight (at day 0) to 1. The relative body weight was plotted at regular intervals and considered a surrogate for evaluation of systemic well-being. There were no significant body weight changes in the seven groups during the experiment (**Figure 4E**), indicating the fewer side effect of the treatments.

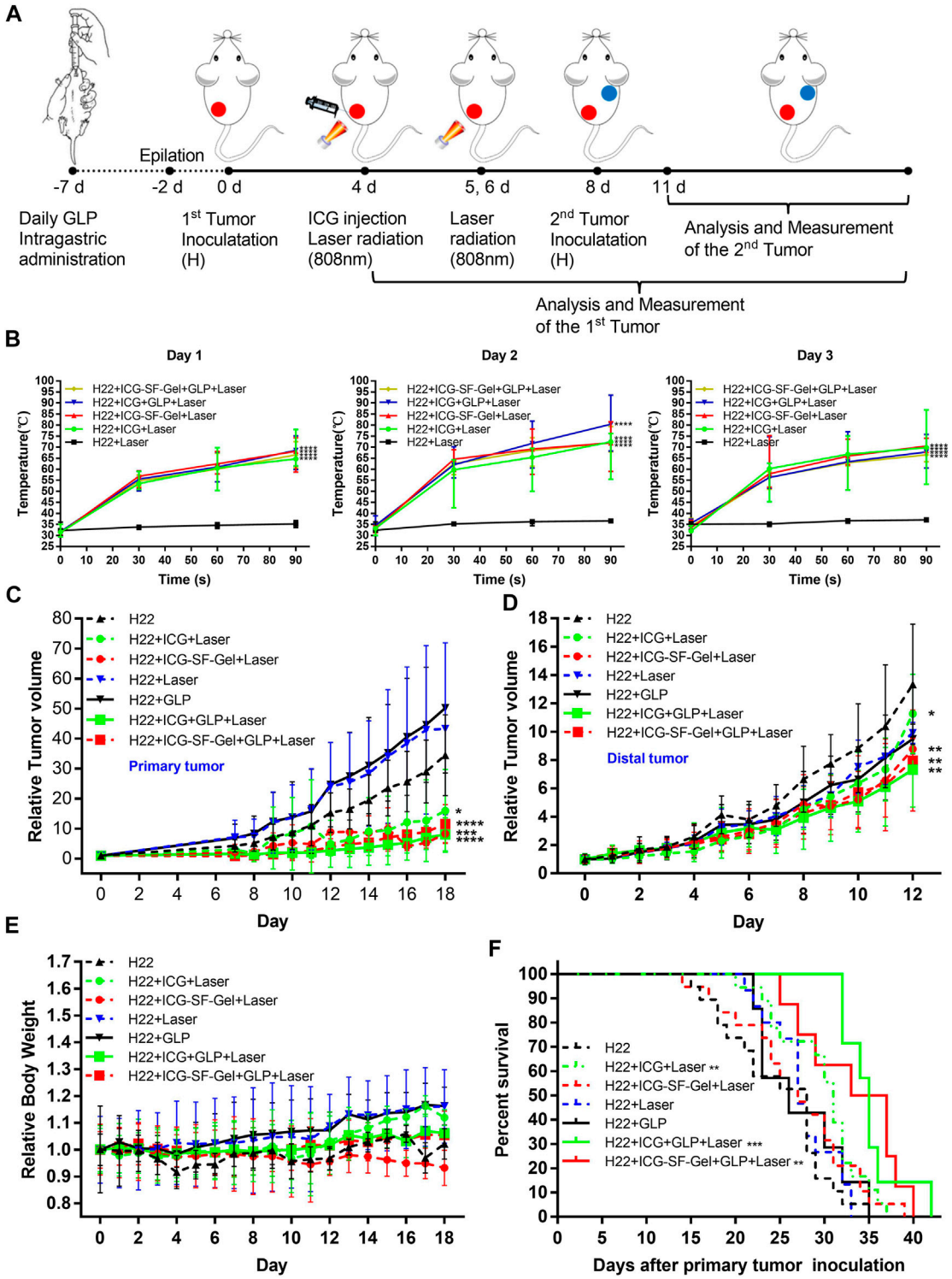


**FIGURE 4 |** Inhibition of the tumor growth *in vivo*. **(A)** Schematic illustration of ICG/ICG-SF-Gel-based photothermal therapy and GLP immunotherapy to inhibit distal tumor growth; **(B)** The temperature changes of tumor area in five groups mice after NIR irradiation during the 3 days NIR irradiation ($n$ = 6–9 mice per group, data are presented as the mean ± SD. Statistical significance was expressed by $^{*}p < 0.05$, $^{**}p < 0.01$, $^{***}p < 0.001$ and $^{****}p < 0.0001$, comparing other groups with the H22 group); **(C–E)** The relative tumor volume of primary tumors **(C)** or distal tumors **(D)** and the relative body weight **(E)** in seven groups mice after different treatments to their primary tumors ($n$ = 10–15 mice per group, data are presented as the mean ± SD. Statistical significance was expressed by $^{*}p < 0.05$, $^{**}p < 0.01$, $^{***}p < 0.001$ and $^{****}p < 0.0001$, comparing other groups with the H22 group); **(F)** The survival curve of seven groups mice after primary tumor inoculation. Survival curves were compared between groups using the log-rank test ($n$ = 7–19 mice per group, data are presented as the mean ± SD. Statistical significance was expressed by $^{*}p < 0.05$, $^{**}p < 0.01$, $^{***}p < 0.001$ and $^{****}p < 0.0001$, comparing other groups with the H22 group).

To evaluate the survival of mice, the mortality of mice was recorded daily. As displayed in **Figure 4F**, ICG-based PTT and GLP immunotherapy significantly resulted in improving the survival time. Compared with the H22 group, the H22 + ICG + Laser group exhibited a significant increase in improving the survival time, and in the H22 + ICG + GLP + Laser group, the survival time increased more obviously, indicating that ICG-based PTT prolonging the survival of mice bearing H22 tumors, and GLP can further prolong the survival time. Meanwhile, Consistent with ICG-based PTT and GLP immunotherapy, ICG-SF-Gel-based PTT and GLP immunotherapy significantly improved the survival time. Compared with the H22 group, the H22 + ICG-SF-Gel + Laser group exhibited no significant increase in improving the survival time, but in the H22 + ICG-SF-Gel + GLP + Laser group, the survival time increased significantly, indicating that ICG-SF-Gel-based PTT prolonging the survival of mice with the combination of GLP.

## The Distal Antitumor Mechanism of Indocyanine Green/Indocyanine Green and Silk Fibroin Gel-based Photothermal Therapy and Ganoderma Lucidum Polysaccharides Immunotherapy

As a promising natural source of immunomodulatory, GLP exerts the antitumor action by stimulating immune function (Sohretoglu and Huang, 2018; Wang et al., 2018). We introduced GLP immunotherapy to improve the distal antitumor efficiency of tumor-associated antigens produced *in situ* after photothermal ablation of primary tumors, and to inhibit the development of tumors.

To explore the antitumor mechanism of ICG/ICG-SF-Gel-based PTT and GLP immunotherapy, the tumors from different treatment groups of mice 7 days after the distal tumor inoculation were collected for HE staining and immunohistochemical staining.

First, to explore the effect of photothermal ablation, the morphological and pathological changes of primary tumors from different treatment groups of mice 7 days after the distal tumor inoculation were analyzed through HE staining. As shown in **Figure 5A**, the H22 group displayed robust tumor tissues with no necrosis and had rich normal capillaries. Binucleated cells with large nuclei and dense chromatin were frequently observed, indicating rapid tumor growth. In contrast, cell shrinkage and nuclear fragmentation were evident in H22 + ICG + Laser, H22 + ICG-SF-Gel + Laser, H22 + ICG + GLP + Laser and H22 + ICG-SF-Gel + GLP + Laser groups, revealing that PTT based on ICG/ICG-SF-Gel could induce tumor necrosis. Besides, more tumor necrosis and fragmentation in nuclei with evident cytoplasmic separation from nuclei were found in H22 + ICG + GLP + Laser and H22 + ICG-SF-Gel + GLP + Laser groups, indicating that GLP could enhance the photothermal ablation efficacy. These results suggested that PTT based on ICG/ICG-SF-Gel could achieve the effect of photothermal ablation and GLP could enhance the photothermal ablation efficacy.

Then, the morphological changes, pathological changes, and cell proliferation of distal tumors after different treatments were analyzed through HE staining and Ki-67 immunohistochemical staining. As shown in **Figure 5B**, the H22 group had large areas of confluent tumor cells with little or no tumor tissue necrosis. Consistent with the primary tumors, cell shrinkage and nuclear fragmentation were observed in distal tumors after PTT based on ICG/ICG-SF-Gel, and GLP-assisted PTT led to more tumor necrosis. Besides, compared with ICG-based PTT, PTT based on ICG-SF-Gel led to more tumor necrosis, indicating that PTT based on ICG-SF-Gel have a stronger inhibitory effect on distal tumor growth than ICG-based PTT. Ki-67 is a nuclear protein expressed in proliferating mammalian cells, suggesting the high proliferation potential of the tumor cells (Sobecki et al., 2016). Ki-67 immunohistochemical staining results revealed that PTT based on ICG/ICG-SF-Gel inhibited the cell proliferation of distal tumors and GLP enhanced the inhibition effect. Compared with ICG-based PTT, ICG-SF-Gel-based PTT enhanced the inhibition of cell proliferation (**Figures 5C,G**). All these results suggested that PTT based on ICG/ICG-SF-Gel could inhibit the cell proliferation of distal tumors and GLP could enhance the inhibition efficacy.

Some studies have revealed that GLP reduces the expression of some signaling molecules in the phosphoinositide 3-kinase (PI3K)/AKT/mammalian target of rapamycin (mTOR) signaling pathways which play a key regulatory function in proliferation at both gene and protein levels (Suarez-Arroyo et al., 2013). In the follow-up work, we will explore whether this signaling pathway is involved in our study.

Caspase-3 is a key executioner in apoptosis which is involved in the growth stimulation (Huang et al., 2011). BAX is a pro-apoptotic gene, it has been proposed that GLP enhances the anti-cancer effects by up-regulation of BAX (Huang et al., 2010). Bcl-2 is a proto-oncogene, which can inhibit apoptosis, mainly because bcl-2 regulates a variety of cell apoptosis-related protein activity, such as by Caspase-3 (Ola et al., 2011). It was reported that GLP induced HUVECs apoptosis directly by decreasing anti-apoptotic protein Bcl-2 expression (Cao and Lin, 2006). It is recognized that GLP can induce apoptosis in cancer cells by regulating the expression of bcl-2 (Martínez-Montemayor et al., 2011). To explore whether cell apoptosis plays a role in ICG/ICG-SF-Gel-based PTT and GLP immunotherapy, the distal tumors from different treatment groups of mice 7 days after the inoculation of the distal tumor were analyzed through immunohistochemical staining of Caspase-3, BAX, and bcl-2. Compared with the H22 group, distal tumors treated with PTT based on ICG/ICG-SF-Gel displayed a more obvious expression of Caspase-3 and BAX, and GLP increased the expression, demonstrated that GLP could increase cell apoptosis of distal tumors induced by PTT based on ICG/ICG-SF-Gel. Compared with ICG-based PTT, ICG-SF-Gel-based PTT increased the expression of Caspase-3 and BAX, indicating that ICG-SF-Gel-based PTT could induce cell apoptosis of distal tumor more effectively than ICG-based PTT (**Figures 5D,E,H,I**). Compared with the H22 group, distal tumors treated with PTT based on ICG/ICG-SF-Gel displayed lower expression of bcl-2 and GLP decreased the expression, demonstrated that PTT based on ICG/ICG-SF-Gel could inhibit the expression of apoptosis inhibitor gene and GLP could enhance the inhibitory effect. Compared

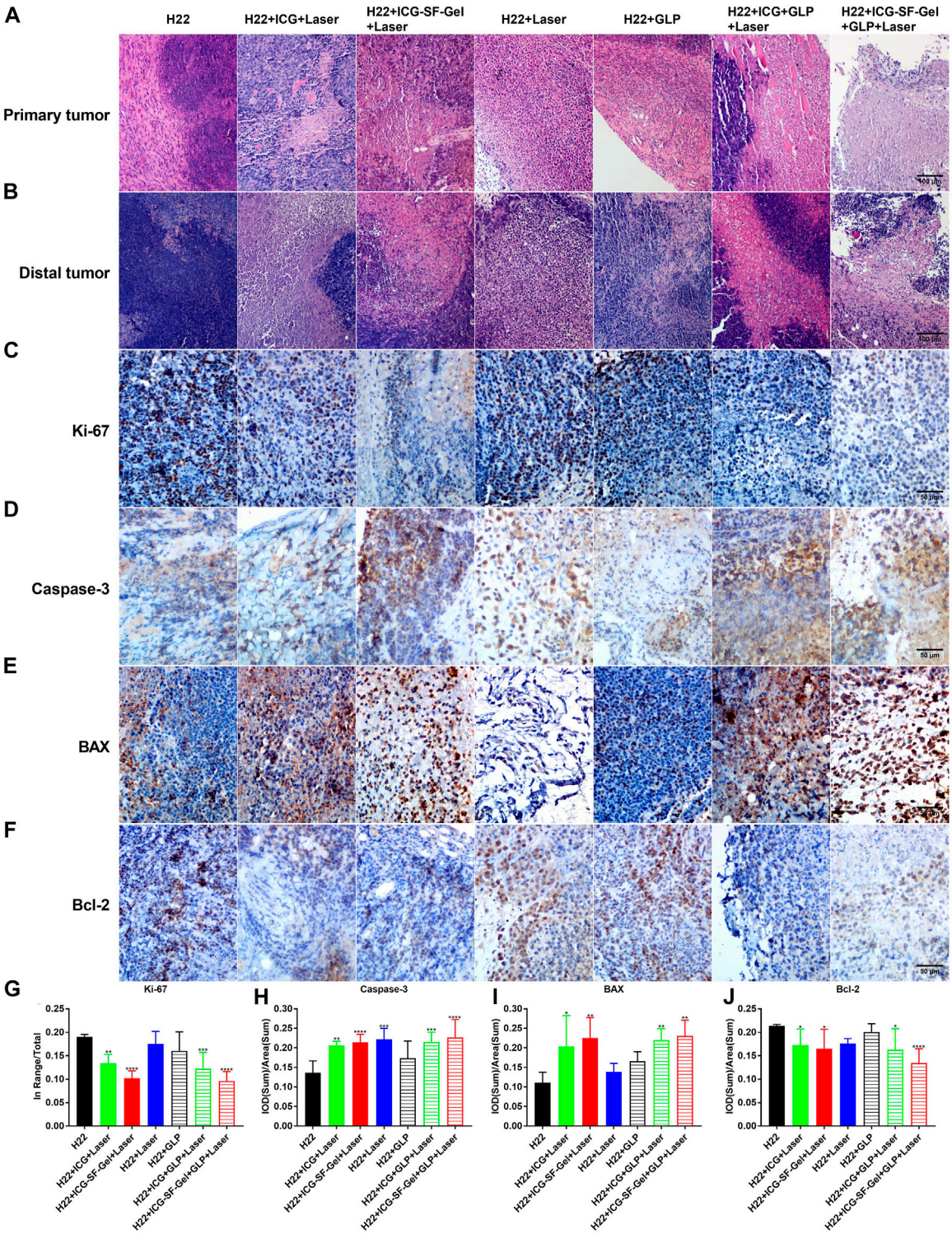


**FIGURE 5 |** Morphological changes, pathological changes, and cell proliferation of tumor tissues after different treatments. **(A,B)** The Haematoxylin-eosin staining of primary tumors **(A)** and distal tumors **(B)** collected from different treated groups of mice 7 days after the distal tumor inoculation (The same row shared the same scale bar: 100 μm); **(C–F)** Immunohistochemical staining of Ki-67 **(C)**, Caspase-3 **(D)**, BAX **(E)** and Bcl-2 **(F)** of distal tumors collected from different treated groups of mice 7 days after the distal tumor inoculation (The same row shared the same scale bar: 50 μm) and quantitative analysis of Ki-67 **(G)**, Caspase-3 **(H)**, BAX **(I)** and Bcl-2 **(J)** ($n$ = 4 mice per group, data are presented as the mean ± SD. Statistical significance was expressed by $^{*}p < 0.05$, $^{**}p < 0.01$, $^{***}p < 0.001$ and $^{****}p < 0.0001$, comparing other groups with the H22 group).

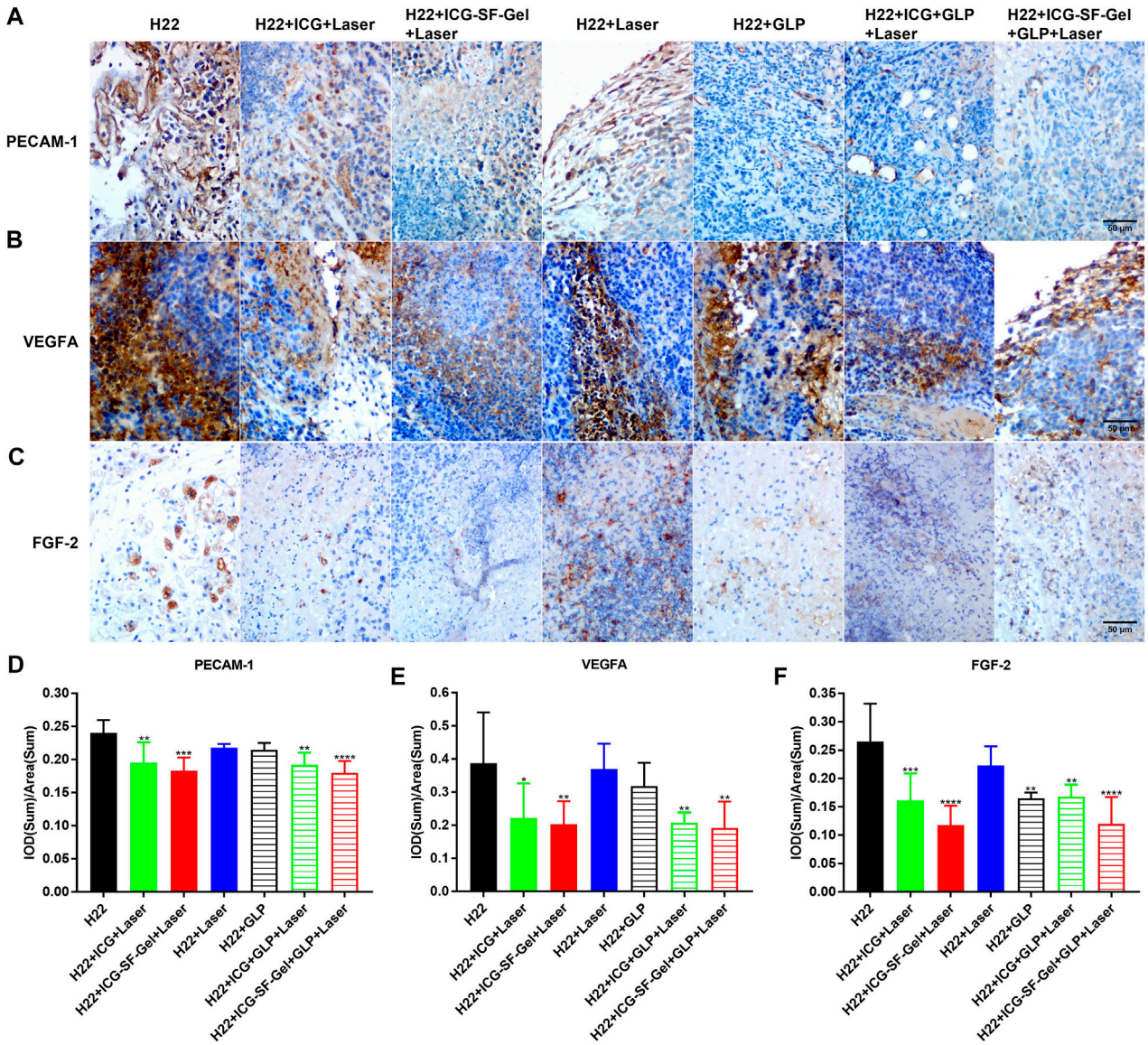


**FIGURE 6 |** The angiogenesis of distal tumors after different treatments. **(A–C)** Immunohistochemical staining of PECAM-1 **(A)**, VEGFA **(B)** and FGF-2 **(C)** of distal tumors collected from different treated groups of mice 7 days after the distal tumor inoculation (The same row shared the same scale bar: 50 μm) and quantitative analysis of PECAM-1 **(D)**, VEGFA **(E)** and FGF-2 **(F)** ($n$ = 4 mice per group, data are presented as the mean ± SD. Statistical significance was expressed by $^{*}p < 0.05$, $^{**}p < 0.01$, $^{***}p < 0.001$ and $^{****}p < 0.0001$, comparing other groups with the H22 group).

with ICG-based PTT, ICG-SF-Gel-based PTT decreased the expression of bcl-2, indicating that ICG-SF-Gel-based PTT could inhibit the expression of apoptosis inhibitor genes more effectively than ICG-based PTT (**Figures 5F,J**). GLP may up-regulate the expression of BAX, inhibit the expression of Bcl-2, and then activate the expression of Caspase-3, thus enhancing the apoptosis of distal tumors. All in all, these results pointed out that ICG-SF-Gel-based PTT could increase cell apoptosis of distal tumors more effectively than ICG-based PTT, and GLP could enhance the pro-apoptosis efficacy.

Platelet endothelial cell adhesion molecule-1 (PECAM-1) is a transmembrane glycoprotein member expressed on endothelial cells, which has been shown to play an important role in angiogenesis (Cao et al., 2009). Fibroblast growth factor-2 (FGF-2) and vascular endothelial growth factor (VEGF) were also involved in angiogenesis, and FGF-2 was reported to stimulate endothelial cell growth and enhances angiogenesis (Bikfalvi, 1999). Besides, GLP has been reported to inhibit angiogenesis by reducing the expression of VEGF (Sohretoglu and Huang, 2018). Therefore, angiogenesis of distal tumors from different treatment groups of mice 7 days after the inoculation of the distal tumor was analyzed through immunohistochemical staining of PECAM-1, VEGFA, and FGF-2. Compared with the H22 group, distal tumors treated with PTT based on ICG/ICG-

SF-Gel displayed lower expression of PECAM-1 and VEGFA, and GLP decreased the expression more obviously, suggested that PTT based on ICG/ICG-SF-Gel could inhibit angiogenesis and GLP could enhance the inhibitory efficacy (**Figures 6A,B,D,E**). Compared with ICG-based PTT, ICG-SF-Gel-based PTT decreased the expression of PECAM-1, VEGFA, and FGF-2, indicating that ICG-SF-Gel-based PTT could inhibit angiogenesis more effectively than ICG-based PTT. (**Figures 6A–F**). These results demonstrated that ICG-SF-Gel-based PTT could inhibit angiogenesis more effectively than ICG-based PTT, and GLP could enhance the anti-angiogenic efficacy. GLP may inhibit angiogenesis by inhibiting the proliferation of vascular endothelial cells and the production of PECAM-1, VEGFA and FGF-2, thus inhibiting the growth of distal tumors.

It has been established that the immune system plays an important role in tumorigenesis (Baxevanis et al., 2009), and photothermal immunotherapy is a promising treatment combining PTT and immunotherapy (Yata et al., 2017). PTT utilizes heat generated by optical absorbing agents under NIR light to dissolve tumor cells, induced apoptosis or necrosis of tumor cells based on hyperthermia (Zhang et al., 2014). Then, tumor cell necrosis releases tumor-associated antigens, triggering specific antitumor immunity and clearing the residual tumor (Guo et al., 2014). As a promising natural source of immunomodulatory, GLP activates the antitumor immune response and enhances immune function (Sohretoglu and Huang, 2018; Wang et al., 2018). TNF-α is an important marker in the activation of cellular immunity (Xiang et al., 2015), CD68 is a pan-marker of macrophages, IL-1β and IL-6 are important proinflammatory cytokines secreted by M1 macrophages (Zong et al., 2019). IL-13 is a Th2 cytokine that plays a critical role in a novel immunoregulatory pathway in which natural killer T cells suppress tumor immunosurveillance (Terabe et al., 2000; Terabe et al., 2004). It was reported that GLP could activate bone marrow-derived macrophages to produce immunomodulatory substances, such as TNF-α, IL-1β and IL-6 (Wang et al., 1997; Zhang et al., 2010).

To investigate whether the immune system plays an important role in ICG/ICG-SF-Gel-based PTT and GLP immunotherapy, the distal tumors from different treatment groups of mice 7 days after the distal tumor inoculation were analyzed through immunohistochemical staining of TNF-α, CD68, IL-1β, IL-6 and IL-13. Compared with the H22 group, distal tumors treated with PTT based on ICG/ICG-SF-Gel displayed a more obvious expression of TNF-α and GLP increased expression, suggesting that PTT based on ICG/ICG-SF-Gel could increase cellular immunity and GLP could enhance cellular immunity induced by PTT based on ICG/ICG-SF-Gel. Compared with ICG-based PTT, ICG-SF-Gel-based PTT increased the expression of TNF-α, indicating that ICG-SF-Gel-based PTT could induce cellular immunity more effectively than ICG-based PTT (**Figures 7A,F**). Compared with the H22 group, distal tumors treated with PTT based on ICG-SF-Gel displayed a more obvious expression of CD68 and GLP increased the expression of CD68 induced by ICG/ICG-SF-Gel based PTT, indicating that PTT based on ICG-SF-Gel could increase the infiltration of macrophages and GLP could enhance the infiltration of macrophages induced by ICG/ICG-SF-Gel based PTT (**Figures 7E,J**). Compared with the H22 group, distal tumors treated with PTT based on ICG/ICG-SF-Gel displayed a more obvious expression of IL-1β and GLP increased the expression of IL-1β induced by ICG-based PTT, indicating that PTT based on ICG/ICG-SF-Gel could increase the infiltration of M1 type macrophages and GLP could enhance the infiltration of M1 type macrophages induced by ICG-based PTT (**Figures 7B,G**). Compared with the H22 group, distal tumors treated with PTT based on ICG/ICG-SF-Gel displayed a more obvious expression of IL-6 and GLP increased expression, suggesting that PTT based on ICG/ICG-SF-Gel could increase the infiltration of M1 type macrophages and GLP could enhance the infiltration of M1 type macrophages induced by PTT based on ICG/ICG-SF-Gel (**Figures 7C,H**). Compared with the H22 group, distal tumors treated with PTT based on ICG/ICG-SF-Gel decreased the expression of IL-13 and GLP decreased the expression more obviously, indicating that PTT based on ICG/ICG-SF-Gel could inhibit the down-regulation of tumor immunosurveillance induced by IL-13 and GLP could enhance the inhibitory efficacy (**Figures 7D,I**). All these results suggested that the immune system plays an important role in ICG/ICG-SF-Gel-based PTT and GLP immunotherapy and GLP could enhance immune function. GLP may promote the secretion of IL-6, IL-1β and TNF-α by activating CD68 macrophages, reduce the inhibition of IL-13 secreted by natural killer T cells on tumor immune surveillance, strengthen the immune function of the body, and thus inhibit the growth of distal tumors.

Due to COVID-19 and other reasons, our experimental animals and cells suffered severe losses, which limited our research methods to immunohistochemical staining, unable to use other research methods to support the experimental results. Therefore, In the follow-up work, we will use more experimental methods to support the experimental results and conduct further research.

## CONCLUSION

In summary, we extracted SF from the Bombyx mori cocoons, prepared ICG-SF-Gel by ultrasonic oscillation and prepared GLP by heating dissolution. The UV absorbance of ICG and ICG-SF solution indicating that the successful encapsulation of ICG in SF solution and SF did not affect the UV absorbance of ICG. *In vitro* results showed that ICG could convert light to heat and ICG-SF-Gel may converge and accelerate the photothermal effect. To confirm the photothermal transformation of ICG and ICG-SF-Gel *in vivo*, we established a subcutaneous bilateral hepatic tumor model and shown a similar result. To investigate the antitumor efficiency, the primary and distal tumor growth rate and the mortality of mice were recorded. Results showed that PTT based on ICG/ICG-SF-Gel inhibited the growth of primary tumors and GLP could enhance the photothermal ablation efficacy. ICG-based PTT inhibited the growth of distal tumors and GLP could enhance the inhibitory effect. ICG-SF-Gel-based PTT had a stronger inhibitory effect on tumor growth than ICG-based PTT. ICG-based PTT and GLP therapy significantly resulted in improving the survival time. ICG-SF-Gel-based PTT with GLP can improve the survival time. And there were no significant body weight changes in the seven groups,

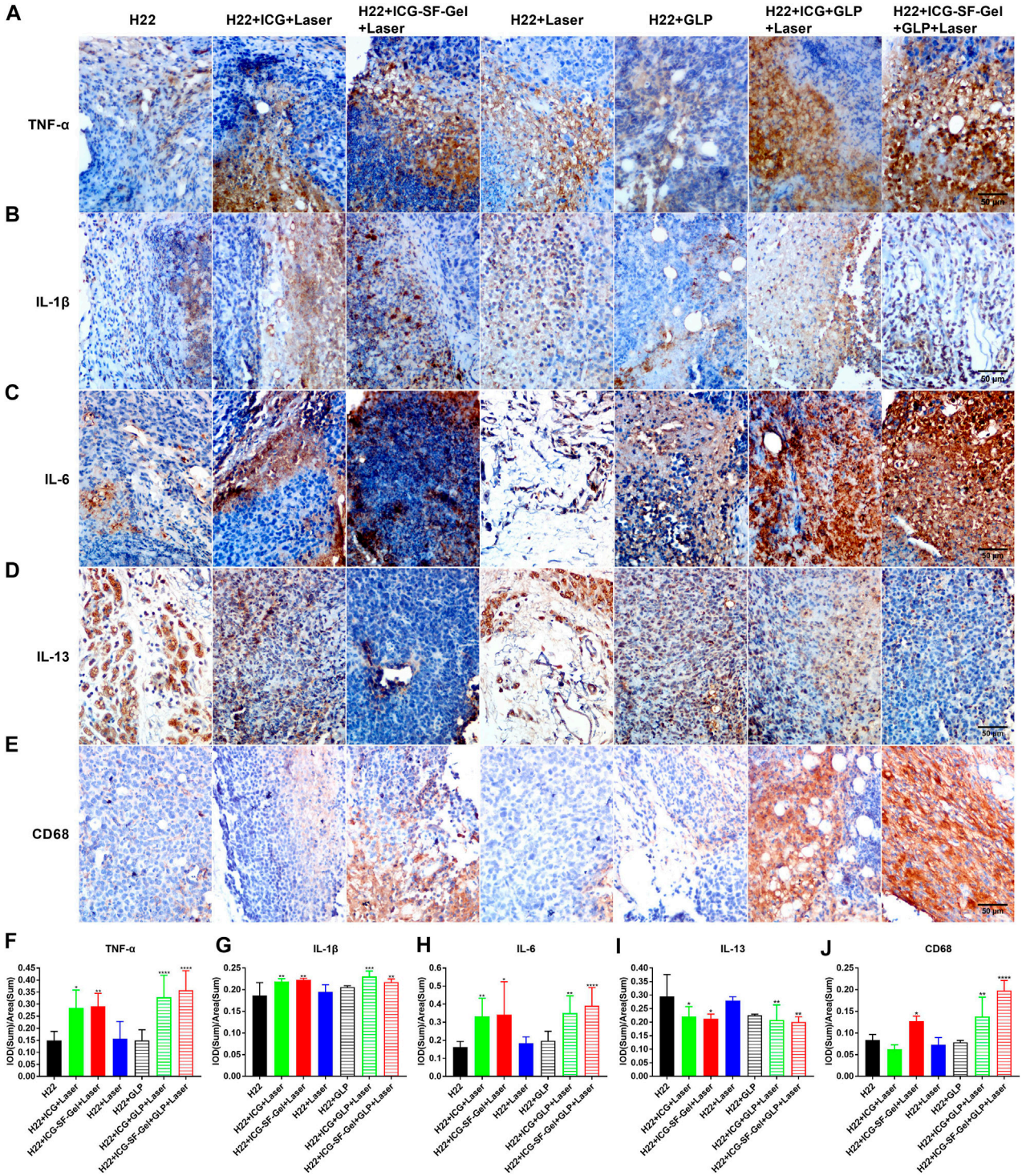


**FIGURE 7 |** The immune index of distal tumors after different treatments. **(A–E)** Immunohistochemical staining of TNF-α **(A)**, IL-1β **(B)**, IL-6 **(C)**, IL-13 **(D)** and CD68 **(E)** of distal tumors collected from different treated groups of mice 7 days after the distal tumor inoculation (The same row shared the same scale bar: 50 μm) and quantitative analysis of TNF-α **(F)**, IL-1β **(G)**, IL-6 **(H)**, IL-13 **(I)** and CD68 **(J)** ($n$ = 4 mice per group, data are presented as the mean ± SD. Statistical significance was expressed by $^{*}p < 0.05$, $^{**}p < 0.01$, $^{***}p < 0.001$ and $^{****}p < 0.0001$, comparing other groups with the H22 group).

indicating the fewer side effect of the treatments. To explore the distal antitumor mechanism of ICG/ICG-SF-Gel-based PTT and GLP immunotherapy, the distal tumors from different treatments were collected for HE staining and immunohistochemical staining of Ki-67, Caspase-3, BAX, bcl-2, PECAM-1, VEGFA, FGF-2, TNF-α, CD68, IL-1β, IL-6 and IL-13. Results showed that ICG/ICG-SF-Gel-based PTT induce tumor necrosis and GLP enhanced the photothermal efficacy. ICG/ICG-SF-Gel-based PTT inhibited cell proliferation and angiogenesis, induced cell apoptosis, enhanced cellular immunity, and GLP enhanced these effects. All in all, our results demonstrated that GLP could enhance the distal antitumor effect of PTT in hepatoma-bearing mice through immunomodulatory, anti-proliferative, pro-apoptotic and anti-angiogenic. The combination of PTT and immunomodulator GLP immunotherapy is potential photothermal immunotherapy on HCC.

## DATA AVAILABILITY STATEMENT

The raw data supporting the conclusion of this article will be made available by the authors, without undue reservation.

## ETHICS STATEMENT

The animal study was reviewed and approved by The Animal Experimentation Ethics Committee of Wenzhou Medical University.

## AUTHOR CONTRIBUTIONS

Investigation, Q-HX, M-QT, MY, RC, and D-LZ; writing-original draft preparation, Q-HX; writing-review and editing, Q-HX; supervision, C-TL and Y-ZZ; project administration, Y-ZZ; funding acquisition, QY, H-LX, and Y-ZZ. All authors have read and agreed to the published version of the manuscript.

## FUNDING

This research was supported by Zhejiang Provincial Natural Science Foundation (Grant Nos. LY19H180001, LQ19H300001 and LY20H300002), the key research and development program of Zhejiang province (Grant No. 2018C03013), Zhejiang provincial program for the cultivation of high-level innovative health talents (Y-ZZ), Wenzhou innovative technology project for high-level talents (Y-ZZ) and Wenzhou municipal science and technology bureau (Grant Nos. Y20190177, Y20180183).

## SUPPLEMENTARY MATERIAL

The Supplementary Material for this article can be found online at: https://www.frontiersin.org/articles/10.3389/fphar.2021.648708/full#supplementary-material

## REFERENCES

Baxevanis, C. N., Perez, S. A., and Papamichail, M. (2009). Cancer Immunotherapy. *Crit. Rev. Clin. Lab. Sci.* 46 (4), 167–189. doi:10.1080/10408360902937809

Bikfalvi, A. (1999). [Role of Fibroblast Growth Factor-2 in Tumor Angiogenesis]. *Pathol. Biol. (Paris)* 47 (4), 364–367.

Bray, F., Ferlay, J., Soerjomataram, I., Siegel, R. L., Torre, L. A., and Jemal, A. (2018). Global Cancer Statistics 2018: GLOBOCAN Estimates of Incidence and Mortality Worldwide for 36 Cancers in 185 Countries. *CA: A Cancer J. Clinicians* 68 (6), 394–424. doi:10.3322/caac.21492

Cao, G., Fehrenbach, M. L., Williams, J. T., Finklestein, J. M., Zhu, J.-X., and Delisser, H. M. (2009). Angiogenesis in Platelet Endothelial Cell Adhesion Molecule-1-Null Mice. *Am. J. Pathol.* 175 (2), 903–915. doi:10.2353/ajpath.2009.090206

Cao, Q.-z., and Lin, Z.-B. (2006). Ganoderma Lucidum Polysaccharides Peptide Inhibits the Growth of Vascular Endothelial Cell and the Induction of VEGF in Human Lung Cancer Cell. *Life Sci.* 78 (13), 1457–1463. doi:10.1016/j.lfs.2005.07.017

Carreno, B. M., Magrini, V., Becker-Hapak, M., Kaabinejadian, S., Hundal, J., Petti, A. A., et al. (2015). A Dendritic Cell Vaccine Increases the Breadth and Diversity of Melanoma Neoantigen-specific T Cells. *Science* 348 (6236), 803–808. doi:10.1126/science.aaa3828

Chang, Y. H., Yang, J. S., Yang, J. L., Wu, C. L., Chang, S. J., Lu, K. W., et al. (2009). Gandoderma Lucidum Extract Promotes Immune Responses in normal BALB/c Mice *In Vivo*. *In Vivo* 23 (5), 755–759. doi:10.1089/hum.2009.006

Chen, Q., Wang, C., Zhan, Z., He, W., Cheng, Z., Li, Y., et al. (2014). Near-infrared Dye Bound Albumin with Separated Imaging and Therapy Wavelength Channels for Imaging-Guided Photothermal Therapy. *Biomaterials* 35 (28), 8206–8214. doi:10.1016/j.biomaterials.2014.06.013

Chen, Q., Xu, L., Liang, C., Wang, C., Peng, R., and Liu, Z. (2016). Photothermal Therapy with Immune-Adjuvant Nanoparticles Together with Checkpoint Blockade for Effective Cancer Immunotherapy. *Nat. Commun.* 7, 13193. doi:10.1038/ncomms13193

Cicchelero, L., de Rooster, H., and Sanders, N. N. (2014). Various Ways to Improve Whole Cancer Cell Vaccines. *Expert Rev. Vaccin.* 13 (6), 721–735. doi:10.1586/14760584.2014.911093

Compte, M., Harwood, S. L., Muñoz, I. G., Navarro, R., Zonca, M., Perez-Chacon, G., et al. (2018). A Tumor-Targeted Trimeric 4-1bb-Agonistic Antibody Induces Potent Anti-tumor Immunity without Systemic Toxicity. *Nat. Commun.* 9 (1), 4809. doi:10.1038/s41467-018-07195-w

DeFrancesco, L. (2014). CAR-T Cell Therapy Seeks Strategies to Harness Cytokine Storm. *Nat. Biotechnol.* 32 (7), 604. doi:10.1038/nbt0714-604

Deng, K., Hou, Z., Deng, X., Yang, P., Li, C., and Lin, J. (2015). Enhanced Antitumor Efficacy by 808 Nm Laser-Induced Synergistic Photothermal and Photodynamic Therapy Based on a Indocyanine-Green-Attached W18O49Nanostructure. *Adv. Funct. Mater.* 25 (47), 7280–7290. doi:10.1002/adfm.201503046

Ellebaek, E., Andersen, M. H., Svane, I. M., and Straten, P. t. (2012). Immunotherapy for Metastatic Colorectal Cancer: Present Status and New Options. *Scand. J. Gastroenterol.* 47 (3), 315–324. doi:10.3109/00365521.2012.640831

Fang, R. H., Hu, C.-M. J., Luk, B. T., Gao, W., Copp, J. A., Tai, Y., et al. (2014). Cancer Cell Membrane-Coated Nanoparticles for Anticancer Vaccination and Drug Delivery. *Nano Lett.* 14 (4), 2181–2188. doi:10.1021/nl500618u

Gao, Y., Gao, H., Chan, E., Tang, W., Xu, A., Yang, H., et al. (2005). Antitumor Activity and Underlying Mechanisms of Ganopoly, the Refined Polysaccharides Extracted from Ganoderma Lucidum, in Mice. *Limm* 34 (2), 171–198. doi:10.1081/imm-200055813

Goncalves, M. D., Lu, C., Tutnauer, J., Hartman, T. E., Hwang, S.-K., Murphy, C. J., et al. (2019). High-fructose Corn Syrup Enhances Intestinal Tumor Growth in Mice. *Science* 363 (6433), 1345–1349. doi:10.1126/science.aat8515

Gubin, M. M., Zhang, X., Schuster, H., Caron, E., Ward, J. P., Noguchi, T., et al. (2014). Checkpoint Blockade Cancer Immunotherapy Targets Tumour-specific Mutant Antigens. *Nature* 515 (7528), 577–581. doi:10.1038/nature13988

Guo, L., Yan, D. D., Yang, D., Li, Y., Wang, X., Zalewski, O., et al. (2014). Combinatorial Photothermal and Immuno Cancer Therapy Using Chitosan-Coated Hollow Copper Sulfide Nanoparticles. *ACS Nano* 8 (6), 5670–5681. doi:10.1021/nn5002112

Hoos, A. (2007). A Clinical Development Paradigm for Cancer Vaccines and Related Biologics. *Eur. J. Cancer Supplements* 5 (9), 5–7. doi:10.1016/j.ejcsup.2007.09.031

Huang, C.-Y., Chen, J. Y.-F., Wu, J.-E., Pu, Y.-S., Liu, G.-Y., Pan, M.-H., et al. (2010). Ling-Zhi Polysaccharides Potentiate Cytotoxic Effects of Anticancer Drugs against Drug-Resistant Urothelial Carcinoma Cells. *J. Agric. Food Chem.* 58 (15), 8798–8805. doi:10.1021/jf1020158

Huang, Q., Li, F., Liu, X., Li, W., Shi, W., Liu, F.-F., et al. (2011). Caspase 3-mediated Stimulation of Tumor Cell Repopulation during Cancer Radiotherapy. *Nat. Med.* 17 (7), 860–866. doi:10.1038/nm.2385

Hynynen, K., and Lulu, B. A. (1990). Hyperthermia in Cancer Treatment. *Invest. Radiol.* 25 (7), 824–834. doi:10.1097/00004424-199007000-00014

Kim, D. K., Kim, J. I., Hwang, T. I., Sim, B. R., and Khang, G. (2017). Bioengineered Osteoinductive Broussonetia kazinoki/Silk Fibroin Composite Scaffolds for Bone Tissue Regeneration. *ACS Appl. Mater. Inter.* 9 (2), 1384–1394. doi:10.1021/acsami.6b14351

Kun, S. (2015). Nanoparticle-based Immunotherapy for Cancer. *ACS nano* 1 (9). 16-30. doi:10.1021/nn5062029

Ledford, H. (2013). Immunotherapy's Cancer Remit Widens. *Nature* 497 (7451), 544. doi:10.1038/497544a

Ledford, H. (2015). Therapeutic Cancer Vaccine Survives Biotech Bust. *Nature* 519 (7541), 17–18. doi:10.1038/nature.2015.16990

Lin, Z. B., and Zhang, H. N. (2004). Anti-tumor and Immunoregulatory Activities of Ganoderma Lucidum and its Possible Mechanisms. *Acta Pharmacol. Sin* 25 (11), 1387–1395. doi:10.1016/j.ejphar.2004.09.008

Martínez-Montemayor, M. M., Acevedo, R. R., Otero-Franqui, E., Cubano, L. A., and Dharmawardhane, S. F. (2011). Ganoderma Lucidum (Reishi) Inhibits Cancer Cell Growth and Expression of Key Molecules in Inflammatory Breast Cancer. *Nutr. Cancer* 63 (7), 1085–1094. doi:10.1080/01635581.2011.601845

Matsumoto, A., Chen, J., Collette, A. L., Kim, U.-J., Altman, G. H., Cebe, P., et al. (2006). Mechanisms of Silk Fibroin Sol–Gel Transitions. *J. Phys. Chem. B* 110 (43), 21630–21638. doi:10.1021/jp056350v

Maude, S. L., Frey, N., Shaw, P. A., Aplenc, R., Barrett, D. M., Bunin, N. J., et al. (2014). Chimeric Antigen Receptor T Cells for Sustained Remissions in Leukemia. *N. Engl. J. Med.* 371 (16), 1507–1517. doi:10.1056/NEJMoa1407222

Momin, N., Mehta, N. K., Bennett, N. R., Ma, L., Palmeri, J. R., Chinn, M. M., et al. (2019). Anchoring of Intratumorally Administered Cytokines to Collagen Safely Potentiates Systemic Cancer Immunotherapy. *Sci. Transl. Med.* 11 (498), eaaw2614. doi:10.1126/scitranslmed.aaw2614

Montero, E., Alonso, L., Perez, R., and Lage, A. (2007). Interleukin-2 Mastering Regulation in Cancer and Autoimmunity. *Ann. N.Y Acad. Sci.* 1107, 239–250. doi:10.1196/annals.1381.026

Ola, M. S., Nawaz, M., and Ahsan, H. (2011). Role of Bcl-2 Family Proteins and Caspases in the Regulation of Apoptosis. *Mol. Cel Biochem* 351 (1-2), 41–58. doi:10.1007/s11010-010-0709-x

Palucka, K., and Banchereau, J. (2014). Cancer Immunotherapy via Dendritic Cells. *Interaction of Immune and Cancer Cells* 12 (4), 75–89. doi:10.1007/978-3-7091-1300-4_4

Restifo, N. P., Dudley, M. E., and Rosenberg, S. A. (2012). Adoptive Immunotherapy for Cancer: Harnessing the T Cell Response. *Nat. Rev. Immunol.* 12 (4), 269–281. doi:10.1038/nri3191

Ribas, A., and Wolchok, J. D. (2018). Cancer Immunotherapy Using Checkpoint Blockade. *Science* 359 (6382), 1350–1355. doi:10.1126/science.aar4060

Rojas, J. E. U., Gerbelli, B. B., Ribeiro, A. O., Nantes-Cardoso, I. L., Giuntini, F., and Alves, W. A. (2019). Silk Fibroin Hydrogels for Potential Applications in Photodynamic Therapy. *Biopolymers* 110 (2), e23245. doi:10.1002/bip.23245

Rongshou, Z., Kexin, S., Siwei, Z., Hongmei, Z., Xiaonong, Z., Ru, C., et al. (2019). Report of Cancer Epidemiology in China. *Chin. J. Oncol.* 41 (1), 19–28. doi:10.3760/cma.j.issn.0253-3766.2019.01.005

Shah, N. N., and Fry, T. J. (2019). Mechanisms of Resistance to CAR T Cell Therapy. *Nat. Rev. Clin. Oncol.* 16 (6), 372–385. doi:10.1038/s41571-019-0184-6

Sliwkowski, M. X., and Mellman, I. (2013). Antibody Therapeutics in Cancer. *Science* 341 (6151), 1192–1198. doi:10.1126/science.1241145

Sobecki, M., Mrouj, K., Camasses, A., Parisis, N., Nicolas, E., Llères, D., et al. (2016). The Cell Proliferation Antigen Ki-67 Organises Heterochromatin. *Elife* 5. doi:10.7554/eLife.13722

Sohretoglu, D., and Huang, S. (2018). Ganoderma Lucidum Polysaccharides as an Anti-cancer Agent. *Acamc* 18 (5), 667–674. doi:10.2174/1871520617666171113121246

Suarez-Arroyo, I. J., Rosario-Acevedo, R., Aguilar-Perez, A., Clemente, P. L., Cubano, L. A., Serrano, J., et al. (2013). Anti-tumor Effects of Ganoderma Lucidum (Reishi) in Inflammatory Breast Cancer in *In Vivo* and *In Vitro* Models. *PLoS One* 8 (2), e57431. doi:10.1371/journal.pone.0057431

Tabrizian, P., Jibara, G., Shrager, B., Schwartz, M., and Roayaie, S. (2015). Recurrence of Hepatocellular Cancer after Resection. *Ann. Surg.* 261 (5), 947–955. doi:10.1097/SLA.0000000000000710

Terabe, M., Matsui, S., Noben-Trauth, N., Chen, H., Watson, C., Donaldson, D. D., et al. (2000). NKT Cell-Mediated Repression of Tumor Immunosurveillance by IL-13 and the IL-4R-STAT6 Pathway. *Nat. Immunol.* 1 (6), 515–520. doi:10.1038/82771

Terabe, M., Park, J. M., and Berzofsky, J. A. (2004). Role of IL-13 in Regulation of Anti-tumor Immunity and Tumor Growth. *Cancer Immunol. Immunother.* 53 (2), 79–85. doi:10.1007/s00262-003-0445-0

Twumasi-Boateng, K., Pettigrew, J. L., Kwok, Y. Y. E., Bell, J. C., and Nelson, B. H. (2018). Oncolytic Viruses as Engineering Platforms for Combination Immunotherapy. *Nat. Rev. Cancer* 18 (7), 419–432. doi:10.1038/s41568-018-0009-4

Wang, C., Shi, S., Chen, Q., Lin, S., Wang, R., Wang, S., et al. (2018). Antitumor and Immunomodulatory Activities of Ganoderma Lucidum Polysaccharides in Glioma-Bearing Rats. *Integr. Cancer Ther.* 17 (3), 674–683. doi:10.1177/1534735418762537

Wang, S.-Y., Hsu, M.-L., Hsu, H.-C., Lee, S.-S., Shiao, M.-S., Ho, C.-K., et al. (1997). The Anti-tumor Effect of Ganoderma Lucidum Is Mediated by Cytokines Released from Activated Macrophages and T Lymphocytes. *Int. J. Cancer* 70 (6), 699–705. doi:10.1002/(sici)1097-0215(19970317)70:6<699::aid-ijc12>3.0.co;2-5

Weng, C.-J., and Yen, G.-C. (2010). The *In Vitro* and *In Vivo* Experimental Evidences Disclose the Chemopreventive Effects of Ganoderma Lucidum on Cancer Invasion and Metastasis. *Clin. Exp. Metastasis* 27 (5), 361–369. doi:10.1007/s10585-010-9334-z

Xiang, J., Xu, L., Gong, H., Zhu, W., Wang, C., Xu, J., et al. (2015). Antigen-Loaded Upconversion Nanoparticles for Dendritic Cell Stimulation, Tracking, and Vaccination in Dendritic Cell-Based Immunotherapy. *ACS Nano* 9 (6), 6401–6411. doi:10.1021/acsnano.5b02014

Xu, H.-L., ZhuGe, D.-L., Chen, P.-P., Tong, M.-Q., Lin, M.-T., Jiang, X., et al. (2018). Silk Fibroin Nanoparticles Dyeing Indocyanine green for Imaging-Guided Photo-thermal Therapy of Glioblastoma. *Drug Deliv.* 25 (1), 364–375. doi:10.1080/10717544.2018.1428244

Yao, Q., Lan, Q.-H., Jiang, X., Du, C.-C., Zhai, Y.-Y., Shen, X., et al. (2020). Bioinspired Biliverdin/silk Fibroin Hydrogel for Antiglioma Photothermal Therapy and Wound Healing. *Theranostics* 10 (25), 11719–11736. doi:10.7150/thno.47682

Yata, T., Takahashi, Y., Tan, M., Nakatsuji, H., Ohtsuki, S., Murakami, T., et al. (2017). DNA Nanotechnology-Based Composite-type Gold Nanoparticle-Immunostimulatory DNA Hydrogel for Tumor Photothermal Immunotherapy. *Biomaterials* 146, 136–145. doi:10.1016/j.biomaterials.2017.09.014

You, J., Zhang, R., Xiong, C., Zhong, M., Melancon, M., Gupta, S., et al. (2012). Effective Photothermal Chemotherapy Using Doxorubicin-Loaded Gold Nanospheres that Target EphB4 Receptors in Tumors. *Cancer Res.* 72 (18), 4777–4786. doi:10.1158/0008-5472.CAN-12-1003

Yucel, T., Lovett, M. L., and Kaplan, D. L. (2014). Silk-based Biomaterials for Sustained Drug Delivery. *J. Controlled Release* 190, 381–397. doi:10.1016/j.jconrel.2014.05.059

Zhang, J., Tang, Q., Zhou, C., Jia, W., Da Silva, L., Nguyen, L. D., et al. (2010). GLIS, a Bioactive Proteoglycan Fraction from Ganoderma Lucidum, Displays Anti-tumour Activity by Increasing Both Humoral and Cellular Immune Response. *Life Sci.* 87 (19-22), 628–637. doi:10.1016/j.lfs.2010.09.026

Zhang, Z., Wang, J., Nie, X., Wen, T., Ji, Y., Wu, X., et al. (2014). Near Infrared Laser-Induced Targeted Cancer Therapy Using Thermoresponsive Polymer

Encapsulated Gold Nanorods. *J. Am. Chem. Soc.* 136 (20), 7317–7326. doi:10.1021/ja412735p

Zhou, F., Wu, S., Song, S., Chen, W. R., Resasco, D. E., and Xing, D. (2012). Antitumor Immunologically Modified Carbon Nanotubes for Photothermal Therapy. *Biomaterials* 33 (11), 3235–3242. doi:10.1016/j.biomaterials.2011.12.029

Zhu, G., Zhang, F., Ni, Q., Niu, G., and Chen, X. (2017). Efficient Nanovaccine Delivery in Cancer Immunotherapy. *ACS Nano* 11 (3), 2387–2392. doi:10.1021/acsnano.7b00978

Zong, Z., Zou, J., Mao, R., Ma, C., Li, N., Wang, J., et al. (2019). M1 Macrophages Induce PD-L1 Expression in Hepatocellular Carcinoma Cells through IL-1β Signaling. *Front. Immunol.* 10, 1643. doi:10.3389/fimmu.2019.01643

**Conflict of Interest:** The authors declare that the research was conducted in the absence of any commercial or financial relationships that could be construed as a potential conflict of interest.

frontiers in Oncology

REVIEW
published: 08 July 2021
doi: 10.3389/fonc.2021.698946

# Role of Sex in the Therapeutic Targeting of p53 Circuitry

*Francesca Mancini[1*†], Ludovica Giorgini[2,3†], Emanuela Teveroni[1], Alfredo Pontecorvi[3‡] and Fabiola Moretti[2*‡]*

*[1] Research Unit on Human Reproduction, International Scientific Institute Paul VI, Fondazione Policlinico A. Gemelli, IRCCS, Rome, Italy, [2] Institute of Biochemistry and Cell Biology, National Research Council of Italy, Monterotondo, Italy, [3] Catholic University of the Sacred Heart of Rome, Fondazione Policlinico A. Gemelli, IRCCS, Rome, Italy*

Sex profoundly affects cancer incidence and susceptibility to therapy, with sex hormones highly contributing to this disparity. Various studies and omics data suggest a relationship between sex and the oncosuppressor p53 circuitry, including its regulators MDM2 and MDM4. Association of this network with genetic variation underlies sex-related altered cancer risk, age of onset, and cancer sensitivity to therapy. Moreover, sex-related factors, mainly estrogenic hormones, can affect the levels and/or function of the p53 network both in hormone-dependent and independent cancer. Despite this evidence, preclinical and clinical studies aimed to evaluate p53 targeted therapy rarely consider sex and related factors. This review summarizes the studies reporting the relationship between sex and the p53 circuitry, including its associated regulators, MDM2 and MDM4, with particular emphasis on estrogenic hormones. Moreover, we reviewed the evaluation of sex/hormone in preclinical studies and clinical trials employing p53-target therapies, and discuss how patients' sex and hormonal status could impact these therapeutic approaches.

**Keywords: cancer therapy, p53, sex, estrogen, MDM2, MDM4**

OPEN ACCESS

***Edited by:***
*Aniello Cerrato, Istituto per l'Endocrinologia e l'oncologia "Gaetano Salvatore (CNR), Italy*

***Reviewed by:***
*Lawrence Panasci, Segal Cancer Centre, Canada*
*Francesca Maffei, University of Bologna, Italy*

****Correspondence:***
*Fabiola Moretti*
*fabiola.moretti@cnr.it*
*Francesca Mancini*
*mancini.chicca@gmail.com*

*†These authors share first authorship*

*‡These authors share last authorship*

***Specialty section:***
*This article was submitted to Pharmacology of Anti-Cancer Drugs, a section of the journal Frontiers in Oncology*

***Received:*** *22 April 2021*
***Accepted:*** *16 June 2021*
***Published:*** *08 July 2021*

***Citation:***
*Mancini F, Giorgini L, Teveroni E, Pontecorvi A and Moretti F (2021) Role of Sex in the Therapeutic Targeting of p53 Circuitry. Front. Oncol. 11:698946. doi: 10.3389/fonc.2021.698946*

## INTRODUCTION

Cancer statistics reveal sex (meant as biological factors) differences in incidence, therapy response, and mortality of many cancers (1). The majority of these tumors, excluding sex-related prostate ovary and breast cancer, present a higher incidence, increased invasive property, and cancer death in males compared to female, even after correction for environmental exposures and risk habits, as smoking and alcohol consumption, more common among men (2). Primarily, genetic factors residing on sex chromosomes contribute to these disparities (3). Indeed, the X chromosome contains various genes involved in oncogenesis (4). Since a percentage of genes is not silenced in inactivated X-chromosome, their higher expression levels in females compared to males may underlie cancer differences (4, 5).

Additionally, an important factor contributing to sexual differentiation is the circulating sex hormones with a strong relevance of estrogen (6, 7). Women have a higher risk of developing lung cancer upon smoking than men. Various studies suggest that the interaction between tobacco carcinogens and endogenous and exogenous sex steroids may be relevant (8). Nonetheless, this disparity persists among adults aged 85 and older, thus beyond the women's reproductive age (9).

The levels of intra-tissue sex hormones determined by local production of the estrogen (intracrinology) are assuming great importance in many hormone-related tumors (10, 11). Finally, epigenetic modification of DNA is different in the two sexes with DNA methylation enhanced in various organs of experimental feminine rodents. Since cancer is linked to epigenetic dysregulation, these differences play an important function, too [reviewed in (5)].

All these factors can variously affect molecular pathways involved in oncogenesis. The p53 pathway is one of the most relevant in tumor development and therapy response, and p53 is a crucial oncosuppressor in both humans and rodents (12, 13). TP53 gene is mutated in about 50% of human cancers, while the protein is inactivated in tumors bearing wild-type p53 (wt-p53). One of the most frequent inactivation mechanisms of wt-p53 is the overexpression of its negative regulators, MDM2 and MDM4 (also MDMX). These two proteins form a heterodimer that controls p53 activity and levels. In addition, the two proteins function singularly towards p53 with different outcomes depending on the tissue (14, 15). Given its relevance, re-activation of wt-p53 oncosuppressive activity is a field of intense study. In tumors retaining wt-p53, most of the approaches target the inhibitory proteins MDM2/MDM4, either singularly or in combination [reviewed in (16, 17)]. These approaches apply mainly to solid tumors as myeloma, melanoma, and liposarcoma, although some trials have also been applied to acute myeloid leukemia (AML) (for details, see *Therapies Directed to wt-p53 Re-Activation*). Unfortunately, at present, none of these therapeutic approaches have reached the patient's bed.

Over time, different studies have demonstrated crosstalk between p53/MDM2/MDM4 and sex. Although p53 and its regulators MDM2 and MDM4 genes reside on autosomes, genes associated with p53 circuitry reside on the X chromosome, affecting its function in a sex-related manner. Moreover, genetic variations in the p53/MDM2/MDM4 genes (in the promoter, 3′UTR region, introns, or coding sequence) are responsive to hormone status, affecting p53/MDM4/MDM2 levels and function. Despite all these data, sex differences are not consistently evaluated in preclinical and clinical trials targeting the p53 circuitry.

In this review, we summarize data regarding sex-related factors associated with wt-p53, MDM2, and MDM4. Particularly, we recapitulate the sex-related factors that can affect p53 function by acting on p53 itself or its regulators MDM2 and MDM4. Moreover, we will review sex differences in therapeutic approaches aimed to reactivate wt-p53 and discuss how the consideration of sex could affect the results of these approaches.

## EFFECTS OF SEX ON P53 CIRCUITRY

### p53

Given the importance of the oncosuppressor p53 in counteracting cancer development, many studies investigated the association of p53 status with sex-related genetic factors and the potential effect of sex-related factors on p53 function.

#### Genetic Factors

A direct association of p53 status with sex-associated cancer difference has been reported in various tumors. In lung cancer, p53 mutations are more frequent in females than in males [reviewed in (8)]. Also, females carrying mutant p53 have an increased risk of developing adrenocortical carcinoma (ACC), suggesting that the p53 oncosuppressive activity impacts ACC development more strongly in females than in males (18). Since ACC risk is also increased in females of pediatric age (19), factors other than sex hormones likely affect p53 function in ACC in a sex-related way (5). At present, these factors have not been identified.

In exon 4 of the p53 gene, the SNP-R72P is present (**Table 1**). The R72 variant possesses higher ability to induce apoptosis compared to P72 [reviewed in (20)]. A hospital-based case–control study of hepatocellular carcinoma (HCC) development in a Turkish population demonstrated that the P72 homozygote ($p53^{Pro/Pro}$) is associated with increased HCC risk in males but not in females (21). A similar association of the variant alleles (P/R + P/P) has been found with a particular squamous cell carcinoma (Kangri cancer) in Indian male subjects (22). These studies suggest that the penetrance/efficacy of the $p53^{Pro/Pro}$ variant is different among male and female subjects. Which factors, genetic or hormonal, alter the $p53^{Pro/Pro}$ activity is currently unknown. It has been proposed that biallelic expression of X-linked tumor-suppressor genes in females explains a portion of the reduced cancer incidence in females compared to males across various tumor types (4). Recently, Haupt and collaborators reported X-linked genes associated with the p53 network. Starting from bio-informatic analyses, they showed that in many non-reproductive cancer histotypes, p53 mutation is more frequent in males than in females with a concomitant lower survival rate (23). Then, they identified X-linked genes encoding for proteins essential for genomic fidelity that are connected to p53. Due to the chromosome X inactivation, females are protected from these gene germline mutations, while males are exposed to a higher risk because they have only a single copy of the X chromosome. The underlying hypothesis is that this link brings to enhanced selection of p53 inactivation in men. This phenomenon is not evident in hormone-dependent tumors since in male breast cancer the frequency of p53 inactivation is reduced compared to females (24). Molecular proof of the ability of these X-linked genes to confer p53-mediated increased protection from cancer in the female gender has not yet been provided.

#### Hormone Activity

Many studies investigated the effect of sex hormones, especially estrogen, on p53 function (25). The picture deriving from these studies is very complex, in some cases reporting opposite results. An important factor that may contribute to this inconsistency is the type of estrogen receptor involved. Indeed, estrogen activity is mediated by the membrane-bound G protein-coupled estrogen

**TABLE 1** | Summary of p53, MDM2, MDM4 SNPs relevant to cancer in a sex/hormone-related way.

| Gene name | SNP | Variant | Location | Genetic consequence | Cytogenetic region | Alleles | Minor allele | MAF (minor allele frequency)[§] | SNP-linked cancer* |
|---|---|---|---|---|---|---|---|---|---|
| P53 | SNP-R72P | rs1042522 | chr17:7676154 | Missense variant | 17p13.1 | G>A/G>C/G>T | G | G = 0.4571 (1,000G) | Hepatocellular carcinoma (HCC), squamous cell carcinoma (Kangri cancer) |
| MDM2 | SNP309 | rs2279744 | chr12:68808800 | Intron variant | 12q15 | T>G | G | G = 0.3666 (1,000G) | Diffuse large B cell lymphoma, soft tissue sarcoma, ER+ invasive ductal adenocarcinoma (IDC), colorectal cancer, pancreatic ductal adenocarcinoma (PDAC), skin squamous cell carcinoma |
| MDM2 | SNP285 | rs117039649 | chr12:68808776 | Intron variant | 12q15 | G>C | C | C = 0.0134 (1 000G) | |
| MDM2 | SNP55 | rs2870820 | chr12:68808546 | Intron variant | 12q15 | C>T | T | T = 0.2322 | Colon cancer |
| MDM4 | SNP34091 | rs4245739 | chr1:204549714 | 3' UTR | 1q32.1 | C>A/C>G/C>T | C | C = 0.2141 (1,000G) | ER$^-$ breast cancer, prostate cancer, ovarian cancers |
| MDM4 | SNPrs2290854 | rs2290854 | chr1:204546897 | Intron variant | 1q32.1 | A>C/A>G | A | A = 0.4607 (1,000G) | BRCA-1-associated breast cancer |
| MDM4 | SNPrs4252707 | rs4252707 | chr1:204539019 | Intron variant | 1q32.1 | G>A | A | A = 0.2196 | Glioma |

*[§]MAF (minor allele frequency) from 1,000 Genomes from 26 different populations divided into five super populations: African, Ad Mixed American, East Asian, European, South Asian; *Tumor histotypes in which the SNP is associated with increased cancer risk.*

receptor 1 (GPER or GP3R0) and the nuclear estrogen receptors (ERs) $\alpha$ and $\beta$ (ER$\alpha$, ER$\beta$), with ER$\beta$ often exhibiting opposite activity to ER$\alpha$. Hormone-stimulated nuclear ERs translocate into the nucleus and direct transcription as homo- and heterodimers or as partners of other transcription factors (indirect genomic signaling) (26). Additionally, the two nuclear receptor genes (named ESR1 and ESR2 corresponding to ER$\alpha$ and ER$\beta$, respectively) originate alternative forms that can interact with the full-length receptors and repress their function. Therefore, the studies performed by stimulation with 17$\beta$-estradiol (E2, the primary estrogenic hormone that interacts with all estrogen receptors) without characterization of the receptor and the ER$\alpha$ and ER$\beta$ isoforms present in the system can be variously interpreted. An additional factor that adds complexity to the interpretation of estrogen activity towards p53 is the positive regulation of MDM2 levels by estrogens (see relative paragraph *MDM2*). Since MDM2 is a negative regulator of p53, the fine-tuning of MDM2 and p53 by estrogens can result in different outcomes.

Since ER$\alpha$ is a critical therapeutic target in hormone-responsive breast and endometrial cancers, many data described in literature investigated the interplay between p53 and ER$\alpha$. Particularly, since p53 mutation is not common in estrogen-responsive breast cancer, accounting for about 20% of tumors (27, 28), many studies focused on this tissue.

Two main and opposite estrogenic hormone activities towards p53 have been described: a positive activity at different levels and a repressive activity mainly related to p53-transcriptional function.

### *Cooperative Estrogen-p53 Activity*

As concerns the mechanism of cooperation, there are various studies from Olivier's group (29–31). In cell lines derived from breast cancer MCF7 cells, they demonstrated that estrogen through endogenous ER$\alpha$ increases p53 levels and enhances p53-mediated response to DNA damage. They further showed that focal adhesion kinase (FAK), a critical regulator of adhesion and motility, is downregulated by p53 in response to E2 (31). These studies have been further confirmed by Berger and colleagues, who demonstrated that the p53 promoter contains four ER$\alpha$ responsive elements (ERE) (32). Accordingly, knockdown of ER$\alpha$ leads to decreased p53 mRNA and protein levels and its targets, MDM2 and p21. This results in increased colony formation in an estrogen-free medium upon a cytostatic dose (100–400 nM) of doxorubicin (32). Of note, these authors demonstrate that the ER$\beta$ receptor is not involved since its exogenous expression does not alter p53 levels and activity. In support of this data, Klaus and colleagues analyzed the radiation-responsiveness of the mammary epithelium in ovariectomized mice upon E2 and progesterone (P) treatment (33). These hormones activate the p53 response to radiation in terms of increased p21. Also, by comparing the mammary epithelium of BALB/c mice with different p53 status (Trp53$^{+/+}$, Trp53$^{+/-}$, Trp53$^{-/-}$), they demonstrated that E + P upregulated p53 nuclear levels and apoptosis upon ionizing radiation, also in the haploinsufficient background (BALB/c Trp53$^{+}$/$^{-}$) (34). Interestingly, parity acted similarly and delayed the onset of spontaneous mammary tumors in these mice, confirming a protective role of hormones towards breast cancer development.

Similar data were obtained by Sivaraman using the rat model (35). Importantly, epidemiologic studies show that women with full-term pregnancy have a significantly reduced risk of developing $ER^+$ breast cancer (36). In agreement with these studies, Kupperwasser and colleagues reported that mare serum gonadotropin (PMSG) and human gonadotropin (hCG) treatment increases p53 nuclear fraction leading to enhanced mammary gland apoptosis following ionizing radiation (37). Interestingly, a recent proteome analysis of MCF-7 cells demonstrated that estrogen modulates cyto-nuclear shuttling; in response to estrogen, dynamic subcellular redistribution of proteins is the major phenomenon compared to the alteration of protein levels (38). Overall, this data strongly supports that estrogen enhances the oncosuppressive function of p53 in the breast tissue. Also, in another normal epithelial context as Young Adult Mouse Colon cells (YAMC), estrogen induces p53 downstream targets as PUMA, Bcl-2-associated X protein (Bax), and Noxa, and sensitizes cells to p53-mediated apoptosis (39), extending the cooperative function of p53 and estrogen in another epithelium. The good prognosis of $ER\alpha^+$/wt-p53 breast cancer can also be related to a cooperative activity between these two factors. To integrate this hypothesis, p53 inhibits ER$\alpha$ transcriptional activity on synthetic estrogen-responsive elements (40), suggesting a tumor-suppressive function of p53 towards ER$\alpha$ in hormone-activated signaling pathways.

This data raises a question about the consequences on p53 of anti-estrogenic therapies in breast cancer (41). Since these drugs antagonize ER function, they should reduce p53 oncosuppressive activity. The observation that anti-estrogenic therapy displays partial agonist activity in a gene-specific and tissue-specific manner partly solves this issue (42). In this regard, Olivier's group demonstrated that 4-hydroxy-tamoxifen (OHT), a selective estrogen receptor modulator (SERM), suppresses cell proliferation more effectively in breast cancer cell lines bearing wild-type p53 compared to cells with mutated p53. Furthermore, p53 expression levels have been reported as a positive prognostic factor for OHT treatment (43). Conversely, the activity of fulvestrant (ICI 182,780), a selective estrogen receptor degrader (SERD) that acts by inducing degradation of nuclear estrogen receptors is independent of p53 status (30). This data suggests that the p53-estrogen crosstalk is differently affected by estrogen, OHT, and fulvestrant, and supports the efficacy of anti-estrogenic therapies in wt-p53 breast cancer.

By considering hepatic tissue, Pok and colleagues showed that testosterone positively regulates hepatocyte cell cycle regulators and reduces p53 and p21, while E2 plays the opposite effect (44). Accordingly, in liver cancer cell lines, E2, *via* ER$\alpha$, activates the transcription of p53 and its target miR-23a, promoting p53-dependent apoptosis and, in turn, inhibiting HCC development (45). Since men are more susceptible than women to hepatocellular carcinoma (HCC) at age <60 years (46), this data supports a protective role of estrogenic hormones in liver cancer risk and highlights a possible mechanism by which sex hormones contribute to establishing the male prevalence of hepatocarcinoma.

Few studies analyzed the effects of ER$\beta$ on p53. In colon cancer cell lines, ER$\beta$ overexpression enhances p53 levels and activity through p14ARF-mediated downregulation of MDM2. Of note, this cell outcome was observed in many but not all colon cancer cell lines analyzed. The reason for these results remains unexplained (47). Similarly, in the human colon metastatic LoVo cell line, overexpression of ER$\beta$ enhances p53-mediated apoptosis in an estrogen-dependent manner (48). Overall, these studies indicate a proapoptotic function and anti-oncogenic activity of ER$\beta$ towards p53 although in tissues other than the breast.

### *Antagonistic Estrogen-p53 Activity*

Opposite to this view, Das's group reported that ER$\alpha$ inhibits p53 function on some transcriptional targets (49). The model proposed by these authors is that ER$\alpha$ and p53 cooperatively bind on the promoters of some p53-targets genes at whose levels ER$\alpha$ represses p53 activity. In most of these studies, cell outcome is not reported, so they are not entirely comparable to previous studies. One limitation of these studies is that they are often based on ER$\alpha$ overexpression. Indeed, in MCF7 without ER$\alpha$ overexpression, endogenous ER$\alpha$ does not affect p53 transcriptional function following E2 or fulvestrant treatments (50). A further explanation can derive from studies of Brown's group (51). They demonstrated in MCF7 that E2 and OHT reduce the apoptosis induced by cytotoxic high dose of doxorubicin (10 μM) whereas fulvestrant is inefficacious. Using genome-wide approaches, they reported the modulation of a subset of p53 and ER target genes, but not changes of p53 levels and its binding to these gene promoters. This data suggests that different p53 targets can be variously regulated upon specific estrogen treatments, leading to different cell outcomes. Also, Lewandowski and collaborators reported an antagonistic activity of estrogen towards p53. In MCF7 cells, E2, through ER$\alpha$, mediates the relocalization of p53 from the nucleus to the cytoplasm, inhibiting its transcriptional activity as revealed by decreased p21 levels. This, in turn, results in reduced sensitivity of MCF7 to TNF-mediated cell death while ER$\beta$ behaves oppositely, antagonizing cytoplasmic relocalization of p53 (52). Interestingly, a study from Bargonetti's group demonstrated that in MCF7, estrogen-induced cell proliferation and downregulation of p21 are p53-independent but MDM2 dependent (53). Therefore, E2-induced p21 modulation as a marker of p53 activity can be misleading. Moreover, the different crosstalk between ER$\alpha$ and p53 could also be ascribed to specific treatments, such as cytostatic (32) *vs.* cytotoxic (49) doses of doxorubicin, $\gamma$-irradiation (33), or TNFα (51).

## MDM2

MDM2 protein is involved in a negative feedback loop with p53, by which p53 activates transcription of the MDM2 oncogene, which in turn inhibits p53 activity. This loop is essential to maintain both proteins at moderate levels and reset cell behavior after p53 activation. Due to their intertwined role, an unbalanced expression or activity of MDM2 is involved in cancer, and many studies highlighted sex-related factors leading to unbalanced

MDM2 (15). Additionally, MDM2 regulates targets other than p53, which also have relevance to cancer (54).

### Genetic Factors

The expression of the MDM2 gene is probably the best example of sex-mediated regulation of p53 circuitry in cancer. An initial report from Blaydes's group demonstrated the activation of the MDM2 P2 promoter by the AP1-ETS transcription factors in an ER$\alpha$ dependent manner (55). Subsequently, Bond and colleagues identified the SNP309 T/G within this promoter (56) (**Table 1**). The SNP309G variant extends the length of the DNA binding site for specificity protein 1 (Sp1), increasing the affinity for this transcriptional factor. As a result, Sp1 increases MDM2 levels, leading to an attenuation of the oncosuppressive p53 activity. This SNP is indeed associated with an early age of cancer diagnosis. Since Sp1 is a co-transcriptional factor of ERs, the authors demonstrated that SNP309 accelerates the age of onset of various cancer types (diffuse large B cell lymphoma, soft tissue sarcoma, invasive ductal breast carcinoma, IDC)—in female but not in male patients (57). Accordingly, this sex difference is associated with $ER^+$ but not $ER^-$ invasive ductal breast carcinoma and is more evident in non-menopausal women. Similar data were reported for colorectal cancer, in which female SNP309G carriers were diagnosed with cancer earlier than those carrying the wild-type gene (58). Other studies evidenced the relevance of this SNP in a p53-independent way due to the ubiquitin ligase activity of MDM2 towards other targets (53, 59, 60). Overall, this data underlies the role of the estrogen-mediated pathway on MDM2 function through SNP309. At odds with this data, some studies did not find an association between SNP309 and estrogen status on cancer risk [reviewed in (61)]. Although, in many cases, the authors did not take into account the sex and the hormone levels, a resolving study from Lønning's group defined the presence of the additional SNP285G>C, which antagonizes the Sp1 binding to SNP309 (**Table 1**) (62). The presence of this SNP reduces the risk of both ovarian and breast cancers, highlighting the relevance of MDM2 fine-tuning for cancer development.

Further complexity has been recently added by Lozano's group, who demonstrated that MDM2 SNP309G exhibits tissue-specific regulation and different impacts on cancer risk (63). Accordingly, Grochola and colleagues showed that in pancreatic ductal adenocarcinoma (PDAC), the SNP309G is associated with earlier onset in men but not in women. They attributed this effect to the function of Sp1 as a coactivator of androgen receptors present in PDAC (64).

In 2015, Kato's group identified an additional SNP in MDM2-P2 promoter, the SNP55 (rs2870820, C/T) (65). Both SNP55T and SNP55C bind Sp1, whereas only the C allelic variant creates an additional consensus sequence for the transcriptional factor NF-kB. The NF-kB p50/p50 homodimer interferes with Sp1 transcriptional activity, as demonstrated by Hirano and colleagues (66). In the context of MDM2, this results in transcriptional repression of the gene (65). Therefore, this SNP further contributes to fine-tuning MDM2 levels. Subsequently, Helwa and colleagues reported that women with SNP55TT or SNP55TC genotype have a higher risk of colon cancer, particularly left-sided colon cancer, than those with SNP55CC genotype (66). Conversely, this SNP does not seem to affect breast, lung, prostate, and endometrial cancer risk (66). In a recent study, the same group analyzed the impact of the combination of all three SNPs and reported that the SNP55T allele variant is associated with a lower risk of endometrial cancer in women carrying the SNP285G and SNP309T. At the same time, this haplotype is not correlated with the risk of ovarian cancer (67).

These results collectively validate the MDM2 SNPs as important cancer modifiers by attenuating the cell-protective activity of p53 or p53-independent pathways. To date, the characterization of these SNPs in the application of MDM2-target therapies has not been reported.

### Hormone Activity

Besides the effect of the hormone on MDM2 transcription through SNPs, other studies evidenced a regulation of MDM2 by the estrogenic pathway at the protein levels. ER$\alpha$ stabilizes MDM2 since the use of fulvestrant significantly reduces the MDM2 half-life. Particularly, fulvestrant decreased basal expression of MDM2 through increased protein turnover in the absence of E2 (68). This in turn, increases cell apoptosis and sensitivity of MCF7 breast cancer cells to chemotherapic drugs, doxorubicin, paclitaxel, and etoposide (68). Accordingly, high levels of MDM2 are detected in $ER\alpha^+$ breast carcinoma (69). In a reciprocal fashion, Cavailles's group demonstrated MDM2 activity towards ER$\alpha$: MDM2 interacts with ER$\alpha$ and p53 and induces ER$\alpha$ degradation through its ubiquitin ligase activity in a ligand-independent manner (70). Conversely, in a p53-independent way, Bargonetti's group reported the ability of MDM2 to facilitate the estrogen-mediated activation of cell proliferation (53), suggesting different activities of MDM2 dependent on p53 background.

The overall positive effects of estrogenic hormones on MDM2, at the mRNA and protein levels, suggest that anti-estrogenic therapies in breast cancer could synergize with MDM2-targeted drugs.

## MDM4

MDM4 is a double-faced p53 regulator: it cooperates with MDM2 in inhibiting p53, thus behaving as an oncogenic factor. Conversely, under DNA damage conditions, it cooperates with p53 and promotes cell apoptosis (71, 72). MDM4 also possesses a p53-independent function by suppressing the mTOR-mediated pathway (73, 74). Of relevance, the proapoptotic activities reside on the cytoplasmic fraction of MDM4 (75, 76). Accordingly, most tumors show high levels of MDM4 in the nuclear compartment (77). Wide-genome studies reported the association of specific SNPs in the MDM4 gene with hormone-mediated cancer and estrogen receptor-negative breast tumors, suggesting that the presence of ERs may select for a particular MDM4 gene status.

### Genetic Factors

Despite the description of various SNPs in the MDM4 gene (78), the majority of data focused on the SNP 34091 (A > C) in the 3′

UTR region of human MDM4 (**Table 1**). Data collected from the Collaborative Oncological Gene-environment (COGS) showed a significant association of this SNP with hormone-dependent cancers (79–81). This SNP located 32 bp downstream of the stop codon should create an illegitimate binding site for miR-887 (80, 82) and has-miR-191, a miRNA often expressed in tumor tissues, leading to downregulation of MDM4 in the MDM4-C variant (83). Unexpectedly, the SNP34091C variant is associated with increased risk of breast cancer, high-grade ovarian cancer (HGSOC), and prostate cancer suggesting a specific sensitivity of these hormone-dependent cancers to presumably low MDM4 levels (79, 84). SNP34091C is associated with increased cancer risk only in ER-negative breast cancer, suggesting that the presence of ERs interferes with MDM4 activity (79, 85). Additionally, in ER-negative breast cancer and HGSOC, the presence of this SNP is not correlated to the status of p53, suggesting that ERs interfere with MDM4 p53-independent activities. This data is in agreement with the cytoplasmic proapoptotic function of MDM4. The ER ability to re-localize MDM4 in the nucleus would abrogate the MDM4 cytoplasmic anti-oncogenic function. Accordingly, many human tumors express nuclear MDM4 (77). Other studies on ovarian cancer reported contradictory results. Wynendaele reported an association of the AA haplotype with reduced overall survival of ovarian carcinoma. Conversely, Gansmo reported an association of C variant with HGSOC (84). A possible explanation raised by these last authors is that in HGSOC, p53 is mutated in almost 90% of tumors. Therefore, the effect of this variant is mediated *via* pathways other than p53 (84).

The association between hormone-related pathways and this SNP is supported by the observation that it does not alter colon- and lung-cancer risk in a large population-based control study (86). Of merit, this study distinguished male and female patients compared to male and female controls. Association with prostate cancer was not found, although some authors reported a trend of association of the C allele with higher prostate cancer aggressiveness (87).

At odds with the previous study, other authors reported a reduced cancer risk for the SNP34091C variant in esophageal squamous cell carcinoma and non-Hodgkin lymphoma (88, 89). Information on ERs status in these studies is not available and cannot be entirely compared to previous results. Additionally, the different geographic populations (Caucasian *vs.* Chinese) may underlie this discrepancy. Indeed, the frequency of the MDM4-SNP34091 is different between these two populations (90). Finally, other miRNAs may affect SNP function (91).

Additional SNPs have been identified in other cancer types. Couch and colleagues reported the association of the minor allele of MDM4 SNP rs2290854 with breast cancer risk in mutant BRCA1 carriers, suggesting that this MDM4 variant can be a modifying factor for breast cancer in this mutant background (92) (**Table 1**). Also, in this case, this SNP is associated with $ER^-$ but not $ER^+$ breast cancer. Moreover, two recent papers analyzed the sex-related association of various MDM4 SNP with glioma in the European and Chinese populations (93, 94). The authors evidenced the association of the A allele of a novel MDM4 SNP (rs4252707) (**Table 1**) with the increased risk of this tumor. However, although the higher frequency of glioma in males, they did not find an association with sex.

### Hormone Activity

Lozano's group was the first to demonstrate a dissimilar activity of overexpressed MDM4 between male and female mice (95). Her group reported a higher incidence of multiple tumors and a decreased animal survival in Mdm4 transgenic p53-null males but not in females, indicating sexual dimorphism of Mdm4 activity, at least in rodents. Using the same animal model, our group demonstrated that in a wt-p53 background, Mdm4 promotes tumor development following DNA damage in a sex-independent way, indicating that Mdm4 oncogenic properties are not affected by sex. In contrast, there is increased chemotherapy sensitivity in Mdm4-overexpressing male but not in female mice. Molecular analysis demonstrated that E2 re-localizes MDM4 in the nucleus, antagonizing the cytoplasmic MDM4-mediated DNA damage response (96). Noteworthy, treatment of animals with fulvestrant rescues MDM4-mediated proapoptotic activity and increases tumor sensitivity to chemotherapy. Accordingly, MDM4 nuclear localization and intra-tumor estrogen availability correlate with decreased platinum sensitivity and apoptosis and predict poor disease-free survival in human HGSOC. A specular finding was reported by Das's group (97). They showed that ER$\alpha$ is a positive regulator of MDM4 oncogenic activity, and treatment of tumor cells with ER inhibitors (fulvestrant or OHT) reduces MDM4 protein levels. Overall, this data indicates that sex and/or ER$\alpha$ regulate MDM4 activity. Depending on p53 background, they can result in opposite outcomes. The assessment of sex/hormone status in MDM4-target therapy could confirm the relevance of these factors in drug efficacy and suggest the potential usefulness of combinatorial treatments.

## THERAPIES DIRECTED TO WT-P53 RE-ACTIVATION

In the last decades, different therapeutic approaches were developed to reactivate wt-p53 functions in cancer. Peptides and small molecule compounds were described to target the critical inhibitory binding of MDM2 and MDM4 to p53 or to stimulate p53 by acting on the protein itself [reviewed in (16, 98, 99)].

Compounds in the p53 network that entered clinical trials are summarized in **Table 2**. Among them, the majority refers to phase I studies that evaluate safety and tolerability, with few or no results about the efficacy of the therapies. Despite the low number of patients usually enrolled in phase I, none of these trials reported the hormone/gender status in their evaluations. Here, we briefly reviewed the active clinical trials suggesting the potential role of sex/hormone.

P28 is a peptide derived from the Azurin, a *Pseudomonas aeruginosa* redox protein that exerts an antiproliferative activity towards cancer cells by inhibiting COP-1 mediated

**TABLE 2** | Strategies for wt-p53 re-activation, which entered clinical trial phases.

| Compound | Drug | Mechanism of action | Clinical trial ID (Phase) |
|---|---|---|---|
| **p28** | Peptide | Inhibition of COP1-mediated p53 ubiquitination | NCT00914914 (I), NCT01975116 (I) |
| **ALRN-6924** | Peptide | Dual inhibition of MDM2 and MDM4 interaction with p53 | NCT02264613 (I,IIa), NCT03725436 (I), NCT02909972 (I,Ib), NCT03654716 (I) |
| **RG7112** **RO5045337** | Small molecule | Binds MDM2 and prevents MDM2/P53 interaction | NCT01677780 (I), NCT01164033(I), NCT01143740(I), NCT01605526(I), NCT00623870(I), NCT00559533(I), NCT01635296(I) |
| **RG7388** **RO5503781** | Small molecule | Binds MDM2 and prevents MDM2/P53 interaction | NCT02407080 (I), NCT02828930 (I), NCT02633059 (I,II), NCT02545283 (III), NCT02624986 (Ib, II), NCT01901172 (I), NCT01773408 (I), NCT01462175 (I) |
| **SAR405838** **MI-77301** | Small molecule | Mimics p53 key amino acids involved in MDM2 binding | NCT01636479 (I), NCT01985191 (I) |
| **CGM097** | Small molecule | Mimics p53 key amino acids involved in MDM2 binding | NCT01760525 (I) |
| **MK-8242** **SCH 900242** | Small molecule | Inhibition of MDM2 interaction with p53 | NCT01463696 (I), NCT01451437 (I) |
| **AMG232** | Small molecule | Inhibition of MDM2 interaction with p53 | NCT02016729 (Ib), NCT03031730 (I), NCT01723020 (I), NCT02110355 (Ib,IIa) |
| **DS-3032b** | Small molecule | Inhibition of MDM2 interaction with p53 | NCT02579824 (I), NCT02319369 (I), NCT01877382 (I) |
| **HDM201** | Small molecule | Inhibition of MDM2 interaction with p53 | NCT02343172 (Ib,II), NCT02143635 (I), NCT02780128 (I), NCT02601378 (I), NCT03940352 (I), NCT03714958 (I), NCT04496999 (I), NCT04116541 (II), NCT04097821 (I,II), NCT02890069 (I) |

**Data from ClinicalTrials.gov. National Library of Medicine:** http://www.clinicaltrials.gov

ubiquitination of p53, thus in an MDM2/MDM4 independent way (100, 101). In a Phase I study (NCT00914914), p28 proved preliminary evidence of anti-tumor activity in patients with melanoma and colon cancer (**Table 2**). Although no results regarding gender are displayed (102), P28 efficacy towards these non-hormone mediated cancers might suggest that COP-1 mediated regulation of p53 is not affected by hormone status. Accordingly, a second Phase I study NCT01975116 established safety in children with recurrent or refractory central nervous system cancer (CNS) (103). Comparing this peptide efficacy in males and females could highlight the potential effects of genetic factor/s on p53 function.

ALRN-6924 is a peptide that targets both MDM2 and MDM4 and prevents their binding to p53 (104). Phase I studies evaluated safety in acute myeloid leukemia (AML), myelodysplastic syndrome (MDS), and solid cancers (**Table 2**). Two recent trials are recruiting patients to evaluate the safety and efficacy of ALRN-6924 in combination with drugs used in chemotherapy as Cytarabine for patients with leukemia (NCT03654716) or Paclitaxel for those with breast cancer (NCT03725436). The results of this last trial could be of interest to evaluate the relevance of ERs in p53 circuitry since the inclusion criteria are breast cancer carrying wt-p53 and positive for ERs.

RG7112 and RG7388, two derivatives of cis-imidazoline molecule known as "nutlin", are under testing in clinical trials (**Table 2**). RG7112, despite promising results in terms of p53 activation, was dropped because of significant toxicity (105). RG7388, known as Idasanutlin, is a nutlin analog with a higher affinity and specificity for MDM2. This compound underwent several clinical trials, including phase II and phase III trials in combination with chemotherapy or novel therapies as monoclonal antibodies and other new anticancer small molecules (**Table 2**). Based on the relevance of ER$\alpha$ in MDM2 levels, the efficacy of this drug could be increased in those tumors previously shown more sensitive to SNP variations.

Spirooxindole-based compound mimics the p53 key amino acids that bind MDM2. MI-77301 from Sanofi (106) and the substituted dihydroisoquinolinone derivative CGM097 from Novartis, entered in phase I clinical trials (**Table 2**). For both compounds, the anti-tumor activity has been verified in preclinical studies (107), whereas no results have been reported from clinical trials. Of interest, p53 status is not sufficient to predict CGM097 sensitivity in a panel of 477 cell lines from the Cancer Cell Line Encyclopedia (CCLE). In the 13 gene signature predicting CGM097 response, MDM2 levels are the most significant predictor (108). Given the relevance of ER/hormone status in affecting MDM2 levels, the assessment of hormone status could be relevant in the analysis of the efficacy of these compounds in the related clinical trials.

MK-8242 from Merck is a small-molecules that inhibits MDM2 interaction with p53 and can induce growth arrest at very low concentration (109). In the NCT01463696 trial, three of 47 patients with liposarcoma showed a partial response, and 31 patients stable disease (110) (**Table 2**). Since 60% of these patients are males, it would be interesting to re-evaluate the results by separate analysis of patients based on sex/hormone status.

AMG232 by Amgen is a piperidinone-derived compound that acts as a potent inhibitor of the MDM2–p53 complex and shows high anti-tumor activity in xenograft models (111). This compound underwent several clinical trials, including phases I and II, as single or combination treatments for solid tumors, AML, myeloma, and melanoma (**Table 2**), but its effects have never been evaluated in the light of sex/hormones.

DS3032b developed by Daiichi Sankyo showed stable disease in 77% of patients with solid tumors (112) and reduced bone marrow blasts after the first cycle in half patients and complete remission in two patients with hematological malignancies.

HDM201 developed by Novartis is an imidazopyrrolidinone analog that inhibits the P53–MDM2 interaction with high

efficiency. It was able to induce p53 dependent apoptosis and tumor regression in xenograft tumor models (113). Many clinical studies are ongoing in patients with wild-type p53 tumors of different histotypes such as AML, solid tumors, and multiple myeloma (**Table 2**). Some results of clinical benefit from these trials have been reported: approximately 25–30% of patients had a partial response or stable disease, although the tumor histotypes are not specified (114).

Many of the tumors under these clinical trials—including myeloma and lymphoma—show sex differences, with male prevalence. Evaluating these drugs in terms of sex and/or hormone status could give valuable information for more personalized medicine.

## DISCUSSION

Although sex is an important factor in determining cancer development, progression, and sensitivity to therapy, sex-based studies of cancer biology and treatment are still largely insufficient, and the factors driving the sex-related cancer disparity remain to be clarified. Even after recommendations from NIH and other funding agencies to consider sex and gender at all levels of biomedical research, animal studies and clinical trials that distinguish gender populations are few (115). P53-target therapies do not make an exception, as demonstrated by **Table 2**. None of those clinical trials reported separate results for men and women or considered the hormonal status of patients. Still, many studies demonstrate that p53 activity is affected by sex-related genetic and/or hormone determinants. This review reflects the abundance and complexity of the sex-related molecular factors that affect p53 response in human tumors. Based on the data here reviewed, nowadays, it is difficult to predict which genetic or hormonal factors could contribute to defining a more personalized application of single or combinatorial treatments.

For this reason, evaluation of sex/hormones in preclinical studies and clinical trials could help clarify the factors that finally affect p53 function *in vivo* and could guide future molecular studies besides drive a more appropriate and successful application of these therapies. Indeed, "false" negative or positive results could be due to the confounding effects of mixed backgrounds. As stated by Clayton and Collins, "inadequate inclusion of female cells and animals in experiments and inadequate analysis of data by sex may well contribute to the troubling rise of reproducibility in preclinical biomedical research" (115).

Inclusion of sex/hormone status in the analysis of p53 data could open the possibility of combinatorial treatments with anti-hormone or other target therapies. Based on the beneficial effect of SERM on tumors with wt-p53 and possible depressing activity of MDM2 levels, a combinatorial treatment of SERM therapy with p53-reactivating drugs in breast cancer could be hypothesized. Accordingly, Rozeboom and colleagues recently suggested a new clinical trial based on triple therapy with a BCL2 inhibitor (venetoclax), an anti-estrogen (tamoxifen/fulvestrant), and an MDM2 inhibitor (AMG-232/MI-77301) in the $ER^+$/WT *TP53* metastatic breast cancer setting (116). Finally, the ascertainment of sex/hormone and p53 crosstalk could guide different drug dosages and improve safety-toxicity drug features. This is particularly relevant given the more active immune response in females than males and the well-known required lower doses of heart disease drugs in females compared to men (117, 118).

## AUTHOR CONTRIBUTIONS

FMa, LG, ET, and FMo wrote the manuscript. AP revised the manuscript. FMo conceived and reviewed the manuscript. All authors contributed to the article and approved the submitted version.

## FUNDING

This study was supported by grant from Italian Association for Cancer Research (AIRC) under IG 2018—ID. 21814 project—P.I. Moretti Fabiola.

## ACKNOWLEDGMENTS

We thank Dr. Donato Civitareale for critical reading and useful suggestion.

## REFERENCES

1. Siegel RL, Miller KD, Fuchs HE, Jemal A. Cancer Statistics, 2021. *CA: A Cancer J Clin* (2021) 71(1):7–33. doi: 10.3322/caac.21654
2. Wisnivesky JP, Halm EA. Sex Differences in Lung Cancer Survival: Do Tumors Behave Differently in Elderly Women? *J Clin Oncol Off J Am Soc Clin Oncol* (2007) 25(13):1705–12. doi: 10.1200/JCO.2006.08.1455
3. Lopes-Ramos CM, Quackenbush J, DeMeo DL. Genome-Wide Sex and Gender Differences in Cancer. *Front Oncol* (2020) 10:2486–503. doi: 10.3389/fonc.2020.597788
4. Dunford A, Weinstock DM, Savova V, Schumacher SE, Cleary JP, Yoda A, et al. Tumor-Suppressor Genes That Escape From X-Inactivation Contribute to Cancer Sex Bias. *Nat Genet* (2017) 49(1):10–6. doi: 10.1038/ng.3726
5. Rubin JB, Lagas JS, Broestl L, Sponagel J, Rockwell N, Rhee G, et al. Sex Differences in Cancer Mechanisms. *Biol Sex Dif* (2020) 11(1):1–29. doi: 10.1186/s13293-020-00291-x
6. Clocchiatti A, Cora E, Zhang Y, Dotto GP. Sexual Dimorphism in Cancer. *Nat Rev Cancer* (2016) 16(5):330–9. doi: 10.1038/nrc.2016.30
7. Thomas C, Gustafsson JA. The Different Roles of ER Subtypes in Cancer Biology and Therapy. *Nat Rev Cancer* (2011) 11(8):597–608. doi: 10.1038/nrc3093
8. Stapelfeld C, Dammann C, Maser E. Sex-Specificity in Lung Cancer Risk. *Int J Cancer* (2020) 146(9):2376–82. doi: 10.1002/ijc.32716
9. DeSantis CE, Miller KD, Dale W, Mohile SG, Cohen HJ, Leach CR, et al. Cancer Statistics for Adults Aged 85 Years and Older, 2019. *CA: A Cancer J Clin* (2019) 69(6):452–67. doi: 10.3322/caac.21577

10. Konings G, Brentjens L, Delvoux B, Linnanen T, Cornel K, Koskimies P, et al. Intracrine Regulation of Estrogen and Other Sex Steroid Levels in Endometrium and Non-Gynecological Tissues; Pathology, Physiology, and Drug Discover. *Front Pharmacol* (2018) 9:940. doi: 10.3389/fphar.2018.00940
11. Labrie F. Intracrinology and Menopause: The Science Describing the Cell-Specific Intracellular Formation of Estrogens and Androgens From DHEA and Their Strictly Local Action and Inactivation in Peripheral Tissues. *Menopause (New York NY)* (2019) 26(2):220–4. doi: 10.1097/GME.0000000000001177
12. Wasylishen AR, Lozano G. Attenuating the P53 Pathway in Human Cancers: Many Means to the Same End. *Cold Spring Harb Perspect Med* (2016) 6(8): a026211. doi: 10.1101/cshperspect.a026211
13. Joerger AC, Fersht AR. The P53 Pathway: Origins, Inactivation in Cancer, and Emerging Therapeutic Approache. *Annu Rev Biochem* (2016) 85:375–404. doi: 10.1146/annurev-biochem-060815-014710
14. Zhang Y, Xiong S, Li Q, Hu S, Tashakori M, Van Pelt C, et al. Tissue-Specific and Age-Dependent Effects of Global MDM2 Loss. *J Pathol* (2014) 233 (4):380–91. doi: 10.1002/path.4368
15. Karni-Schmidt O, Lokshin M, Prives C. The Roles of MDM2 and MDMX in Cance. *Annu Rev Pathol* (2016) 11:617–44. doi: 10.1146/annurev-pathol-012414-040349
16. Teveroni E, Luca R, Pellegrino M, Ciolli G, Pontecorvi A, Moretti F. Peptides and Peptidomimetics in the P53/MDM2/MDM4 Circuitry - A Patent Review. *Expert Opin Ther Patents* (2016) 26(12):1417–29. doi: 10.1080/13543776.2017.1233179
17. Sanz G, Singh M, Peuget S, Selivanova G. Inhibition of P53 Inhibitors: Progress, Challenges and Perspectives. *J Mol Cell Biol* (2019) 11(7):586–99. doi: 10.1093/jmcb/mjz075
18. Audenet F, Méjean A, Chartier-Kastler E, Rouprêt M. Adrenal Tumours Are More Predominant in Females Regardless of Their Histological Subtype: A Review. *World J Urol* (2013) 31(5):1037–43. doi: 10.1007/s00345-012-1011-1
19. Ribeiro RC, Pinto EM, Zambetti GP. Familial Predisposition to Adrenocortical Tumors: Clinical and Biological Features and Management Strategies. *Best Pract Res Clin Endocrinol Metab* (2010) 24(3):477–90. doi: 10.1016/j.beem.2010.03.002
20. Whibley C, Pharoah PD, Hollstein M. P53 Polymorphisms: Cancer Implications. *Nat Rev Cancer* (2009) 9(2):95–107. doi: 10.1038/nrc2584
21. Sümbül AT, Akkız H, Bayram S, Bekar A, Akgöllü E, Sandıkçı M. P53 Codon 72 Polymorphism Is Associated With Susceptibility to Hepatocellular Carcinoma in the Turkish Population: A Case-Control Study. *Mol Biol Rep* (2012) 39(2):1639–47. doi: 10.1007/s11033-011-0903-2
22. Pandith AA, Khan NP, Rashid N, Azad N, Zaroo I, Hafiz A, et al. Impact of Codon 72 Arg > Pro Single Nucleotide Polymorphism in TP53 Gene in the Risk of Kangri Cancer: A Case Control Study in Kashmi. *Tumour Biol J Int Soc Oncodev Biol Med* (2012) 33(4):927–33. doi: 10.1007/s13277-012-0318-2
23. Haupt S, Caramia F, Herschtal A, Soussi T, Lozano G, Chen H, et al. Identification of Cancer Sex-Disparity in the Functional Integrity of P53 and Its X Chromosome Network. *Nat Commun* (2019) 10(1):5385–96. doi: 10.1038/s41467-019-13266-3
24. Moelans CB, de Ligt J, van der Groep P, Prins P, Besselink NJM, Hoogstraat M, et al. The Molecular Genetic Make-Up of Male Breast Cancer. *Endocrine-Related Cancer* (2019) 26(10):779–94. doi: 10.1530/ERC-19-0278
25. Berger C, Qian Y, Chen X. The P53-Estrogen Receptor Loop in Cancer. *Curr Mol Med* (2013) 13(8):1229–40. doi: 10.2174/15665240113399900065
26. Fuentes N, Silveyra P. Estrogen Receptor Signaling Mechanisms. *Adv Protein Chem Struct Biol* (2019) 116:135–70. doi: 10.1016/bs.apcsb.2019.01.001
27. *Welcome - IARC TP53 Database 2016* . Available at: http://p53.iarc.fr/.
28. Pharoah PD, Day NE, Caldas C. Somatic Mutations in the P53 Gene and Prognosis in Breast Cancer: A Meta-Analysis. *Br J Cancer* (1999) 80 (12):1968–73. doi: 10.1038/sj.bjc.6690628
29. Fernández-Cuesta L, Anaganti S, Hainaut P, Olivier M. Estrogen Levels Act as a Rheostat on P53 Levels and Modulate P53-Dependent Responses in Breast Cancer Cell Lines. *Breast Cancer Res Treat* (2011) 125(1):35–42. doi: 10.1007/s10549-010-0819-x
30. Fernandez-Cuesta L, Anaganti S, Hainaut P, Olivier M. P53 Status Influences Response to Tamoxifen But Not to Fulvestrant in Breast Cancer Cell Lines. *Int J Cancer* (2011) 128(8):1813–21. doi: 10.1002/ijc.25512
31. Anaganti S, Fernández-Cuesta L, Langerød A, Hainaut P, Olivier M. P53-Dependent Repression of Focal Adhesion Kinase in Response to Estradiol in Breast Cancer Cell-Lines. *Cancer Letters* (2011) 300(2):215–24. doi: 10.1016/j.canlet.2010.10.008
32. Berger CE, Qian Y, Liu G, Chen H, Chen X. P53, a Target of Estrogen Receptor (ER) α, Modulates DNA Damage-Induced Growth Suppression in ER-Positive Breast Cancer Cells. *J Biol Chem* (2012) 287(36):30117–27. doi: 10.1074/jbc.M112.367326
33. Becker KA, Lu S, Dickinson ES, Dunphy KA, Mathews L, Schneider SS, et al. Estrogen and Progesterone Regulate Radiation-Induced P53 Activity in Mammary Epithelium Through TGF-Beta-Dependent Pathways. *Oncogene* (2005) 24(42):6345–53. doi: 10.1038/sj.onc.1208787
34. Dunphy KA, Blackburn AC, Yan H, O'Connell LR, Jerry DJ. Estrogen and Progesterone Induce Persistent Increases in P53-Dependent Apoptosis and Suppress Mammary Tumors in BALB/c-Trp53+/- Mice. *Breast Cancer Res BCR* (2008) 10(3):R43. doi: 10.1186/bcr2094
35. Sivaraman L, Conneely OM, Medina D, O'Malley BW. P53 Is a Potential Mediator of Pregnancy and Hormone-Induced Resistance to Mammary Carcinogenesis. *Proc Natl Acad Sci USA* (2001) 98(22):12379–84. doi: 10.1073/pnas.221459098
36. Fortner RT, Sisti J, Chai B, Collins LC, Rosner B, Hankinson SE, et al. Parity, Breastfeeding, and Breast Cancer Risk by Hormone Receptor Status and Molecular Phenotype: Results From the Nurses' Health Studie. *Breast Cancer Res BCR* (2019) 21(1):40. doi: 10.1186/s13058-019-1119-y
37. Kuperwasser C, Pinkas J, Hurlbut GD, Naber SP, Jerry DJ. Cytoplasmic Sequestration and Functional Repression of P53 in the Mammary Epithelium Is Reversed by Hormonal Treatment. *Cancer Res* (2000) 60 (10):2723–29.
38. Pinto G, Alhaiek AA, Amadi S, Qattan AT, Crawford M, Radulovic M, et al. Systematic Nucleo-Cytoplasmic Trafficking of Proteins Following Exposure of MCF7 Breast Cancer Cells to Estradiol. *J Proteome Res* (2014) 13(2):1112–27. doi: 10.1021/pr4012359
39. Weige CC, Allred KF, Armstrong CM, Allred CD. P53 Mediates Estradiol Induced Activation of Apoptosis and DNA Repair in Non-Malignant Colonocytes. *J Steroid Biochem Mol Biol* (2012) 128(3-5):113–20. doi: 10.1016/j.jsbmb.2011.10.010
40. Yu CL, Driggers P, Barrera-Hernandez G, Nunez SB, Segars JH, Cheng S. The Tumor Suppressor P53 Is a Negative Regulator of Estrogen Receptor Signaling Pathways. *Biochem Biophys Res Commun* (1997) 239(2):617–20. doi: 10.1006/bbrc.1997.7522
41. Lewis-Wambi JS, Jordan VC. Estrogen Regulation of Apoptosis: How Can One Hormone Stimulate and Inhibit? *Breast Cancer Res BCR* (2009) 11 (3):206. doi: 10.1186/bcr2255
42. Traboulsi T, El EM, Gleason JL, Mader S. Antiestrogens: Structure-Activity Relationships and Use in Breast Cancer Treatment. *J Mol Endocrinol* (2017) 58(1):R15–31. doi: 10.1530/JME-16-0024
43. Coates AS, Millar EK, O'Toole SA, Molloy TJ, Viale G, Goldhirsch A, et al. Prognostic Interaction Between Expression of P53 and Estrogen Receptor in Patients With Node-Negative Breast Cancer: Results From IBCSG Trials VIII and IX. *Breast Cancer Res BCR* (2012) 14(6):R143. doi: 10.1186/bcr3348
44. Pok S, Barn VA, Wong HJ, Blackburn AC, Board P, Farrell GC, et al. Testosterone Regulation of Cyclin E Kinase: A Key Factor in Determining Gender Differences in Hepatocarcinogenesis. *J Gastroenterol Hepatol* (2016) 31(6):1210–9. doi: 10.1111/jgh.13232
45. Huang FY, Wong DK, Seto WK, Lai CL, Yuen MF. Estradiol Induces Apoptosis via Activation of miRNA-23a and P53: Implication for Gender Difference in Liver Cancer Development. *Oncotarget* (2015) 6(33):34941–52. doi: 10.18632/oncotarget.5472
46. El-Serag HB. Hepatocellular Carcinoma. *N Engl J Med* (2011) 365(12):1118–27. doi: 10.1056/NEJMra1001683
47. Hartman J, Edvardsson K, Lindberg K, Zhao C, Williams C, Ström A, et al. Tumor Repressive Functions of Estrogen Receptor Beta in SW480 Colon Cancer Cells. *Cancer Res* (2009) 69(15):6100–6. doi: 10.1158/0008-5472.CAN-09-0506
48. Hsu HH, Cheng SF, Wu CC, Chu CH, Weng YJ, Lin CS, et al. Apoptotic Effects of Over-Expressed Estrogen Receptor-Beta on LoVo Colon Cancer Cell Is Mediated by P53 Signalings in a Ligand-Dependent Manner. *Chin J Physiol* (2006) 49(2):110–6.
49. Liu W, Konduri SD, Bansal S, Nayak BK, Rajasekaran SA, Karuppayil SM, et al. Estrogen Receptor-Alpha Binds P53 Tumor Suppressor Protein

Directly and Represses Its Function. *J Biol Chem* (2006) 281(15):9837–40. doi: 10.1074/jbc.C600001200
50. Sayeed A, Konduri SD, Liu W, Bansal S, Li F, Das GM. Estrogen Receptor Alpha Inhibits P53-Mediated Transcriptional Repression: Implications for the Regulation of Apoptosis. *Cancer Res* (2007) 67(16):7746–55. doi: 10.1158/0008-5472.CAN-06-3724
51. Bailey ST, Shin H, Westerling T, Liu XS, Brown M. Estrogen Receptor Prevents P53-Dependent Apoptosis in Breast Cancer. *Proc Natl Acad Sci USA* (2012) 109(44):18060–5. doi: 10.1073/pnas.1018858109
52. Lewandowski SA, Thiery J, Jalil A, Leclercq G, Szczylik C, Chouaib S. Opposite Effects of Estrogen Receptors Alpha and Beta on MCF-7 Sensitivity to the Cytotoxic Action of TNF and P53 Activity. *Oncogene* (2005) 24 (30):4789–98. doi: 10.1038/sj.onc.1208595
53. Brekman A, Singh KE, Polotskaia A, Kundu N, Bargonetti J. A P53-Independent Role of Mdm2 in Estrogen-Mediated Activation of Breast Cancer Cell Proliferation. *Breast Cancer Res BCR* (2011) 13(1):R3. doi: 10.1186/bcr2804
54. Hu L, Zhang H, Bergholz J, Sun S, Xiao ZX. MDM2/MDMX: Master Negative Regulators for P53 and RB. *Mol Cell Oncol* (2016) 3(2):e1106635. doi: 10.1080/23723556.2015.1106635
55. Phelps M, Darley M, Primrose JN, Blaydes JP. P53-Independent Activation of the Hdm2-P2 Promoter Through Multiple Transcription Factor Response Elements Results in Elevated Hdm2 Expression in Estrogen Receptor Alpha-Positive Breast Cancer Cells. *Cancer Res* (2003) 63(10):2616–23.
56. Bond GL, Hu W, Bond EE, Robins H, Lutzker SG, Arva NC, et al. A Single Nucleotide Polymorphism in the MDM2 Promoter Attenuates the P53 Tumor Suppressor Pathway and Accelerates Tumor Formation in Humans. *Cell* (2004) 119(5):591–602. doi: 10.1016/j.cell.2004.11.022
57. Bond GL, Hirshfield KM, Kirchhoff T, Alexe G, Bond EE, Robins H, et al. MDM2 SNP309 Accelerates Tumor Formation in a Gender-Specific and Hormone-Dependent Manner. *Cancer Res* (2006) 66(10):5104–10. doi: 10.1158/0008-5472.CAN-06-0180
58. Alhopuro P, Ylisaukko-Oja SK, Koskinen WJ, Bono P, Arola J, Järvinen HJ, et al. The MDM2 Promoter Polymorphism SNP309–>G and the Risk of Uterine Leiomyosarcoma, Colorectal Cancer, and Squamous Cell Carcinoma of the Head and Neck. *J Med Genet* (2005) 42(9):694–8. doi: 10.1136/jmg.2005.031260
59. Nayak MS, Yang JM, Hait WN. Effect of a Single Nucleotide Polymorphism in the Murine Double Minute 2 Promoter (SNP309) on the Sensitivity to Topoisomerase II-Targeting Drugs. *Cancer Res* (2007) 67(12):5831–9. doi: 10.1158/0008-5472.CAN-06-4533
60. Kundu N, Brekman A, Kim JY, Xiao G, Gao C, Bargonetti J. Estrogen-Activated MDM2 Disrupts Mammary Tissue Architecture Through a P53-Independent Pathway. *Oncotarget* (2017) 8(29):47916–30. doi: 10.18632/oncotarget.18147
61. Bond GL, Levine AJ. A Single Nucleotide Polymorphism in the P53 Pathway Interacts With Gender, Environmental Stresses and Tumor Genetics to Influence Cancer in Humans. *Oncogene* (2007) 26(9):1317–23. doi: 10.1038/sj.onc.1210199
62. Knappskog S, Bjørnslett M, Myklebust LM, Huijts PE, Vreeswijk MP, Edvardsen H, et al. The MDM2 Promoter SNP285C/309G Haplotype Diminishes Sp1 Transcription Factor Binding and Reduces Risk for Breast and Ovarian Cancer in Caucasian. *Cancer Cell* (2011) 19(2):273–82. doi: 10.1016/j.ccr.2010.12.019
63. Ortiz GJ, Li Y, Post SM, Pant V, Xiong S, Larsson CA, et al. Contrasting Effects of an Mdm2 Functional Polymorphism on Tumor Phenotypes. *Oncogene* (2018) 37(3):332–40. doi: 10.1038/onc.2017.344
64. Grochola LF, Müller TH, Bond GL, Taubert H, Udelnow A, Würl P. MDM2 SNP309 Associates With Accelerated Pancreatic Adenocarcinoma Formation. *Pancreas* (2010) 39(1):76–80. doi: 10.1097/MPA.0b013e3181b9f105
65. Okamoto K, Tsunematsu R, Tahira T, Sonoda K, Asanoma K, Yagi H, et al. SNP55, a New Functional Polymorphism of MDM2-P2 Promoter, Contributes to Allele-Specific Expression of MDM2 in Endometrial Cancers. *BMC Med Genet* (2015) 16:67. doi: 10.1186/s12881-015-0216-8
66. Helwa R, Gansmo LB, Romundstad P, Hveem K, Vatten L, Ryan BM, et al. MDM2 Promoter SNP55 (Rs2870820) Affects Risk of Colon Cancer But Not Breast-, Lung-, or Prostate Cancer. *Sci Rep* (2016) 6:33153. doi: 10.1038/srep33153
67. Helwa R, Gansmo LB, Bjørnslett M, Halle MK, Werner HMJ, Romundstad P, et al. Impact of MDM2 Promoter SNP55 (Rs2870820) on Risk of Endometrial and Ovarian Cancer. *Biomarkers* (2021) 26(4):302–8. doi: 10.1080/1354750X.2021.1891291
68. Dolfi SC, Jäger AV, Medina DJ, Haffty BG, Yang JM, Hirshfield KM. Fulvestrant Treatment Alters MDM2 Protein Turnover and Sensitivity of Human Breast Carcinoma Cells to Chemotherapeutic Drugs. *Cancer Lett* (2014) 350(1-2):52–60. doi: 10.1016/j.canlet.2014.04.009
69. Sheikh MS, Shao ZM, Hussain A, Fontana JA. The P53-Binding Protein MDM2 Gene is Differentially Expressed in Human Breast Carcinoma. *Cancer Res* (1993) 53(14):3226–8.
70. Duong V, Boulle N, Daujat S, Chauvet J, Bonnet S, Neel H, et al. Differential Regulation of Estrogen Receptor Alpha Turnover and Transactivation by Mdm2 and Stress-Inducing Agents. *Cancer Res* (2007) 67(11):5513–21. doi: 10.1158/0008-5472.CAN-07-0967
71. Mancini F, Di Conza G, Monti O, Macchiarulo A, Pellicciari R, Pontecorvi A, et al. Puzzling Over MDM4-P53 Network. *Int J Biochem Cell Biol* (2010) 42(7):1080–3. doi: 10.1016/j.biocel.2010.04.010
72. Chen SH, Forrester W, Lahav G. Schedule-Dependent Interaction Between Anticancer Treatments. *Science* (2016) 351(6278):1204–8. doi: 10.1126/science.aac5610
73. Mancini F, Teveroni E, Di Conza G, Monteleone V, Arisi I, Pellegrino M, et al. MDM4 Actively Restrains Cytoplasmic Mtorc1 by Sensing Nutrient Availability. *Mol Cancer* (2017) 16:13. doi: 10.1186/s12943-017-0626-7
74. Kon N, Wang D, Li T, Jiang L, Qiang L, Gu W. Inhibition of Mdmx (Mdm4) In Vivo Induces Anti-Obesity Effects. *Oncotarget* (2018) 9(7):7282–97. doi: 10.18632/oncotarget.23837
75. Mancini F, Moretti F. Mitochondrial MDM4 (MDMX) An Unpredicted Role in the P53-Mediated Intrinsic Apoptotic Pathway. *Cell Cycle* (2009) 8 (23):3854–9. doi: 10.4161/cc.8.23.10089
76. Mancini F, Pieroni L, Monteleone V, Luca R, Fici L, Luca E, et al. MDM4/HIPK2/p53 Cytoplasmic Assembly Uncovers Coordinated Repression of Molecules With Anti-Apoptotic Activity During Early DNA Damage Response. *Oncogene* (2016) 35(2):228–40. doi: 10.1038/onc.2015.76
77. Gembarska A, Luciani F, Fedele C, Russell EA, Dewaele M, Villar S, et al. MDM4 Is a Key Therapeutic Target in Cutaneous Melanoma. *Nat Med* (2012) 18(8):1239–47. doi: 10.1038/nm.2863
78. Atwal GS, Kirchhoff T, Bond EE, Montagna M, Menin C, Bertorelle R, et al. Altered Tumor Formation and Evolutionary Selection of Genetic Variants in the Human MDM4 Oncogene. *Proc Natl Acad Sci USA* (2009) 106 (25):10236–41. doi: 10.1073/pnas.0901298106
79. Garcia-Closas M, Couch FJ, Lindstrom S, Michailidou K, Schmidt MK, Brook MN, et al. Genome-Wide Association Studies Identify Four ER Negative-Specific Breast Cancer Risk Loci. *Nat Genet* (2013) 45(4):392–8, 398e1-2. doi: 10.1038/ng.2561
80. Eeles RA, Olama AA, Benlloch S, Saunders EJ, Leongamornlert DA, Tymrakiewicz M, et al. Identification of 23 New Prostate Cancer Susceptibility Loci Using the iCOGS Custom Genotyping Array. *Nat Genet* (2013) 45(4):385–91, 391e1–2. doi: 10.1038/ng.2560
81. Sakoda LC, Jorgenson E, Witte JS. Turning of COGS Moves Forward Findings for Hormonally Mediated Cancers. *Nat Genet* (2013) 45(4):345–8. doi: 10.1038/ng.2587
82. Stegeman S, Moya L, Selth LA, Spurdle AB, Clements JA, Batra J. A Genetic Variant of MDM4 Influences Regulation by Multiple microRNAs in Prostate Cancer. *Endocr Relat Cancer* (2015) 22(2):265–76. doi: 10.1530/ERC-15-0013
83. Wynendaele J, Bohnke A, Leucci E, Nielsen SJ, Lambertz I, Hammer S, et al. An Illegitimate microRNA Target Site Within the 3' UTR of MDM4 Affects Ovarian Cancer Progression and Chemosensitivity. *Cancer Res* (2010) 70 (23):9641–9. doi: 10.1158/0008-5472.CAN-10-0527
84. Gansmo LB, Bjornslett M, Halle MK, Salvesen HB, Dorum A, Birkeland E, et al. The MDM4 SNP34091 (Rs4245739) C-Allele Is Associated With Increased Risk of Ovarian-But Not Endometrial Cancer. *Tumour Biol* (2016) 37(8):10697–702. doi: 10.1007/s13277-016-4940-2
85. Milne RL, Kuchenbaecker KB, Michailidou K, Beesley J, Kar S, Lindstrom S, et al. Identification of Ten Variants Associated With Risk of Estrogen-Receptor-Negative Breast Cancer. *Nat Genet* (2017) 49(12):1767–78. doi: 10.1038/ng.3785
86. Gansmo LB, Romundstad P, Birkeland E, Hveem K, Vatten L, Knappskog S, et al. MDM4 SNP34091 (Rs4245739) and Its Effect on Breast-, Colon-,

Lung-, and Prostate Cancer Risk. *Cancer Med* (2015) 4(12): 1901–7. doi: 10.1002/cam4.555
87. Kotarac N, Dobrijevic Z, Matijasevic S, Savic-Pavicevic D, Brajuskovic G. Association of KLK3, VAMP8 and MDM4 Genetic Variants Within microRNA Binding Sites With Prostate Cancer: Evidence From Serbian Populatio. *Pathol Oncol Res POR* (2020) 26(4):2409–23. doi: 10.1007/s12253-020-00839-7
88. Fan C, Wei J, Yuan C, Wang X, Jiang C, Zhou C, et al. The Functional TP53 Rs1042522 and MDM4 Rs4245739 Genetic Variants Contribute to Non-Hodgkin Lymphoma Risk. *PloS One* (2014) 9(9):e107047. doi: 10.1371/journal.pone.0107047
89. Zhou L, Zhang X, Li Z, Zhou C, Li M, Tang X, et al. Association of a Genetic Variation in a miR-191 Binding Site in MDM4 With Risk of Esophageal Squamous Cell Carcinoma. *PloS One* (2013) 8(5):e64331. doi: 10.1371/journal.pone.0064331
90. Abecasis GR, Auton A, Brooks LD, DePristo MA, Durbin RM, Handsaker RE, et al. An Integrated Map of Genetic Variation From 1,092 Human Genomes. *Nature* (2012) 491(7422):56–65. doi: 10.1038/nature11632
91. Anwar SL, Wulaningsih W, Watkins J. Profile of the Breast Cancer Susceptibility Marker Rs4245739 Identifies a Role for miRNAs. *Cancer Biol Med* (2017) 14(4):387–95. doi: 10.20892/j.issn.2095-3941.2017.0050
92. Couch FJ, Wang X, McGuffog L, Lee A, Olswold C, Kuchenbaecker KB, et al. Genome-Wide Association Study in BRCA1 Mutation Carriers Identifies Novel Loci Associated With Breast and Ovarian Cancer Risk. *PloS Genet* (2013) 9(3):e1003212. doi: 10.1371/journal.pgen.1003212
93. Sun P, Yan F, Fang W, Zhao J, Chen H, Ma X, et al. MDM4 Contributes to the Increased Risk of Glioma Susceptibility in Han Chinese Population. *Sci Rep* (2018) 8(1). doi: 10.1038/s41598-018-29468-6
94. Melin BS, Barnholtz-Sloan JS, Wrensch MR, Johansen C, Il'yasova D, Kinnersley B, et al. Genome-Wide Association Study of Glioma Subtypes Identifies Specific Differences in Genetic Susceptibility to Glioblastoma and Non-Glioblastoma Tumors. *Nat Genet* (2017) 49(5):789–4. doi: 10.1038/ng.3823
95. Xiong S, Pant V, Zhang Y, Aryal NK, You MJ, Kusewitt D, et al. The P53 Inhibitor Mdm4 Cooperates With Multiple Genetic Lesions in Tumourigenesis. *J Pathol* (2017) 241(4):501–10. doi: 10.1002/path.4854
96. Luca R, di Blasio G, Gallo D, Monteleone V, Manni I, Fici L, et al. Estrogens Counteract Platinum-Chemosensitivity by Modifying the Subcellular Localization of MDM4. *Cancers (Basel)* (2019) 11(9):1349. doi: 10.3390/cancers11091349
97. Swetzig WM, Wang J, Das GM. Estrogen Receptor Alpha (Erα/ESR1) Mediates the P53-Independent Overexpression of MDM4/MDMX and MDM2 in Human Breast Cancer. *Oncotarget* (2016) 7(13):16049–69. doi: 10.18632/oncotarget.7533
98. Skalniak L, Surmiak E, Holak TA. A Therapeutic Patent Overview of MDM2/X-Targeted Therapies (2014-2018). *Expert Opin Ther Patents* (2019) 29(3):151–70. doi: 10.1080/13543776.2019.1582645
99. Duffy MJ, Synnott NC, O'Grady S, Crown J. Targeting P53 for the Treatment of Cancer. *Semin Cancer Biol* (2020) S1044-579X(20). doi: 10.1016/j.semcancer.2020.07.005
100. Yamada T, Goto M, Punj V, Zaborina O, Chen ML, Kimbara K, et al. Bacterial Redox Protein Azurin, Tumor Suppressor Protein P53, and Regression of Cancer. *Proc Natl Acad Sci USA* (2002) 99(22):14098–103. doi: 10.1073/pnas.222539699
101. Punj V, Bhattacharyya S, Saint-Dic D, Vasu C, Cunningham EA, Graves J, et al. Bacterial Cupredoxin Azurin as an Inducer of Apoptosis and Regression in Human Breast Cancer. *Oncogene* (2004) 23(13):2367–78. doi: 10.1038/sj.onc.1207376
102. Warso MA, Richards JM, Mehta D, Christov K, Schaeffer C, Rae Bressler L, et al. A First-in-Class, First-in-Human, Phase I Trial of P28, a Non-HDM2-Mediated Peptide Inhibitor of P53 Ubiquitination in Patients With Advanced Solid Tumours. *Br J Cancer* (2013) 108(5):1061–70. doi: 10.1038/bjc.2013.74
103. Lulla RR, Goldman S, Yamada T, Beattie CW, Bressler L, Pacini M, et al. Phase 1 Trial of P28 (NSC745104), a Non-HDM2-Mediated Peptide Inhibitor of P53 Ubiquitination in Pediatric Patients With Recurrent or Progressive Central Nervous System Tumors: A Pediatric Brain Tumor Consortium Studu. *Neuro Oncol* (2016) 18(9):1319–25. doi: 10.1093/neuonc/now047
104. Carvajal LA, Neriah DB, Senecal A, Benard L, Thiruthuvanathan V, Yatsenko T, et al. Dual Inhibition of MDMX and MDM2 as a Therapeutic Strategy in Leukemia. *Sci Trans Med* (2018) 10(436):eaao3003. doi: 10.1126/scitranslmed.aao3003
105. Andreeff M, Kelly KR, Yee K, Assouline S, Strair R, Popplewell L, et al. Results of the Phase I Trial of RG7112, a Small-Molecule MDM2 Antagonist in Leukemia. *Clin Cancer Res Off J Am Assoc Cancer Res* (2016) 22(4):868–76. doi: 10.1158/1078-0432.CCR-15-0481
106. Wang S, Sun W, Zhao Y, McEachern D, Meaux I, Barrière C, et al. SAR405838: An Optimized Inhibitor of MDM2-P53 Interaction That Induces Complete and Durable Tumor Regression. *Cancer Res* (2014) 74 (20):5855–65. doi: 10.1158/0008-5472.CAN-14-0799
107. Holzer P, Masuya K, Furet P, Kallen J, Valat-Stachyra T, Ferretti S, et al. Discovery of a Dihydroisoquinolinone Derivative (NVP-CGM097): A Highly Potent and Selective MDM2 Inhibitor Undergoing Phase 1 Clinical Trials in P53wt Tumor. *J Medicinal Chem* (2015) 58(16):6348–58. doi: 10.1021/acs.jmedchem.5b00810
108. Jeay S, Gaulis S, Ferretti S, Bitter H, Ito M, Valat T, et al. A Distinct P53 Target Gene Set Predicts for Response to the Selective P53-HDM2 Inhibitor NVP-Cgm097. *eLife* (2015) 4:e06498. doi: 10.7554/eLife.06498
109. Ravandi F, Gojo I, Patnaik MM, Minden MD, Kantarjian H, Johnson-Levonas AO, et al. A Phase I Trial of the Human Double Minute 2 Inhibitor (MK-8242) in Patients With Refractory/Recurrent Acute Myelogenous Leukemia (AM). *Leukemia Res* (2016) 48:92–100. doi: 10.1016/j.leukres.2016.07.004
110. Wagner AJ, Banerji U, Mahipal A, Somaiah N, Hirsch H, Fancourt C, et al. Phase I Trial of the Human Double Minute 2 Inhibitor MK-8242 in Patients With Advanced Solid Tumor. *J Clin Oncol Off J Am Soc Clin Oncol* (2017) 35 (12):1304–11. doi: 10.1200/JCO.2016.70.7117
111. Sun D, Li Z, Rew Y, Gribble M, Bartberger MD, Beck HP, et al. Discovery of AMG 232, a Potent, Selective, and Orally Bioavailable MDM2-P53 Inhibitor in Clinical Development. *J Medicinal Chem* (2014) 57(4):1454–72. doi: 10.1021/jm401753e.
112. DiNardo CD, Rosenthal J, Andreeff M, Zernovak O, Kumar P, Gajee R, et al. Phase 1 Dose Escalation Study of MDM2 Inhibitor DS-3032b in Patients With Hematological Malignancies - Preliminary Results | Blood | American Society of Hematology. *Blood* (2016) 128:593. doi: 10.1182/blood.V128.22.593.593
113. Ferretti S, Rebmann R, Berger M, Santacroce F , Albrecht G, Pollehn K, et al. Insights Into the Mechanism of Action of NVP-HDM201, a Differentiated and Versatile Next-Generation Small-Molecule Inhibitor of Mdm2, Under Evaluation in Phase I Clinical Trials. *Cancer Res* (2016) 76(14):1224. doi: 10.1158/1538-7445.AM2016-1224
114. Hyman D, Chatterjee M, Langenberg MHG, Lin CC, Suarez C, Tai D, et al. Dose- and Regimen-Finding Phase I Study of NVP-HDM201 in Patients (Pts) With TP53 Wild-Type (Wt) Advanced Tumors. *Eur J Cancer* (2016) 69:S128–S9. doi: 10.1016/S0959-8049(16)32982-3
115. Clayton JA, Collins FS. Policy: NIH to Balance Sex in Cell and Animal Studies. *Nature* (2014) 509(7500):282–3. doi: 10.1038/509282a
116. Rozeboom B, Dey N, De P. ER+ Metastatic Breast Cancer: Past, Present, and a Prescription for an Apoptosis-Targeted Future. *Am J Cancer Res* (2019) 9 (12):2821–31.
117. Mauvais-Jarvis F, Bairey M N, Barnes PJ, Brinton RD, Carrero JJ, DeMeo DL, et al. Sex and Gender: Modifiers of Health, Disease, and Medicine. *Lancet (Lond Eng)* (2020) 396(10250):565–82. doi: 10.1016/S0140-6736(20)31561-0
118. Irelli A, Sirufo MM, D'Ugo C, Ginaldi L, De Martinis M. Sex and Gender Influences on Cancer Immunotherapy Response. *Biomedicines* (2020) 8 (7):232. doi: 10.3390/biomedicines8070232

**Conflict of Interest:** The authors declare that the research was conducted in the absence of any commercial or financial relationships that could be construed as a potential conflict of interest.

frontiers in Oncology

ORIGINAL RESEARCH
published: 14 July 2021
doi: 10.3389/fonc.2021.692497

# The Basic Research of the Combinatorial Therapy of ABT-199 and Homoharringtonine on Acute Myeloid Leukemia

*Yuanfei Shi[1†], Jing Ye[2,3†], Ying Yang[4], Yanchun Zhao[1], Huafei Shen[1], Xiujin Ye[1] and Wanzhuo Xie[1*]*

[1] Department of Hematology, The First Affiliated Hospital, College of Medicine, Zhejiang University, Hangzhou, China, [2] Sports Medicine Department, Beijing Key Laboratory of Sports Injuries, Peking University Third Hospital, Beijing, China, [3] Institute of Sports Medicine, Peking University, Beijing, China, [4] Department of Gynaecology and Obstetrics, Northwest Women's and Children's Hospital, Xi'an, China

OPEN ACCESS

**Edited by:**
Daniela Spano,
National Research Council (CNR), Italy

**Reviewed by:**
Yuan Tang,
University of Toledo,
United States
Jie Meng,
Chinese Academy of Medical Sciences and Peking Union Medical College, China

***Correspondence:**
Wanzhuo Xie
xiewanzhuo@zju.edu.cn

[†]These authors have contributed equally to this work

**Specialty section:**
This article was submitted to Pharmacology of Anti-Cancer Drugs, a section of the journal Frontiers in Oncology

**Received:** 08 April 2021
**Accepted:** 28 June 2021
**Published:** 14 July 2021

**Citation:**
Shi Y, Ye J, Yang Y, Zhao Y, Shen H, Ye X and Xie W (2021) The Basic Research of the Combinatorial Therapy of ABT-199 and Homoharringtonine on Acute Myeloid Leukemia. Front. Oncol. 11:692497. doi: 10.3389/fonc.2021.692497

**Background:** Existing research shows that ABT-199, as a first-line drug, have been widely used in hematological malignancies, especially in leukemia, but the clinical efficacy of single drug therapy was limited part of the reason was that BCL-2 inhibitors failure to target other anti-apoptotic BCL-2 family proteins, such as MCL-1. In this case, combination therapy may be a promising way to overcome this obstacle. Here, we investigate the preclinical efficacy of a new strategy combining ABT-199 with homoharringtonine (HHT), a selective inhibitor of MCL-1 may be a promising approach for AML treatment as these two molecules are important in apoptosis.

**Methods:** A Cell Counting Kit-8 (CCK8) assay and flow cytometry were used to determine the half-maximal inhibitory concentration (IC50) value and cell apoptosis rate, respectively. The flow cytometry results showed that combined treatment with HHT and ABT-199 caused apoptosis in AML patient samples (n=5) but had no effect on normal healthy donor samples (n=11). Furthermore, we used a Western blot assay to explore the mechanism underlying the efficacy of HHT combined with ABT-199. Finally, antileukemic activity was further evaluated *in vivo* xenograft model.

**Results:** Our results indicated that ABT-199 combined with HHT significantly inhibited cell growth and promoted apoptosis in both AML cell lines and primary AML tumors in a dose- and time-dependent manner. Moreover, HHT combined with ABT-199 suppressed AML cell growth and progression *in vivo* xenograft model.

**Conclusions:** Our research found that HHT combined with ABT-199 exerted its anti-leukemia effect by inducing apoptosis through the treatment of AML *in vitro* and *in vivo*.

**Keywords: ABT-199, homoharringtonine, cancer, acute myeloid leukemia, combinatorial therapy, molecular mechanisms, basic research**

## INTRODUCTION

Acute myeloid leukemia (AML) is a common and severe type of acute leukemia, especially in adults. In the United States, nearly 20,000 patients suffer from AML every year. Worse still, AML causes over 10,000 deaths per year. The 5-year survival rates, which are 65% for children and 26% for adults, remain quite low (1, 2). It has been reported that apoptosis evasion is associated with tumorigenesis and drug resistance (3). The upregulation of antiapoptotic BCL-2 family members and MCL-1 functions are two typical approaches exploited by cancer cells to escape apoptosis (4).

Targeted therapy has emerged as a promising treatment strategy for AML, which is resistant to chemotherapy. BCL-2 plays an important role in chemoresistance as an effective antiapoptotic protein (5, 6). Targeting BCL-2 with BH3 mimetics, such as ABT-199 (venetoclax), shows superior effects on lymphoma, especially when combined with homoharringtonine (HHT) (7).

ABT-199, a selective inhibitor of BCL-2, shows remarkable efficacy in a large number of cancers (6, 8). The emergence of ABT-199 provides an opportunity to study the function of BCL-2 inhibition. Other studies have shown that targeting BCL-2 *via* ABT-199 can effectively induce apoptosis in AML. Furthermore, overexpression of MCL-1, another antiapoptotic protein, renders leukemia cells resistant to both ABT and its predecessor ABT-737 (9, 10).

HHT, an omacetaxine mepesuccinate, has been widely studied and used in China as a classic antileukemic drug. However, the precise targets of HHT remain unclear (11, 12). Our findings indicated that HHT could potentiate the cytotoxicity of ABT-199 to leukemia cells. Moreover, a regimen combining ABT-199 with HHT was highly active against primary cells obtained from patients with refractory or relapsed AML.

## MATERIALS AND METHODS

### Chemicals and Reagents

ABT-199 was purchased from Selleck Chemicals (Houston, TX, USA). HHT (Zhejiang Minsheng Pharmaceutical, Zhejiang, China) was dissolved in sterile phosphate-buffered saline (PBS) at 1 mg/mL and stored at -20°C. HHT was diluted to the required concentrations in subsequent experiments with culture medium.

### Cell Culture

AML cell lines (OCL-AML2, OCL-AML3, MOLM-13, and MV4-11) were purchased from the American Type Culture Collection (ATCC, Manassas, VA, USA). Cells were cultured in a humidified incubator at 37°C and 5% $CO_2$ in RPMI 1640 medium (HyClone, Logan, UT, USA) containing 10% fetal bovine serum (FBS) (Gemini, Sacramento, CA, USA).

### Patient Samples

Primary AML cells were extracted from patients newly diagnosed with AML at the Department of Hematology, the First Affiliated Hospital of Zhejiang University. Bone marrow samples were collected from healthy hematopoietic stem cell transplantation donors (n=11). The characteristics of the patients with AML are shown in **Table 3**. The experiment was conducted by the guidelines of the Declaration of Helsinki and was approved by the Ethics Committee of the Faculty of the First Affiliated Hospital of Zhejiang University. IRB approval information is shown in **Supplemental 4**.

### Cell Viability Assay

The cytotoxic effects of ABT-199 and HHT on AML cell lines were determined by a Cell Counting Kit-8 (CCK8; Dojindo, Kumamoto, Japan) assay. Cells (2×10 (4) cells/well) were seeded in 96-well plates containing 100 μL growth medium and treated with designated doses of ABT-199 or HHT alone or in combination at 37°C in a humidified 5% $CO_2$-95% air incubator for 24 h or 48 h; the optical densities (O.D.s) at the dual wavelengths of 450/630 nm were determined using a microplate reader (BIO-TEK EPOCH, USA).

### *In Vitro* Clonogenicity Assay

To evaluate colony-forming abilities following drug treatment, OCL-AML2, OCL-AML3, and MOLM-13 cells ($2\times10^5$/well) in the logarithmic growth phase were seeded in 24-well plates and then treated with 80 nM ABT-199 or 16 nM HHT alone or both molecules. After 24 h, the cells were washed and further cultured in complete methylcellulose medium at a cell density of 500 cells/well in 3.5-cm dishes for 14 days. Colonies consisting of at least 50 cells were counted and analyzed for clonogenicity.

### Apoptosis Assay

To assess apoptosis, OCL-AML2, OCL-AML3, MOLM-13, and MV4-11 cells were cultured and treated with different doses of ABT-199 or HHT alone or in combination for 24 h or 48 h and then double-labeled with Annexin-V-FITC/PI (eBioscience, San Diego, California, USA) for 20 min at room temperature in the dark according to the manufacturer's instructions. The stained cells were analyzed with a NovoCyte flow cytometer (ACEA Biosciences, Inc.) with NovoExpress software. Apoptotic cells were defined as Annexin-V positive.

### Western Blot Analysis

Cell lysates were prepared using RIPA protein lysis buffer (Beyotime, Nantong, China). MOLM-13 cells ($2\times10^5$/mL) were cultured with 5 nM ABT-199 or 4 nM HHT alone or the two drugs in combination for 24 h because no obvious apoptosis was observed at this time. The specific antibodies used in this study included those specific for β-actin, MCL-1, Caspase-3, BCL-2, FLT3, and (rabbit monoclonal antibodies, 1:1000, Cell Signaling Technology). Proteins were detected by the addition of horseradish peroxidase (HRP)-conjugated secondary antibody. Signals were detected using the ECL Western Blotting Detection Kit (Gene-Flow, Staffordshire, UK).

### Xenograft Tumor Model

Twenty-four female NOD/SCID mice (4-6 weeks of age, nonpregnant, female, and 16-18 g) were purchased from the Nanjing Biomedical Research Institute of Nanjing University (Nanjing, China). OCL-AML3 cells ($5\times10^6$) were subcutaneously injected into the front-left region of the NOD/SCID mice. When tumor volumes reached approximately 75 $mm^3$, the mice were

randomly divided into four groups: the vehicle, ABT-199, HHT, and combination groups (n=5). The mice were treated with the vehicle (the same volume of normal saline), ABT-199 (50 mg/kg/day), HHT (1.0 mg/kg/day), or the corresponding doses of ABT-199 and HHT by oral gavage for 2 successive weeks. Tumor volume (V) was determined by the equation $V = (L \times W^2)/2$, where L is tumor length and W is tumor width.

## Statistical Analysis

Statistical analyses were conducted using Prism software v6.0 (GraphPad Software, La Jolla, CA, USA); at least three independent experiments were performed and compared using Student's t-test. Multigroup comparisons were performed using one-way analysis of variance (ANOVA) followed by the Bonferroni *post hoc* test. Survival was estimated using Kaplan-Meier analysis and compared using the log-rank test. We used Calcusyn v2.0 software to calculate the "combination index" (CI) of the drug combination treatment to describe synergism (CI < 1), addictive effect (CI = 1), or antagonism (CI > 1) (13). P values < 0.05 were considered statistically significant. Statistical analyses were performed using SPSS 20.0 software (La Jolla, CA).

# RESULTS

## Combination of ABT-199 and HHT Exerted Antileukemic Activity in Diverse AML Cell Lines

First, we used an MTT assay to examine the viability of AML cell lines treated with ABT-199 or HHT alone or in combination. The concentrations of ABT-199 and HHT are shown in **Figures 1A–H**. We found that AML cell lines treated with both ABT-199 and HHT showed a much better inhibitory effect especially in OCL-AML2, OCL-AML3, MOLM-13, and MV4-11cell lines with FLT3-ITD mutation than those treated with each reagent alone in a time-dependent manner. The half-maximal inhibitory concentration (IC50) values (**Table 1**) of ABT-199 and HHT were lower at 48 h than at 24 h in all cell lines (P < 0.001). Percent viabilities of the DMSO-treated control of the ABT-199 and HHT in the ratios (3:1 and 7:1) were shown in the **Supplemental Figures 1**, **2**.

## Combination Treatment With ABT-199 and HHT Synergistically Induced Apoptosis in Both AML Cell Lines and Primary AML Samples

We investigated the effects of ABT-199 and HHT alone or in combination on AML cell lines. OCL-AML2, OCL-AML3, MOLM13, and MV4-11 cells were exposed to the indicated concentrations of ABT-199 with or without HHT for 24 h or 48 h. As shown in **Figure 2A**, ABT-199 or HHT alone was unable to induce apoptosis, while the combination could significantly increase apoptosis in all of the tested AML cell lines. Combination index (CI) values were calculated according to the median effect method of Chou and Talala (**Table 2**). A CI value of less than 1.0 indicates a synergistic effect. Then, we further confirmed the antileukemic activity of ABT-199 combined with HHT in primary samples (n=5). The clinical characteristics of the donor AML patients are summarized in **Table 3**. Consistent with the antileukemic activity of ABT-199 plus HHT observed in the AML cell lines (**Figures 2B–E**), exposure of primary AML cells to ABT-199 and HHT resulted in remarkable apoptosis (**Figure 2F**). In contrast, the combination of ABT-199 and HHT displayed minimal toxicity to normal peripheral blood mononuclear cells obtained from healthy donors (n=11) (**Figure 2G**). The CI value of other ratios of ABT-199 and HHT were shown in the **Supplemental Figure 3**(**3:1**) and **Supplemental Figure 4** (**7:1**). The CI values are listed in **Supplemental Table 1**. These findings indicated that the combination of ABT-199 and HHT might be a promising therapy for AML that spares normal hematopoietic cells.

## Effects of ABT-199 Combined With HHT on Colony Formation

Clonogenicity assays were carried out to investigate whether ABT-199 combined with HHT affects the clonogenic capacity of AML cells. Therefore, OCL-AML2, OCL-AML3, and MOLM-13 cells were treated with the indicated concentrations of ABT-199 or HHT alone or in combination for 24 h. Neither ABT-199 (80 nM) nor HHT (16 nM) alone diminished the colony formation abilities of the OCL-AML2, OCL-AML3, and MOLM-13 cells (**Figures 3A–C**). The colony formation of MV4-11 was listed in the **Supplemental Figure 5**. However, when the combination of ABT-199 and HHT was given, the colony-forming units decreased remarkably (P<0.001 *vs.* control, ABT-199 alone, or HHT alone).

## Combination Therapy With ABT-19 and HHT Was More Active Than Either Monotherapy in a Xenograft Mouse Model

To validate that the joint effects of ABT-199 and HHT measured *in vitro* translate into a difference in tumor responsiveness *in vivo*, we established a xenograft mouse model by subcutaneous injection of OCL-AML3 cells. As we expected, the results were consistent with those of the *in vitro* experiments. Mice treated with ABT-199 combined with HHT showed a remarkably reduced tumor burden (**Figures 4A–C**). Moreover, the combined treatment group showed little lethal toxicity (**Figure 4D**). Consistently, histopathological analysis revealed a remarkable reduction in leukemia cell infiltration into tumor tissue in the combination group (**Figure 4E**). In brief, the combination regimen of ABT-199 and HHT was more effective than the corresponding single-agent treatments in inhibiting AML growth and progression.

## ABT-199 Combined With HHT Modulated MCL-1 Phosphorylation by Inhibiting p-ERK and Activating BAX

To better understand the underlying mechanism of the reductions in BCL-2 and MCL-1, Western blotting was performed, and the results showed that the reductions in the MCL-1 protein levels in AML cell lines treated with HHT might be mediated through proteasome degradation. ABT-199 has been reported to associate with BAX. We found that ABT-199 combined with HHT reduced MCL-1 level but increased BAX level. In addition, compared with ABT-199 or HHT alone, combination treatment produced more p-ERK degradation. The results showed that ABT-199 combined with HHT

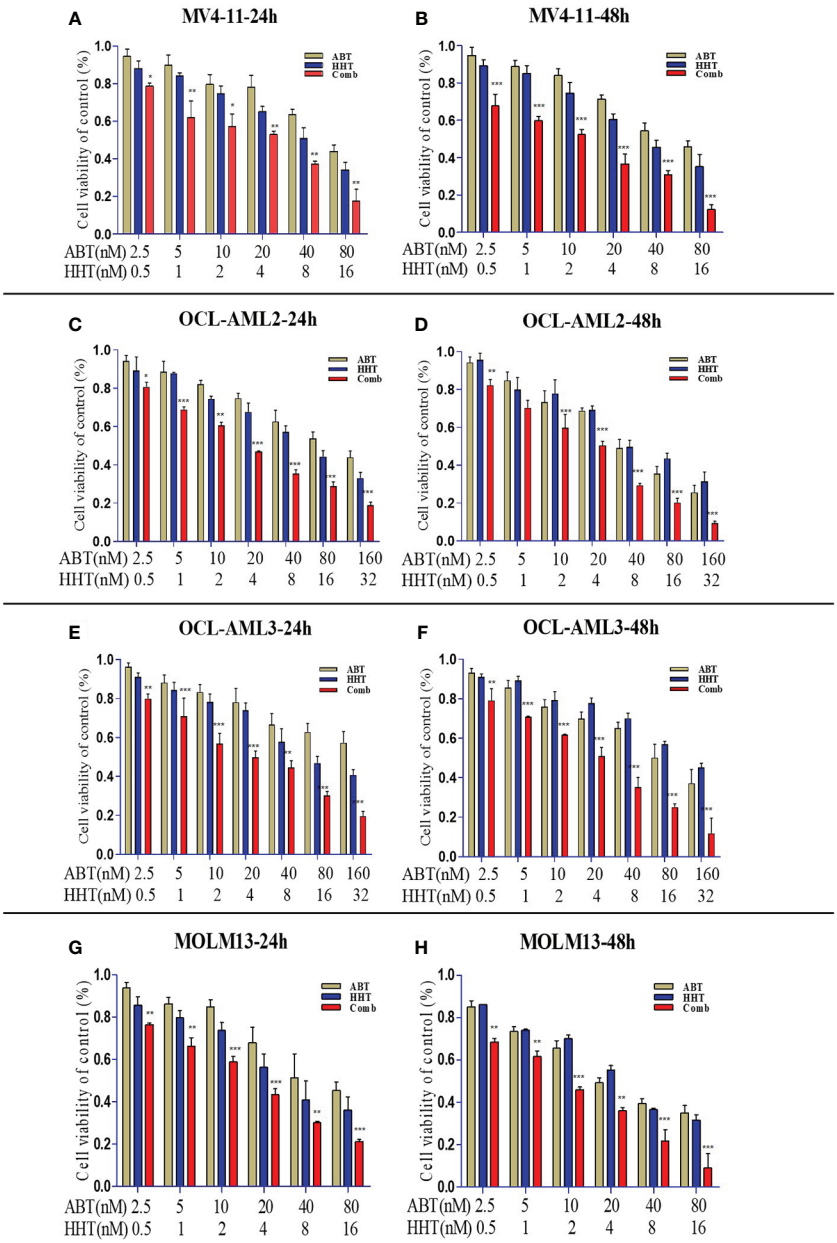


**FIGURE 1** | AML cell lines (OCL-AML2, OCL-AML3, MOLM13, and MV4-11) were treated with various doses of ABT-199 or HHT alone or in combination for 24 h or 48 h **(A–H)**. The percent viability is normalized to the percent viability of the DMSO-treated control. Values are expressed as the mean ± S.D. @ of three independent experiments (*P < 0.05, **P < 0.01, and ***P < 0.001).

**TABLE 1** | $IC_{50}$ values of ABT-199 and HHT as single agent in AML cells.

| AML cell lines | $IC_{50}$ at 24h(nM) | | $IC_{50}$ at 48h(nM) | |
|---|---|---|---|---|
| | ABT-199 | HHT | ABT-199 | HHT |
| MV4-11 | 12.54 ± 2.69 | 10.15 ± 1.82 | 9.07 ± 1.30 | 5.32 ± 1.21 |
| MOLM13 | 9.81 ± 1.13 | 6.060 ± 0.84 | 2.86 ± 1.51 | 1.54 ± 0.89 |
| OCL-AML2 | 126.2 ± 2.43 | 65.00 ± 1.96 | 15.67 ± 0.65 | 4.67 ± 0.79 |
| OCL-AML3 | 34.1 ± 0.49 | 23.94 ± 0.53 | 3.87 ± 0.69 | 4.85 ± 0.83 |

*IC50: Half maximal inhibitory concentration.*

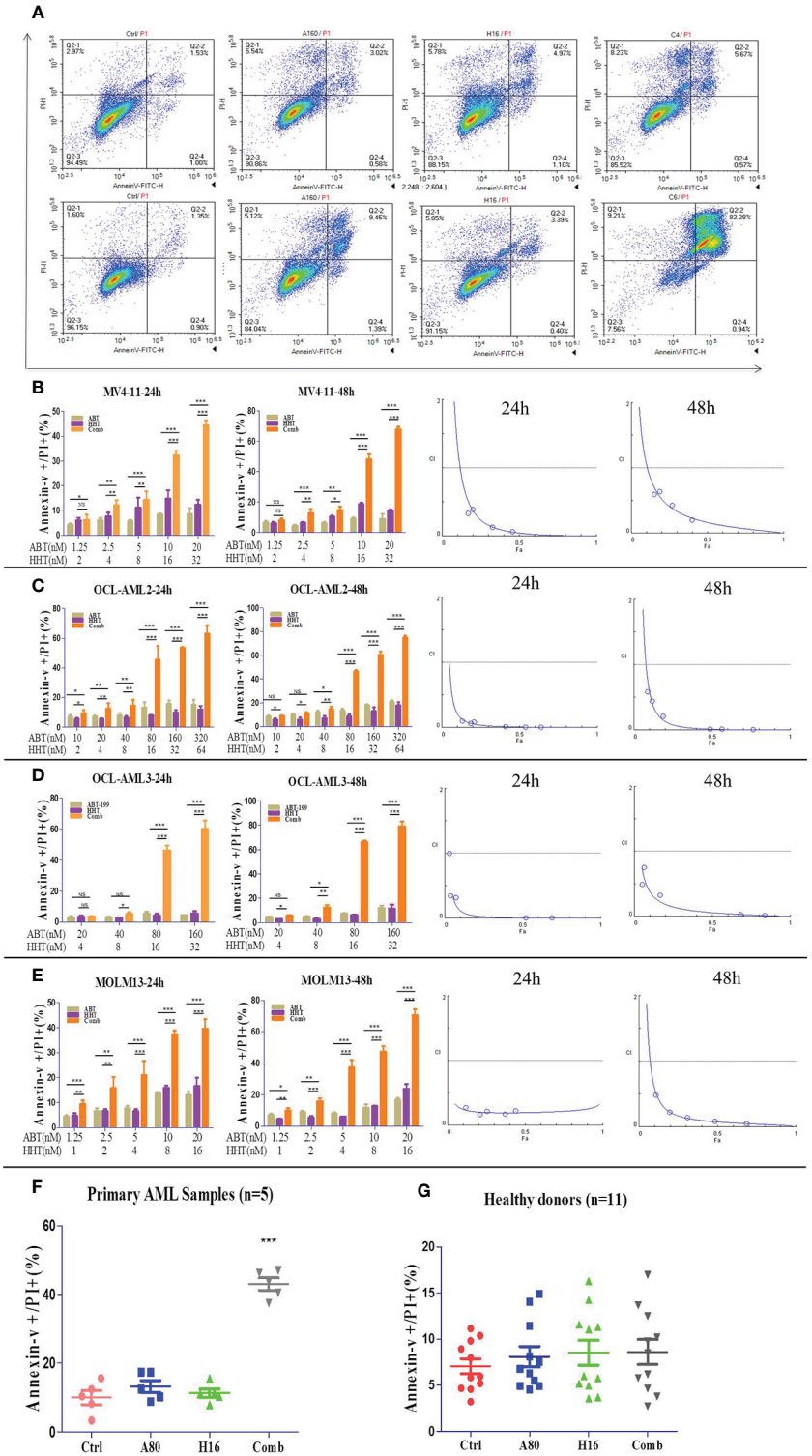


**FIGURE 2** | The percentage of apoptotic cells was examined with a NovoCyte flow cytometer. ABT-199 combined with HHT resulted in significant increases in the apoptosis rate in AML cell lines **(A)**. The same results were observed in primary leukemia samples **(B–F)**. The combination regimen exhibited minimal toxicity to normal peripheral blood mononuclear cells obtained from healthy donors **(G)** (*P < 0.05, **P < 0.01, and ***P < 0.001; NS, not significant).

**TABLE 2 |** The effect of synergistic inhibition in AML cell lines.

| **MV4-11** | | | | | |
|---|---|---|---|---|---|
| **Concentration (nM)** | | **24h** | | **48h** | |
| ABT-199 | HHT | Fa | CI | Fa | CI |
| 1.25 | 2 | 0.352 | 5.011 | 0.446 | 0.253 |
| 2.5 | 4 | 0.553 | 0.322 | 0.528 | 0.321 |
| 5 | 8 | 0.582 | 0.383 | 0.660 | 0.620 |
| 10 | 16 | 0.642 | 0.120 | 0.573 | 0.071 |
| 20 | 32 | 0.703 | 0.061 | 0.694 | 0.023 |
| MOLM13 | | | | | |
| Concentration (nM) | | 24h | | 48h | |
| ABT-199 | HHT | Fa | CI | Fa | CI |
| 1.25 | 1 | 0.121 | 0.2705 | 0.110 | 0.4823 |
| 2.5 | 2 | 0.210 | 0.1653 | 0.197 | 0.2216 |
| 5 | 4 | 0.256 | 0.2125 | 0.312 | 0.1411 |
| 10 | 8 | 0.374 | 0.1711 | 0.485 | 0.0845 |
| 20 | 16 | 0.442 | 0.2184 | 0.687 | 0.0467 |
| OCL-AML2 | | | | | |
| Concentration (nM) | | 24h | | 48h | |
| ABT-199 | HHT | Fa | CI | Fa | CI |
| 10 | 2 | 0.135 | 0.097 | 0.089 | 0.584 |
| 20 | 4 | 0.188 | 0.061 | 0.121 | 0.441 |
| 40 | 8 | 0.207 | 0.083 | 0.189 | 0.205 |
| 80 | 16 | 0.413 | 0.011 | 0.488 | 0.009 |
| 160 | 32 | 0.541 | 0.005 | 0.566 | 0.008 |
| 320 | 64 | 0.641 | 0.003 | 0.766 | 0.001 |
| OCL-AML3 | | | | | |
| Concentration (nM) | | 24h | | 48h | |
| ABT-199 | HHT | Fa | CI | Fa | CI |
| 10 | 2 | 0.039 | 0.341 | 0.054 | 0.489 |
| 20 | 4 | 0.033 | 0.992 | 0.064 | 0.753 |
| 40 | 8 | 0.075 | 0.312 | 0.168 | 0.318 |
| 80 | 16 | 0.522 | 0.003 | 0.648 | 0.028 |
| 160 | 32 | 0.688 | 0.002 | 0.838 | 0.014 |

*CI, Combination index.*
*Fa, Fractional inhibition.*

**TABLE 3 |** The characteristics of 5 cases diagnosed with *de novo* or refractory/relapsed acute myeloid leukemia.

| **Patient** | **Sex** | **Age** | **Cell count(10^9)** | | | **LDH(U/L)** | **Karyo-type** | **Molecular features** |
|---|---|---|---|---|---|---|---|---|
| **No.** | | **(yr)** | **WBC** | **HB** | **PLT** | | | |
| 1 | F | 44 | 28.1X10^9/L | 66.0g/L | 73.0X10^9/L | 256/L | 46, XY | No |
| 2 | M | 29 | 54.15 | 77.0 | 43.0 | 255 | 46, XY, t(11;19) | No |
| 3 | M | 27 | 20.50 | 69.0 | 63 | 691 | 46, t(8;21) | AML-ETO |
| 4 | M | 62 | 44.43 | 43.0 | 204 | 226 | ND | No |
| 5 | M | 65 | 49.29 | 162 | 43.0 | 432 | 46, XY | No |

modulated MCL-1 phosphorylation by inhibiting p-ERK and activating BAX (**Figure 5A**).

## ABT-199 Combined With HHT Downregulated the FLT3/Stat5/MCL-1 Signaling Cascade

To investigate the cytotoxicity mechanism of ABT-199 combined with HHT in AML cells, potential signals were further analyzed by Western blot analysis. As we have mentioned above ABT-199 combined with HHT are sensitive to FLT3 mutant cell lines so ABT-199 combined with HHT markedly reduced the phosphorylation of FLT3 in the MOLM13 cell line (**Figure 5B**). However, the FLT3 downstream signaling molecules total Stat5 did not significantly change. Our results showed that ABT-199 combined with HHT yielded substantial reductions in the levels of p-FLT3 and p-Stat5 in MOLM13 cells. The total and phosphorylation protein of FLT3 and STAT in a FLT3 ITD-negative cell line were shown in **Figure 5C**.

# DISCUSSION

Chemotherapy is currently one of the main approaches for AML therapy. However, most targeted agents concentrate on upstream

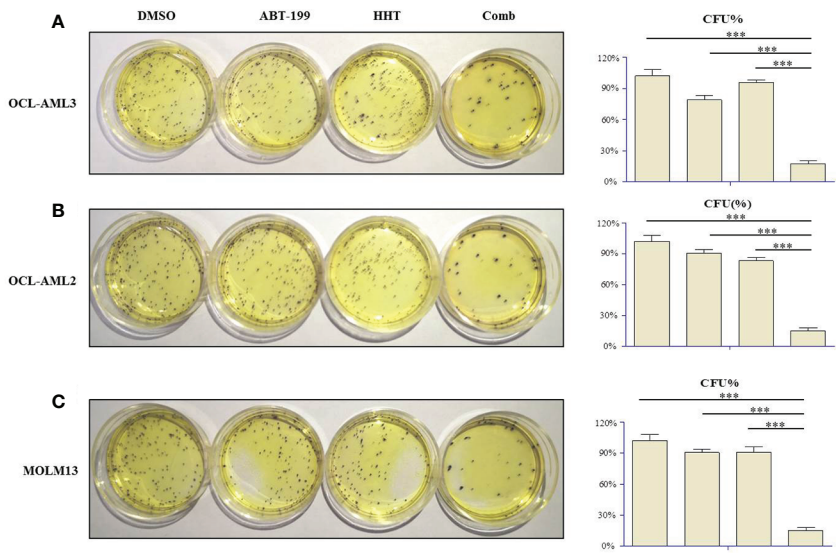


**FIGURE 3** | The numbers of colony-forming units (CFU) produced by OCL-AML2, OCL-AML3, and MOLM13 cells exposed to ABT-199 alone (80 nM) or in combination with HHT (16 nM) in a methylcellulose culture system for 24 h **(A–C)**. The percentage of CFU was determined by counting colonies (≥50 cells). Data are presented as the mean ± S.D. @ of three independent experiments. (*P < 0.05, **P < 0.01, and ***P < 0.001).

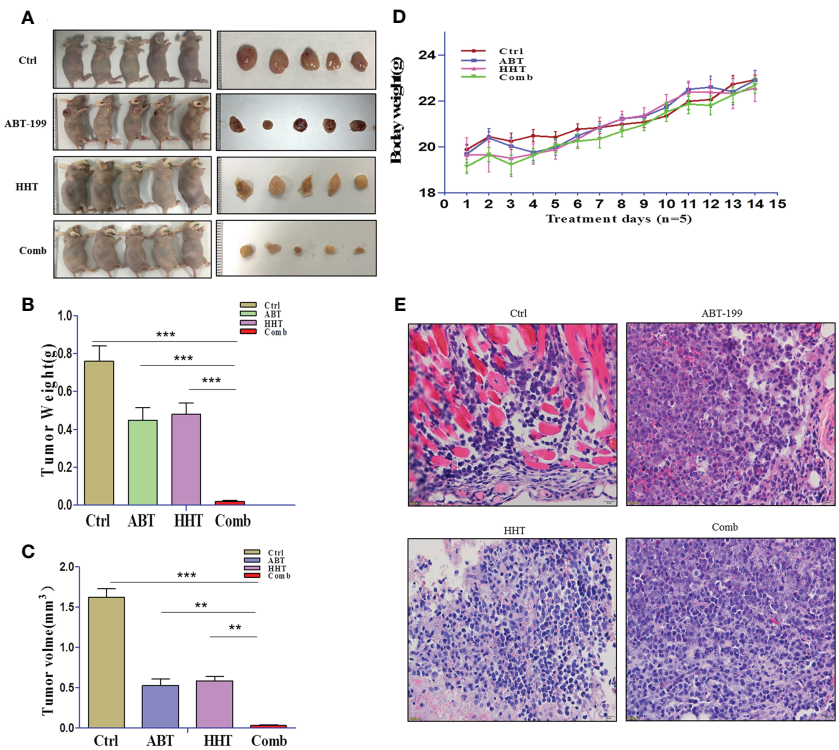


**FIGURE 4** | The antitumor potency of ABT-199 combined with HHT was evaluated in OCL-AML3 cell line-derived mouse xenograft models (n = 5 per group). Compared with each agent alone, the combination of ABT-199 with HHT significantly decreased the tumor burden, including tumor size and weight **(A–C)**. Mouse body weight was measured every other day. **(D)** Bone marrow from mice was embedded in paraffin and stained with H&E. Scale bar, 25 μm. Data represent the mean ± S.D. *P < 0.05 *vs* the cotreatment groups **(E)**. (*P < 0.05, **P < 0.01, and ***P < 0.001).

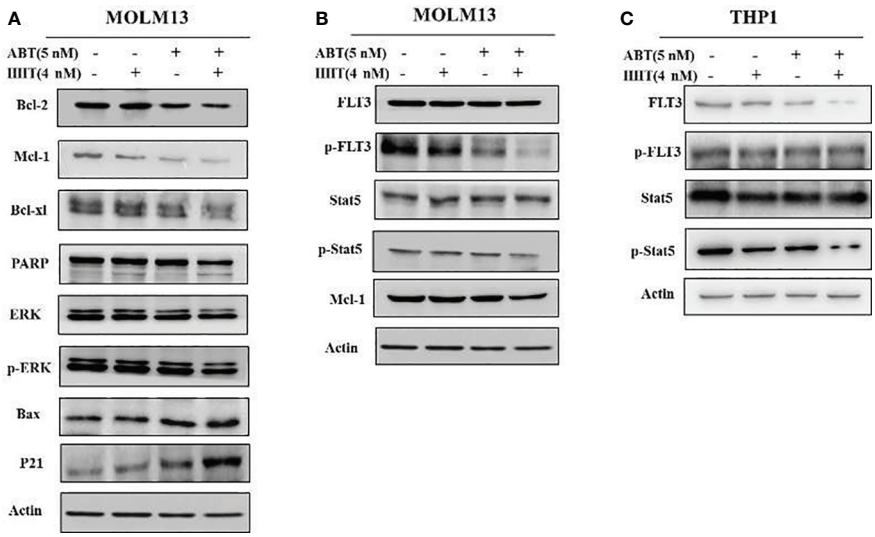


**FIGURE 5** | In the MOLM-13 cell lines, compared with each agent alone, ABT-199 combined with HHT downregulated MCL-1, p-ERK expression **(A)**. Strikingly, our results also showed that cotreatment with ABT-199 and HHT inhibited the FLT3/Stat5/MCL-1 signaling cascade, and the protein levels of p-FLT3, p-Stat5, and MCL-1 were determined by Western blotting **(B)**. The total and phosphorylation protein of FLT3 and STAT in a FLT3 ITD-negative cell line were shown by Western blot **(C)**.

nodes in cancer signaling pathways. Drug resistance and severe side effects as well as relatively low overall survival limit the use of traditional chemotherapeutic drugs (14, 15). Drug resistance is usually inevitable, particularly for monotherapies utilizing targeted compounds, due to complex cancer signaling pathways (16, 17). Studies have shown that FLT3-ITD MR is related to complete remission (CR) and overall survival (OS) in AML patients. Furthermore, FLT3-ITD MR may act as an independent prognostic factor for OS in non-M3 AML patients. Classifying risk grades based on FLT3-ITD MR is crucial for individualized treatment and prognostic evaluation. Concordantly, monotherapy with ABT-199 has a finite efficacy because of the absence of triggering of BH3-only protein expression and compensatory upregulation of MCL-1 expression (18, 19). Combining two agents is an effective way to reduce the dose used at this stage. An ideal combination of two drugs would be able to enhance proapoptotic effects, such as inducing the expression of the Bax protein. According to our research, we found that ABT-199 combined with HHT exerted superior synergistic lethality in AML cell lines.

HHT, a natural alkaloid derived from Cephalotaxus, is widely applied for AML therapy in China (12, 20–23). Recently, some researchers launched a national, multicenter, randomized, double-blinded, prospective phase III clinical trial to study the effect of an HHT-based induction regimen on *de novo* AML patients. The results showed that the HHT-based regimen achieved a relatively high completion rate and prolonged overall survival (24). Additionally, HHT plays an important role in the treatment of chronic myeloid leukemia (CML). In 2010, FAD evaluated the use of HHT in relapsed/refractory CML. Clinical research on the mechanisms of action of HHT has found different mechanisms, including binding with the small subunit of the ribosome and interfering with the process of translation to inhibit protein synthesis (25). However, adverse events have been observed to be similar in all groups studied (26). Tumor recurrence and drug resistance are associated with high expression of anti-apoptotic proteins, such as MCL-1, that have been increasingly recognized as important targets in cancer therapy (8). In addition, because the MCL-1 protein has a short half-life, it can be easily cleaved by activated caspases during apoptotic cell death (27). Numerous experiments have shown that co-treatment with other antitumor therapeutics can reduce the level of MCL-1. It was recently reported that the anti-apoptotic activity of MCL-1 is necessary for the development and sustained growth of AML (28). If a drug can effectively inhibit MCL-1, then it should have some effects on AML.

BCL-2 was initially found in lymphoid cancer cells. A large number of studies on BCL-2 have been conducted in lymphoid cells, in which BCL-2 is highly expressed (29, 30). In our research, we found that selective, on-target BCL-2 inhibition was a superior method for the clinical treatment of AML (31). It should be noted that even AML myeloblasts that are not sensitive to conventional chemotherapy appear to be quite sensitive to BCL-2 inhibitors (32). Thus, the BCL-2 inhibitor ABT-199, an effective chemotherapeutic agent, has been used in the clinic. In our research, we found that Bax expression was dramatically upregulated, whereas BCL-2 and MCL-1 levels were downregulated in ABT-199 plus HHT combination-treated cells, leading to a dramatic increase in the cleavage of caspase-3, which may be one of the ways that HHT enhances the promotive effect of ABT-199 on apoptosis in AML cell lines.

Our results found that ABT-199 combined with HHT could inhibit those with FLT3-ITD mutant of AML cell proliferation by inducing apoptosis in a dose- and time-dependent manner. Furthermore, the possible mechanism revealed inhibition of the

antiapoptotic proteins BCL-2 and MCL-1 and activation of caspase family members, such as caspase-3 and caspase-9. Cell cycle blockade inhibits DNA synthesis, thereby inhibiting cell proliferation and promoting antileukemic effects (33). The critical role of PI3K signaling in the progression of numerous tumors, including leukemia, has been well reported (34, 35). Strikingly, we revealed that ABT-199 combined with HHT could effectively inhibit the expression of p-FLT3 and its downstream signaling proteins, p-Stat5 and MCL-1, inducing apoptosis in AML cell lines.

Interestingly, according to the IC50 value, we observed a phenomenon in which MV4-11 and MOLM13 cells carried the FLT3-ITD mutation and exhibited increased sensitivity to ABT-199, especially when combined with HHT. It has been reported that HHT affects the FLT3-STAT5 signaling pathway (36). Our research showed that HHT, especially in combination with ABT-199, had a significant effect on the FLT3 signaling pathway by downregulating the phosphorylation of FLT3 and STAT5. In this study, the combination of ABT-199 and HHT exerted promising antileukemic effects at the lower tested doses. The low but effective doses of ABT-199 combined with HHT likely observed *in vitro* may produce tolerance advantages *in vivo*. Overall, our study provided a rationale for a novel combination approach to cure AML. Besides, our research indicated that HHT could strengthen the antileukemic effect of ABT-199 *in vitro* and *in vivo*. In addition, we also discussed the potential mechanisms of the two drugs. Therefore, our findings provide a strong rationale for a phase I/II clinical trial with ABT-199 and HHT combination treatment of AML patients.

## CONCLUSION

Taken together, our research results show that ABT-199 combined with HHT exerts antileukemic activity *in vitro* and *in vivo*, likely through inhibiting the expression of BCL-2 and MCL-1, as well as the FLT3-STAT5 signaling pathway, and provide potential benefits and a clinical application approach for ABT-199 and HHT in AML patients.

## DATA AVAILABILITY STATEMENT

The original contributions presented in the study are included in the article/**Supplementary Material**. Further inquiries can be directed to the corresponding author.

## ETHICS STATEMENT

The animal study was reviewed and approved by Department of Hematology, The First Affiliated Hospital, College of Medicine, Zhejiang University.

## AUTHOR CONTRIBUTIONS

YS and JY performed the experiments and analysis of data. YY and HS collected primary AML samples and interpret data and wrote the manuscript. XY and WX contributed to study design, data analysis, and interpretation and manuscript revision. All authors contributed to the article and approved the submitted version.

## FUNDING

This work was supported in part by the Research Plan of the National Natural Science Foundation of China (No. 81372256).

## SUPPLEMENTARY MATERIAL

The Supplementary Material for this article can be found online at: https://www.frontiersin.org/articles/10.3389/fonc.2021.692497/full#supplementary-material

## REFERENCES

1. O'Dwyer K, Freyer DR, Horan JT. Treatment Strategies for Adolescent and Young Adult Patients With Acute Myeloid Leukemia. *Blood* (2018) 132:362–8. doi: 10.1182/blood-2017-12-778472
2. Walter RB, Estey EH. Management of Older or Unfit Patients With Acute Myeloid Leukemia. *Leukemia* (2015) 29:770–5. doi: 10.1038/leu.2014.216
3. Hanahan D, Weinberg RA. Hallmarks of Cancer: The Next Generation. *Cell* (2011) 144:646–74. doi: 10.1016/j.cell.2011.02.013
4. Ding Q, Zhang Z, Liu J-J, Jiang N, Zhang J, Ross TM, et al. Discovery of RG7388, a Potent and Selective P53-MDM2 Inhibitor in Clinical Development. *J Med Chem* (2013) 56:5979–83. doi: 10.1021/jm400487c
5. Czabotar PE, Lessene G, Strasser A, Adams JM. Control of Apoptosis by the BCL-2 Protein Family: Implications for Physiology and Therapy. *Nat Rev Mol Cell Biol* (2014) 15:49–63. doi: 10.1038/nrm3722
6. Delbridge AR, Grabow S, Strasser A, Vaux DL. Thirty Years of BCL-2: Translating Cell Death Discoveries Into Novel Cancer Therapies. *Nat Rev Cancer* (2016) 16:99–109. doi: 10.1038/nrc.2015.17
7. Klanova M, Andera L, Brazina J, Svadlenka J, Benesova S, Soukup J, et al. Targeting of BCL2 Family Proteins With ABT-199 and Homoharringtonine Reveals BCL2- and MCL1-Dependent Subgroups of Diffuse Large B-Cell Lymphoma. *Clin Cancer Res* (2016) 22:1138–49. doi: 10.1158/1078-0432.CCR-15-1191
8. Hata AN, Engelman JA, Faber AC. The BCL2 Family: Key Mediators of the Apoptotic Response to Targeted Anticancer Therapeutics. *Cancer Discov* (2015) 5:475–87. doi: 10.1158/2159-8290.CD-15-0011
9. Konopleva M, Contractor R, Tsao T, Samudio I, Ruvolo PP, Kitada S, et al. Mechanisms of Apoptosis Sensitivity and Resistance to the BH3 Mimetic ABT-737 in Acute Myeloid Leukemia. *Cancer Cell* (2006) 10:375–88. doi: 10.1016/j.ccr.2006.10.006
10. Kruiswijk F, Labuschagne CF, Vousden KH. p53 in Survival, Death and Metabolic Health: A Lifeguard With a Licence to Kill. *Nat Rev Mol Cell Biol* (2015) 16:393–405. doi: 10.1038/nrm4007
11. Lu S, Wang J. Homoharringtonine and Omacetaxine for Myeloid Hematological Malignancies. *J Hematol Oncol* (2014) 7:2. doi: 10.1186/1756-8722-7-2
12. Feldman E, Arlin Z, Ahmed T, Mittelman A, Puccio C, Chun H, et al. Homoharringtonine Is Safe and Effective for Patients With Acute Myelogenous Leukemia. *Leukemia* (1992) 6:1185–8. doi: 10.1002/hon.2900100607
13. Chou TC, Talalay P. Quantitative Analysis of Dose-Effect Relationships: The Combined Effects of Multiple Drugs or Enzyme Inhibitors. *Adv Enzyme Regul* (1984) 22:27–55. doi: 10.1016/0065-2571(84)90007-4

14. Chandarlapaty S. Negative Feedback and Adaptive Resistance to the Targeted Therapy of Cancer. *Cancer Discov* (2012) 2:311–9. doi: 10.1158/2159-8290.CD-12-0018
15. Trusolino L, Bertotti A. Compensatory Pathways in Oncogenic Kinase Signaling and Resistance to Targeted Therapies: Six Degrees of Separation. *Cancer Discovery* (2012) 2:876–80. doi: 10.1158/2159-8290.CD-12-0400
16. Winter AM, Landsburg DJ, Mato AR, Isaac K, Hernandez-Ilizaliturri FJ, Reddy N, et al. A Multi-Institutional Outcomes Analysis of Patients With Relapsed or Refractory DLBCL Treated With Ibrutinib. *Blood* (2017) 130:1676–9. doi: 10.1182/blood-2017-05-786988
17. Wang ML, Blum KA, Martin P, Goy A, Auer R, Kahl BS, et al. Long-Term Follow-Up of MCL Patients Treated With Single-Agent Ibrutinib: Updated Safety and Efficacy Results. *Blood* (2015) 126:739–45. doi: 10.1182/blood-2015-03-635326
18. Chen J, Jin S, Abraham V, Huang X, Liu B, Mitten MJ, et al. The Bcl-2/Bcl-X (L)/Bcl-w Inhibitor, Navitoclax, Enhances the Activity of Chemotherapeutic Agents In Vitro and *In Vivo*. *Mol Cancer Ther* (2011) 10:2340–9. doi: 10.1158/1535-7163.MCT-11-0415
19. Mason KD, Khaw SL, Rayeroux KC, Chew E, Lee EF, Fairlie WD, et al. The BH3 Mimetic Compound, ABT-737, Synergizes With a Range of Cytotoxic Chemotherapy Agents in Chronic Lymphocytic Leukemia. *Leukemia* (2009) 23:2034–41. doi: 10.1038/leu.2009.151
20. Rawlings DJ, Saffran DC, Tsukada S, Largaespada DA, Grimaldi JC, Cohen L, et al. Mutation of Unique Region of Bruton's Tyrosine Kinase in Immunodeficient XID Mice. *Science* (1993) 261:358–61. doi: 10.1126/science.8332901
21. Cephalotaxine Esters in the Treatment of Acute Leukemia. A Preliminary Clinical Assessment. *Chin Med J (Engl)* (1976) 2:263–72.
22. Harringtonine in Acute Leukemias. Clinical Analysis of 31 Cases. *Chin Med J (Engl)* (1977) 3:319–24.
23. Rai KR, Holland KF, Glidewell OJ, Weinberg V, Brunner K, Obrecht JP, et al. Treatment of Acute Myelocytic Leukemia: A Study by Cancer and Leukemia Group B. *Blood* (1981) 58:1203–12. doi: 10.1182/blood.V58.6.1203.bloodjournal5861203
24. Wang J, Lü S, Yang J, Song X, Chen L, Huang C, et al. A Homoharringtonine-Based Induction Regimen for the Treatment of Elderly Patients With Acute Myeloid Leukemia: a Single Center Experience From China. *J Hematol Oncol* (2009) 2:32. doi: 10.1186/1756-8722-2-32
25. Fresno M, Jimenez A, Vazquez D. Inhibition of Translation in Eukaryotic Systems by Harringtonine. *Eur J Biochem* (1977) 72:323–30. doi: 10.1111/j.1432-1033.1977.tb11256.x
26. Thomas JD, Sideras P, Smith CI, Vorechovský I, Chapman V, Paul WE. Colocalization of X-Linked Agammaglobulinemia and X-Linked Immunodeficiency Genes. *Science* (1993) 261:355–8. doi: 10.1126/science.8332900
27. Opferman JT. Unraveling MCL-1 Degradation. *Cell Death Differ* (2006) 13:1260–2. doi: 10.1038/sj.cdd.4401978
28. Glaser SP, Lee EF, Trounson E, Bouillet P, Wei A, Fairlie WD, et al. Anti-Apoptotic Mcl-1 Is Essential for the Development and Sustained Growth of Acute Myeloid Leukemia. *Genes Dev* (2012) 26:120–5. doi: 10.1101/gad.182980.111
29. Tsujimoto Y, Finger LR, Yunis J, Nowell PC, Croce CM. Cloning of the Chromosome Breakpoint of Neoplastic B Cells With the T(14;18) Chromosome Translocation. *Science* (1984) 226:1097–9. doi: 10.1126/science.6093263
30. Del Gaizo Moore V, Schlis KD, Sallan SE, Armstrong SA, Letai A. BCL-2 Dependence and ABT-737 Sensitivity in Acute Lymphoblastic Leukemia. *Blood* (2008) 111:2300–9. doi: 10.1182/blood-2007-06-098012
31. Souers AJ, Leverson JD, Boghaert ER, Ackler SL, Catron ND, Chen J, et al. Abt-199, a Potent and Selective BCL-2 Inhibitor, Achieves Antitumor Activity While Sparing Platelets. *Nat Med* (2013) 19:202–8. doi: 10.1038/nm.3048
32. Vaillant F, Merino D, Lee L, Breslin K, Pal B, Ritchie ME, et al. Targeting BCL-2 With the BH3 Mimetic ABT-199 in Estrogen Receptor-Positive Breast Cancer. *Cancer Cell* (2013) 24:120–9. doi: 10.1016/j.ccr.2013.06.002
33. Huang S, Pan J, Jin J, Li C, Li X, Huang J, et al. Abivertinib, a Novel BTK Inhibitor: Anti-Leukemia Effects and Synergistic Efficacy With Homoharringtonine in Acute Myeloid Leukemia. *Cancer Lett* (2019) 461:132–43. doi: 10.1016/j.canlet.2019.07.008
34. Pei R, Si T, Lu Y, Zhou JX, Jiang L. Salvianolic Acid A, a Novel PI3K/Akt Inhibitor, Induces Cell Apoptosis and Suppresses Tumor Growth in Acute Myeloid Leukemia. *Leuk Lymphoma* (2018) 59:1959–67. doi: 10.1080/10428194.2017.1399314
35. Nepstad I, Reikvam H, Brenner AK, Bruserud O, Hatfield KJ. Resistance to the Antiproliferative In Vitro Effect of PI3K-Akt-mTOR Inhibition in Primary Human Acute Myeloid Leukemia Cells Is Associated With Altered Cell Metabolism. *Int J Mol Sci* (2018) 19:1–18. doi: 10.3390/ijms19020382
36. Tong H, Ren Y, Zhang F, Jin J. Homoharringtonine Affects the JAK2-STAT5 Signal Pathway Through Alteration of Protein Tyrosine Kinase Phosphorylation in Acute Myeloid Leukemia Cells. *Eur J Haematol* (2008) 81:259–66. doi: 10.1111/j.1600-0609.2008.01116.x

**Conflict of Interest:** The authors declare that the research was conducted in the absence of any commercial or financial relationships that could be construed as a potential conflict of interest.

frontiers in Oncology

ORIGINAL RESEARCH
published: 16 July 2021
doi: 10.3389/fonc.2021.692592

# A Personalized Therapeutics Approach Using an *In Silico Drosophila Patient Model* Reveals Optimal Chemo- and Targeted Therapy Combinations for Colorectal Cancer

*Mahnoor Naseer Gondal*[1], *Rida Nasir Butt*[1], *Osama Shiraz Shah*[1], *Muhammad Umer Sultan*[1], *Ghulam Mustafa*[1], *Zainab Nasir*[1], *Risham Hussain*[1], *Huma Khawar*[1], *Romena Qazi*[2], *Muhammad Tariq*[3], *Amir Faisal*[4] *and Safee Ullah Chaudhary*[1]*

[1] Biomedical Informatics Research Laboratory, Department of Biology, Lahore University of Management Sciences, Lahore, Pakistan, [2] Department of Pathology, Shaukat Khanum Memorial Cancer Hospital and Research Centre, Lahore, Pakistan, [3] Epigenetics Laboratory, Department of Biology, Lahore University of Management Sciences, Lahore, Pakistan, [4] Cancer Therapeutics Laboratory, Department of Biology, Lahore University of Management Sciences, Lahore, Pakistan

OPEN ACCESS

**Edited by:**
*Aniello Cerrato, Istituto per l'Endocrinologia e l'oncologia "Gaetano Salvatore, Consiglio Nazionale Delle Ricerche (CNR), Italy*

**Reviewed by:**
*Yiorgos Apidianakis, University of Cyprus, Cyprus*
*Dakang Xu, Shanghai Jiao Tong University, China*

***Correspondence:**
*Safee Ullah Chaudhary*
*safee.ullah.chaudhary@gmail.com*

**Specialty section:**
*This article was submitted to Pharmacology of Anti-Cancer Drugs, a section of the journal Frontiers in Oncology*

**Received:** *08 April 2021*
**Accepted:** *30 June 2021*
**Published:** *16 July 2021*

**Citation:**
*Gondal MN, Butt RN, Shah OS, Sultan MU, Mustafa G, Nasir Z, Hussain R, Khawar H, Qazi R, Tariq M, Faisal A and Chaudhary SU (2021) A Personalized Therapeutics Approach Using an In Silico Drosophila Patient Model Reveals Optimal Chemo- and Targeted Therapy Combinations for Colorectal Cancer. Front. Oncol. 11:692592. doi: 10.3389/fonc.2021.692592*

*In silico* models of biomolecular regulation in cancer, annotated with patient-specific gene expression data, can aid in the development of novel personalized cancer therapeutic strategies. *Drosophila melanogaster* is a well-established animal model that is increasingly being employed to evaluate such preclinical personalized cancer therapies. Here, we report five Boolean network models of biomolecular regulation in cells lining the *Drosophila* midgut epithelium and annotate them with colorectal cancer patient-specific mutation data to develop an *in silico Drosophila Patient Model* (DPM). We employed cell-type-specific RNA-seq gene expression data from the FlyGut-*seq* database to annotate and then validate these networks. Next, we developed three literature-based colorectal cancer case studies to evaluate cell fate outcomes from the model. Results obtained from analyses of the proposed DPM help: (i) elucidate cell fate evolution in colorectal tumorigenesis, (ii) validate cytotoxicity of nine FDA-approved CRC drugs, and (iii) devise optimal personalized treatment combinations. The personalized network models helped identify synergistic combinations of paclitaxel-regorafenib, paclitaxel-bortezomib, docetaxel-bortezomib, and paclitaxel-imatinib for treating different colorectal cancer patients. Follow-on therapeutic screening of six colorectal cancer patients from cBioPortal using this drug combination demonstrated a 100% increase in apoptosis and a 100% decrease in proliferation. In conclusion, this work outlines a novel roadmap for decoding colorectal tumorigenesis along with the development of personalized combinatorial therapeutics for preclinical translational studies.

**Keywords: personalized *in silico* cancer models, Boolean network models, cancer systems biology, preclinical *in silico* drug screening, combinatorial therapeutics**

## INTRODUCTION

Cancer development is a multistep process that is driven by a heterogeneous combination of somatic mutations at the genetic and epigenetic levels (1, 2). Specific mutations in oncogenes (3) and tumor suppressor genes (4), that result in their activation and inactivation, respectively, manifest themselves at the tissue level in the form of polyps, multi-layering, and metastasis (1, 5, 6). These system-level properties resulting from heterogeneous biomolecular aberrations and dysregulated cellular processes are abstracted as "*hallmarks of cancer*" (1, 6). The heterogeneity exhibited by cancer cells stems from factors such as genomic instability, clonal evolution, and variations in the microenvironment (7, 8). This fosters plasticity in cancer cells which lead to drug resistance – a leading impediment in the treatment of the disease (7–9). As a result, despite major research initiatives and resultant advancements in decoding the molecular basis of cancer, a comprehensive treatment for the disease still alludes researchers. The limited therapeutic regimens approved by the Food and Drug Administration (FDA) (10–12) exhibit variable efficacies across patients besides a multitude of toxic side effects and, multi-drug resistance (13). Towards designing efficacious personalized cancer therapeutics, recent advances in high-throughput omics-based approaches complemented by patient-specific gene expression data can provide significant assistance (14, 15). Several online databases and portals including cBioPortal (16), The Cancer Genome Atlas (TCGA) (17), and International Cancer Genome Consortium (ICGC) (18) amongst others (19, 20) provide such freely available datasets. However, effective and seamless utilization of such patient-specific genomic data to design personalized cancer therapies is still a fledgling area.

Researchers are increasingly employing whole-animal models (21–24) such a mouse, zebrafish, and fruit fly for preclinical *in vivo* validation of therapeutic hypotheses generated from personalized preclinical studies. Amongst the animal models, *Drosophila melanogaster* has become a popular platform for gene manipulation, investigating site-specific changes in the genome, and high-throughput whole-animal screening (14, 25). Importantly, a comparative study of the human and fly genome showed around 75% of disease-causing genes in humans are conserved in *Drosophila* (24, 26). Additionally, ease of handling and significantly lower genetic redundancy imparts further advantage to the employment of fly models (27). As a result, over 50 different data repositories, and tools are now available for hosting data on the fly genome, RNAi screens, and expression data including FlyGut-*seq* (28), and *FlyAtlas* (29) databases. Specifically in the case of cancer, several *in vivo* studies have been designed to elicit novel therapeutic targets using the *Drosophila* model system (30–33). One salient example is the validation of indomethacin, which is reported to enhance human Adenomatous Polyposis Coli (*hAPC*) induced phenotype in *Drosophila* eye (34) and therefore, employed for treating colorectal cancer (CRC). Vandetanib, another approved targeted therapy that was also validated by using the *Drosophila* system, suppressed Ret activity, and was later approved for medullary thyroid carcinoma (MTC) (30). However, a major shortcoming of using such mono-therapeutic agents for cancer treatment stems from the tumor heterogeneity which results in the selection of resistant cells (35, 36) besides acting specifically on singular pathways. To overcome these issues, multiple therapeutic agents acting on multiple pathways in synergy can significantly increase drug efficacy, besides lowering the therapeutic dosage (36). To evaluate high-efficacy synergistic drug combinations, researchers have employed the *Drosophila* model in preclinical studies to elicit optimal drug combinations (32, 33). The *Drosophila* Lung Cancer Model by Levine et al. (32) helped identify trametinib and fluvastatin as combinatorial drug therapy for lung cancer. Further, an EGFR induced lung tumor model was also designed in *Drosophila* which assisted in providing an alternative combination of drugs for lung cancer treatment through screening an FDA-approved compound library (33). However, combinatorial therapies pose unique challenges such as multidrug resistance in chemotherapy (13) and cross drug resistance (37, 38) besides the continuing need for higher therapeutic efficacies (39). Towards tackling these issues, researchers are now 'personalizing' live animal platforms for employment in preclinical studies to design efficacious therapeutic regimens. For instance, a comprehensive state-of-the-art *in vivo Drosophila Patient Model* (DPM) using a personalized therapeutics approach was described in flies (40). This particular study involved genetic manipulation of the fly genome to induce mutations specific to KRAS-mutant metastatic colorectal cancer. Combinatorial therapies were then given to the transgenic flies, harboring mutations that were identified in the patient, to discover high-efficacy synergistic drug combinations.

Here, we propose a novel computational framework in the form of an *in silico Drosophila Patient Model* (DPM), for developing personalized drug combinations for CRC patients. This framework is designed such that it can facilitate the modeling and analysis of patient-specified CRC network models along with evaluation of combinatorial therapeutic strategies (41, 42). We have constructed five biomolecular network models of cells regulating the maintenance of adult *Drosophila* midgut epithelium lining. These include multipotent intestinal stem cells (ISCs) (43–47), enteroblasts (EBs) (48), enterocytes (ECs), enteroendocrine cells (EEs) (49–53), and visceral muscle (VM) cells (54). Next, we evaluated each network's ability to program cell fates under *normal* conditions as well as under minor perturbations. The ISCs are under the regulation of two sub-regions at the time of division; Apical and Basal (52). In our study, we have incorporated this information and analyzed ISC network under Apical and Basal regulation by changing inputs to the network. The networks including ISC's under Apical and Basal regulation, EB, and EC, were then subjected to three types of inputs including physiological inputs (referred to as "*normal*"), aberrant inputs such that the fly homeostatic midgut regulation is perturbed (referred to as "*stress*"), and oncogenic inputs (referred to as "*cancer*"). The cell fate outcomes under *normal* and *cancer* conditions were validated against published literature. The individual output

node propensities for the *normal* case were also validated against RNA-seq gene expression values taken from the FlyGut-*seq* (28) database. Additionally, three literature-based case studies were constructed to further validate the proposed *in silico* DPM. The first case study replicates colorectal tumorigenesis under progressive mutations using Martorell et al.'s CRC model (55). In the second case study, we employed Markstein et al.'s (56) model to perform therapeutic interventions to validate the cytotoxicity of nine FDA-approved drugs. Finally, in the third case study, we reproduced Bangi et al.'s KRAS-mutant CRC model (40) for evaluating optimal personalized drug treatment combinations by incorporating key patient-specific mutations into our model followed by combinatorial therapeutic screening. Building on these case studies, we devised a novel synergistic combination of a chemotherapeutic agent and a targeted therapy i.e., paclitaxel-regorafenib, paclitaxel-bortezomib, docetaxel-bortezomib, and paclitaxel-imatinib for treating six CRC patients taken from cBioPortal (16), while four patients were treated with only targeted therapy. The results obtained from combinatorial chemo- and targeted therapies show up to a 100% increase in anti-cancerous cell fates such as apoptosis and a 100% reduction in tumorigenesis promoting cell fates such as hyper-proliferation.

Taken together, we propose a computational framework in the form of an *in silico* DPM to provide personalized CRC therapeutics. This approach can help reduce the overall cancer treatment cost by facilitating the development of higher efficacy combinatorial therapies for colorectal cancer.

# RESULTS

## Network Construction and Robustness Analysis of Regulatory Homeostasis in *Drosophila melanogaster* Midgut

To investigate the biomolecular signaling regulating the homeostasis in *Drosophila melanogaster* midgut (**Supplementary Figure 1**), we undertook an extensive literature survey and constructed five cell-type-specific rules-based network models (*details in* **Supplementary Tables 1–5**). Each model corresponds to one of the five cellular phenotypes lining the *Drosophila* midgut including intestinal stem cells (ISCs) (43–47), enteroblasts (EBs) (48), enterocytes (ECs), enteroendocrine cells (EEs) (49–53), and visceral muscle (VM) (54). The schematic of pathway integration in each network model is provided in **Supplementary Figures 2–6**. ISC network contains 48 nodes and 70 edges, EB consists of 45 nodes and 65 edges, EC and EE comprise 39 nodes and 55 edges, and VM contains 42 nodes and 57 edges (**Figures 1A–D**).

Next, to evaluate the biological plausibility of each network, we assessed the network response under *normal* input node values taken from the FlyGut-*seq* database (28) (*see Materials and Methods*). Our results show that the biomolecular network of ISC cells programmed apoptosis (with a propensity of 0.332), extrusion (0.188), proliferation (0.131), and differentiation/EB fate (0.131). EB network exhibited apoptosis (0.379), and extrusion (0.230). In the case of the EC network, apoptosis and dpp production were both programmed with propensities of 0.331, while for VM network apoptosis and dpp production cell fate program with 0.398 propensity (**Figure 1E**).

To determine the robustness of cell fate programming by each type of cell, we induced a 10% perturbation in the input stimuli and observed the network response. The highest variation in cell fates was exhibited in apoptosis (SEM 0.0006), delta production (SEM 0.0012), multilayering (0.0014), and WNT target genes (0.0009) for ISC, EB, EC, and VM, respectively (**Supplementary Figure 7**). The robust cell fate programming results indicate that all five networks are biologically plausible as they exhibited robustness against random perturbations and are hence feasible for employment in onward analyses (57, 58) (**Supplementary Table 6**).

## Evaluation and Validation of Biomolecular Network Models Under *Normal, Stress* and *Colon Cancer* Conditions

To investigate and evaluate the proposed normal networks under *normal, stress*, and *cancerous* conditions (construed as a combination of inputs), Deterministic Analysis (DA) was performed (59) (**Supplementary Table 7**). Results from our analyses (**Figure 2**) revealed that under *normal* conditions, ISC's Apical regulation programmed apoptosis, extrusion, proliferation, and differentiation (or EB fate) with propensities of 0.295, 0.178, 0.130, and 0.130, respectively (**Supplementary Table 8**) (see *Materials and Methods*). Under *stress* conditions, the propensity for proliferation, delta production, apoptosis, and differentiation increased to 0.141, 0.074 (from 0.062 in *normal* conditions), 0.344, and 0.141, respectively. Lastly, in *cancerous* conditions, propensities for multi-layering increased to 0.207, while proliferation, delta production decreased to 0.089 and 0.014, respectively. The results were again validated from the literature which supports that normal ISCs in *stress* conditions are known to undergo higher proliferation (60–62) and since delta is a marker for proliferation, its value increases as well (63–65). However, in the case of *cancer* conditions such as nutrient deprivation, etc., normal cells exhibit lowered proliferation (66, 67). Literature reports also that ISCs upon encountering extreme *stress*, exhibit epithelium multi-layering, augmented by overgrowth (68, 69) (**Supplementary Figures 8–10**).

For the ISC network under Basal regulation and in *normal* conditions (**Supplementary Table 7**), the cell fate outcomes included apoptosis, differentiation (or EE fate), and extrusion, with propensities of 0.353, 0.303, and 0.094, respectively (**Supplementary Table 8**). Under *stress*, apoptosis, proliferation, and delta production increased to 0.375, 0.069 (from 0.045 in *normal* conditions), and 0.102 (from 0.089 in *normal* conditions), respectively. For *cancer* conditions, the propensity of apoptosis, proliferation, and delta production decreased to 0.353, 0.017, and 0.000, respectively, whereas multi-layering increased to 0.353. Stressful cellular environments are known to increase the apoptosis rate (70–72). In absence of mutations, *normal* cells residing in toxic and oncogenic environments reduce their proliferation rate and delta production (63–67). Cell division rate, moreover, needs to be balanced with cell turnover and

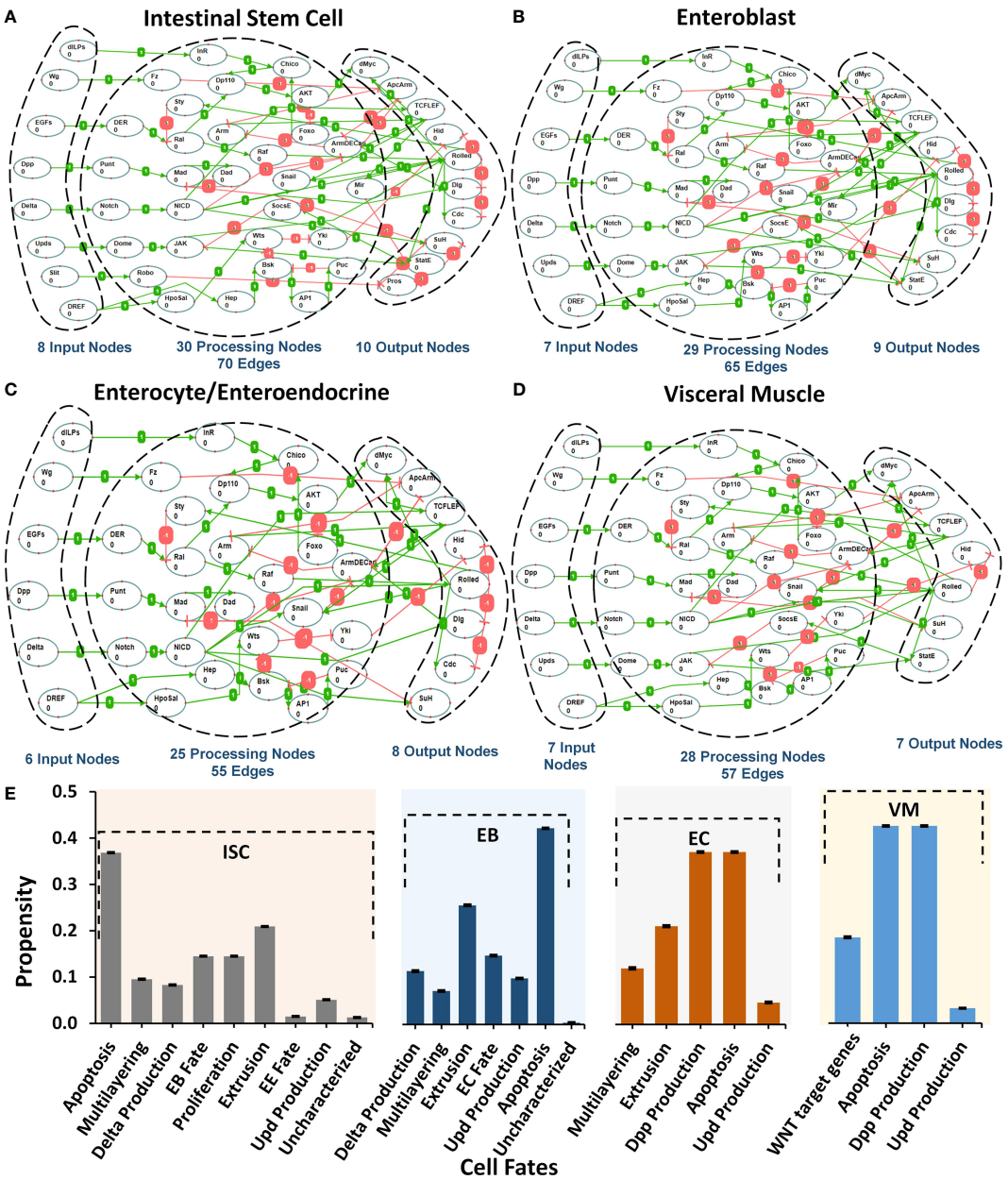


**FIGURE 1** | Regulatory schema of networks for the five cell types present in Drosophila melanogaster midgut. **(A–D)** The mapping between inputs, processing, and output nodes present in the biomolecular network models of five cell types i.e. ISC, EB, EC/EE, and VM. **(E)** Cellular fate propensities for ISC, EBs, ECs, and VM, along with their respective SEMs.

apoptosis so when proliferation slows down so does cell death (70, 71) (**Supplementary Figures 11–13**).

Next, we evaluated cell fate programming of the EB network under *normal* conditions (**Supplementary Table 7**). The results showed apoptosis, extrusion, and differentiation (or EC fate) cell fates with propensities of 0.381, 0.229, and 0.133, respectively (**Supplementary Table 8**). However, under *stress* conditions, the propensity for apoptosis and multi-layering increased to 0.450 and 0.109, respectively, whereas, extrusion and differentiation (or EC fate) decreased to 0.166, and 0.080, respectively. Under *cancerous* conditions, the salient cell fates programmed included multi-layering, apoptosis, and extrusion with propensities of 0.351, 0.394, and 0.124, respectively. Also, differentiation was suppressed to 0.000 due to toxic cellular environments. The trend in cell fate propensities under *cancerous* conditions also exhibited multi-layering (68, 69) along with low delta production and extrusion (**Supplementary Figures 14–16**). This corroborates with published literature stating that delta is a known marker

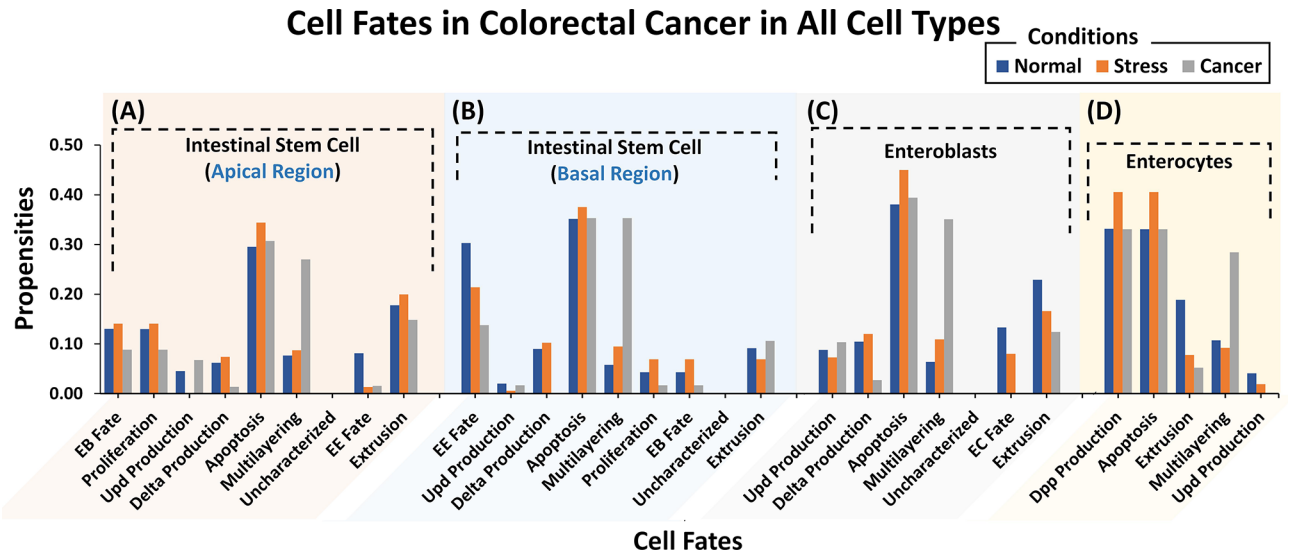


**FIGURE 2** | Cell fate propensities for intestinal stem cells (ISCs) under Apical and Basal regulation, enteroblasts (EBs), and enterocytes (ECs) in *normal, stress*, and *cancer* conditions. **(A)** ISC's under Apical regulation adopt eight different cell fates in three ambient conditions. In *normal* conditions, the highest propensity was observed for apoptosis followed by extrusion, proliferation, and EB fate, in order. In the case of *stress*, the highest propensity is that of apoptosis, followed by extrusion, EB fate, and proliferation. In cancer, the highest propensity is that of apologies followed by multi-layering and extrusion. **(B)** ISCs under Basal regulation program eight different cell fates with the highest propensity being for apoptosis fate in *normal*, *stress*, and *cancer* conditions. **(C)** Six cellular fates in EB, with the highest propensity for apoptosis in *normal*, *stress*, and *cancer* conditions. **(D)** Five cellular fates in EC, with the highest propensity for dpp production and apoptosis in *normal, stress*, and *cancer* conditions. Uncharacterized cell fate has a 0.000 propensity in all conditions and every network.

for ISC and in the case of ISC proliferation, is reduced along with delta production (63–67) in *cancer* conditions.

Moreover, the EC network was also analyzed for response under *normal* conditions (**Supplementary Table 7**). The emergent cell fates included dpp production, apoptosis, and extrusion with propensities of 0.331, 0.331, and 0.189, respectively (**Supplementary Table 8**). Under *stress*, the extrusion rate decreased to 0.078, while dpp production and apoptosis both increased to 0.406, respectively. Dpp signaling is also known to increase under *stress* conditions to promote cell division (73). Under *cancer* conditions, however, an increase in propensities of multi-layering (0.284) was observed which is in agreement with published studies (68, 69) (**Supplementary Figures 17–19**).

Lastly, a comparison of output node values for ISC, EB, and EC networks under *normal* conditions was performed against experimental RNA-seq data from the FlyGut-*seq* database (28). Note that due to the paucity of regulatory dynamics in the literature on EE and VM, we could not evaluate their networks further. The output node propensities for ISC, EB, and EC were found to be comparable with values from the FlyGut-*seq* database (28) (**Figure 3** and **Supplementary Table 9**). The full names of nodes in the network are mentioned in **Supplementary Table 10**.

## Case Study 1 – Investigating Colorectal Tumorigenesis Under Progressive Mutations in *Drosophila* Midgut

To decode the emergent cell fates during initiation and progression of colorectal cancer (CRC) in the adult *Drosophila* midgut, two salient driver mutations (55) in adenomatous polyposis coli (Apc, in WNT pathway) (74) and Ras (in the EGFR pathway) (75) were incorporated into the ISC network. These mutations were initially incorporated to act individually and later simultaneously (**Supplementary Figure 20**). The emergent cell fates in the control case (without mutations) included apoptosis, proliferation, and differentiation, along with loss of polarity, multi-layering, and extrusion with propensities of 0.296, 0.130, 0.130, 0.00, 0.077, and 0.179, respectively. Upon incorporation of Apc mutation into the ISC network, a slight decrease in apoptosis and proliferation was observed as their propensities decreased to 0.256 and 0.112, respectively. Differentiation and extrusion also got reduced to 0.112 and 0.151, respectively, while multi-layering increased to 0.256, and loss of polarity remained unaffected. Next, upon introducing Ras mutation, a decrease in apoptosis (0.210) and an increase in proliferation (0.148) was observed, which indicated cellular overgrowth. Furthermore, in line with Martorell et al. (55), loss of polarity and extrusion increased to 0.080 and 0.210, respectively.

On the other hand, the concurrent incorporation of Apc and Ras mutations resulted in hyper-proliferation and overgrowth as apoptosis decreased to 0.173 and proliferation increased to 0.173. The differentiation rate was observed to be 0.112 and loss of polarity, multi-layering and extrusion increased to 0.061, 0.173, and 0.173, respectively. Hence, with concurrent mutations in Apc and Ras, the emergent cell fates started exhibiting the hallmarks of cancer including abnormal proliferation and loss of differentiation, etc. (76). These results were also coherent with

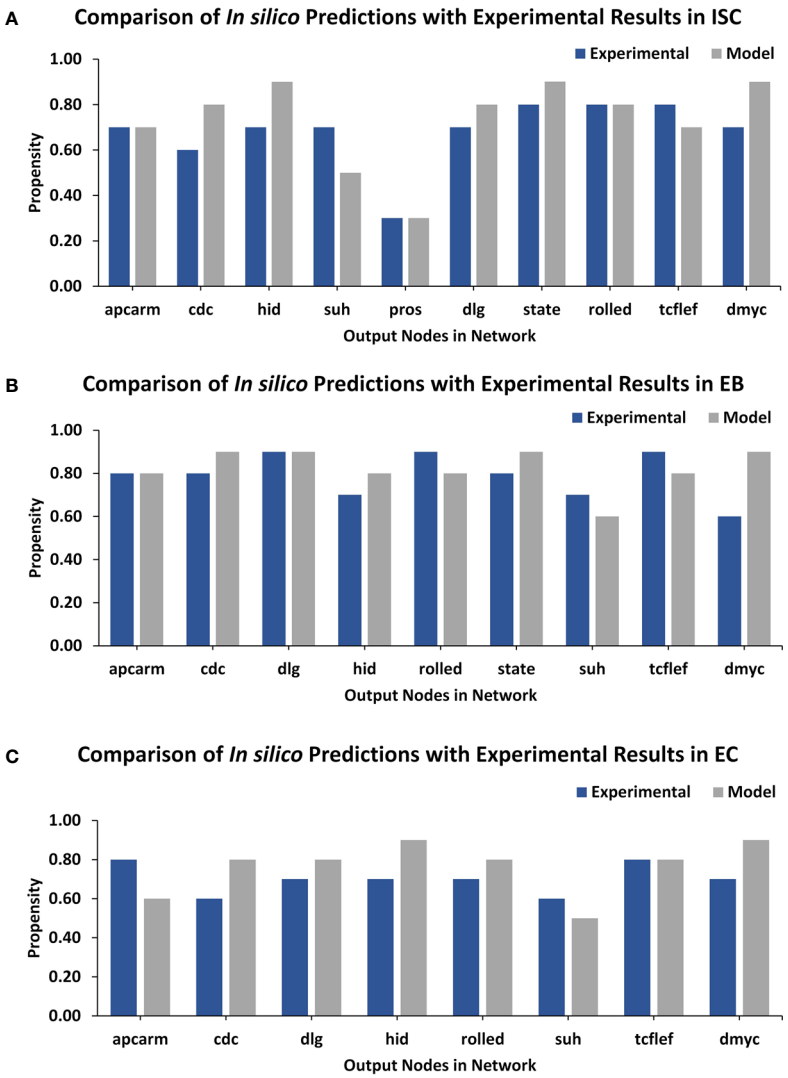


**FIGURE 3** | TISON output nodes propensities (*in silico* results) validation from FlyGut-seq database (*in vivo* results). **(A)** Comparison of ten output nodes propensities in ISC network: adenomatous polyposis coli (Apc2), cdc42 (Cdc42), head involution defective (hid), suppressor of hairless (Su(H)), prospero (pros), discs large 1 (dlg1), signal-transducer and activator of transcription protein at 92E (Stat92E), rolled (rl), pangolin (pan), and dMyc (myc). **(B)** Comparison of nine output nodes propensities in EB network: adenomatous polyposis coli (Apc2), cdc42 (Cdc42), discs large 1 (dlg1), head involution defective (hid), rolled (rl), signal-transducer, and activator of transcription protein at 92E (Stat92E), suppressor of hairless (Su(H)), pangolin (pan), and dMyc (myc). **(C)** Comparison of eight output nodes propensities in EC network: adenomatous polyposis coli (Apc2), cdc42 (Cdc42), discs large 1 (dlg1), head involution defective (hid), rolled (rl), suppressor of hairless (Su(H)), pangolin (pan) and dMyc (myc) (**Supplementary Table 10**).

both the experimental findings reported by Martorell et al. (55) (**Figure 4** and **Supplementary Table 11**) and differential gene expression data (**Supplementary Table 12**).

## Case Study 2 – Therapeutic Evaluation of Raf-Mutation in *Drosophila* Midgut Using Targets From the Literature

Introduction of gain-of-function Raf-specific driver mutations in our ISC network enabled the replication of Markstein et al.'s (56) therapeutic screen towards a comparative cancer recurrence evaluation of nine FDA-approved drugs. In their gain-of-function Raf tumor model, Markstein and colleagues had classified FDA-approved drugs into class I and II drugs. According to the study class, I drugs induced cancer reversal in mutated cells without affecting the wild-type cells, in contrast, class II drugs induced cancerous phenotype in wild-type cells (**Supplementary Table 13**). The result of our network analysis of the control case exhibited proliferation and apoptosis with propensities of 0.157 and 0.286, respectively. However, after the induction of Raf mutations, the proliferation (0.162) rate increased along with a decrease in apoptosis (0.175). Treatment of a Raf-mutated network using class I drugs led to a decrease in

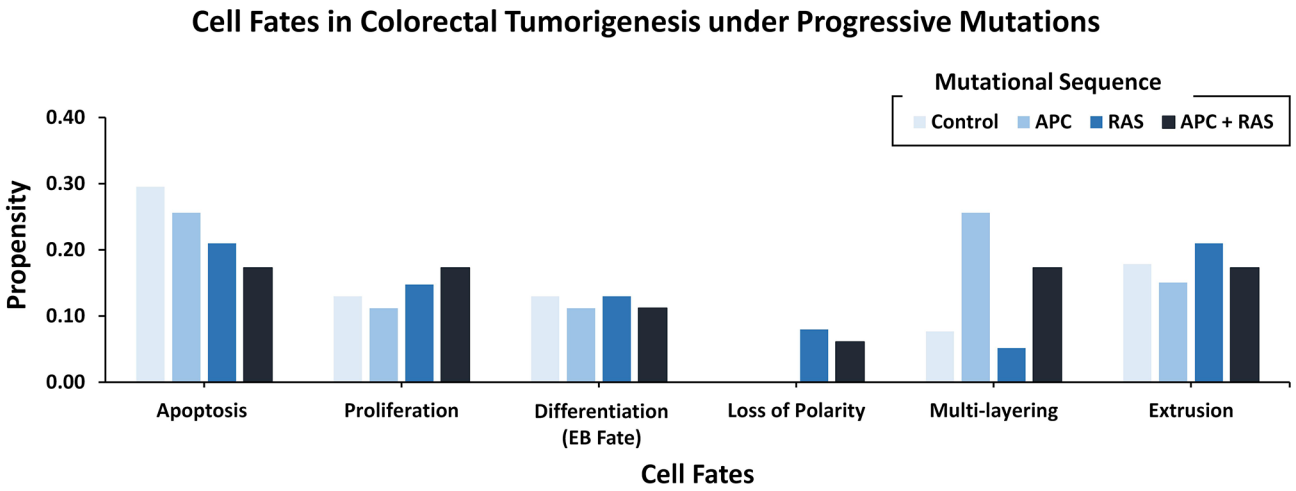


**FIGURE 4** | Cell fate outcomes after the introduction of progressive CRC mutations and their validation against Martorell et al.'s Drosophila CRC model. A high rate of extrusion and loss of polarity was observed in Apc-Ras as well as Ras clones. Alongside, an increased proliferation rate with a decreased apoptosis and differentiation is also highlighted by Martorell et al. in their in *vivo* model.

proliferation (0.089) and an increase in apoptosis (0.263). For the wild type in comparison with the control, almost no effect was observed on apoptosis, which remained steady at 0.283 whereas a slight decrease was observed in proliferation (0.130). This confirmed the action of class I drugs which act to substantially reduce cancerous fates in cancer without having a major impact on wild-type cells.

Alternatively, in the case of class II drugs, the wild type also exhibited hyper-proliferation after therapy with its propensity reaching up to 0.191, and apoptosis increased to 0.336. Importantly, for the mutated network, drug action continued its activities with the propensity of proliferation reaching 0.175 and apoptosis at 0.306. These results suggest that class II drugs are indeed associated with drug cytotoxicity as they induced malignancy in normal cells under therapy. This confirms Markstein et al.'s study which hypothesized that the extracellular environment in animal models is crucial in drug delivery and cytotoxicity (**Figure 5** and **Supplementary Table 14**).

## Case Study 3 – Employing the *In Silico Drosophila Patient Model* (DPM) for Personalized Therapeutics

Towards developing a *Drosophila-based* platform for employment in orchestrating patient-centric cancer therapeutics, we adopted Bangi et al.'s (40) *in vivo Drosophila Patient Model* (DPM). The *in vivo* model was first translated into an *in silico* DPM which incorporated patient-specific mutations from Bangi et al.'s study. These mutations included eight tumor suppressors: Apc, Tp53, Fbxw7, Tgfbr2, Smarca4, Fat4, Mapk14, and Cdh1, along with one oncogenic mutation in Kras (**Supplementary Table 15**). After inducing these patient-specific mutations into the ISC network (through direct and indirect target identification), we administered trametinib and zoledronate in different combinations to observe the most efficacious therapeutic effect. Our results showed that in control (i.e. healthy cells), the cell fate propensities for proliferation and apoptosis came out to be 0.130 and 0.294, respectively. Upon induction of mutations, proliferation increased to 0.200 and apoptosis decreased to 0.200, respectively. Next, with the administration of trametinib, an inhibitor of MEK kinase (mitogen-activated protein kinase kinase), used to treat patients with Kras mutation, the propensities for proliferation decreased to 0.000, whereas apoptosis increased to 0.386 (**Figure 6A**). With the administration of zoledronate, the cell fate propensities came out to be 0.130 for proliferation and 0.324 in the case of apoptosis (**Figure 6B**). Next, with the induction of zoledronate in combination with trametinib, a decrease in proliferation to 0.000 and an increase in apoptosis to 0.386 was observed (**Figure 6C**). Interestingly, augmentation of therapy with in tandem administration of trametinib, zoledronate, and trametinib with zoledronate showed proliferation to decrease to 0.000 and apoptosis to increase to 0.400 propensities (**Figure 6D**). These results exhibited cancer reversion on the administration of the drug combination and corroborate with Bangi et al.'s findings.

## Identification and Evaluation of Personalized Therapeutics for CRC Patients Using *In Silico* DPM

Towards developing personalized combinatorial therapies for treating colorectal cancer patients, we coupled our *in silico* DPM with patient-specific gene expression data from cBioPortal (16) (**Supplementary Table 16**). Patient-specific potential druggable targets were identified (from the 48 nodes in the ISC network) and their oncogenic cell fate ("apoptosis" and "proliferation" rates) propensities were obtained using the DA pipeline (**Supplementary Table 17**). Next, we employed PanDrugs (77) - an online database that prioritizes direct and indirect

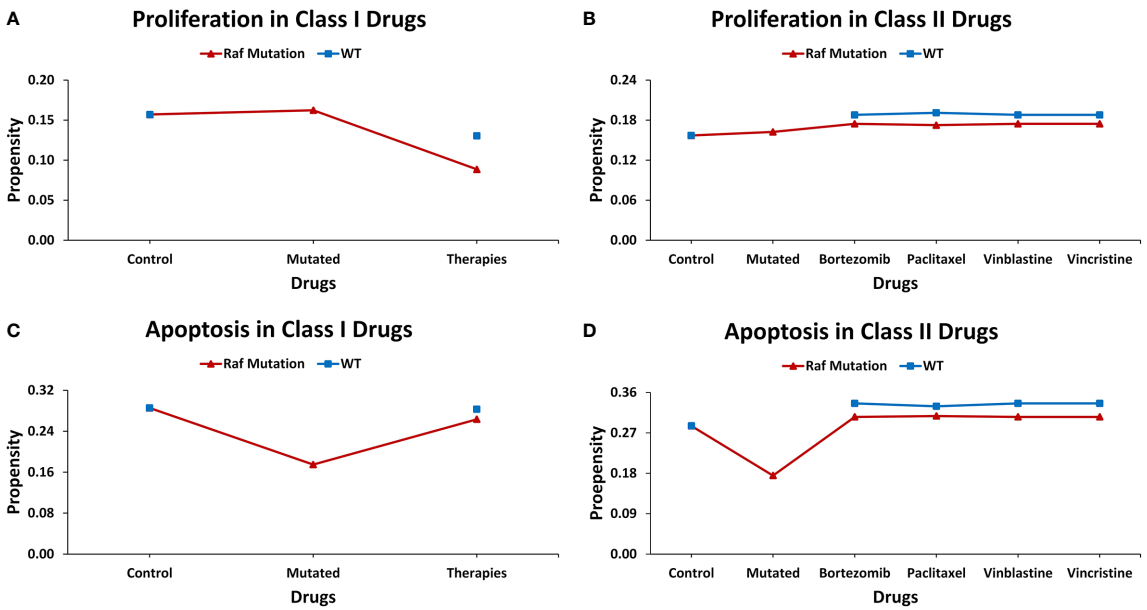


**FIGURE 5** | Evaluating cell fates under therapeutic screens taken from Markstein et al.'s *Drosophila* model. **(A)** The effect of class I drugs on cell proliferation in wild type and mutated networks, **(B)** The effect of class II drugs on cell proliferation in wild type and mutated networks, **(C)** The effect of class I drugs on apoptosis in wild type and mutated networks, **(D)** The effect of class II drugs on apoptosis in wild type and mutated network.

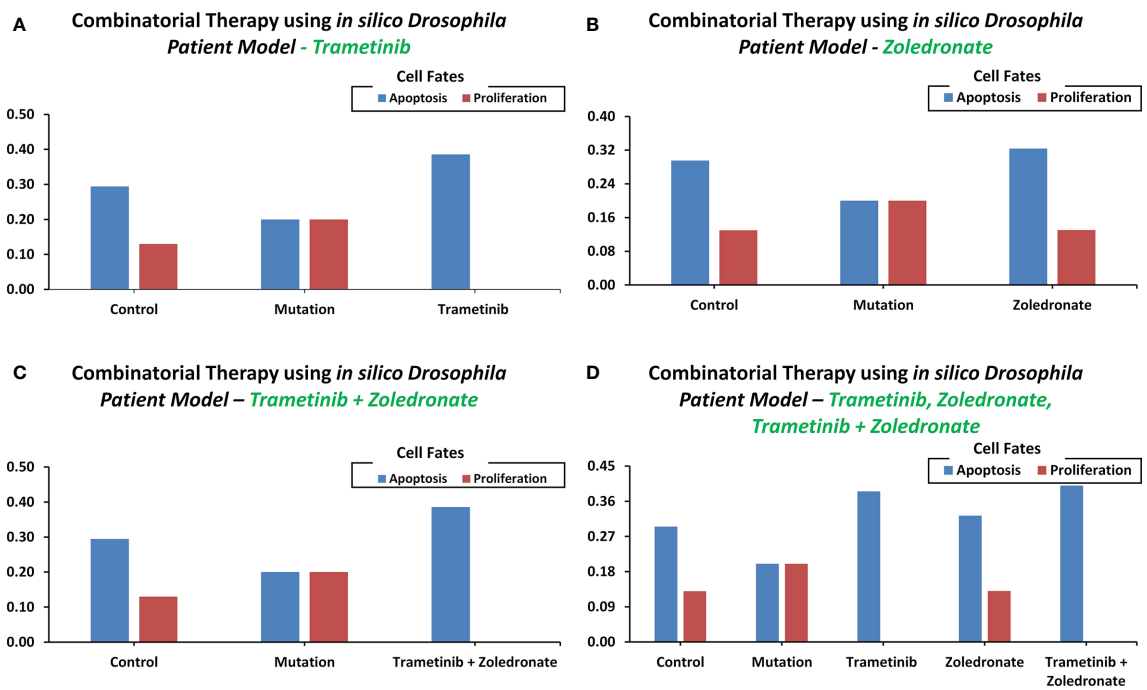


**FIGURE 6** | Cell fate propensities were obtained from the *in vivo Drosophila Patient Model* using Bangi et al.'s study. Cell fate propensities under **(A)** control, mutated, and therapy (Trametinib), **(B)** control, mutated, and therapy (Zoledronate), **(C)** control, mutated, and therapy (Trametinib + Zoledronate), **(D)** control, mutated, and therapy (Trametinib, Zoledronate, and Trametinib + Zoledronate).

targeting of genomic mutations, to search for "*druggable genes*" in our networks. Each node was then queried in the database to find out the drugs that targeted them directly or indirectly (**Supplementary Tables 18, 19**). The results from this exercise elicited chemotherapy (paclitaxel/docetaxel) and targeted therapies (regorafenib, bortezomib, imatinib) depending on patient-specific mutations (**Supplementary Table 20**). Follow up literature review showed that these drugs and their combinations are currently being used in several studies and clinical trials (78–86). Specifically, the combination of the paclitaxel-regorafenib was evaluated for treating advanced esophagogastric cancer (78), and the paclitaxel-bortezomib combination was used in metastatic solid tumors (87). While the docetaxel-bortezomib combination was evaluated for metastatic breast cancer (79), Non-Small Cell Lung Cancer (NSCLC) (80, 81), and prostate cancer (82). Paclitaxel-imatinib combination was tested in metastatic solid tumors (83), NSCLC (84), and ovarian cancer (85).

To test the efficacy of these drug combinations in CRC patients, we administered these therapies using the proposed *in silico* DPMs to ten patients with colorectal adenocarcinoma obtained from cBioPortal (16). To implement the simultaneous action of chemotherapy wherein the drug introduces widespread inhibition of mitosis by stabilizing polymerized microtubules and not allowing them to function during cell division for that, we surveyed the existing literature on microtubule targeting (**Supplementary Table 21**, **Supplementary Figure 21**) and embedded it into ISC network (**Supplementary Table 22**) to study the behavior of microtubule stabilization-induced cell fates in chemotherapy. The resultant network consists of 54 nodes and 83 edges (**Supplementary Figure 22**). Our results from combinatorial chemo- and targeted therapy using an extended network showed up to a 100% increase in apoptosis cell fate and a 100% decrease in proliferation rate (**Figure 7** and **Supplementary Table 23**).

## MATERIALS AND METHODS

The following sub-sections provide details of the methodology employed at each step of the study. The overall workflow of the study is outlined in **Supplementary Figure 23**.

### Data Collection and Boolean Modeling of Five Cell-Type-Specific Networks in *Drosophila* Midgut

To construct the biomolecular network models involved in the cellular regulation of *Drosophila* midgut, a comprehensive review of the existing literature and databases was undertaken. The databases employed included the Kyoto Encyclopedia of Genes and Genomes (KEGG) (88), Drosophila Interactions Database (DroID) (89), and data repositories such as FlyGut-*seq* (28). Alongside, network models of *Drosophila* by Giot et al. (90), Formstecher et al. (91), and Toku et al. were used to construct five rule-based Boolean biomolecular networks of the conserved signaling pathways in intestinal stem cells (ISCs) (43–47), enteroblasts (EBs) (48), enterocytes (ECs), enteroendocrine cells (EEs) (49–53), and visceral muscle (VM) cells (54). Nine major pathways involved in maintaining the overall homeostatic nature of the fly midgut were selected from the available literature. These included Notch (92), BMP (92), EGFR (93), WNT (94), JAK-STAT (94, 95), JNK (96), HIPPO (97), Insulin (63), and/or Robo (98) pathways for each cell type lining the midgut. The network steady states were used to

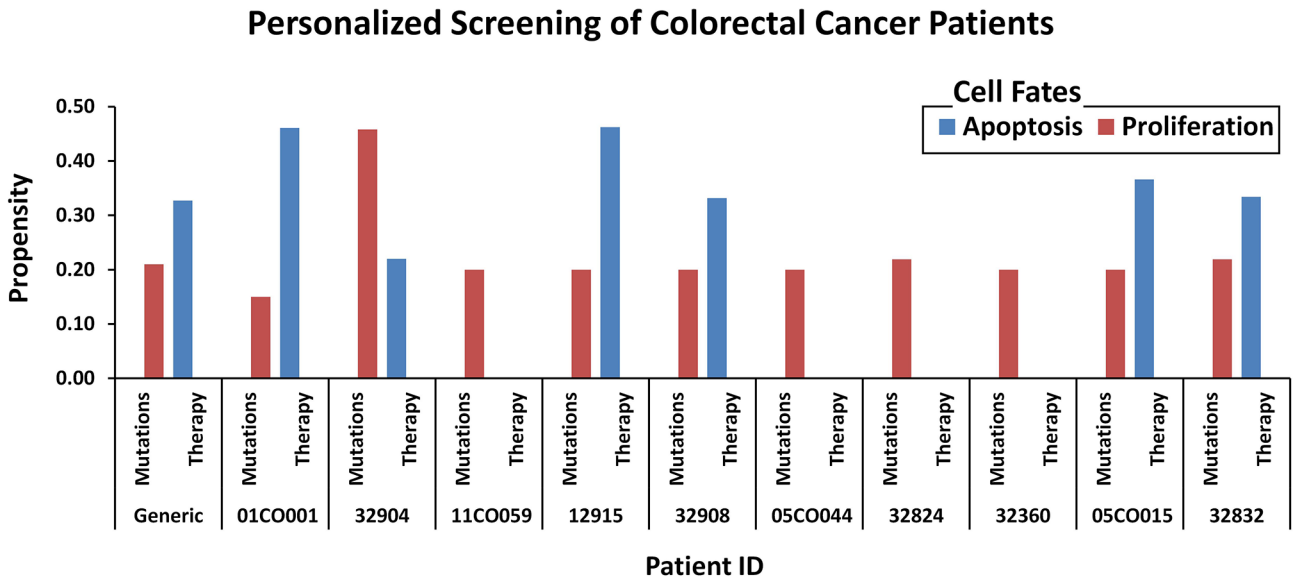


**FIGURE 7** | Comparison of oncogenic cell fate propensities obtained from personalized screening. Personalized screening of ten colorectal cancer patients. Patient ID and mutation data were extracted from cBioPortal and cell fates for apoptosis and proliferation were plotted to observe before and after therapy results.

program cell fate outcomes such as cellular differentiation, proliferation, apoptosis, EC fate determination, etc. Boolean equations (59) were used to model the regulation of each node in the biomolecular network. TISON (99), an in-house theatre for *in silico* systems oncology was used to translate Boolean rules into network models (see **Supplementary Data**, **Supplementary Table 24** for video tutorial).

## Robustness Analysis

To validate the biological plausibility of the proposed networks, a robustness analysis was performed (see **Supplementary Table 24** for video tutorial). Physiological conditions were maintained during this process and the input node values were taken from the FlyGut-*seq* database (28). The *normal* node states for ISC, EB, EC, and VM were perturbed by ±10%. Bootstrapping was employed on 10,000 network states. The means and standard deviations of the emergent cell fates were then calculated and the standard error of means (SEM) was plotted for each cell fate to determine the biological plausibility of the scale-free networks (100) (see **Supplementary Data 1**).

## Deterministic Analysis

The Boolean networks have been analyzed using the Deterministic Analysis (DA) (59) pipeline reported in ATLANTIS (101) and TISON (99) (see **Supplementary Table 24** for video tutorial). The results from DA were used to program "cell fate attractors" which are biological states that a cell can take, along with computation of their propensities (probability of their occurrence). Three different input files are used in this process which includes (i) network file, (ii) fixed node states file, and (iii) cell fate classification file. The network file contains the Boolean rules defining the biomolecular networks. The fixed node states file contained fixed values for generating environmental conditions such as normal, stress, or cancer conditions. The cell fate classification file is used to map network states onto the biological cell fates in the light of particular cell fate markers (101) (**Supplementary Table 25**). For network analysis, the DA pipeline starts with a set of initial network states. To achieve a steady state, logical rules, and state transition functions are employed. Upon reaching a steady-state a cell fate attractor is formed. This attractor can represent a specific cell fate with a cell fate propensity or basin size ratio. Bootstrapping was employed on 10,000 network states. TISON's *Therapeutics Editor* (TE) was used to undertake therapeutic evaluation on the network using the DA pipeline, with mutation and drug data integrated (see **Supplementary Table 24** for video tutorial). Fixed node states for *normal* conditions were obtained from the FlyGut-*seq* database while for cancer conditions, literature was surveyed to find out if the pathway is up or downregulated. For *stress*, abnormal values were abstracted by perturbing the stimuli from *normal* conditions (see **Supplementary Data 2**).

## Network Annotation Using Flygut-seq Database

Towards annotating networks with experimental values, the FlyGut-*seq* database was employed. For that, an RNA-seq dataset consisting of rpkm values was exported from the database. Data were extracted for the relevant genes present in our networks (ISC, EB, and EC) using their biological names (**Supplementary Table 10**). Expression data across the five regions of the midgut (i.e. R1, R2, R3, R4, and R5) (102) was normalized for each gene in specific cells. The normalized values were taken as *normal* input fixed node states for onward analyses. The normalized values were also used to compare the output node propensities from DA that was performed under *normal* input conditions (**Supplementary Table 9**, for details, see **Supplementary Data 2**).

## Cell Fate Data Collection for Case Studies and Their Validation

To validate and exemplify our network models, we used three literature-based case studies on colorectal tumorigenesis in *Drosophila* melanogaster. For case study 1, data including cell fates under Apc and Ras single and simultaneous mutations were obtained from Martorell et al.'s model (55). The differential gene expression screens and data were also obtained from Martorell et al. (see **Supplementary Data 3**). TISON's TE was used to implement the mutations in our network using TE's horizontal therapy pipeline. For case study 2, therapeutic screens including the existing list of FDA-approved drugs for targeting ISC in *Drosophila* were adapted from Markstein et al.'s (56) study. Existing databases on drugs and drug-gene interactions such as PharmacoDB (103), PanDrugs (77), OncoKB (104), and DGIdb (105), etc (106, 107) were then used to identify target nodes in our ISC network, which were also mentioned in Markstein et al.'s study. TE was employed to deliver drug data into the CRC mutated network using TE's vertical therapy pipeline (see **Supplementary Data 4**). For case study 3, patient-specific mutations, along with combinatorial therapy drug candidates were taken from Bangi et al.'s (40) study. Drug databases were used to identify target nodes in the ISC network mentioned in Bangi et al.'s study. Drugs that did not have direct targets in the network were implemented indirectly using literature-based mechanisms (see **Supplementary Data 5**).

## Development of an *In Silico Drosophila Patient Model* (DPM) and Its Validation

Towards devising a novel drug combination for the treatment of colorectal tumorigenesis, we performed an exhaustive evaluation of each node in our ISC network using TISON's TE. For that, we started with the sensitivity analysis of both tumor suppressor genes and oncogenes involved in CRC using data from existing databases and literature (55, 103, 106, 107) against patient-specific mutations taken from cBioPortal (16). The therapeutic screening was performed by upregulating the tumor suppressors and downregulating the oncogenes (**Supplementary Table 26**), to evaluate potential drug combination targets using the PanDrugs (77) database, a platform that prioritizes direct and indirect targeting of genomic mutations (see **Supplementary Data 6**).

## Combination of Chemotherapy and Targeted Therapy to Treat CRC Patients

To induce the effect of chemotherapy we carried an extensive survey of the existing literature and constructed a microtubule

network. The microtubule network was incorporated by integrating 6 nodes and 13 interactions to the ISC network. The resultant network contained 54 nodes and 83 interactions. This integrated network was then utilized for chemotherapeutic screening. The combinatorial personalized therapy was used to treat the CRC patients, in a vertical therapy scheme through targeting specific nodes in our ISC network in light of patient-specific mutations. DA pipeline was used to carry out the therapeutic evaluation (see **Supplementary Data 6**).

## DISCUSSION

Combinatorial therapies have created avenues for enhanced treatment of colorectal cancer (CRC) through drug synergy (108). Translational studies using omics-based data can help develop efficacious drug combinations for individualized CRC treatment. In particular, *in silico* Boolean models that utilize omics datasets can facilitate the process of developing and evaluating different drug combination therapies for the treatment of CRC (109–111). In this work, we propose a novel *in silico Drosophila Patient Model* (DPM), a computational framework for devising personalized therapeutic combinations for CRC patients. For that, we have constructed Boolean network models of five cell types present in *Drosophila* midgut: (i) intestinal stem cell, (ii) enteroblast, (iii) enterocyte, (iv) enteroendocrine, and (iv) visceral muscles (**Figures 1A–D**). We have used these networks to systematically induct tumorigenesis in *Drosophila* midgut tissue followed by therapeutic interventions for tumor reversion and restoration of physiological homeostasis (**Figure 2**). We then employed the ISC networks to create an *in silico* DPM for identifying optimal combinatorial therapeutics to treat CRC in humans. Our modeling pipeline provides a novel roadmap to annotate Boolean network models with patient data towards developing personalized medicine for CRC patients.

Several network models of biomolecular regulation in *Drosophila* have been reported for investigating the regulatory dynamics in cancer (90, 91, 112–114). Specifically, such applications of adult *Drosophila* midgut models are particularly useful in investigating CRC due to cellular and organizational similarities between *Drosophila* midgut and the human colon. More so, the biomolecular signaling pathways involved in maintaining homeostasis and differentiation are also conserved in both. This has given impetus to the development and utilization of *Drosophila* midgut models for investigating human colorectal cancer (115, 116). As a result, fly-based midgut models have been employed to investigate tissue homeostasis (117), multi-step tumorigenesis (55), epithelium renewal and regeneration upon bacterial infection or tissue damage (118), and its effect on mature and undifferentiated epithelial cells during intestinal cancer initiation (119). However, the employment of *Drosophila* midgut networks has hitherto remained unannotated with patient-specific mutation to study tumorigenesis in CRC thus limiting their translational potential. In this study, we have employed three literature-based case studies on *in vivo Drosophila* model to investigate CRC, employing *in silico* approaches. In our first case study, we used a fly-based network model to help investigate colorectal tumorigenesis under progressive mutations; the results from our analysis were validated against Martorell's CRC model (55) (**Figure 4**). The results from our second case study helped elucidate cytotoxicity in nine FDA-approved drugs (**Figure 5**) and conformed with Markstein et al.'s (56) hypothesis that the extracellular environment plays a crucial role in animal models for evaluating drug delivery and cytotoxicity. Next, for the third case study, we used Bangi et al.'s *in vivo* DPM to perform personalized therapy for KRAS-mutant metastatic colorectal cancer patient (40) (**Figure 6**), which re-confirmed the potential of combinatorial treatment; trametinib, zoledronate followed by trametinib in combination with zoledronate.

Onwards, we have performed personalized therapeutics by incorporating patient-specific mutation data into our model towards devising novel combinatorial treatments. For that, we took patient-specific data on ten patients with colorectal adenocarcinoma obtained from cBioPortal (16) to annotate our network model (**Supplementary Table 16**). We then undertook an exhaustive screening towards identifying efficacious target nodes for each patient which was based on the node's pro-apoptotic and anti-proliferation cell fate propensities after therapy (**Supplementary Table 17**). We used the PanDrugs database (77) to identify these target nodes in existing drugs. In light of our personalized screening step, we discovered that four patients can respond well to targeted therapy (imatinib, regorafenib, and everolimus), whereas for the rest a synergistic combination of chemotherapy (paclitaxel/docetaxel) and targeted therapy (imatinib, regorafenib, and bortezomib) was a more efficacious treatment (**Supplementary Table 20**). Literature also supports our finding that CRC treatment using a combination of chemo- and targeted therapy can provide efficacious results compared to conventional chemotherapy alone (119, 120). Specifically, the combination of the paclitaxel-regorafenib was evaluated for treating advanced esophagogastric cancer (78), and the paclitaxel-bortezomib combination was used in metastatic solid tumors (87). While the docetaxel-bortezomib combination was evaluated for metastatic breast cancer (79), Non-Small Cell Lung Cancer (NSCLC) (80, 81), and prostate cancer (82). Paclitaxel-imatinib combination was tested in metastatic solid tumor (83), NSCLC (84), and ovarian cancer (85, 86). However, further validation of these prognostic drug combinations in large-scale clinical cohorts will be required to test these drug combinations suggested by our study. In unison, our findings suggest that the proposed translational approach is effective in optimizing existing therapies.

Limitations of this study include utilizing abstracted *in silico* Boolean models (59) which are only qualitative. Moreover, analysis of EE and VM networks remained limited due to a lack of substantive literature. In this work, to overcome exponential computational complexity due to network size, we pruned each network to a minimum while maintaining biological cell fate outcomes. Additionally, ISC-EB-EC

interplay is pivotal in determining cell fates, especially for intestinal stem cells in *Drosophila* midgut, however, due to network-level analysis strategy employed in the study, we are currently unable to investigate cellular interplays as well as continuous lineage tracking for various cell types. Since our networks are independent of each other we can only elucidate individual cell fates programmed by each network at a time.

Several assumptions have been made for constructing this model. Firstly, since *Drosophila* midgut comprises of several regions with differential niches and context specific cellular processes (42), for the sake of computational scalability, we have not incorporated *Drosophila* midgut compartmentalization in our model. In view of the exponential relation between computational complexity and network size, we have kept the network size to a minimum by reducing path lengths between critical nodes through removing intermediary nodes. Integrated multi-omics information e.g., from genomics, transcriptomics, and proteomics level was assumed to act on the same time-scale, towards undertaking network analysis.

With regards to drugs, we search the nodes (genes) in our network in PanDrugs database for selecting and prioritizing potential drugs that can efficaciously target the selected nodes. The assumptions made by PanDrugs for declaring a gene-drug relationship, include: for targeted therapies, the genes-drug relationship that PanDrugs provides is a direct relationship, and that the targeted drugs acting directly on the nodes in the network are without any off target pleotropic effects. PanDrugs's drug prioritization scheme can improve if it also takes into account protein interaction networks, pathway activity, multi-omics information, however, its search is limited to genome-level information only. Moreover, each drug is able to act on all the possible transcriptomic isoforms of a gene, where necessary.

Additionally, during the personalized screening of patients, non-druggable nodes could not be evaluated further due to unsubstantive literature on their employment as drugs. Moreover, some of the genes present in the human genome do not have exact homologs in *Drosophila's* genes list, which can limit the study's translational capabilities.

Onwards, the proposed *in silico* DPM can be extended to perform probabilistic analysis by converting rules to the weights-based network which can also cater to external perturbations and noise into the system. Further investigations need to be carried out to predict novel druggable genes (direct targets, biomarkers, and pathway members not available in PanDrugs database) for employment in developing new drug combinations. The network models developed can also be extended to multi-scale models towards incorporating spatiotemporal regulations of colorectal cancer. Further verifications with a greater patient sample size can help achieve a better understanding of the relationship between patient-specific data in connection to therapeutic combinations. Moreover, result verification can be enhanced with wet lab validation of the proposed synergistic drug combinations outlined by our computational framework.

Taken together, our preclinical *in silico* DPM not only captures the regulatory homeostasis of fly midgut but also presents a novel framework to personalize Boolean network models towards their employment in personalized cancer therapeutic interventions.

## DATA AVAILABILITY STATEMENT

The original contributions presented in the study are included in the article/**Supplementary Material**. Further inquiries can be directed to the corresponding author.

## AUTHOR CONTRIBUTIONS

SC designed and supervised the study. MG carried out the literature review, construction of the model, and undertook the analyses. SC, MG, and RN designed the personalized treatment pipeline, SC, MG, RN, ZN, and HK drafted the manuscript. OS helped construct Boolean networks. RH critically reviewed the model development and performed validations, RQ, MT, and AF assisted in the study design and manuscript development. All authors contributed to the article and approved the submitted version.

## FUNDING

This work was supported by the National ICT-R&D Fund (SRG-209), RF-NCBC-015, NGIRI-2020-4771, HEC (21-30SRGP/R&D/HEC/2014, 20-2269/NRPU/R&D/HEC/12/4792 and 20-3629/NRPU/R&D/HEC/14/585), TWAS (RG 14-319 RG/ITC/AS_C) and LUMS (STG-BIO-1008, FIF-BIO-2052, FIF-BIO-0255, SRP-185-BIO, SRP-058-BIO and FIF-477-1819-BIO) grants.

## SUPPLEMENTARY MATERIAL

The Supplementary Material for this article can be found online at: https://www.frontiersin.org/articles/10.3389/fonc.2021.692592/full#supplementary-material

## REFERENCES

1. Hanahan D, Weinberg RA. Hallmarks of Cancer: The Next Generation. *Cell* (2011) 144(5):646–74. doi: 10.1016/j.cell.2011.02.013
2. Baylin SB, Jones PA. A Decade of Exploring the Cancer Epigenome — Biological and Translational Implications. *Nat Rev Cancer* (2011) 11 (10):726–34. doi: 10.1038/nrc3130
3. Bild AH, Yao G, Chang JT, Wang Q, Potti A, Chasse D, et al. Oncogenic Pathway Signatures in Human Cancers as a Guide to Targeted Therapies. *Nature* (2006) 439(7074):353–7. doi: 10.1038/nature04296
4. Harris CC, Hollstein M. Clinical Implications of the p53 Tumor-Suppressor Gene. *N Engl J Med* (1993) 329(18):1318–27. doi: 10.1056/NEJM199310283291807
5. Haggitt RC, Glotzbach RE, Soffer EE, Wruble LD. Prognostic Factors in Colorectal Carcinomas Arising in Adenomas: Implications for Lesions Removed by Endoscopic Polypectomy. *Gastroenterology* (1985) 89(2):328–36. doi: 10.1016/0016-5085(85)90333-6
6. Hanahan D, Weinberg RA. The Hallmarks of Cancer. *Cell* (2000) 100(1):57–70. doi: 10.1016/s0092-8674(00)81683-9
7. Meacham CE, Morrison SJ. Tumour Heterogeneity and Cancer Cell Plasticity. *Nature* (2013) 501(7467):328–37. doi: 10.1038/nature12624

8. Dagogo-Jack I, Shaw AT. Tumour Heterogeneity and Resistance to Cancer Therapies. *Nat Rev Clin Oncol* (2018) 15(2):81–94. doi: 10.1038/nrclinonc.2017.166
9. Szakács G, Paterson JK, Ludwig JA, Booth-Genthe C, Gottesman MM. Targeting Multidrug Resistance in Cancer. *Nat Rev Drug Discov* (2006) 5 (3):219–34. doi: 10.1038/nrd1984
10. Ocana A, Pandiella A, Siu LL, Tannock IF. Preclinical Development of Molecular-Targeted Agents for Cancer. *Nat Rev Clin Oncol* (2011) 8(4):200–9. doi: 10.1038/nrclinonc.2010.194
11. DiMasi JA, Reichert JM, Feldman L, Malins A. Clinical Approval Success Rates for Investigational Cancer Drugs. *Clin Pharmacol Ther* (2013) 94 (3):329–35. doi: 10.1038/clpt.2013.117
12. Zamboni WC, Torchilin V, Patri AK, Hrkach J, Stern S, Lee R, et al. Best Practices in Cancer Nanotechnology: Perspective From NCI Nanotechnology Alliance. *Clin Cancer Res* (2012) 18(12):3229–41. doi: 10.1158/1078-0432.CCR-11-2938
13. Gottesman MM, Fojo T, Bates SE. Multidrug Resistance in Cancer: Role of ATP–dependent Transporters. *Nat Rev Cancer* (2002) 2(1):48–58. doi: 10.1038/nrc706
14. Kasai Y, Cagan R. Drosophila as a Tool for Personalized Medicine: A Primer. *Per Med* (2010) 7(6):621–32. doi: 10.2217/pme.10.65
15. Grandori C, Kemp CJ. Personalized Cancer Models for Target Discovery and Precision Medicine. *Trends Cancer* (2018) 4(9):634–42. doi: 10.1016/j.trecan.2018.07.005
16. Gao J, Aksoy BA, Dogrusoz U, Dresdner G, Gross B, Sumer SO, et al. Integrative Analysis of Complex Cancer Genomics and Clinical Profiles Using the Cbioportal. *Sci Signal* (2013) 6(269):pl1. doi: 10.1126/scisignal.2004088
17. Lee HJ, Palm J, Grimes SM, Ji HP. The Cancer Genome Atlas Clinical Explorer: A Web and Mobile Interface for Identifying Clinical-Genomic Driver Associations. *Genome Med* (2015) 7(1):1–14. doi: 10.1186/s13073-015-0226-3
18. Zhang J, Baran J, Cros A, Guberman JM, Haider S, Hsu J, et al. International Cancer Genome Consortium Data Portal—A One-Stop Shop for Cancer Genomics Data. *Database* (2011) 2011:bar026. doi: 10.1093/database/bar026
19. Papatheodorou I, Fonseca NA, Keays M, Tang YA, Barrera E, Bazant W, et al. Expression Atlas: Gene and Protein Expression Across Multiple Studies and Organisms. *Nucleic Acids Res* (2018) 46(D1):D246–51. doi: 10.1093/nar/gkx1158
20. Benson DA, Cavanaugh M, Clark K, Karsch-Mizrachi I, Lipman DJ, Ostell J, et al. Genbank. *Nucleic Acids Res* (2013) 41(D1):D36–42. doi: 10.1093/nar/gks1195
21. Morgan MM, Johnson BP, Livingston MK, Schuler LA, Alarid ET, Sung KE, et al. Personalized *In Vitro* Cancer Models to Predict Therapeutic Response: Challenges and a Framework for Improvement. *Pharmacol Ther* (2016) 165:79–92. doi: 10.1016/j.pharmthera.2016.05.007
22. Lieschke GJ, Currie PD. Animal Models of Human Disease: Zebrafish Swim Into View. *Nat Rev Genet* (2007) 8(5):353–67. doi: 10.1038/nrg2091
23. Olive KP, Tuveson DA. The Use of Targeted Mouse Models for Preclinical Testing of Novel Cancer Therapeutics. *Clin Cancer Res* (2006) 12(18):5277–87. doi: 10.1158/1078-0432.CCR-06-0436
24. Pandey UB, Nichols CD. Human Disease Models in Drosophila Melanogaster and the Role of the Fly in Therapeutic Drug Discovery. *Pharmacol Rev* (2011) 63(2):411–36. doi: 10.1124/pr.110.003293
25. Adams MD, Celniker SE, Holt RA, Evans CA, Gocayne JD, Amanatides PG, et al. The Genome Sequence of Drosophila Melanogaster. *Science* (2000) 287 (5461):2185–95. doi: 10.1126/science.287.5461.2185
26. Reiter LT. A Systematic Analysis of Human Disease-Associated Gene Sequences in Drosophila Melanogaster. *Genome Res* (2001) 11(6):1114–25. doi: 10.1101/gr.169101
27. Mirzoyan Z, Sollazzo M, Allocca M, Valenza AM, Grifoni D, Bellosta P. Drosophila Melanogaster: A Model Organism to Study Cancer. *Front Genet* (2019) 10:51. doi: 10.3389/fgene.2019.00051
28. Dutta D, Dobson AJ, Houtz PL, Gläßer C, Revah J, Korzelius J, et al. Regional Cell-Specific Transcriptome Mapping Reveals Regulatory Complexity in the Adult Drosophila Midgut. *Cell Rep* (2015) 12(2):346–58. doi: 10.1016/j.celrep.2015.06.009
29. Chintapalli VR, Wang J, Dow JAT. Using FlyAtlas to Identify Better Drosophila Melanogaster Models of Human Disease. *Nat Genet* (2007) 39 (6):715–20. doi: 10.1038/ng2049
30. Vidal M, Wells S, Ryan A, Cagan R. ZD6474 Suppresses Oncogenic RET Isoforms in a Drosophila Model for Type 2 Multiple Endocrine Neoplasia Syndromes and Papillary Thyroid Carcinoma. *Cancer Res* (2005) 65 (9):3538–41. doi: 10.1158/0008-5472.CAN-04-4561
31. Bangi E, Garza D, Hild M. In Vivo Analysis of Compound Activity and Mechanism of Action Using Epistasis in Drosophila. *J Chem Biol* (2011) 4 (2):55–68. doi: 10.1007/s12154-010-0051-5
32. Levine BD, Cagan RL. Drosophila Lung Cancer Models Identify Trametinib Plus Statin as Candidate Therapeutic. *Cell Rep* (2016) 14(6):1477–87. doi: 10.1016/j.celrep.2015.12.105
33. Bossen J, Uliczka K, Steen L, Pfefferkorn R, Mai MM-Q, Burkhardt L, et al. An EGFR-Induced Drosophila Lung Tumor Model Identifies Alternative Combination Treatments. *Mol Cancer Ther* (2019) 18(9):1659–68. doi: 10.1158/1535-7163.MCT-19-0168
34. Bhandari P, Shashidhara LS. Studies on Human Colon Cancer Gene APC by Targeted Expression in Drosophila. *Oncogene* (2001) 20(47):6871–80. doi: 10.1038/sj.onc.1204849
35. Palmer AC, Sorger PK. Combination Cancer Therapy Can Confer Benefit *Via* Patient-to-Patient Variability Without Drug Additivity or Synergy. *Cell* (2017) 171(7):1678–91. doi: 10.1016/j.cell.2017.11.009
36. Chen S-H, Lahav G. Two Is Better Than One; Toward a Rational Design of Combinatorial Therapy. *Curr Opin Struct Biol* (2016) 41:145–50. doi: 10.1016/j.sbi.2016.07.020
37. Yardley DA. Drug Resistance and the Role of Combination Chemotherapy in Improving Patient Outcomes. *Int J Breast Cancer* (2013) 2013:137414. doi: 10.1155/2013/137414
38. Aird RE, Cummings J, Ritchie AA, Muir M, Morris RE, Chen H, et al. In Vitro and *In Vivo* Activity and Cross Resistance Profiles of Novel Ruthenium (II) Organometallic Arene Complexes in Human Ovarian Cancer. *Br J Cancer* (2002) 86(10):1652–7. doi: 10.1038/sj.bjc.6600290
39. Murayama T, Gotoh N. Patient-Derived Xenograft Models of Breast Cancer and Their Application. *Cells* (2019) 8(6):621. doi: 10.3390/cells8060621
40. Bangi E, Ang C, Smibert P, Uzilov AV, Teague AG, Antipin Y, et al. A Personalized Platform Identifies Trametinib Plus Zoledronate for a Patient With KRAS-mutant Metastatic Colorectal Cancer. *Sci Adv* (2019) 5(5): eaav6528. doi: 10.1126/sciadv.aav6528
41. Passini E, Britton OJ, Lu HR, Rohrbacher J, Hermans AN, Gallacher DJ, et al. Human in Silico Drug Trials Demonstrate Higher Accuracy Than Animal Models in Predicting Clinical Pro-Arrhythmic Cardiotoxicity. *Front Physiol* (2017) 8:668. doi: 10.3389/fphys.2017.00668
42. Richardson HE, Willoughby L, Humbert PO. Screening for Anti-Cancer Drugs in Drosophila. *eLS* (2015) 1–14. doi: 10.1002/9780470015902.a0022535
43. Micchelli CA, Perrimon N. Evidence That Stem Cells Reside in the Adult Drosophila Midgut Epithelium. *Nature* (2006) 439(7075):475–79. doi: 10.1038/nature04371
44. Ohlstein B, Spradling A. The Adult Drosophila Posterior Midgut Is Maintained by Pluripotent Stem Cells. *Nature* (2006) 439(7075):470–4. doi: 10.1038/nature04333
45. Takashima S, Adams KL, Ortiz PA, Ying CT, Moridzadeh R, Younossi-Hartenstein A, et al. Development of the Drosophila Entero-Endocrine Lineage and Its Specification by the Notch Signaling Pathway. *Dev Biol* (2011) 353(2):161–72. doi: 10.1016/j.ydbio.2011.01.039
46. Ohlstein B, Spradling A. Multipotent Drosophila Intestinal Stem Cells Specify Daughter Cell Fates by Differential Notch Signaling. *Science* (2007) 315(5814):988–92. doi: 10.1126/science.1136606
47. Lee M, Vasioukhin V. Cell Polarity and Cancer – Cell and Tissue Polarity as a non-Canonical Tumor Suppressor. *J Cell Sci* (2008) 121(8):1141–50. doi: 10.1242/jcs.016634
48. Pasco MY, Loudhaief R, Gallet A. The Cellular Homeostasis of the Gut: What the Drosophila Model Points Out. *Histol Histopathol* (2015) 30 (3):277–92. doi: 10.14670/HH-30.277
49. Loza-coll MA, Southall TD, Sandall SL, Brand AH, Jones DL. Regulation of Drosophila Intestinal Stem Cell Maintenance and Differentiation by the Transcription Factor Escargot. *EMBO J* (2014) 33(24):2983–96. doi: 10.15252/embj.201489050

50. Zeng X, Hou SX. Enteroendocrine Cells are Generated From Stem Cells Through a Distinct Progenitor in the Adult Drosophila Posterior Midgut. *Development* (2015) 142(4):644–53. doi: 10.1242/dev.113357
51. Macara IG, McCaffrey L. Cell Polarity in Morphogenesis and Metastasis. *Philos Trans R Soc Lond B Biol Sci* (2013) 368(1629):20130012. doi: 10.1098/rstb.2013.0012
52. Guo Z, Ohlstein B. Bidirectional Notch Signaling Regulates Drosophila Intestinal Stem Cell Multipotency. *Science* (2015) 350(6263):927. doi: 10.1126/science.aab0988
53. Snoeck V, Goddeeris B, Cox E. The Role of Enterocytes in the Intestinal Barrier Function and Antigen Uptake. *Microbes Infect* (2005) 7(7–8):997–1004. doi: 10.1016/j.micinf.2005.04.003
54. Wolfstetter G, Shirinian M, Stute C, Grabbe C, Hummel T, Baumgartner S, et al. Fusion of Circular and Longitudinal Muscles in Drosophila is Independent of the Endoderm But Further Visceral Muscle Differentiation Requires a Close Contact Between Mesoderm and Endoderm. *Mech Dev* (2009) 126(8–9):721–36. doi: 10.1016/j.mod.2009.05.001
55. Martorell Ò, Merlos-Suárez A, Campbell K, Barriga FM, Christov CP, Miguel-Aliaga I, et al. Conserved Mechanisms of Tumorigenesis in the Drosophila Adult Midgut. *PloS One* (2014) 9(2):e88413. doi: 10.1371/journal.pone.0088413
56. Markstein M, Dettorre S, Cho J, Neumuller RA, Craig-Muller S, Perrimon N. Systematic Screen of Chemotherapeutics in Drosophila Stem Cell Tumors. *Proc Natl Acad Sci* (2014) 111(12):4530–5. doi: 10.1073/pnas.1401160111
57. Stone L. The Feasibility and Stability of Large Complex Biological Networks: A Random Matrix Approach. *Sci Rep* (2018) 8(1):1–12. doi: 10.1038/s41598-018-26486-2
58. Kwon Y-K, Cho K-H. Quantitative Analysis of Robustness and Fragility in Biological Networks Based on Feedback Dynamics. *Bioinformatics* (2008) 24 (7):987–94. doi: 10.1093/bioinformatics/btn060
59. Glass L, Kauffman SA. The Logical Analysis of Continuous, Non-Linear Biochemical Control Networks. *J Theor Biol* (1973) 39(1):103–29. doi: 10.1016/0022-5193(73)90208-7
60. Chatterjee M, Ip YT. Pathogenic Stimulation of Intestinal Stem Cell Response in Drosophila. *J Cell Physiol* (2009) 220(3):664–71. doi: 10.1002/jcp.21808
61. Wang L, Ryoo HD, Qi Y, Jasper H. PERK Limits Drosophila Lifespan by Promoting Intestinal Stem Cell Proliferation in Response to ER Stress. *PloS Genet* (2015) 11(5):e1005220. doi: 10.1371/journal.pgen.1005220
62. Rodriguez-Fernandez IA, Qi Y, Jasper H. Loss of a Proteostatic Checkpoint in Intestinal Stem Cells Contributes to Age-Related Epithelial Dysfunction. *Nat Commun* (2019) 10(1):1–15. doi: 10.1038/s41467-019-08982-9
63. Amcheslavsky A, Jiang J, Ip YT. Tissue Damage-Induced Intestinal Stem Cell Division in Drosophila. *Cell Stem Cell* (2009) 4(1):49–61. doi: 10.1016/j.stem.2008.10.016
64. Jiang H, Patel PH, Kohlmaier A, Grenley MO, McEwen DG, Edgar BA. Cytokine/Jak/Stat Signaling Mediates Regeneration and Homeostasis in the Drosophila Midgut. *Cell* (2009) 137(7):1343–55. doi: 10.1016/j.cell.2009.05.014
65. Cordero JB, Stefanatos RK, Myant K, Vidal M, Sansom OJ. Non-Autonomous Crosstalk Between the Jak/Stat and Egfr Pathways Mediates Apc1-Driven Intestinal Stem Cell Hyperplasia in the Drosophila Adult Midgut. *Development* (2012) 139(24):4524–35. doi: 10.1242/dev.078261
66. McLeod CJ, Wang L, Wong C, Jones DL. Stem Cell Dynamics in Response to Nutrient Availability. *Curr Biol* (2010) 20(23):2100–5. doi: 10.1016/j.cub.2010.10.038
67. Goodlad RA, Wright NA. The Effects of Starvation and Refeeding on Intestinal Cell Proliferation in the Mouse. *Virchows Arch B* (1984) 45 (1):63–73. doi: 10.1007/BF02889852
68. Schell JC, Wisidagama DR, Bensard C, Zhao H, Wei P, Tanner J, et al. Control of Intestinal Stem Cell Function and Proliferation by Mitochondrial Pyruvate Metabolism. *Nat Cell Biol* (2017) 19(9):1027–36. doi: 10.1038/ncb3593
69. Rojas Villa SE, Meng FW, Biteau B. Zfh2 Controls Progenitor Cell Activation and Differentiation in the Adult Drosophila Intestinal Absorptive Lineage. *PloS Genet* (2019) 15(12):e1008553. doi: 10.1371/journal.pgen.1008553
70. Koren E, Yosefzon Y, Ankawa R, Soteriou D, Jacob A, Nevelsky A, et al. ARTS Mediates Apoptosis and Regeneration of the Intestinal Stem Cell Niche. *Nat Commun* (2018) 9(1):1–17. doi: 10.1038/s41467-018-06941-4
71. Tower J. Stress and Stem Cells. *Wiley Interdiscip Rev Dev Biol* (2012) 1 (6):789–802. doi: 10.1002/wdev.56
72. Bach SP, Renehan AG, Potten CS. Stem Cells: The Intestinal Stem Cell as a Paradigm. *Carcinogenesis* (2000) 21(3):469–76. doi: 10.1093/carcin/21.3.469
73. Pérez-Garijo A, Martín FA, Struhl G, Morata G. Dpp Signaling and the Induction of Neoplastic Tumors by Caspase-Inhibited Apoptotic Cells in Drosophila. *Proc Natl Acad Sci USA* (2005) 102(49):17664–9. doi: 10.1073/pnas.0508966102
74. Sancho E, Batlle E, Clevers H. Signaling Pathways in Intestinal Development and Cancer. *Annu Rev Cell Dev Biol* (2004) 20:695–723. doi: 10.1146/annurev.cellbio.20.010403.092805
75. Gou H-F, Li X, Qiu M, Cheng K, Li L-H, Dong H, et al. Epidermal Growth Factor Receptor (EGFR)-RAS Signaling Pathway in Penile Squamous Cell Carcinoma. *PloS One* (2013) 8(4):e62175. doi: 10.1371/journal.pone.0062175
76. Oberley LW, Oberley TD, Buettner GR. Cell Differentation, Aging and Cancer: The Possible Roles of Superoxide and Superoxide Dismutases. *Med Hypotheses* (1980) 6(3):249–68. doi: 10.1016/0306-9877(80)90123-1
77. Piñeiro-Yáñez E, Reboiro-Jato M, Gómez-López G, Perales-Patón J, Troulé K, Rodríguez JM, et al. PanDrugs: A Novel Method to Prioritize Anticancer Drug Treatments According to Individual Genomic Data. *Genome Med* (2018) 10(1):1–11. doi: 10.1186/s13073-018-0546-1
78. Khurshed M, Stroes CI, Schokker S, van der Woude S, Mathôt R, Slingerland M, et al. Regorafenib in Combination With Paclitaxel for Beyond First-Line Treatment of Advanced Esophagogastric Cancer (REPEAT): A Phase Ib Trial With Expansion Cohort. *Ann Oncol* (2019) 30(October):v307. doi: 10.1093/annonc/mdz247.124
79. Awada A, Albanell J, Canney PA, Dirix LY, Gil T, Cardoso F, et al. Bortezomib/Docetaxel Combination Therapy in Patients With Anthracycline-Pretreated Advanced/Metastatic Breast Cancer: A Phase I/II Dose-Escalation Study. *Br J Cancer* (2008) 98(9):1500–7. doi: 10.1038/sj.bjc.6604347
80. Lara PN, Koczywas M, Quinn DI, Lenz HJ, Davies AM, Lau DHM, et al. Bortezomib Plus Docetaxel in Advanced Non-Small Cell Lung Cancer and Other Solid Tumors: A Phase I California Cancer Consortium Trial. *J Thorac Oncol* (2006) 1(2):126–34. doi: 10.1016/s1556-0864(15)31527-6
81. Fanucchi MP, Fossella FV, Belt R, Natale R, Fidias P, Carbone DP, et al. Randomized Phase II Study of Bortezomib Alone and Bortezomib in Combination With Docetaxel in Previously Treated Advanced non-Small-Cell Lung Cancer. *J Clin Oncol Off J Am Soc Clin Oncol* (2006) 24(31):5025–33. doi: 10.1200/JCO.2006.06.1853
82. Dreicer R, Petrylak D, Agus D, Webb I, Roth B. Phase I/II Study of Bortezomib Plus Docetaxel in Patients With Advanced Androgen-Independent Prostate Cancer. *Clin Cancer Res An Off J Am Assoc Cancer Res* (2007) 13(4):1208–15. doi: 10.1158/1078-0432.CCR-06-2046
83. Pishvaian MJ, Slack R, Koh EY, Beumer JH, Hartley ML, Cotarla I, et al. A Phase I Clinical Trial of the Combination of Imatinib and Paclitaxel in Patients With Advanced or Metastatic Solid Tumors Refractory to Standard Therapy. *Cancer Chemother Pharmacol* (2012) 70(6):843–53. doi: 10.1007/s00280-012-1969-9
84. Bauman JE, Eaton KD, Wallace SG, Carr LL, Lee S-J, Jones DV, et al. A Phase II Study of Pulse Dose Imatinib Mesylate and Weekly Paclitaxel in Patients Aged 70 and Over With Advanced Non-Small Cell Lung Cancer. *BMC Cancer* (2012) 12(1):1–8. doi: 10.1186/1471-2407-12-449
85. Safra T, Andreopoulou E, Levinson B, Borgato L, Pothuri B, Blank S, et al. Weekly Paclitaxel With Intermittent Imatinib Mesylate (Gleevec): Tolerance and Activity in Recurrent Epithelial Ovarian Cancer. *Anticancer Res* (2010) 30(9):3243–7.
86. Iqbal N, Iqbal N. Imatinib: A Breakthrough of Targeted Therapy in Cancer. *Chemother Res Pract* (2014) 2014:357027. doi: 10.1155/2014/357027
87. Ramaswamy B, Bekaii-Saab T, Schaaf LJ, Lesinski GB, Lucas DM, Young DC, et al. A Dose-Finding and Pharmacodynamic Study of Bortezomib in Combination With Weekly Paclitaxel in Patients With Advanced Solid Tumors. *Cancer Chemother Pharmacol* (2010) 66(1):151–8. doi: 10.1007/s00280-009-1145-z
88. Kanehisa M. Kegg: Kyoto Encyclopedia of Genes and Genomes. *Nucleic Acids Res* (2000) 28(1):27–30. doi: 10.1093/nar/28.1.27

89. Yu J, Pacifico S, Liu G, Finley RL. DroID: The Drosophila Interactions Database, a Comprehensive Resource for Annotated Gene and Protein Interactions. *BMC Genomics* (2008) 9(1):1–9. doi: 10.1186/1471-2164-9-461
90. Giot L, Bader JS, Brouwer C, Chaudhuri A, Kuang B, Li Y, et al. A Protein Interaction Map of Drosophila Melanogaster. *Science* (2003) 302 (5651):1727–36. doi: 10.1126/science.1090289
91. Formstecher E, Aresta S, Collura V, Hamburger A, Meil A, Trehin A, et al. Protein Interaction Mapping: A Drosophila Case Study. *Genome Res* (2005) 15(3):376–84. doi: 10.1101/gr.2659105
92. Vinson KE, George DC, Fender AW, Bertrand FE, Sigounas G. The Notch Pathway in Colorectal Cancer. *Int J Cancer* (2016) 138(8):1835–42. doi: 10.1002/ijc.29800
93. Buchon N, Broderick NA, Kuraishi T, Lemaitre B. Drosophila EGFR Pathway Coordinates Stem Cell Proliferation and Gut Remodeling Following Infection. *BMC Biol* (2010) 8(1):1–19. doi: 10.1186/1741-7007-8-152
94. Xu N, Wang SQ, Tan D, Gao Y, Lin G, Xi R. Egfr, Wingless and JAK/STAT Signaling Cooperatively Maintain Drosophila Intestinal Stem Cells. *Dev Biol* (2011) 354(1):31–43. doi: 10.1016/j.ydbio.2011.03.018
95. Slattery ML, Lundgreen A, Kadlubar SA, Bondurant KL, Wolff RK. JAK/STAT/SOCS-Signaling Pathway and Colon and Rectal Cancer. *Mol Carcinog* (2013) 52(2):155–66. doi: 10.1002/mc.21841
96. Tamamouna V, Panagi M, Theophanous A, Demosthenous M, Michail M, Papadopoulou M, et al. Evidence of Two Types of Balance Between Stem Cell Mitosis and Enterocyte Nucleus Growth in the Drosophila Midgut. *Development* (2020) 147(11):dev189472. doi: 10.1242/dev.189472
97. Karpowicz P, Perez J, Perrimon N. The Hippo Tumor Suppressor Pathway Regulates Intestinal Stem Cell Regeneration. *Development* (2010) 137 (24):4135–45. doi: 10.1242/dev.060483
98. Huang T, Kang W, Cheng ASL, Yu J, To KF. The Emerging Role of Slit-Robo Pathway in Gastric and Other Gastro Intestinal Cancers. *BMC Cancer* (2015) 15(1):1–9. doi: 10.1186/s12885-015-1984-4
99. Gondal MN, Sultan MU, Arif A, Rehman A, Awan HA, Arshad Z, et al. TISON: A Next-Generation Multi-Scale Modeling Theatre for in Silico Systems Oncology. *BioRxiv* (2021). doi: 10.1101/2021.05.04.442539
100. Darabos C, Cunto F, Tomassini M, Moore JH, Provero P. Additive Functions in Boolean Models of Gene Regulatory Network Modules. *PloS One* (2011) 6 (11):e25110. doi: 10.1371/journal.pone.0025110
101. Shah OS, Chaudhary MFA, Awan HA, Fatima F, Arshad Z, Amina B, et al. Atlantis - Attractor Landscape Analysis Toolbox for Cell Fate Discovery and Reprogramming. *Sci Rep* (2018) 8(1):1–11. doi: 10.1038/s41598-018-22031-3
102. Buchon N, Osman D, David FPA, Yu Fang H, Boquete J-P, Deplancke B, et al. Morphological and Molecular Characterization of Adult Midgut Compartmentalization in Drosophila. *Cell Rep* (2013) 3(5):1725–38. doi: 10.1016/j.celrep.2013.04.001
103. Smirnov P, Kofia V, Maru A, Freeman M, Ho C, El-Hachem N, et al. PharmacoDB: An Integrative Database for Mining In Vitro Anticancer Drug Screening Studies. *Nucleic Acids Res* (2018) 46(D1):D994–1002. doi: 10.1093/nar/gkx911
104. Chakravarty D, Gao J, Phillips SM, Kundra R, Zhang H, Wang J, et al. Oncokb: A Precision Oncology Knowledge Base. *JCO Precis Oncol* (2017) 1:1–16. doi: 10.1200/PO.17.00011
105. Griffith M, Griffith OL, Coffman AC, Weible JV, McMichael JF, Spies NC, et al. Dgidb: Mining the Druggable Genome. *Nat Methods* (2013) 10 (12):1209–10. doi: 10.1038/nmeth.2689
106. Yang W, Soares J, Greninger P, Edelman EJ, Lightfoot H, Forbes S, et al. Genomics of Drug Sensitivity in Cancer (Gdsc): A Resource for Therapeutic Biomarker Discovery in Cancer Cells. *Nucleic Acids Res* (2013) 41(D1):955–61. doi: 10.1093/nar/gks1111
107. Wishart DS, Feunang YD, Guo AC, Lo EJ, Marcu A, Grant JR, et al. DrugBank 5.0: A Major Update to the DrugBank Database for 2018. *Nucleic Acids Res* (2018) 46(D1):D1074–82. doi: 10.1093/nar/gkx1037
108. Wang Z, Wei Y, Fang G, Hong D, An L, Jiao T, et al. Colorectal Cancer Combination Therapy Using Drug and Gene Co-Delivered, Targeted Poly (Ethylene Glycol)-ϵ-Poly(Caprolactone) Nanocarriers. *Drug Des Devel Ther* (2018) 12:3171–80. doi: 10.2147/DDDT.S175614
109. Arshad OA, Datta A. Towards Targeted Combinatorial Therapy Design for the Treatment of Castration-Resistant Prostate Cancer. *BMC Bioinf* (2017) 18(4):5–15. doi: 10.1186/s12859-017-1522-2
110. Steinway SN, Zañudo JGT, Michel PJ, Feith DJ, Loughran TP, Albert R. Combinatorial Interventions Inhibit Tgfβ-Driven Epithelial-to-Mesenchymal Transition and Support Hybrid Cellular Phenotypes. *NPJ Syst Biol Appl* (2015) 1(1):1–12. doi: 10.1038/npjsba.2015.14
111. Cho S-H, Park S-M, Lee H-S, Lee H-Y, Cho K-H. Attractor Landscape Analysis of Colorectal Tumorigenesis and Its Reversion. *BMC Syst Biol* (2016) 10(1):96. doi: 10.1186/s12918-016-0341-9
112. Liu J, Ghanim M, Xue L, Brown CD, Iossifov I, Angeletti C, et al. Analysis of Drosophila Segmentation Network Identifies a JNK Pathway Factor Overexpressed in Kidney Cancer. *Science* (2009) 323(5918):1218–22. doi: 10.1126/science.1157669
113. Toku AE, Tekir SD, Özbayraktar FBK, Ülgen Ö. Reconstruction and Crosstalk of Protein-Protein Interaction Networks of Wnt and Hedgehog Signaling in Drosophila Melanogaster. *Comput Biol Chem* (2011) 35(5):282–92. doi: 10.1016/j.compbiolchem.2011.07.002
114. Schönborn JW, Jehrke L, Mettler-Altmann T, Beller M. Flysilico: Flux Balance Modeling of Drosophila Larval Growth and Resource Allocation. *Sci Rep* (2019) 9(1):1–16. doi: 10.1038/s41598-019-53532-4
115. Jiang H, Grenley MO, Bravo M-J, Blumhagen RZ, Edgar BA. EGFR/Ras/MAPK Signaling Mediates Adult Midgut Epithelial Homeostasis and Regeneration in Drosophila. *Cell Stem Cell* (2011) 8(1):84–95. doi: 10.1016/j.stem.2010.11.026
116. Casali A, Batlle E. Intestinal Stem Cells in Mammals and Drosophila. *Cell Stem Cell* (2009) 4(2):124–7. doi: 10.1016/j.stem.2009.01.009
117. Lucchetta EM, Ohlstein B. The Drosophila Midgut: A Model for Stem Cell Driven Tissue Regeneration. *Wiley Interdiscip Rev Dev Biol* (2012) 1(5):781–8. doi: 10.1002/wdev.51
118. Buchon N, Broderick NA, Chakrabarti S, Lemaitre B. Invasive and Indigenous Microbiota Impact Intestinal Stem Cell Activity Through Multiple Pathways in Drosophila. *Genes Dev* (2009) 23(19):2333–44. doi: 10.1101/gad.1827009
119. Apidianakis Y, Pitsouli C, Perrimon N, Rahme L. Synergy Between Bacterial Infection and Genetic Predisposition in Intestinal Dysplasia. *Proc Natl Acad Sci USA* (2009) 106(49):20883–8. doi: 10.1073/pnas.0911797106
120. Rodriguez J, Zarate R, Bandres E, Viudez A, Chopitea A, Garcia-Foncillas J, et al. Combining Chemotherapy and Targeted Therapies in Metastatic Colorectal Cancer. *World J Gastroenterol WJG* (2007) 13(44):5867. doi: 10.3748/wjg.v13.i44.5867


**Conflict of Interest:** The authors declare that the research was conducted in the absence of any commercial or financial relationships that could be construed as a potential conflict of interest.

frontiers in Oncology

ORIGINAL RESEARCH
published: 22 July 2021
doi: 10.3389/fonc.2021.705384

# Wnt/β-Catenin Inhibition Disrupts Carboplatin Resistance in Isogenic Models of Triple-Negative Breast Cancer

*Willy Antoni Abreu de Oliveira[1†], Stijn Moens[2†], Youssef El Laithy[1], Bernard K. van der Veer[3], Paraskevi Athanasouli[1], Emanuela Elsa Cortesi[4], Maria Francesca Baietti[5], Kian Peng Koh[3], Juan-Jose Ventura[4], Frédéric Amant[2,6], Daniela Annibali[2,7‡] and Frederic Lluis[1*‡]*

[1] Stem Cell Institute, Department of Development and Regeneration, Katholieke Universiteit (KU) Leuven, Leuven, Belgium, [2] Leuven Cancer Institute (LKI), Department of Oncology, Gynecological Oncology Lab 3000, KU Leuven, Leuven, Belgium, [3] Stem Cell Institute, Department of Development and Regeneration, Laboratory for Stem Cell and Developmental Epigenetics, KU Leuven, Leuven, Belgium, [4] Translational Cell and Tissue Research – Department of Imaging & Pathology, KU Leuven, Leuven, Belgium, [5] Leuven Kanker Instituut (LKI) Leuven Cancer Institute - Trace, KU Leuven, Leuven, Belgium, [6] Centre for Gynecologic Oncology Amsterdam (CGOA), Antoni Van Leeuwenhoek-Netherlands Cancer Institute (AvL-NKI), University Medical Center (UMC), Amsterdam, Netherlands, [7] Division of Oncogenomics, Oncode Institute, The Netherlands Cancer Institute, Amsterdam, Netherlands

Triple-Negative Breast Cancer (TNBC) is the most aggressive breast cancer subtype, characterized by limited treatment options and higher relapse rates than hormone-receptor-positive breast cancers. Chemotherapy remains the mainstay treatment for TNBC, and platinum salts have been explored as a therapeutic alternative in neo-adjuvant and metastatic settings. However, primary and acquired resistance to chemotherapy in general and platinum-based regimens specifically strongly hampers TNBC management. In this study, we used carboplatin-resistant in vivo patient-derived xenograft and isogenic TNBC cell-line models and detected enhanced Wnt/β-catenin activity correlating with an induced expression of stem cell markers in both resistant models. In accordance, the activation of canonical Wnt signaling in parental TNBC cell lines increases stem cell markers' expression, formation of tumorspheres and promotes carboplatin resistance. Finally, we prove that Wnt signaling inhibition resensitizes resistant models to carboplatin both in vitro and in vivo, suggesting the synergistic use of Wnt inhibitors and carboplatin as a therapeutic option in TNBC. Here we provide evidence for a prominent role of Wnt signaling in mediating resistance to carboplatin, and we establish that combinatorial targeting of Wnt signaling overcomes carboplatin resistance enhancing chemotherapeutic drug efficacy.

**Keywords: triple negative breast cancer, WNT pathway, platinum-resistance, cancer stem cells, patient-derived xenograft models**

OPEN ACCESS

***Edited by:***
*Daniela Spano, Institute of Biochemistry and Cell Biology, (CNR), Italy*

***Reviewed by:***
*Laura Cerchia, Istituto per l'Endocrinologia e l'oncologia "Gaetano Salvatore (CNR), Italy*
*Radhika Nair, Rajiv Gandhi Centre for Biotechnology, India*

***Correspondence:**
*Frederic Lluis*
*frederic.lluisvinas@kuleuven.be*

*[†]These authors have contributed equally to this work*

*[‡]These authors share last authorship*

***Specialty section:***
*This article was submitted to Pharmacology of Anti-Cancer Drugs, a section of the journal Frontiers in Oncology*

***Received:*** *05 May 2021*
***Accepted:*** *28 June 2021*
***Published:*** *22 July 2021*

***Citation:***
*Abreu de Oliveira WA, Moens S, El Laithy Y, van der Veer BK, Athanasouli P, Cortesi EE, Baietti MF, Koh KP, Ventura J-J, Amant F, Annibali D and Lluis F (2021) Wnt/β-Catenin Inhibition Disrupts Carboplatin Resistance in Isogenic Models of Triple-Negative Breast Cancer. Front. Oncol. 11:705384. doi: 10.3389/fonc.2021.705384*

## INTRODUCTION

Triple-negative breast cancer (TNBC) is a molecular subtype of breast cancer characterized by the lack of expression of estrogen-receptor, progesterone-receptor, and human epidermal growth factor receptor type 2 (1). TNBC accounts for 10-20% of all breast cancer cases, occurring with higher frequency in younger women, presenting with higher grade and mitotic counts than non-TNBCs, low differentiation, and frequent lymph node involvement, ultimately contributing to poor prognosis (1, 2).

The lack of hormone- and growth factor-receptors render chemotherapy the primary systemic treatment for TNBC. Interestingly, TNBC patients have high response rates to neoadjuvant chemotherapy, achieving pathological complete response (pCR) more frequently than those bearing non-TNBCs (3). Nonetheless, TNBC patients experience lower progression-free- and overall survival rates and higher distant metastatic relapse frequency than non-TNBC patients, highlighting the critical need for alternative therapeutic approaches (3).

The Food and Drugs Administration of the United States of America first approved platinum salts, namely cisplatin, to treat metastatic testicular cancer, ovarian cancer, and bladder cancer between 1978 and 1979 (4). Since then, the use of platinum-based chemotherapy has grown and is now applied in many other cancer types. Preclinical studies have highlighted that TNBC is particularly sensitive to DNA damaging agents (5, 6). For that reason, platinum salts – DNA-crosslinking agents – have gained traction as potential additions to the therapeutic toolbox for TNBC. Phase-II and Phase-III clinical trials have demonstrated the benefits of including carboplatin (CAR) in neoadjuvant regimens for TNBC (7–10). Importantly, pCR with neoadjuvant treatment is a robust predictor of survival in TNBC (3). However, chemotherapy-treated TNBC patients are likely to acquire resistance, and patients with residual disease (RD) have worsened prognosis and experience low survival rates, particularly within the first three years ensuing treatment (3).

During the last decades, our knowledge of platinum's mechanism of action has increased significantly. Nonetheless, how cancer overcomes platinum-mediated cytotoxicity still holds unanswered questions. Several studies have shed light on how cancer cells adapt to platinum-based treatment by restoring DNA damage repair, increasing tolerance to DNA damage, decreasing its intracellular uptake and accumulation, and regulating apoptosis and autophagy (11). Chemotherapy resistance is also known to be induced and maintained by adaptations in pro-survival and anti-apoptotic signaling pathways. Like other chemotherapeutic agents, alterations of such cellular dynamics also affect platinum-based treatments. Several studies have demonstrated the involvement of NOTCH (12), MEK (13), Hedgehog (14), EGFR (15), among others, in mediating resistance to platinum in different cancer types. Also, cancer cells with stem cell-like properties have been described to significantly influence the response to different chemotherapeutic agents, including platinum compounds (16–19). Cancer stem cells constitute a subpopulation of cancer cells with tumorigenic and self-renewal capacities and are considered desirable therapeutic targets since their intrinsic cellular properties contribute extensively to treatment failure (20–22). Breast cancer stem cells were first isolated in 2003 based on cell surface markers CD44 and CD24 (23). Since then, many studies have demonstrated their tumorigenic and drug-resistance capacities, highlighting the need to develop therapeutic approaches that deplete this population (6, 24–26).

The Wnt/β-catenin signaling pathway is a developmental signaling cascade with a prominent role in cancer (27). It is initiated when Wnt ligands (secreted lipid-modified signaling molecules) bind the receptor complex at the cell membrane. A series of events ensues, culminating in the inhibition of glycogen synthase kinase 3 beta (GSK3β), and the subsequent cytoplasmic accumulation of β-catenin, the critical mediator protein of Wnt signaling. This accumulation leads to the nuclear translocation of β-catenin, eliciting Wnt target genes' expression by interacting with different transcription factors. In the absence of Wnt ligands, β-catenin is constitutively phosphorylated by GSK3β and targeted for proteasomal degradation (28). Notably, Wnt is known to govern several cellular functions with the potential to contribute to chemotherapy resistance. Such functions include the control and regulation of proliferation (29), DNA damage repair (30), inhibition of apoptosis (31), and maintenance and regulation of embryonic, somatic, and cancer stem cell properties (32). Different studies have demonstrated Wnt pathway involvement in the mediation of platinum resistance in various cancer types, including squamous cell carcinoma (33, 34) and ovarian cancer (35). However, its involvement in platinum resistance in TNBC is not known.

To study how TNBCs acquire resistance to carboplatin treatment, we used a pair of isogenic carboplatin-sensitive and -resistant TNBC cell lines. Transcriptomic analysis was performed to gain insight into biological signaling pathways underlying acquired carboplatin resistance *in vitro*, leading to the identification of Wnt signaling as a candidate resistant-mediating pathway. Additionally, the resistant cell line displayed enhanced expression of pluripotency markers and stem cell features compared to the parental, carboplatin-sensitive cells.

*In vitro* pharmacological and genetic manipulation of Wnt signaling was employed to assess drug response alterations and stem cell potential functionally. Inducing Wnt signaling in parental non-resistant TNBC cell lines elicited the expression of pluripotency markers observed in isogenic resistant cells and enhanced stem cell features *in vitro*. Moreover, inhibition of Wnt activity in resistant cells resensitized them to carboplatin and hindered tumorsphere formation. Finally, carboplatin-resistant patient-derived xenograft (PDX) models were used to test the effect of *in vivo* Wnt inhibition on platinum-response. Similar to what we observed *in vitro*, inhibition of Wnt reduced expression of cancer stem cell markers and drastically reduced resistance to carboplatin treatment *in vivo*.

Altogether, our results suggest the potential for Wnt signaling inhibition in combination with carboplatin as a strategy to prevent or overcome platinum resistance in TNBC patients.

# MATERIALS AND METHODS

## Cell Lines, Cell Culture, and Treatments

MDA-MB-468 (ATCC-HTB-132) and MDA-MB-231 (ATCC HTB-26) were maintained in DMEM high glucose (Gibco 41965039) supplemented with 10% fetal bovine serum, 1mM sodium pyruvate (Gibco, 11360070), 1X non-essential amino acids (Gibco, 11140035), 100 µg/mL penicillin-streptomycin (Gibco, 15140163) and 0.01mM 2-mercaptoethanol (Gibco, 31350010).

Unless otherwise specified in the text, all carboplatin treatments (CAR, Hospira UK, Ltd) were done at 2 µM for MDA-MB-468 cells and 35 µM for MDA-MB-231 cells. Small molecule Wnt activator CHIR99021 (CHIR, Sigma, SML1046) was administered to cells in DMSO (Sigma, D2650) at 4 µM. Small molecule Wnt inhibitor LGK-974 (LGK, Selleckchem, S7143) was, unless otherwise specified, administered at 200 nM in DMSO.

Carboplatin resistance was induced in MDA-MB-468 cells by continued maintenance in carboplatin containing medium, starting at a concentration of 0.4 µM. The concentration of carboplatin was increased in 9 increments until reaching 2 µM, once unhindered cell growth was obtained at each concentration level, allowing a 48h carboplatin-free recovery period with each splitting (35).

## Lentiviral Particle Production and Transduction

Lentiviruses were produced according to the RNAi Consortium (TRC) protocol available from the Broad Institute (https://portals.broadinstitute.org/gpp/public/resources/protocols). In brief, $5x10^5$ HEK293T cells seeded per well in 6-well plates and transfected the following day with 750 µg pCMV-dR8.91, 250 µg pCMV-VSV-G, and 1 µg of the specific lentiviral expression or silencing constructs using FugeneHD (Promega, E2311) in Opti-MEM (Gibco, 31985070). One day after, the culture medium was replaced. The same day, lentivirus-recipient cells were plated in 6-well plates at a density of $5x10^4$ cells per well. Lentivirus-containing medium was collected from HEK293T cells 48h and 72h after transfection and added to recipient cancer cells after being filtered. Two days after infection, cells were washed thoroughly with PBS, medium refreshed, and appropriate selection antibiotics applied.

For overexpression of ΔN90-β-catenin, we used pLV-beta-catenin ΔN90 (Addgene, #36985) and pPRIME-CMV-NEO-recipient (CTRL, Addgene, #11659). For β-catenin shRNA mediated silencing, we used pXL002-ishRNA-beta-catenin-1 (Addgene, #36297) and pXL004-ishRNA-scramble (Addgene, #36311). For Wnt fluorescent reporter assay, we used 7TGP (Addgene, #24305).

## *In Vitro* Carboplatin Response

For IC50 experiments, we seeded $2.5x10^4$ cells per well in 12-well plates. Cells were treated with increasing concentrations of CAR (0.02 to 200 µM for MDA-MB-468 and 0.35 to 3500 µM for MDA-MB-231) for 72 hours. Viability was assessed by manual cell counting using a Neubauer hemocytometer using trypan blue for dead cell exclusion. Cell viability was determined as a percentage of untreated cells, and non-linear regressions of [CAR] *vs.* normalized-response were fitted using GraphPad Prism v.8.0.1. to mathematically determine the IC50.

## Flow Cytometry

For annexin V apoptosis analysis, cells were detached and resuspended in annexin V binding buffer (BD Pharmigen, 51-66121E) and incubated for 15 minutes at room temperature with APC-conjugated AnnexinV (Thermo-eBioscience, BMS306APC-100). After incubation, cells were diluted in binding buffer containing 100 nM of 4',6-diamidino-2-phenylindole (DAPI). Unstained and single-stained (annexin V and DAPI) were used as gating controls.

For ALDH activity assays, cells were detached, washed in PBS, and stained using the AldeRed ALDH detection assay kit (Merck SRC150) according to manufacturer specifications.

For immunolabeling of CD44 and CD24, cells were detached, washed twice in PBS with 4% FBS, and incubated with CD44-PE (BD Pharmigen, 555479) and CD24-APC (Invitrogen, 17-4714-81) antibodies according to manufacturer specifications at room temperature. After incubations, cells were washed twice in PBS with FBS and resuspended in PBS containing 4% FBS and 100 nM of DAPI. Cells incubated with PE- and APC- conjugated isotype-antibodies and single-stained cells were used as gating controls.

All data were collected on a BD FACS Canto II at the KU Leuven Flow Cytometry Core and analyzed using FlowJo v.10.6.2.

## SDS-PAGE and Western Blot

For western blot, cells were collected and washed in PBS before being pelleted. Then, cells were lysed on ice with RIPA buffer (150 mM NaCl, 1% Nonidet P40, 0.5% sodium deoxycholate, 0.1% dodecyl sulfate, 50 mM Tris-HCL, pH 8.0) containing a cocktail of protease and phosphatase inhibitors (Sigma, #P5726, #P0044, #P8340). Lysates were centrifuged at 16,000x g for 10 minutes at 4°C to discard insoluble material, and protein concentration was determined using the Bradford method. For SDS-PAGE, 30 µg of protein were mixed with 4x Laemmli buffer (240 mM Tris/HCL pH 6.8, 8% SDS, 0.04% bromophenol blue, 5% 2-mercaptoethanol, 40% glycerol) and denatured for 5 minutes at 96°C prior to electrophoretic protein separation. Resolved protein extracts were transferred to PVDF membranes (BIORAD, 162-0177). Transfer success was assessed with Ponceau S solution, and membranes were blocked with 5% non-fat milk or 5% BSA in TBS-T (0.1% Tween-20®) for 60 minutes. After blocking, membranes were incubated with primary antibodies at 4°C overnight. The day after, membranes were washed 3 times with PBS-T for 10 minutes and incubated with secondary HRP-conjugated antibodies. Immunolabeled proteins were detected with Supersignal West Pico chemiluminescent kit (Fisher Scientific, 34077) on autoradiography film (Santa Cruz, SC-201697). The primary antibodies used were active rabbit anti-non-phosphorylated β-catenin (CellSignaling Technologies, #19807S), mouse anti-total β-catenin (BD, #610154), mouse anti-β-actin (Santa Cruz, #47778).

## Next-Generation mRNA Sequencing

Total RNA was obtained from cells using the GenElute mammalian total RNA miniprep kit (Sigma, RTN350-1KT) for mRNA sequencing. According to the manufacturer's specifications, libraries were prepared from 250 ng of total RNA using the KAPA stranded mRNA-seq kit (Roche, KK8421). KAPA-single index adapters (Roche, KK8700) were added to A-tailed cDNA, and libraries were amplified by 12 cycles. Finally, libraries were purified on Agencourt AMPure XP beads (Beckman Coulter, A63881). Libraries were controlled for fragment size using the High Sensitivity DNA analysis kit (Agilent, 5067-4626) on an Agilent Bioanalyzer 2100. Each library was diluted to 4 nM and pooled for single-end 50-bp sequencing on an Illumina Hiseq4000 20 – 27 million reads per sample (22 million reads on average).

Adapters, polyA tails, and bad quality reads (Phred score > 20) were trimmed using Trim Galore! (v0.6.4_dev) with default parameters. Reads were aligned to the transcriptome and quantified using Salmon (v0.14.1) (36) with default parameters using GENCODE release 36 of the human reference transcriptome sequences and the comprehensive gene annotation. Subsequently, the counts were imported into R (v4.0.2) using tximport (v1.18.0) and differentially expressed genes were defined using DEseq2 (v1.30.0) (37) and log fold changes corrected using "ashr" method (38) (FDR adjusted p.val < 0.05 & |log2(fold change)| > 1.5). TPM values were also calculated using tximport.

## Functional Enrichment Analysis and Enrichment Maps

Datasets GSE103668 and E-MTAB-7083 were downloaded from the GeneExpression Omnibus and ArrayExpress public repositories, respectively. Differentially expressed genes with |log2(fold-change)| >1 and p-value < 0.05 were obtained using limma (v3.26.8) R package in R (v4.02) and by using the limma method on NetworkAnalyst (39). Differentially expressed genes were ranked by fold-change for Gene Set Enrichment Analysis (GSEA v4.1.0) using weighted enrichment statistic and KEGG, Hallmarks, and Wikipathways gene sets. Additionally, we used custom gene sets comprised of human embryonic stem cell-related genes (M1871: BENPORATH_ES1 and M4241: BENPORATH_ES2), pluripotency transcription factor target genes (M14573: BENPORATH_NOS_TARGETS), and cancer progenitor genes (ENGELMANN_CANCER_PROGENITORS_UP) obtained from www.gsea-msigdb.org. The statistical significance threshold was set at FDR<0.1 or ($p$<0.5 ∧ FDR<0.25). Additionally, gProfiler (https://biit.cs.ut.ee/gprofiler/gost) was used to assess the function of ranked DEGs using the ranked query mode and Benjamini-Hochberg FDR thresholding. GSEA and gProfiler analysis outputs were fed to the EnrichmentMap app on Cytoscape (v3.8.1) to generate visualizations of enriched biological features and pathways following published protocols (40). Differentially expressed genes from RNA-sequencing were processed for functional analysis and visualization in the same way, except for GSEA, differentially expressed genes were ranked by the absolute value of fold change (41).

## Real-Time Quantitative Polymerase Chain Reaction and Gene Expression Analysis

For RT-qPCR, total RNA was extracted using the GenElute mammalian total RNA miniprep kit from Sigma (Sigma, RTN350-1KT) according to the manufacturer's instructions, and DNA was digested during RNA extraction using on-column DNAse (Sigma, On-Column DNAse I digestion set, DNASE70). cDNA was synthesized from 500 ng of total RNA using the BIORAD iScript cDNA synthesis kit (BIORAD, CAT#1708891). Quantitative real-time PCR reactions were set up in technical triplicates with Platinum SYBR Green qPCR SuperMix-UDG (Invitrogen, 11733-046) on a ViiA7 Real-Time PCR System (Thermo Scientific). Expression levels were normalized to housekeeping genes (HKG) GAPDH and RPL19. Statistical testing of differences in expression between samples was carried out on relative-expression values ($2^{-\Delta CT}$). In some figures, mRNA expression values are represented as fold-change for convenience of interpretation, although statistical testing was performed on relative expression values ($2^{-\Delta CT}$).

## Tumorsphere Formation Assays

For tumorsphere formation assays, cells were collected as described above, washed, counted, and resuspended in serum-free tumorsphere assay medium containing DMEM/F12, 1x B27 (Thermo, 12587010), 10ng/mL bFGF, (Peprotech, 100-18b) 20 ng/mL EGF (Peprotech, AF-100-15), and 2% growth-factor reduced matrigel (Corning, 734-0268). Cells were seeded at a density of 1000 cells/mL in ultra-low attachment 6-well plates and allowed seven days to grow. On the 7$^{th}$ day, spheres were collected and centrifuged at 50g for 10 minutes, resuspended, and transferred to 96-well plates. Plates were briefly centrifuged at 50g for 1 minute to pull down larger spheroids (>60 μm) which were counted using a tally counter.

## Immunohistochemistry

Tumor samples were dissected, washed in saline, and either snap-frozen in OCT compound (VWR 361603E) or fixed in 4% formalin for 24 hours. Frozen tissue was cut at 10 μm thickness using a cryostat and mounted on superfrost microscope slides (Thermo Scientific, °J1800AMNZ). Formalin-fixed tissue was embedded in paraffin and sectioned at 4 μm thickness using a microtome. Frozen and FFPE sections were stained with hematoxylin and eosin (HE), using a Leica Autostainer XL (Leica Microsystems), or stained in immunohistochemistry (IHC). In brief, frozen sections were fixed in acetone and preserved at -80°C until use. Slides were thawed at room temperature for 15 minutes and rehydrated in PBS. FFPE sections were deparaffinized in Leica Autostainer XL (Leica Microsystems) and pre-treated in citrate buffer (EnVision FLEX Target Retrieval Solution Low pH, Agilent-Dako, K8005) using a PT Link module (Dako), according to manufacturer's instructions. For IHC, tumor sections were incubated with Envision Flex Peroxidase-Blocking Reagent (Dako, S202386-2) for at least 5 minutes, rinsed three times in wash buffer (Dako, K800721-2), and blocked with 5% bovine serum albumin (BSA) for 45 min at room temperature. After overnight incubation with

anti-human Ki67 antibody (Abcam, EPR3610 clone, 1:1500) at 4°C, slides were incubated with HPR-conjugated secondary antibodies (Agilent, K400311-2) for 30 min. Tissue sections were stained with 3,3'-diaminobenzidine solution (DAB; Liquid DAB+ Substrate Chromogen System, K346889-2, Dako), counterstained with hematoxylin, and mounted using an automated coverslipper machine (Leica CV5030, Leica Biosystems). Pictures were acquired using a Zeiss Axiovision microscope. Quantification of Ki67+ cells was performed in at least 5 random 20x fields per sample using QuPath 0.2.3 (42).

## Tunel Staining and Pan-Cytokeratin Immunofluorescent Staining

For TUNEL staining, cryopreserved tumor samples were cryosectioned at 10 μM thick and mounted on superfrost microscope slides. Slides were stored at -80°C and stained using the Click-iT Plus TUNEL (ThermoFisher C10617) according to the manufacturer's instructions. After TUNEL staining, slides were blocked with 5% normal donkey serum in PBS (Gibco, 10010-050) for one hour and incubated overnight at 4°C with rabbit anti-pan-cytokeratin polyclonal antibody (Abcam ab217916 1:400). The following day, slides were washed three times in PBS containing 0.01% Triton X-100 and incubated for 2 hours with AlexaFluor conjugated donkey anti-rabbit secondary antibody (Abcam ab150073 1:1000). After secondary antibody incubation, slides were washed three times with PBS containing 0.01% Triton X-100 and mounted with ProLong™ Gold Antifade Mountant with DAPI (P36931, Thermo Fisher Scientific). Images were acquired using a Leica Sp8x confocal microscope. TUNEL positive/pan-cytokeratin positive cells were quantified in at least eight randomly sampled 10x fields per sample using QuPath 0.2.3.

## PDX Models

BRC016 (primary, grade III, TNBC) was established at the University Hospital UZ Leuven and is available from Trace, the KU Leuven/LKI PDX Platform (https://www.uzleuven-kuleuven.be/lki/trace/trace-leuven-pdx-platform). C4O was previously obtained from a carboplatin treatment-refractory BRC016 tumor. Briefly, 10 BRC016 TNBC tumor-bearing NMRI-Fox1nu nude mice (Taconic) were treated intraperitoneally with 50 mg/kg carboplatin, once weekly for three weeks. The carboplatin dose chosen was based on previous studies of carboplatin-response in our lab and other groups (35, 43–45). Nine out of ten mice had a complete response to treatment. One mouse had delayed and incomplete response, bearing a residual tumor mass that became unresponsive to further carboplatin treatment and eventually resumed growth. In a previously published study, the regrown tumor was harvested and implanted on nude mice for propagation, re-testing, and confirmation of carboplatin resistance (35). Treatment experiments included 24 mice implanted with C4O tumor fragments. When tumors reached a volume of approximately 300 $mm^3$, mice were randomly assigned to placebo (vehicle), CAR (50 mg/kg), LGK (2 mg/kg), or CAR+LGK (50 mg/kg + 2 mg/kg) treatment groups. Carboplatin was administered once a week intraperitoneally, and LGK974 was administered daily by oral gavage. Treatments were carried out for three weeks, and body weight was closely monitored throughout treatment Tumors were measured every 48 hours with digital calipers, and volume was estimated as $V = L \times W^2 \times \pi/6$ (L: length, W: width). All animals were euthanized at the end of three weeks of treatment, and tumors were collected for downstream analysis.

## Statistical Analysis

All data were analyzed using GraphPad Prism 8, except for transcriptomic datasets. Unless otherwise specified, comparisons between two groups were tested for statistical significance using unpaired t-tests with Welch correction. Comparisons between multiple groups were performed using a one-way analysis of variance (ANOVA). Comparisons between multiple groups across multiple time points were performed using two-way ANOVA. All statistical testing was corrected for multiple comparisons, using the Holm-Sidak method when comparing samples based on experimental design or the Tukey method when testing the comparison between all means in a dataset. For the reader's convenience, all statistical tests and sample sizes are indicated in the figure legends.

# RESULTS

## Carboplatin-Resistant TNBC Cells Are Characterized by Enhanced WNT/β-Catenin Pathway Activity, Stem Cell Marker Expression, and Tumorsphere Formation Capacity

To explore the mechanisms of *in vitro* carboplatin resistance in TNBC, we generated an isogenic carboplatin-resistant cell line (468'R) (**Figure 1A**) by exposing MDA-MB-468 cells to carboplatin treatment in incremental cycles.

Half-maximal inhibitory concentration (IC50) profiles for carboplatin were determined for both parental (468'P) and 468'R cells (**Figure 1B**). 468'R cells displayed a 5-fold increase in IC50, thereby functionally confirming a significant increase in carboplatin resistance. When treated with vehicle, we did not observe differences in proliferation between resistant and parental cells. However, when treated with CAR, 468'R cells displayed unhindered proliferation capacity in striking contrast to parental cells (**Figure 1C**). Additionally, we did not find differences in Ki67 expression in standard culture conditions between cell lines (**Supplementary Figure 1A**). Altogether, these results suggest that differences in proliferation rate cannot justify resistance in 468'R cells compared to the parental, sensitive cell line. Flow-cytometric analysis of apoptosis further corroborated the establishment of the carboplatin-resistant phenotype. When exposed to 2 μM for 72 hours, 468'P stained positively and significantly for the apoptosis marker annexin V (47), whereas no significant increase in apoptotic cells was observed in 468'R (**Figure 1D**).

To study the underlying mechanisms of carboplatin resistance, we performed transcriptome analysis by next-

generation mRNA sequencing in 468'P and 468'R cells. We used the ranked differentially expressed genes (**Supplementary Table 1**) followed by one-tailed Gene Set Enrichment Analysis (GSEA) (41) to identify changes in signaling pathways (Hallmarks, KEGG and Wikipathways). GSEA analysis identified alterations in several key cancer-related processes, such as epithelial-mesenchymal-transition (Hallmarks) and PPAR and P53 signaling (KEGG) (**Supplementary Table 1**). However, Wnt signaling was consistently enriched across the two databases (**Figure 1E**) with a clear differential expression pattern across the two cell lines (**Supplementary Figure 1B**). Moreover, enrichment maps of Wikipathway database terms highlighted a cluster of gene sets comprising Wnt signaling and pluripotency regulation (**Figure 1F**), suggesting a potential acquisition or enrichment of stem cell features in carboplatin resistant cells.

To further understand the differences in stem cell transcriptional features between 468'R and 468'P cells, we compared our transcriptomic data with curated gene sets comprised of genes found overexpressed in human embryonic stem cells (hESC) and cancer stem cells (26, 46). Interestingly, 468'R seems to be transcriptionally closer to embryonic and cancer stem cells than 468'P as determined by GSEA (**Figure 1G**). In addition, we compared our transcriptomic data with a gene set comprised of targets of pluripotency transcription factors NANOG, OCT4, and SOX2 in hESCs determined by chromatin immunoprecipitation followed by DNA sequencing (26). GSEA revealed enrichment of pluripotency transcription factor target genes in 468'R cells, supporting the putative acquisition of stem cell features in this cell line (**Figure 1H**).

To functionally validate the observed differences in Wnt/β-catenin signaling between 468'R and 468'P cells, we analyzed protein levels of non-phosphorylated (active) β-catenin. Importantly, western-blot analysis of total protein extracts in baseline untreated conditions revealed strong enrichment of active β-catenin in 468'R cells compared to the parental counterpart, thereby confirming the functional activation of Wnt signaling in drug-resistant cells (**Figure 1I**). Moreover, the accumulation of active β-catenin was accompanied by transcriptional activation of Wnt-reporter activity (**Supplementary Figure 1C**).

To quantify differences in frequency of putative cancer stem cell populations in both cell lines, we used flow cytometry to assess the enzymatic activity of aldehyde dehydrogenases (ALDH) and the expression level of the cell surface markers CD44 and CD24. Both methods have been used to identify, quantify, and isolate putative cancer stem cells from different cancer types. High ALDH activity and CD44/CD24 expression ratio in TNBC have been shown to correlate with enhanced tumorigenesis and metastatic potential as wells as radio- and chemotherapy resistance (23, 25, 48). Flow cytometric analysis showed significant differences in ALDH positive (**Figure 1J**) and $CD44^{+}/CD24^{-}$ cells (**Figure 1K**), with 468'R cells expressing higher levels of both markers. Gene expression analysis also revealed an enrichment of the core pluripotency regulators *OCT4, NANOG*, and *cMYC*, as well as cancer stem cell marker *LGR5* (49) (**Figure 1L**).

We performed a tumorsphere formation assay to functionally evaluate differences in cancer stem cell properties and *in vitro* tumor-initiating capacity. *In vitro* growth in non-adherent conditions has been described as an exclusive capability of cancer stem cells, thereby functioning as a surrogate measure of *in vitro* tumor-initiating capacity and as a method to enrich cancer stem cells (50). Importantly, in line with our stemness-related gene expression data and flow cytometry analysis of ALDH activity and CD44/CD24 expression, we observed a significantly higher tumorsphere formation frequency in 468'R cells compared to 468'P (**Figure 1M**).

Altogether, the transcriptomic evidence for alterations in Wnt signaling, and presumably stem cell features, between 468'R and 468'P cells suggests the possibility of its involvement in mediating carboplatin resistance in our isogenic cell line.

## Pharmacological Activation of Wnt Signaling in 468'P Cells, Disrupts Carboplatin-Response and Enhances Stemness and Pluripotency Marker Expression

We hypothesized that modulation of Wnt signaling in the parental 468'P cell line could recapitulate the carboplatin-resistant phenotype and increase the expression level of pluripotency and stem cell-related genes. To test this hypothesis, we treated 468'P with a small molecule inhibitor of GSK3, CHIR99021 (CHIR), thereby preventing β-catenin degradation and activating the Wnt/β-catenin pathway. To confirm Wnt signaling activation, we used a lentiviral fluorescent reporter of canonical Wnt transcriptional activity (TOPGFP) (51). 468'P displayed low basal levels of Wnt-reporter activity but promptly induced the reporter upon GSK3β inhibition, with almost 100% of cells becoming GFP positive within 12 hours of treatment (**Figure 2A**).

We observed a significant rescue of survival when treating 468'P with CHIR combined with carboplatin (**Figure 2B**). Carboplatin-induced apoptosis was also significantly reduced when cells were co-treated with CHIR and CAR, as determined by flow cytometric analysis of Annexin V positivity (**Figure 2C**). Also, GSK3β inhibition led to the upregulation of *OCT4* and *NANOG* pluripotency markers (**Figure 2D**).

Similar results were observed by inhibiting GSK3β on a second TNBC cell line (MDA-MB-231) (**Supplementary Figures 2A, B**), suggesting this effect is not cell line-specific.

## β-Catenin Overexpression Induces Carboplatin Resistance in 468'P and Enhances Stem Cell Features

GSK3 is a multi-substrate serine-threonine kinase that regulates a multitude of signaling pathways (52). As such, we proceeded to investigate whether the effects of pharmacological activation of Wnt signaling on stemness and carboplatin resistance observed upon GSK3 inhibition could also be induced by direct overexpression of β-catenin. To achieve this, we transduced 468'P cells with a lentiviral vector encoding a truncated, constitutively

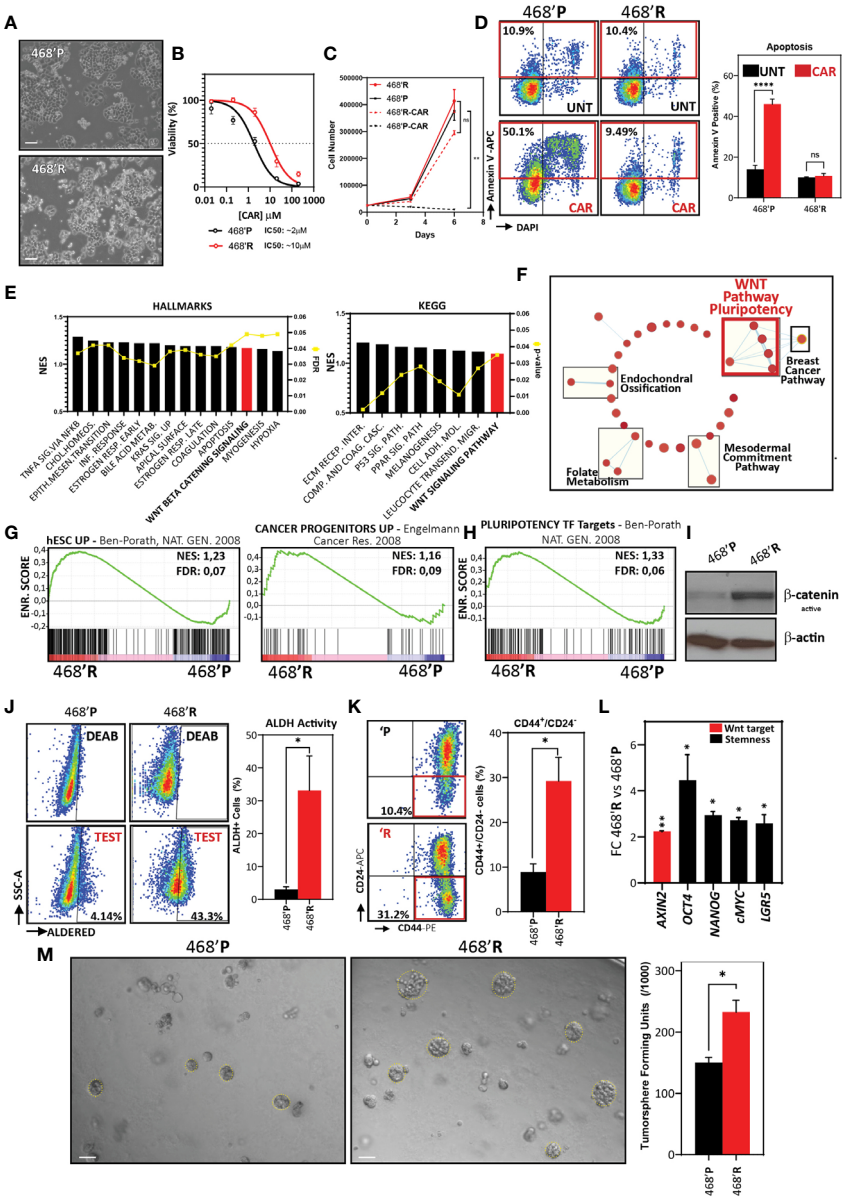


**FIGURE 1** | *Carboplatin-resistant TNBC cells are characterized by enhanced WNT/β-catenin pathway activity, stem cell marker expression, and tumorsphere formation capacity*. **(A)** Phase contrast microscope images of 468'P and 468'R cells. Scale bar: 100 µm. **(B)** Non-linear fit model of [CAR] µM *vs* normalized response for IC50 determination. (468'P: n=6, $R^2$ = 0.92) (468'R: n=4, $R^2$ = 0.95). **(C)** Growth curve and statistical analysis for 468'P and 468'R cells treated with VEH or CAR using two-way ANOVA. Statistical significance is reported for day 6 of treatment (n=4). **(D)** Representative flow cytometry scatterplots of annexin V staining of cells treated with 2 µM CAR for 72 hours (left) and respective statistical analysis (right) using multiple t-tests corrected for multiple comparisons with the Holms-Sidak method (n=3). **(E)** Enriched gene sets from Hallmarks and KEGG databases by one-tailed GSEA ranked by Normalized enrichment score (NES), illustrating pathways most significantly deregulated between 468'P and 468'R. **(F)** Enrichment map of one-tailed GSEA hits from Wikipathways database. Rectangles highlight clusters of gene sets with significant overlap and are labeled using AutoAnnotate on Cytoscape. **(G)** GSEA of hESCs (26) (left) and Cancer Progenitor (46) (right) gene sets in 468'R *vs* 468'P cells. **(H)** GSEA of NANOG, OCT4, and SOX2 target genes determined by ChIP-SEQ in hESC's (26) in 468'R *vs*. 468'P cells. **(I)** Western blot of active non-phosphorylated β-catenin in 468'P and 468'R. β-actin was used as the loading control. **(J)** Representative scatterplots of flow cytometric analysis of aldehyde dehydrogenase activity (left). DEAB panels refer to internal controls in which ALDH activity is blocked with diethylaminobenzaldehyde to determine the background signal generated by unconverted ALDH substrate. TEST panels refer to the experimental samples where substrate for fluorimetric determination of ALDH activity is supplied. TEST samples are normalized to background fluorescence measured in DEAB internal controls and presented as the mean + standard error of the mean percentage of ALDH+ cells in 468'R (n=5) and 468'P (n=7) (right). Welch's t-test. **(K)** Representative scatterplots of flow cytometric analysis of CD44-PE and CD24-APC immunolabeling (left) and corresponding statistical analysis of the mean percentage of $CD44^{+}/CD24^{-}$ cells (right; n=3). Welch's t-test. **(L)** qRT-PCR of Wnt target AXIN2 and stem cell markers in 468'R cells *vs*. 468'P (n=4). Multiple t-tests. **(M)** Representative brightfield images of tumorspheres generated from 468'P and 468'R cells (left, scale bar: 50 µm) and statistical analysis of mean tumorsphere forming units (number of spheres/number of seeded single cells) (right; n=3). Welch's t-test. (Barplots represent mean + SEM. *$p < 0.05$; **$p < 0.01$; ****$p < 0.0001$; ns, non significant).

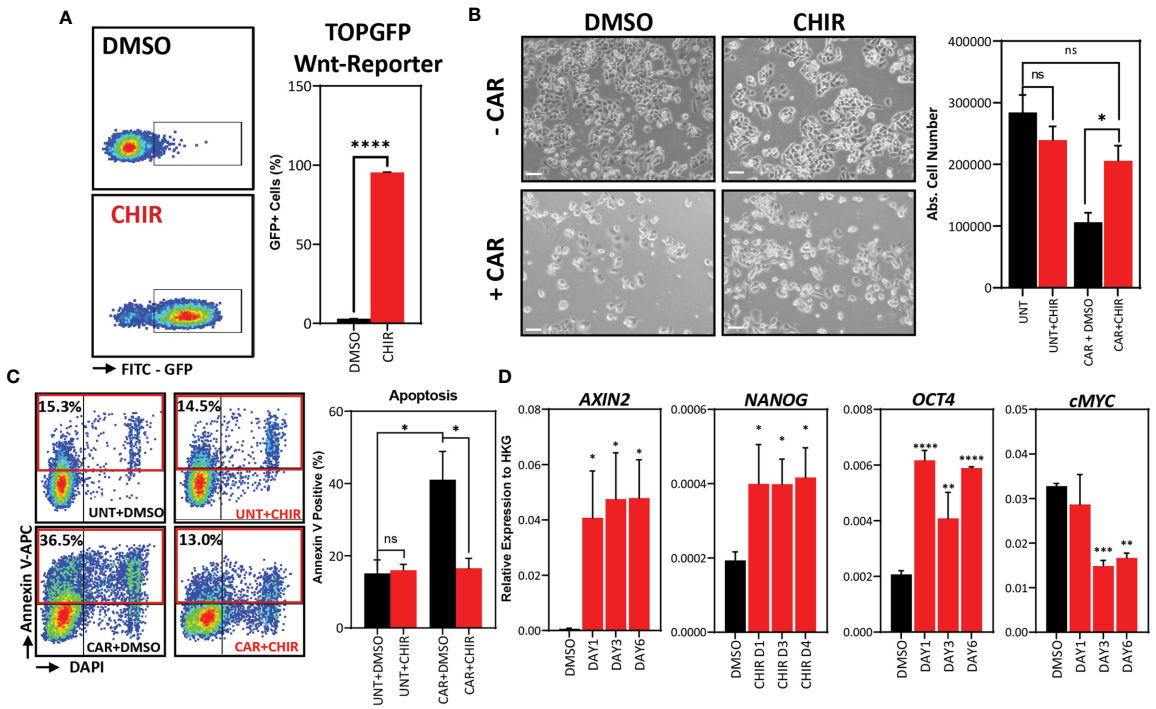


**FIGURE 2** | *Pharmacological in vitro Wnt induction prevents carboplatin-induced apoptosis and upregulates stem cell marker expression*. **(A)** Representative flow cytometry scatterplots (left) of Wnt-reporter MDA-MB-468 TOPGFP cells treated with vehicle (DMSO) or GSK3 inhibitor (CHIR, 4 μM) for 12 hours and statistical analysis of the mean frequency of GFP+ cells using Welch's t-test (right, n=3). **(B)** Phase-contrast microscopy images of 468'P cells treated with or without carboplatin in the presence of CHIR or DMSO (left, scale bar: 100 μm) and statistical analysis of absolute cell numbers after 72 hours of each treatment using One-way ANOVA corrected for multiple comparisons using the Holm-Sidak method (n=4). **(C)** Representative flow cytometry scatterplots of annexin V staining of 468'P cells (left) treated with or without carboplatin in the presence of DMSO or CHIR (4 μM) for 72 hours and statistical analysis of the mean frequency of annexin V positive cells (right) using one-way ANOVA corrected for multiple comparisons using the Holm-Sidak method (n=3). **(D)** Relative mRNA expression of Wnt target and stem cell markers upon 72-hour treatment with DMSO or CHIR (4 μM) in 468'P cells (n=3). Multiple t-tests with Holm-Sidak correction for multiple comparisons. (Barplots represent mean + SEM. *$p < 0.05$; **$p < 0.01$; ***$p < 0.001$; ****$p < 0.0001$; ns, non significant).

active mutant β-catenin (ΔN90-β-catenin) (53), generating β-catenin overexpressing cells (468'OE) (**Figure 3A**).

We then performed mRNA-sequencing to investigate biological processes altered by overexpression of β-catenin in TNBC cells. Differentially expressed genes (**Supplementary Table 2**) were ranked by fold-change and analyzed by GSEA using the Wikipathways database. We detected an interesting enrichment of gene sets related to both pluripotency and differentiation, namely Embryonic Stem Cell Pluripotency Pathways (M39530: WP_ESC_PLURIPOTENCY_PATHWAY) and Wnt signaling in pluripotency (M39387: WP_WNT_SIGNALING_PATHWAY_AND_PLURIPOTENCY) (**Figure 3B**). In addition, GSEA revealed a significant correlation between the transcriptional profile of 468'OE cells and hESC and pluripotency transcription factor gene sets (**Supplementary Figure 3A**).

468'OE displayed increased carboplatin resistance in comparison with 468'CTRL cells (empty lentiviral vector) (IC50 468'OE: ~7 μM *vs*. IC50 468'CTRL: ~1.5 μM) (**Figure 3C**). Accordingly, flow cytometric analysis revealed that upon overexpression of active β-catenin, 468'OE cells fail to induce apoptosis when challenged with carboplatin, displaying Annexin V positivity frequencies at the same level of untreated cells (**Figure 3D**). These data confirm the direct involvement of β-catenin in the acquisition of *in vitro* carboplatin resistance in TNBC.

Next, we probed gene expression of Wnt targets and pluripotency and cancer stem cell markers by RT-qPCR. As observed with pharmacological activation of Wnt, β-catenin overexpression also induced a significant upregulation of pluripotency markers *OCT4* and *NANOG* but also *cMYC* and *LGR5* (**Figure 3E**).

Further, in accordance with the increased expression of pluripotency and stemness-related genes, flow cytometric analysis of ALDH activity (**Figure 3F**) and CD44/CD24 expression (**Figure 3G**) corroborated the presumptive induction of an enhanced cancer stem cell phenotype upon overexpression of β-catenin in TNBC cells.

Finally, we investigated whether overexpression of β-catenin functionally endows TNBC cells with enhanced tumorsphere formation capacity. Indeed, 468'OE cells displayed a significantly higher sphere-forming efficiency when grown in 3D suspension culture conditions, confirming that β-catenin overexpression functionally enhances *in vitro* stem cell properties in TNBC cell lines (**Figure 3H**).

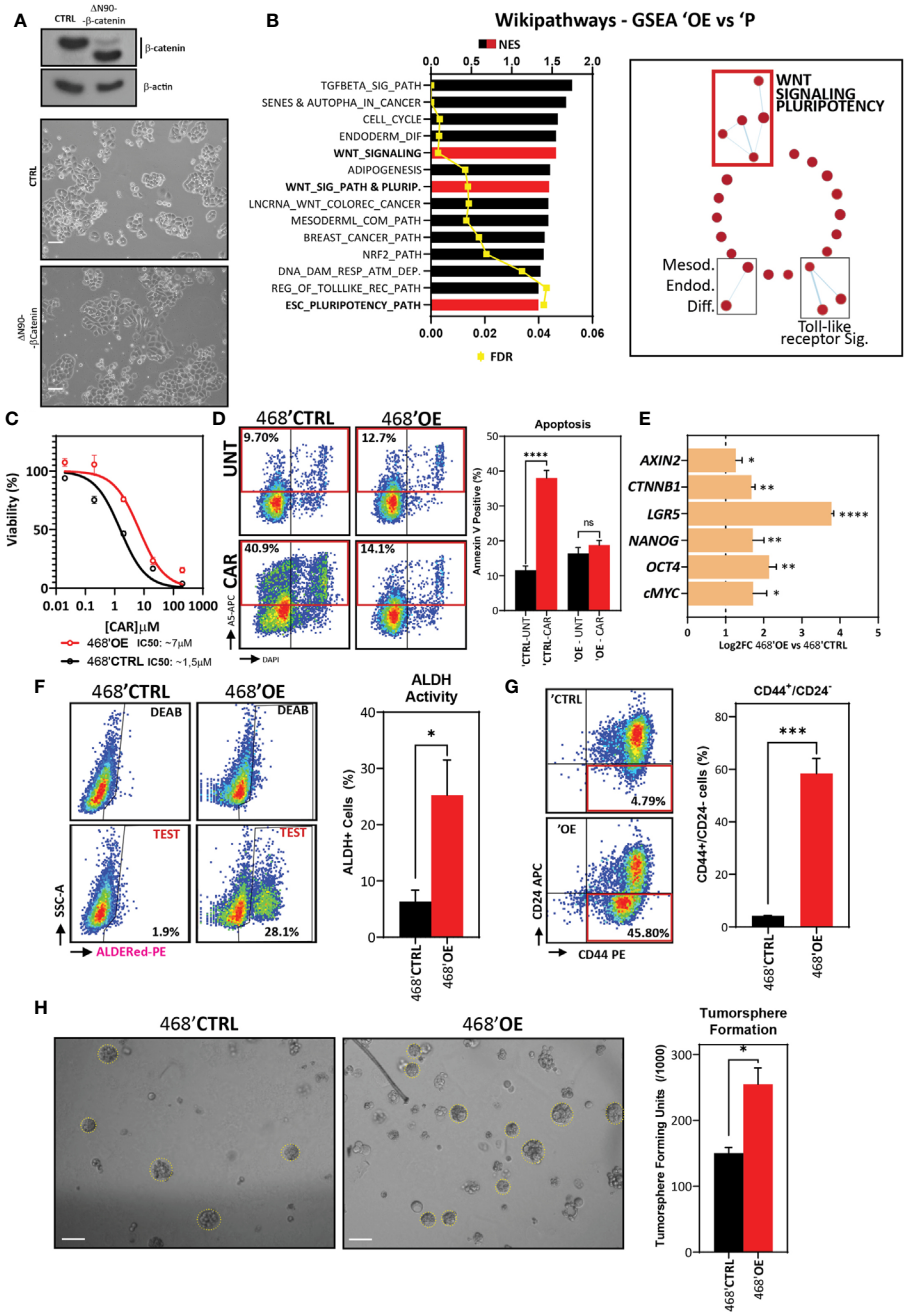


**FIGURE 3** | β-catenin overexpression in 468'P induces carboplatin-resistance, pluripotency-related gene expression, and cancer stem cell features. **(A)** Western blot (top) of total β-catenin in MDA-MB-468 cells transduced with an empty vector or truncated, constitutively active β-catenin isoform ΔN90 and phase-contrast microscopy (down). **(B)** Enriched gene sets from Wikipathways database by one-tailed GSEA of ranked DEGs between 468'OE and 468'P sorted by normalized enrichment score (left) and enrichment map illustrating pathways most significantly different between 468'OE and 468'P (right). **(C)** Non-linear fit model of [CAR] *vs*. normalized response for IC50 determination. (468'OE: n=6, $R^2$ = 0.92; 468'CTRL: n=6, $R^2$ = 0.95). **(D)** Representative flow cytometry scatterplots of annexin V staining (left) of 468'CTRL and 468'OE cells treated with carboplatin 2 μM for 72h and statistical analysis of the mean frequency of annexin V positive cells using one-way ANOVA corrected for multiple comparisons using the Holm-Sidak method (right, n=3). **(E)** mRNA level fold change (Log2) of CTNNB1 (β-catenin), Wnt target AXIN2, and stem cell markers in 468'OE cells *vs*. 468'CTRL (n=4). Multiple t-tests with Holms-Sidak correction for multiple comparisons. **(F)** Representative scatterplots of flow cytometric analysis of aldehyde dehydrogenase activity (left) and statistical analysis of the mean percentage of ALDH+ cells in 468'OE (n=5) and 468'CTRL (n=5) using Welch's t-test (right). **(G)** Representative scatterplots of flow cytometric analysis of CD44-PE and CD24-APC immunolabeling (left) and corresponding statistical analysis of the mean percentage of $CD44^+/CD24^-$ cells using Welch's t-test (right; n=3). **(H)** Representative brightfield images of tumorspheres generated from 468'CTRL and 468'OE cells (left, scale bar: 50 μm) and statistical analysis of mean tumorsphere forming units (number of spheres/number of seeded single cells) using Welch's t-test (right; n=3). (Barplots represent mean + SEM. *$p < 0.05$; **$p < 0.01$; ***$p < 0.001$; ****$p < 0.0001$; ns, non significant).

The overexpression of ΔN90-β-catenin on MDA-MB-231 cells yielded the same effect with a roughly 10-fold increase in the IC50 of carboplatin, as well as increased ALDH activity and tumorsphere formation capacity (**Supplementary Figures 3B–F**).

## Wnt Inhibition Disrupts Carboplatin Resistance in 468'R Cells and Downregulates Cancer Stem Cell and Pluripotency Marker Expression

Wnt signaling is deregulated in 468'R cells, and β-catenin overexpression on parental cells confirmed its role in mediating the carboplatin-resistant stem-like phenotype. Given these observations, we hypothesized that inhibition of Wnt signaling could restore sensitivity in 468'R cells. To that end, we used LGK974 (LGK), a small molecule inhibitor of the endoplasmic reticulum palmitoyltransferase porcupine (PORCN). This enzyme is responsible for processing Wnt ligands for secretion, mediating a crucial step of Wnt-dependent signaling (54).

Combinatorial treatment of 468'R cells with 2 μM of CAR and increasing concentrations of LGK resulted in carboplatin-sensitivity in a dose-dependent manner, starting at 200 nM of the Wnt inhibitor (**Figure 4A**). Interestingly, LGK treatment alone (200 nM) was insufficient to induce apoptosis in both 468'R and 468'P. However, when added to carboplatin, LGK induced strong annexin V positivity in 468'R cells, indicating rescue of carboplatin sensitivity in the resistant cell line (**Figure 4B**).

Gene expression analysis by qPCR of LGK-treated 468'R cells confirmed downregulation of Wnt signaling by reduced expression of Wnt target *AXIN2*. More importantly, LGK severely reduced transcript levels of pluripotency markers *OCT4*, *NANOG*, and *cMYC*, both in the presence or absence of carboplatin (**Figure 4C**). These results corroborate the hypothesis that Wnt primes TNBC cells for carboplatin resistance by maintaining a stem-cell-like phenotype.

## Inducible β-Catenin Knockdown Resensitizes 468'R Cells to Carboplatin and Disrupts Expression of Stem Cell Markers and Tumorsphere Formation Capacity

Next, we investigated whether cancer stem cell markers and function could be manipulated by directly disrupting β-catenin making use of doxycycline (DOX) inducible short-hairpin RNA targeting *CTNNB1* (β-catenin) transcripts in 468'R cells (iCTNNB1-KD) (55).

Gene expression analysis by RT-qPCR confirmed a reduction of roughly 90% in *CTNNB1* transcripts upon DOX treatment of iCTNNB1-KD cells whereas, as expected, cells expressing inducible scrambled shRNA (iSCRMBL) maintained basal β-catenin transcript levels (**Figure 5A**). Notably, DOX-induced β-catenin knockdown led to a robust reduction of pluripotency and cancer stem cell markers, confirming the role of β-catenin in maintaining their high expression (**Figure 5A**).

Next, we investigated the effect of β-catenin knockdown on *in vitro* carboplatin response by determining the IC50 for 468'R iCTNNB1-KD cells in the presence or absence of DOX. Suppressing the expression of β-catenin had a remarkable effect on carboplatin resistance. DOX-treated iCTNNB1-KD cells displayed a substantial reduction in measured IC50 compared to non-induced cells (IC50 -DOX: ~11 μM *vs*. IC50 +DOX: ~1 μM) (**Figure 5B**). Importantly, 468'R iSCRMBL cells displayed no significant changes in IC50 (-DOX: ~13 μM *vs*. +DOX: ~11 μM) (**Supplementary Figure 4**). Additionally, when exposed to the IC50 of 468'P cells, 468'R iCTNNB1-KD cells strongly induced apoptosis in the presence of DOX, while no difference was observed in iSCRMBL cells (**Figure 5C**).

Finally, we assessed the effect of β-catenin suppression on tumorsphere formation as a functional readout for stem cell activity. In line with the downregulation of stem cell marker expression in the presence of DOX, iCTNNB1-KD cells displayed a significantly lower tumorsphere forming frequency when β-catenin shRNA was induced. On the other hand, differences upon the induction of SCRMBL shRNA were negligible (**Figure 5D**).

## Wnt Inhibition Disrupts *In Vivo* Carboplatin Resistance in a Carboplatin-Resistant TNBC Patient-Derived Xenograft

Patient-derived xenografts are essential *in vivo models* of human neoplasms. Moreover, PDX models retain with excellent fidelity histological and molecular features of originating tumors, representing essential tools for assessing drug resistance and response (56–58).

To study whether, like in 468'R cells, *in vivo* PORCN inhibition with LGK re-establishes carboplatin sensitivity, we used an isogenic carboplatin-resistant TNBC PDX (C4O) obtained from a previously chemotherapy-sensitive model (BRC016) (35). In brief, ten mice bearing BRC016 tumors were treated with 50 mg/kg of carboplatin once weekly for three weeks. Nine out of ten BRC016-bearing mice achieved a complete response to treatment with no tumors detectable. However, one tumor displayed a late response and became resistant to further treatment despite undergoing a substantial volume reduction. The non-responder xenograft eventually regrew from the post-treatment residual tumor (**Figure 6A**). Material from the regrown tumor was collected to establish an isogenic model of carboplatin-resistant TNBC (C4O) and gene expression analysis revealed changes in Wnt signaling target *AXIN2* and pluripotency and stem markers *NANOG*, *OCT4*, *SOX2*, and *LGR5* (**Figure 6B**).

*In vivo* carboplatin resistance was maintained in subsequent generations of transplanted C4O PDX models. We detected no significant differences in mean final tumor volumes in animals treated with vehicle or 50 mg/kg carboplatin, administered once weekly intraperitoneally, for three weeks (**Supplementary Figure 5A**). However, combinatorial treatment with daily dosing of PORCN inhibitor LGK drastically reduced C4O tumor growth (**Figure 6C** and **Supplementary Figure 5A**). LGK was well tolerated both as mono-therapy and in combination with carboplatin, and no significant changes in

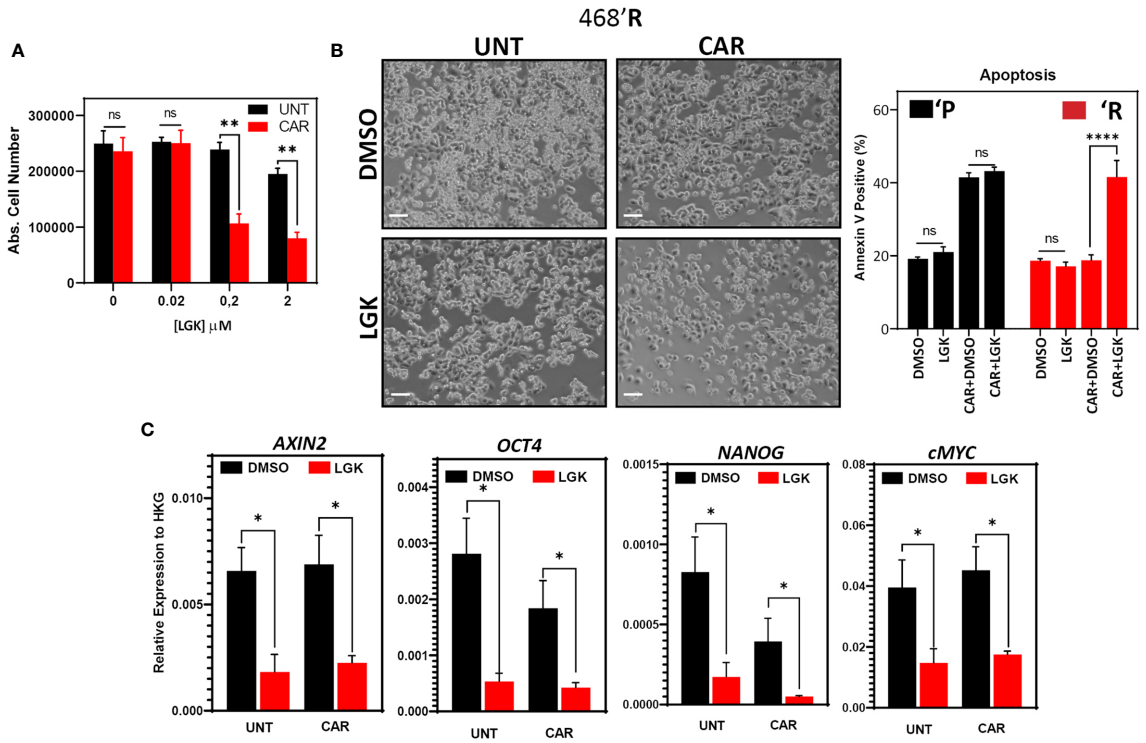


**FIGURE 4** | *Wnt inhibitor LGK974 disrupts carboplatin resistance and pluripotency gene expression.* **(A)** Absolute cell number of 468'R cells treated for 72 hours with increasing concentrations of LGK974 in the presence or absence of 2 µM carboplatin. Multiple t-tests (n=3). **(B)** Phase-contrast microscopy of 468'R cells treated for 72 hours with 200 nM LGK974 or DMSO in the presence or absence of 2 µM carboplatin (left). Mean frequency of annexin V positive cells in 468'P and 468'R cells treated with or without 200 nM LGK974 in presence or absence of 2 µM carboplatin showing the resensitization of 468'R cells to carboplatin when co-treated with Wnt inhibitor (right, n=3). One-way Anova with correction for multiple comparisons using the Holm-Sidak method. **(C)** Relative mRNA expression of Wnt target and stem cell markers upon 72-hour treatment with DMSO or 200 nM LGK974 with or without 2 µM carboplatin in 468'R cells (n=3). Multiple t-tests: Unt *vs*. Unt+LGK & CAR *vs*. CAR+LGK. (Barplots represent mean + SEM. *$p < 0.05$; **$p < 0.01$; ****$p < 0.0001$; ns, non significant).

mouse body weight were observed during treatment (**Supplementary Figure 5B**). Interestingly, LGK or CAR alone could not reduce C4O growth (**Figure 6C**), and no significant differences in mean final tumor volumes between VEH, CAR, and LGK-treated animals were observed. Importantly, we did not find differences in Ki67 positivity between any treatment arms, indicating that reduced tumor growth in CAR+LGK treated animals was not due to differences in proliferation (**Supplementary Figure 5C**).

Gene expression analysis by RT-PCR revealed that similar to what we observed upon treating 468'R cells with LGK, inhibition of PORCN in C4O led to the depletion of pluripotency marker expression both in the presence or absence of carboplatin (**Figure 6D**).

Finally, given the absence of alterations in the expression of Ki67, we sought out to understand whether the drastic reduction in tumor growth in animals treated with the combination of CAR and LGK could be due to increased apoptotic cell death. For this, we performed fluorescent terminal deoxynucleotidyl transferase dUTP nick end labeling (TUNEL) to detect DNA fragmentation as a readout of apoptosis. We combined TUNEL staining with human pan-cytokeratin immunolabeling to enable quantification of apoptotic signal specifically in cancer cells. No differences in TUNEL positivity were measured in VEH, LGK, and CAR-treated animals. However, animals treated with the combination of CAR and LGK displayed a significant increase in apoptotic TUNEL signal (**Figure 6E**).

## Wnt Signaling Is Deregulated in Patients With Platinum-Resistant TNBCs and High-Grade Serous Ovarian Cancer

To understand whether alterations in Wnt signaling are prevalent in platinum-resistant human TNBCs, we analyzed a public RNA microarray dataset (GSE103668) comprised of 21 pre-treatment samples from TNBC patients treated with cisplatin and bevacizumab (59). Due to the scarcity of additional platinum-treated TNBC transcriptomic data available in public repositories, we decided to include a supplementary dataset from high-grade serous ovarian cancer (HGSOC) (E-MTAB-7083) (**Figure 7A**). The reason for this choice lies in the extensive use of platinum-based chemotherapy in this type of cancer and the striking overlap in clinical and molecular features between HGSOC and TNBC (61).

The available clinical metadata was analyzed in both datasets to classify patients based on response to treatment, and differential gene expression was calculated between responders

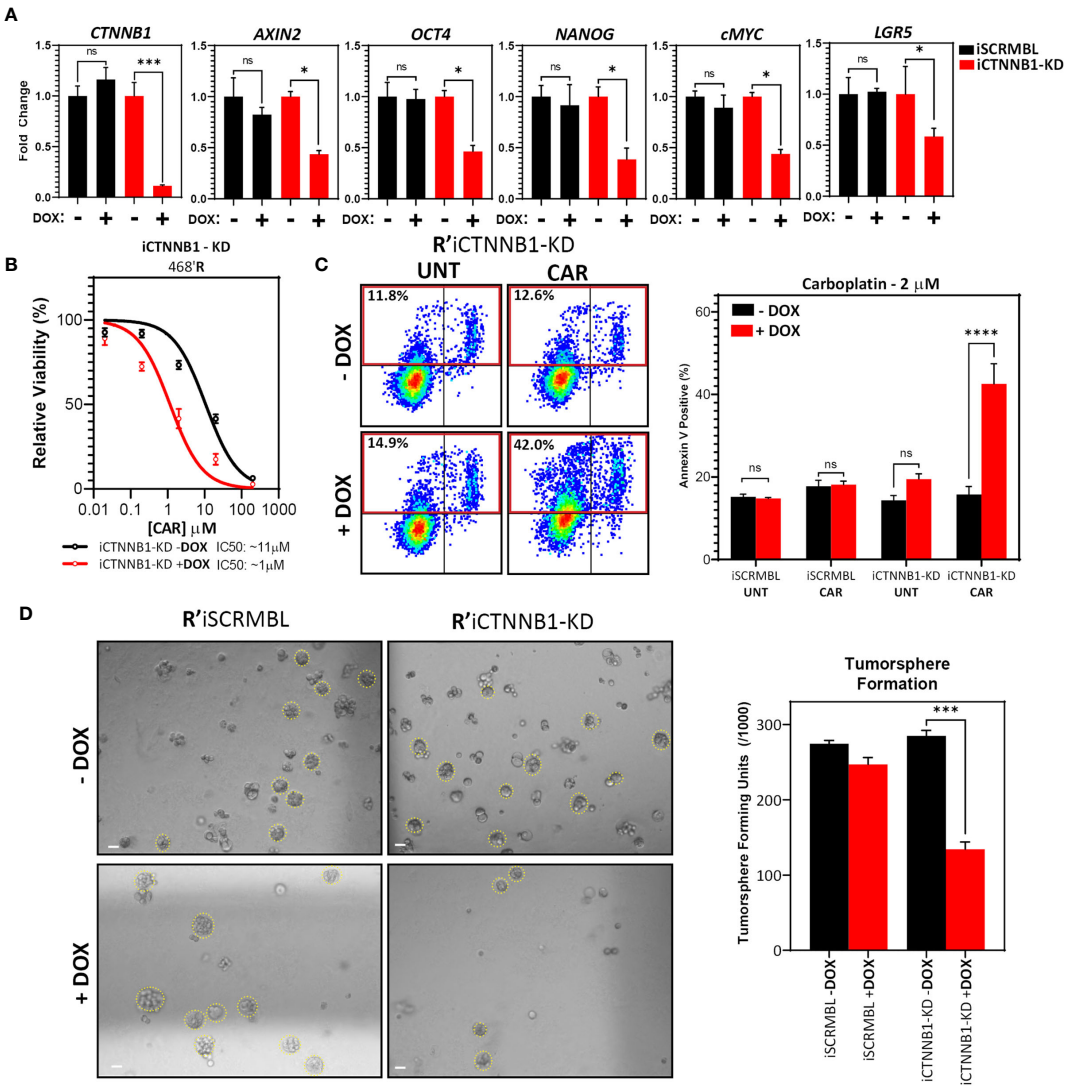


**FIGURE 5** | *Inducible β-catenin shRNA disrupts carboplatin-resistance and stem cell function in 468'R cells*. **(A)** Relative mRNA expression level of *CTNNB1* (β-catenin) and Wnt target and pluripotency markers in 468'R cells transduced with inducible CTNNB1-targeting or SCRMBL shRNAs, in the presence or absence of doxycycline (n=3). Welch's t-test (Dox *vs*. no Dox). **(B)** Non-linear fit model of [CAR] *vs* normalized response for IC50 determination in iCTNNB1-KD cells in presence or absence of doxycyclin. (n=3, $R^2$ + DOX: 0.93, $R^2$ - DOX: 0.95). **(C)** Representative scatterplots of flow cytometric analysis of apoptosis by annexin V staining of 468'R iCTNNB1-KD and 468'R iSCRBML cells treated with or without 2 μM carboplatin for 72h in presence or absence of doxycycline (left) and corresponding statistical analysis of the mean frequency of annexin V positive cells (right, n=6). One-way Anova with correction for multiple comparisons using the Holm-Sidak method. **(D)** Representative brightfield images of tumorspheres generated from 468'R iSCRMBL and 468'R iCTNNB1-KD cells (left, scale bar: 50 μm) and statistical analysis of mean tumorsphere forming units (number of spheres/number of seeded single cells) (right; n=3). Welch's t-test (Dox *vs*. no Dox). (Barplots represent mean + SEM. *$p < 0.05$; **$p < 0.001$; ***$p < 0.0001$; ns, non significant).

and non-responders. Interestingly, GSEA analysis on ranked differentially expressed genes using the KEGG database retrieved Wnt signaling as one of the top enriched terms with False Discovery Rate (FDR) <10% in TNBC and HGSOC patients with no response to platinum therapy (**Figure 7B**). Other enriched KEGG terms comprised biological processes such as focal adhesion, extracellular matrix interaction, and other signaling pathways such as TGFβ and Hedgehog. Enrichment maps of GSEA hits for both datasets contained distinctive Wnt-related clusters involving gene sets with overlapping enriched genes such as "Melanogenesis" and "Basal Cell Carcinoma" for TNBC patients and HGSOC with the addition of "Hedgehog Signaling Pathway" in the latter (**Figure 7C**). To obtain a broader perspective of the function of differentially expressed genes, we performed functional enrichment analysis for both datasets using gProfiler to retrieve enriched gene ontology, Reactome, and Wikipathway gene sets to build enrichment maps. We obtained a distinctive cluster of Wnt-related terms in both datasets, including regulating both canonical and non-canonical Wnt signaling in TNBC and

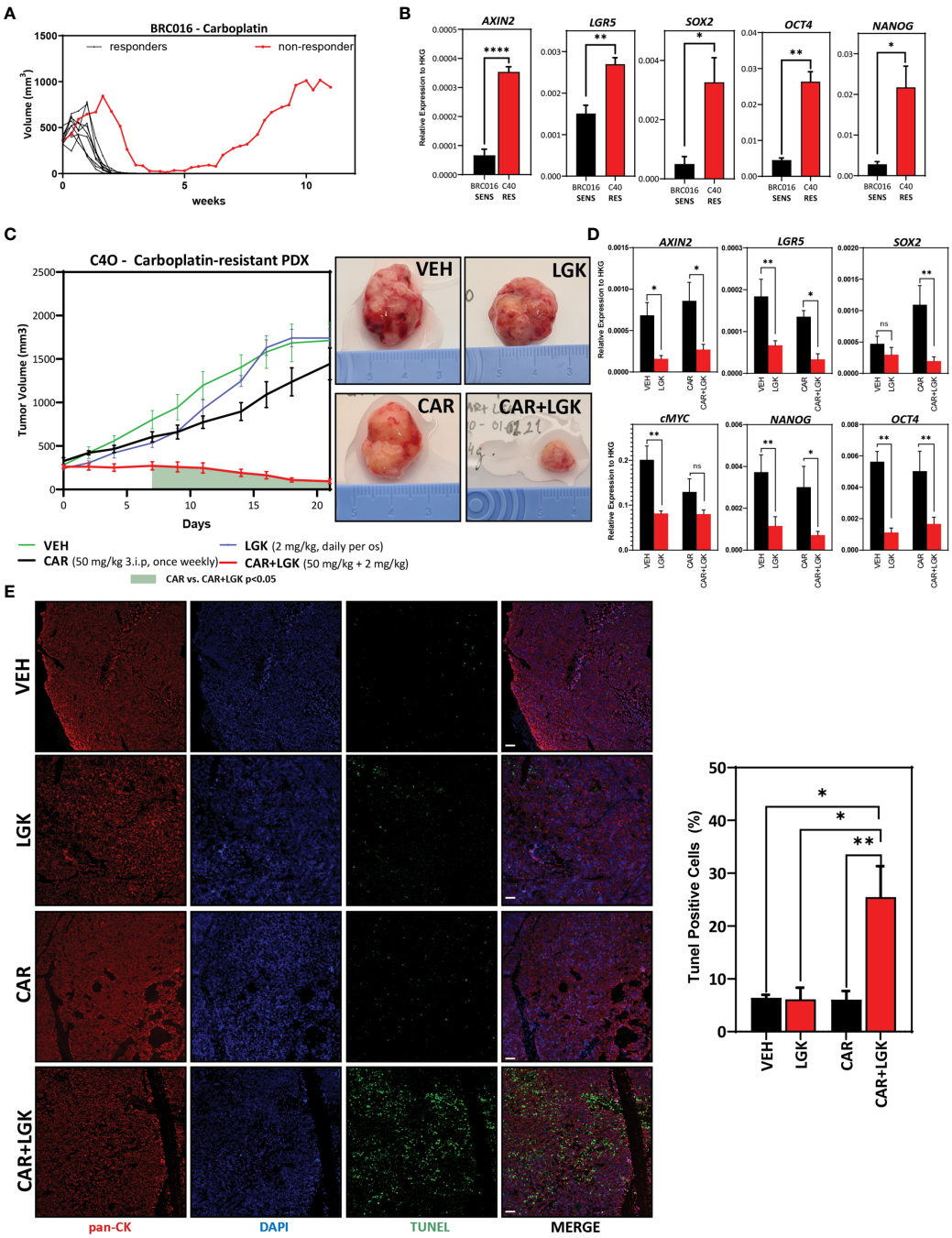


**FIGURE 6** | *WNT inhibition disrupts in vivo carboplatin-resistance in a carboplatin-resistant TNBC Patient-Derived Xenograft*. **(A)** Tumor growth curves of carboplatin-sensitive BRC016 TNBC PDX model. Nine out of 10 mice show a complete response to treatment. One animal (red line) had a very delayed response and still had residual tumor mass after three weeks of treatment. The residual xenograft resumed growth after carboplatin treatment was stopped. This tumor was collected to establish a carboplatin-resistant model (C4O). **(B)** Comparative gene expression analysis by qRT-PCR of Wnt target AXIN2 and stem cell markers in BRC016 carboplatin-sensitive PDX and the C4O carboplatin-resistant isogenic PDX (n=4). Welch's t-test. **(C)** Tumor growth curves of C4O carboplatin-resistant PDX treated with VEH, LGK974, CAR, or CAR+LGK showing reduced tumor growth in the combinatorial treatment arm (VEH, CAR, CAR+LGK n=6 and LGK n=5) (left). Two-way ANOVA with Tukey correction. The green-shadowed area under the curve represents highlights the time points in which the difference between CAR and CAR+LGK is statistically significant. Representative photographs of tumors in each treatment arm at day 21 of treatment (right). **(D)** mRNA level fold change (Log2) *vs*. VEH treatment (no carboplatin and no Wnt inhibitor) in tumors dissected at treatment endpoint (21 days) (n=3). Multiple t-tests (VEH *vs*. LGK and CAR *vs*. CAR+LGK). **(E)** Representative confocal microscopy images (left) of TUNEL staining in green and human pan-cytokeratin immunolabeling in red and respective quantification and statistical analysis of TUNEL positive cells (VEH n=4, LGK n=4, CAR & CAR+LGK n=6). One-way ANOVA with correction for multiple comparisons using the Holm-Sidak method. (Barplots represent mean + SEM. *$p < 0.05$; **$p < 0.01$; ****$p < 0.0001$; ns, non significant).

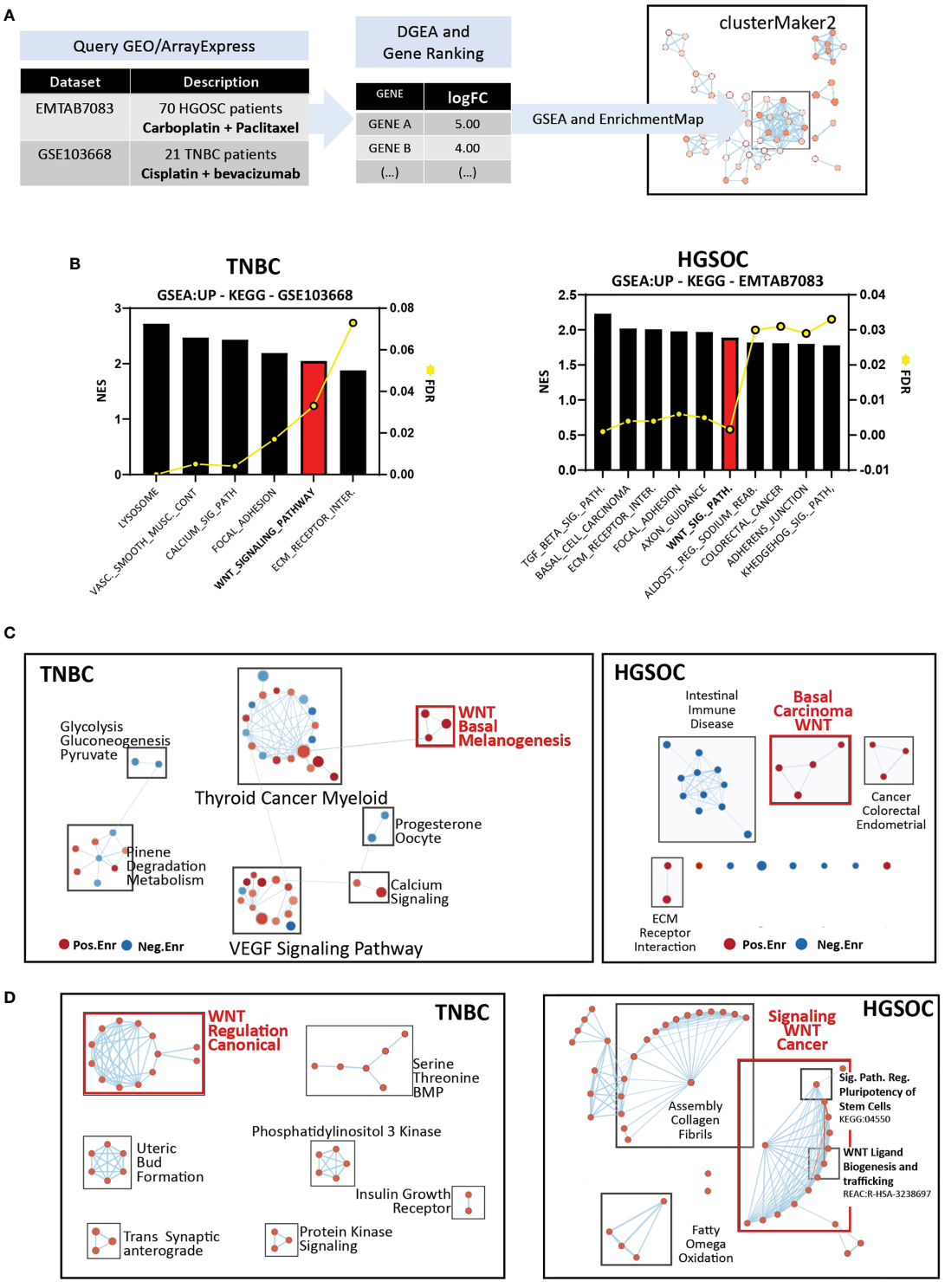


**FIGURE 7** | Wnt signaling is deregulated in patients with platinum-resistant TNBCs, high-grade serous ovarian cancer, and isogenic cisplatin-resistant ovarian cancer cell lines. **(A)** Summary of datasets and analysis methodology used. Functional enrichment and mapping as previously reported (40, 41, 60). **(B)** Enriched KEGG gene sets in patients with platinum-resistant TNBC (left) and HGSOC (right). **(C)** Enrichment maps for visualization of enriched KEGG gene sets in patients with platinum-resistant TNBC (left) and HGSOC (right). **(D)** Enrichment maps for visualization of gProfiler functional enrichment analysis of ranked, upregulated DEGs in patients with platinum-resistant TNBC (left) and HGSOC (right).

regulating pluripotency and Wnt ligand biogenesis and secretion in HGSOC (**Figure 7D**).

Altogether, these results highlight Wnt signaling's importance in mediating platinum resistance in human TNBC and suggest transversal resistance mechanisms across TNBC and HGSOC.

## DISCUSSION

Primary and acquired resistance to chemotherapy poses a critical hurdle in the treatment of cancer. This is particularly important in TNBC due to the relatively limited therapeutic toolbox available and the daunting clinical characteristics of this disease. In the continued absence of targeted molecular therapies, we must strive to improve response to current therapeutic options given the high probability of shorter survival when pCR is not achieved. The use of platinum compounds in combination with other agents or as a standalone treatment in TNBC is still under intense investigation but already shows the potential to improve pCR rates in this breast cancer subtype. However, how TNBCs specifically develop resistance to platinum-based treatment is still a poorly understood process.

In this study, we used an isogenic carboplatin-resistant TNBC cell line and used next-generation mRNA sequencing to identify transcriptomic differences between sensitive and resistant cells. Functional enrichment analysis indicated, among others, the existence of profound differences in transcription of Wnt signaling and pluripotency-related genes. Active β-catenin protein levels, together with pluripotency transcription factor and cancer stem cell marker expression, confirmed enrichment of Wnt signaling and stem cell features in resistant cells. Importantly, resistant cells displayed significantly higher *in vitro* tumorsphere formation efficiency, a strong indicator of the functional acquisition of cancer stem cell features which could underly chemotherapy resistance. However, further *in vivo* characterization of this model of carboplatin resistance should be performed to validate enrichment tumor-initiating capacity thoroughly.

Nonetheless, we deemed the observed *in vitro* enrichment in Wnt signaling, and stem cell features significant since there is a link between this pathway and cancer stem cell biology and tumorigenesis. In addition, several studies have demonstrated the involvement of this pathway in mediating resistance to chemotherapy and radiation in different types of cancer, including breast (30, 34, 62–64). Wnt signaling is also known to specifically mediate platinum resistance in endometrial cancer (65), ovarian (66), and oral squamous cell carcinoma (67). However, little is known regarding the role of Wnt signaling in mediating resistance to platinum in TNBC. Interestingly, Wnt is often deregulated in breast cancers, particularly TNBCs, despite the negligible frequency of mutations in Wnt pathway components. Significantly, Wnt activation is associated with poor clinical outcomes in TNBC (68).

Based on the transcriptomic data herein generated, we hypothesized that stem-cell gene expression and carboplatin resistance could be induced on parental MDA-MB-468 cells by manipulating Wnt signaling. For this, we first used CHIR, a small molecule inhibitor of GSK3β, thereby activating Wnt. Our results showed a significant increase in pluripotency marker expression and reduced apoptosis upon concomitant treatment with Wnt agonist and carboplatin. Past studies regarding the role of this multi-substrate kinase in treatment resistance are rather intriguing. While our results confirm other studies that report the enrichment of stem cell features upon GSK3β inhibition (69, 70), they seem to contradict reports of GSK3 inhibition leading to reduction of tumor growth and apoptosis (71–73). However, it is essential to note that GSK3 regulates several pathways and a myriad of cellular functions. In addition, its' role in cancer is not only complex but also controversial since it has both tumor-suppressing and tumor-promoting functions (74). One example of its' tumor-suppressor capabilities is through its' inhibitory role on the Wnt signaling pathway, with the expression of kinase-inactive mutants leading to oncogenic conversion of epidermal cells (75). On the other hand, GSK3β is overexpressed in certain cancers such as colon, liver, and pancreas. In the latter, depletion of GSK3β was shown to drastically reduce tumor growth, highlighting the pro-tumoral effects of GSK3β (76). Given this, it is highly likely that the different outcomes of GSK3β inhibition may be specific to different tissues and cancer types.

Nonetheless, by overexpressing β-catenin in parental cells, we could replicate the phenotype of the isogenic carboplatin-resistant cells and GSK3 inhibition extensively. Specifically, β-catenin overexpression induced a significant increase in expression of pluripotency markers and induced carboplatin resistance, highlighting the role of Wnt pathway activation on drug resistance in TNBC.

To further validate the role of Wnt signaling and specifically β-catenin in mediating carboplatin resistance in TNBC, we made use of another TNBC cell line: MDA-MB-231. Several studies report the enrichment of cancer stem cell features such as high expression of the CD44+/CD24- immunophenotype in these cells (25, 77). Both pharmacological activation of Wnt and β-catenin overexpression successfully induced pluripotency marker expression and enhanced resistance to carboplatin. Additionally, β-catenin overexpression significantly enhanced ALDH activity and tumorsphere formation. These are interesting observations given the pre-existing enrichment in CD44+/CD24- in this cell line.

Nonetheless, another study has established a clear correlation between enhanced Wnt activity and enriched cancer stem cell potential in MDA-MB-231 cells (78). Importantly, in standard culture conditions, these cells display very low Wnt transcriptional activity but respond robustly to exogenous Wnt activation. This suggests some level of phenotypic plasticity that can be further skewed towards a more stem-like state by high levels of Wnt activation.

Inhibition of Wnt ligand secretion using LGK in isogenic carboplatin-resistant cells disrupted stem cell markers' expression and reversed resistance. Interestingly, inhibition of Wnt ligand secretion alone was insufficient to induce apoptosis in either carboplatin sensitive or resistant cells, despite severely

downregulating stem cell marker expression. This indicates that Wnt secretory signals are not necessarily essential for the survival of either sensitive or resistant cells, but rather that these signals prime the latter for survival upon challenge by carboplatin. Secreted Wnt-ligands originating from cells of the tumor microenvironment have been shown to significantly contribute to resistance by mediating immune evasion, cancer progression, and cancer stem cell maintenance (79). We here provide *in vitro* evidence for cancer cells themselves being an additional source of resistant-mediating Wnt-ligands in a cell-autonomous manner. Understanding which cancer cell-derived ligands are being secreted and their influence over other cell types associated with the tumor microenvironment would prove beneficial for developing novel therapeutic approaches and discovering new biomarkers for drug response.

LGK prevents the secretion of all Wnt ligands by inhibiting the palmitoyl acyltransferase PORCN. In vertebrates, the Wnt family of lipid-modified secreted signaling proteins comprises 19 members, conferring a great deal of complexity to this pathway. Wnt signaling includes a canonical or Wnt/β-catenin dependent pathway and the non-canonical or β-catenin-independent pathway (80). For that reason, it was essential to determine whether LGK-induced carboplatin sensitivity was mediated directly by β-catenin. Silencing β-catenin downregulated stem cell marker expression and dramatically reversed resistance to carboplatin, phenocopying LGK effects, and directly implicating canonical Wnt signaling in the maintenance of carboplatin resistance.

Inhibition of Wnt ligand secretion, namely through the inhibition of PORCN, has been under scrutiny during the last decade as a potential therapeutic approach for different types of cancer. LGK specifically has shown excellent preclinical efficacy in Wnt-addicted models (81) and is under examination in phase I clinical trial for several Wnt-dependent solid malignancies, including TNBC (NCT01351103) (82). We evaluated whether this molecule could resensitize an *in vivo* model of carboplatin-resistant TNBC. Previous studies reported that LGK alone significantly reduces the growth of a murine mouse mammary tumor-Wnt3 model (81). To our surprise, daily dosing of LGK alone had no impact on tumor growth. This is analogous to what we observed when treating carboplatin-resistant cells with LGK alone. Importantly, we observed a significant reduction of tumor growth in animals treated with a combination of daily LGK and weekly carboplatin.

The resistance we observe in our models is likely multifactorial, and Wnt is probably one of several deregulated processes which ultimately contribute to it. Nonetheless, it is crucial to consider that Wnt signaling has an overarching set of functions that lead to chemotherapy resistance. Fischer and colleagues demonstrated that in colorectal cancer PDX models, monoclonal antibodies targeting RSPO3 (a potent Wnt-signaling enhancer that binds LGR5 to potentiate Wnt activation by reducing Wnt-receptor turnover) had a strong synergistic effect against tumor growth when administered in combination with paclitaxel (83). However, when anti-RSPO3 antibodies were administered alone, they failed to reduce tumor progression. Interestingly, anti-RSPO3 administration alone significantly decreased the frequency of cancer stem cells, despite the absence of deleterious effects on tumor viability. The combinatorial treatment further decreased cancer stem cell frequency, and a surge in differentiated paclitaxel-sensitive cells was observed. An earlier study reports a very similar effect in breast cancer xenografts treated with antibodies targeting Frizzled (Wnt-ligand receptors) and taxanes, where antibody treatment alone had a limited effect on tumor growth and combined with taxanes resulted in a potent synergism (84). We report a similar therapeutic dynamic with LGK in our resistant models of TNBC, wherein LGK or β-catenin knockdown disturb stem cell functions without affecting *in vitro* tumorsphere formation and proliferation and *in vivo* tumor growth.

In addition to regulating and maintaining cancer stem cells, Wnt is known to mediate chemotherapy and radiotherapy resistance in non-stem cancer cells. One example is the enhancement of DNA damage repair in ovarian cancers (85, 86). Moreover, Wnt directly regulates the transcription of several genes encoding proteins associated with resistance to chemotherapy in diverse cancer types, such as *MDR1* (Multi-drug resistance protein 1, also known as ABCB1), Survivin, and MMP7 (87). However, lower expression levels of these proteins could likely have no deleterious effects in cancer cells in the absence of cytotoxic aggression by chemotherapeutic agents.

We thus hypothesize that the synergistic effect of LGK and carboplatin is likely mediated by the combination of a shift in population dynamics from a cancer stem cell-like state to a generally more differentiated and drug-sensitive phenotype. This effect compounds with the repression of other resistance-inducing features that are non-exclusive of stem cells, thereby enhancing the response to treatment upon exposure to exogenous stressors.

Finally, we were able to identify similarities in transcriptional profiles of patients with platinum-refractory ovarian and triple-negative breast neoplasms. Wnt signaling deregulation is a common denominator in both datasets we analyzed. Given the overlapping clinical and molecular features of both cancer types, it would be interesting to investigate whether transversal resistance mechanisms exist for other therapies and other cancers. There is growing evidence that different cancers harbor rare stem cell populations, significantly contributing to therapy resistance and relapse. In addition, in many cancer types, Wnt/β-catenin is enriched in cancer stem cells.

Interestingly, Wnt activation is also coupled with a poor prognosis in several cancers, possibly indicating the existence of a common role for Wnt signaling in cancer stem cell regulation across different neoplastic diseases and suggesting that a common therapeutic approach focusing on cancer stem cell eradication could be effective in a wide variety of cancers. This warrants the necessity for developing and characterizing isogenic *in vitro* and *in vivo* models of resistance and the preclinical evaluation of Wnt-targeting molecules and their effect on cancer stem cell-mediated treatment resistance in other cancer types.

Altogether, this study demonstrates that response to platinum can be improved, and stable *in vitro* and *in vivo* resistance can be reversed by a combinatorial approach to TNBC treatment which leverages the inhibition of Wnt signaling to disrupt resistance-inducing cancer stem cell functions.

## DATA AVAILABILITY STATEMENT

The datasets presented in this study can be found in online repositories. The names of the repository/repositories and accession number(s) can be found below: https://www.ebi.ac.uk/arrayexpress/E-MTAB-10337.

## ETHICS STATEMENT

Tumor tissue for PDX implantation was acquired from a patient who provided written informed consent, and the procedure was approved by the Commission of Medical Ethics of the University Hospitals Leuven (approval numbers S54185 and ML8713). The PDX models herein used are now banked at the Trace Patient Derived Tumor Xenograft Platform of UZ Leuven/KU Leuven. All animal experiments were performed at the Trace PDX platform and were approved by the Ethics Committee Research UZ/KU Leuven (approval number P038/2015). Experiments with cell lines were approved by the Ethische Comissie Onderzoek UZ/KU Leuven (S65166).

## AUTHOR CONTRIBUTIONS

WO and FL conceived and designed the study. SM generated *in-vitro* models of carboplatin resistance and the carboplatin-resistant C4O PDX under the supervision of DA and FA. YL generated the transgenic cell lines used in this study. WO and SM conducted all *in vivo* experimental work. EC conducted immunohistochemistry experiments. BV performed RNA-sequencing differential expression analysis, and WO performed downstream functional enrichment and visualizations. WO and partially YL carried out all flow-cytometry experiments. PA performed Western blots. WO carried out the remainder of the experimental work. Data analysis and figure preparation were performed by WO and reviewed by SM, DA, and FL. The manuscript was written by WO and reviewed, and approved by all authors. FL secured funding and supervised and guided experimental work and manuscript preparation. BV, KK, J-JV, MB and FA made comments on formatting, editing, and data analysis. All authors contributed to the article and approved the submitted version. WO and SM are co-first authors. DA and FL are co-last authors.

## FUNDING

WO and BV are funded by the Research Foundation-Flanders with Ph.D. fellowships 1155619N and 11E7920N, respectively. EC holds a fellowship from Stichting Tegen Kanker – the Belgian Foundation against Cancer (FAF-F/2016/822, fellowship number ZKD2498-00-W02). The authors would like to extend their gratitude to the Research Foundation – Flanders (FWO) for the G091521N grant (FL and DA) and to Jo Van Biesbroeck, the breast cancer research fund Nadine de Beauffort and the KU Leuven Research Fund (C24/17/073) for funding the development of the models used in this research study (FA). FA is a senior researcher for the Research Foundation-Flanders (FWO). Trace staff is supported by the Stichting Tegen Kanker grant 2016-054.

## ACKNOWLEDGMENTS

We want to show our gratitude to Anchel de Jaime Soguero for his critical review of the manuscript. We also sincerely thank the Trace Leuven PDX platform for its help in setting up mouse experiments. Trace is part of the EuroPDX consortium.

## SUPPLEMENTARY MATERIAL

The Supplementary Material for this article can be found online at: https://www.frontiersin.org/articles/10.3389/fonc.2021.705384/full#supplementary-material

**Supplementary Table 1 |** Differentially expressed genes and GSEA of 468'R *vs*. 468'P.

**Supplementary Table 2 |** Differentially expressed genes and GSEA of 468'OE *vs*. 468'P.

**Supplementary Table 3 |** Primer List.

**Supplementary Figure 1 | (A)** Representative histogram of flow cytometry Ki67 frequency in 468'P and 468'R cells (left) and statistical analysis (n=3). **(B)** Expression heatmap of Wnt-related genes from the WNT Pathway Pluripotency cluster from **Figure 1F**. **(C)** Flow cytometry analysis of TOPGFP-Wnt reporter activity in 468'P and 468'R cells (n=3). (Barplots represent mean + SEM. **p <0.05, **p<0.01, ***p<0.001, ****p<0.0001*, ns= non significant).

**Supplementary Figure 2 | (A)** Phase-contrast microscopy (left, scale bar: 100 μm) of MDA-MB-231 cells treated for 72 hours with 35 μM Carboplatin in the presence or absence of 4 μM CHIR and statistical analysis of mean absolute cell numbers (n=4). One-way ANOVA with correction for multiple comparisons using the Holm-Sidak method. **(B)** mRNA level fold change (Log2) Wnt target *AXIN2*, and stem cell markers in MDA-MB-231 cells treated with 4 μM CHIR vs. DMSO (n=1, average of technical replicates). (Barplots represent mean + SEM. **p <0.05, **p<0.01, ***p<0.001, ****p<0.0001*, ns= non significant).

**Supplementary Figure 3 | (A)** GSEA of hESCs (26) (left), Cancer Progenitor (46) (center), and pluripotency transcription target gene sets (26) (right) in 468'OE *vs* 468'P cells. **(B)** Phase-contrast microscopy (scale bar: 100 μm) of control MDA-MB-23 and 231'OE (Δn90 β-catenin overexpression). **(C)** Western blot of total β-catenin in MDA-MB-231 cells transduced with an empty vector or truncated, constitutively active β-catenin isoform ΔN90. β-actin was used as a loading control. **(D)** Non-linear fit model of [CAR] *vs*. normalized response for IC50 determination (right). (n=2) **(E)** Representative scatterplots of flow cytometric analysis of aldehyde dehydrogenase activity (left) and statistical analysis of the mean percentage of ALDH+ cells in 231'OE and 231'Ctrl cells using Welch's t-test (n=5) (right). **(F)** Representative brightfield images of tumorspheres generated from 231'Ctrl and 231'OE cells (left, scale bar: 100 μm) and statistical analysis of mean tumorsphere forming units (number of spheres/number of seeded single cells) (right; n=3). Welch's t-test. (Barplots represent mean + SEM. **p <0.05, **p<0.01, ***p<0.001, ****p<0.0001*, ns = non significant).

**Supplementary Figure 4 |** Non-linear fit model of [CAR] *vs*. normalized response for IC50 determination (right) in 468'R cells transduced with inducible scrambled non-targeting shRNAs in the presence or absence of DOX. (n=2).

**Supplementary Figure 5 | (A)** Final tumor volumes of VEH (n=6), LGK (n=5), CAR (n=6) and CAR+LGK (n=6) treated mice. One way-ANOVA with Holm-Sidak

correction for multiple comparisons. **(B)** Bodyweight change in percentage of initial treatment bodyweight for VEH (n=6), LGK (n=5), CAR (n=6) and CAR+LGK (n=6) treated mice. No statistically significant changes detected by two way ANOVA. **(C)** Representative brightfield microscopy (20x magnification) of tumor sections labeled with anti-human Ki67 (left) and corresponding statistical analysis of the mean frequency of Ki67 positive cells. (VEH, CAR, CAR+LGK n=6 and LGK n=4). One-way ANOVA with Holm-Sidak correction for multiple comparisons. (Barplots represent mean + SEM. *$p < 0.05$, **$p < 0.01$, ***$p < 0.001$, ****$p < 0.0001$, ns = non significant).

## REFERENCES


1. Carey L, Winer E, Viale G, Cameron D, Gianni L. Triple-Negative Breast Cancer: Disease Entity or Title of Convenience? *Nat Rev Clin Oncol* (2010) 7:683–92. doi: 10.1038/nrclinonc.2010.154
2. Marra A, Trapani D, Viale G, Criscitiello C, Curigliano G. Practical Classification of Triple-Negative Breast Cancer: Intratumoral Heterogeneity, Mechanisms of Drug Resistance, and Novel Therapies. *NPJ Breast Cancer* (2020) 6:1–16. doi: 10.1038/s41523-020-00197-2
3. Liedtke C, Mazouni C, Hess KR, André F, Tordai A, Mejia JA, et al. Response to Neoadjuvant Therapy and Long-Term Survival in Patients With Triple-Negative Breast Cancer. *J Clin Oncol* (2008) 26:1275–81. doi: 10.1200/JCO.2007.14.4147
4. Rottenberg S, Disler C, Perego P. The Rediscovery of Platinum-Based Cancer Therapy. *Nat Rev Cancer* (2021) 21:37–50. doi: 10.1038/s41568-020-00308-y
5. Turner NC, Reis-Filho JS, Russell AM, Springall RJ, Ryder K, Steele D, et al. BRCA1 Dysfunction in Sporadic Basal-Like Breast Cancer. *Oncogene* (2007) 26:2126–32. doi: 10.1038/sj.onc.1210014
6. Shafee N, Smith CR, Wei S, Kim Y, Mills GB, Hortobagyi GN, et al. Cancer Stem Cells Contribute to Cisplatin Resistance in Brca1/p53-Mediated Mouse Mammary Tumors. *Cancer Res* (2008) 68:3243–50. doi: 10.1158/0008-5472.CAN-07-5480
7. Von Minckwitz G, Schneeweiss A, Loibl S, Salat C, Denkert C, Rezai M, et al. Neoadjuvant Carboplatin in Patients With Triple-Negative and HER2-Positive Early Breast Cancer (GeparSixto; GBG 66): A Randomised Phase 2 Trial. *Lancet Oncol* (2014) 15:747–56. doi: 10.1016/S1470-2045(14)70160-3
8. Sikov WM, Berry DA, Perou CM, Singh B, Cirrincione CT, Tolaney SM, et al. Impact of the Addition of Carboplatin and/or Bevacizumab to Neoadjuvant Once-Per-Week Paclitaxel Followed by Dose-Dense Doxorubicin and Cyclophosphamide on Pathologic Complete Response Rates in Stage II to III Triple-Negative Breast Cancer: CALGB 40603 (A. *J Clin Oncol* (2015) 33:13–21. doi: 10.1200/JCO.2014.57.0572
9. Loibl S, O'Shaughnessy J, Untch M, Sikov WM, Rugo HS, McKee MD, et al. Addition of the PARP Inhibitor Veliparib Plus Carboplatin or Carboplatin Alone to Standard Neoadjuvant Chemotherapy in Triple-Negative Breast Cancer (BrighTNess): A Randomised, Phase 3 Trial. *Lancet Oncol* (2018) 19:497–509. doi: 10.1016/S1470-2045(18)30111-6
10. Iwase M, Ando M, Aogi K, Aruga T, Inoue K, Shimomura A, et al. Long-Term Survival Analysis of Addition of Carboplatin to Neoadjuvant Chemotherapy in HER2-Negative Breast Cancer. *Breast Cancer Res Treat* (2020) 180:687–94. doi: 10.1007/s10549-020-05580-y
11. Zhou J, Kang Y, Chen L, Wang H, Liu J, Zeng S, et al. The Drug-Resistance Mechanisms of Five Platinum-Based Antitumor Agents. *Front Pharmacol* (2020) 11:343. doi: 10.3389/fphar.2020.00343
12. Wang L, Jin F, Qin A, Hao Y, Dong Y, Ge S, et al. Targeting Notch1 Signaling Pathway Positively Affects the Sensitivity of Osteosarcoma to Cisplatin by Regulating the Expression and/or Activity of Caspase Family. *Mol Cancer* (2014) 13:139. doi: 10.1186/1476-4598-13-139
13. Jin L, Chun J, Pan C, Li D, Lin R, Alesi GN, et al. MAST1 Drives Cisplatin Resistance in Human Cancers by Rewiring Craf-Independent MEK Activation. *Cancer Cell* (2018) 34:315–30.e7. doi: 10.1016/j.ccell.2018.06.012
14. Seidl C, Panzitt K, Bertsch A, Brcic L, Schein S, Mack M, et al. MicroRNA-182-5p Regulates Hedgehog Signaling Pathway and Chemosensitivity of Cisplatin-Resistant Lung Adenocarcinoma Cells *via* Targeting GLI2. *Cancer Lett* (2020) 469:266–76. doi: 10.1016/j.canlet.2019.10.044
15. Atkinson CJ, Kawamata F, Liu C, Ham S, Győrffy B, Munn AL, et al. EGFR and Prion Protein Promote Signaling *via* FOXO3a-KLF5 Resulting in Clinical Resistance to Platinum Agents in Colorectal Cancer. *Mol Oncol* (2019) 13:725–37. doi: 10.1002/1878-0261.12411
16. Akrap N, Andersson D, Bom E, Gregersson P, Ståhlberg A, Landberg G. Identification of Distinct Breast Cancer Stem Cell Populations Based on Single-Cell Analyses of Functionally Enriched Stem and Progenitor Pools. *Stem Cell Rep* (2016) 6:121–36. doi: 10.1016/j.stemcr.2015.12.006
17. Pattabiraman DR, Weinberg RA. Tackling the Cancer Stem Cells — What Challenges Do They Pose? *Nat Rev Drug Discov* (2014) 13:497–512. doi: 10.1038/nrd4253
18. Moore N, Lyle S. Quiescent, Slow-Cycling Stem Cell Populations in Cancer: A Review of the Evidence and Discussion of Significance. *J Oncol* (2011) 2011:1–11. doi: 10.1155/2011/396076
19. Koury J, Zhong L, Hao J. Targeting Signaling Pathways in Cancer Stem Cells for Cancer Treatment. *Stem Cells Int* (2017) 2017:1–10. doi: 10.1155/2017/2925869
20. Badve S, Nakshatri H. Breast-Cancer Stem Cells-Beyond Semantics. *Lancet Oncol* (2012) 13:e43–8. doi: 10.1016/S1470-2045(11)70191-7
21. Clevers H. The Cancer Stem Cell: Premises, Promises and Challenges. *Nat Med* (2011) 17:313–9. doi: 10.1038/nm.2304
22. Yang F, Xu J, Tang L, Guan X. Breast Cancer Stem Cell: The Roles and Therapeutic Implications. *Cell Mol Life Sci* (2017) 74:951–66. doi: 10.1007/s00018-016-2334-7
23. Al-Hajj M, Wicha MS, Benito-Hernandez A, Morrison SJ, Clarke MF. Prospective Identification of Tumorigenic Breast Cancer Cells. *Proc Natl Acad Sci* (2003) 100:3983–8. doi: 10.1073/pnas.0530291100
24. Wei W, Lewis MT. Identifying and Targeting Tumor-Initiating Cells in the Treatment of Breast Cancer. *Endocr Relat Cancer* (2015) 22:R135–55. doi: 10.1530/ERC-14-0447
25. Li W, Ma H, Zhang J, Zhu L, Wang C, Yang Y. Unraveling the Roles of CD44/CD24 and ALDH1 as Cancer Stem Cell Markers in Tumorigenesis and Metastasis. *Sci Rep* (2017) 7:1–15. doi: 10.1038/s41598-017-14364-2
26. Ben-Porath I, Thomson MW, Carey VJ, Ge R, Bell GW, Regev A, et al. An Embryonic Stem Cell–Like Gene Expression Signature in Poorly Differentiated Aggressive Human Tumors. *Nat Genet* (2008) 40:499–507. doi: 10.1038/ng.127
27. Zhan T, Rindtorff N, Boutros M. Wnt Signaling in Cancer. *Oncogene* (2017) 36:1461–73. doi: 10.1038/onc.2016.304
28. Van Der Wal T, Van Amerongen R. Walking the Tight Wire Between Cell Adhesion and WNT Signalling: A Balancing Act for β-Catenin: A Balancing Act for CTNNB1. *Open Biol* (2020) 10:1–15. doi: 10.1098/rsob.200267rsob200267
29. Niehrs C, Acebron SP. Mitotic and Mitogenic Wnt Signalling. *EMBO J* (2012) 31:2705–13. doi: 10.1038/emboj.2012.124
30. Jun S, Jung YS, Suh HN, Wang W, Kim MJ, Oh YS, et al. LIG4 Mediates Wnt Signalling-Induced Radioresistance. *Nat Commun* (2016) 7:1–13. doi: 10.1038/ncomms10994
31. Chen S, Guttridge DC, You Z, Zhang Z, Fribley A, Mayo MW, et al. Wnt-1 Signaling Inhibits Apoptosis by Activating β-Catenin/T Cell Factor-Mediated Transcription. *J Cell Biol* (2001) 152:87–96. doi: 10.1083/jcb.152.1.87
32. Malanchi I, Santamaria-Martínez A, Susanto E, Peng H, Lehr HA, Delaloye JF, et al. Interactions Between Cancer Stem Cells and Their Niche Govern Metastatic Colonization. *Nature* (2012) 481:85–91. doi: 10.1038/nature10694
33. Roy S, Kar M, Roy S, Padhi S, Kumar A, Thakur S, et al. Inhibition of CD44 Sensitizes Cisplatin-Resistance and Affects Wnt/β-Catenin Signaling in HNSCC Cells. *Int J Biol Macromol* (2020) 149:501–12. doi: 10.1016/j.ijbiomac.2020.01.131
34. Xie S-L, Fan S, Zhang S-Y, Chen W-X, Li Q-X, Pan G-K, et al. SOX8 Regulates Cancer Stem-Like Properties and Cisplatin-Induced EMT in Tongue Squamous Cell Carcinoma by Acting on the Wnt/β-Catenin Pathway. *Int J Cancer* (2018) 142:1252–65. doi: 10.1002/ijc.31134
35. Moens S, Zhao P, Baietti MF, Marinelli O, Van Haver D, Impens F, et al. The Mitotic Checkpoint Is a Targetable Vulnerability of Carboplatin-Resistant Triple Negative Breast Cancers. *Sci Rep* (2021) 11:1–13. doi: 10.1038/s41598-021-82780-6
36. Patro R, Duggal G, Love MI, Irizarry RA, Kingsford C. Salmon Provides Fast and Bias-Aware Quantification of Transcript Expression. *Nat Methods* (2017) 14:417–9. doi: 10.1038/nmeth.4197

37. Love MI, Huber W, Anders S. Moderated Estimation of Fold Change and Dispersion for RNA-Seq Data With Deseq2. *Genome Biol* (2014) 15:1–21. doi: 10.1186/s13059-014-0550-8
38. Stephens M. False Discovery Rates: A New Deal. *Biostatistics* (2017) 18:275–94. doi: 10.1093/biostatistics/kxw041
39. Zhou G, Soufan O, Ewald J, Hancock REW, Basu N, Xia J. NetworkAnalyst 3.0: A Visual Analytics Platform for Comprehensive Gene Expression Profiling and Meta-Analysis. *Nucleic Acids Res* (2019) 47:W234–41. doi: 10.1093/nar/gkz240
40. Müller AC, Giambruno R, Weißer J, Májek P, Hofer A, Bigenzahn JW, et al. Pathway Enrichment Analysis and Visualization of Omics Data Using G: Profiler, GSEA, Cytoscape and EnrichmentMap. *Nat Protoc* (2019) 22:924–34. doi: 10.1038/s41596-018-0103-9
41. Yoon S, Kim SY, Nam D. Improving Gene-Set Enrichment Analysis of RNA-Seq Data With Small Replicates. *PloS One* (2016) 11:1–16. doi: 10.1371/journal.pone.0165919
42. Bankhead P, Loughrey MB, Fernández JA, Dombrowski Y, McArt DG, Dunne PD, et al. QuPath: Open Source Software for Digital Pathology Image Analysis. *Sci Rep* (2017) 7:1–7. doi: 10.1038/s41598-017-17204-5
43. Schrauwen S, Coenegrachts L, Cattaneo A, Hermans E, Lambrechts D, Amant F. The Antitumor Effect of Metformin With and Without Carboplatin on Primary Endometrioid Endometrial Carcinoma *In Vivo*. *Gynecol Oncol* (2015) 138:378–82. doi: 10.1016/j.ygyno.2015.06.006
44. Depreeuw J, Hermans E, Schrauwen S, Annibali D, Coenegrachts L, Thomas D, et al. Characterization of Patient-Derived Tumor Xenograft Models of Endometrial Cancer for Preclinical Evaluation of Targeted Therapies. *Gynecol Oncol* (2015) 139:118–26. doi: 10.1016/j.ygyno.2015.07.104
45. Herath NI, Berthault N, Thierry S, Jdey W, Lienafa MC, Bono F, et al. Preclinical Studies Comparing Efficacy and Toxicity of DNA Repair Inhibitors, Olaparib, and AsiDNA, in the Treatment of Carboplatin-Resistant Tumors. *Front Oncol* (2019) 9:1097. doi: 10.3389/fonc.2019.01097
46. Engelmann K, Shen H, Finn OJ. MCF7 Side Population Cells With Characteristics of Cancer Stem/Progenitor Cells Express the Tumor Antigen MUC1. *Cancer Res* (2008) 68:2419–26. doi: 10.1158/0008-5472.CAN-07-2249
47. Koopman G, Reutelingsperger CP, Kuijten GA, Keehnen RM, Pals ST, van Oers MH. Annexin V for Flow Cytometric Detection of Phosphatidylserine Expression on B Cells Undergoing Apoptosis. *Blood* (1994) 84:1415–20. doi: 10.1182/blood.V84.5.1415.1415
48. Croker AK, Allan AL. Inhibition of Aldehyde Dehydrogenase (ALDH) Activity Reduces Chemotherapy and Radiation Resistance of Stem-Like ALDH Hicd44 + Human Breast Cancer Cells. *Breast Cancer Res Treat* (2012) 133:75–87. doi: 10.1007/s10549-011-1692-y
49. Yang L, Xie X, Tang H, Kong Y, Xie X, Chen J, et al. LGR5 Promotes Breast Cancer Progression and Maintains Stem-Like Cells Through Activation of Wnt/β-Catenin Signaling. *Stem Cells* (2015) 33:2913–24. doi: 10.1002/stem.2083
50. Ponti D, Costa A, Zaffaroni N, Pratesi G, Petrangolini G, Coradini D, et al. Isolation and *In Vitro* Propagation of Tumorigenic Breast Cancer Cells With Stem/Progenitor Cell Properties. *Cancer Res* (2005) 65:5506–11. doi: 10.1158/0008-5472.CAN-05-0626
51. Fuerer C, Nusse R. Lentiviral Vectors to Probe and Manipulate the Wnt Signaling Pathway. *PloS One* (2010) 5:e9370. doi: 10.1371/journal.pone.0009370
52. Doble BW, Woodgett JR. GSK-3: Tricks of the Trade for a Multi-Tasking Kinase. *J Cell Sci* (2003) 116:1175–86. doi: 10.1242/jcs.00384
53. Guo W, Keckesova Z, Donaher JL, Shibue T, Tischler V, Reinhardt F, et al. Slug and Sox9 Cooperatively Determine the Mammary Stem Cell State. *Cell* (2012) 148:1015–28. doi: 10.1016/j.cell.2012.02.008
54. Barrott JJ, Cash GM, Smith AP, Barrow JR, Murtaugh LC. Deletion of Mouse Porcn Blocks Wnt Ligand Secretion and Reveals an Ectodermal Etiology of Human Focal Dermal Hypoplasia/Goltz Syndrome. *Proc Natl Acad Sci USA* (2011) 108:12752–7. doi: 10.1073/pnas.1006437108
55. Lian X, Hsiao C, Wilson G, Zhu K, Hazeltine LB, Azarin SM, et al. Robust Cardiomyocyte Differentiation From Human Pluripotent Stem Cells *via* Temporal Modulation of Canonical Wnt Signaling. *Proc Natl Acad Sci* (2012) 109:E1848–57. doi: 10.1073/pnas.1200250109
56. Bruna A, Rueda OM, Greenwood W, Serra V, Garnett MJ. Caldas Correspondence C. A Biobank of Breast Cancer Explants With Preserved Intra-Tumor Heterogeneity to Screen Anticancer Compounds In Brief. *Cell* (2016) 167:260–74. doi: 10.1016/j.cell.2016.08.041
57. Gao H, Korn JM, Ferretti S, Monahan JE, Wang Y, Singh M, et al. High-Throughput Screening Using Patient-Derived Tumor Xenografts to Predict Clinical Trial Drug Response. *Nat Med* (2015) 21:1318–25. doi: 10.1038/nm.3954
58. Woo XY, Giordano J, Srivastava A, Zhao ZM, Lloyd MW, de Bruijn R, et al. Conservation of Copy Number Profiles During Engraftment and Passaging of Patient-Derived Cancer Xenografts. *Nat Genet* (2021) 53:86–99. doi: 10.1038/s41588-020-00750-6
59. Birkbak NJ, Li Y, Pathania S, Greene-Colozzi A, Dreze M, Bowman-Colin C, et al. Overexpression of BLM Promotes DNA Damage and Increased Sensitivity to Platinum Salts in Triple-Negative Breast and Serous Ovarian Cancers. *Ann Oncol* (2018) 29:903–9. doi: 10.1093/annonc/mdy049
60. Raudvere U, Kolberg L, Kuzmin I, Arak T, Adler P, Peterson H, et al. G: Profiler: A Web Server for Functional Enrichment Analysis and Conversions of Gene Lists (2019 Update). *Nucleic Acids Res* (2019) 47:W191–8. doi: 10.1093/nar/gkz369
61. Jönsson JM, Johansson I, Dominguez-Valentin M, Kimbung S, Jönsson M, Bonde JH, et al. Molecular Subtyping of Serous Ovarian Tumors Reveals Multiple Connections to Intrinsic Breast Cancer Subtypes. *PloS One* (2014) 9:1–11. doi: 10.1371/journal.pone.0107643
62. Woodward WA, Chen MS, Behbod F, Alfaro MP, Buchholz TA, Rosen JM. WNT/beta-Catenin Mediates Radiation Resistance of Mouse Mammary Progenitor Cells. *Proc Natl Acad Sci USA* (2007) 104:618–23. doi: 10.1073/pnas.0606599104
63. Martins-Neves SR, Paiva-Oliveira DI, Wijers-Koster PM, Abrunhosa AJ, Fontes-Ribeiro C, Bovée JVMG, et al. Chemotherapy Induces Stemness in Osteosarcoma Cells Through Activation of Wnt/β-Catenin Signaling. *Cancer Lett* (2016) 370:286–95. doi: 10.1016/j.canlet.2015.11.013
64. Jang G-B, Kim J-Y, Cho S-D, Park K-S, Jung J-Y, Lee H-Y, et al. Blockade of Wnt/β-Catenin Signaling Suppresses Breast Cancer Metastasis by Inhibiting CSC-Like Phenotype. *Sci Rep* (2015) 5:12465. doi: 10.1038/srep12465
65. Xie W, Liu N, Wang X, Wei L, Xie W, Sheng X. Wilms' Tumor 1-Associated Protein Contributes to Chemo-Resistance to Cisplatin Through the Wnt/b -Catenin Pathway in Endometrial Cancer. *BioMed Res Inter* (2021) 11:1–13. doi: 10.3389/fonc.2021.598344
66. He S, Wang W, Wan Z, Shen H, Zhao Y, You Z, et al. FAM83B Inhibits Ovarian Cancer Cisplatin Resistance Through Inhibiting Wnt Pathway. *Oncogenesis* (2021) 10. doi: 10.1038/s41389-020-00301-y
67. Mohapatra P, Shriwas O, Mohanty S, Ghosh A, Smita S, Kaushik SR, et al. CMTM6 Drives Cisplatin Resistance by Regulating Wnt Signaling Through ENO-1/AKT/Gsk3β Axis. *JCI Insight* (2021) 6:1–21. doi: 10.1172/jci.insight.143643
68. Geyer FC, Lacroix-Triki M, Savage K, Arnedos M, Lambros MB, MacKay A, et al. β-Catenin Pathway Activation in Breast Cancer Is Associated With Triple-Negative Phenotype But Not With CTNNB1 Mutation. *Mod Pathol* (2011) 24:209–31. doi: 10.1038/modpathol.2010.205
69. Liao S, Gan L, Qin W, Liu C, Mei Z. Inhibition of GSK3 and MEK Induced Cancer Stem Cell Generation *via* the Wnt and MEK Signaling Pathways. *Oncol Rep* (2018) 40:2005–13. doi: 10.3892/or.2018.6600
70. Yang Y, Wang QQ, Bozinov O, Xu RX, Sun YL, Wang SS. GSK–3 Inhibitor CHIR99021 Enriches Glioma Stem–Like Cells. *Oncol Rep* (2020) 43:1479–90. doi: 10.3892/or.2020.7525
71. Yoshino Y, Ishioka C. Inhibition of Glycogen Synthase Kinase-3 Beta Induces Apoptosis and Mitotic Catastrophe by Disrupting Centrosome Regulation in Cancer Cells. *Sci Rep* (2015) 5:1–14. doi: 10.1038/srep13249
72. Dewi FRP, Domoto T, Hazawa M, Kobayashi A, Douwaki T, Minamoto T, et al. Colorectal Cancer Cells Require Glycogen Synthase Kinase-3β for Sustaining Mitosis *via* Translocated Promoter Region (TPR)- Dynein Interaction. *Oncotarget* (2018) 9:13337–52. doi: 10.18632/oncotarget.24344
73. O'Flaherty L, Shnyder SD, Cooper PA, Cross SJ, Wakefield JG, Pardo OE, et al. Tumor Growth Suppression Using a Combination of Taxol-Based Therapy and GSK3 Inhibition in Non-Small Cell Lung Cancer. *PloS One* (2019) 14:1–17. doi: 10.1371/journal.pone.0214610
74. Glibo M, Serman A, Karin-Kujundzic V, Vlatkovic IB, Miskovic B, Vranic S, et al. The Role of Glycogen Synthase Kinase 3 (GSK3) in Cancer With Emphasis on Ovarian Cancer Development and Progression: A

Comprehensive Review. *Bosn J Basic Med Sci* (2021) 21:5–18. doi: 10.17305/bjbms.2020.5036
75. Ma C, Wang J, Gao Y, Gao TW, Chen G, Bower KA, et al. The Role of Glycogen Synthase Kinase 3β in the Transformation of Epidermal Cells. *Cancer Res* (2007) 67:7756–64. doi: 10.1158/0008-5472.CAN-06-4665
76. Zhou W, Wang L, Gou Sm, Wang Tl, Zhang M, Liu T, et al. ShRNA Silencing Glycogen Synthase Kinase-3 Beta Inhibits Tumor Growth and Angiogenesis in Pancreatic Cancer. *Cancer Lett* (2012) 316:178–86. doi: 10.1016/j.canlet.2011.10.033
77. Fillmore CM, Kuperwasser C. Human Breast Cancer Cell Lines Contain Stem-Like Cells That Self-Renew, Give Rise to Phenotypically Diverse Progeny and Survive Chemotherapy. *Breast Cancer Res* (2008) 10:1–13. doi: 10.1186/bcr1982
78. Su Y-J, Chang Y-W, Lin W-H, Liang C-L, Lee J-L. An Aberrant Nuclear Localization of E-Cadherin is a Potent Inhibitor of Wnt/β-Catenin-Elicited Promotion of the Cancer Stem Cell Phenotype. *Oncogenesis* (2015) 4:e157–7. doi: 10.1038/oncsis.2015.17
79. Martin-Orozco E, Sanchez-Fernandez A, Ortiz-Parra I, Ayala-San Nicolas M. WNT Signaling in Tumors: The Way to Evade Drugs and Immunity. *Front Immunol* (2019) 10:2854. doi: 10.3389/fimmu.2019.02854
80. Bejsovec A. Wingless Signaling: A Genetic Journey From Morphogenesis to Metastasis. *Genetics* (2018) 208:1311–36. doi: 10.1534/genetics.117.300157
81. Liu J, Pan S, Hsieh MH, Ng N, Sun F, Wang T, et al. Targeting Wnt-Driven Cancer Through the Inhibition of Porcupine by LGK974. *Proc Nat Acad Sci* (2013) 110:20224–9. doi: 10.1073/pnas.1314239110
82. Novartis. *A Study of LGK974 in Patients With Malignancies Dependent on Wnt Ligands*. ClinicalTrials.gov identifier: NCT01351103 (2021), U.S. National Library of Medicine. Available at: https://clinicaltrials.gov/ct2/show/NCT01351103?id=NCT01351103&draw=2&rank=1&load=cart.
83. Fischer MM, Yeung VP, Cattaruzza F, Hussein R, Yen WC, Murriel C, et al. RSPO3 Antagonism Inhibits Growth and Tumorigenicity in Colorectal Tumors Harboring Common Wnt Pathway Mutations. *Sci Rep* (2017) 7:1–9. doi: 10.1038/s41598-017-15704-y
84. Gurney A, Axelrod F, Bond CJ, Cain J, Chartier C, Donigan L, et al. Wnt Pathway Inhibition *via* the Targeting of Frizzled Receptors Results in Decreased Growth and Tumorigenicity of Human Tumors. *Proc Natl Acad Sci USA* (2012) 109:11717–22. doi: 10.1073/pnas.1120068109
85. Fukumoto T, Zhu H, Nacarelli T, Karakashev S, Fatkhutdinov N, Wu S, et al. N6-Methylation of Adenosine of FZD10 mRNA Contributes to PARP Inhibitor Resistance. *Cancer Res* (2019) 79:2812–20. doi: 10.1158/0008-5472.CAN-18-3592
86. Yamamoto TM, McMellen A, Watson ZL, Aguilera J, Ferguson R, Nurmemmedov E, et al. Activation of Wnt Signaling Promotes Olaparib Resistant Ovarian Cancer. *Mol Carcinog* (2019) 58:1770–82. doi: 10.1002/mc.23064
87. Yuan S, Tao F, Zhang X, Zhang Y, Sun X, Wu D. Role of Wnt/β-Catenin Signaling in the Chemoresistance Modulation of Colorectal Cancer. *BioMed Res Int* (2020) 2020:1–9. doi: 10.1155/2020/9390878

**Conflict of Interest:** The authors declare that the research was conducted in the absence of any commercial or financial relationships that could be construed as a potential conflict of interest.

frontiers in Oncology

REVIEW
published: 26 July 2021
doi: 10.3389/fonc.2021.689131

# Combinatorial Strategies to Target Molecular and Signaling Pathways to Disarm Cancer Stem Cells

*Giuliana Catara, Antonino Colanzi and Daniela Spano* *

*Institute of Biochemistry and Cell Biology, National Research Council, Naples, Italy*

Cancer is an urgent public health issue with a very huge number of cases all over the world expected to increase by 2040. Despite improved diagnosis and therapeutic protocols, it remains the main leading cause of death in the world. Cancer stem cells (CSCs) constitute a tumor subpopulation defined by ability to self-renewal and to generate the heterogeneous and differentiated cell lineages that form the tumor bulk. These cells represent a major concern in cancer treatment due to resistance to conventional protocols of radiotherapy, chemotherapy and molecular targeted therapy. In fact, although partial or complete tumor regression can be achieved in patients, these responses are often followed by cancer relapse due to the expansion of CSCs population. The aberrant activation of developmental and oncogenic signaling pathways plays a relevant role in promoting CSCs therapy resistance. Although several targeted approaches relying on monotherapy have been developed to affect these pathways, they have shown limited efficacy. Therefore, an urgent need to design alternative combinatorial strategies to replace conventional regimens exists. This review summarizes the preclinical studies which provide a proof of concept of therapeutic efficacy of combinatorial approaches targeting the CSCs.

**Keywords: cancer stem cells, cancer, combinatorial strategies, signaling pathways, molecular pathways**

OPEN ACCESS

***Edited by:***
*Hany Omar,*
*University of Sharjah,*
*United Arab Emirates*

***Reviewed by:***
*Sarika Saraswati,*
*Tennessee State University,*
*United States*
*Hyuk-Jin Cha,*
*Seoul National University, South Korea*

***Correspondence:**
*Daniela Spano*
*daniela.spano@ibbc.cnr.it*

***Specialty section:***
*This article was submitted to Pharmacology of Anti-Cancer Drugs, a section of the journal Frontiers in Oncology*

***Received:*** *31 March 2021*
***Accepted:*** *01 July 2021*
***Published:*** *26 July 2021*

***Citation:***
*Catara G, Colanzi A and Spano D (2021) Combinatorial Strategies to Target Molecular and Signaling Pathways to Disarm Cancer Stem Cells. Front. Oncol. 11:689131. doi: 10.3389/fonc.2021.689131*

## INTRODUCTION

Cancer stem cells (CSCs) constitute a cell subpopulation within the tumor whose frequency depends on the tumor type (1) and stage, being the frequency increasing with the tumor malignant progression (2). These cells possess both the ability to unlimited self-renewal and to generate the heterogeneous and differentiated cell lineages that form the tumor bulk (3). In addition, they show enhanced ability to form tumorspheres (4), high tumorigenicity (5) and high metastatic potential (6). CSCs have a leading role on resistance to cancer therapies such as chemotherapy, radiotherapy and molecular targeted therapy (7, 8). In fact, recent findings show that these conventional therapeutic interventions exert selective pressure on tumors (9, 10) resulting in the activation of or selection of cancer cells unresponsive to the treatment that display alternative pathways associated with CSCs properties. High expression level of transmembrane proteins adenosine triphosphate-binding cassette family which efflux anti-tumor drugs out of tumor cells (11), elevated capacity of DNA repair mechanism, increased protection against reactive oxygen species (ROS) and up-regulation of anti-apoptotic pathway (12) constitute a range of CSCs properties that serve chemotherapy and radiotherapy

resistance. In addition to the above-mentioned features, CSCs acquire a transient state of slow proliferation that identifies a population of quiescent cells able to maintain viability in conditions that kill the other cancer cells. However, after the discontinuation of the therapy, the quiescent state is reverted and CSCs can regenerate cancer (13) following the activation of new survival strategies, including new mutations, trans-differentiation or reprogramming (14). Moreover, the radiotherapy induces the Epithelial to Mesenchymal Transition (EMT) program that makes the CSCs more invasive and resistant to the therapy (15, 16).

Developmental signaling pathways [including Wnt, Sonic Hedgehog (Shh) and Notch] and oncogenic cascades (including transforming growth factor-beta (TGF-β), Janus kinase/signal transducer and activator of transcription 3 (JAK/STAT3), phosphatidylinositol 3-kinase/V-Akt murine thymoma viral oncogene/mammalian target of rapamycin (PI3K/AKT/mTOR), Mitogen-activated protein kinase (MAPK) and V-SRC avian sarcoma (Src) have been identified as key players both in CSCs biology maintenance and in cancer therapy resistance (17, 18). The description of these signaling pathways and their roles in defining the biology of CSCs will not be tackled herein and the reader is invited to refer to reviews that widely discuss these topics (17–28). Although several targeted approaches relying on monotherapy have been developed to affect these pathways, they have shown limited efficacy due to the activation of bypass pathway(s) and to the complexity of signaling networks containing feedback loops and cross-talk. For example, bypass activation of mitogen-activated protein kinase kinase (MEK) and/or AKT limits mTOR/PI3K inhibitor therapy (29, 30). Src inhibition rapidly mediates MEK/MAPK induction in preclinical breast cancer models (31, 32) and in high-grade serous ovarian cancer cellular model (33). MEK inhibition induces PI3K pathway in KRAS mutant cancers leading to MEK inhibitor resistance (34). The activation of MAPK-interacting kinase (MNK) signaling in response to mTOR complex1 (mTORC1) inhibition leads to the resistance mechanism in medulloblastoma (35). Therefore, strategies targeting more than one pathway might yield greater, and more durable responses. Similarly, strategies that combine the molecular targeted therapy with chemotherapy or radiotherapy could be more effective. In addition to signaling pathways, tumor-associated antigens, or molecules expressed by CSCs, have been linked to therapeutic resistance. These molecules represent targets for the development of new therapeutic avenues.

This review describes the state of the art of the CSCs-targeted combinatorial therapies investigated in the preclinical studies with a focus on the hematological malignancies and different types of solid tumors. These studies provide a proof of concept of the efficacy of these dual therapeutic approaches, in which the molecular targeted therapy, and/or the chemotherapy and/or the radiotherapy are combined each with other, to fight CSCs (**Figure 1**).

## COMBINATORIAL STRATEGIES IN TREATMENT OF HEMATOLOGICAL MALIGNANCIES CSCs

Combinatorial therapeutic approaches have been investigated in treatment of acute myeloid leukemia (AML) and chronic myeloid leukemia (CML) CSCs.

### Acute Myeloid Leukemia

About 30% of AML patients show *FMS-like tyrosine kinase-3* (*FLT3*)-mutations, which are associated with high levels of β-catenin. This observation suggests that the combined blockade of β-catenin and FLT3 could represent a new therapeutic avenue. Here AML and Leukemia Stem Cell (LSC)/progenitor cell viability is inhibited following treatment with the β-catenin/CBP antagonist C-82 combined with FLT3-tyrosine kinases inhibitor (TKI) sorafenib or quizartinib (36). Pre-treatment with C-82 sensitizes cells to sorafenib or quizartinib, thus resulting in reduced cell viability and induction of apoptosis both in AML cells and LSC/progenitor cells. Similarly, *in vivo* C-82 in combination with sorafenib or quizartinib synergistically acts to promote prolonged survival in mice xenografted with either a *FLT3*-mutated cell line or patient-derived tumor cells (patient-derived xenograft (PDX) mice). Mechanistically, C-82, TKIs or the combination of the two drugs effectively inhibit Wnt/β-catenin targets and FLT3 downstream signaling, with the combinatorial administration being more effective (36). The efficacy of the therapy has been also tested by using PRI724, another β-catenin/CBP antagonist. In addition, the cooperative action supported by blockade of Wnt/β-catenin and FLT3 is also provided by the administration of dual FLT3 and Wnt/β-catenin inhibitor SKLB-677 that suppresses LSCs and has strong anti-leukemia activity in *FLT3*-mutated AML cells (37), thus providing the rationale for the development of clinical trials.

Shh activation is detected in 45% of AML biopsies (38) and plays a role in drug resistance of AML CSCs, thus providing the rationale for selective inhibition of this pathway for AML treatment. Cyclopamine is a Shh inhibitor that does not affect the survival of normal hematopoietic stem cells (39, 40). A therapeutic combinatorial strategy relying on the administration of cyclopamine in the presence of either Lipopolysaccharide (LPS)

**Abbreviations:** CSCs, Cancer stem cells; ALDH1, aldehyde dehydrogenase 1; AML, acute myeloid leukemia; CML, chronic myeloid leukemia; ROS, reactive oxygen species; EMT, Epithelial to Mesenchymal Transition; Shh, Sonic Hedgehog; TGF-β, transforming growth factor-beta; JAK, Janus kinase; STAT3, signal transducer and activator of transcription 3; PI3K, phosphatidylinositol 3-kinase; AKT, V-Akt murine thymoma viral oncogene; mTOR, mammalian target of rapamycin; MAPK, Mitogen-activated protein kinase; Src, V-SRC avian sarcoma; ERK, extracellular signal-regulated kinase; JNK, c-Jun N-terminal kinase; EGFR, epidermal growth factor receptor; MEK, mitogen-activated protein kinase kinase; LSCs, leukemia stem cells; TNBC, triple-negative breast cancer; HCC, hepatocellular carcinoma; PDX, patient-derived xenograft; GSIs, γ-secretase inhibitors; FTIs, farnesyltransferase inhibitors; GBM, glioblastoma; GSCs, glioma stem cells; MNK, MAPK-interacting kinase; mTORC, mTOR complex; NSCLC, non-small cell lung cancer; HNSCC, head and neck squamous cell carcinoma; TMZ, temozolomide; DMC, demethoxycurcumin; TKI, tyrosine kinase inhibitor; PUMA, p53-upregulated modulator of apoptosis; BMI1, B cell specific moloney murine leukemia virus insertion site 1 gene; PAF, PCNA-associated factor; BMX, bone marrow and X-linked; DTIC, dacarbazine; Hsp90, Heat shock protein 90; ECSLCs, esophageal cancer stem-like cells; GSTO1, Glutathione S-transferase omega 1; FDA, Food and Drug Administration; TNF-α, Tumor Necrosis Factor-α; IFNs, interferons.

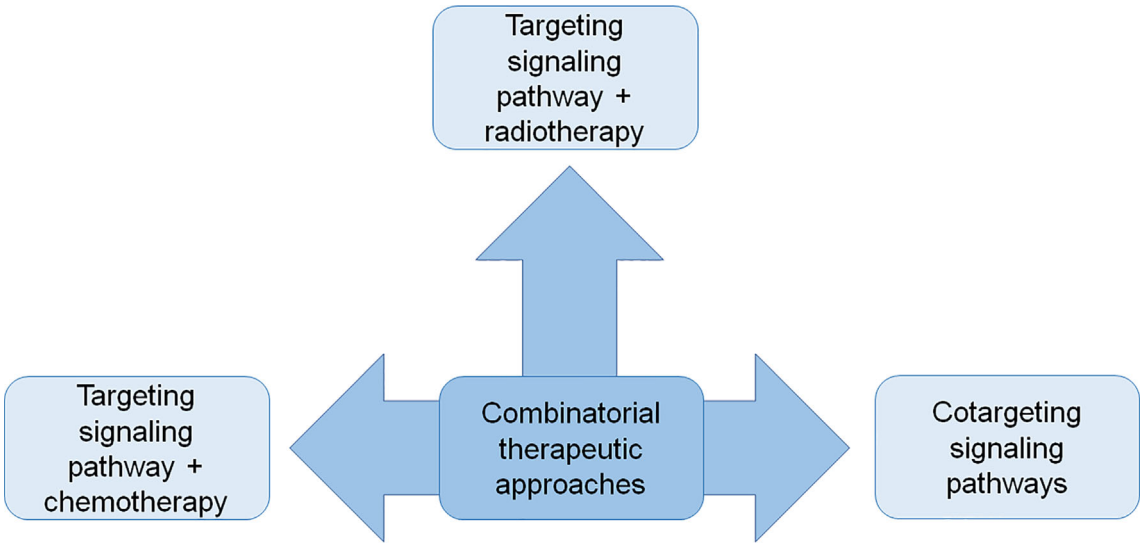


**FIGURE 1** | The schematic diagram shows combinatorial strategies to fight CSCs applied in the preclinical studies described in the text.

or Tumor Necrosis Factor-α (TNF-α) or interferons (IFNs) has been proposed to cure AML patients (41). Here cyclopamine-LPS administration synergistically reduces cell viability respect to a moderate decrease for cells treated with cyclopamine alone or LPS alone and leads to a massive cell apoptosis in THP-1 and U937 cells, AML patients cell lines and AML primary cells. In *in vivo* AML xenograft mouse model, in which U937 cells were injected in severe combined immunodeficient (SCID) mice, combinatorial therapy determines a reduction in tumor growth. Similar results are obtained replacing LPS with TNF-α or IFNs, which allows to reduce the side effects caused by LPS. To exclude an eventual off-target effect another Shh pathway inhibitor, SANT-1, was administered in combination producing same effects. Thus, this synergistic suppressive activity of Shh inhibitors in combination with either LPS or TNF-α or IFNs may be exploited to induce cell death in other types of cancer cells.

Aiming at overcoming resistance of LSCs to chemotherapy in patients with AML, an additional combined therapy targeting Shh signaling components has been proposed by Long and collaborators (42). The study provides evidence that Gli1 could be a promising target for AML therapy. As such, Gli1 is highly abundant in AML $CD34^+$ LSCs and in samples derived from AML patients in comparison to the healthy donors. Targeting Gli1 by the small-molecule inhibitor GANT61 significantly inhibits AML cells growth, suggesting that Gli1 can be considered a promising target to cure AML patients. Of note, co-treatment with Gli1 inhibitor and the generally used anti-leukemic drugs, such as cytarabine or all trans retinoic acid (ATRA), synergistically reduces AML cells viability, showing that pre-treatment with GANT61 promotes sensitization of primary AML $CD34^+$ LSCs to anti-leukemic drugs. These data foster the findings obtained in previous studies where the combination of GANT61 with vincristine reverses chemoresistance in Lucena-1 myeloid leukemia cells (43).

Raf/MEK/ERK (MAPK) cascade is activated in 70%-80% of patients affected by AML and regulates Bcl-2 family proteins by stabilizing anti-apoptotic Mcl-1 and inactivating pro-apoptotic BIM (44, 45). Moreover, MAPK signaling activation contributes to acquired resistance to venetoclax, a strong inhibitor of Bcl-2, which is highly expressed in AML LSCs. Starting from these findings, anti-leukemia effects of concomitant Bcl-2 and MAPK blockade by venetoclax and MEK1/2 inhibitor cobimetinib in AML were investigated (46). The combined treatment suppresses both Bcl-2:BIM and Mcl-1:BIM complexes, enabling release of free BIM to induce apoptosis in AML stem/progenitor population. In addition, the combination significantly suppresses the clonogenic potential of myeloid progenitors compared to either drug alone and importantly minimally affects normal progenitor function (46).

Dasatinib is a highly potent inhibitor of tyrosine kinases, including Src and ABL, approved for treatment of solid tumors and hematological malignancies (47, 48). It was used in combination with natural compounds or chemotherapeutic drugs for CSCs treatment. Dasatinib was found able to enhance both *in vitro* and *in vivo* the sensitivity of AML stem/progenitor cells to chemotherapeutic agents such as daunorubicin, cytarabine and doxorubicin (49). Here the *in vitro* combined treatment results in a significant increase in inhibition of AML stem/progenitor cell proliferation and colony-forming cells compared to single agent treatments. Moreover, the dual treatment significantly enhances the apoptosis of AML stem/progenitor cells (49). In *in vivo* AML mouse model, dasatinib and chemotherapy (cytarabine or doxorubicin) combination shows significantly prolonged survival, indicating improved targeting of AML LSCs (49). On a molecular point of view, in AML stem/progenitors cells, the combination inhibits the activation of AKT and MAPK signaling pathways, while does not affect STAT5 pathway, and enhances the expression levels of

p53 and its target genes, including BAX, p53-upregulated modulator of apoptosis (PUMA), p21, NOXA and DR5. In turn the reduced activation of AKT causes a reduction of HDM2 serine 166 phosphorylation, which is associated with p53 degradation. Therefore, the inhibition of AKT pathway probably represents the molecular mechanism responsible for p53 increased level, which is functional for the elimination of AML stem/progenitor cells treated with dasatinib/chemotherapy combination (49).

The relevance of blockade of PI3K/AKT/mTOR signaling cascade in AML stem cells therapy is highlighted by the combined treatment of active-site mTOR inhibitor MLN0128 and HDAC3 inhibitor vorinostat which stimulates a significantly higher apoptosis induction than the single agents in AML stem cells (50).

### Chronic Myeloid Leukemia

CML is a stem cell disease characterized by the reciprocal translocation t(9;22) that generates the BCR-ABL1 tyrosine kinase oncoprotein. The therapy consists in the administration of BCR-ABL1 TKI, however the TKI resistance occurs in a large number of patients. The molecular mechanisms responsible for TKI resistance consist in the generation of BCR-ABL1 mutations, intrinsic stem cell resistance (51) or, within the native BCR-ABL1 genetic background, in the activation of pro-oncogenic signaling networks and molecules, including AKT, mTOR, MEK, STAT3, STAT5, JAK2, or Src kinases (52–56). In particular, the activation of STAT3 signaling pathway protects CML cells upon TKI-mediated BCR-ABL1 inhibition (54) and confers kinase-independent TKI resistance to primary CML stem and progenitor cells (57). The STAT3 targeting with BP-5-087, a potent and selective STAT3 inhibitor, in combination with TKI imatinib rescues the TKI sensitivity of TKI-resistant CML cell lines and primary CML stem and progenitor cells with no toxicity to normal hematopoietic stem or progenitor cells (57). Therefore, the combined blockade of both BCR-ABL1 and STAT3 significantly decreases the survival and the clonogenic properties of CML stem and progenitor cells with kinase-independent TKI-resistance compared to inhibition of only BCR-ABL1 or only STAT3, thus suggesting that the combination could be a new therapeutic approach for eradicating the TKI-resistant stem cell population in CML affected patients. Based on these results, another combined therapeutic approach that uses the STAT3 potent inhibitor CDDO-Me was assessed in CML treatment. The combination of CDDO-Me and TKI ponatinib induces the apoptosis and reduces the clonogenic ability of both CML stem cells and progenitor cells in a synergistic manner, as a result of the full and simultaneous inhibition of both STAT3 and STAT5 (58). CDDO-Me shows pleiotropic effects; in fact, it, in addition to inhibit STAT3, induces ROS generation, suppresses several survival-related molecules (including AKT, mTOR, and MAPK), and increases the expression of heme-oxygenase-1, a heat-shock-protein that contributes to drug resistance of CML cells (59). For these reasons, the combined inhibition of STAT3, heme-oxygenase-1 and BCR-ABL1, by using CDDO-Me, the heme-oxygenase-1 inhibitor SMA-ZnPP and TKI (dasatinib or ponatinib) respectively, was also investigated. The anti-proliferative effect of the triple-combination in CML cells was superior to single drug treatment or 2-drug treatment (58). Interestingly the CDDO-Me/TKI and CDDO-Me/SMA-ZnPP/TKI combinations do not significantly affect the proliferation of normal bone marrow cells, thus further supporting them as new therapeutic avenues (58).

A summary of the preclinical studies performed on CSCs of hematological tumors is provided in **Table 1**.

## COMBINATORIAL STRATEGIES IN TREATMENT OF SOLID TUMORS CSCs

Combinatorial therapeutic approaches have been investigated in treatment of CSCs from solid tumors including central and sympathetic nervous system tumors, breast cancer, prostate cancer, non-small-cell lung cancer (NSCLC), head and neck squamous cell carcinoma (HNSCC), colorectal cancer, hepatocellular carcinoma (HCC), ovarian cancer, pancreatic cancer and melanoma.

### Tumors of Central and Sympathetic Nervous System

#### Gliomas

Gliomas, the most prevalent primary tumors of the brain and spinal cord, are characterized by the amplification of Gli1, a component of the Shh cascade, following the Ras/NFkB-mediated activation of Shh pathway (60). Therefore, the combinatorial targeting of Shh and Ras/NFkB pathways could represent a new strategy to fight gliomas. Driven by this hypothesis, Dixit and collaborators demonstrated that the combinatorial approach using Shh inhibitor SANT-1 and Ras/NFkB inhibitor guggulsterone is effective in arresting glioma CSCs and non-stem cells proliferation (61). The combined treatment significantly increases glioma CSCs and non-stem cells apoptosis compared to monotherapies, thus resulting in decreased cell viability. On a mechanistic point of view, guggulsterone inhibits Ras and NFkB activities and sensitizes cells to SANT-1-induced apoptosis. To corroborate this finding, the inhibition of Ras or NFkB is sufficient to sensitize glioma CSCs and non-stem cells to SANT-1. Of note, treatment with a combination of SANT-1 and guggulsterone on SVG p12 astroglia cell line does not decrease cell viability, thus suggesting that this combination selectively targets the viability of glioma CSCs and non-stem cells without affecting normal astrocytes (61).

Among the gliomas, glioblastoma (GBM) represents the most common and aggressive tumor of the central nervous system. The current standard of GBM treatment is surgical resection, concurrent and adjuvant chemotherapy with temozolomide (TMZ) and radiotherapy (62). However, the glioma stem cells (GSCs), responsible for GBM malignant growth, therapeutic resistance and recurrence, are not sensitive to TMZ and until now, there are no effective drugs for the clinical treatment of these cells. To develop new therapeutic approaches to fight GBM, the therapeutic efficacy of TMZ and demethoxycurcumin

**TABLE 1** | Combinatorial therapies tested in pre-clinical studies to treat CSCs from acute myeloid leukemia (AML) and chronic myeloid leukemia (CML).

| Tumor | Combinatorial therapy | Molecular target | Phenotypic outcome | Cellular/animal models | References |
|---|---|---|---|---|---|
| Acute myeloid leukemia | C-82/PRI724 + sorafenib/quizartinib | CBP/β-catenin + Tyrosine Kinase FLT3 | Suppression of CSCs proliferation<br>Prolonged survival | AML cells, LSC/progenitor cells<br>Mice xenografted with either a *FLT3*-mutated cell line or PDX cells | (36) |
| Acute myeloid leukemia | Cyclopamine + LPS/TFN-a/IFNs | Smo | Reduction of CSCs viability | THP-1,U937 cells, AML patients cell lines and AML primary cells | (41) |
| | | | Suppression of tumor growth | xenograft mouse model | |
| Acute myeloid leukemia | GANT-61 + cytarabine (Ara-c)/ATRA | Gli1 | Reduction of CSCs viability | AML cells | (42) |
| Acute myeloid leukemia | Cobimetinib + venetoclax | MEK1/2 + Bcl-2 | Induction of apoptosis and inhibition of progenitor clonogenic properties | AML stem/progenitor cells | (46) |
| Acute myeloid leukemia | Dasatinib + daunorubicin/cytarabine/doxorubicin | Src | Inhibition of cell proliferation and colony-forming cells, induction of apoptosis<br>Inhibition of AML stem/progenitor cell proliferation and increase of mice survival | AML stem/progenitor cells<br>AML mouse model | (49) |
| Chronic myeloid leukemia | BP-5-087 + imatinib | STAT3 + BCR-ABL1 | Decrease of survival and clonogenic properties | CML stem and progenitor cells | (57) |
| Chronic myeloid leukemia | CDDO-Me + ponatinib | STAT3 + STAT5 + BCR-ABL1 | Induction of apoptosis and reduction of clonogenic properties | CML stem cells and progenitor cells | (58) |
| Chronic myeloid leukemia | CDDO-Me + SMA-ZnPP + dasatinib/ponatinib | STAT3 + heme-oxygenase-1 + BCR-ABL1 | Inhibition of CML cell proliferation | CML cells | (59) |

(DMC) combination was investigated on GSCs (63). The DMC-TMZ treatment causes a strong impairment of GSCs proliferation due to G0/G1 cell cycle arrest and apoptosis induction. On a molecular point of view, DMC-TMZ combination increases ROS production in GSCs, that in turn promotes the activation of caspase-3 signaling, thus inducing the apoptosis. In addition, the two drugs co-administration leads to a strong reduction of STAT3 signaling pathway activation in GSCs, thus resulting in the inhibition of STAT3 targets genes, including *c-Myc* and *CDC25A* genes, implicated in activating G1 to S cell cycle progression, and *Bcl-2* and *Bcl-xL* genes that promote cell survival (63). In summary, STAT3 signaling blockade caused by DMC-TMZ combinatorial treatment contributes to GSCs growth inhibition and apoptosis, thus representing a new avenue to fight GBM.

GBM shows hyperactivation of Notch signaling, therefore several Notch-targeted therapies based on the γ-secretase inhibitors (GSIs) exploitation have been evaluated either as monotherapy or in combinatorial approaches with other regimens. Currently the GSI RO4929097 has been found effective in the treatment of patients with severe glioma in association with bevacizumab (64). Alternatively, it has been described to act synergistically with chemotherapeutic drugs contributing to reduce the numbers of GBM CSCs (65). One of the most promising approach relies on the combined treatment with GSIs and farnesyltransferase inhibitors (FTIs), the latter evaluated for their potential to cure glioma-affected patients, though with modest outcomes (66, 67). Ma and colleagues have shown that FTIs and GSIs act synergistically on GBM stem cells that become more sensitive to radiation respect to non-stem tumor cells (68). In particular, combined administration of the FTI tipifarnib and the GSI RO4929097 produces anti-proliferative effects and cytotoxicity on $CD133^+$ CSCs respect to single agent treatment. On the contrary, $CD133^-$ cells were resistant to these drugs used either in mono- or combined therapy. Similarly, GBM xenograft tumors treated with the combination show a reduced tumor growth. The dual therapy tested on orthotopic GBM models extends the mice median survival with two cases of durable response. From mechanistic point of view, the synergistic activity of the cure relies on the ability of FTIs to compromise cell-cycle progression prior of the effect exerted by RO4929097, though the molecular mechanism remains not fully elucidated. On the same line of evidence, valuable outcomes have been reached in other trials using FTIs and GSIs in combination with TMZ (69) or treating other cancers types, such as breast and lung cancers (70, 71).

Another combined therapeutic approach uses LY2109761, an inhibitor of TGF-β type I serine/threonine kinase receptor (TGFβR-I), that shows anti-tumor activity in various tumor models (72–74). The combinatorial effects of radiation and LY2109761 were investigated in *in vitro* established human GBM cell lines and GSCs and in *in vivo* subcutaneous and orthotopic tumor models (75). Here the combined treatment significantly enhances the radiation-induced double-strand breaks, inhibits the DNA repair and increases the apoptosis of both GBM and GSCs. Moreover, it reduces the self-renewal and proliferation of GSCs compared to LY2109761 or radiation monotherapy. These data demonstrate that LY2109761 sensitizes both GBM and GSCs toward radiation (75).

On a molecular point of view, combined treatment reduces SMAD2 phosphorylation, thus resulting in the blockade of TGF-β signaling cascade, that in turn affects the expression profiles of genes involved in several functional categories including cellular movement, cell death, and cellular growth and proliferation (75). Furthermore, the combinatorial treatment delays the tumor growth in both GBM subcutaneous and GSCs orthotopic xenograft tumor models and increases the survival of mice bearing orthotopically implanted brain tumor compared to single treatments. In addition, histologic analyses show that LY2109761 inhibits tumor invasion promoted by radiation, reduces tumor microvessel density, and attenuates mesenchymal transition (75). These findings demonstrate the therapeutic efficacy of this approach in *in vitro* and *in vivo* preclinical models of GBM.

Evidence demonstrates that the cross-talk between MEK/ERK and PI3K/mTOR pathways controls the maintenance of self-renewal and tumorigenicity of GBM CSCs (76). Therefore, the therapeutic efficacy of the combinatorial blockade of these signaling cascades was assessed in these cells. Here the combined treatment with PI3K/mTOR inhibitor NVP-BEZ235 and MEK1/2 inhibitors UO126 or SL327 results in suppression of the level of both phospho-ERK and phospho-Akt and in significant reduction of sphere-forming ability, which indicates the impairment of self-renewal ability of CSCs (76). Moreover, the combination induces a higher expression level of the neural marker βIII-tubulin, indicating that the inhibition of those pathways promotes GBM CSCs neural differentiation (76). In *in vivo* xenograft animal models, the GBM CSCs treated with both NVP-BEZ235 and SL327 inhibitors form smaller tumors than GBM CSCs treated with the single agent, with a significant improvement of mice survival (76).

AZD2014 is an inhibitor of mTORC1 and mTORC2 complexes as demonstrated by its ability to decrease the phosphorylation of S6k and 4EBP1, markers of mTORC1 activity, and of AKT, a marker of mTORC2 activity (77). Although AZD2014 alone has slight effect on survival of GBM CSCs, the combination of AZD2014 and radiation decreases the survival of GBM CSCs, thus indicating that the dual inhibition of mTORC1 and mTORC2 complexes sensitizes GBM CSCs to radiotherapy. Mechanistically, AZD2014-induced GBM CSCs radiosensitization involves the impairment of the repair of radiation-induced DNA double strand breaks. Moreover, the combinatorial treatment significantly increases the survival of mice bearing GBM CSCs xenograft brain tumor compared to control and single treatments mice (77).

PI3K signaling cascade is commonly hyperactive in GBM multiforme, which is also characterized by the dysregulation of apoptotic pathway due to the high expression level of anti-apoptotic Bcl-2 family of proteins. Therefore, combined blockade of PI3K pathway and Bcl-2 family of proteins may represent a reasonable therapeutic strategy. With this aim, ABT-263 (Navitoclax), an inhibitor of Bcl-2 and Bcl-xL, was used in combination with GDC-0941, a PI3K inhibitor, for the therapeutic treatment of GBM cells and CSCs (78). On a mechanistic point of view, ABT-263 binding to Bcl-2 and Bcl-xL proteins prevents their interaction with pro-apoptotic Bcl-2 family members, which results in the activation of intrinsic apoptotic cascade. However, ABT-263 poorly inhibits Mcl-1, another member of Bcl-2 family of proteins with anti-apoptotic properties, which confers resistance to ABT-263. The combination of GDC-0941 and ABT-263 significantly reduces the viability of GBM cell lines and the neurosphere formation ability of GSCs compared to single treatments. These data provide evidence that combinatorial treatment not only affects the bulk of the tumor, but also targets the CSCs population within malignant gliomas (78). On a mechanistic point of view, the combination causes a loss in mitochondrial membrane potential, the activation of both initiator caspase-9 and effector caspase-3 and the apoptosis of both GBM cell lines and glioma CSCs. Moreover, Akt pathway induces BAD phosphorylation, thereby inhibiting its pro-apoptotic properties. GDC-0941 dramatically reduces the phosphorylation of AKT and pro-apoptotic BAD proteins and lowers Mcl-1 levels by enhancing its degradation through the proteasome in GBM cell lines and glioma CSCs. In summary, GDC-0941-mediated dephosphorylation of BAD and Mcl-1 reduction render GBM cell lines and glioma CSCs more sensitive to the apoptotic properties of ABT-263 (78).

Some combinatorial therapeutic avenues in GBM CSCs treatment are based on the targeting of molecules specifically expressed by GBM CSCs including PCNA-associated factor (PAF) and bone marrow and X-linked (BMX) nonreceptor tyrosine kinase. PAF is overexpressed in breast cancer and GBM CSCs and controls cancer cell stemness *via* Wnt signaling (79, 80). In addition, PAF promotes CSCs resistance to radiotherapy by interacting with PCNA and regulating PCNA-associated DNA translesion synthesis (79). PAF depletion in combination with radiation compromises self-renewal and radioresistance of GSCs, thus suggesting a new therapeutic approach for GBM treatment (79). In addition, the high expression level of PAF in breast CSCs opens the possibility to design new therapeutic approaches. About the 90% of human GBMs shows high level of expression and activation of BMX (81). Interestingly, BMX is overexpressed in GSCs compared to non-stem tumor cells and neural progenitor cells. The binding of interleukin-6 to gp130 receptor stimulates the BMX mediated-hyperactivation of STAT3 signaling pathway, which in turn promotes the maintenance of GSCs self-renewal and tumorigenic potential (81, 82). In addition, BMX contributes to chemotherapy and radiotherapy cancer cells resistance (83, 84). Ibrutinib inhibits the tyrosine kinase activity of BMX, reduces GSCs proliferation, suppresses GSCs self-renewal potential and tumor sphere formation, and induces GSCs apoptosis (81). *In vivo*, ibrutinib suppresses the tumor growth in mice bearing GSCs-derived orthotopic xenografts, thus improving the mice survival (81). Interestingly, ibrutinib does not affect the ability of neural progenitor cells to form neurosphere; moreover, it selectively targets stem-like glioma cells expressing BMX in GBMs xenograft mice with small impact on neural progenitor cells lacking BMX expression (81). On a molecular point of view, in GSCs ibrutinib treatment strongly reduces the level of active phosphorylated BMX, and in turn the level of active phosphorylated STAT3, thus resulting in the reduction of the expression of STAT3 targets genes (*Nanog* and *Oct4*). This effect is not observed on STAT3 activation in ibrutinib treated neural progenitor cells, further confirming the specificity of ibrutinib on GSCs (81). Based on these data, the therapeutic efficacy of combined ibrutinib and irradiation treatment was analyzed in mice bearing GSCs-derived tumors (81). Here the

ibrutinib and irradiation combination results in a significantly more efficient inhibition of tumor growth and in a longer survival extension compared to ibrutinib and irradiation single agent treatments. This improved therapeutic efficiency of combined treatment is due to a decreased cell proliferation and an increased apoptosis of tumor cells in GSCs-derived xenografts (81).

Diffuse intrinsic pontine glioma (DIPG) is a brainstem pediatric tumor characterized by high molecular heterogeneity (85–87) that leads to classification in cohorts according to high expression of MYCN and Shh or to presence of *H3F3A* mutations (86, 88). DIPG is characterized by hyperactivation of Notch, therefore the administration of Notch inhibitor has been evaluated as a potential therapeutic approach. A sequential combinatorial therapy has been assessed including the MYCN inhibitor JQ1 and the GSI MRK003 with the aim to reduce tumor growth and the resistance to radiotherapy (89). Combined treatment of DIPG cell lines (JHH-DIPG and SU DIPGXIII) shows a reduced cell proliferation with increased apoptotic cell death in a shorter time frame respect to single drug administration. On the other hand, DIPG SF7761 cells are more resistant to combinatorial treatment, even though comparative analyses at molecular level show a general downregulation of MYCN and MYC proteins levels in all the 3 cell lines tested, thereby suggesting that the molecular heterogeneity of DIPG plays an important role in the efficacy of therapy.

A summary of the preclinical studies performed on glioma CSCs is provided in **Table 2**.

## Medulloblastoma

Medulloblastoma is a brain tumor which occurs exclusively in the posterior fossa. Evidence suggests that PI3K and MAPK are reciprocal bypass pathways that can promote resistance to drugs targeting either pathway alone (35). Therefore, the dual inhibition of these pathways could represent a new therapeutic approach. Frank Eckerdt and collaborators demonstrated that the pharmacological blockade of MNK sensitizes medulloblastoma CSCs to targeted PI3Kα inhibition (90). *In vitro* the combined MNK and PI3Kα targeting significantly impairs the neurosphere growth compared to single treatments, and in *in vivo* xenograft animal models it reduces tumor growth and prolongs the mice survival compared to single treatments (90).

A summary of the preclinical study performed on medulloblastoma CSCs is provided in **Supplementary Table 1**.

## Neuroblastoma

Neuroblastoma is an extracranial solid tumor of the sympathetic nervous system. Kwang Woon Kim and collaborators (91) showed that the activation of both AKT2/mTOR and MAPK signaling pathways in neuroblastoma cells is associated with the acquisition of cancer stem like phenotype (characterized by the expression of CD133, SOX2, ALDH, Nestin, Oct4, and Nanog stem cells markers and increased sphere-forming ability) and cisplatin- and radiation-resistance. The blocking of these signaling cascades with specific inhibitors of AKT2 (CCT128930) and MEK (PD98059) results in significantly higher reduction of sphere formation, cell proliferation, and cell migration compared to the single treatments in these cisplatin- and radiation- resistant cells, thus demonstrating the

**TABLE 2** | Combinatorial therapies tested in pre-clinical studies to treat glioma CSCs.

| Tumor | Combinatorial therapy | Molecular target | Phenotypic outcome | Cellular/animal models | References |
|---|---|---|---|---|---|
| Glioma | SANT-1 + Guggulsterone | Smo + Ras/NFkB | Reduction of CSCs viability | Glioma CSCs and non-stem cells | (61) |
| Glioblastoma | Temozolomide + demethoxycurcumin | STAT3 | Inhibition of glioma stem cells proliferation, G0/G1 cell cycle arrest and apoptosis induction | Glioma CSCs | (63) |
| Glioblastoma | Tipifarnib + RO4929097 | Cell cycle<br>Progression factors + Notch | CSCs death<br>Reduction of tumor growth | $CD133^+$ CSCs<br>GBM mouse model | (68) |
| Glioblastoma | LY2109761 + radiation | TGF-β type I receptor | Reduction of CSCs self-renewal and proliferation; induction of apoptosis<br>Delay of tumor growth and increase of mice survival | GBM cell lines and GSCs<br>GBM subcutaneous and GSCs orthotopic xenograft tumor models | (75) |
| Glioblastoma | UO126/SL327 + NVP-BEZ235 | MEK1/2 + PI3K/mTOR | Reduction of CSCs sphere-forming ability, induction of CSCs neural differentiation<br>Inhibition of tumor growth, increase of mice survival | GBM CSCs<br>Xenograft animal models | (76) |
| Glioblastoma | AZD2014 + radiation | mTORC1 and mTORC2 | Decrease of CSCs survival<br>Increase of mice survival | GBM CSCs<br>GBM CSCs xenograft mouse model | (77) |
| Glioblastoma | GDC-0941 + ABT-263 | PI3K + bcl-2 and Bcl-xL | Decrease of CSCs neurosphere formation ability, induction of CSCs apoptosis | GBM cells and CSCs | (78) |
| Glioblastoma<br>Glioblastoma | PAF shRNA + radiation<br>Ibrutinib + radiation | PAF<br>BMX | Decrease of GSCs self-renewal and radioresistance<br>Decrease of GSCs proliferation, suppression of self-renewal and tumor sphere formation, Induction of apoptosis<br>Suppression of tumor growth, increase of mice survival | Glioma stem cells<br>GBM CSCs<br>Mice bearing GSCs-derived orthotopic xenografts | (79)<br>(81) |
| Pediatric diffuse intrinsic pontine glioma | MRK003 + JQ1 | Notch + MYCN | Suppression of CSCs proliferation | JHH-DIPG and SU DIPGXIII cell lines | (89) |

therapeutic efficacy of combined treatment to fight neuroblastoma CSCs (91).

A summary of the preclinical study performed on neuroblastoma CSCs is provided in **Supplementary Table 1**.

## Breast Cancer

The combined therapeutic strategies investigated in breast CSCs treatment are based on the combination of chemotherapeutic agents with molecular targeted therapies.

EW-7197 is TGF-β type I receptor kinase inhibitor which has been proved to be efficient in inhibiting the paclitaxel-induced CSCs properties in breast cancer cell lines and xenograft animal models (92). Paclitaxel treatment induces the increase of intracellular ROS, that in turn promote the EMT (93) through the *Snail* increased expression (92). The EMT increases the population of CSCs, as exemplified by the enhanced expression of pluripotency regulators (*Oct4*, *Nanog*, *Klf4*, *Myc*, and *Sox2*) and stemness markers [$CD44^+$/$CD24^-$ ratio, aldehyde dehydrogenase 1 (ALDH1)] and increased mammosphere-forming efficiency (92). The combinatorial treatment of EW-7197 and paclitaxel suppresses both *in vitro* and *in vivo* paclitaxel-induced ROS increase, Snail expression, EMT, and cancer stem-like properties (exemplified as reduction of the expression of CSCs markers and pluripotency regulators). Furthermore, it improves the therapeutic effect of paclitaxel by decreasing the lung metastasis and increasing the survival time *in vivo* (92).

The chemotherapy-induced CSCs enrichment in triple negative breast cancer (TNBC) is mediated by the reciprocal regulation of ERK and p38 activities (94), thus suggesting that the dual targeting of these pathways could represent a new therapeutic strategy to fight breast CSCs. Driven by this hypothesis Lu and collaborators (94) showed that the pharmacological inhibition of p38 activity by SB203580 blocks paclitaxel-induced expression of Nanog, Sox2, and Klf4 pluripotency factors and abrogates the paclitaxel-induced increase in the percentage of CSCs. Moreover, the combination of paclitaxel and p38 inhibitor LY2228820 significantly affects the tumor grow of mammary fat pad xenograft animal models compared to either drug alone. LY2228820 abrogates paclitaxel-induced increase in CSCs and mammosphere-forming cells and expression of Nanog and Klf4 stemness factors, indicating efficacy of p38 inhibitors, in combination with chemotherapy, in the eradication of breast CSCs (94).

The combination of src inhibitor saracatinib and gemcitabine sensitizes gemcitabine-resistant triple negative breast CSCs, overexpressing Src and its active form p-Src, to gemcitabine through the down-regulation of AKT/c-Jun pathway (95). This combination dramatically reduces the viabilities, survival and colony formation of gemcitabine-resistant breast CSCs compared to single agents (95). Moreover, it increases the expression of pro-apoptotic protein BAX and decreases the level of anti-apoptotic proteins Bcl-xL and Survivin, thus resulting in an enhancement of gemcitabine-induced apoptosis in gemcitabine-resistant breast CSCs than the single treatments (95). In addition, the combinatorial treatment reduces the expression of migration associated proteins p-FAK and MMP-3, thus resulting in impairment of gemcitabine-resistant breast CSCs migration compared to single treatments. Src inhibition combined to gemcitabine dramatically impairs the ability of sphere forming and the expression of CSCs markers, such as CD44 and Oct-4, compared with either agent alone, reflecting the synergistic inhibition of breast cancer stemness (95).

A further study shows the efficacy of combined therapy relying on the pre-treatment with selective WNT antagonists vantictumab (OMP-18R5) or ipafricept (OMP-54F28) followed by the taxane plaxicitin administration (96). Vantictumab (OMP-18R5) and ipafricept (OMP-54F28) impair respectively the binding of WNT to FZD receptors 1,2,5,7 and 8 (97) and to FZD8-Fc, a fusion protein between the extracellular ligand binding domain of FZD8 receptor and Fc domain of human immunoglobulin G1 (IgG1) (97, 98). It is worthy to mention that these antagonist compounds in combination with taxane plaxicitin act synergistically displaying anti-tumor activity on different type of tumor cells by using PDX models such as breast, ovarian and pancreatic cancers (96). In detail, the pre-administration of WNT antagonists sensitizes CSCs to plaxicitin therapy leading to potentiate the drug induced-mitotic cell death (mitotic catastrophe) in tumor cells responsive to the treatment and to reduce the number of CSCs.

In a rare subset of breast CSCs, characterized by high expression of αvβ3 and Slug and low expression of PUMA ($\alpha v\beta 3^+$/$Slug^+$/$PUMA^{Lo}$), Qi Sun and collaborators identified a signaling pathway, consisting of the integrin αvβ3, Src and the transcription factor Slug, responsible for the down-regulation of the expression of the pro-apoptotic molecule PUMA, which results in promoting the survival of breast CSCs and tumor aggressiveness, independently of hormone receptor status or molecular subtype (99). The genetic (by shRNA) or pharmacological (by dasatinib or saracatinib) blockade of Src activity disrupts this signaling axis in CSCs and drives PUMA expression, which in turn leads to decreased mammosphere formation, self-renewal and tumor initiation. Therefore, Src inhibition specifically targets CSCs and decreases breast cancer metastasis *in vivo* (99). Src inhibition is effective in targeting CSCs in anchorage-independent conditions; however, it is relatively ineffective against adherent cells, suggesting the presence of innate resistance factors. Since pro-apoptotic PUMA binds to pro-survival Bcl-2 proteins, limiting its ability to initiate apoptosis, the authors hypothesized that Src inhibition resistance of breast CSCs is mediated by the interaction between PUMA and the pro-survival Bcl-2 family members and the combinatorial inhibition of Src and the appropriate pro-survival Bcl-2 factor should result in the overcoming breast CSCs resistance to Src inhibition, thus resulting in the further improvement of CSCs depletion. As assumed, the Src inhibitor resistance of CSCs is mediated by the interaction between PUMA and the pro-survival Bcl-2 and Bcl-xL factors. The clinically-approved Bcl-2 selective inhibitor venetoclax is able to prevent PUMA binding to Bcl-2, freeing PUMA to induce intrinsic apoptosis. Therefore, the combinatorial treatment with both venetoclax and dasatinib was investigated. This treatment increases the percentage of apoptotic CSCs compared to dasatinib alone treatment, thus resulting in a synergistic reduction of breast CSCs viability (100). In addition, it further

reduces stemness properties, including self-renewal and tumorsphere formation, compared to Src inhibition alone (100).

Glutathione S-transferase omega 1 (GSTO1) plays a major role in detoxification of chemotherapeutic agents in cancer cells. Recently, Lu and collaborators showed that GSTO1 plays a role in specification of the breast CSCs phenotype in response to chemotherapy independently of its enzymatic activity (101). Here the exposure of breast cancer cells to chemotherapy induces HIF-dependent expression of GSTO1, which interacts with ryanodine receptor 1 (RYR1) to increase intracellular $Ca^{2+}$ levels, which in turn activates the PYK2/Src/STAT3 signaling cascade leading to breast CSCs enrichment (101). Thus, it was hypothesized that the genetic (by siRNA) or pharmacological (by inhibitor sulfonamide chalcone S2E) inhibition of GSTO1 in combination with chemotherapy should sensitize the breast CSCs to chemotherapeutic treatment. Actually, combined treatment of GSTO1 inhibitor S2E or siRNA with tamoxifen significantly reduces cell viability, cell migration and mammospheres forming efficiency of breast CSCs compared to single treatments, while increases the breast CSCs apoptosis (102). On the mechanistic point of view, GSTO1 inhibition leads to decreased activation of pro-migration and pro-survival ERK1/2, AKT, p38, Src and STAT3 signaling pathways and drives the activation of the stress kinase JNK, that in turn induces the pro-apoptotic proteins BAX, cytochrome c and cleaved caspase-3 of the mitochondrial apoptosis signaling pathway (102).

A further therapeutic approach using chemotherapy in combination with antibody therapy against the CSCs-associated molecule Nodal was assessed in TNBC cellular models (103). Nodal, an embryonic morphogen of TGF-β superfamily, is a regulator of early embryonic development (103), is highly expressed in several aggressive neoplasms (104) and plays a role in tumor growth, metastasis, CSCs phenotype and resistance to conventional therapy (103, 104). Nodal high expression drives maintenance of self-renewal and is associated to stem cell markers expression in CSCs (105, 106), vice versa the Nodal signaling inhibition causes the reduction of tumorigenesis, metastasis, invasion, angiogenesis, and plastic stem cell phenotype in several cancer types (105, 107–109). Since Nodal is not typically expressed in most normal adult tissues, it represents a potential targetable CSCs-associated molecule. The *in vitro* sequential treatment with doxorubicin, an inducer of DNA damage, followed by anti-Nodal antibody regimen in TNBC cellular models, impairs the cellular stress (p38) and DNA repair (ChK1) pathways, thus resulting in significant cellular growth and viability decrease and significant cell apoptosis increase (103).

A summary of the preclinical studies performed on breast CSCs is provided in **Table 3**.

**TABLE 3** | Combinatorial therapies tested in pre-clinical studies to treat breast CSCs.

| Tumor | Combinatorial therapy | Molecular target | Phenotypic outcome | Cellular/animal models | References |
|---|---|---|---|---|---|
| Breast cancer | EW-7197 + paclitaxel | TGF-β type I receptor | Inhibition of EMT and CSCs properties<br>Inhibition of EMT and CSCs properties; reduction of metastasis; increase of survival | Breast CSCs<br>Xenograft mouse model | (92) |
| Triple negative breast cancer | SB203580/LY2228820 + paclitaxel | p38 | Inhibition of CSCs stemness factors expression, inhibition of CSCs expansion<br>Inhibition of tumor growth | Breast CSCs<br>Xenograft animal models | (94) |
| Breast cancer | Saracatinib + gemcitabine | Src | Reduction of viabilities, survival, colony formation, sphere forming ability and migration of CSCs | Gemcitabine-resistant breast CSCs | (95) |
| Breast cancer | OMP-18R5/OMP-54F28 + plaxicitin | FZD/FZD8-Fc + tubulin | Suppression of tumor growth | Patient-derived xenograft (PDX) models | (96) |
| Breast cancer | Dasatinib + etoposide | Src | Decrease of CSCs population | Breast CSCs | (99) |
| Breast cancer | Dasatinib + venetoclax | Src + Bcl-2 | Induction of CSCs apoptosis, reduction of CSCs self-renewal and tumorsphere formation | Breast CSCs | (100) |
| Breast cancer | GSTO1 siRNA/S2E + tamoxifen | GSTO1 | Decrease of cell viability, cell migration and mammospheres forming efficiency | Breast CSCs | (102) |
| Breast cancer | Doxorubicin + anti-Nodal antibody | Nodal | Decrease of cell growth and viability, induction of apoptosis | TNBC CSCs | (103) |

## Prostate Cancer

Two combinatorial therapeutic approaches were investigated in preclinical studies for treatment of prostate CSCs.

Zhang and collaborators (110) provided a first evidence that the combinatorial treatment of Napabucasin (BBI608), an inhibitor of STAT3 approved for the treatment of metastatic

colorectal carcinoma and pancreatic cancer, with chemotherapeutic agents could improve the chemotherapy efficacy by modulating the sensitivity of CSCs to the drugs. Here the treatment of PC3 prostate cancer cells with different concentrations of docetaxel in combination with Napabucasin results in more effective inhibition of cell proliferation compared to docetaxel alone, thus suggesting that napabucasin could significantly increase the sensitivity of prostate cancer cells to docetaxel by killing drug resistant CSCs.

L Chang and collaborators demonstrated that the radiotherapy resistance in prostate cancer is due to the activation of PI3K/Akt/mTOR signaling pathway, which promotes both the EMT (as exemplified by increased cell migration/invasion, downregulation of epithelial marker and upregulation of mesenchymal markers) and the acquisition of CSCs phenotype (as exemplified by increased expression of CSCs markers and sphere formation ability) (111). The combination of inhibitor BEZ235 (targeting both PI3K and mTOR) with radiation exposure decreases the activation of PI3K/Akt/mTOR cascade (in terms of phosphorylation status of PI3K/Akt/mTOR signaling proteins such as p-Akt, p-mTOR, p-S6K, p-4EBP1), reduces EMT (in terms of increased expression of E-cadherin and decreased expression of N-cadherin, Vimentin, OCT3/4, SOX2 and αSMA), reduces the expression of CSCs markers (including CD44, CD44v6, CD326, ALDH1) and self-renewal proteins (such as Nanog and Snail), stimulates the apoptosis and decreases colony formation ability compared to single treatments, thus suggesting that the dual PI3K/mTOR inhibitor BEZ235 increases radiosensitivity of prostate CSCs (111).

A summary of the preclinical studies performed on prostate CSCs is provided in **Supplementary Table 1**.

## Non-Small-Cell Lung Cancer

The therapeutic efficacy of combination of Napabucasin with chemotherapeutic agents in treatment of prostate CSCs was further corroborated by the study of Lauren MacDonagh and collaborators who analyzed the therapeutic efficacy of Napabucasin-cisplatin combination in non-small-cell lung cancer (NSCLC) CSCs treatment (112). Here Napabucasin reduces the expression of stemness related genes (*Nanog*, *Oct-4*, *Sox-2* and *cMyc*) and CSCs associated genes (*CD133* and *ALDH1*), which results in decrease of CSCs population present in cisplatin resistant NSCLC subtypes (113). Moreover, the combined treatment significantly reduces the proliferation of cisplatin resistant NSCLC subtypes compared to cisplatin-only treated cells, thus suggesting that Napabucasin re-sensitizes the cells to the drug cytotoxic effects (113). In addition, the combined treatment significantly impairs the clonogenic survival of cisplatin resistant NSCLC subtypes compared to Napabucasin-only treated cells and simultaneously increases the percentage of cisplatin resistant apoptotic cells compared to cisplatin alone, thus demonstrating the potential benefit of combining Napabucasin with current chemotherapy drugs, such as cisplatin, to decrease NSCLC cell survival and as a means of overcoming cisplatin resistance (113).

A summary of the preclinical study performed on NSCLC CSCs is provided in **Supplementary Table 1**.

## Head and Neck Squamous Cell Carcinoma

Three combined approaches of molecular targeted therapies with chemotherapy were investigated in *in vitro* preclinical studies in treatment of head and neck squamous cell carcinoma (HNSCC) CSCs. The first strategy combines the p38 inhibitor SB203580 and chemotherapeutic agent cisplatin (114). Here the combined treatment results in a reduction of survival and colony forming ability, increased apoptosis and an impairment of DNA damage response and repair capacity compared to cisplatin alone treatment. This finding suggests that the inhibition of p38 sensitizes HNSCC cells toward cisplatin. Interestingly, SB203580-cisplatin combination significantly reduces CSCs markers expression and tumor spheroid formation compared to cisplatin treated cells, thus showing that the combinatorial treatment impairs CSCs maintenance (114).

The second approach combines the targeting of the stem cell factor BMI1 (B cell specific moloney murine leukemia virus insertion site 1 gene) with cisplatin. BMI1, a core component of the polycomb repressive complex 1, is upregulated in a variety of human cancers and contributes to CSCs self-renewal and chemoresistance (115). Cancer cells in HNSCC are efficiently targeted by cisplatin, while $BMI1^+$ CSCs are not. Therefore, the combined administration of the BMI1 specific inhibitor PTC-209 and cisplatin fights both tumor cells and CSCs thus reducing the $BMI1^+$ CSCs-mediated lymph node metastases (116).

The combination between dasatinib and the mithramycin analog EC-8042 was also investigated in the treatment of HNSCC CSCs (117). Hermida-Prado and collaborators showed that dasatinib and saracatinib, in monotherapy regimes, strongly reduce the phosphorylation levels of active Src and FAK, and inhibit EMT, through the up-regulation of epithelial marker E-Cadherin and concomitant down-regulation of mesenchymal markers vimentin and Snail, thus resulting in a significant inhibition of HNSCC cell migration and invasion. However, both dasatinib and saracatinib fail to eliminate CSCs-enriched tumorsphere cultures of HNSCC cells, as revealed by the significant increase in the expression levels of CSCs markers, including ALDH1A1, SOX2, Nanog1 and Oct4, thus suggesting that these drugs, used as single agents, strongly enhance CSCs properties (117). To counteract the pro-stemness activity of dasatinib, the authors assessed the effects of the dual treatment with dasatinib and EC-8042 on HNSCC cellular and xenograft animal models, based on the observation that a strong decrease of CSCs viability and CSCs-related markers expression was observed in HNSCC (117) and in other cancers (118) treated with the mithramycin analog EC-8042. As a result of the combinatorial treatment, the HNSCC cell invasion ability, the viability of CSCs-enriched tumorspheres and the expression of CSCs-related factors (including ALDH1, SOX2, Nanog, Oct4, c-Myc and Notch1) are significantly affected. On a molecular point of view, the dasatinib-EC-8042 treatment inhibits active Src phosphorylation, Src-dependent phosphorylation and activation of FAK, AKT and p44/42-MAPK and reduces the levels of the EC-8042 target SP1 (118). In *in vivo* HNSCC xenograft animal model, the dual treatment leads to a significant reduction of tumor growth with the concomitant improvement in mice survival when compared to vehicle and dasatinib alone treatments (117). Of note, the significant reduction

in the percentage of Ki67-positive cells, the strong increase in the percentage of apoptotic cells and the remarkable decrease in the CSCs markers (such as ALDH1A1 and SOX2) expression level was observed in tumors from dasatinib-EC-8042 treated mice (117). Furthermore, while tumorsphere formation slightly increases in dasatinib-treated tumors, the tumorspheres-forming ability is significantly inhibited in dasatinib-EC-8042 treated tumors, thus providing evidence that the combined treatment effectively targets CSCs properties in *in vivo* HNSCC animal model. Taken together these findings demonstrate that EC-8042 counteracts the pro-stemness effects of dasatinib on HNSCC cellular and animal models and that the combined dasatinib-EC-8042 treatment benefits from the anti-proliferative, anti-invasive and anti-stemness functions provided by each compound without antagonizing each other.

A summary of the preclinical studies performed on HNSCC CSCs is provided in **Supplementary Table 1**.

## Colorectal Cancer

5-fluorouracil (5-FU) administration remains the most effective regimen for the cure of colorectal cancer-patients (119, 120), despite tumor relapse is encountered after discontinuation of the chemotherapeutic treatment (121). WNT/β-catenin pathway is activated upon 5-FU administration and is involved in the maintenance of colorectal cancer 5-FU-treated CSCs (122). On a mechanistic point of view, the drug modulates p53 activity, which in turn leads to the expression of WNT3 that is a positive regulator of Wnt/β-catenin signaling in colorectal cancer cell lines that harbor wild-type p53, thus contributing to relapse of the tumor (122). As such the administration of the WNT inhibitor LGK-974 combined with 5-FU to patient-derived tumor organoids and patient-derived tumor cells has revealed to be effective in suppressing tumor regrowth after discontinuation of treatment. The combined treatment induces a strong decrease in β-catenin levels, thus resulting in downregulation of WNT signaling pathway. To further determine the pathophysiological importance of WNT inhibition *in vivo*, the effects of 5-FU and LGK-974 combinatorial treatment were evaluated in 3 wild-type PDX mouse models. Both 5-FU monotherapy and combinatorial therapy with LGK-974 and 5-FU effectively reduce tumor growth, whereas co-treatment increases the sensitivity of tumors to 5-FU. Treatment with 5-FU alone, however, increases β-catenin and CSCs markers in the remaining tumor, while concurrent LGK-974 treatment effectively suppresses the effects of 5-FU on the levels of β-catenin and CSCs markers, thus preventing from the recurrence of the tumor. Taken together these findings prompt to consider WNT inhibition and 5-FU treatment as a strategy to overcome poor survival rates in colorectal cancer-patients.

Nautiyal and collaborators showed that the combination of the src inhibitor dasatinib and curcumin is effective in eliminating chemo-resistant colon cancer cells (123). The combined treatment strongly reduces the expression of CSCs markers (*ALDH*, *CD44*, *CD133*, *CD166*) in intestinal adenomas from $APCMin^{+/-}$ mice, thus suggesting that the dual treatment decreases the CSCs population in adenomas (123). *In vitro* dasatinib-curcumin treatment acts synergistically to significantly inhibit the growth of oxaliplatin chemo-resistant colon CSCs, the colonosphere formation, invasion potential and the expression of CSCs markers (such as *CD133*, *CD44*, *CD166* and *ALDH*), thus indicating that it is highly effective in reducing the colon CSCs population and inhibiting CSCs stemness properties (123).

A summary of the preclinical studies performed on colorectal CSCs is provided in **Supplementary Table 1**.

## Hepatocellular Carcinoma

HCC, one of the most common cancers worldwide, is characterized by high biological, molecular and clinical heterogeneity. Among the genes whose regulation appears altered, *CDK1* has been reported to be up-regulated in 46% of HCC tumor tissues and to correlate with poor prognosis of survival. On a molecular point of view, the CDK1/PDK1/β-catenin axis activation is linked to EMT, which in turn leads to an increased capacity of migration. Therefore, the dual blockade of CDK1 and PDK1 may represent a valuable combinatorial therapeutic strategy for HCC CSCs targeting. The administration of the cyclin-dependent kinase inhibitor (CDKI) RO3306 in association with the TKI sorafenib has been found functional to target CSCs in PDX tumor models of HCC (124). The treatment of PDX tumors with RO3306, sorafenib or the combination of the two drugs determines the tumor growth suppression of 75%, 42% and 92% respectively. These results clearly underline the efficacy of the combinatorial therapy and the positive effect of pretreatment with the CDKI in sensitizing CSCs to sorafenib. In particular, western blot analyses reveal the synergistic effect of the drugs combined use in down-regulating the CDK1, PDK1, β-catenin protein levels with the concurrent decrease in the levels of several CSCs stemness proteins, such as Oct4, Sox2 and Nanog (124).

A summary of the preclinical study performed on HCC CSCs is provided in **Supplementary Table 1**.

## Ovarian Cancer

The ovarian cancer is a heterogenous disease in which a multiplicity of distinct malignancies shares a common anatomical site. The high-grade serous subtype predominates in the clinical setting and is responsible for the highest rate of mortality among all forms of ovarian cancer. The prolonged Src inhibitor saracatinib treatment of high-grade serous ovarian cancer cells generates saracatinib-resistant cells, in which the activation of epidermal growth factor receptor (EGFR), HER2/ERBB2 and Raf/MEK signaling kinases was observed (33). Moreover, high expression levels of Src and MAPK active phosphorylated forms were detected in high-grade serous ovarian cancer $ALDH1^+$ CSCs. Therefore, the efficacy of combined Src and MEK inhibition with Src inhibitor saracatinib and MEK1/2 inhibitor selumetinib was investigated (33). The combinatorial treatment inhibits the EGFR-1 and EGFR-2–mediated bypass MEK/MAPK activation observed with saracatinib alone and effectively targets CSCs subpopulation of ovarian cancer. In *in vitro* experiments, the dual treatment reduces $ALDH1^+$ CSCs population and

sphere-forming cell amount more effectively than monotherapies. *In vivo*, it causes a significant inhibition of xenograft tumor growth compared to single drug treatments as a consequence of the drastic reduction of $ALDH1^+$ CSCs population. In fact, tumors dissociated after combined therapy show a significant reduction in $ALDH1^+$ CSCs population and sphere forming cells upon serial xenografting compared to tumors dissociated after monotherapies (33).

A summary of the preclinical study performed on ovarian CSCs is provided in **Supplementary Table 1**.

## Pancreatic Cancer

Pancreatic cancer remains a deadly disease with a very low 5-year survival due to disease recurrence even after surgical resection and/or chemotherapeutic regimes. Therefore, the combinatorial therapy may represent a valuable opportunity. The combination of molecular targeted therapies with chemotherapeutic drugs was investigated in preclinical studies to fight pancreatic CSCs. Duong and collaborators showed that dasatinib sensitizes pancreatic CSCs to gemcitabine (125). In fact, dasatinib-gemcitabine treatment significantly decreases both Src and STAT3 activation (in terms of level of phospho-Src and phospho-STAT3), and the ALDH1A1 level, which in turn promotes the inhibition of CSCs proliferation and survival by the induction of apoptosis through activation of caspase-3/7 and PARP cleavage (125).

Similarly, the inhibition of Nodal signaling in combination with the chemotherapeutic agent gemcitabine induces the apoptosis of pancreatic CSCs, suppresses cells in S phase and *in vivo* tumorigenicity, thus suggesting that Nodal signaling inhibition reverses the chemoresistance of the tumorigenic CSCs population (105). In pancreatic cancer xenograft athymic mouse model, established by the implantation of pancreatic cancer cell line, the combination therapy significantly delays tumor growth and increases the mice survival compared to monotherapies (105). However, engrafted primary human pancreatic cancer tissue with a substantial stroma shows no response to combinatorial therapy, probably due to limited drug delivery. To improve the Nodal inhibitor delivery, a triple combination therapy, in which gemcitabine plus Nodal signaling inhibitor treatment was combined to Shh pathway inhibition, was used. This triple therapy results in the impairment of *in vivo* tumor growth and increase of long-term progression-free survival (105).

A summary of the preclinical studies performed on pancreatic CSCs is provided in **Supplementary Table 1**.

## Melanoma

A therapeutic approach of combination of the anti-Nodal antibody with the chemotherapeutic agent dacarbazine (DTIC) was tested in melanoma cell lines (107). Here, while the DTIC alone treatment induces an increase in cell population expressing Nodal, the sequential treatment with DTIC and anti-Nodal antibody exhibits a striking decrease in the viable cell population and a striking increase in the proportion of programmed cell death. Moreover, the combined treatment results in a significant reduction in cell invasion, thus suggesting that targeting Nodal impairs the invasive ability of DTIC-resistant melanoma cells (107). More interestingly, the combined DTIC and anti-Nodal antibody exposure significantly suppresses the cell proliferation and induces the apoptosis in multicellular tumor spheroid culture (107). Similarly, the treatment of melanoma cell line harboring the active V600E mutation of B-RAF, which is constitutively active in approximately half of the melanoma patients, with B-RAF inhibitor RG7204 (vemurafenib) drives the selection of B-RAF inhibitor-resistant cells. These cells further treated with anti-Nodal antibody exhibit a marked decrease in viability and dramatic increase in cell death, thus showing that Nodal expression maintained in B-RAF inhibitor-resistant cells is also targetable with anti-Nodal antibodies with a significant benefit in therapeutic efficacy of melanoma treatment (107). The efficacy of combination of anti-Nodal antibody and dabrafenib, another inhibitor of B-RAF, was further investigated. Here *in vitro* and *in vivo* experiments were carried out on highly metastatic melanoma cell line and xenograft mice model with active B-RAF (V600E) mutation (126). The combined treatment significantly reduces the Nodal expression, the *in vitro* anchorage-independent colony formation and tumorigenic growth potential, and the *in vivo* lung metastases compared to the single treatments (126).

A summary of the preclinical studies performed on melanoma CSCs is provided in **Supplementary Table 1**.

## Esophageal Cancer

The therapeutic efficacy of the combined targeting of Heat shock protein 90 (Hsp90) and STAT3 was investigated in treatment of esophageal CSCs. Hsp90 is a molecular chaperone which binds to its client proteins to stabilize them and assist in their folding. It is a positive modulator of prostate CSCs, in fact it upregulates stemness markers, promotes self-renewal, and enhances tumor sphere growth (127). Hsp90 inhibition is effective in targeting CSCs in several cancers (127–130). One of the client proteins of Hsp90 is STAT3. The association between Hsp90 and STAT3 is necessary for STAT3 phosphorylation, dimerization, and nuclear translocation (131). This evidence suggests the combinatorial inhibition of Hsp90 and STAT3 as a therapeutic approach in CSCs treatment. To this aim the therapeutic efficacy of the combined treatment of Hsp90 inhibitor SNX-2112 and the sh-mediated knockdown of STAT3 was assessed in esophageal cancer stem-like cells (ECSLCs). Here the dual treatment strongly inhibits the proliferation of ECSLCs, induces G2/M phase arrest and apoptosis of ECSLCs, significantly decreases the colony formation ability and the colony size of ECSLCs compared with shSTAT3 and SNX-2112 alone (132). On a molecular point of view, the combined treatment reduces the levels of phosphorylation of Hsp90 client proteins involved in cell proliferation including p-p38, p-JNK and p-ERK, decreases the mRNA level of adenosine triphosphate-binding cassette transporter super-family *ABCB1* and *ABCG2* and the expression level of pro-survival Bcl-2 protein, and increases the expression level of the pro-apoptotic Bax protein compared with SNX-2112 and shSTAT3 alone groups (132). In addition, the combined treatment significantly reduces the tumor growth in

*in vivo* ECSLCs xenograft tumor models compared to single treatments (132).

A summary of the preclinical study performed on ECSLCs is provided in **Supplementary Table 1**.

## CSCs-CENTERED COMBINATORIAL STRATEGIES: WHICH ARE THE CONCLUDING REMARKS?

The combinatorial strategies herein reported foresee the targeting of developmental and oncogenic signaling pathways that are key players in defining several features of CSCs biology, including self-renewal, stemness, EMT, CSCs dormancy, as well as drug resistance, radio-resistance, tumor initiation and dedifferentiation, widely discussed in many published reviews (17–28).

The molecular mechanisms underlying the combinatorial strategies have been described in detail for each approach (please refer to the text above). In spite of the multiplicity of the strategies, some considerations can be taken into account to better address some common aspects of the topic.

Most of the dual therapies are based on the combination of molecular targeted therapies (for details the reader is referred to **Tables 1–3** and **Supplementary Table 1**). The rationale underlying this combination is based on the evidence of the activation of bypass pathway(s) and the feedback loops and cross-talk occurring. For the sake of simplicity, the following cases are presented as examples. The extensive cross-talk between MAPK and PI3K/AKT/mTOR pathways limits the therapeutic efficacy of the monotherapeutic regimes which target one or the other pathway (29, 30, 34, 35). The combinatorial strategies here reviewed provide a proof of concept that the dual blockade of these pathways by different combinations of molecules as diverse as alpelisib-CGP57380 (90), CCT128930-PD98059 (91) and UO126/SL327-NVP-BEZ235 (76) allows to overcome the activation of bypass pathway, thus resulting in the stronger therapeutic efficacy in CSCs eradication. Similarly, the Src inhibition induced-activation of MAPK signaling cascade (31–33) is overcome by the saracatinib-selumetinib dual treatment (33). The activation of STAT3 signaling pathway upon TKI-mediated BCR-ABL1 inhibition suggests the combinatorial STAT3 and BCR-ABL1 targeting as a new therapeutic avenue to eradicate CML stem and progenitor cells (57, 58). In addition, the concomitant activation of more than one signaling cascade represents the basis for the molecular targeted combinatorial approaches as demonstrated in the case of the combination of the β-catenin/CBP antagonist C-82 and the FLT3-TKI sorafenib or quizartinib in LSC treatment (36).

Other strategies combine the blockade of the anti-apoptotic Bcl-2/Bcl-xL proteins and MAPK or PI3K or Src signaling cascades by the administration of cobimetinib-venetoclax (46), GDC-0941-ABT-263 (78) and dasatinib-venetoclax 100] respectively. In these cases, the rationale for these approaches relies on the ability of MAPK, PI3K and Src signaling to negatively regulate the apoptotic pathway. Indeed, MAPK stabilizes anti-apoptotic Mcl-1 and inactivates pro-apoptotic BIM (44, 45), PI3K stabilizes Mcl-1 and inhibits the pro-apoptotic properties of BAD (78), Src down-regulates pro-apoptotic PUMA (100), thus promoting CSCs survival (for more details see the text). Therefore, the apoptosis is strongly stimulated by dual inhibition treatment rather than single treatment regimes.

Related to combinatorial strategies including chemotherapeutic drugs, their use as single agents in cancer treatment activates signaling pathways that promote the enrichment in CSCs population. This is the case of paclitaxel and gemcitabine which induce the activation of p38 and Src signaling respectively, thus resulting in CSCs increase (94, 95). This mechanism of action justifies the dual combination of SB203580 or LY2228820 with paclitaxel (94) and the dual combination of saracatinib with gemcitabine (95) as new therapeutic avenues to fight CSCs. Similarly, the ability of 5-FU to activate Wnt signaling cascade represents the rationale for the dual 5-FU/LGK-974 treatment as a new approach in CSCs therapy (122). Accordingly, the combinatorial strategies based on the use of chemotherapeutic agents in combination with inhibitors of specific signaling pathways have been developed to overcome this drawback and to foster the effect of chemotherapy. Examples are provided by the combination of chemotherapeutic drugs, interfering with DNA-related physiologic functions, such as mitosis (paclitaxel, docetaxel), DNA synthesis (cytarabine (Ara-c), etoposide, gemcitabine, daunorubicin, doxorubicin), DNA repair (cisplatin) or DNA transcription (EC-8042), with the inhibitors of different signaling pathways (including Wnt, TGF-β, MAPK, STAT, Sonic Hedgehog, Src, PI3K/AKT/mTOR) playing key roles in CSCs survival, proliferation, self-renewal and EMT (42, 49, 92, 94–96, 110, 112–114, 117, 122, 125).

On the same line of evidence, the radiotherapy induces the activation of signaling pathways, such as TGF-β and PI3K/AKT/mTOR, which promote EMT and CSCs stemness. Therefore, the radiotherapy regime combined with the inhibition of these signaling cascades represents the rationale behind few therapeutic strategies herein described, such as radiation-LY2109761 (75), radiation-AZD2014 (77), radiation-BEZ235 (111) (for details the reader is referred to the text).

## DISCUSSION

Accumulating evidence from studies in cancer shows that the CSCs, although constitute a rare cell subpopulation within the tumor bulk, represent the major cause of cancer therapy failure and tumor relapse. Therefore, these cells have become attractive candidate for preclinical studies to define promising targeted therapies in the treatment of cancer. Indeed, different CSCs-centered anti-cancer strategies have been assessed that foresee the targeting CSCs specific surface markers and tumor microenvironment, the inhibition of ATP-binding cassette transporters, the switching off CSCs self-renewal and survival signaling pathways and immunotherapy (133, 134). In addition,

more recent developments include nano-drug delivery systems, mitochondrion targeting, autophagy and hyperthermia (134). Herein, the description of the combinatorial strategies between the molecular targeted therapy and the chemotherapy or the radiotherapy to fight CSCs is reviewed. The preclinical studies presented in this review demonstrate that the therapeutic strategies based both on the combination of two molecular targeted therapies and on the combination of molecular targeted therapy with chemotherapy or radiotherapy result in a more effective targeting of CSCs compared to the single treatments. The most common mechanism through which these dual strategies affect CSCs relies on their eradication due to the induction of the apoptosis (**Figure 2A**), although a case of induction of CSCs differentiation is also reported (76) (**Figure 2B**). On a biological point of view, these combinatorial approaches impair some distinguishing features of CSCs, including proliferation and viability, self-renewal, clonogenic and sphere-forming potential and anti-apoptotic pathway activation, thus resulting in the reduction of CSCs radio- and chemo-resistance (the reader is referred to **Tables 1–3** and **Supplementary Table 1**).

The preclinical studies herein described have been performed on some hematological malignancies, including the AML and CML, and on some solid tumor types, mainly tumors of nervous system and breast cancers. Few studies of combinatorial avenues have been carried out on other cancers, including HCC, prostate cancer, pancreatic cancer, NSCLC, HNSCC, colorectal cancer, melanoma and ovarian cancer. The promising results achieved by the CSCs-treatment of these types of tumors strongly suggest

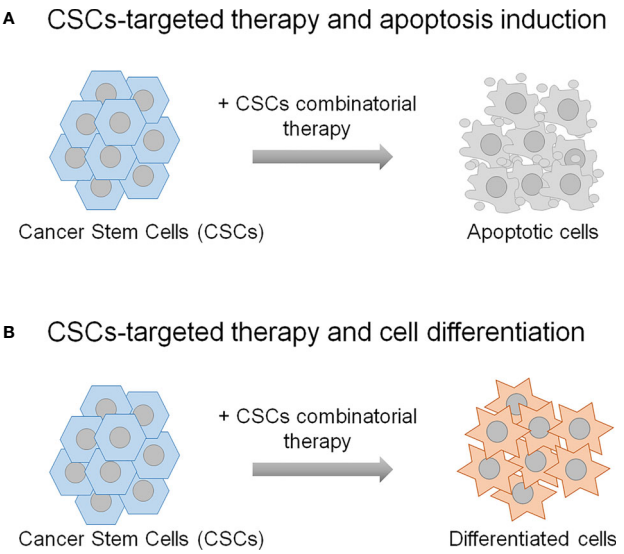


**FIGURE 2** | The schematic representation shows the mechanisms underlying the CSCs combinatorial strategies applied in the preclinical studies described in the text. CSCs-targeting can result in their eradication **(A)**, or differentiation **(B)**. The remaining non-stem tumor cells are thought to be sensitive to the conventional chemo- and radio-therapies.

to further extend the combinatorial therapeutic approaches to the treatment of additional cancers. In addition, preclinical studies demonstrate that some therapeutic combinations selectively affect CSCs and non-stem tumor cells without impact on normal stem cells, thus further supporting them as new therapeutic avenues (46, 58, 61, 81). Of note, the preclinical studies here presented show that some Food and Drug Administration (FDA)-approved drugs/inhibitors (such as Napabucasin, dasatinib, tipifarnib, venetoclax and sorafenib), already used in clinic for cancer treatment, in combination with clinically-approved chemotherapeutic agents (including cisplatin, paclitaxel, 5-FU, docetaxel) or radiation regimes effectively affect CSCs from different tumors. Among these, Napabucasin, a STAT3 inhibitor approved for the treatment of metastatic colorectal carcinoma and pancreatic cancer, is an example. In combination with chemotherapeutic drugs (docetaxel or cisplatin) it sensitizes prostate and NSCLC CSCs to chemotherapy. Taken together these achievements suggest that the therapeutic combinatorial strategies can be translated to clinical trials.

However, it is worthy to mention that some FDA-approved drugs/inhibitors, such as dasatinib and saracatinib, with proven powerful anti-tumor properties in preclinical studies, have shown limited clinical efficacy once translated in cancer patient's treatment (135–139). Of note, these two drugs enhance the CSCs properties in the HNSCC cellular models (117) and, more importantly, dasatinib fails to eliminate CSCs-enriched tumorspheres or to impair tumor growth in HNSCC xenograft models (117). On the same line of evidence, dasatinib worsens the effect of cetuximab in combination with radiotherapy in HNSCC xenograft models (140) and saracatinib does not affect tumor growth but impairs invasion and lymph node metastasis in HNSCC xenograft model (141). In clinical settings, these two drugs do not demonstrate any significant effect as single agents in patients with operable, recurrent and/or metastatic HNSCC (142–144). The deleterious pro-stemness activities exerted by dasatinib and saracatinib in HNSCC cell lines could envisaged as the main cause for the lack of clinical efficacy in HNSCC patients when used in monotherapeutic regimes. Similarly, dasatinib in combination with quercetin worsens the progression of liver disease, in a mouse model of obesity- and age- dependent liver disease, which fully recapitulates the non-alcoholic fatty disease (NAFLD) and HCC (145). In contrast to these findings, dasatinib inhibits the expression of CSCs marker SOX2 and tumorsphere formation in NSCLC cells (146, 147). These findings clearly demonstrate the contradictory effects of dasatinib suggesting that the observed anti-CSCs therapeutic efficacy is tumor-dependent, and thus an adequate patient stratification is required to select the patients who may benefit from dasatinib treatment.

Although the combinatorial treatments are promising strategies for CSCs-targeted therapies, the molecular heterogeneity of tumors adds another layer of complexity. Indeed, the molecular heterogeneity requires the targeting of specific signaling molecules according to the dysregulated signaling pathways, as exemplified in the case of breast, glioma and AML CSCs for which more than one

combinatorial approach has been proven to be successful in cancer treatment. Therefore, the understanding of molecular and signaling networks active in each tumor subtype and in related CSCs is a relevant issue to be addressed. The implementation of –omic techniques, contributing to dissect the molecular heterogeneity of the tumors, provides the tools for defining personalized-therapeutic treatments.

A further consideration regards the cellular and animal models used in the preclinical studies. In fact, the most of these studies have been performed *in vitro* on CSCs from established tumor cell lines or from patients' tumor specimens. Given the roles played by tumor microenvironment in defining tumor and CSCs properties, more appropriate models should be developed in further studies, including PDXs and organoids, to investigate the therapeutic efficacy of combinatorial approaches. The relevance of tumor microenvironment in defining both the CSCs properties and the therapeutic efficacy of the anti-CSCs combinatorial therapies is highlighted by the triple therapy that combines the Shh pathway inhibitor with Nodal inhibitor and gemcitabine to impair the pancreatic PDX tumor growth *in vivo* (105). Similarly, Cazet and collaborators demonstrated that Hedgehog ligand-activated cancer-associated fibroblasts provide an environment that promotes the tumor cells to acquire a chemoresistant stem-like phenotype (148). The treatment with the SMO inhibitors, reverting the cancer-associated fibroblasts gene expression changes induced by Hedgehog signaling, sensitizes the tumors to docetaxel chemotherapy in TNBC cells- and patient-derived xenograft animal models, thus resulting in inhibition of tumor growth and increased mice survival (148). In addition, the SMO inhibitor-docetaxel combined treatment was effective in treating a proportion of women with metastatic disease who had previously failed on taxane chemotherapy (148). These findings are further corroborated by the recent study of Brown and collaborators (149) who performed an *ex vivo* translational study on tumors dissected from ovarian cancer patients treated with metformin, a modulator of cellular metabolism, and matched non-metformin-treated control patients. Their findings demonstrate not only that metformin-treated tumors exhibit a significant reduction in CSCs population and are more sensitive to cisplatin treatment *ex vivo* compared to non-metformin-treated tumors, but also that metformin may impair stemness indirectly *via* an impact on tumor microenvironment. Indeed, metformin induces epigenetic changes in the cancer-associated mesenchymal stem cells, which prevents the ability of these cells to drive the chemoresistance *ex vivo* (149).

Drug specificity, selectivity and the related drug treatment side-effects are additional issues to be considered in designing new therapeutic avenues. For example, GSIs are not selective for Notch given that they may target a variety of γ-secretase substrates as well with different cellular outcomes (150). In addition, clinical trials using GSIs frequently counted drug-related side-effects (151). Therefore, there is an urgent need to develop more selective, potent and healthy drugs. For such a purpose, since several FDA-approved drugs have repurposing effects, they could constitute a further repertoire of potential anti-cancer agents. Indeed, one of the most promising repurposing approaches relies on the administration of antibiotics in combination with chemotherapy. In line with this approach, linezolid, a bactericidal antibiotic with the ability to induce a block in protein translation at mito-ribosomes with consequent alteration of mitochondrial functions, has been recently proposed in combination with the autophagy inhibitor HCQ as valuable strategy in TNBC anticancer therapy (152). Of note, concomitant treatment with linezolid and HCQ reduces tumor size in TNBC xenograft mice and colony formation in parental TNBC cells, and corresponding chemoresistant cells and CSCs compared to the linezolid alone treatment (control) (152). Similarly, a recent clinical pilot study was performed to assess the efficacy of antibiotic treatment in anticancer strategy (153). Given the important role of mitochondrial metabolism in CSCs, the FDA-approved doxycycline inhibitor was administered in short term pre-operative treatment (14 days before surgery) with the aim to follow the CSCs reduction in a small group of early breast cancer patients. The expression of known biomarkers of stemness, mitochondria, cell proliferation, apoptosis and neo-angiogenesis was analyzed in pre-operative specimens and matched surgical specimens. After doxycycline treatment, surgical tumor samples showed a significant decrease in the expression level of the stemness markers CD44 and ALDH1 respect to matched pre-operative and pre-doxycycline samples. Differently, the levels of markers of mitochondria, proliferation, apoptosis, and neo-angiogenesis were found similar in all the analyzed specimens (153). Although a further clinical study involving a larger number of patients should be performed to validate these preliminary data, this small-scale clinical study suggests that the mitochondrial functions inhibition may represent a new potential strategy for the CSCs eradication. In addition, the application of the Artificial Intelligence (154), a new emerging technology in drug discovery field, will implement the number of candidate molecules to be screened in order to design new combinatorial therapeutic avenues.

Taken together the combinatorial strategies described herein represent a starting point for future studies to design CSCs-targeted and personalized therapies.

## AUTHOR CONTRIBUTIONS

GC and DS discussed, wrote, and approved the manuscript. AC discussed and approved the manuscript. All authors contributed to the article and approved the submitted version.

## FUNDING

This article was funded by Italian Association for Cancer Research (AIRC, Milan, Italy), IG 2017 id. 20095 to Antonino Colanzi.

## SUPPLEMENTARY MATERIAL

The Supplementary Material for this article can be found online at: https://www.frontiersin.org/articles/10.3389/fonc.2021.689131/full#supplementary-material

## REFERENCES


1. Visvader JE, Lindeman GJ. Cancer Stem Cells in Solid Tumours: Accumulating Evidence and Unresolved Questions. *Nat Rev Cancer* (2008) 8(10):755–68. doi: 10.1038/nrc2499
2. Zhang D, Tang DG, Rycaj K. Cancer Stem Cells: Regulation Programs, Immunological Properties and Immunotherapy. *Semin Cancer Biol* (2018) 52(Pt 2):94–106. doi: 10.1016/j.semcancer.2018.05.001
3. Clarke MF, Dick JE, Dirks PB, Eaves CJ, Jamieson CHM, Jones DL, et al. Cancer Stem Cells–Perspectives on Current Status and Future Directions: AACR Workshop on Cancer Stem Cells. *Cancer Res* (2006) 66(19):9339–44. doi: 10.1158/0008-5472.CAN-06-3126
4. Weiswald LB, Bellet D, Dangles-Marie V. Spherical Cancer Models in Tumor Biology. *Neoplasia* (2015) 17(1):1–15. doi: 10.1016/j.neo.2014.12.004
5. Dick JE. Breast Cancer Stem Cells Revealed. *Proc Natl Acad Sci USA* (2003) 100(7):3547–9. doi: 10.1073/pnas.0830967100
6. Pardal R, Clarke MF, Morrison SJ. Applying the Principles of Stem-Cell Biology to Cancer. *Nat Rev Cancer* (2003) 3(12):895–902. doi: 10.1038/nrc1232
7. Clevers H. The Cancer Stem Cell: Premises, Promises and Challenges. *Nat Med* (2011) 17(3):313–9. doi: 10.1038/nm.2304
8. Skvortsova I, Debbage P, Kumar V, Skvortsov S. Radiation Resistance: Cancer Stem Cells (Cscs) and Their Enigmatic Pro-Survival Signaling. *Semin Cancer Biol* (2015) 35:39–44. doi: 10.1016/j.semcancer.2015.09.009
9. Liu L, Yang L, Yan W, Zhai J, Pizzo DP, Chu P, et al. Chemotherapy Induces Breast Cancer Stemness in Association With Dysregulated Monocytosis. *Clin Cancer Res* (2018) 24(10):2370–82. doi: 10.1158/1078-0432.CCR-17-2545
10. Lee SY, Jeong EK, Ju MK, Jeon HM, Kim MY, Kim CH, et al. Induction of Metastasis, Cancer Stem Cell Phenotype, and Oncogenic Metabolism in Cancer Cells by Ionizing Radiation. *Mol Cancer* (2017) 16(1):10. doi: 10.1186/s12943-016-0577-4
11. Begicevic RR, Falasca M. Abc Transporters in Cancer Stem Cells: Beyond Chemoresistance. *Int J Mol Sci* (2017) 18(11):2362–84. doi: 10.3390/ijms18112362
12. Steinbichler TB, Dudás J, Skvortsov S, Ganswindt U, Riechelmann H, Skvortsova II, et al. Therapy Resistance Mediated by Cancer Stem Cells. *Semin Cancer Biol* (2018) 53:156–67. doi: 10.1016/j.semcancer.2018.11.006
13. De Angelis ML, Francescangeli F, La Torre F, Zeuner A. Stem Cell Plasticity and Dormancy in the Development of Cancer Therapy Resistance. *Front Oncol* (2019) 9:626. doi: 10.3389/fonc.2019.00626
14. Shen MM, Abate-Shen C. Molecular Genetics of Prostate Cancer: New Prospects for Old Challenges. *Genes Dev* (2010) 24(18):1967–2000. doi: 10.1101/gad.1965810
15. Chi HC, Tsai CY, Tsai MM, Yeh CT, Lin KH. Roles of Long Noncoding RNAs in Recurrence and Metastasis of Radiotherapy-Resistant Cancer Stem Cells. *Int J Mol Sci* (2017) 18(9):1903–31. doi: 10.3390/ijms18091903
16. Phillips TM, McBride WH, Pajonk F. The Response of CD24(-/low)/CD44+ Breast Cancer-Initiating Cells to Radiation. *J Natl Cancer Inst* (2006) 98 (24):1777–85. doi: 10.1093/jnci/djj495
17. Takebe N, Miele L, Harris PJ, Jeong W, Bando H, Kahn M, et al. Targeting Notch, Hedgehog, and Wnt Pathways in Cancer Stem Cells: Clinical Update. *Nat Rev Clin Oncol* (2015) 12(8):445–64. doi: 10.1038/nrclinonc.2015.61
18. Marquardt S, Solanki M, Spitschak A, Vera J, Pützer BM. Emerging Functional Markers for Cancer Stem Cell-Based Therapies: Understanding Signaling Networks for Targeting Metastasis. *Semin Cancer Biol* (2018) 53:90–109. doi: 10.1016/j.semcancer.2018.06.006
19. Espinosa-Sánchez A, Suárez-Martínez E, Sánchez-Díaz L, Carnero A. Therapeutic Targeting of Signaling Pathways Related to Cancer Stemness. *Front Oncol* (2020) 10:1533. doi: 10.3389/fonc.2020.01533
20. Liu S, Ren J, Ten Dijke P. Targeting Tgfβ Signal Transduction for Cancer Therapy. *Signal Transduct Target Ther* (2021) 6(1):8. doi: 10.1038/s41392-020-00436-9
21. Dorritie KA, Redner RL, Johnson DE. STAT Transcription Factors in Normal and Cancer Stem Cells. *Adv Biol Regul* (2014) 56:30–44. doi: 10.1016/j.jbior.2014.05.004
22. Xia P, Xu XY. Pi3k/Akt/mTOR Signaling Pathway in Cancer Stem Cells: From Basic Research to Clinical Application. *Am J Cancer Res* (2015) 5 (5):1602–9.
23. Healy FM, Prior IA, MacEwan DJ. The Importance of Ras in Drug Resistance in Cancer. *Br J Pharmacol* (2021). doi: 10.1111/bph.15420
24. Tan FH, Putoczki TL, Stylli SS, Luwor RB. The Role of STAT3 Signaling in Mediating Tumor Resistance to Cancer Therapy. *Curr Drug Targets* (2014) 15(14):1341–53. doi: 10.2174/1389450115666141120104146
25. Semba T, Sammons R, Wang X, Xie X, Dalby KN, Ueno NT, et al. Jnk Signaling in Stem Cell Self-Renewal and Differentiation. *Int J Mol Sci* (2020) 21(7):2613. doi: 10.3390/ijms21072613
26. Matozaki T, Kotani T, Murata Y, Saito Y. Roles of Src Family Kinase, Ras, and mTOR Signaling in Intestinal Epithelial Homeostasis and Tumorigenesis. *Cancer Sci* (2021) 112(1):16–21. doi: 10.1111/cas.14702
27. Shah AN, Gallick GE. Src, Chemoresistance and Epithelial to Mesenchymal Transition: Are They Related? *Anticancer Drugs* (2007) 18(4):371–5. doi: 10.1097/CAD.0b013e32801265d7
28. Bhanumathy KK, Balagopal A, Vizeacoumar FS, Vizeacoumar FJ, Freywald A, Giambra V, et al. Protein Tyrosine Kinases: Their Roles and Their Targeting in Leukemia. *Cancers (Basel)* (2021) 13(2):184. doi: 10.3390/cancers13020184
29. O'Reilly KE, Rojo F, She QB, Solit D, Mills GB, Smith D, et al. mTOR Inhibition Induces Upstream Receptor Tyrosine Kinase Signaling and Activates Akt. *Cancer Res* (2006) 66(3):1500–8. doi: 10.1158/0008-5472.CAN-05-2925
30. Carracedo A, Ma L, Teruya-Feldstein J, Rojo F, Salmena L, Alimonti A, et al. Inhibition of mTORC1 Leads to MAPK Pathway Activation Through a PI3K-Dependent Feedback Loop in Human Cancer. *J Clin Invest* (2008) 118 (9):3065–74. doi: 10.1172/JCI34739
31. Chen Y, Guggisberg N, Jorda M, Gonzalez-Angulo A, Hennessy B, Mills GB, et al. Combined Src and Aromatase Inhibition Impairs Human Breast Cancer Growth In Vivo and Bypass Pathways Are Activated in AZD0530-resistant Tumors. *Clin Cancer Res* (2009) 15(10):3396–405. doi: 10.1158/1078-0432.CCR-08-3127
32. Chen Y, Alvarez EA, Azzam D, Wander SA, Guggisberg N, Jordà M, et al. Combined Src and ER Blockade Impairs Human Breast Cancer Proliferation In Vitro and *In Vivo*. *Breast Cancer Res Treat* (2011) 128(1):69–78. doi: 10.1007/s10549-010-1024-7
33. Simpkins F, Jang K, Yoon H, Hew KE, Kim M, Azzam DJ, et al. Dual Src and MEK Inhibition Decreases Ovarian Cancer Growth and Targets Tumor Initiating Stem-Like Cells. *Clin Cancer Res* (2018) 24(19):4874–86. doi: 10.1158/1078-0432.CCR-17-3697
34. Wee S, Jagani Z, Xiang KX, Loo A, Dorsch M, Yao YM, et al. PI3K Pathway Activation Mediates Resistance to MEK Inhibitors in KRAS Mutant Cancers. *Cancer Res* (2009) 69(10):4286–93. doi: 10.1158/0008-5472.CAN-08-4765
35. Bell JB, Eckerdt F, Dhruv HD, Finlay D, Peng S, Kim S, et al. Differential Response of Glioma Stem Cells to Arsenic Trioxide Therapy Is Regulated by MNK1 and mRNA Translation. *Mol Cancer Res* (2018) 16(1):32–46. doi: 10.1158/1541-7786.MCR-17-0397
36. Jiang X, Mak PY, Mu H, Tao W, Mak DH, Kornblau S, et al. Disruption of Wnt/beta-Catenin Exerts Antileukemia Activity and Synergizes With FLT3 Inhibition in FLT3-Mutant Acute Myeloid Leukemia. *Clin Cancer Res* (2018) 24(10):2417–29. doi: 10.1158/1078-0432.CCR-17-1556
37. Ma S, Yang LL, Niu T, Cheng C, Zhong L, Zheng MW, et al. Sklb-677, An FLT3 and Wnt/beta-Catenin Signaling Inhibitor, Displays Potent Activity in Models of FLT3-Driven Aml. *Sci Rep* (2015) 5:15646. doi: 10.1038/srep15646
38. Bai LY, Chiu CF, Lin CW, Hsu NY, Lin CL, Lo WJ, et al. Differential Expression of Sonic Hedgehog and Gli1 in Hematological Malignancies. *Leukemia* (2008) 22(1):226–8. doi: 10.1038/sj.leu.2404978
39. Hofmann I, Stover EH, Cullen DE, Mao J, Morgan KJ, Lee BH, et al. Hedgehog Signaling Is Dispensable for Adult Murine Hematopoietic Stem Cell Function and Hematopoiesis. *Cell Stem Cell* (2009) 4(6):559–67. doi: 10.1016/j.stem.2009.03.016
40. Gao J, Graves S, Koch U, Liu S, Jankovic V, Buonamici S, et al. Hedgehog Signaling Is Dispensable for Adult Hematopoietic Stem Cell Function. *Cell Stem Cell* (2009) 4(6):548–58. doi: 10.1016/j.stem.2009.03.015
41. Lu FL, Yu CC, Chiu HH, Liu HE, Chen SY, Lin S, et al. Sonic Hedgehog Antagonists Induce Cell Death in Acute Myeloid Leukemia Cells With the Presence of Lipopolysaccharides, Tumor Necrosis Factor-Alpha, or Interferons. *Invest New Drugs* (2013) 31(4):823–32. doi: 10.1007/s10637-012-9908-5

42. Long B, Wang LX, Zheng FM, Lai SP, Xu DR, Hu Y, et al. Targeting GLI1 Suppresses Cell Growth and Enhances Chemosensitivity in CD34+ Enriched Acute Myeloid Leukemia Progenitor Cells. *Cell Physiol Biochem* (2016) 38 (4):1288–302. doi: 10.1159/000443075
43. Queiroz KC, Ruela-de-Sousa RR, Fuhler GM, Aberson HL, Ferreira CV, Peppelenbosch MP, et al. Hedgehog Signaling Maintains Chemoresistance in Myeloid Leukemic Cells. *Oncogene* (2010) 29(48):6314–22. doi: 10.1038/onc.2010.375
44. Konopleva M, Milella M, Ruvolo P, Watts JC, Ricciardi MR, Korchin B, et al. MEK Inhibition Enhances ABT-737-Induced Leukemia Cell Apoptosis Via Prevention of ERK-Activated MCL-1 Induction and Modulation of MCL-1/BIM Complex. *Leukemia* (2012) 26(4):778–87. doi: 10.1038/leu.2011.287
45. Pei XY, Dai Y, Tenorio S, Lu J, Harada H, Dent P, et al. MEK1/2 Inhibitors Potentiate UCN-01 Lethality in Human Multiple Myeloma Cells Through a Bim-Dependent Mechanism. *Blood* (2007) 110(6):2092–101. doi: 10.1182/blood-2007-04-083204
46. Han L, Zhang Q, Dail M, Shi C, Cavazos A, Ruvolo VR, et al. Concomitant Targeting of BCL2 With Venetoclax and MAPK Signaling With Cobimetinib in Acute Myeloid Leukemia Models. *Haematologica* (2020) 105(3):697–707. doi: 10.3324/haematol.2018.205534
47. Schenone S, Brullo C, Musumeci F, Botta M, et al. Novel Dual Src/Abl Inhibitors for Hematologic and Solid Malignancies. *Expert Opin Investig Drugs* (2010) 19(8):931–45. doi: 10.1517/13543784.2010.499898
48. Araujo J, Logothetis C. Dasatinib: A Potent SRC Inhibitor in Clinical Development for the Treatment of Solid Tumors. *Cancer Treat Rev* (2010) 36(6):492–500. doi: 10.1016/j.ctrv.2010.02.015
49. Dos Santos C, McDonald T, Ho YW, Liu H, Lin A, Forman SJ, et al. The Src and c-Kit Kinase Inhibitor Dasatinib Enhances p53-Mediated Targeting of Human Acute Myeloid Leukemia Stem Cells by Chemotherapeutic Agents. *Blood* (2013) 122(11):1900–13. doi: 10.1182/blood-2012-11-466425
50. Zeng Z, Wang RY, Qiu YH, Mak DH, Coombes K, Yoo SY, et al. MLN0128, a Novel mTOR Kinase Inhibitor, Disrupts Survival Signaling and Triggers Apoptosis in AML and AML Stem/Progenitor Cells. *Oncotarget* (2016) 7 (34):55083–97. doi: 10.18632/oncotarget.10397
51. Valent P. Emerging Stem Cell Concepts for Imatinib-Resistant Chronic Myeloid Leukaemia: Implications for the Biology, Management, and Therapy of the Disease. *Br J Haematol* (2008) 142(3):361–78. doi: 10.1111/j.1365-2141.2008.07197.x
52. Coppo P, Flamant S, De Mas V, Jarrier P, Guillier M, Bonnet ML, et al. Bcr-ABL Activates STAT3 *Via* JAK and MEK Pathways in Human Cells. *Br J Haematol* (2006) 134(2):171–9. doi: 10.1111/j.1365-2141.2006.06161.x
53. Stella S, Tirrò E, Conte E, Stagno F, Di Raimondo F, Manzella L, et al. Suppression of Survivin Induced by a BCR-ABL/JAK2/STAT3 Pathway Sensitizes Imatinib-Resistant CML Cells to Different Cytotoxic Drugs. *Mol Cancer Ther* (2013) 12(6):1085–98. doi: 10.1158/1535-7163.MCT-12-0550
54. Traer E, MacKenzie R, Snead J, Agarwal A, Eiring AM, O'Hare T, et al. Blockade of JAK2-Mediated Extrinsic Survival Signals Restores Sensitivity of CML Cells to ABL Inhibitors. *Leukemia* (2012) 26(5):1140–3. doi: 10.1038/leu.2011.325
55. Warsch W, Walz C, Sexl V. JAK of All Trades: JAK2-STAT5 as Novel Therapeutic Targets in BCR-ABL1+ Chronic Myeloid Leukemia. *Blood* (2013) 122(13):2167–75. doi: 10.1182/blood-2013-02-485573
56. Zimmerman EI, Dollins CM, Crawford M, Grant S, Nana'Sinkam SP, Richards KL, et al. Lyn Kinase-Dependent Regulation of miR181 and Myeloid Cell Leukemia-1 Expression: Implications for Drug Resistance in Myelogenous Leukemia. *Mol Pharmacol* (2010) 78(5):811–7. doi: 10.1124/mol.110.066258
57. Eiring AM, Page BDG, Kraft IL, Mason CC, Vellore NA, Resetca D, et al. Combined STAT3 and BCR-ABL1 Inhibition Induces Synthetic Lethality in Therapy-Resistant Chronic Myeloid Leukemia. *Leukemia* (2015) 29(3):586–97. doi: 10.1038/leu.2014.245
58. Gleixner KV, Schneeweiss M, Eisenwort G, Berger D, Herrmann H, Blatt K, et al. Combined Targeting of STAT3 and STAT5: A Novel Approach to Overcome Drug Resistance in Chronic Myeloid Leukemia. *Haematologica* (2017) 102(9):1519–29. doi: 10.3324/haematol.2016.163436
59. Mayerhofer M, Florian S, Krauth MT, Aichberger KJ, Bilban M, Marculescu R, et al. Identification of Heme Oxygenase-1 as a Novel BCR/ABL-Dependent Survival Factor in Chronic Myeloid Leukemia. *Cancer Res* (2004) 64(9):3148–54. doi: 10.1158/0008-5472.can-03-1200
60. Kinzler KW, Bigner SH, Bigner DD, Trent JM, Law ML, O'Brien SJ, et al. Identification of an Amplified, Highly Expressed Gene in a Human Glioma. *Science* (1987) 236(4797):70–3. doi: 10.1126/science.3563490
61. Dixit D, Ghildiyal R, Anto NP, Ghosh S, Sharma V, Sen E, et al. Guggulsterone Sensitizes Glioblastoma Cells to Sonic Hedgehog Inhibitor SANT-1 Induced Apoptosis in a Ras/NFkappaB Dependent Manner. *Cancer Lett* (2013) 336(2):347–58. doi: 10.1016/j.canlet.2013.03.025
62. Stupp R, Mason WP, van den Bent MJ, Weller M, Fisher B, Taphoorn MJ, et al. Radiotherapy Plus Concomitant and Adjuvant Temozolomide for Glioblastoma. *N Engl J Med* (2005) 352(10):987–96. doi: 10.1056/NEJMoa043330
63. Shi L, Fei X, Wang Z. Demethoxycurcumin Was Prior to Temozolomide on Inhibiting Proliferation and Induced Apoptosis of Glioblastoma Stem Cells. *Tumour Biol* (2015) 36(9):7107–19. doi: 10.1007/s13277-015-3427-x
64. Pan E, Supko JG, Kaley TJ, Butowski NA, Cloughesy T, Jung J, et al. Phase I Study of RO4929097 With Bevacizumab in Patients With Recurrent Malignant Glioma. *J Neurooncol* (2016) 130(3):571–9. doi: 10.1007/s11060-016-2263-1
65. Xu DD, Zhou PJ, Wang Y, Zhang L, Fu WY, Ruan BB, et al. Reciprocal Activation Between STAT3 and miR-181b Regulates the Proliferation of Esophageal Cancer Stem-Like Cells Via the CYLD Pathway. *Mol Cancer* (2016) 15(1):40. doi: 10.1186/s12943-016-0521-7
66. Nghiemphu PL, Wen PY, Lamborn KR, Drappatz J, Robins HI, Fink K, et al. A Phase I Trial of Tipifarnib With Radiation Therapy, With and Without Temozolomide, for Patients With Newly Diagnosed Glioblastoma. *Int J Radiat Oncol Biol Phys* (2011) 81(5):1422–7. doi: 10.1016/j.ijrobp.2010.07.1997
67. Yust-Katz S, Liu D, Yuan Y, Liu V, Kang S, Groves M, et al. Phase 1/1b Study of Lonafarnib and Temozolomide in Patients With Recurrent or Temozolomide Refractory Glioblastoma. *Cancer* (2013) 119(15):2747–53. doi: 10.1002/cncr.28031
68. Ma Y, Cheng Z, Liu J, Torre-Healy L, Lathia JD, Nakano I, et al. Inhibition of Farnesyltransferase Potentiates NOTCH-Targeted Therapy Against Glioblastoma Stem Cells. *Stem Cell Rep* (2017) 9(6):1948–60. doi: 10.1016/j.stemcr.2017.10.028
69. Yahyanejad S, King H, Iglesias VS, Granton PV, Barbeau LM, van Hoof SJ, et al. NOTCH Blockade Combined With Radiation Therapy and Temozolomide Prolongs Survival of Orthotopic Glioblastoma. *Oncotarget* (2016) 7(27):41251–64. doi: 10.18632/oncotarget.9275
70. Lagadec C, Vlashi E, Alhiyari Y, Phillips TM, Bochkur Dratver M, Pajonk F, et al. Radiation-Induced Notch Signaling in Breast Cancer Stem Cells. *Int J Radiat Oncol Biol Phys* (2013) 87(3):609–18. doi: 10.1016/j.ijrobp.2013.06.2064
71. Mizugaki H, Sakakibara-Konishi J, Ikezawa Y, Kikuchi J, Kikuchi E, Oizumi S, et al. gamma-Secretase Inhibitor Enhances Antitumour Effect of Radiation in Notch-Expressing Lung Cancer. *Br J Cancer* (2012) 106(12):1953–9. doi: 10.1038/bjc.2012.178
72. Melisi D, Ishiyama S, Sclabas GM, Fleming JB, Xia Q, Tortora G, et al. LY2109761, a Novel Transforming Growth Factor Beta Receptor Type I and Type II Dual Inhibitor, as a Therapeutic Approach to Suppressing Pancreatic Cancer Metastasis. *Mol Cancer Ther* (2008) 7(4):829–40. doi: 10.1158/1535-7163.MCT-07-0337
73. Fransvea E, Angelotti U, Antonaci S, Giannelli G. Blocking Transforming Growth Factor-Beta Up-Regulates E-Cadherin and Reduces Migration and Invasion of Hepatocellular Carcinoma Cells. *Hepatology* (2008) 47(5):1557–66. doi: 10.1002/hep.22201
74. Zhang B, Halder SK, Zhang S, Datta PK. Targeting Transforming Growth Factor-Beta Signaling in Liver Metastasis of Colon Cancer. *Cancer Lett* (2009) 277(1):114–20. doi: 10.1016/j.canlet.2008.11.035
75. Zhang M, Kleber S, Röhrich M, Timke C, Han N, Tuettenberg J, et al. Blockade of TGF-Beta Signaling by the TGFbetaR-I Kinase Inhibitor LY2109761 Enhances Radiation Response and Prolongs Survival in Glioblastoma. *Cancer Res* (2011) 71(23):7155–67. doi: 10.1158/0008-5472.CAN-11-1212
76. Sunayama J, Matsuda K, Sato A, Tachibana K, Suzuki K, Narita Y, et al. Crosstalk Between the PI3K/mTOR and MEK/ERK Pathways Involved in

the Maintenance of Self-Renewal and Tumorigenicity of Glioblastoma Stem-Like Cells. *Stem Cells* (2010) 28(11):1930–9. doi: 10.1002/stem.521
77. Kahn J, Hayman TJ, Jamal M, Rath BH, Kramp T, Camphausen K, et al. The mTORC1/mTORC2 Inhibitor AZD2014 Enhances the Radiosensitivity of Glioblastoma Stem-Like Cells. *Neuro Oncol* (2014) 16(1):29–37. doi: 10.1093/neuonc/not139
78. Pareja F, Macleod D, Shu C, Crary JF, Canoll PD, Ross AH, et al. PI3K and Bcl-2 Inhibition Primes Glioblastoma Cells to Apoptosis Through Downregulation of Mcl-1 and Phospho-BAD. *Mol Cancer Res* (2014) 12 (7):987–1001. doi: 10.1158/1541-7786.MCR-13-0650
79. Ong DST, Hu B, Ho YW, Sauvé CG, Bristow CA, Wang Q, et al. PAF Promotes Stemness and Radioresistance of Glioma Stem Cells. *Proc Natl Acad Sci USA* (2017) 114(43):E9086–95. doi: 10.1073/pnas.1708122114
80. Wang X, Jung YS, Jun S, Lee S, Wang W, Schneider A, et al. Paf-Wnt Signaling-Induced Cell Plasticity Is Required for Maintenance of Breast Cancer Cell Stemness. *Nat Commun* (2016) 7:10633. doi: 10.1038/ncomms10633
81. Shi Y, Guryanova OA, Zhou W, Liu C, Huang Z, Fang X, et al. Ibrutinib Inactivates BMX-STAT3 in Glioma Stem Cells to Impair Malignant Growth and Radioresistance. *Sci Transl Med* (2018) 10(443):1–13. doi: 10.1126/scitranslmed.aah6816
82. Guryanova OA, Wu Q, Cheng L, Lathia JD, Huang Z, Yang J, et al. Nonreceptor Tyrosine Kinase BMX Maintains Self-Renewal and Tumorigenic Potential of Glioblastoma Stem Cells by Activating STAT3. *Cancer Cell* (2011) 19(4):498–511. doi: 10.1016/j.ccr.2011.03.004
83. Fox JL, Storey A. Bmx Negatively Regulates BAK Function, Thereby Increasing Apoptotic Resistance to Chemotherapeutic Drugs. *Cancer Res* (2015) 75(7):1345–55. doi: 10.1158/0008-5472.CAN-14-1340
84. Zhang Z, Zhu W, Zhang J, Guo L, et al. Tyrosine Kinase Etk/BMX Protects Nasopharyngeal Carcinoma Cells From Apoptosis Induced by Radiation. *Cancer Biol Ther* (2011) 11(7):690–8. doi: 10.4161/cbt.11.7.15060
85. Ballester LY, Wang Z, Shandilya S, Miettinen M, Burger PC, Eberhart CG, et al. Morphologic Characteristics and Immunohistochemical Profile of Diffuse Intrinsic Pontine Gliomas. *Am J Surg Pathol* (2013) 37(9):1357–64. doi: 10.1097/PAS.0b013e318294e817
86. Sturm D, Witt H, Hovestadt V, Khuong-Quang DA, Jones DT, Konermann C, et al. Hotspot Mutations in H3F3A and IDH1 Define Distinct Epigenetic and Biological Subgroups of Glioblastoma. *Cancer Cell* (2012) 22(4):425–37. doi: 10.1016/j.ccr.2012.08.024
87. Paugh SW, Stocco G, Evans WE. Pharmacogenomics in Pediatric Leukemia. *Curr Opin Pediatr* (2010) 22(6):703–10. doi: 10.1097/MOP.0b013e32833fde85
88. Khuong-Quang DA, Buczkowicz P, Rakopoulos P, Liu XY, Fontebasso AM, Bouffet E, et al. K27M Mutation in Histone H3.3 Defines Clinically and Biologically Distinct Subgroups of Pediatric Diffuse Intrinsic Pontine Gliomas. *Acta Neuropathol* (2012) 124(3):439–47. doi: 10.1007/s00401-012-0998-0
89. Taylor IC, Hütt-Cabezas M, Brandt WD, Kambhampati M, Nazarian J, Chang HT, et al. Disrupting NOTCH Slows Diffuse Intrinsic Pontine Glioma Growth, Enhances Radiation Sensitivity, and Shows Combinatorial Efficacy With Bromodomain Inhibition. *J Neuropathol Exp Neurol* (2015) 74(8):778–90. doi: 10.1097/NEN.0000000000000216
90. Eckerdt F, Bell JB, Beauchamp EM, Clymer J, Blyth GT, Kosciuczuk EM, et al. Potent Antineoplastic Effects of Combined Pi3kalpha-Mnk Inhibition in Medulloblastoma. *Mol Cancer Res* (2019) 17(6):1305–15. doi: 10.1158/1541-7786.MCR-18-1193
91. Kim KW, Kim JY, Qiao J, Clark RA, Powers CM, Correa H, et al. Dual-Targeting AKT2 and ERK in Cancer Stem-Like Cells in Neuroblastoma. *Oncotarget* (2019) 10(54):5645–59. doi: 10.18632/oncotarget.27210
92. Park SY, Kim MJ, Park SA, Kim JS, Min KN, Kim DK, et al. Combinatorial TGF-Beta Attenuation With Paclitaxel Inhibits the Epithelial-to-Mesenchymal Transition and Breast Cancer Stem-Like Cells. *Oncotarget* (2015) 6(35):37526–43. doi: 10.18632/oncotarget.6063
93. Cannito S, Novo E, di Bonzo LV, Busletta C, Colombatto S, Parola M, et al. Epithelial-Mesenchymal Transition: From Molecular Mechanisms, Redox Regulation to Implications in Human Health and Disease. *Antioxid Redox Signal* (2010) 12(12):1383–430. doi: 10.1089/ars.2009.2737
94. Lu H, Tran L, Park Y, Chen I, Lan J, Xie Y, et al. Reciprocal Regulation of DUSP9 and DUSP16 Expression by HIF1 Controls ERK and P38 MAP Kinase Activity and Mediates Chemotherapy-Induced Breast Cancer Stem Cell Enrichment. *Cancer Res* (2018) 78(15):4191–202. doi: 10.1158/0008-5472.CAN-18-0270
95. Wu ZH, Lin C, Liu MM, Zhang J, Tao ZH, Hu XC, et al. Src Inhibition can Synergize With Gemcitabine and Reverse Resistance in Triple Negative Breast Cancer Cells Via the AKT/c-Jun Pathway. *PloS One* (2016) 11(12):e0169230. doi: 10.1371/journal.pone.0169230
96. Fischer MM, Cancilla B, Yeung VP, Cattaruzza F, Chartier C, Murriel CL, et al. WNT Antagonists Exhibit Unique Combinatorial Antitumor Activity With Taxanes by Potentiating Mitotic Cell Death. *Sci Adv* (2017) 3(6): e1700090. doi: 10.1126/sciadv.1700090
97. Gurney A, Axelrod F, Bond CJ, Cain J, Chartier C, Donigan L, et al. Wnt Pathway Inhibition Via the Targeting of Frizzled Receptors Results in Decreased Growth and Tumorigenicity of Human Tumors. *Proc Natl Acad Sci USA* (2012) 109(29):11717–22. doi: 10.1073/pnas.1120068109
98. Jimeno A, Gordon M, Chugh R, Messersmith W, Mendelson D, Dupont J, et al. A First-in-Human Phase I Study of the Anticancer Stem Cell Agent Ipafricept (Omp-54F28), A Decoy Receptor for Wnt Ligands, in Patients With Advanced Solid Tumors. *Clin Cancer Res* (2017) 23(24):7490–7. doi: 10.1158/1078-0432.CCR-17-2157
99. Sun Q, Lesperance J, Wettersten H, Luterstein E, DeRose YS, Welm A, et al. Proapoptotic PUMA Targets Stem-Like Breast Cancer Cells to Suppress Metastasis. *J Clin Invest* (2018) 128(1):531–44. doi: 10.1172/JCI93707
100. Sun Q, Wang Y, Desgrosellier JS. Combined Bcl-2/Src Inhibition Synergize to Deplete Stem-Like Breast Cancer Cells. *Cancer Lett* (2019) 457:40–6. doi: 10.1016/j.canlet.2019.05.004
101. Lu H, Chen I, Shimoda LA, Park Y, Zhang C, Tran L, et al. Chemotherapy-Induced Ca(2+) Release Stimulates Breast Cancer Stem Cell Enrichment. *Cell Rep* (2017) 18(8):1946–57. doi: 10.1016/j.celrep.2017.02.001
102. Manupati K, Debnath S, Goswami K, Bhoj PS, Chandak HS, Bahekar SP, et al. Glutathione S-Transferase Omega 1 Inhibition Activates JNK-Mediated Apoptotic Response in Breast Cancer Stem Cells. *FEBS J* (2019) 286 (11):2167–92. doi: 10.1111/febs.14813
103. Bodenstine TM, Chandler GS, Seftor RE, Seftor EA, Hendrix MJ. Plasticity Underlies Tumor Progression: Role of Nodal Signaling. *Cancer Metastasis Rev* (2016) 35(1):21–39. doi: 10.1007/s10555-016-9605-5
104. Margaryan NV, Hazard-Jenkins H, Salkeni MA, Smolkin MB, Coad JA, Wen S, et al. The Stem Cell Phenotype of Aggressive Breast Cancer Cells. *Cancers (Basel)* (2019) 11(3):340–50. doi: 10.3390/cancers11030340
105. Lonardo E, Hermann PC, Mueller MT, Huber S, Balic A, Miranda-Lorenzo I, et al. Nodal/Activin Signaling Drives Self-Renewal and Tumorigenicity of Pancreatic Cancer Stem Cells and Provides a Target for Combined Drug Therapy. *Cell Stem Cell* (2011) 9(5):433–46. doi: 10.1016/j.stem.2011.10.001
106. Gong Y, Guo Y, Hai Y, Yang H, Liu Y, Yang S, et al. Nodal Promotes the Self-Renewal of Human Colon Cancer Stem Cells Via an Autocrine Manner Through Smad2/3 Signaling Pathway. *BioMed Res Int* (2014) 2014:364134. doi: 10.1155/2014/364134
107. Hardy KM, Strizzi L, Margaryan NV, Gupta K, Murphy GF, Scolyer RA, et al. Targeting Nodal in Conjunction With Dacarbazine Induces Synergistic Anticancer Effects in Metastatic Melanoma. *Mol Cancer Res* (2015) 13 (4):670–80. doi: 10.1158/1541-7786.MCR-14-0077
108. Strizzi L, Hardy KM, Margaryan NV, Hillman DW, Seftor EA, Chen B, et al. Potential for the Embryonic Morphogen Nodal as a Prognostic and Predictive Biomarker in Breast Cancer. *Breast Cancer Res* (2012) 14(3): R75. doi: 10.1186/bcr3185
109. Quail DF, Siegers GM, Jewer M, Postovit LM. Nodal Signalling in Embryogenesis and Tumourigenesis. *Int J Biochem Cell Biol* (2013) 45 (4):885–98. doi: 10.1016/j.biocel.2012.12.021
110. Zhang Y, Jin Z, Zhou H, Ou X, Xu Y, Li H, et al. Suppression of Prostate Cancer Progression by Cancer Cell Stemness Inhibitor Napabucasin. *Cancer Med* (2016) 5(6):1251–8. doi: 10.1002/cam4.675
111. Chang L, Graham PH, Hao J, Ni J, Bucci J, Cozzi PJ, et al. Acquisition of Epithelial-Mesenchymal Transition and Cancer Stem Cell Phenotypes Is Associated With Activation of the PI3K/Akt/mTOR Pathway in Prostate Cancer Radioresistance. *Cell Death Dis* (2013) 4:e875. doi: 10.1038/cddis.2013.407
112. MacDonagh L, Gallagher MF, Ffrench B, Gasch C, Breen E, Gray SG, et al. Targeting the Cancer Stem Cell Marker, Aldehyde Dehydrogenase 1, to

Circumvent Cisplatin Resistance in NSCLC. *Oncotarget* (2017) 8(42):72544–63. doi: 10.18632/oncotarget.19881
113. MacDonagh L, Gray SG, Breen E, Cuffe S, Finn SP, O'Byrne KJ, et al. BBI608 Inhibits Cancer Stemness and Reverses Cisplatin Resistance in NSCLC. *Cancer Lett* (2018) 428:117–26. doi: 10.1016/j.canlet.2018.04.008
114. Roy S, Roy S, Kar M, Padhi S, Saha A, Anuja K, et al. Role of P38 MAPK in Disease Relapse and Therapeutic Resistance by Maintenance of Cancer Stem Cells in Head and Neck Squamous Cell Carcinoma. *J Oral Pathol Med* (2018) 47(5):492–501. doi: 10.1111/jop.12707
115. Siddique HR, Saleem M. Role of BMI1, a Stem Cell Factor, in Cancer Recurrence and Chemoresistance: Preclinical and Clinical Evidences. *Stem Cells* (2012) 30(3):372–8. doi: 10.1002/stem.1035
116. Chen D, Wu M, Li Y, Chang I, Yuan Q, Ekimyan-Salvo M, et al. Targeting BMI1(+) Cancer Stem Cells Overcomes Chemoresistance and Inhibits Metastases in Squamous Cell Carcinoma. *Cell Stem Cell* (2017) 20(5):621–34.e6. doi: 10.1016/j.stem.2017.02.003
117. Hermida-Prado F, Villaronga MÁ, Granda-Díaz R, Del-Río-Ibisate N, Santos L, Hermosilla M, et al. The SRC Inhibitor Dasatinib Induces Stem Cell-Like Properties in Head and Neck Cancer Cells That Are Effectively Counteracted by the Mithralog Ec-8042. *J Clin Med* (2019) 8(8):1157. doi: 10.3390/jcm8081157
118. Tornin J, Martinez-Cruzado L, Santos L, Rodriguez A, Núñez LE, Oro P, et al. Inhibition of SP1 by the Mithramycin Analog EC-8042 Efficiently Targets Tumor Initiating Cells in Sarcoma. *Oncotarget* (2016) 7(21):30935–50. doi: 10.18632/oncotarget.8817
119. Fevr T, Robine S, Louvard D, Huelsken J, et al. Wnt/Beta-Catenin Is Essential for Intestinal Homeostasis and Maintenance of Intestinal Stem Cells. *Mol Cell Biol* (2007) 27(21):7551–9. doi: 10.1128/MCB.01034-07
120. Carethers JM. Systemic Treatment of Advanced Colorectal Cancer: Tailoring Therapy to the Tumor. *Therap Adv Gastroenterol* (2008) 1(1):33–42. doi: 10.1177/1756283X08093607
121. Sinicrope FA, Foster NR, Thibodeau SN, Marsoni S, Monges G, Labianca R, et al. DNA Mismatch Repair Status and Colon Cancer Recurrence and Survival in Clinical Trials of 5-Fluorouracil-Based Adjuvant Therapy. *J Natl Cancer Inst* (2011) 103(11):863–75. doi: 10.1093/jnci/djr153
122. Cho YH, Ro EJ, Yoon JS, Mizutani T, Kang DW, Park JC, et al. 5-FU Promotes Stemness of Colorectal Cancer *Via* P53-Mediated WNT/beta-Catenin Pathway Activation. *Nat Commun* (2020) 11(1):5321. doi: 10.1038/s41467-020-19173-2
123. Nautiyal J, Kanwar SS, Yu Y, Majumdar AP. Combination of Dasatinib and Curcumin Eliminates Chemo-Resistant Colon Cancer Cells. *J Mol Signal* (2011) 6:7. doi: 10.1186/1750-2187-6-7
124. Wu CX, Wang XQ, Chok SH, Man K, Tsang SHY, Chan ACY, et al. Blocking CDK1/PDK1/beta-Catenin Signaling by CDK1 Inhibitor RO3306 Increased the Efficacy of Sorafenib Treatment by Targeting Cancer Stem Cells in a Preclinical Model of Hepatocellular Carcinoma. *Theranostics* (2018) 8 (14):3737–50. doi: 10.7150/thno.25487
125. Duong HQ, Yi YW, Kang HJ, Bae I, Jang YJ, Kwak SJ, et al. Combination of Dasatinib and Gemcitabine Reduces the ALDH1A1 Expression and the Proliferation of Gemcitabine-Resistant Pancreatic Cancer MIA PaCa-2 Cells. *Int J Oncol* (2014) 44(6):2132–8. doi: 10.3892/ijo.2014.2357
126. Hendrix MJ, Kandela I, Mazar AP, Seftor EA, Seftor RE, Margaryan NV, et al. Targeting Melanoma With Front-Line Therapy Does Not Abrogate Nodal-Expressing Tumor Cells. *Lab Invest* (2017) 97(2):176–86. doi: 10.1038/labinvest.2016.107
127. Nolan KD, Kaur J, Isaacs JS. Secreted Heat Shock Protein 90 Promotes Prostate Cancer Stem Cell Heterogeneity. *Oncotarget* (2017) 8(12):19323–41. doi: 10.18632/oncotarget.14252
128. White PT, Subramanian C, Zhu Q, Zhang H, Zhao H, Gallagher R, et al. Novel HSP90 Inhibitors Effectively Target Functions of Thyroid Cancer Stem Cell Preventing Migration and Invasion. *Surgery* (2016) 159(1):142–51. doi: 10.1016/j.surg.2015.07.050
129. Stivarou T, Stellas D, Vartzi G, Thomaidou D, Patsavoudi E, et al. Targeting Highly Expressed Extracellular HSP90 in Breast Cancer Stem Cells Inhibits Tumor Growth In Vitro and *In Vivo*. *Cancer Biol Ther* (2016) 17(8):799–812. doi: 10.1080/15384047.2016.1195041
130. Subramanian C, Kovatch KJ, Sim MW, Wang G, Prince ME, Carey TE, et al. Novel C-Terminal Heat Shock Protein 90 Inhibitors (KU711 and Ku757) Are Effective in Targeting Head and Neck Squamous Cell Carcinoma Cancer Stem Cells. *Neoplasia* (2017) 19(12):1003–11. doi: 10.1016/j.neo.2017.09.003
131. Bocchini CE, Kasembeli MM, Roh SH, Tweardy DJ. Contribution of Chaperones to STAT Pathway Signaling. *JAKSTAT* (2014) 3(3):e970459. doi: 10.4161/21623988.2014.970459
132. Xu DD, Chen SH, Zhou PJ, Wang Y, Zhao ZD, Wang X, et al. Suppression of Esophageal Cancer Stem-Like Cells by SNX-2112 Is Enhanced by STAT3 Silencing. *Front Pharmacol* (2020) 11:532395. doi: 10.3389/fphar.2020.532395
133. Barbato L, Bocchetti M, Di Biase A, Regad T, et al. Cancer Stem Cells and Targeting Strategies. *Cells* (2019) 8(8):926. doi: 10.3390/cells8080926
134. Du FY, Zhou QF, Sun WJ, Chen GL. Targeting Cancer Stem Cells in Drug Discovery: Current State and Future Perspectives. *World J Stem Cells* (2019) 11(7):398–420. doi: 10.4252/wjsc.v11.i7.398
135. Creedon H, Brunton VG. Src Kinase Inhibitors: Promising Cancer Therapeutics? *Crit Rev Oncog* (2012) 17(2):145–59. doi: 10.1615/critrevoncog.v17.i2.20
136. Schuetze SM, Bolejack V, Choy E, Ganjoo KN, Staddon AP, Chow WA, et al. Phase 2 Study of Dasatinib in Patients With Alveolar Soft Part Sarcoma, Chondrosarcoma, Chordoma, Epithelioid Sarcoma, or Solitary Fibrous Tumor. *Cancer* (2017) 123(1):90–7. doi: 10.1002/cncr.30379
137. Scott AJ, Song EK, Bagby S, Purkey A, McCarter M, Gajdos C, et al. Evaluation of the Efficacy of Dasatinib, a Src/Abl Inhibitor, in Colorectal Cancer Cell Lines and Explant Mouse Model. *PLoS One* (2017) 12(11): e0187173. doi: 10.1371/journal.pone.0187173
138. Kalinsky K, Lee S, Rubin KM, Lawrence DP, Iafrarte AJ, Borger DR, et al. A Phase 2 Trial of Dasatinib in Patients With Locally Advanced or Stage IV Mucosal, Acral, or Vulvovaginal Melanoma: A Trial of the ECOG-ACRIN Cancer Research Group (E2607). *Cancer* (2017) 123(14):2688–97. doi: 10.1002/cncr.30663
139. Parseghian CM, Parikh NU, Wu JY, Jiang ZQ, Henderson L, Tian F, et al. Dual Inhibition of EGFR and c-Src by Cetuximab and Dasatinib Combined With FOLFOX Chemotherapy in Patients With Metastatic Colorectal Cancer. *Clin Cancer Res* (2017) 23(15):4146–54. doi: 10.1158/1078-0432.CCR-16-3138
140. Baro M, de Llobet LI, Figueras A, Skvortsova I, Mesia R, Balart J, et al. Dasatinib Worsens the Effect of Cetuximab in Combination With Fractionated Radiotherapy in FaDu- and A431-Derived Xenografted Tumours. *Br J Cancer* (2014) 111(7):1310–8. doi: 10.1038/bjc.2014.432
141. Ammer AG, Kelley LC, Hayes KE, Evans JV, Lopez-Skinner LA, Martin KH, et al. Saracatinib Impairs Head and Neck Squamous Cell Carcinoma Invasion by Disrupting Invadopodia Function. *J Cancer Sci Ther* (2009) 1 (2):52–61. doi: 10.4172/1948-5956.1000009
142. Brooks HD, Glisson BS, Bekele BN, Johnson FM, Ginsberg LE, El-Naggar A, et al. Phase 2 Study of Dasatinib in the Treatment of Head and Neck Squamous Cell Carcinoma. *Cancer* (2011) 117(10):2112–9. doi: 10.1002/cncr.25769
143. Fury MG, Baxi S, Shen R, Kelly KW, Lipson BL, Carlson D, et al. Phase II Study of Saracatinib (AZD0530) for Patients With Recurrent or Metastatic Head and Neck Squamous Cell Carcinoma (HNSCC). *Anticancer Res* (2011) 31(1):249–53.
144. Bauman JE, Duvvuri U, Gooding WE, Rath TJ, Gross ND, Song J, et al. Randomized, Placebo-Controlled Window Trial of EGFR, Src, or Combined Blockade in Head and Neck Cancer. *JCI Insight* (2017) 2(6):e90449. doi: 10.1172/jci.insight.90449
145. Raffaele M, Kovacovicova K, Frohlich J, Lo Re O, Giallongo S, Oben JA, et al. Mild Exacerbation of Obesity- and Age-Dependent Liver Disease Progression by Senolytic Cocktail Dasatinib + Quercetin. *Cell Commun Signal* (2021) 19(1):44. doi: 10.1186/s12964-021-00731-0
146. Singh S, Trevino J, Bora-Singhal N, Coppola D, Haura E, Altiok S, et al. EGFR/Src/Akt Signaling Modulates Sox2 Expression and Self-Renewal of Stem-Like Side-Population Cells in Non-Small Cell Lung Cancer. *Mol Cancer* (2012) 11:73. doi: 10.1186/1476-4598-11-73
147. Bhummaphan N, Pongrakhananon V, Sritularak B, Chanvorachote P. Cancer Stem Cell-Suppressing Activity of Chrysotoxine, A Bibenzyl From Dendrobium Pulchellum. *J Pharmacol Exp Ther* (2018) 364(2):332–46. doi: 10.1124/jpet.117.244467
148. Cazet AS, Hui MN, Elsworth BL, Wu SZ, Roden D, Chan CL, et al. Targeting Stromal Remodeling and Cancer Stem Cell Plasticity Overcomes Chemoresistance in Triple Negative Breast Cancer. *Nat Commun* (2018) 9 (1):2897. doi: 10.1038/s41467-018-05220-6

149. Brown JR, Chan DK, Shank JJ, Griffith KA, Fan H, Szulawski R, et al. Phase II Clinical Trial of Metformin as a Cancer Stem Cell-Targeting Agent in Ovarian Cancer. *JCI Insight* (2020) 5(11):e133247. doi: 10.1172/jci.insight.133247
150. Haapasalo A, Kovacs DM. The Many Substrates of Presenilin/Gamma-Secretase. *J Alzheimers Dis* (2011) 25(1):3–28. doi: 10.3233/JAD-2011-101065
151. Stockhausen MT, Kristoffersen K, Poulsen HS. The Functional Role of Notch Signaling in Human Gliomas. *Neuro Oncol* (2010) 12(2):199–211. doi: 10.1093/neuonc/nop022
152. Abad E, García-Mayea Y, Mir C, Sebastian D, Zorzano A, Potesil D, et al. Common Metabolic Pathways Implicated in Resistance to Chemotherapy Point to a Key Mitochondrial Role in Breast Cancer. *Mol Cell Proteomics* (2019) 18(2):231–44. doi: 10.1074/mcp.RA118.001102
153. Scatena C, Roncella M, Di Paolo A, Aretini P, Menicagli M, Fanelli G, et al. Doxycycline, an Inhibitor of Mitochondrial Biogenesis, Effectively Reduces Cancer Stem Cells (Cscs) in Early Breast Cancer Patients: A Clinical Pilot Study. *Front Oncol* (2018) 8:452. doi: 10.3389/fonc.2018.00452
154. Issa NT, Stathias V, Schürer S, Dakshanamurthy S. Machine and Deep Learning Approaches for Cancer Drug Repurposing. *Semin Cancer Biol* (2021) 68:132–42. doi: 10.1016/j.semcancer.2019.12.011

**Conflict of Interest:** DS is a topic editor of the research topic: Combinatorial approaches for cancer treatment: from basic to translational research.

The remaining author declares that the research was conducted in the absence of any commercial or financial relationships that could be construed as a potential conflict of interest.

**Publisher's Note:** All claims expressed in this article are solely those of the authors and do not necessarily represent those of their affiliated organizations, or those of the publisher, the editors and the reviewers. Any product that may be evaluated in this article, or claim that may be made by its manufacturer, is not guaranteed or endorsed by the publisher.

frontiers in Oncology

SYSTEMATIC REVIEW
published: 29 July 2021
doi: 10.3389/fonc.2021.700407

# Targeting Hypoxia: Hypoxia-Activated Prodrugs in Cancer Therapy

*Yue Li*[1,2,3], *Long Zhao*[1,3] *and Xiao-Feng Li*[1,3]*

[1] Department of Nuclear Medicine, The Second Clinical Medical College, Jinan University (Shenzhen People's Hospital), Shenzhen, China, [2] The First Affiliated Hospital, Jinan University, Guangzhou, China, [3] Department of Nuclear Medicine, The First Affiliated Hospital of Southern University of Science and Technology, Shenzhen, China

Hypoxia is an important characteristic of most solid malignancies, and is closely related to tumor prognosis and therapeutic resistance. Hypoxia is one of the most important factors associated with resistance to conventional radiotherapy and chemotherapy. Therapies targeting tumor hypoxia have attracted considerable attention. Hypoxia-activated prodrugs (HAPs) are bioreductive drugs that are selectively activated under hypoxic conditions and that can accurately target the hypoxic regions of solid tumors. Both single-agent and combined use with other drugs have shown promising antitumor effects. In this review, we discuss the mechanism of action and the current preclinical and clinical progress of several of the most widely used HAPs, summarize their existing problems and shortcomings, and discuss future research prospects.

**Keywords: hypoxia, hypoxia-activated prodrugs, tirapazamine, AQ4N, PR-104, EO9, TH-302, SN30000**

OPEN ACCESS

***Edited by:***
*George Mattheolabakis, University of Louisiana at Monroe, United States*

***Reviewed by:***
*Chia-Che Chang, National Chung Hsing University, Taiwan*
*Saartjie Roux, Nelson Mandela University, South Africa*

***Correspondence:**
*Xiao-Feng Li*
*linucmed@hotmail.com*

***Specialty section:***
*This article was submitted to Pharmacology of Anti-Cancer Drugs, a section of the journal Frontiers in Oncology*

***Received:*** *26 April 2021*
***Accepted:*** *09 July 2021*
***Published:*** *29 July 2021*

***Citation:***
*Li Y, Zhao L and Li X-F (2021) Targeting Hypoxia: Hypoxia-Activated Prodrugs in Cancer Therapy. Front. Oncol. 11:700407. doi: 10.3389/fonc.2021.700407*

## INTRODUCTION

Hypoxia is a hallmark of a wide variety of solid tumors. In tumors, hypoxia arises due to a mismatch between oxygen delivery and consumption. Hypoxia is closely related to tumor progression, metastasis, therapeutic resistance, and poor prognosis (1). Hypoxia in tumor microenvironment leads to the transcriptional induction of a series of genes. The most important factor mediating this response is the hypoxia-inducible factor-1 (HIF-1), which extensively participates in glucose metabolism, angiogenesis, apoptosis, tumor metastasis and therapeutic resistance (2). Under hypoxic condition, HIF-1α regulates the switch from oxidative phosphorylation to anaerobic glycolysis, by activating the expression of glucose transporter 1 and 3 (GLUT-1 and GLUT-3) and related glycolytic enzymes (3). By regulating its downstream angiogenesis related genes, such as vascular endothelial growth factor (VEGF), basic fibroblast growth factor (bFGF), matrix metalloproteinases (MMPs), HIF-1α is widely involved in every step of angiogenesis, including endothelial progenitor cells recruitment and their differentiation to endothelial cells and smooth muscle cells, degradation of extracellular matrix, and the stability of peripheral cells (4). HIF-1α could induce apoptosis by regulating p53, Bcl-2, BNIP-3 and other genes (5). Through induction of MMPs, E-cadherin, CXCR4, CA9, HIF could promote tumor invasion and metastasis by regulating epithelial-to-mesenchymal transition (EMT) (6).

Tumor cells response to hypoxia depends in part on the duration of exposure. Hypoxic tumor cells may undergo necrosis, but some of the tumor cells may adjust to hypoxic stress and survive, which is also mediated by HIF-1α, resulting in a more aggressive phenotype and therapeutic resistance (5). Hypoxia and HIF could induce cell cycle arrest and hypoxic tumor cells generally

have a relatively low proliferation rate (7, 8), while radiotherapy or chemotherapy mainly act on proliferating cells (9–11). Therefore, the hypoxic regions of tumors are usually insensitive to current radiotherapy and chemotherapy, and treatments targeting the hypoxic regions may provide additional clinical benefits. To this end, increasing efforts have been focused on the development of agents that selectively target and kill hypoxic tumor cells.

Hypoxia-activated prodrugs (HAPs), also referred to as bioreductive drugs, are compounds that can be selectively reduced by specific reductases under hypoxic conditions to form cytotoxic agents that precisely target hypoxic tumor cells and have little toxicity to normal tissue. At present, several classes of HAPs have been developed, including quinones, nitroaromatics, aliphatic N-oxides and hetero-aromatic N-oxides. The most representative ones are tirapazamine, AQ4N (banoxantrone), PR-104, EO9 (apaziquone), TH-302 (evofosfamide), and SN30000 (**Figure 1**). This review puts a special emphasis on the past achievements as well as limitations of HAPs and attempts to analyze the potential reasons for unsuccessful clinical trials, with the aim of guiding future investigations into optimizing the use of this therapeutic approach.

## TIRAPAZAMINE

Tirapazamine (SR-4233, WIN 59075) [3-amino-1,2,4-benzotriazine-1,4 dioxide], the first hypoxia-activated prodrug, was reported in 1986 (12). Through one-electron reduction, the prodrug can generate an oxidative radical, which will diffuse into hypoxic regions and cause oxidative damage (13) (**Figure 2**). Cytochrome P-450 (CYP) is the main catalytic reductase involved in the reduction of tirapazamine (14). Although evidence showed that tirapazamine is a substrate for NAD(P)H: (quinone acceptor) oxidoreductase (DT-diaphorase) (15), the amount of DT-diaphorase expression in cells did not affect their sensitivity to tirapazamine (16).

Tirapazamine kills hypoxic cells by inducing chromosome aberrations and DNA double-strand breaks (17). Chromosome breaks caused by tirapazamine were more damaging and difficult to repair (18). Under hypoxic conditions, tirapazamine causes damage to both purine and pyrimidine residues in double-stranded DNA. DNA base damage was dominated by formation of formamidopyrimidine and 5-hydroxy-6-hydropyrimidine (19, 20). The DNA damaging activity of tirapazamine mainly results from radicals generated within the nucleus but not in the cytoplasm (21). Tirapazamine can induce acute changes in energy metabolism and intracellular pH in tumors (22). Skarsgard et al. (23) found that tirapazamine-induced DNA damage was pH-dependent (more effective at acidic pH) and could be repaired by certain gene products including uvrC and exonuclease III (24). The affinity of tirapazamine for hypoxic tissues was confirmed by many researchers but Durand and Olive demonstrated that this selectivity of tirapazamine was much lower *in vivo* (3 fold higher than aerobic) than that observed *in vitro* (50-500 fold) (25). Under aerobic conditions, tirapazamine can still induce cell cycle interruption and apoptosis, which may lead to its aerobic toxicity (26).

In preclinical studies, tirapazamine effectively inhibited tumor colony-forming *in vitro*, especially in hypoxic cells (27). Tirapazamine induced cell cycle arrest and apoptosis, and down-regulated HIF-1α, CA-IX and VEGF expression (28, 29). Brown (30) suggested that the activity of tirapazamine was p53-independent, but Yang's study on neuroblastoma revealed that tirapazamine had clinical activity only in p53-functional neuroblastoma (31). Zeman and Brown published a series of reports focusing on the radiosensitization effects of tirapazamine. They reported that tirapazamine enhanced radiation-induced

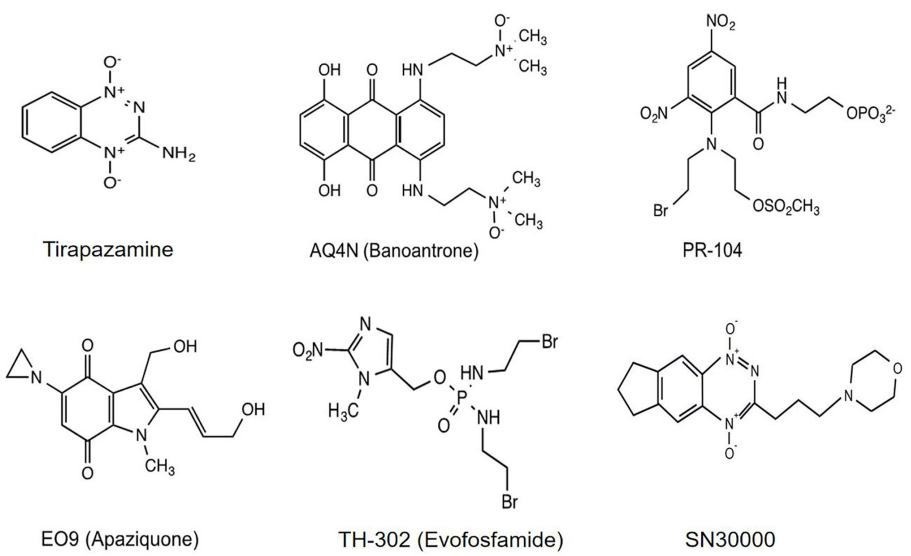


**FIGURE 1** | Chemical structures of representative HAPs.

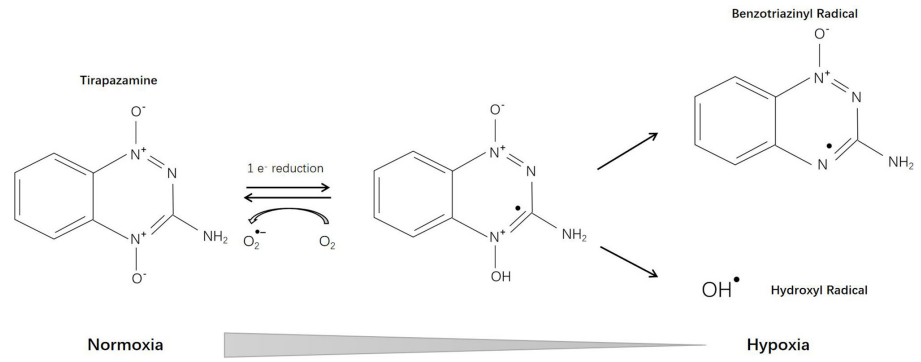


**FIGURE 2** | Reductive reaction of tirapazamine.

antineoplastic effects while sparing normal tissues (12, 32–38). As flavone acetic acid (FAA) reduces the blood supply of tumors, tirapazamine in combination with FAA could significantly enhance the antineoplastic efficacy of both drugs (39). Many studies have investigated the synergistic effect of tirapazamine and chemotherapy (such as cyclophosphamide, cisplatin, paclitaxel, etc.) or radioimmunotherapy (40–45). Tirapazamine, together with hyperthermia, electric pulses, etc. also exhibited encouraging antineoplastic efficacy (46–49). However, studies conducted by Adam et al. (50, 51) demonstrated that tirapazamine plus cisplatin and/or irradiation significantly increased toxicity and mortality.

In clinical trials, the reported adverse events associated with tirapazamine included muscle cramping, ototoxicity, granulocytopenia, nausea and vomiting, etc. (52, 53). Most phase 1 and 2 clinical trials have shown encouraging antineoplastic efficacy and tolerable toxicity (54–60). However, others, as well as two phase 3 clinical studies showed little benefit or significant toxicity (61–65).

## AQ4N

AQ4N [1,4-bis{[2-(dimethylamino-N-oxide)ethyl]amino}-5,8-dihydroxyanthracene-9,10-dione], an aliphatic N-oxide, was first reported in 1993 (66). Its prodrug has no intrinsic DNA binding affinity and thus is non-toxic. Under hypoxic conditions, AQ4N can be activated into AQ4 (with an intermediate product AQ4M) through a two-electron reduction mediated by CYP, which is DNA-affinic and possesses 1000-fold cytotoxic potency compared with its prodrug (**Figure 3**). During the subsequent decade, Patterson and his team deeply investigated the pharmacology of AQ4N. They demonstrated that AQ4N combined with radiotherapy or chemotherapy (cisplatin, cyclophosphamide, thiotepa, mitoxantrone) showed enhanced antineoplastic effects (67–70). In 2003, they proposed a gene-directed enzyme prodrug therapy (GDEPT) strategy using CYPs in order to facilitate the bioreduction of AQ4N (71). Other researchers also investigated the activation of AQ4N by different types of CYPs and nitric oxide synthase (NOS) (72–75).

Many researchers have confirmed that AQ4N exerts antitumor effects in preclinical models of pancreatic cancer (76), bladder cancer and lung cancer (77), prostate cancer (78), gliosarcoma (79), etc., in both single-agent and combined chemotherapy, and in radiotherapy. Gieling et al. (80) demonstrated that AQ4N was more effective toward metastases in a fibrosarcoma-bearing mouse model (subcutaneous KHT tumors). Trédan et al. compared the penetration capacity of AQ4N and mitoxantrone through multi-layer cell cultures and

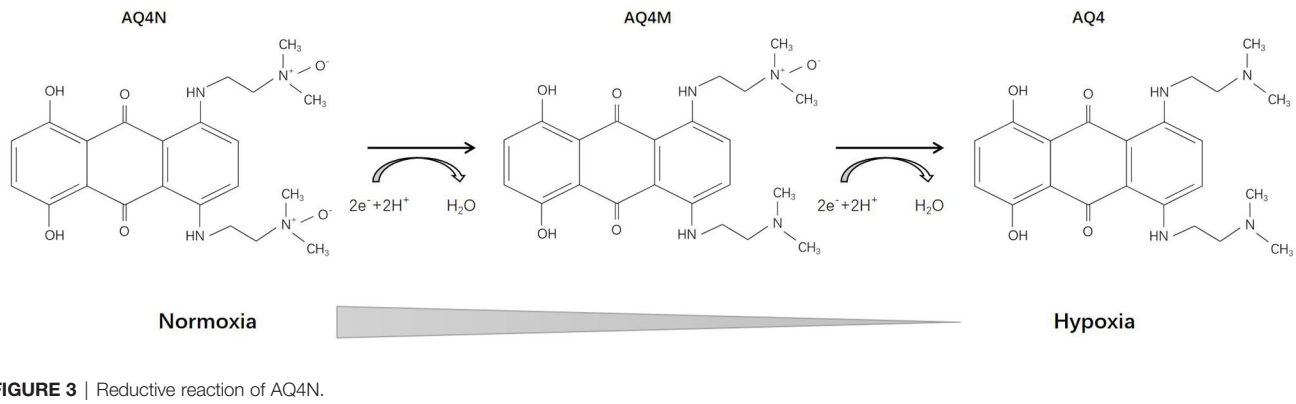


**FIGURE 3** | Reductive reaction of AQ4N.

tumor xenografts, and found that AQ4N could penetrate deeply into the hypoxic regions of the tumor and that combination therapy of AQ4N with mitoxantrone showed decreased tumor growth (81). There is also evidence showed that AQ4N had anti-angiogenic effects (82, 83).

The first phase 1 study of AQ4N was reported in 2007, in which 22 esophageal carcinoma patients received an AQ4N infusion followed by fractionated radiotherapy (84). Three of 22 patients had > 50% reductions in tumor volume and 9 had stable disease without dose-limiting toxicity. Albertella et al. enrolled 32 patients with different malignancies in a phase 1 study, and demonstrated that AQ4N was activated selectively in hypoxic regions of tumors and that it can penetrate the blood-brain barrier (85). No objective antitumor effect was observed in another phase 1 clinical study conducted by Papadopoulos et al. (86).

In recent years, a series of new therapeutic strategies have been under development, including combination therapy with AQ4N and photodynamic therapy (PDT), vascular-targeted photodynamic therapy (VTP) (87–92). Feng et al. (93) developed a treatment strategy that combined PDT with AQ4N. Using an AQ4N-64Cu-hCe6-liposome *in vivo* PET probe, they were able to monitor tumor hypoxia status after illumination with light-emitting diode light and demonstrated that utilization of PDT-induced hypoxia to trigger hypoxia-targeted therapy achieved significant antineoplastic effects. Zhang et al. (94) showed that AQ4N combined with starvation therapy (by using stealth liposomes to deliver glucose oxidase together with prodrugs) exhibited similar enhancement of antitumor effects. These methodologies provide new insights for future cancer diagnosis and therapy.

## PR-104

PR-104 is a 3,5-dinitrobenzamide-2-mustard. The water-soluble phosphate PR-104 can transform to a more lipophilic prodrug PR-104A (3,5-dinitrobenzamide-2-nitrogen mustard) systemically, and then, under hypoxic conditions, it can be further activated by reduction to PR-104H (5-hydroxylamine) and PR-104M (5-amine), allowing it to act as a DNA interstrand cross-linking agent in hypoxic cells and exert cytotoxic effects (95) (**Figure 4**). The reduction reaction is catalyzed anaerobically mainly by NADPH-cytochrome P450 reductase (96). There are studies demonstrating that PR-104 may also be reduced by aldo-keto reductase (AKR) 1C3 anaerobically, which might cause systemic toxicity (97, 98). The sensitivity of PR-104 depends on the oxygenation status, reductase activity, and DNA repair ability (99). Two studies have revealed the bystander effect of PR-104 (100, 101).

In *in vitro* studies, the antitumor efficacy of PR-104 has been investigated in cervical squamous cell carcinoma (SiHa cells), ovarian carcinoma (A2780 cells), non-small cell lung carcinoma (H1299 and A549 cells), colorectal carcinoma (RKO and HCT116 cells), hepatocellular carcinoma, etc., PR-104 as a single agent or in combination with radiotherapy or chemotherapy has shown different degrees of antineoplastic effects (95, 102–104).

In clinical trials, however, no or only partial responses were observed, but with obvious toxicities, mainly thrombocytopenia and neutropenia (105–108). However, PR-104 showed advantages in the treatment of leukemia. Evidence showed that in acute lymphoblastic leukemia, T-cell acute lymphoblastic leukemia, and acute myeloid leukemia, PR-104 decreased

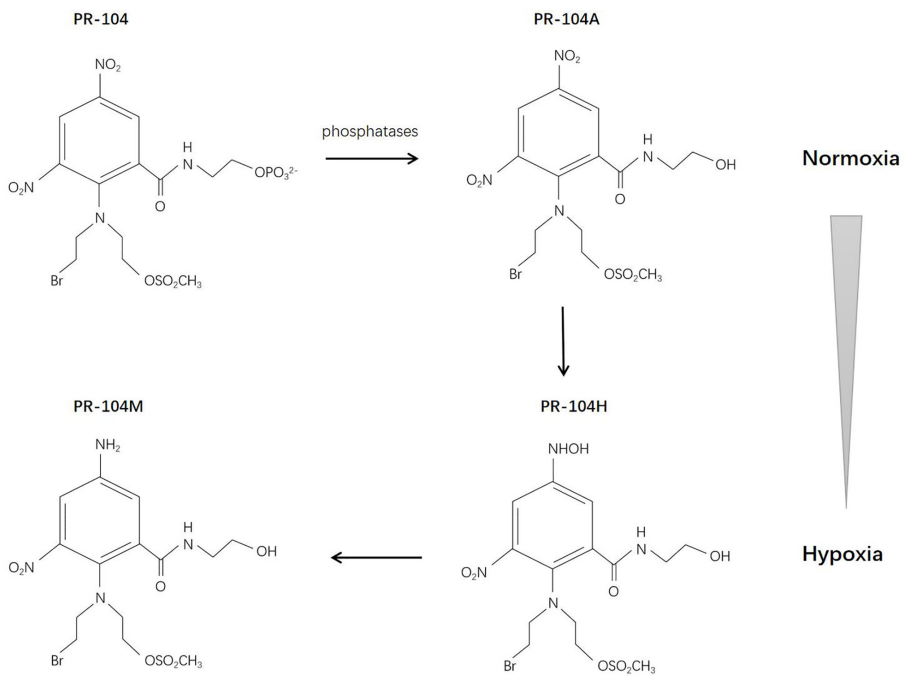


**FIGURE 4** | Reductive reaction of PR-104.

tumor burden and prolonged survival in pre-clinical studies (109), and also was associated with disease response in a phase I/II clinical trial (110). The expression of AKR1C3 can be used as a biomarker to predict response to PR-104 and patients screening (111).

## EO9 (APAZIQUONE)

EO9 (Apaziquone) [3-hydroxy-5-aziridinyl-1-methyl-2(1H-indole-4,7-dione)prop-beta-en-alpha-ol], which is structurally related to mitomycin C, was first reported 1989 and has been deeply investigated since then. Pharmacological studies have shown that DT-diaphorase plays a vital role in the reduction of EO9 prodrug (112), implying that detection of DT-diaphorase activity might predict the sensitivity of certain tumors to EO9 (113–115) (**Figure 5**).

*In vitro*, EO9 was proved effective toward colon adenocarcinoma cells, melanoma cells, central nervous system tumors, renal cancer cells, oral squamous cell carcinoma, and lung cancer cells (including NSCLC and certain cell lines of small cell lung cancer). *In vivo*, gastric and colorectal adenocarcinoma, ovarian carcinoma, and breast carcinoma were sensitive while leukemia was found to be resistant to EO9 (116–118). Certain inducers such as 1,2-dithiole-3-thiones (D3T) could enhance DT-diaphorase activity, thereby increasing the sensitivity of EO9 (119, 120). However, some researchers pointed out that *in vitro* studies on DT-diaphorase activity are different from *in vivo* studies, and may result in different sensitivity measurements (121). Further pharmacological studies have shown that in the presence of oxygen, DT-diaphorase reduces EO9 through 2-electron reduction, and the product is hydroquinone; while under hypoxic conditions, EO9 undergoes 1-electron reduction, and the product is semiquinone, which is more toxic than hydroquinone (122, 123). Therefore, EO9 may be more effective for hypoxic solid tumors (124, 125). Studies have also shown that the anti-tumor effect of EO9 is pH-dependent, and may exert a tumor suppressor effect in tumor areas with low pH (pH5.5-7.0) (126).

For clinical trials, nephrotoxicity and proteinuria were observed in both phase 1 and phase 2 clinical studies, but only partial response or stable disease was achieved (127–131). The reason for these unsatisfactory results may be attributed to the instability of both semiquinone and hydroquinone, with a short half-life and poor permeability, which will be quickly removed *in vivo* (131–134). However, this special pharmacokinetic profile is ideal for local treatment (135, 136). Intravesical instillation of EO9 was well tolerated and effective for superficial bladder cancer, manifested by a higher complete remission rate and a lower recurrence rate (137–139). A recent study pointed out that EO9 may be inactivated by hematuria, which suggests that the timing of medication should be selected with this in mind in the design of future phase 3 clinical trials (140).

## TH-302 (EVOFOSFAMIDE)

TH-302 (Evofosfamide), a second-generation HAP, consists of a 2-nitroimidazole moiety linked to bromo-iso-phosphoramide mustard (Br-IPM). Br-IPM is a DNA cross-linking agent. Under hypoxic conditions through a 2-nitroimidazole reduction reaction, TH-302 prodrug releases Br-IPM and perform cytotoxic effect (141) (**Figure 6**). Cytochrome P450 oxidoreductase (POR) also plays an important role in the reduction reaction and is the main determinant of cell sensitivity to TH-302 (142). Thus, the efficacy of TH-302 is highly dependent on the tumor type (143).

Many researchers have reported the antitumor efficacy of TH-302 as a single agent in malignancies including multiple myeloma, osteosarcoma, chondrosarcoma, neuroblastoma, rhabdomyosarcoma, breast cancer, non-small cell lung cancer, head and neck tumors, acute myeloid leukemia, etc. (144–152). The effect of TH-302 on spherical cells was significantly enhanced (153) and its activity was related to tumor hypoxic fractions (154), indicating that TH-302 had high hypoxic selectivity. The reported antineoplastic mechanisms include DNA fragmentation, cell cycle arrest, down-regulation of hypoxia-inducible factor-1α expression, etc.

In addition to monotherapy, TH-302 also showed synergistic effects with many traditional chemotherapy drugs, including doxorubicin, topotecan, paclitaxel, cisplatin, docetaxel, pemetrexed, irinotecan, gemcitabine, and temozolomide (155–157). TH-302 was able to inhibit the reoxygenation and

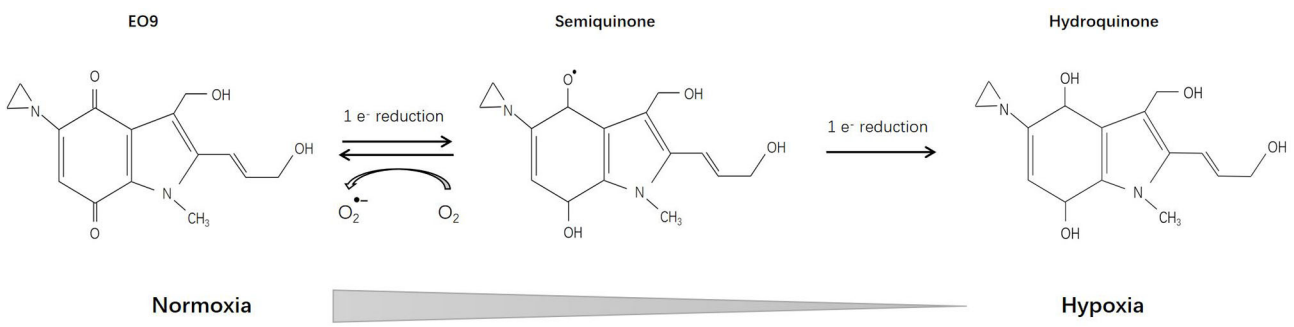


**FIGURE 5** | Reductive reaction of EO9.

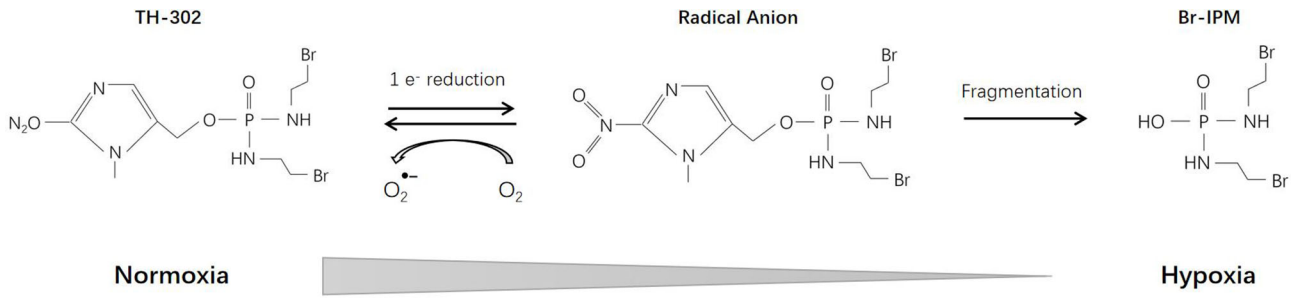


**FIGURE 6** | Reductive reaction of TH-302.

proliferation of hypoxic tumor cells that survived chemotherapy (158). Studies also revealed that the application of hypoxia inducers, such as Chk1 inhibitor, mTOR inhibitor, hydralazine, and pyruvate, enhanced the efficacy of TH-302 (159–161). TH-302 also has a radiosensitization effect. It exerts a synergistic effect when combined with radiotherapy (162–164). TH-302 has been shown to be beneficial in combination with conventional transarterial chemoembolization (cTACE) (165); anti-angiogenic therapy, such as VEGF-A inhibitor, sunitinib, and pazopanib (166–168); molecular targeted therapy, such as sorafenib and erlotinib (169, 170); and immunotherapy, such as CTLA-4 and PD-1 blockade (171, 172), where it also exerted a significant tumor inhibition effect. Recent evidence suggests that TH-302 can not only kill hypoxic pancreatic cancer cells, but also has the ability to improve the oxygenation status of residual tumor cells, so it may be useful to enhance the effect of radiotherapy and chemotherapy (173).

Since 2007, TH-302 has been in clinical trials. The main toxicities reported were skin and/or mucosal toxicity, thrombocytopenia, neutropenia, and myelosuppression (174–177). Several phase 1/2 clinical trials have reported encouraging results. For several types of tumors, including soft tissue sarcoma, pancreatic cancer, glioblastoma, and papillomavirus-negative head and neck squamous cell carcinoma, etc, TH-302 alone or in combination with other therapies showed varying degrees of antineoplastic activity (171, 175–178). It showed limited efficacy in the treatment of leukemia and failed in two phase 3 clinical trials (179–181). Researchers analyzed the possible reasons, including the lack of patient screening based on tumor hypoxia status (182, 183), antagonism between drugs (184), and drug formulation changes (185). Further research is still in progress.

## SN30000

SN30000 [3-(3-Morpholinopropyl)-7,8-dihydro-6H-indeno[5,6-e][1,2,4]triazine 1,4-dioxide], previously known as CEN-209, is a second-generation benzotriazine-N-oxide hypoxia-activated prodrug and a modified analogue of tirapazamine (**Figure 7**). Currently, it is still in the stage of preclinical research. Several studies have confirmed that SN30000 possesses similar pharmacological mechanisms (186) to tirapamine, but is superior in terms of antineoplastic effects and hypoxia selectivity (187).

Mao et al. (188) proved that, compared with monolayer tumor cells, SN30000 has higher activity on tumor spheroids, and when combined with radiation, it can cause significant tumor spheroid growth delay. Moreover, when used together with or before gemcitabine, SN30000 can effectively inhibit the proliferation of reoxygenated tumor cells (189). EF5 binding may be a promising biomarker for hypoxia stratification and SN30000 treatment response assessment (190, 191).

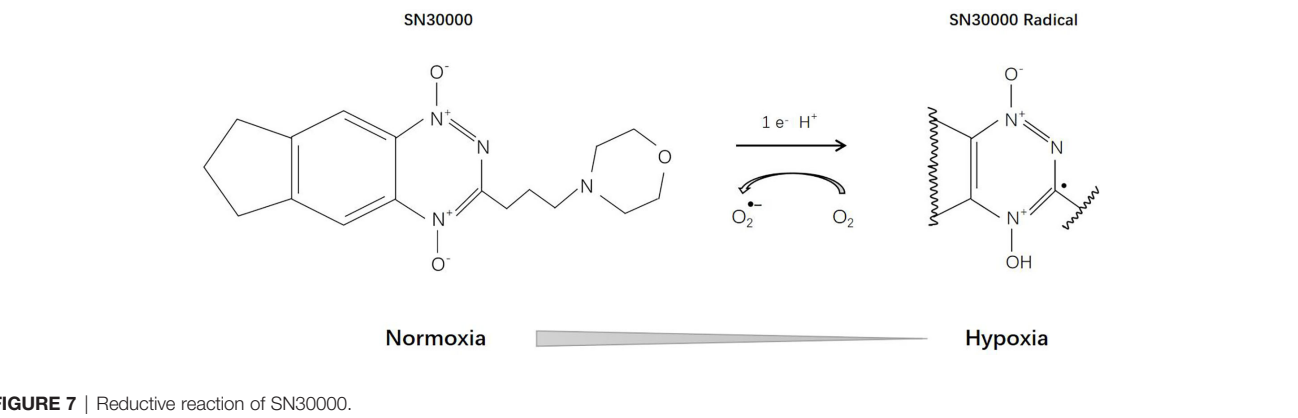


**FIGURE 7** | Reductive reaction of SN30000.

**TABLE 1** | Summary points.

| Summary points |
|---|
| Current Research Status: |
| •At present, the research of HAPS is mostly limited to the curative effect of macroscopic solid tumors. However, the results are not satisfactory. |
| •Evidence showed that hypoxic tumor cells could only survive for 2-3 days *in vivo*, suggesting that *in vivo* hypoxic cells are destined to enter necrosis *in vivo* and that hypoxia-targeting therapy of macroscopic tumors should be revisited. |
| Suggestions For Future Investigations: |
| •Our experimental evidence showed that micro-metastases (< 1 mm in diameter) and tumor cells in ascites and pleural effusion were severely hypoxic and in low proliferation state. |
| •They were insensitivity to traditional radiotherapy and chemotherapy. |
| •Micro-metastases (< 1 mm in diameter) and tumor cells in ascites and pleural effusion are more suitable therapeutic targets for HAPs. |

## CONCLUSIONS AND SUGGESTIONS FOR FUTURE INVESTIGATIONS

Since the 1980s, HAPs have been developed and validated step by step, from preclinical to clinical. Despite their antineoplastic effects, their drawbacks and limitations have also been revealed by many studies. Here, we summarize the past experience and the latest research progress, and propose the following directions for future research (**Table 1**):

First, screening methods need to be developed based on tumor hypoxia to select the best candidates for this type of therapy. A growing number of studies have shown that PET/CT imaging can be an effective method to monitor HAPs uptake and therapeutic response (148, 190, 192). Second, biomarkers to predict drug sensitivity are needed. Since HAP is a bioreductive drug, it requires specific enzymes to complete the reduction reaction. Therefore, the detection of specific enzymes can play a role in predicting drug sensitivity (112, 142). In addition, experiments conducted by our group and others showed that hypoxic tumor cells could only survive for 2-3 days *in vivo* (193, 194), suggesting that *in vivo* hypoxic cells are destined to enter necrosis *in vivo* and that hypoxia-targeting therapy of macroscopic tumors should be revisited.

Hypoxia is not only a characteristic of macroscopic tumors. In 2007, Li et al. reported that peritoneal disseminated micrometastases (< 1 mm in diameter) were severely hypoxic and in low proliferation state (7, 8, 195–197). This hypoxic state of early micrometastases likely confers insensitivity to traditional radiotherapy and chemotherapy, making them suitable therapeutic targets for HAPs. HAPs may have the potential to prevent them from developing into macroscopic tumors, thereby reducing the metastatic rate of tumors. Our group is working to further confirm the efficacy of HAPs on such tumors and its effect on early tumor metastasis.

## DATA AVAILABILITY STATEMENT

The original contributions presented in the study are included in the article/supplementary files. Further inquiries can be directed to the corresponding author.

## AUTHOR CONTRIBUTIONS

YL performed the literature search and wrote the manuscript. LZ performed the literature search and figure editing. X-FL contributed to write and revise the manuscript. All authors contributed to the article and approved the submitted version.

## ACKNOWLEDGMENTS

The authors' research is supported in part by a grant from Shenzhen People's Hospital for "Climbing" Program (X-FL), and a Shenzhen Science and Technology Project grant (JCYJ20190806151003583) (X-FL). We thank Libby Cone, MD, MA, from Effective Medical English (www.effectivemedicalenglish.com/cone@effectivemedicalenglish) for editing a draft of this manuscript.

## REFERENCES

1. Evans SM, Koch CJ. Prognostic Significance of Tumor Oxygenation in Humans. *Cancer Lett* (2003) 195(1):1–16. doi: 10.1016/s0304-3835(03)00012-0
2. Challapalli A, Carroll L, Aboagye EO. Molecular Mechanisms of Hypoxia in Cancer. *Clin Transl Imaging* (2017) 5(3):225–53. doi: 10.1007/s40336-017-0231-1
3. Bristow RG, Hill RP. Hypoxia and Metabolism. Hypoxia, DNA Repair and Genetic Instability. *Nat Rev Cancer* (2008) 8(3):180–92. doi: 10.1038/nrc2344
4. Carmeliet P, Jain RK. Molecular Mechanisms and Clinical Applications of Angiogenesis. *Nature* (2011) 19473(7347):298–307. doi: 10.1038/nature10144
5. Lum JJ, Bui T, Gruber M, Gordan JD, DeBerardinis RJ, Covello KL, et al. The Transcription Factor HIF-1alpha Plays a Critical Role in the Growth Factor-Dependent Regulation of Both Aerobic and Anaerobic Glycolysis. *Genes Dev* (2007) 21(9):1037–49. doi: 10.1101/gad.1529107
6. Joseph JP, Harishankar MK, Pillai AA, Devi A. Hypoxia Induced EMT: A Review on the Mechanism of Tumor Progression and Metastasis in OSCC. *Oral Oncol* (2018) 80:23–32. doi: 10.1016/j.oraloncology.2018.03.004
7. Li XF, Carlin S, Urano M, Russell J, Ling CC, O'Donoghue JA. Visualization of Hypoxia in Microscopic Tumors by Immunofluorescent Microscopy. *Cancer Res* (2007) 67(16):7646–53. doi: 10.1158/0008-5472.CAN-06-4353
8. Li XF, O'Donoghue JA. Hypoxia in Microscopic Tumors. *Cancer Lett* (2008) 264(2):172–80. doi: 10.1016/j.canlet.2008.02.037
9. Horsman MR, Overgaard J. The Impact of Hypoxia and Its Modification of the Outcome of Radiotherapy. *J Radiat Res* (2016) 57(Suppl 1):i90–8. doi: 10.1093/jrr/rrw007
10. Manoochehri Khoshinani H, Afshar S, Najafi R. Hypoxia: A Double-Edged Sword in Cancer Therapy. *Cancer Invest* (2016) 34(10):536–45. doi: 10.1080/07357907.2016.1245317
11. Kim JY, Lee JY. Targeting Tumor Adaption to Chronic Hypoxia: Implications for Drug Resistance, and How it Can be Overcome. *Int J Mol Sci* (2017) 18(9):1854. doi: 10.3390/ijms18091854
12. Zeman EM, Brown JM, Lemmon MJ, Hirst VK, Lee WW. Sr-4233: A New Bioreductive Agent With High Selective Toxicity for Hypoxic Mammalian Cells. *Int J Radiat Oncol Biol Phys* (1986) 12(7):1239–42. doi: 10.1016/0360-3016(86)90267-1
13. Laderoute K, Wardman P, Rauth AM. Molecular Mechanisms for the Hypoxia-Dependent Activation of 3-Amino-1,2,4-Benzotriazine-1,4-Dioxide (Sr 4233). *Biochem Pharmacol* (1988) 37(8):1487–95. doi: 10.1016/0006-2952(88)90010-x
14. Saunders MP, Patterson AV, Chinje EC, Harris AL, Stratford IJ. NADPH: Cytochrome C (P450) Reductase Activates Tirapazamine (SR4233) to Restore Hypoxic and Oxic Cytotoxicity in an Aerobic Resistant Derivative

of the A549 Lung Cancer Cell Line. *Br J Cancer* (2000) 82(3):651–6. doi: 10.1054/bjoc.1999.0977
15. Riley RJ, Workman P. Enzymology of the Reduction of the Potent Benzotriazine-di-N-oxide Hypoxic Cell Cytotoxin SR 4233 (WIN 59075) by NAD(P)H: (Quinone Acceptor) Oxidoreductase (EC 1.6.99.2) Purified From Walker 256 Rat Tumour Cells. *Biochem Pharmacol* (1992) 43(2):167–74. doi: 10.1016/0006-2952(92)90274-m
16. Patterson AV, Robertson N, Houlbrook S, Stephens MA, Adams GE, Harris AL, et al. The Role of DT-diaphorase in Determining the Sensitivity of Human Tumor Cells to Tirapazamine (Sr 4233). *Int J Radiat Oncol Biol Phys* (1994) 29(2):369–72. doi: 10.1016/0360-3016(94)90291-7
17. Elwell JH, Siim BG, Evans JW, Brown JM. Adaptation of Human Tumor Cells to Tirapazamine Under Aerobic Conditions: Implications of Increased Antioxidant Enzyme Activity to Mechanism of Aerobic Cytotoxicity. *Biochem Pharmacol* (1997) 54(2):249–57. doi: 10.1016/s0006-2952(97)00171-8
18. Wang J, Biedermann KA, Brown JM. Repair of DNA and Chromosome Breaks in Cells Exposed to SR 4233 Under Hypoxia or to Ionizing Radiation. *Cancer Res* (1992) 52(16):4473–7. doi: 10.1002/1097-0142(19920815)70:4<903::AID-CNCR2820700432>3.0.CO;2
19. Kotandeniya D, Ganley B, Gates KS. Oxidative DNA Base Damage by the Antitumor Agent 3-amino-1,2,4-benzotriazine 1,4-Dioxide (Tirapazamine). *Bioorg Med Chem Lett* (2002) 12(17):2325–9. doi: 10.1016/s0960-894x(02)00468-7
20. Birincioglu M, Jaruga P, Chowdhury G, Rodriguez H, Dizdaroglu M, Gates KS. Dna Base Damage by the Antitumor Agent 3-amino-1,2,4-benzotriazine 1,4-Dioxide (Tirapazamine). *J Am Chem Soc* (2003) 125(38):11607–15. doi: 10.1021/ja0352146
21. Evans JW, Yudoh K, Delahoussaye YM, Brown JM. Tirapazamine Is Metabolized to Its DNA-Damaging Radical by Intranuclear Enzymes. *Cancer Res* (1998) 58(10):2098–101.
22. Aboagye EO, Dillehay LE, Bhujwalla ZM, Lee DJ. Hypoxic Cell Cytotoxin Tirapazamine Induces Acute Changes in Tumor Energy Metabolism and Ph: A 31p Magnetic Resonance Spectroscopy Study. *Radiat Oncol Investig* (1998) 6(6):249–54. doi: 10.1002/(SICI)1520-6823(1998)6:6<249::AID-ROI1>3.0.CO;2-C
23. Skarsgard LD, Vinczan A, Skwarchuk MW, Chaplin DJ. The Effect of Low Ph and Hypoxia on the Cytotoxic Effects of SR4233 and Mitomycin C *In Vitro*. *Int J Radiat Oncol Biol Phys* (1994) 29(2):363–7. doi: 10.1016/0360-3016(94)90290-9
24. Koch CJ. Unusual Oxygen Concentration Dependence of Toxicity of SR-4233, a Hypoxic Cell Toxin. *Cancer Res* (1993) 53(17):3992–7. doi: 10.1007/BF01518522
25. Durand RE, Olive PL. Physiologic and Cytotoxic Effects of Tirapazamine in Tumor-Bearing Mice. *Radiat Oncol Investig* (1997) 5(5):213–9. doi: 10.1002/(SICI)1520-6823(1997)5:5<213::AID-ROI1>3.0.CO;2-0
26. Lin PS, Ho KC, Yang SJ. Tirapazamine (SR 4233) Interrupts Cell Cycle Progression and Induces Apoptosis. *Cancer Lett* (1996) 105(2):249–55. doi: 10.1016/0304-3835(96)04292-9
27. Hanauske AR, Ross M, Degen D, Hilsenbeck SG, Von Hoff DD. *In Vitro* Activity of the Benzotriazine Dioxide SR 4233 Against Human Tumour Colony-Forming Units. *Eur J Cancer* (1993) 29A(3):423–5. doi: 10.1016/0959-8049(93)90400-a
28. Hong B, Lui VW, Hui EP, Ng MH, Cheng SH, Sung FL, et al. Hypoxia-Targeting by Tirapazamine (Tpz) Induces Preferential Growth Inhibition of Nasopharyngeal Carcinoma Cells With Chk1/2 Activation. *Invest New Drugs* (2011) 29(3):401–10. doi: 10.1007/s10637-009-9356-z
29. Govaert KM, Nijkamp MW, Emmink BL, Steller EJ, Minchinton AI, Kranenburg O, et al. Effects of Tirapazamine on Experimental Colorectal Liver Metastases After Radiofrequency Ablation. *Br J Surg* (2012) 99(4):567–75. doi: 10.1002/bjs.8668
30. Brown JM. Exploiting Tumour Hypoxia and Overcoming Mutant P53 With Tirapazamine. *Br J Cancer* (1998) 77(Suppl 4):12–4. doi: 10.1038/bjc.1998.430
31. Yang B, Reynolds CP. Tirapazamine Cytotoxicity for Neuroblastoma is p53 Dependent. *Clin Cancer Res* (2005) 11(7):2774–80. doi: 10.1158/1078-0432.CCR-04-2382
32. Brown JM, Lemmon MJ. Potentiation by the Hypoxic Cytotoxin SR 4233 of Cell Killing Produced by Fractionated Irradiation of Mouse Tumors. *Cancer Res* (1990) 50(24):7745–9. doi: 10.1002/1097-0142(19901215)66:12<2673::AID-CNCR2820661235>3.0.CO
33. Minchinton AI, Brown JM. Enhancement of the Cytotoxicity of SR 4233 to Normal and Malignant Tissues by Hypoxic Breathing. *Br J Cancer* (1992) 66(6):1053–8. doi: 10.1038/bjc.1992.409
34. el-Said A, Menke D, Dorie MJ, Brown JM. Comparison of the Effectiveness of Tirapazamine and Carbogen With Nicotinamide in Enhancing the Response of a Human Tumor Xenograft to Fractionated Irradiation. *Radiat Oncol Investig* (1999) 7(3):163–9. doi: 10.1002/(SICI)1520-6823(1999)7:3<163::AID-ROI5>3.0.CO;2-M
35. Shibata T, Shibamoto Y, Sasai K, Oya N, Murata R, Takagi T, et al. Comparison of *In Vivo* Efficacy of Hypoxic Cytotoxin Tirapazamine and Hypoxic Cell Radiosensitizer Ku-2285 in Combination With Single and Fractionated Irradiation. *Jpn J Cancer Res* (1996) 87(1):98–104. doi: 10.1111/j.1349-7006.1996.tb00206.x
36. Friery OP, Hejmadi MV, McKeown SR. Dna Damage Induced in T50/80 Tumour Cells Following Exposure to the Bioreductive Drug Tirapazamine in Combination With a Single Dose of Radiation (12gy). *Biochem Soc Trans* (1997) 25(1):135S. doi: 10.1042/bst025135s
37. Zhang M, Stevens G. Effect of Radiation and Tirapazamine (Sr-4233) on Three Melanoma Cell Lines. *Melanoma Res* (1998) 8(6):510–5. doi: 10.1097/00008390-199812000-00006
38. Masunaga SI, Tano K, Sanada Y, Sakurai Y, Tanaka H, Suzuki M, et al. Effect of Tirapazamine, Metformin or Mild Hyperthermia on Recovery From Radiation-Induced Damage in Pimonidazole-Unlabeled Quiescent Tumor Cells. *World J Oncol* (2017) 8(5):137–46. doi: 10.14740/wjon1058w
39. Cliffe S, Taylor ML, Rutland M, Baguley BC, Hill RP, Wilson WR. Combining Bioreductive Drugs (SR 4233 or SN 23862) With the Vasoactive Agents Flavone Acetic Acid or 5,6-Dimethylxanthenone Acetic Acid. *Int J Radiat Oncol Biol Phys* (1994) 29(2):373–7. doi: 10.1016/0360-3016(94)90292-5
40. Masunaga S, Ono K, Hori H, Shibata T, Suzuki M, Kinashi Y, et al. Effects of Bioreductive Agents, Tirapazamine and Mitomycin C, on Quiescent Cell Populations in Solid Tumors, Evaluated by Micronucleus Assay. *Jpn J Cancer Res* (1997) 88(9):907–14. doi: 10.1111/j.1349-7006.1997.tb00468.x
41. Weitman S, Mangold G, Marty J, Dexter D, Hilsenbeck S, Rake J, et al. Evidence of Enhanced *In Vivo* Activity Using Tirapazamine With Paclitaxel and Paraplatin Regimens Against the MV-522 Human Lung Cancer Xenograft. *Cancer Chemother Pharmacol* (1999) 43(5):402–8. doi: 10.1007/s002800050914
42. Jounaidi Y, Waxman DJ. Combination of the Bioreductive Drug Tirapazamine With the Chemotherapeutic Prodrug Cyclophosphamide for P450/P450-Reductase-Based Cancer Gene Therapy. *Cancer Res* (2000) 60(14):3761–9. doi: 10.1016/S0165-4608(00)00214-4
43. Masunaga S, Ono K, Hori H, Suzuki M, Kinashi Y, Takagaki M, et al. Change in Oxygenation Status in Intratumour Total and Quiescent Cells Following Gamma-Ray Irradiation, Tirapazamine Administration, Cisplatin Injection and Bleomycin Treatment. *Br J Radiol* (2000) 73(873):978–86. doi: 10.1259/bjr.73.873.11064652
44. Doloff JC, Khan N, Ma J, Demidenko E, Swartz HM, Jounaidi Y. Increased Tumor Oxygenation and Drug Uptake During Anti-Angiogenic Weekly Low Dose Cyclophosphamide Enhances the Anti-Tumor Effect of Weekly Tirapazamine. *Curr Cancer Drug Targets* (2009) 9(6):777–88. doi: 10.2174/156800909789271503
45. Wilder RB, Langmuir VK, Mendonca HL, Goris ML, Knox SJ. Local Hyperthermia and SR 4233 Enhance the Antitumor Effects of Radioimmunotherapy in Nude Mice With Human Colonic Adenocarcinoma Xenografts. *Cancer Res* (1993) 53(13):3022–7. doi: 10.1007/BF01517047
46. Masunaga S, Nagasawa H, Uto Y, Hori H, Nagata K, Suzuki M, et al. The Usefulness of Mild Temperature Hyperthermia Combined With Continuous Tirapazamine Administration Under Reduced Dose-Rate Irradiation With Gamma-Rays. *Int J Hyperthermia* (2007) 23(1):29–35. doi: 10.1080/02656730601135366
47. Masunaga S, Liu Y, Sakurai Y, Tanaka H, Suzuki M, Kondo N, et al. Usefulness of Combined Treatment With Continuous Administration of Tirapazamine and Mild Temperature Hyperthermia in γ-Ray Irradiation in Terms of Local Tumour Response and Lung Metastatic Potential. *Int J Hyperthermia* (2012) 28(7):636–44. doi: 10.3109/02656736.2012.714517
48. Broekgaarden M, Weijer R, van Wijk AC, Cox RC, Egmond MR, Hoebe R, et al. Photodynamic Therapy With Liposomal Zinc Phthalocyanine and

Tirapazamine Increases Tumor Cell Death *Via* DNA Damage. *J BioMed Nanotechnol* (2017) 13(2):204–20. doi: 10.1166/jbn.2017.2327
49. Lin WH, Yeh SH, Yeh KH, Chen KW, Cheng YW, Su TH, et al. Hypoxia-Activated Cytotoxic Agent Tirapazamine Enhances Hepatic Artery Ligation-Induced Killing of Liver Tumor in HBx Transgenic Mice. *Proc Natl Acad Sci USA* (2016) 113(42):11937–42. doi: 10.1073/pnas.1613466113
50. Adam M, Ottenjann S, Künzel G, Busch R, Erhardt W, Nieder C, et al. Evaluation of the Toxicity of Tirapazamine Plus Cisplatin in a Mouse Tumor Model. *Strahlenther Onkol* (2006) 182(4):231–9. doi: 10.1007/s00066-006-1506-z
51. Adam M, Bayer C, Henke J, Grosu A, Molls M, Nieder C. Tirapazamine Plus Cisplatin and Irradiation in a Mouse Model: Improved Tumor Control at the Cost of Increased Toxicity. *J Cancer Res Clin Oncol* (2008) 134(2):137–46. doi: 10.1007/s00432-007-0260-7
52. Johnson CA, Kilpatrick D, von Roemeling R, Langer C, Graham MA, Greenslade D, et al. Phase I Trial of Tirapazamine in Combination With Cisplatin in a Single Dose Every 3 Weeks in Patients With Solid Tumors. *J Clin Oncol* (1997) 15(2):773–80. doi: 10.1200/JCO.1997.15.2.773
53. Hoff PM, Saad ED, Ravandi-Kashani F, Czerny E, Pazdur R. Phase I Trial of I.V. Administered Tirapazamine Plus Cyclophosphamide. *Anticancer Drugs* (2001) 12(6):499–503. doi: 10.1097/00001813-200107000-00002
54. Lara PNJr, Frankel P, Mack PC, Gumerlock PH, Galvin I, Martel CL, et al. Tirapazamine Plus Carboplatin and Paclitaxel in Advanced Malignant Solid Tumors: A California Cancer Consortium Phase I and Molecular Correlative Study. *Clin Cancer Res* (2003) 9(12):4356–62. doi: 10.1093/carcin/bgg164
55. Aquino VM, Weitman SD, Winick NJ, Blaney S, Furman WL, Kepner JL, et al. Phase I Trial of Tirapazamine and Cyclophosphamide in Children With Refractory Solid Tumors: A Pediatric Oncology Group Study. *J Clin Oncol* (2004) 22(8):1413–9. doi: 10.1200/JCO.2004.07.111
56. Cohen EE, Rosine D, Haraf DJ, Loh E, Shen L, Lusinchi A, et al. Phase I Trial of Tirapazamine, Cisplatin, and Concurrent Accelerated Boost Reirradiation in Patients With Recurrent Head and Neck Cancer. *Int J Radiat Oncol Biol Phys* (2007) 67(3):678–84. doi: 10.1016/j.ijrobp.2006.09.056
57. Smith HO, Jiang CS, Weiss GR, Hallum AV 3rd, Liu PY, Robinson WR 3rd, et al. Tirapazamine Plus Cisplatin in Advanced or Recurrent Carcinoma of the Uterine Cervix: A Southwest Oncology Group Study. *Int J Gynecol Cancer* (2006) 16(1):298–305. doi: 10.1111/j.1525-1438.2006.00339.x
58. Reck M, von Pawel J, Nimmermann C, Groth G, Gatzemeier U. Phase II-trial of Tirapazamine in Combination With Cisplatin and Gemcitabine in Patients With Advanced Non-Small-Cell-Lung-Cancer (NSCLC). *Pneumologie* (2004) 58(12):845–9. doi: 10.1055/s-2004-830056
59. Covens A, Blessing J, Bender D, Mannel R, Morgan M. Gynecologic Oncology Group. A Phase II Evaluation of Tirapazamine Plus Cisplatin in the Treatment of Recurrent Platinum-Sensitive Ovarian or Primary Peritoneal Cancer: A Gynecologic Oncology Group Study. *Gynecol Oncol* (2006) 100(3):586–90. doi: 10.1016/j.ygyno.2005.09.032
60. Maluf FC, Leiser AL, Aghajanian C, Sabbatini P, Pezzulli S, Chi DS, et al. Phase II Study of Tirapazamine Plus Cisplatin in Patients With Advanced or Recurrent Cervical Cancer. *Int J Gynecol Cancer* (2006) 16(3):1165–71. doi: 10.1111/j.1525-1438.2006.00454.x
61. Ghatage P, Sabagh H. Is There a Role for Tirapazamine in the Treatment of Cervical Cancer? *Expert Opin Drug Metab Toxicol* (2012) 8(12):1589–97. doi: 10.1517/17425255.2012.730518
62. Rischin D, Narayan K, Oza AM, Mileshkin L, Bernshaw D, Choi J, et al. Phase 1 Study of Tirapazamine in Combination With Radiation and Weekly Cisplatin in Patients With Locally Advanced Cervical Cancer. *Int J Gynecol Cancer* (2010) 20(5):827–33. doi: 10.1111/IGC.0b013e3181dc827e
63. Le QT, Taira A, Budenz S, Jo Dorie M, Goffinet DR, Fee WE, et al. Mature Results From a Randomized Phase II Trial of Cisplatin Plus 5-Fluorouracil and Radiotherapy With or Without Tirapazamine in Patients With Resectable Stage IV Head and Neck Squamous Cell Carcinomas. *Cancer* (2006) 106(9):1940–9. doi: 10.1002/cncr.21785
64. Williamson SK, Crowley JJ, Lara PNJr, McCoy J, Lau DH, Tucker RW, et al. Phase III Trial of Paclitaxel Plus Carboplatin With or Without Tirapazamine in Advanced Non-Small-Cell Lung Cancer: Southwest Oncology Group Trial S0003. *J Clin Oncol* (2005) 23(36):9097–104. doi: 10.1200/JCO.2005.01.3771
65. Rischin D, Peters LJ, O'Sullivan B, Giralt J, Fisher R, Yuen K, et al. Tirapazamine, Cisplatin, and Radiation Versus Cisplatin and Radiation for Advanced Squamous Cell Carcinoma of the Head and Neck (Trog 02.02, Headstart): A Phase III Trial of the Trans-Tasman Radiation Oncology Group. *J Clin Oncol* (2010) 28(18):2989–95. doi: 10.1200/JCO.2009.27.4449
66. Patterson LH. Rationale for the Use of Aliphatic N-oxides of Cytotoxic Anthraquinones as Prodrug DNA Binding Agents: A New Class of Bioreductive Agent. *Cancer Metastasis Rev* (1993) 12(2):119–34. doi: 10.1007/bf00689805
67. McKeown SR, Hejmadi MV, McIntyre IA, McAleer JJ, Patterson LH. AQ4N: An Alkylaminoanthraquinone N-Oxide Showing Bioreductive Potential and Positive Interaction With Radiation *In Vivo*. *Br J Cancer* (1995) 72(1):76–81. doi: 10.1038/bjc.1995.280
68. Hejmadi MV, McKeown SR, Friery OP, McIntyre IA, Patterson LH, Hirst DG. DNA Damage Following Combination of Radiation With the Bioreductive Drug AQ4N: Possible Selective Toxicity to Oxic and Hypoxic Tumour Cells. *Br J Cancer* (1996) 73(4):499–505. doi: 10.1038/bjc.1996.87
69. Patterson LH, McKeown SR, Ruparelia K, Double JA, Bibby MC, Cole S, et al. Enhancement of Chemotherapy and Radiotherapy of Murine Tumours by AQ4N, a Bioreductively Activated Anti-Tumour Agent. *Br J Cancer* (2000) 82(12):1984–90. doi: 10.1054/bjoc.2000.1564
70. Gallagher R, Hughes CM, Murray MM, Friery OP, Patterson LH, Hirst DG, et al. The Chemopotentiation of Cisplatin by the Novel Bioreductive Drug AQ4N. *Br J Cancer* (2001) 85(4):625–9. doi: 10.1054/bjoc.2001.1975
71. McCarthy HO, Yakkundi A, McErlane V, Hughes CM, Keilty G, Murray M, et al. Bioreductive GDEPT Using Cytochrome P450 3A4 in Combination With AQ4N. *Cancer Gene Ther* (2003) 10(1):40–8. doi: 10.1038/sj.cgt.7700522
72. Nishida CR, Lee M, de Montellano PR. Efficient Hypoxic Activation of the Anticancer Agent AQ4N by CYP2S1 and CYP2W1. *Mol Pharmacol* (2010) 78(3):497–502. doi: 10.1124/mol.110.065045
73. Xiao Y, Shinkyo R, Guengerich FP. Cytochrome P450 2S1 Is Reduced by NADPH-cytochrome P450 Reductase. *Drug Metab Dispos* (2011) 39(6):944–6. doi: 10.1124/dmd.111.039321
74. Bebenek IG, Solaimani P, Bui P, Hankinson O. CYP2S1 Is Negatively Regulated by Corticosteroids in Human Cell Lines. *Toxicol Lett* (2012) 209(1):30–4. doi: 10.1016/j.toxlet.2011.11.020
75. Mehibel M, Singh S, Cowen RL, Williams KJ, Stratford IJ. Radiation Enhances the Therapeutic Effect of Banoxantrone in Hypoxic Tumour Cells With Elevated Levels of Nitric Oxide Synthase. *Oncol Rep* (2016) 35(4):1925–32. doi: 10.3892/or.2016.4555
76. Lalani AS, Alters SE, Wong A, Albertella MR, Cleland JL, Henner WD. Selective Tumor Targeting by the Hypoxia-Activated Prodrug AQ4N Blocks Tumor Growth and Metastasis in Preclinical Models of Pancreatic Cancer. *Clin Cancer Res* (2007) 13(7):2216–25. doi: 10.1158/1078-0432.CCR-06-2427
77. Williams KJ, Albertella MR, Fitzpatrick B, Loadman PM, Shnyder SD, Chinje EC, et al. *In Vivo* Activation of the Hypoxia-Targeted Cytotoxin AQ4N in Human Tumor Xenografts. *Mol Cancer Ther* (2009) 8(12):3266–75. doi: 10.1158/1535-7163.MCT-09-0396
78. Ming L, Byrne NM, Camac SN, Mitchell CA, Ward C, Waugh DJ, et al. Androgen Deprivation Results in Time-Dependent Hypoxia in LNCaP Prostate Tumours: Informed Scheduling of the Bioreductive Drug AQ4N Improves Treatment Response. *Int J Cancer* (2013) 132(6):1323–32. doi: 10.1002/ijc.27796
79. Manley EJr, Waxman DJ. Impact of Tumor Blood Flow Modulation on Tumor Sensitivity to the Bioreductive Drug Banoxantrone. *J Pharmacol Exp Ther* (2013) 344(2):368–77. doi: 10.1124/jpet.112.200089
80. Gieling RG, Fitzmaurice RJ, Telfer BA, Babur M, Williams KJ. Dissemination *Via* the Lymphatic or Angiogenic Route Impacts the Pathology, Microenvironment and Hypoxia-Related Drug Response of Lung Metastases. *Clin Exp Metastasis* (2015) 32(6):567–77. doi: 10.1007/s10585-015-9728-z
81. Trédan O, Garbens AB, Lalani AS, Tannock IF. The Hypoxia-Activated ProDrug AQ4N Penetrates Deeply in Tumor Tissues and Complements the Limited Distribution of Mitoxantrone. *Cancer Res* (2009) 69(3):940–7. doi: 10.1158/0008-5472.CAN-08-0676
82. Raghava S, Kompella UB. AQ4, an Antitumor Anthracenedione, Inhibits Endothelial Cell Proliferation and Vascular Endothelial Growth Factor Secretion: Implications for the Therapy of Ocular Neovascular Disorders. *Eur J Pharmacol* (2007) 568(1-3):68–74. doi: 10.1016/j.ejphar.2007.04.044

83. O'Rourke M, Ward C, Worthington J, McKenna J, Valentine A, Robson T, et al. Evaluation of the Antiangiogenic Potential of AQ4N. *Clin Cancer Res* (2008) 14(5):1502–9. doi: 10.1158/1078-0432.CCR-07-1262
84. Steward WP, Middleton M, Benghiat A, Loadman PM, Hayward C, Waller S, et al. The Use of Pharmacokinetic and Pharmacodynamic End Points to Determine the Dose of AQ4N, a Novel Hypoxic Cell Cytotoxin, Given With Fractionated Radiotherapy in a Phase I Study. *Ann Oncol* (2007) 18(6):1098–103. doi: 10.1093/annonc/mdm120
85. Albertella MR, Loadman PM, Jones PH, Phillips RM, Rampling R, Burnet N, et al. Hypoxia-Selective Targeting by the Bioreductive Prodrug AQ4N in Patients With Solid Tumors: Results of a Phase I Study. *Clin Cancer Res* (2008) 14(4):1096–104. doi: 10.1158/1078-0432.CCR-07-4020
86. Papadopoulos KP, Goel S, Beeram M, Wong A, Desai K, Haigentz M, et al. A Phase 1 Open-Label, Accelerated Dose-Escalation Study of the Hypoxia-Activated Prodrug AQ4N in Patients With Advanced Malignancies. *Clin Cancer Res* (2008) 14(21):7110–5. doi: 10.1158/1078-0432.CCR-08-0483
87. Shen S, Wu Y, Li K, Wang Y, Wu J, Zeng Y, et al. Versatile Hyaluronic Acid Modified AQ4N-Cu(II)-gossypol Infinite Coordination Polymer Nanoparticles: Multiple Tumor Targeting, Highly Efficient Synergistic Chemotherapy, and Real-Time Self-Monitoring. *Biomaterials* (2018) 154:197–212. doi: 10.1016/j.biomaterials.2017.11.001
88. Zhang D, Wu M, Cai Z, Liao N, Ke K, Liu H, et al. Chemotherapeutic Drug Based Metal-Organic Particles for Microvesicle-Mediated Deep Penetration and Programmable Ph/NIR/Hypoxia Activated Cancer Photochemotherapy. *Adv Sci (Weinh)* (2018) 5(2):1700648. doi: 10.1002/advs.201700648
89. Luan X, Guan YY, Liu HJ, Lu Q, Zhao M, Sun D, et al. A Tumor Vascular-Targeted Interlocking Trimodal Nanosystem That Induces and Exploits Hypoxia. *Adv Sci (Weinh)* (2018) 5(8):1800034. doi: 10.1002/advs.201800034
90. He Z, Dai Y, Li X, Guo D, Liu Y, Huang X, et al. Hybrid Nanomedicine Fabricated From Photosensitizer-Terminated Metal-Organic Framework Nanoparticles for Photodynamic Therapy and Hypoxia-Activated Cascade Chemotherapy. *Small* (2019) 15(4):e1804131. doi: 10.1002/smll.201804131
91. Li X, Zhao Y, Jiang W, Li S, Zhan M, Liu H, et al. Ultralong Circulating Choline Phosphate Liposomal Nanomedicines for Cascaded Chemo-Radiotherapy. *Biomater Sci* (2019) 7(4):1335–44. doi: 10.1039/c9bm00051h
92. Ji Y, Lu F, Hu W, Zhao H, Tang Y, Li B, et al. Tandem Activated Photodynamic and Chemotherapy: Using pH-Sensitive Nanosystems to Realize Different Tumour Distributions of Photosensitizer/Prodrug for Amplified Combination Therapy. *Biomaterials* (2019) 219:119393. doi: 10.1016/j.biomaterials.2019.119393
93. Feng L, Cheng L, Dong Z, Tao D, Barnhart TE, Cai W, et al. Theranostic Liposomes With Hypoxia-Activated Prodrug to Effectively Destruct Hypoxic Tumors Post-Photodynamic Therapy. *ACS Nano* (2017) 11(1):927–37. doi: 10.1021/acsnano.6b07525
94. Zhang R, Feng L, Dong Z, Wang L, Liang C, Chen J, et al. Glucose & Oxygen Exhausting Liposomes for Combined Cancer Starvation and Hypoxia-Activated Therapy. *Biomaterials* (2018) 162:123–31. doi: 10.1016/j.biomaterials.2018.02.004
95. Singleton RS, Guise CP, Ferry DM, Pullen SM, Dorie MJ, Brown JM, et al. DNA Cross-Links in Human Tumor Cells Exposed to the Prodrug PR-104A: Relationships to Hypoxia, Bioreductive Metabolism, and Cytotoxicity. *Cancer Res* (2009) 69(9):3884–91. doi: 10.1158/0008-5472.CAN-08-4023
96. Guise CP, Wang AT, Theil A, Bridewell DJ, Wilson WR, Patterson AV. Identification of Human Reductases That Activate the Dinitrobenzamide Mustard Prodrug PR-104A: A Role for NADPH:cytochrome P450 Oxidoreductase Under Hypoxia. *Biochem Pharmacol* (2007) 74(6):810–20. doi: 10.1016/j.bcp.2007.06.014
97. Guise CP, Abbattista MR, Singleton RS, Holford SD, Connolly J, Dachs GU, et al. The Bioreductive Prodrug PR-104A Is Activated Under Aerobic Conditions by Human Aldo-Keto Reductase 1C3. *Cancer Res* (2010) 70(4):1573–84. doi: 10.1158/0008-5472.CAN-09-3237
98. Gu Y, Guise CP, Patel K, Abbattista MR, Li J, Sun X, et al. Reductive Metabolism of the Dinitrobenzamide Mustard Anticancer Prodrug PR-104 in Mice. *Cancer Chemother Pharmacol* (2011) 67(3):543–55. doi: 10.1007/s00280-010-1354-5
99. Gu Y, Patterson AV, Atwell GJ, Chernikova SB, Brown JM, Thompson LH, et al. Roles of DNA Repair and Reductase Activity in the Cytotoxicity of the Hypoxia-Activated Dinitrobenzamide Mustard PR-104A. *Mol Cancer Ther* (2009) 8(6):1714–23. doi: 10.1158/1535-7163.MCT-08-1209
100. Hicks KO, Myint H, Patterson AV, Pruijn FB, Siim BG, Patel K, et al. Oxygen Dependence and Extravascular Transport of Hypoxia-Activated Prodrugs: Comparison of the Dinitrobenzamide Mustard PR-104A and Tirapazamine. *Int J Radiat Oncol Biol Phys* (2007) 69(2):560–71. doi: 10.1016/j.ijrobp.2007.05.049
101. Foehrenbacher A, Patel K, Abbattista MR, Guise CP, Secomb TW, Wilson WR, et al. The Role of Bystander Effects in the Antitumor Activity of the Hypoxia-Activated Prodrug Pr-104. *Front Oncol* (2013) 3:263. doi: 10.3389/fonc.2013.00263
102. Cairns RA, Bennewith KL, Graves EE, Giaccia AJ, Chang DT, Denko NC. Pharmacologically Increased Tumor Hypoxia Can be Measured by 18F-Fluoroazomycin Arabinoside Positron Emission Tomography and Enhances Tumor Response to Hypoxic Cytotoxin PR-104. *Clin Cancer Res* (2009) 15(23):7170–4. doi: 10.1158/1078-0432.CCR-09-1676
103. Graves EE, Vilalta M, Cecic IK, Erler JT, Tran PT, Felsher D, et al. Hypoxia in Models of Lung Cancer: Implications for Targeted Therapeutics. *Clin Cancer Res* (2010) 16(19):4843–52. doi: 10.1158/1078-0432.CCR-10-1206
104. Abbattista MR, Jamieson SM, Gu Y, Nickel JE, Pullen SM, Patterson AV, et al. Pre-Clinical Activity of PR-104 as Monotherapy and in Combination With Sorafenib in Hepatocellular Carcinoma. *Cancer Biol Ther* (2015) 16(4):610–22. doi: 10.1080/15384047.2015.1017171
105. Jameson MB, Rischin D, Pegram M, Gutheil J, Patterson AV, Denny WA, et al. A Phase I Trial of PR-104, a Nitrogen Mustard Prodrug Activated by Both Hypoxia and Aldo-Keto Reductase 1C3, in Patients With Solid Tumors. *Cancer Chemother Pharmacol* (2010) 65(4):791–801. doi: 10.1007/s00280-009-1188-1
106. McKeage MJ, Gu Y, Wilson WR, Hill A, Amies K, Melink TJ, et al. A Phase I Trial of PR-104, a Pre-Prodrug of the Bioreductive Prodrug PR-104A, Given Weekly to Solid Tumour Patients. *BMC Cancer* (2011) 11:432. doi: 10.1186/1471-2407-11-432
107. McKeage MJ, Jameson MB, Ramanathan RK, Rajendran J, Gu Y, Wilson WR, et al. Pr-104 a Bioreductive Pre-Prodrug Combined With Gemcitabine or Docetaxel in a Phase Ib Study of Patients With Advanced Solid Tumours. *BMC Cancer* (2012) 12:496. doi: 10.1186/1471-2407-12-496
108. Abou-Alfa GK, Chan SL, Lin CC, Chiorean EG, Holcombe RF, Mulcahy MF, et al. Pr-104 Plus Sorafenib in Patients With Advanced Hepatocellular Carcinoma. *Cancer Chemother Pharmacol* (2011) 68(2):539–45. doi: 10.1007/s00280-011-1671-3
109. Benito J, Shi Y, Szymanska B, Carol H, Boehm I, Lu H, et al. Pronounced Hypoxia in Models of Murine and Human Leukemia: High Efficacy of Hypoxia-Activated Prodrug PR-104. *PLoS One* (2011) 6(8):e23108. doi: 10.1371/journal.pone.0023108
110. Konopleva M, Thall PF, Yi CA, Borthakur G, Coveler A, Bueso-Ramos C, et al. Phase I/II Study of the Hypoxia-Activated Prodrug PR104 in Refractory/Relapsed Acute Myeloid Leukemia and Acute Lymphoblastic Leukemia. *Haematologica* (2015) 100(7):927–34. doi: 10.3324/haematol.2014.118455
111. Moradi Manesh D, El-Hoss J, Evans K, Richmond J, Toscan CE, Bracken LS, et al. AKR1C3 Is a Biomarker of Sensitivity to PR-104 in Preclinical Models of T-Cell Acute Lymphoblastic Leukemia. *Blood* (2015) 126(10):1193–202. doi: 10.1182/blood-2014-12-618900
112. Walton MI, Sugget N, Workman P. The Role of Human and Rodent DT-Diaphorase in the Reductive Metabolism of Hypoxic Cell Cytotoxins. *Int J Radiat Oncol Biol Phys* (1992) 22(4):643–7. doi: 10.1016/0360-3016(92)90495-4
113. Smitskamp-Wilms E, Giaccone G, Pinedo HM, van der Laan BF, Peters GJ. DT-Diaphorase Activity in Normal and Neoplastic Human Tissues; an Indicator for Sensitivity to Bioreductive Agents? *Br J Cancer* (1995) 72(4):917–21. doi: 10.1038/bjc.1995.433
114. Fitzsimmons SA, Workman P, Grever M, Paull K, Camalier R, Lewis AD. Reductase Enzyme Expression Across the National Cancer Institute Tumor Cell Line Panel: Correlation With Sensitivity to Mitomycin C and EO9. *J Natl Cancer Inst* (1996) 88(5):259–69. doi: 10.1093/jnci/88.5.259
115. Smitskamp-Wilms E, Peters GJ, Pinedo HM, van Ark-Otte J, Giaccone G. Chemosensitivity to the Indoloquinone EO9 Is Correlated With DT-diaphorase Activity and Its Gene Expression. *Biochem Pharmacol* (1994) 47(8):1325–32. doi: 10.1016/0006-2952(94)90330-1

116. Hendriks HR, Pizao PE, Berger DP, Kooistra KL, Bibby MC, Boven E, et al. EO9: A Novel Bioreductive Alkylating Indoloquinone With Preferential Solid Tumour Activity and Lack of Bone Marrow Toxicity in Preclinical Models. *Eur J Cancer* (1993) 29A(6):897–906. doi: 10.1016/s0959-8049(05)80434-4
117. Roed H, Aabo K, Vindeløv L, Spang-Thomsen M, Christensen IB, Hansen HH. *In Vitro* and *In Vivo* Evaluation of the Indoloquinone EO-9 (NSC 382 459) Against Human Small Cell Carcinoma of the Lung. *Eur J Cancer Clin Oncol* (1989) 25(8):1197–201. doi: 10.1016/0277-5379(89)90415-x
118. Srivastava G, Somasundaram RT, Walfish PG, Ralhan R. Anticancer Activity of Apaziquone in Oral Cancer Cells and Xenograft Model: Implications for Oral Cancer Therapy. *PLoS One* (2015) 10(7):e0133735. doi: 10.1371/journal.pone.0133735
119. Begleiter A, Leith MK, Curphey TJ, Doherty GP. Induction of DT-diaphorase in Cancer Chemoprevention and Chemotherapy. *Oncol Res* (1997) 9(6-7):371–82. doi: 10.1016/0031-9422(91)83448-T
120. Doherty GP, Leith MK, Wang X, Curphey TJ, Begleiter A. Induction of DT-diaphorase by 1,2-dithiole-3-thiones in Human Tumour and Normal Cells and Effect on Anti-Tumour Activity of Bioreductive Agents. *Br J Cancer* (1998) 77(8):1241–52. doi: 10.1038/bjc.1998.209
121. Collard J, Matthew AM, Double JA, Bibby MC. EO9: Relationship Between DT-Diaphorase Levels and Response *In Vitro* and *In Vivo*. *Br J Cancer* (1995) 71(6):1199–203. doi: 10.1038/bjc.1995.233
122. Plumb JA, Workman P. Unusually Marked Hypoxic Sensitization to Indoloquinone EO9 and Mitomycin C in a Human Colon-Tumour Cell Line That Lacks DT-diaphorase Activity. *Int J Cancer* (1994) 56(1):134–9. doi: 10.1002/ijc.2910560124
123. Bailey SM, Wyatt MD, Friedlos F, Hartley JA, Knox RJ, Lewis AD, et al. Involvement of DT-diaphorase (Ec 1.6.99.2) in the DNA Cross-Linking and Sequence Selectivity of the Bioreductive Anti-Tumour Agent EO9. *Br J Cancer* (1997) 76(12):1596–603. doi: 10.1038/bjc.1997.603
124. Bando T, Kasahara K, Shibata K, Numata Y, Heki U, Shirasaki H, et al. Cytotoxicity of a Novel Indoloquinone Eo9 in Hypoxic Non-Small-Cell Lung-Cancer Cell-Lines. *Int J Oncol* (1995) 7(4):789–93. doi: 10.3892/ijo.7.4.789
125. Robertson N, Haigh A, Adams GE, Stratford IJ. Factors Affecting Sensitivity to EO9 in Rodent and Human Tumour Cells *In Vitro*: DT-diaphorase Activity and Hypoxia. *Eur J Cancer* (1994) 30A(7):1013–9. doi: 10.1016/0959-8049(94)90134-1
126. Phillips RM, Hulbert PB, Bibby MC, Sleigh NR, Double JA. *In Vitro* Activity of the Novel Indoloquinone EO-9 and the Influence of Ph on Cytotoxicity. *Br J Cancer* (1992) 65(3):359–64. doi: 10.1038/bjc.1992.73
127. McLeod HL, Graham MA, Aamdal S, Setanoians A, Groot Y, Lund B. Phase I Pharmacokinetics and Limited Sampling Strategies for the Bioreductive Alkylating Drug EO9. Eortc Early Clinical Trials Group. *Eur J Cancer* (1996) 32A(9):1518–22. doi: 10.1016/0959-8049(96)00120-7
128. Aamdal S, Lund B, Koier I, Houten M, Wanders J, Verweij J. Phase I Trial With Weekly EO9, a Novel Bioreductive Alkylating Indoloquinone, by the EORTC Early Clinical Study Group (Ecsg). *Cancer Chemother Pharmacol* (2000) 45:85–8. doi: 10.1007/PL00006748
129. Pavlidis N, Hanauske AR, Gamucci T, Smyth J, Lehnert M, te Velde A, et al. A Randomized Phase II Study With Two Schedules of the Novel Indoloquinone EO9 in Non-Small-Cell Lung Cancer: A Study of the EORTC Early Clinical Studies Group (Ecsg). *Ann Oncol* (1996) 7(5):529–31. doi: 10.1093/oxfordjournals.annonc.a010645
130. Dirix LY, Tonnesen F, Cassidy J, Epelbaum R, ten Bokkel Huinink WW, Pavlidis N, et al. EO9 Phase II Study in Advanced Breast, Gastric, Pancreatic and Colorectal Carcinoma by the EORTC Early Clinical Studies Group. *Eur J Cancer* (1996) 32A(11):2019–22. doi: 10.1016/0959-8049(96)00226-2
131. Schellens JH, Dombernowsky P, Cassidy J, Epelbaum R, Dirix L, Cox EH, et al. Population Pharmacokinetics and Dynamics in Phase II Studies of the Novel Bioreductive Alkylating Cytotoxic Indoloquinone EO9. *Anticancer Drugs* (2001) 12(7):583–90. doi: 10.1097/00001813-200108000-00004
132. Butler J, Spanswick VJ, Cummings J. The Autoxidation of the Reduced Forms of EO9. *Free Radic Res* (1996) 25(2):141–8. doi: 10.3109/10715769609149919
133. Phillips RM, Hendriks HR, Peters GJ. Eortc-Pharmacology and Molecular Mechanism Group. EO9 (Apaziquone): From the Clinic to the Laboratory and Back Again. *Br J Pharmacol* (2013) 168(1):11–8. doi: 10.1111/j.1476-5381.2012.01996.x
134. Phillips RM, Hendriks HR, Sweeney JB, Reddy G, Peters GJ. Efficacy, Pharmacokinetic and Pharmacodynamic Evaluation of Apaziquone in the Treatment of Non-Muscle Invasive Bladder Cancer. *Expert Opin Drug Metab Toxicol* (2017) 13(7):783–91. doi: 10.1080/17425255.2017.1341490
135. Caramés Masana F, de Reijke TM. The Efficacy of Apaziquone in the Treatment of Bladder Cancer. *Expert Opin Pharmacother* (2017) 18 (16):1781–8. doi: 10.1080/14656566.2017.1392510
136. Puri R, Palit V, Loadman PM, Flannigan M, Shah T, Choudry GA, et al. Phase I/II Pilot Study of Intravesical Apaziquone (EO9) for Superficial Bladder Cancer. *J Urol* (2006) 176(4 Pt 1):1344–8. doi: 10.1016/j.juro.2006.06.047
137. Karsh L, Shore N, Saltzstein D, Bhat G, Reddy G, Allen LF, et al. Integrated Results of Two Multicenter, Randomised, Placebo Controlled, Double Blind, Phase 3 Trials (SPI-611/612) of Single Dose Intravesical Apaziquone Immediately Following Resection in Patients With Nonmuscle Invasive Bladder Cancer. *J Urol* (2016) 95(Supplement):e290. doi: 10.1016/j.juro.2016.02.847
138. Witjes JA, Karsh L, Soloway M, Bhat G, Reddy G, Allen Y, et al. MP13-07 Improved Efficacy of Adjuvant, Single Dose Intravesical Apaziquone by Timing Post-Resection in Two Double Blind, Randomised, Placebo-Controlled Phase 3 Studies in Non-Muscle Invasive Bladder Cancer. *J Urol* (2016) 195(Supplement):e136. doi: 10.1016/j.juro.2016.02.2488
139. Karsh L, Shore N, Soloway M, Bhat G, Reddy G, Leu SY, et al. Double-Blind, Randomized, Placebo-Controlled Studies Evaluating Apaziquone (E09, Qapzola™) Intravesical Instillation Post Transurethral Resection of Bladder Tumors for the Treatment of Low-risk Non-Muscle Invasive Bladder Cancer. *Bladder Cancer* (2018) 4(3):293–301. doi: 10.3233/BLC-180166
140. Phillips RM, Loadman PM, Reddy G. Inactivation of Apaziquone by Haematuria: Implications for the Design of Phase III Clinical Trials Against Non-Muscle Invasive Bladder Cancer. *Cancer Chemother Pharmacol* (2019) 83(6):1183–9. doi: 10.1007/s00280-019-03812-7
141. Duan JX, Jiao H, Kaizerman J, Stanton T, Evans JW, Lan L, et al. Potent and Highly Selective Hypoxia-Activated Achiral Phosphoramidate Mustards as Anticancer Drugs. *J Med Chem* (2008) 51(8):2412–20. doi: 10.1021/jm701028q
142. Hunter FW, Young RJ, Shalev Z, Vellanki RN, Wang J, Gu Y, et al. Identification of P450 Oxidoreductase as a Major Determinant of Sensitivity to Hypoxia-Activated Prodrugs. *Cancer Res* (2015) 75 (19):4211–23. doi: 10.1158/0008-5472.CAN-15-1107
143. Nytko KJ, Grgic I, Bender S, Ott J, Guckenberger M, Riesterer O, et al. The Hypoxia-Activated Prodrug Evofosfamide in Combination With Multiple Regimens of Radiotherapy. *Oncotarget* (2017) 8(14):23702–12. doi: 10.18632/oncotarget.15784
144. Hu J, Handisides DR, Van Valckenborgh E, De Raeve H, Menu E, Vande Broek I, et al. Targeting the Multiple Myeloma Hypoxic Niche With Th-302, a Hypoxia-Activated Prodrug. *Blood* (2010) 116(9):1524–7. doi: 10.1182/blood-2010-02-269126
145. Liapis V, Labrinidis A, Zinonos I, Hay S, Ponomarev V, Panagopoulos V, et al. Hypoxia-Activated Pro-Drug Th-302 Exhibits Potent Tumor Suppressive Activity and Cooperates With Chemotherapy Against Osteosarcoma. *Cancer Lett* (2015) 357(1):160–9. doi: 10.1016/j.canlet.2014.11.020
146. Voissiere A, Jouberton E, Maubert E, Degoul F, Peyrode C, Chezal JM, et al. Development and Characterization of a Human Three-Dimensional Chondrosarcoma Culture for *In Vitro* Drug Testing. *PLoS One* (2017) 12 (7):e0181340. doi: 10.1371/journal.pone.0181340
147. Zhang L, Marrano P, Wu B, Kumar S, Thorner P, Baruchel S. Combined Antitumor Therapy With Metronomic Topotecan and Hypoxia-Activated Prodrug, Evofosfamide, in Neuroblastoma and Rhabdomyosarcoma Preclinical Models. *Clin Cancer Res* (2016) 22(11):2697–708. doi: 10.1158/1078-0432.CCR-15-1853
148. Stokes AM, Hart CP, Quarles CC. Hypoxia Imaging With PET Correlates With Antitumor Activity of the Hypoxia-Activated Prodrug Evofosfamide (Th-302) in Rodent Glioma Models. *Tomography* (2016) 2(3):229–37. doi: 10.18383/j.tom.2016.00259
149. Liapis V, Zinonos I, Labrinidis A, Hay S, Ponomarev V, Panagopoulos V, et al. Anticancer Efficacy of the Hypoxia-Activated Prodrug Evofosfamide (TH-302) in Osteolytic Breast Cancer Murine Models. *Cancer Med* (2016) 5 (3):534–45. doi: 10.1002/cam4.599

150. Sun JD, Liu Q, Ahluwalia D, Ferraro DJ, Wang Y, Jung D, et al. Comparison of Hypoxia-Activated Prodrug Evofosfamide (TH-302) and Ifosfamide in Preclinical Non-Small Cell Lung Cancer Models. *Cancer Biol Ther* (2016) 17 (4):371–80. doi: 10.1080/15384047.2016.1139268
151. Huang Y, Tian Y, Zhao Y, Xue C, Zhan J, Liu L, et al. Efficacy of the Hypoxia-Activated Prodrug Evofosfamide (TH-302) in Nasopharyngeal Carcinoma *In Vitro* and *In Vivo*. *Cancer Commun (Lond)* (2018) 38(1):15. doi: 10.1186/s40880-018-0285-0
152. Portwood S, Lal D, Hsu YC, Vargas R, Johnson MK, Wetzler M, et al. Activity of the Hypoxia-Activated Prodrug, TH-302, in Preclinical Human Acute Myeloid Leukemia Models. *Clin Cancer Res* (2013) 19(23):6506–19. doi: 10.1158/1078-0432.CCR-13-0674
153. Meng F, Evans JW, Bhupathi D, Banica M, Lan L, Lorente G, et al. Molecular and Cellular Pharmacology of the Hypoxia-Activated Prodrug Th-302. *Mol Cancer Ther* (2012) 11(3):740–51. doi: 10.1158/1535-7163.MCT-11-0634
154. Sun JD, Liu Q, Wang J, Ahluwalia D, Ferraro D, Wang Y, et al. Selective Tumor Hypoxia Targeting by Hypoxia-Activated Prodrug TH-302 Inhibits Tumor Growth in Preclinical Models of Cancer. *Clin Cancer Res* (2012) 18 (3):758–70. doi: 10.1158/1078-0432.CCR-11-1980
155. Sun JD, Liu Q, Ahluwalia D, Li W, Meng F, Wang Y, et al. Efficacy and Safety of the Hypoxia-Activated Prodrug TH-302 in Combination With Gemcitabine and Nab-Paclitaxel in Human Tumor Xenograft Models of Pancreatic Cancer. *Cancer Biol Ther* (2015) 16(3):438–49. doi: 10.1080/15384047.2014.100300
156. Ham SL, Joshi R, Luker GD, Tavana H. Engineered Breast Cancer Cell Spheroids Reproduce Biologic Properties of Solid Tumors. *Adv Healthc Mater* (2016) 5(21):2788–98. doi: 10.1002/adhm.201600644
157. Liapis V, Zysk A, DeNichilo M, Zinonos I, Hay S, Panagopoulos V, et al. Anticancer Efficacy of the Hypoxia-Activated Prodrug Evofosfamide Is Enhanced in Combination With Proapoptotic Receptor Agonists Against Osteosarcoma. *Cancer Med* (2017) 6(9):2164–76. doi: 10.1002/cam4.1115
158. Saggar JK, Tannock IF. Chemotherapy Rescues Hypoxic Tumor Cells and Induces Their Reoxygenation and Repopulation-An Effect That is Inhibited by the Hypoxia-Activated Prodrug Th-302. *Clin Cancer Res* (2015) 21 (9):2107–14. doi: 10.1158/1078-0432.CCR-14-2298
159. Meng F, Bhupathi D, Sun JD, Liu Q, Ahluwalia D, Wang Y, et al. Enhancement of Hypoxia-Activated Prodrug TH-302 Anti-Tumor Activity by Chk1 Inhibition. *BMC Cancer* (2015) 15:422. doi: 10.1186/s12885-015-1387-6
160. Sun JD, Ahluwalia D, Liu Q, Li W, Wang Y, Meng F, et al. Combination Treatment With Hypoxia-Activated Prodrug Evofosfamide (TH-302) and mTOR Inhibitors Results in Enhanced Antitumor Efficacy in Preclinical Renal Cell Carcinoma Models. *Am J Cancer Res* (2015) 5(7):2139–55.
161. Wojtkowiak JW, Cornnell HC, Matsumoto S, Saito K, Takakusagi Y, Dutta P, et al. Pyruvate Sensitizes Pancreatic Tumors to Hypoxia-Activated Prodrug Th-302. *Cancer Metab* (2015) 3(1):2. doi: 10.1186/s40170-014-0026-z
162. Takakusagi Y, Kishimoto S, Naz S, Matsumoto S, Saito K, Hart CP, et al. Radiotherapy Synergizes With the Hypoxia-Activated Prodrug Evofosfamide: *In Vitro* and *In Vivo* Studies. *Antioxid Redox Signal* (2018) 28(2):131–40. doi: 10.1089/ars.2017.7106
163. Hajj C, Russell J, Hart CP, Goodman KA, Lowery MA, Haimovitz-Friedman A, et al. A Combination of Radiation and the Hypoxia-Activated Prodrug Evofosfamide (Th-302) is Efficacious Against a Human Orthotopic Pancreatic Tumor Model. *Transl Oncol* (2017) 10(5):760–5. doi: 10.1016/j.tranon.2017.06.010
164. Spiegelberg L, van Hoof SJ, Biemans R, Lieuwes NG, Marcus D, Niemans R, et al. Evofosfamide Sensitizes Esophageal Carcinomas to Radiation Without Increasing Normal Tissue Toxicity. *Radiother Oncol* (2019) 141:247–55. doi: 10.1016/j.radonc.2019.06.034
165. Duran R, Mirpour S, Pekurovsky V, Ganapathy-Kanniappan S, Brayton CF, Cornish TC, et al. Preclinical Benefit of Hypoxia-Activated Intra-Arterial Therapy With Evofosfamide in Liver Cancer. *Clin Cancer Res* (2017) 23 (2):536–48. doi: 10.1158/1078-0432.CCR-16-0725
166. Yoon C, Chang KK, Lee JH, Tap WD, Hart CP, Simon MC, et al. Multimodal Targeting of Tumor Vasculature and Cancer Stem-Like Cells in Sarcomas With VEGF-A Inhibition, HIF-1α Inhibition, and Hypoxia-Activated Chemotherapy. *Oncotarget* (2016) 7(28):42844–58. doi: 10.18632/oncotarget
167. Kumar S, Sun JD, Zhang L, Mokhtari RB, Wu B, Meng F, et al. Hypoxia-Targeting Drug Evofosfamide (Th-302) Enhances Sunitinib Activity in Neuroblastoma Xenograft Models. *Transl Oncol* (2018) 11(4):911–9. doi: 10.1016/j.tranon.2018.05.004
168. Riedel RF, Meadows KL, Lee PH, Morse MA, Uronis HE, Blobe GC, et al. Phase I Study of Pazopanib Plus TH-302 in Advanced Solid Tumors. *Cancer Chemother Pharmacol* (2017) 79(3):611–9. doi: 10.1007/s00280-017-3256-2
169. Benito J, Ramirez MS, Millward NZ, Velez J, Harutyunyan KG, Lu H, et al. Hypoxia-Activated Prodrug Th-302 Targets Hypoxic Bone Marrow Niches in Preclinical Leukemia Models. *Clin Cancer Res* (2016) 22(7):1687–98. doi: 10.1158/1078-0432.CCR-14-3378
170. Lindsay D, Garvey CM, Mumenthaler SM, Foo J. Leveraging Hypoxia-Activated Prodrugs to Prevent Drug Resistance in Solid Tumors. *PLoS Comput Biol* (2016) 12(8):e1005077. doi: 10.1371/journal.pcbi.1005077
171. Jamieson SM, Tsai P, Kondratyev MK, Budhani P, Liu A, Senzer NN, et al. Evofosfamide for the Treatment of Human Papillomavirus-Negative Head and Neck Squamous Cell Carcinoma. *JCI Insight* (2018) 3(16):e122204. doi: 10.1172/jci.insight.122204
172. Jayaprakash P, Ai M, Liu A, Budhani P, Bartkowiak T, Sheng J, et al. Targeted Hypoxia Reduction Restores T Cell Infiltration and Sensitizes Prostate Cancer to Immunotherapy. *J Clin Invest* (2018) 128(11):5137–49. doi: 10.1172/JCI96268
173. Kishimoto S, Brender JR, Chandramouli GVR, Saida Y, Yamamoto K, Mitchell JB, et al. Hypoxia-Activated Prodrug Evofosfamide Treatment in Pancreatic Ductal Adenocarcinoma Xenografts Alters the Tumor Redox Status to Potentiate Radiotherapy. *Antioxid Redox Signal* (2020). doi: 10.1089/ars.2020.8131
174. Weiss GJ, Infante JR, Chiorean EG, Borad MJ, Bendell JC, Molina JR, et al. Phase 1 Study of the Safety, Tolerability, and Pharmacokinetics of TH-302, a Hypoxia-Activated Prodrug, in Patients With Advanced Solid Malignancies. *Clin Cancer Res* (2011) 17(9):2997–3004. doi: 10.1158/1078-0432.CCR-10-3425
175. Chawla SP, Cranmer LD, Van Tine BA, Reed DR, Okuno SH, Butrynski JE, et al. Phase II Study of the Safety and Antitumor Activity of the Hypoxia-Activated Prodrug TH-302 in Combination With Doxorubicin in Patients With Advanced Soft Tissue Sarcoma. *J Clin Oncol* (2014) 32(29):3299–306. doi: 10.1200/JCO.2013.54.3660
176. Borad MJ, Reddy SG, Bahary N, Uronis HE, Sigal D, Cohn AL, et al. Randomized Phase II Trial of Gemcitabine Plus TH-302 *Versus* Gemcitabine in Patients With Advanced Pancreatic Cancer. *J Clin Oncol* (2015) 33 (13):1475–81. doi: 10.1200/JCO.2014.55.7504
177. Brenner A, Zuniga R, Sun JD, Floyd J, Hart CP, Kroll S, et al. Hypoxia-Activated Evofosfamide for Treatment of Recurrent Bevacizumab-Refractory Glioblastoma: A Phase I Surgical Study. *Neuro Oncol* (2018) 20(9):1231–9. doi: 10.1093/neuonc/noy015
178. Laubach JP, Liu CJ, Raje NS, Yee AJ, Armand P, Schlossman RL, et al. A Phase I/Ii Study of Evofosfamide, A Hypoxia-Activated Prodrug With or Without Bortezomib in Subjects With Relapsed/Refractory Multiple Myeloma. *Clin Cancer Res* (2019) 25(2):478–86. doi: 10.1158/1078-0432
179. Badar T, Handisides DR, Benito JM, Richie MA, Borthakur G, Jabbour E, et al. Phase I Study of Evofosfamide, an Investigational Hypoxia-Activated Prodrug, in Patients With Advanced Leukemia. *Am J Hematol* (2016) 91 (8):800–5. doi: 10.1002/ajh.24415
180. Van Cutsem E, Lenz HJ, Furuse J, Tabernero J, Heinemann V, Ioka T, et al. Maestro: A Randomized, Double-Blind Phase III Study of Evofosfamide (Evo) in Combination With Gemcitabine (Gem) in Previously Untreated Patients (Pts) With Metastatic or Locally Advanced Unresectable Pancreatic Ductal Adenocarcinoma (PDAC). *J Clin Oncol* (2016) 34(15_suppl):4007. doi: 10.1200/JCO.2016.34.15_suppl.4007
181. Tap WD, Papai Z, Van Tine BA, Attia S, Ganjoo KN, Jones RL, et al. Doxorubicin Plus Evofosfamide *Versus* Doxorubicin Alone in Locally Advanced, Unresectable or Metastatic Soft-Tissue Sarcoma (TH CR-406/SARC021): An International, Multicentre, Open-Label, Randomised Phase 3 Trial. *Lancet Oncol* (2017) 18(8):1089–103. doi: 10.1016/S1470-2045(17)30381-9
182. Domenyuk V, Liu X, Magee D, Gatalica Z, Stark A, Kennedy P, et al. Poly-Ligand Profiling Differentiates Pancreatic Cancer Patients According to Treatment Benefit From Gemcitabine+Placebo *Versus* Gemcitabine+Evofosfamide and Identifies Candidate Targets. *Ann Oncol* (2018) 29(suppl_5):mdy151.131. doi: 10.1093/annonc/mdy151.131
183. Li Y, Zhao L, Li XF. The Hypoxia-Activated Prodrug TH-302: Exploiting Hypoxia in Cancer Therapy. *Front Pharmacol* (2021) 12:636892. doi: 10.3389/fphar.2021.636892

184. Anderson RF, Li D, Hunter FW. Antagonism in Effectiveness of Evofosfamide and Doxorubicin Through Intermolecular Electron Transfer. *Free Radic Biol Med* (2017) 113:564–70. doi: 10.1016/j.freeradbiomed.2017.10.385
185. Higgins JP, Sarapa N, Kim J, Poma E. Unexpected Pharmacokinetics of Evofosfamide Observed in Phase III MAESTRO Study. *J Clin Oncol* (2018) 36(15_suppl):2568. doi: 10.1200/JCO.2018.36.15_suppl.2568
186. Hunter FW, Wang J, Patel R, Hsu HL, Hickey AJ, Hay MP, et al. Homologous Recombination Repair-Dependent Cytotoxicity of the Benzotriazine Di-N-Oxide CEN-209: Comparison With Other Hypoxia-Activated Prodrugs. *Biochem Pharmacol* (2012) 83(5):574–85. doi: 10.1016/j.bcp.2011.12.005
187. Hicks KO, Siim BG, Jaiswal JK, Pruijn FB, Fraser AM, Patel R, et al. Pharmacokinetic/Pharmacodynamic Modeling Identifies SN30000 and SN29751 as Tirapazamine Analogues With Improved Tissue Penetration and Hypoxic Cell Killing in Tumors. *Clin Cancer Res* (2010) 16(20):4946–57. doi: 10.1158/1078-0432.CCR-10-1439
188. Mao X, McManaway S, Jaiswal JK, Patel PB, Wilson WR, Hicks KO, et al. An Agent-Based Model for Drug-Radiation Interactions in the Tumour Microenvironment: Hypoxia-Activated Prodrug SN30000 in Multicellular Tumour Spheroids. *PLoS Comput Biol* (2018) 14(10):e1006469. doi: 10.1371/journal.pcbi.1006469
189. Mao X, McManaway S, Jaiswal JK, Hong CR, Wilson WR, Hicks KO. Schedule-Dependent Potentiation of Chemotherapy Drugs by the Hypoxia-Activated Prodrug Sn30000. *Cancer Biol Ther* (2019) 20(9):1258–69. doi: 10.1080/15384047.2019.1617570
190. Chitneni SK, Bida GT, Yuan H, Palmer GM, Hay MP, Melcher T, et al. 18f-Ef5 PET Imaging as an Early Response Biomarker for the Hypoxia-Activated Prodrug SN30000 Combined With Radiation Treatment in a Non-Small Cell Lung Cancer Xenograft Model. *J Nucl Med* (2013) 54(8):1339–46. doi: 10.2967/jnumed.112.116293
191. Wang J, Foehrenbacher A, Su J, Patel R, Hay MP, Hicks KO, et al. The 2-Nitroimidazole EF5 Is a Biomarker for Oxidoreductases That Activate the Bioreductive Prodrug CEN-209 Under Hypoxia. *Clin Cancer Res* (2012) 18 (6):1684–95. doi: 10.1158/1078-0432.CCR-11-2296
192. Grkovski M, Fanchon L, Pillarsetty NVK, Russell J, Humm JL. 18F-Fluoromisonidazole Predicts Evofosfamide Uptake in Pancreatic Tumor Model. *EJNMMI Res* (2018) 8(1):53. doi: 10.1186/s13550-018-0409-1
193. Cui YL, Wang X, Li XF. (18)F-Fluoromisonidazole PET Reveals Spatial and Temporal Heterogeneity of Hypoxia in Mouse Models of Human Non-Small-Cell Lung Cancer. *Future Oncol* (2015) 11(20):2841–9. doi: 10.2217/fon.15.205
194. Ljungkvist AS, Bussink J, Kaanders JH, Rijken PF, Begg AC, Raleigh JA, et al. Hypoxic Cell Turnover in Different Solid Tumor Lines. *Int J Radiat Oncol Biol Phys* (2005) 62(4):1157–68. doi: 10.1016/j.ijrobp.2005.03.049
195. Li XF, Sun X, Ma Y, Suehiro M, Zhang M, Russell J, et al. Detection of Hypoxia in Microscopic Tumors Using 131I-Labeled Iodo-Azomycin Galactopyranoside (131I-IAZGP) Digital Autoradiography. *Eur J Nucl Med Mol Imaging* (2010) 37(2):339–48. doi: 10.1007/s00259-009-1310-y
196. Li XF, Ma Y, Sun X, Humm JL, Ling CC, O'Donoghue JA. High 18F-FDG Uptake in Microscopic Peritoneal Tumors Requires Physiologic Hypoxia. *J Nucl Med* (2010) 51(4):632–8. doi: 10.2967/jnumed.109.071233
197. Huang T, Civelek AC, Zheng H, Ng CK, Duan X, Li J, et al. (18)F-Misonidazole PET Imaging of Hypoxia in Micrometastases and Macroscopic Xenografts of Human Non-Small Cell Lung Cancer: A Correlation With Autoradiography and Histological Findings. *Am J Nucl Med Mol Imaging* (2013) 3(2):142–53.

**Conflict of Interest:** The authors declare that the research was conducted in the absence of any commercial or financial relationships that could be construed as a potential conflict of interest.

**Publisher's Note:** All claims expressed in this article are solely those of the authors and do not necessarily represent those of their affiliated organizations, or those of the publisher, the editors and the reviewers. Any product that may be evaluated in this article, or claim that may be made by its manufacturer, is not guaranteed or endorsed by the publisher.

frontiers in Pharmacology

ORIGINAL RESEARCH
published: 04 August 2021
doi: 10.3389/fphar.2021.712181

# Metformin Potentiates the Effects of Anlotinib in NSCLC *via* AMPK/mTOR and ROS-Mediated Signaling Pathways

*Zhongling Zhu[1†], Teng Jiang[1†], Huirong Suo[2†], Shan Xu[1], Cai Zhang[1], Guoguang Ying[3] and Zhao Yan[1,4*]*

[1]Department of Clinical Pharmacology, Tianjin Medical University Cancer Institute and Hospital, National Clinical Research Center for Cancer, Key Laboratory of Cancer Prevention and Therapy, Tianjin's Clinical Research Center for Cancer, Tianjin, China, [2]Department of Pharmacy, The Second Hospital of Tianjin Medical University, Tianjin, China, [3]Department of Tumor Cell Biology, Tianjin Medical University Cancer Institute and Hospital, National Clinical Research Center for Cancer, Key Laboratory of Cancer Prevention and Therapy, Tianjin's Clinical Research Center for Cancer, Tianjin, China, [4]Department of Continuing Education and Science and Technology Service, China Anti-cancer Association, Tianjin, China

OPEN ACCESS

**Edited by:**
Aniello Cerrato,
Consiglio Nazionale Delle Ricerche (CNR), Italy

**Reviewed by:**
Ganesh Prasad Mishra,
Swami Vivekanand Subharti University, India
Gamal Eldein Fathy Abd-Ellatef Abd-Elrahman,
National Research Centre (Egypt), Egypt

***Correspondence:**
Zhao Yan
yanzhaopaper@163.com

[†]These authors have contributed equally to this work.

**Specialty section:**
This article was submitted to Pharmacology of Anti-Cancer Drugs, a section of the journal Frontiers in Pharmacology

**Received:** 20 May 2021
**Accepted:** 21 July 2021
**Published:** 04 August 2021

**Citation:**
Zhu Z, Jiang T, Suo H, Xu S, Zhang C, Ying G and Yan Z (2021) Metformin Potentiates the Effects of Anlotinib in NSCLC via AMPK/mTOR and ROS-Mediated Signaling Pathways. Front. Pharmacol. 12:712181. doi: 10.3389/fphar.2021.712181

Anlotinib is a novel multi-targeted tyrosine kinase inhibitor with activity against soft tissue sarcoma, small cell lung cancer, and non-small cell lung cancer (NSCLC). Potentiating the anticancer effect of anlotinib in combination strategies remains a clinical challenge. Metformin is an oral agent that is used as a first-line therapy for type 2 diabetes. Interesting, metformin also exerts broad anticancer effects through the activation of AMP-activated protein kinase (AMPK) and inhibition of mammalian target of rapamycin (mTOR). Here, we evaluated the possible synergistic effect of anlotinib and metformin in NSCLC cells. The results showed that metformin enhanced the antiproliferative effect of anlotinib. Moreover, anlotinib combined with metformin induced apoptosis and oxidative stress, which was associated with the activation of AMPK and inhibition of mTOR. Reactive oxygen species (ROS)- mediated p38/JNK MAPK and ERK signaling may be involved in the anticancer effects of this combination treatment. Our results show that metformin potentiates the efficacy of anlotinib *in vivo* by increasing the sensitivity of NSCLC cells to the drug. These data provide a potential rationale for the combination of anlotinib and metformin for the treatment of patients with NSCLC or other cancers.

**Keywords: non-small cell lung cancer, anlotinib, metformin, AMP-activated protein kinase, reactive oxygen species**

## INTRODUCTION

Lung cancer is the leading cause of cancer-related death, accounting for over 1.7 million deaths per year worldwide (Bray et al., 2018). Approximately 85% of all lung cancers are non-small cell lung cancer (NSCLC). Most patients with NSCLC have advanced disease or local metastasis at diagnosis, and the 5-years overall survival rate is less than 20% (Hirsch et al., 2017). In recent years, checkpoint inhibitors and inhibitors of constitutively active EGFR, ALK, or ROS1 receptor tyrosine kinases (RTKs) have markedly improved tumor responses and clinical outcomes in patients with NSCLC (Hirsch et al., 2017; Assi et al., 2018).

Anlotinib is a novel, multitargeted tyrosine kinase inhibitor that has activity against a range of RTKs involved in vascularization and tumor progression, including VEGFR-1, -2, and -3; FGFR-1,

-2, -3, and -4; c-kit; and PDGFR-α and -β (Shen et al., 2018; Gao et al., 2020). Several clinical trials have demonstrated that anlotinib is well tolerated and has promising efficacy in patients with solid tumors, including advanced NSCLC, soft tissue sarcoma, medullary thyroid carcinoma, esophageal squamous cell carcinoma, and metastatic renal cell carcinoma (Chi et al., 2018; Sun et al., 2018; Zhou et al., 2019; Ma et al., 2020; Wu et al., 2020; Huang et al., 2021). In phase III clinical trials, the median overall survival for patients with advanced NSCLC who progressed after treatment with at least two lines of prior systemic chemotherapy had increased by 3.3 months (Han et al., 2018). Based on these data, anlotinib was approved by the China National Medical Products Administration for third-line or further treatment of advanced NSCLC in 2018 (Syed, 2018).

The biguanide metformin is a first-line oral anti-diabetic drug. Several studies have shown that metformin inhibits cancer cell growth and induces both cell cycle arrest and apoptosis (Alimova et al., 2009; Dowling et al., 2011). Treatment with metformin has been reported to suppress the growth of tumor xenografts in nude mice (Wheaton et al., 2014). However, the mechanisms underlying these effects are poorly understood. It is known that metformin inhibits complex I of the mitochondrial electron transport chain (Fontaine, 2018), resulting in an increase in the intracellular AMP/ATP ratio and indirect activation of AMP-activated protein kinase (AMPK). AMPK activation promotes metabolic flexibility and net ATP conservation through multiple mechanisms, including activation of catabolic pathways, inhibition of anabolic processes that consume ATP, induction of autophagy, and maintenance of NADPH homeostasis to buffer reactive oxygen species (ROS). Retaining AMPK activity may protect tumor cells from bioenergetic catastrophe and provide them with a selective growth advantage under stress. Conversely, AMPK activation can inhibit mTOR signaling, leading to decreased HIFα-driven metabolism of glucose and glutamine (Faubert et al., 2015). Metformin can also exert anti-tumor effects through AMPK-independent pathways (Kalender et al., 2010).

Metformin was previously reported to increase the sensitivity of cancer cells to targeted therapies and chemotherapies (Zhang and Guo, 2016; Deng et al., 2019). Multiple combinations of metformin with targeted agents, such as gefitinib, trastuzumab, and temsirolimus, are currently being tested in phase I/II clinical trials (Khawaja et al., 2016; Zhang and Guo, 2016; Martin-Castillo et al., 2018). Here, we report the synergistic effect of anlotinib in combination with metformin *in vitro* and *in vivo*. We observed AMPK activation and inhibition of the downstream mTOR pathway, which may partly explain the synergistic cytotoxic effect. In addition, ROS-mediated p38/JNK MAPK and ERK signaling may be involved in the anticancer effect of the combination.

# MATERIALS AND METHODS

## Reagents

Anlotinib was kindly provided by Chia Tai Tian Qing Pharmaceutical Group Co., Ltd (Nanjing, China). Metformin, 3- (4,5-dimethylthiazol-2-yl)-2,5-diphenyltetrazolium bromide (MTT), methanol, crystal violet, and phosphate-buffered saline (PBS) were purchased from Solarbio Bioscience & Technology Co. Ltd (Beijing, China). Hoechst 33342, propidium iodide (PI), 2,7-dichlorodihydrofluorescein diacetate (DCFH-DA), and SDS lysis buffer were obtained from Beyotime Biotechnology Co., Ltd (Shanghai, China). Dulbecco's modified Eagle's medium (DMEM), fetal bovine serum (FBS), trypsin, and penicillin/streptomycin were purchased from Invitrogen (Carlsbad, CA, United States).

## Cell Culture

The human lung cell lines A549 and H460 were obtained from American Type Culture Collection (Manassas, VA, United States) and were authenticated *via* DNA sequencing on an ABI 3730xl genetic analyzer. The cells were grown in DMEM supplemented with 10% heat-inactivated FBS, 100 units/ml penicillin, and 100 μg/ml streptomycin in a humidified atmosphere with 5% $CO_2$ at 37°C.

## MTT Cell Viability Assay

Cells were seeded in 96-well culture plates at a density of 1–3 × $10^3$ cells/well. After 24 h, various concentrations of anlotinib (range, 0–20 μmol/L), metformin (range, 0–20 mmol/L), or both were added to the cells. After 72 h of incubation, 5 mg/ml MTT was added to each well and incubated for 4 h. The supernatants were carefully aspirated and the formazan crystals were dissolved in DMSO. Absorbance was recorded at 570 nm using a microplate reader.

## Colony Formation Assay

For clonogenic survival studies, 300 cells were seeded in 12-well plates and exposed to different treatments for 48 h. After 10–14 days of incubation, the colonies were fixed in cold methanol for 6 min and then stained with 1% crystal violet solution for 30 min. Colonies containing more than 50 cells were counted. Percent colony formation was calculated by comparison to that in untreated cultures, which was set to 100%. Thus, the percent colony formation of treated cells was calculated as follows: colony formation by treated cells/colony formation by untreated cells × 100.

## Apoptosis Assay

The apoptosis assay was performed using Hoechst 33342/PI fluorescence double staining. Briefly, A549 and H460 cells were seeded at approximately 50% confluence in six-well cell culture plates. Thereafter, cells were incubated with anlotinib (10 μM), metformin (10 mM), or both for 24 h. Finally, the treated cells were stained with Hoechst 33342 (10 μg/ml) and PI (5 μg/ml) at 37°C for 15 min and then imaged using fluorescence microscopy.

## Western Blot Analysis

Cells were washed with ice-cold PBS and lysed with SDS lysis buffer. The protein concentration in the lysates was determined using BCA reagent (Pierce, Rockford, IL, United States). The proteins were separated *via* SDS-polyacrylamide gel

electrophoresis and then electrotransferred onto PVDF membranes (Millipore, Bedford, MA, United States). The membranes were blocked with 5% nonfat milk and incubated overnight at 4°C with primary antibodies against AMPK (#5832), phospho-AMPK (Thr172) (#2535), mTOR (#2983), phospho-mTOR (Ser2448) (#5536), acetyl-CoA carboxylase (ACC) (#3676), phospho-ACC (Ser79) (#3661), hypoxia-inducible factor 1α (HIF1α) (#36169), extracellular signal-regulated kinase (ERK1/2) (#4695), phospho-ERK1/2 (Thr202/Tyr204) (#4370), c-Jun NH 2-terminal kinase (JNK) (#9252), phospho-JNK (Thr183/Tyr185) (#4668), p38 (#8690), phospho-p38 (#4511) (Thr180/Tyr182), Bax (#5023), Bcl-2(#2870), cleaved caspase-3 (#9664), and cleaved PARP (#5625), which were purchased from Cell Signaling Technology (Danvers, MA, USA).Antibodies against $\beta$-actin (sc-47778) were purchased from Santa Cruz Biotechnology (Santa Cruz, CA, United States). After washing, the membranes were incubated with IRDye-conjugated anti-rabbit or anti-mouse IgG antibodies (LI-COR Biosciences, Lincoln, NE, United States). The proteins were visualized using an Odyssey LI-COR infrared imaging system.

## ROS Staining

Intracellular hydrogen peroxide was detected using a DCFH-DA fluorescent probe. Cells were cultured in six-well plates and treated as indicated. Cells were washed twice with PBS and then incubated with 10 μM DCFH-DA and 10 μg/ml Hoechst 33342 at 37°C for 30 min and then imaged using fluorescence microscopy.

## Determination of Intracellular ATP and the $NADP^+$/NADPH Ratio

Relative intracellular ATP levels and the $NADP^+$/NADPH ratio were determined using assay kits (Beyotime Biotechnology, Jiangsu, China) according to the manufacturer's instructions. Briefly, cells were cultured in six-well plates and treated as indicated. At harvest, the cells were washed twice with PBS and lysed in lysis buffer. After centrifugation at 12,000 × *g* at 4°C for 5 min, the supernatant was collected. Intracellular ATP levels were determined using a luminescent plate reader. The protein concentration was quantified using BCA reagent to normalize protein levels for calculating ATP content.

To determine the $NADP^+$/NADPH ratio, the cells were washed twice with PBS and lysed in NADP extraction buffer. Following centrifugation at 12,000 × *g* at 4°C for 10 min, the supernatants were collected and analyzed to quantify the $NADP^+$/NADPH ratio according to the manufacturer's instructions.

## Mouse Xenografts *in vivo*

Four-week-old female BALB/c nude mice were purchased from Beijing HFK Bioscience Co., Ltd (Beijing, China). The animals were maintained under controlled environmental conditions: 22–28°C, 60–70% relative humidity, and a 12 h dark/light cycle with water ad libitum. A549 cells ($3 \times 10^6$ cells) were intravenously injected into the left hind flanks of nude mice (n = 6 mice per group). Tumor volume was calculated using formula $V = (a \times b^2)/2$, where $a$ is the tumor length and $b$ is the tumor width. When the tumor volume reached approximately 100 $mm^3$, the mice were randomly assigned to the control [treated with vehicle (sterile PBS)], anlotinib (0.75 mg/kg), metformin (250 mg/kg), or combination (anlotinib plus metformin) groups. Anlotinib and metformin were intragastrically administered daily for 28 consecutive days. Tumor growth was monitored and measured twice per week using a Vernier caliper. Tumors were removed from the mice after 28 days of treatment. The relative tumor volume (RTV) was calculated as the ratio of the tumor volume at time $t$ to the tumor volume at the start of treatment. Inhibition rates are expressed as the ratio of the RTV of the treatment group (TRTV) to the RTV of the control group (CRTV) by dividing the RTV of each treatment group by the RTV of the control group, and then multiplying the quotient by 100 (TRTV/CRTV%). All protocols were approved by the Laboratory Animal Ethics Committee of Tianjin Medical University Cancer Institute and Hospital.

## Statistical Analysis

In the xenograft experiment, randomization was performed using a computer-generated sequence of random numbers. In other experiments, randomization was not performed. Data are presented as the mean ± SE from three independent experiments. Data were analyzed using GraphPad Prism 5.01. Mean values were compared using the unpaired Student's $t$-test. Normality distribution was assessed using the Shapiro-Wilk test. The combination index (CI) was calculated using CompuSyn software (Biosoft, Cambridge, United Kingdom). Statistical significance was set at $p < 0.05$ (*) or $p < 0.01$ (**).

# RESULTS

## Metformin Potentiates the Antiproliferative Effect of Anlotinib in NSCLC Cells

To examine the potential synergistic effect of anlotinib and metformin on cancer cell proliferation, we studied this drug combination in the NSCLC cell lines A549 and H460 using MTT and colony formation assays. As shown in **Figure 1A**, although each agent alone inhibited the proliferation of A549 and H46 cells, the combination had the strongest antiproliferative effect. The CI values were calculated using cytotoxicity data from the MTT assay. The results revealed that the CI values were less than one in both cell lines (**Figure 1B**). A CI value < 1 indicates drug synergism. The addition of metformin reduced the half-maximal inhibitory concentration of anlotinib by 2.7-fold in A549 cells and by 4. 0-fold in H460 cells (**Figure 1C**). We also tested this combination in a 14-days colony formation assay. Similarly, combined treatment with anlotinib and metformin synergistically suppressed colony formation in both A549 and H460 cells (**Figure 1D**). These data indicate that the antiproliferative effects of anlotinib and metformin are strongly synergistic in A549 and H460 cells.

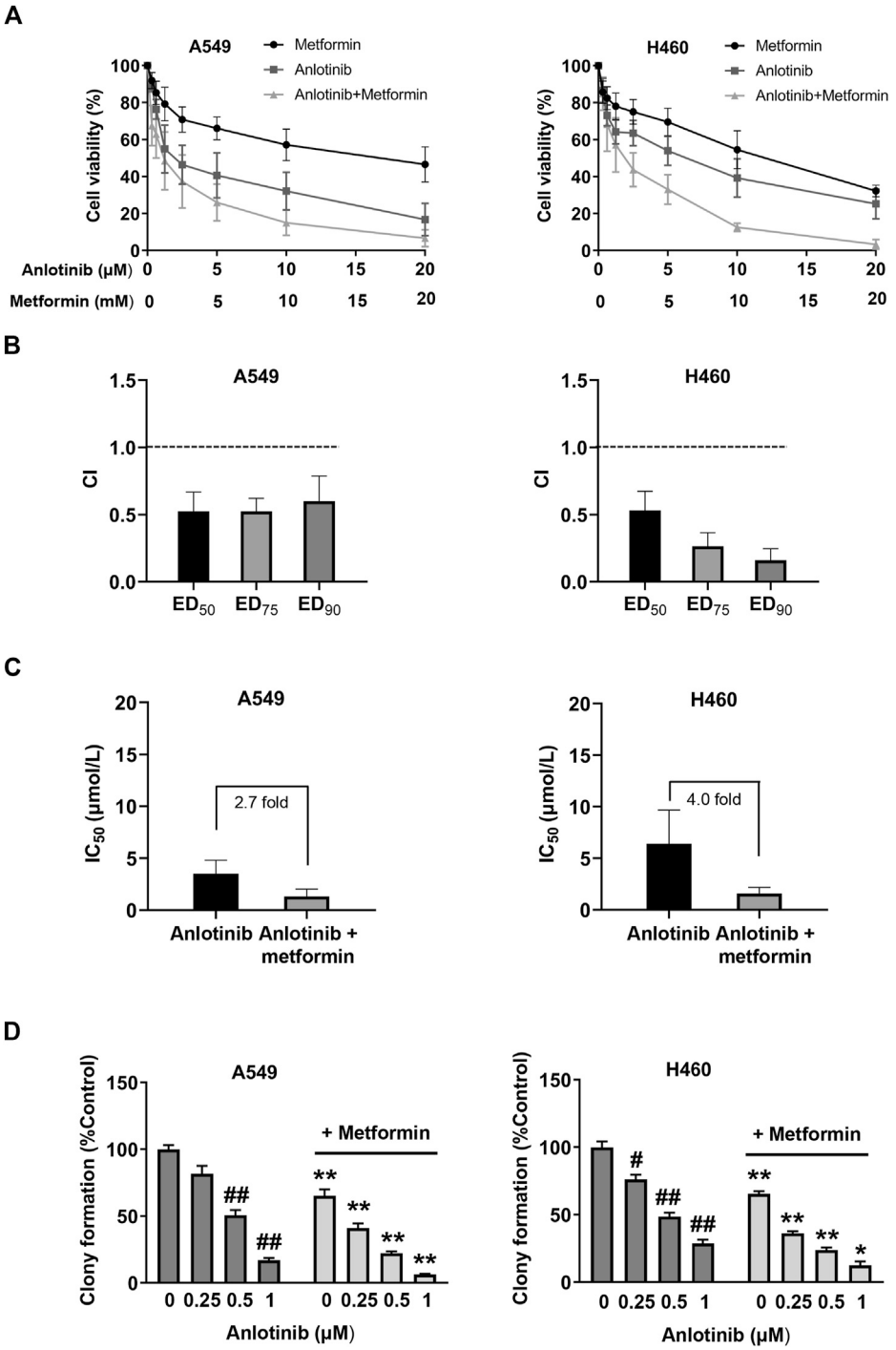


**FIGURE 1 |** Metformin enhances the cytotoxicity of anlotinib in non-small cell lung cancer (NSCLC) cells **(A)** A549 and H460 NSCLC cells were treated with anlotinib (range, 0–20 μmol/L), metformin (range, 0–20 mmol/L), or both for 3 days. Cell viability (%) was determined using the MTT assay **(B)** The CI values were determined for effective dose (ED) $ED_{50}$, $ED_{75}$, and $ED_{90}$. Columns represent data from triplicate analyses ±SE **(C)** The $IC_{50}$ of anlotinib in A549 and H460 cells was reduced by the addition of metformin **(D)** A549 and H460 cells were exposed to the indicated concentrations of anlotinib alone or anlotinib combined with metformin (0.5 mM) for 48 h. Colony-forming efficiency was determined 10–14 days later. Data are presented as means ± SE from three independent experiments. Statistical significance was analyzed using unpaired Student's *t*-test; $^{*}p < 0.05$, $^{**}p < 0.01$ compared with anlotinib alone; $\#p < 0.05$, $\#\#p < 0.01$ compared with the untreated control group.

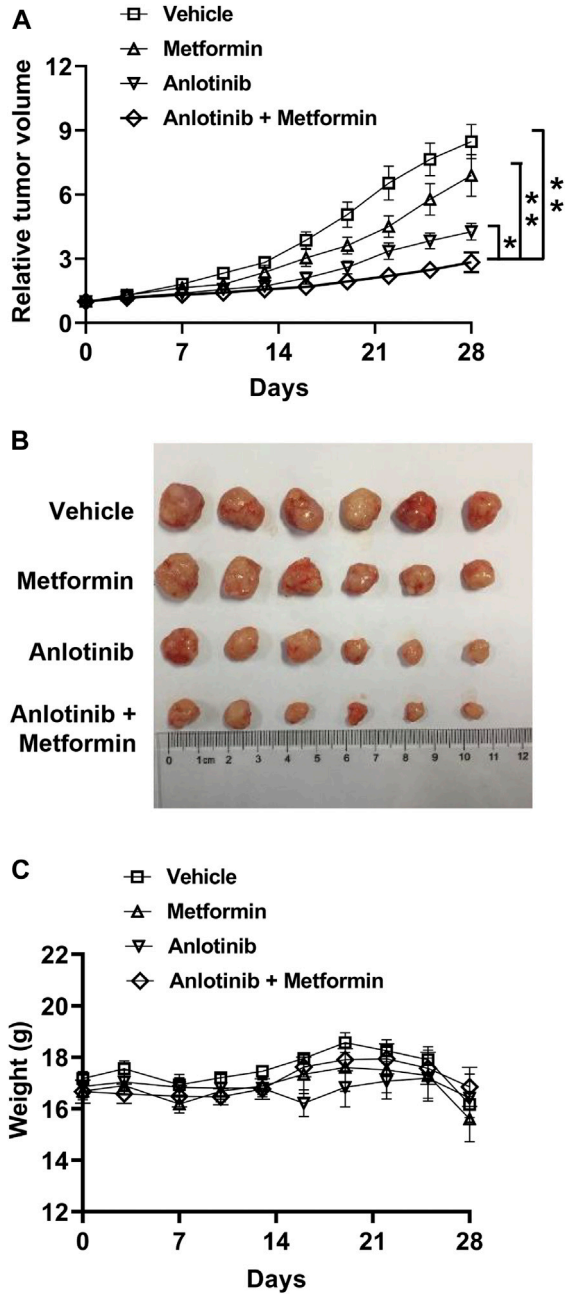


**FIGURE 2 |** Metformin potentiates the efficacy of anlotinib in a xenograft model **(A)** Mice with H460 xenografts were randomly divided into four groups and treated for 28 consecutive days with vehicle (squares), anlotinib (triangles), metformin (inverted triangles), or both anlotinib and metformin (diamonds) as described in the *Materials and Methods* **(B)** The sizes of the xenografts at the end of experiment **(C)** Body weight was measured every 3 days. Data are presented as means ± SE (n = 6 per group). Statistical significance was analyzed using the unpaired Student's *t*-test; $^{*}p < 0.05$, $^{**}p < 0.01$.

## Metformin Enhances the Efficacy of Anlotinib in Tumor Xenografts

We evaluated whether combination treatment with metformin enhanced the antitumor effects of anlotinib using A549 xenografts. Nude mice bearing A549 xenografts were randomized and treated either with anlotinib (0.75 mg/kg), metformin (250 mg/kg), or both. Although anlotinib and metformin as monotherapies decreased tumor growth when compared with the control, the combination treatment potentiated the antitumor effects of each single treatment (**Figures 2A,B**), indicating that the cytotoxicity of anlotinib in the xenograft model was enhanced by the addition of metformin. No significant weight loss was observed in any of the treatment groups, suggesting that the toxicity of the combination was acceptable (**Figure 2C**).

## Anlotinib in Combination with Metformin Induces Cell Apoptosis

We examined the effects of anlotinib and metformin on cell apoptosis *via* Hoechst 33342/PI double staining under a fluorescence microscope. As shown in **Figures 3A,B**, higher numbers of apoptotic and necrotic cells, with condensation of nuclear chromatin and fragmentation, were detected in cells treated with the combination of anlotinib and metformin compared to cells treated with monotherapy. We then determined the expression levels of the apoptosis-related proteins Bcl-2, Bax, caspase 3, and PARP using western blot analysis. The level of Bax protein was substantially increased in response to combination treatment, whereas the expression of Bcl-2 was reduced. We also found that the combination treatment induced caspase 3 and PARP cleavage to an even greater extent (**Figures 3C,D**). These results suggested that the combination treatment likely induced the Bcl-2/Bax-caspase signaling pathway.

## The Synergistic Effect of Anlotinib and Metformin is Mediated by AMPK Activation and mTOR Inhibition

To clarify the mechanisms underlying the antiproliferative effects of the combination treatment, we studied the effects of the combined treatment on the AMPK and mTOR pathways. Our results showed that anlotinib treatment alone induced phosphorylation of AMPKα at Thr-172. Importantly, AMPK activation increased significantly when anlotinib was combined with metformin (**Figure 4**). AMPK activation has been shown to reduce cell proliferation, at least in part, by inhibiting mTOR signaling. We found that the combination treatment had a synergistic effect on the suppression of mTOR phosphorylation. It has been reported that acetyl-coA carboxylase (ACC), which plays an important role in the biosynthesis and oxidation of fatty acids, is a downstream substrate of AMPK signaling. Indeed, we found that phosphorylation of ACC at Ser79 was markedly increased when cells were treated with both anlotinib and metformin (**Figures 4A,B**). Previous studies indicated that metformin might inhibit tumor growth by inhibiting complex I of the respiratory chain and decreasing ATP production. Interestingly, as shown in **Figures 4C,D** the generation of intracellular ATP in A549 and H460 cells was markedly

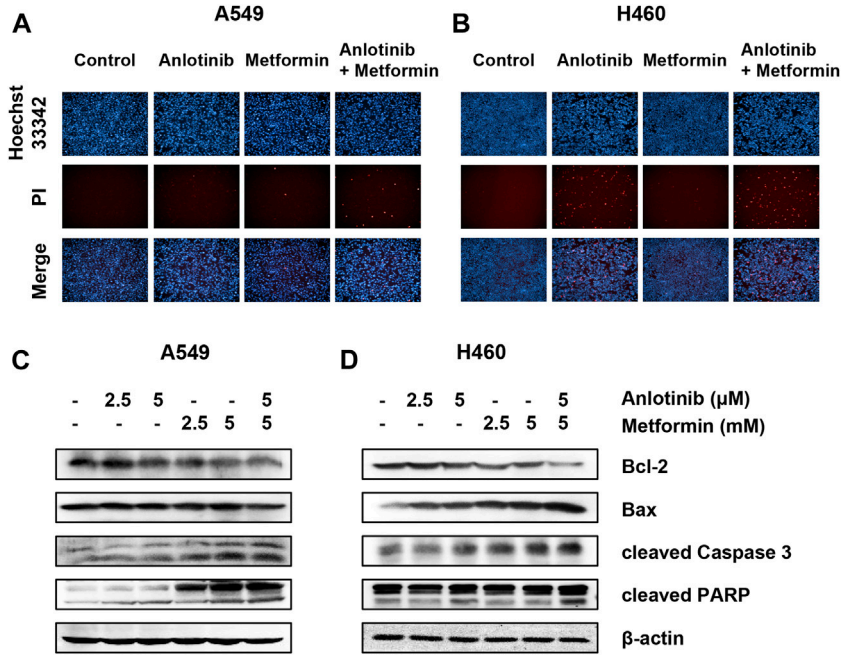


**FIGURE 3 |** Anlotinib with metformin synergistically induces apoptosis. A549 **(A)** and H460 **(B)** cells were incubated with anlotinib (10 μM), metformin (10 mM), or both for 24 h. After Hoechst 33342 (bright blue color) and PI (red color) double staining, the morphological changes in cells undergoing apoptosis and necrosis were observed under a fluorescence microscope. A549 **(C)** and H460 **(D)** cells were treated with the indicated concentrations of anlotinib, metformin, or both for 24 h. Cell lysates were immunoblotted with antibodies against Bcl-2, Bax, cleaved caspase 3, and PARP.

inhibited by exposure to anlotinib in a concentration-dependent manner. In addition, the combination treatment resulted in a lower intracellular ATP levels, suggesting that anlotinib and metformin synergistically inhibited the production of intracellular ATP. HIF-1 transcriptionally promotes anaerobic glycolysis, leading to increased ATP production. Therefore, we next examined HIF-1α expression in treated cells and found that the expression of HIF-1α was markedly inhibited in both A549 and H460 cells exposed to the combination treatment under normoxic conditions (**Figures 4A,B**). These data suggest that the synergistic effect of anlotinib and metformin is related to regulation of the AMPK/mTOR signaling pathway.

## The Combination of Anlotinib and Metformin Promotes Oxidative Stress

ROS plays a crucial role in cell apoptosis signaling pathways. Therefore, we examined whether ROS is involved in the cytotoxic effects of anlotinib. The changes in total ROS production were estimated using a cell-permeable probe DCFH-DA. The fluorescence signals for DCF were markedly enhanced in cells treated with anlotinib and metformin compared to the signals in cells treated with anlotinib or metformin alone (**Figures 5A,B**). Intracellular $NADP^+$/NADPH is believed to be a critical redox couple against oxidative stress. Anlotinib significantly increased the ratio of intracellular $NADP^+$/NADPH in both cell types. The effect of anlotinib on the $NADP^+$/NADPH ratio was potentiated in the presence of metformin, indicating that the combination treatment regulated intracellular redox homeostasis and promoted switching to the oxidative state (**Figures 5C,D**). These results indicate that the combination treatment induced oxidative stress in A549 and H460 cells.

## Anlotinib Combined with Metformin Stimulates the Kinase Activities of p38, JNK, and ERK1/2 Kinases

ROS play a critical role in cell death *via* regulation of the mitogen-activated protein kinase (MAPK) family. Here, we studied the effects of anlotinib and metformin both alone and in combination on the kinase activities of ERK1/2, p38, and JNK. Our results showed that the combination treatment exerted a synergistic effect on p38, JNK, and ERK1/2 activation (**Figure 6**). Thus, these results indicate that anlotinib in combination with metformin enhances the phosphorylation of p38, JNK, and ERK1/2, which may be mediated by ROS.

# DISCUSSION

The anticancer effect of anlotinib has been reported to be associated with its function as a multikinase inhibitor in angiogenic signaling pathways. Anlotinibalso suppresses tumor growth by blocking c-Kit, RET, Aurora-B, c-FMS, and DDR1

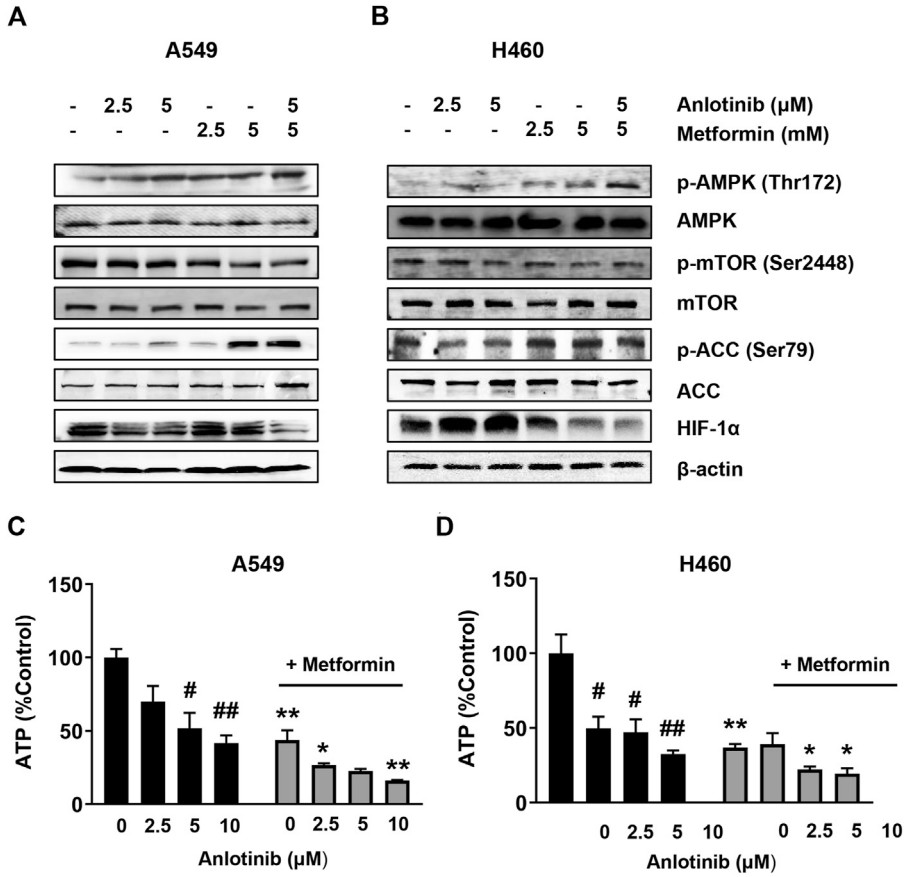


**FIGURE 4 |** Anlotinib in combination with metformin promotes the activation of AMPK and inhibition of mTOR. A549 **(A)** and H460 **(B)** cells were treated with the indicated concentrations of anlotinib, metformin, or both for 24 h. Cell lysates were harvested and immunoblotted with the indicated antibodies. A549 **(C)** and H460 **(D)** were exposed to the indicated concentrations of anlotinib alone or anlotinib and metformin (5 mM) for 24 h. Relative intracellular ATP levels were determined using an assay kit according to the manufacturer's instructions. Data are presented as means ± SE from three independent experiments. Statistical significance was analyzed using unpaired Student's *t*-test; $^{*}p < 0.05$, $^{**}p < 0.01$ compared with anlotinib alone; $\#p < 0.05$, $\#\#p < 0.01$ compared with the untreated control group.

(Sun et al., 2016). In this study, we revealed that metformin could augment the cytotoxic effects of anlotinib. The enhanced synergistic effect of anlotinib and metformin inhibited the proliferation of NSCLC cells both *in vitro* and *in vivo*. The concentrations of anlotinib and metformin administrated in our *in vitro* and *in vivo* experiments are equal to concentrations administrated in previous studies (Chen et al., 2012; Xie et al., 2020), though higher than the therapeutic doses in humans. Low concentrations of metformin (typically 0.1–0. 3 mM) selectively inhibited cancer stem cells, but these low doses had little effect on the proliferation of cancer cells (Ben et al., 2010). The combination treatment increased PARP1 cleavage, caspase-3 cleavage, and the Bax/Bcl-2 ratio, suggesting that the combination treatment triggered apoptosis, possibly mediated by the mitochondrial-dependent pathway.

Previous studies have mostly focused on the effects of anlotinib on angiogenesis and proliferation (Song F. et al., 2020). Comparatively, little attention has been paid to the effects of anlotinib on energy metabolism. In this study, we found that anlotinib significantly decreased the ATP content in NSCLC cells. It is known that decreased ATP can activate AMPK, which inhibits growth by blocking the mTOR pathway (Faubert et al., 2015). Metformin has been shown to reduce cell proliferation through the activation of AMPK and inactivation of mTOR signaling (Rocha et al., 2011; Storozhuk et al., 2013). In our study, we found that anlotinib activated AMPK, downregulated mTOR phosphorylation, and induced apoptosis. Importantly, metformin, as an indirect AMPK activator, potentiates the effects of anlotinib on the AMPK and mTOR signaling pathways. In agreement with our findings, Groenendijk et al. showed that sorafenib synergizes with metformin in NSCLC through the activation of the AMPK pathway (Groenendijk et al., 2015).

As signaling molecules, ROS play a crucial role in cell death signal transduction pathways. Excessive ROS can cause damage to biomacromolecules and promote autophagy, apoptosis, or necrosis (Wong et al., 2010). The $NADP^{+}$/NADPH redox couple is involved in buffering ROS and sustaining antioxidant defenses (Aon et al., 2010). Recently, Yang et al. reported that anlotinib can directly inhibit the proliferation of and induce apoptosis in pancreatic cancer cells through ROS-activated ER stress *via* PERK/p-eIF2α/ATF4

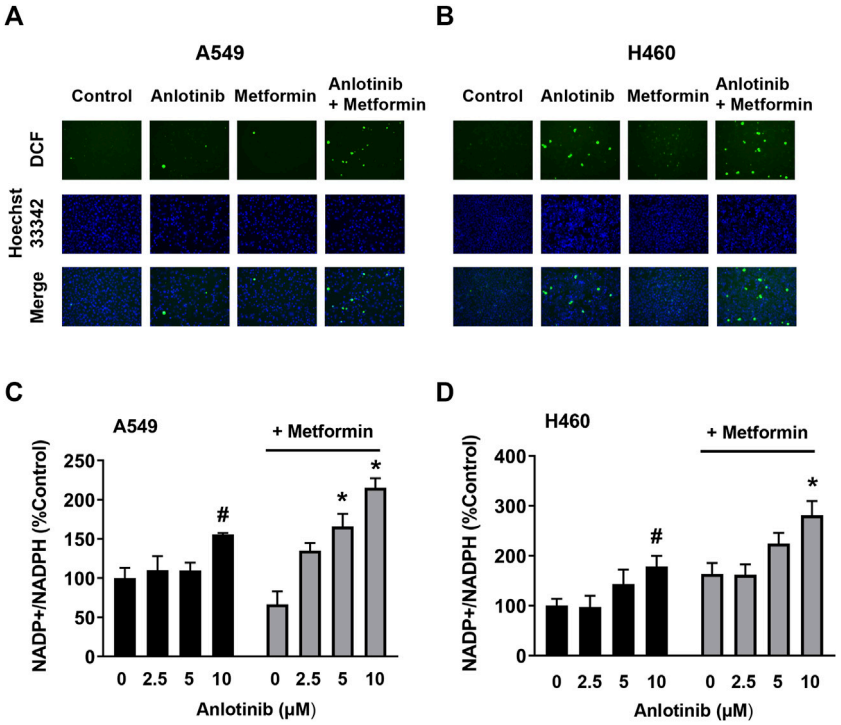


**FIGURE 5 |** Anlotinib combined with metformin increased intracellular ROS levels and the $NADP^+$/NADPH ratio. A549 **(A)** and H460 **(B)** cells were incubated with anlotinib (5 μM), metformin (5 mM), or both for 24 h. After DCF (green color) and Hoechst 33342 (bright blue color) double staining, cellular DCF fluorescence was observed under a fluorescence microscope. A549 **(C)** and H460 **(D)** cells were exposed to the indicated concentrations of anlotinib or anlotinib and metformin (5 mM) for 24 h. The $NADP^+$/NADPH ratio was measured in A549 and H460 cells using an assay kit, as described in the *Materials and Methods*. Data are presented as means ± SE from three independent experiments. Statistical significance was analyzed using unpaired Student's *t*-test; $^*p < 0.05$ compared with anlotinib alone; $\#p < 0.05$ compared with the untreated control group.

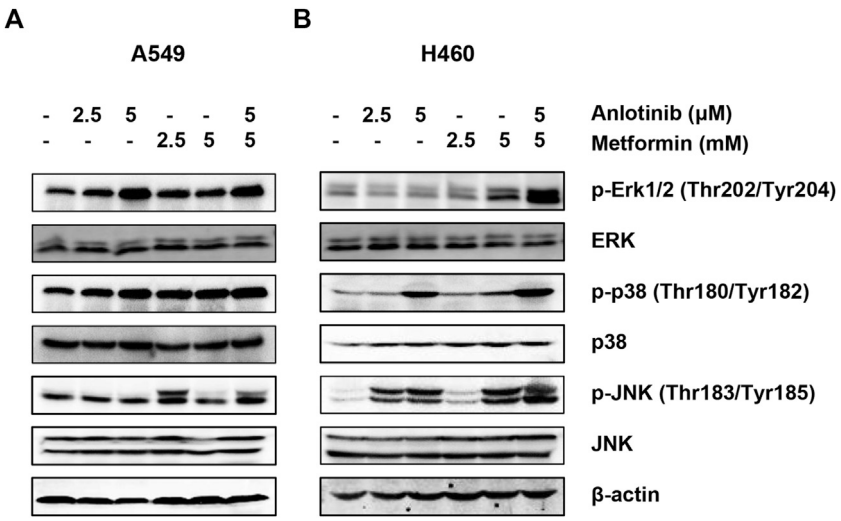


**FIGURE 6 |** Anlotinib combined with metformin increases the phosphorylation of ERK1/2, p38, and JNK. A549 **(A)** and H460 **(B)** cells were incubated with the indicated concentrations of anlotinib, metformin, or both for 24 h. Cell lysates were immunoblotted with antibodies against pERK1/2 and ERK1/2, p-p38 and p38, and pJNK and JNK.

(Yang L. et al., 2020). Similarly, we found that anlotinib or metformin increased ROS production and the $NADP^+$/NADPH ratio in NSCLC cells, indicating that anlotinib or metformin can disrupt intracellular redox homeostasis and induce oxidative stress. Moreover, the combination treatment stimulated ROS generation to an even greater extent. Growing evidence has shown that members of the MAPK family, including p38 MAPK, JNK, and ERK, are critically involved inthe oxidative stress response (El-Najjar et al., 2010). The p38 MAPK and JNK pathways are related to apoptosis, yet activation of ERK is also related to cell survival (Zhang et al., 2019). However, many studies have shown that activation of ERK can promote cell death *via* apoptotic pathways and cell cycle arrest (Wang et al., 2000; Tang et al., 2002; Song Y. et al., 2020). These effects require sustained activation of ERK in specific subcellular compartments (Wang et al., 2000). In our study, we observed that anlotinib increased the phosphorylation of ERK1/2, p38, and JNK, and these increases in phosphorylation were greatest when cells were treated with both anlotinib and metformin. These data suggest that anlotinib-induced apoptosis may be the result of elevated intracellular ROS, which may function as upstream regulators of the p38/JNK MAPK and ERK pathways. In contrast, other studies have shown that anlotinib attenuates ERK activation in diverse cancer cells (Yang Q. et al., 2020; Hu et al., 2020; Lian et al., 2020). Cagnol et al. reported that ERK activity depends on the presence of ROS (Cagnol and Chambard, 2010). Differences in intracellular ROS levels and patterns of ROS accumulation may contribute to this inconsistency.

Thus, several mechanisms may contribute to the synergistic anticancer effect of anlotinib and metformin. The first involves decreased ATP-induced AMPK activation and mTOR inhibition. Additionally, ROS-mediated induction of p38/JNK MAPK and ERK signaling may be involved.

## CONCLUSION

Metformin increases the sensitivity of NSCLC cells to anlotinib both *in vitro* and *in vivo*, providing a potential rationale for the combination of anlotinib with metformin for patients with NSCLC or other cancers.

## DATA AVAILABILITY STATEMENT

The original contributions presented in the study are included in the article/supplementary materials, further inquiries can be directed to the corresponding author.

## ETHICS STATEMENT

The animal study was reviewed and approved by Laboratory Animal Ethics Committee of Tianjin Medical University Cancer Institute and Hospital.

## AUTHOR CONTRIBUTIONS

ZZ and ZY designed the research. TJ, HS and SX performed the experiments and collected data. ZZ, TJ, SX and CZ conducted data analysis. ZZ wrote the paper. ZY and GY revised the paper. All authors reviewed the manuscript.

## FUNDING

This work was supported by the National Natural Science Foundation of China (No. 81402481) and Tianjin Science and Technology Plan Project (No. 18ZXXYSY00070).

## REFERENCES

Alimova, I. N., Liu, B., Fan, Z., Edgerton, S. M., Dillon, T., Lind, S. E., et al. (2009). Metformin Inhibits Breast Cancer Cell Growth, colony Formation and Induces Cell Cycle Arrest *In Vitro*. *Cell Cycle* 8 (6), 909–915. doi:10.4161/cc.8.6.7933

Aon, M. A., Cortassa, S., and O'Rourke, B. (2010). Redox-optimized ROS Balance: a Unifying Hypothesis. *Biochim. Biophys. Acta (Bba) - Bioenerg.* 1797 (6-7), 865–877. doi:10.1016/j.bbabio.2010.02.016

Assi, H. I., Kamphorst, A. O., Moukalled, N. M., and Ramalingam, S. S. (2018). Immune Checkpoint Inhibitors in Advanced Non-small Cell Lung Cancer. *Cancer* 124 (2), 248–261. doi:10.1002/cncr.31105

Ben Sahra, I., Le Marchand-Brustel, Y., Tanti, J. F., and Bost, F. (2010). Metformin in Cancer Therapy: a New Perspective for an Old Antidiabetic Drug?. *Mol. Cancer Ther.* 9 (5), 1092–1099. doi:10.1158/1535-7163.MCT-09-1186

Bray, F., Ferlay, J., Soerjomataram, I., Siegel, R. L., Torre, L. A., and Jemal, A. (2018). Global Cancer Statistics 2018: GLOBOCAN Estimates of Incidence and Mortality Worldwide for 36 Cancers in 185 Countries. *CA: A Cancer J. Clinicians* 68 (6), 394–424. doi:10.3322/caac.21492

Cagnol, S., and Chambard, J. C. (2010). ERK and Cell Death: Mechanisms of ERK-Induced Cell Death - Apoptosis, Autophagy and Senescence. *FEBS J.* 277 (1), 2–21. doi:10.1111/j.1742-4658.2009.07366.x

Chen, G., Xu, S., Renko, K., and Derwahl, M. (2012). Metformin Inhibits Growth of Thyroid Carcinoma Cells, Suppresses Self-Renewal of Derived Cancer Stem Cells, and Potentiates the Effect of Chemotherapeutic Agents. *J. Clin. Endocrinol. Metab.* 97 (4), E510–E520. doi:10.1210/jc.2011-1754

Chi, Y., Fang, Z., Hong, X., Yao, Y., Sun, P., Wang, G., et al. (2018). Safety and Efficacy of Anlotinib, a Multikinase Angiogenesis Inhibitor, in Patients with Refractory Metastatic Soft-Tissue Sarcoma. *Clin. Cancer Res.* 24, 5233–5238. doi:10.1158/1078-0432.CCR-17-3766

Deng, J., Peng, M., Wang, Z., Zhou, S., Xiao, D., Deng, J., et al. (2019). Novel Application of Metformin Combined with Targeted Drugs on Anticancer Treatment. *Cancer Sci.* 110 (1), 23–30. doi:10.1111/cas.13849

Dowling, R. J., Goodwin, P. J., and Stambolic, V. (2011). Understanding the Benefit of Metformin Use in Cancer Treatment. *BMC Med.* 9, 33. doi:10.1186/1741-7015-9-33

El-Najjar, N., Chatila, M., Moukadem, H., Vuorela, H., Ocker, M., Gandesiri, M., et al. (2010). Reactive Oxygen Species Mediate Thymoquinone-Induced Apoptosis and Activate ERK and JNK Signaling. *Apoptosis* 15 (2), 183–195. doi:10.1007/s10495-009-0421-z

Faubert, B., Vincent, E. E., Poffenberger, M. C., and Jones, R. G. (2015). The AMP-Activated Protein Kinase (AMPK) and Cancer: Many Faces of a Metabolic Regulator. *Cancer Lett.* 356 (2), 165–170. doi:10.1016/j.canlet.2014.01.018

Fontaine, E. (2018). Metformin-Induced Mitochondrial Complex I Inhibition: Facts, Uncertainties, and Consequences. *Front. Endocrinol.* 9, 753. doi:10.3389/fendo.2018.00753

Gao, Y., Liu, P., and Shi, R. (2020). Anlotinib as a Molecular Targeted Therapy for Tumors (Review). *Oncol. Lett.* 20 (2), 1001–1014. doi:10.3892/ol.2020.11685

Groenendijk, F. H., Mellema, W. W., van der Burg, E., Schut, E., Hauptmann, M., Horlings, H. M., et al. (2015). Sorafenib Synergizes with Metformin in NSCLC through AMPK Pathway Activation. *Int. J. Cancer* 136 (6), 1434–1444. doi:10.1002/ijc.29113

Han, B., Li, K., Wang, Q., Zhang, L., Shi, J., Wang, Z., et al. (2018). Effect of Anlotinib as a Third-Line or Further Treatment on Overall Survival of Patients with Advanced Non-small Cell Lung Cancer. *JAMA Oncol.* 4 (11), 1569. doi:10.1001/jamaoncol.2018.3039

Hirsch, F. R., Scagliotti, G. V., Mulshine, J. L., Kwon, R., Curran, W. J., Wu, Y.-L., et al. (2017). Lung Cancer: Current Therapies and New Targeted Treatments. *The Lancet* 389 (10066), 299–311. doi:10.1016/S0140-6736(16)30958-8

Hu, H., Liu, Y., Tan, S., Xie, X. X., He, J., Luo, F., et al. (2020). Anlotinib Exerts Anti-cancer Effects on KRAS-Mutated Lung Cancer Cell through Suppressing the MEK/ERK Pathway. *Cmar* 12, 3579–3587. doi:10.2147/CMAR.S243660

Huang, J., Xiao, J., Fang, W., Lu, P., Fan, Q., Shu, Y., et al. (2021). Anlotinib for Previously Treated Advanced or Metastatic Esophageal Squamous Cell Carcinoma: A Double-blind Randomized Phase 2 Trial. *Cancer Med.* 10 (5), 1681–1689. doi:10.1002/cam4.3771

Kalender, A., Selvaraj, A., Kim, S. Y., Gulati, P., Brûlé, S., Viollet, B., et al. (2010). Metformin, Independent of AMPK, Inhibits mTORC1 in a Rag GTPase-dependent Manner. *Cel. Metab.* 11 (5), 390–401. doi:10.1016/j.cmet.2010.03.014

Khawaja, M. R., Nick, A. M., Madhusudanannair, V., Fu, S., Hong, D., Mcquinn, L. M., et al. (2016). Phase I Dose Escalation Study of Temsirolimus in Combination with Metformin in Patients with Advanced/refractory Cancers. *Cancer Chemother. Pharmacol.* 77 (5), 973–977. doi:10.1007/s00280-016-3009-7

Lian, Z., Du, W., Zhang, Y., Fu, Y., Liu, T., Wang, A., et al. (2020). Anlotinib Can Overcome Acquired Resistance to EGFR-TKIs *via* FGFR1 Signaling in Non-small Cell Lung Cancer without Harboring EGFR T790M Mutation. *Thorac. Cancer* 11 (7), 1934–1943. doi:10.1111/1759-7714.13485

Ma, J., Song, Y., Shou, J., Bai, Y., Li, H., Xie, X., et al. (2020). Anlotinib for Patients with Metastatic Renal Cell Carcinoma Previously Treated with One Vascular Endothelial Growth Factor Receptor-Tyrosine Kinase Inhibitor: A Phase 2 Trial. *Front. Oncol.* 10, 664. doi:10.3389/fonc.2020.00664

Martin-Castillo, B., Pernas, S., Dorca, J., Álvarez, I., Martínez, S., Pérez-Garcia, J. M., et al. (2018). A Phase 2 Trial of Neoadjuvant Metformin in Combination with Trastuzumab and Chemotherapy in Women with Early HER2-Positive Breast Cancer: the METTEN Study. *Oncotarget* 9 (86), 35687–35704. doi:10.18632/oncotarget.26286

Rocha, G. Z., Dias, M. M., Ropelle, E. R., Osório-Costa, F., Rossato, F. A., Vercesi, A. E., et al. (2011). Metformin Amplifies Chemotherapy-Induced AMPK Activation and Antitumoral Growth. *Clin. Cancer Res.* 17 (12), 3993–4005. doi:10.1158/1078-0432.CCR-10-2243

Shen, G., Zheng, F., Ren, D., Du, F., Dong, Q., Wang, Z., et al. (2018). Anlotinib: a Novel Multi-Targeting Tyrosine Kinase Inhibitor in Clinical Development. *J. Hematol. Oncol.* 11 (1), 120. doi:10.1186/s13045-018-0664-7

Song, F., Hu, B., Cheng, J.-W., Sun, Y.-F., Zhou, K.-Q., Wang, P.-X., et al. (2020a). Anlotinib Suppresses Tumor Progression *via* Blocking the VEGFR2/PI3K/AKT cascade in Intrahepatic Cholangiocarcinoma. *Cell Death Dis* 11 (7), 573. doi:10.1038/s41419-020-02749-7

Song, Y., Sun, X., Duan, F., He, C., Wu, J., Huang, X., et al. (2020b). SYPL1 Inhibits Apoptosis in Pancreatic Ductal Adenocarcinoma *via* Suppression of ROS-Induced ERK Activation. *Front. Oncol.* 10, 1482. doi:10.3389/fonc.2020.01482

Storozhuk, Y., Hopmans, S. N., Sanli, T., Barron, C., Tsiani, E., Cutz, J.-C., et al. (2013). Metformin Inhibits Growth and Enhances Radiation Response of Non-small Cell Lung Cancer (NSCLC) through ATM and AMPK. *Br. J. Cancer* 108 (10), 2021–2032. doi:10.1038/bjc.2013.187

Sun, Y., Du, F., Gao, M., Ji, Q., Li, Z., Zhang, Y., et al. (2018). Anlotinib for the Treatment of Patients with Locally Advanced or Metastatic Medullary Thyroid Cancer. *Thyroid* 28 (11), 1455–1461. doi:10.1089/thy.2018.0022

Sun, Y., Niu, W., Du, F., Du, C., Li, S., Wang, J., et al. (2016). Safety, Pharmacokinetics, and Antitumor Properties of Anlotinib, an Oral Multi-Target Tyrosine Kinase Inhibitor, in Patients with Advanced Refractory Solid Tumors. *J. Hematol. Oncol.* 9 (1), 105. doi:10.1186/s13045-016-0332-8

Syed, Y. Y. (2018). Anlotinib: First Global Approval. *Drugs* 78 (10), 1057–1062. doi:10.1007/s40265-018-0939-x

Tang, D., Wu, D., Hirao, A., Lahti, J. M., Liu, L., Mazza, B., et al. (2002). ERK Activation Mediates Cell Cycle Arrest and Apoptosis after DNA Damage Independently of P53. *J. Biol. Chem.* 277 (15), 12710–12717. doi:10.1074/jbc.M111598200

Wang, X., Martindale, J. L., and Holbrook, N. J. (2000). Requirement for ERK Activation in Cisplatin-Induced Apoptosis. *J. Biol. Chem.* 275 (50), 39435–39443. doi:10.1074/jbc.M004583200

Wheaton, W. W., Weinberg, S. E., Hamanaka, R. B., Soberanes, S., Sullivan, L. B., Anso, E., et al. (2014). Metformin Inhibits Mitochondrial Complex I of Cancer Cells to Reduce Tumorigenesis. *eLife* 3. doi:10.7554/eLife.02242

Wong, C. H., Iskandar, K. B., Yadav, S. K., Hirpara, J. L., Loh, T., and Pervaiz, S. (2010). Simultaneous Induction of Non-canonical Autophagy and Apoptosis in Cancer Cells by ROS-dependent ERK and JNK Activation. *PLoS One* 5 (4), e9996. doi:10.1371/journal.pone.0009996

Wu, D., Nie, J., Hu, W., Dai, L., Zhang, J., Chen, X., et al. (2020). A Phase II Study of Anlotinib in 45 Patients with Relapsed Small Cell Lung Cancer. *Int. J. Cancer* 147, 3453–3460. doi:10.1002/ijc.33161

Xie, J., Ye, J., Cai, Z., Luo, Y., Zhu, X., Deng, Y., et al. (2020). GPD1 Enhances the Anticancer Effects of Metformin by Synergistically Increasing Total Cellular Glycerol-3-Phosphate. *Cancer Res.* 80 (11), 2150–2162. doi:10.1158/0008-5472.CAN-19-2852

Yang, L., Zhou, X., Sun, J., Lei, Q., Wang, Q., Pan, D., et al. (2020a). Reactive Oxygen Species Mediate Anlotinib-Induced Apoptosis *via* Activation of Endoplasmic Reticulum Stress in Pancreatic Cancer. *Cel. Death Dis.* 11 (9), 766. doi:10.1038/s41419-020-02938-4

Yang, Q., Ni, L., Imani, S., Xiang, Z., Hai, R., Ding, R., et al. (2020b). Anlotinib Suppresses Colorectal Cancer Proliferation and Angiogenesis *via* Inhibition of AKT/ERK Signaling Cascade. *Cmar* 12, 4937–4948. doi:10.2147/CMAR.S252181

Zhang, G., He, J., Ye, X., Zhu, J., Hu, X., Shen, M., et al. (2019). β-Thujaplicin Induces Autophagic Cell Death, Apoptosis, and Cell Cycle Arrest through ROS-Mediated Akt and P38/ERK MAPK Signaling in Human Hepatocellular Carcinoma. *Cel. Death Dis.* 10 (4), 255. doi:10.1038/s41419-019-1492-6

Zhang, H. H., and Guo, X. L. (2016). Combinational Strategies of Metformin and Chemotherapy in Cancers. *Cancer Chemother. Pharmacol.* 78 (1), 13–26. doi:10.1007/s00280-016-3037-3

Zhou, A. P., Bai, Y., Song, Y., Luo, H., Ren, X. B., Wang, X., et al. (2019). Anlotinib versus Sunitinib as First-Line Treatment for Metastatic Renal Cell Carcinoma: A Randomized Phase II Clinical Trial. *Oncol.* 24 (8), e702–e708. doi:10.1634/theoncologist.2018-0839

**Conflict of Interest:** The authors declare that the research was conducted in the absence of any commercial or financial relationships that could be construed as a potential conflict of interest.

**Publisher's Note:** All claims expressed in this article are solely those of the authors and do not necessarily represent those of their affiliated organizations, or those of the publisher, the editors and the reviewers. Any product that may be evaluated in this article, or claim that may be made by its manufacturer, is not guaranteed or endorsed by the publisher.

frontiers in Oncology

REVIEW
published: 24 November 2021
doi: 10.3389/fonc.2021.712505

# Navigating Multi-Scale Cancer Systems Biology Towards Model-Driven Clinical Oncology and Its Applications in Personalized Therapeutics

*Mahnoor Naseer Gondal*[1,2] *and Safee Ullah Chaudhary*[1]*

[1] *Biomedical Informatics Research Laboratory, Department of Biology, Syed Babar Ali School of Science and Engineering, Lahore University of Management Sciences, Lahore, Pakistan,* [2] *Department of Computational Medicine and Bioinformatics, University of Michigan, Ann Arbor, MI, United States*

Rapid advancements in high-throughput omics technologies and experimental protocols have led to the generation of vast amounts of scale-specific biomolecular data on cancer that now populates several online databases and resources. Cancer systems biology models built using this data have the potential to provide specific insights into complex multifactorial aberrations underpinning tumor initiation, development, and metastasis. Furthermore, the annotation of these single- and multi-scale models with patient data can additionally assist in designing personalized therapeutic interventions as well as aid in clinical decision-making. Here, we have systematically reviewed the emergence and evolution of (i) repositories with scale-specific and multi-scale biomolecular cancer data, (ii) systems biology models developed using this data, (iii) associated simulation software for the development of personalized cancer therapeutics, and (iv) translational attempts to pipeline multi-scale panomics data for data-driven *in silico* clinical oncology. The review concludes that the absence of a generic, zero-code, panomics-based multi-scale modeling pipeline and associated software framework, impedes the development and seamless deployment of personalized *in silico* multi-scale models in clinical settings.

**Keywords: multi-scale cancer modeling, personalized cancer therapeutics, cancer systems biology, data-driven oncology, *in silico* cancer systems oncology, predictive systems oncology**

OPEN ACCESS

***Edited by:***
*George Mattheolabakis, University of Louisiana at Monroe, United States*

***Reviewed by:***
*Andrei Leitao, University of São Paulo, Brazil*
*Ulf Schmitz, James Cook University, Australia*

***Correspondence:**
*Safee Ullah Chaudhary*
*safee.ullah.chaudhary@gmail.com*

***Specialty section:***
*This article was submitted to Pharmacology of Anti-Cancer Drugs, a section of the journal Frontiers in Oncology*

***Received:*** *20 May 2021*
***Accepted:*** *26 October 2021*
***Published:*** *24 November 2021*

***Citation:***
*Gondal MN and Chaudhary SU (2021) Navigating Multi-Scale Cancer Systems Biology Towards Model-Driven Clinical Oncology and Its Applications in Personalized Therapeutics. Front. Oncol. 11:712505. doi: 10.3389/fonc.2021.712505*

## 1 INTRODUCTION

In 1971, President Richard Nixon declared his euphemistic "*war on cancer*" through the promulgation of the National Cancer Act (1). Five decades later, despite ground-breaking discoveries and advancements in the field of cancer systems biology, a definitive and affordable cure for all types of cancer still evades humankind (2). Numerous "breakthrough" treatments have also gone on to exhibit adverse side effects (3, 4) that lower patients' quality of life (QoL) or have reported degrading efficacies (5). At the heart of this problem lies our limited understanding of the bewildering multifactorial biomolecular complexity as well as patient-centricity of cancer.

Recent advances in biomolecular cancer research have helped factor system-level oncological manifestations into mutations across genetic, transcriptomic, proteomic, and metabolomic scales (6–9) that also act in concert (10, 11). Crosstalk between multi-scale pathways comprising of these oncogenic mutations can further exacerbate the etiology of the disease (7, 12–14). The combination of mutational diversity and interplay between the constituent pathways adds genetic heterogeneity and phenotypic plasticity in cancer cells (15, 16). Hanahan and Weinberg (17, 18) summarized this heterogeneity and plasticity into "*Hallmarks of Cancer*" – a set of progressively acquired traits during the development of cancer.

Experimental techniques such as high-throughput next-generation sequencing, and mass spectrometry-based proteomics are now providing specific spatiotemporal cues on patient-specific biomolecular aberrations involved in cancer development and growth. The voluminous high-throughput patient data coupled with the remarkable complexity of the disease has given impetus to data integrative *in silico* cancer modeling and therapeutic evaluation approaches (19). Specifically, scale-specific molecular insights into key regulators underpinning each hallmark of cancer are now helping unravel the complex dynamics of the disease (20) besides creating avenues for personalized therapeutics (21, 22). In this review, we will evaluate the emergence, evolution, and integration of multiscale cancer data towards building coherent and biologically plausible *in silico* models and their integrative analysis for employment in personalized cancer treatment in clinical settings. The review concludes by highlighting the need of integrating and modeling multi-omics data and associated software pipelines for employment in developing personalized therapeutics.

# 2 SCALE-SPECIFIC BIOMOLECULAR DATA AND ITS APPLICATIONS IN CANCER

Rapid advancements in molecular biology research, particularly in high-throughput genomics (23), transcriptomics (24), and proteomics (25) have resulted in the generation of big data on spatiotemporal measurements of scale-specific biomolecules (**Figure 1A**) in physiological as well as pathological contexts (26, 27). This vast and complex spatiotemporal data is expected to exceed 40 exabytes by 2025 (28) and is currently populating several online databases and repositories. These databases can be broadly categorized into seven salient database sub-types: biomolecules (29–31), pathways (32–34), networks (35–37), cellular environment (38, 39), cell lines (40–43), histopathological images (44–46), and mutations, and drug (47–52) databases, which are discussed below.

## 2.1 Biomolecular Databases

Biomolecular and clinical data generated from large-scale omics approaches for cancer research can be divided into four sub-categories: (i) genome, (ii) transcriptome, (iii) proteome, and (iv) metabolome (53).

### 2.1.1 Genome-Scale Databases

The foremost endeavor to collect and organize large-scale genomics data into coherent and accessible repositories led to the establishment of GenBank in 1986 (54) (**Figure 1B**, **Table S1**). This open-access resource now forms one of the largest public databases for nucleotide sequences from large-scale sequencing projects comprising over 300,000 species (55, 56). In a salient study employing GenBank, Diez et al. (57) screened breast and ovarian cancer families with mutations in BRCA1 and BRCA2 genes and its distribution in the Spanish population. Medrek et al. (58) employed microarray profile sets from GenBank to analyze gene levels for CD163 and CD68 in different breast cancer patient groups. The study established the need for localization of tumor-associated macrophages as a prognostic marker for breast cancer patients. To date, GenBank remains a comprehensive nucleotide database; however, its data heterogeneity poses a significant challenge in its employment in the development of personalized cancer therapeutics. Towards an improved data stratification and retrieval of genome-scale data, in 2002, Hubbard et al. (59) launched the Ensembl genome database. Ensembl provides a comprehensive resource for human genome sequences capable of automatic annotation and organization of large-scale sequencing data. Amongst various genome-wide studies utilizing Ensembl, Easton et al. (60) used this database to extract human sequence information to identify novel breast cancer susceptibility loci. Patient-specificity (10, 11) and mutational diversity (19) in cancer can manifest across spatiotemporal scales. Hence, the availability of patient-specific data for each type of cancer can furnish valuable insights into the biomolecular foundation of the disease. In an attempt to provide cancer type-specific mutation data, Wellcome Trust's Sanger Institute developed Catalogue of Somatic Mutations in Cancer (COSMIC) (61) database. COSMIC comprises of 10,000 somatic mutations from 66,634 clinical samples. Schubbert et al. (62) employed COSMIC's mutation data to investigate Ras activity in cancers as well as developmental disorders. The study concluded that the duration, as well as the strength of hyperactive Ras signaling controls the probability of tumorigenesis. Similarly, Weir et al. (63) utilized COSMIC data on tumor-suppressor and proto-oncogenes in the study to characterize the genome of lung adenocarcinomas. The systematic copy-number analysis with SNP data indicated that several lung cancer genes remain to be elucidated and characterized.

### 2.1.2 Transcriptome-Scale Databases

Gene-level information can facilitate the development of personalized cancer models; however, gene expression may vary from cell to cell and across cancer patients. As a result, cancer patients have divergent genetic signatures and transcript-level information. Hence, high-throughput transcriptomic data has the potential to provide valuable insights into the transcriptomic complexity in cancer cells and can be useful in investigating cell state, physiology, and relevant biological events

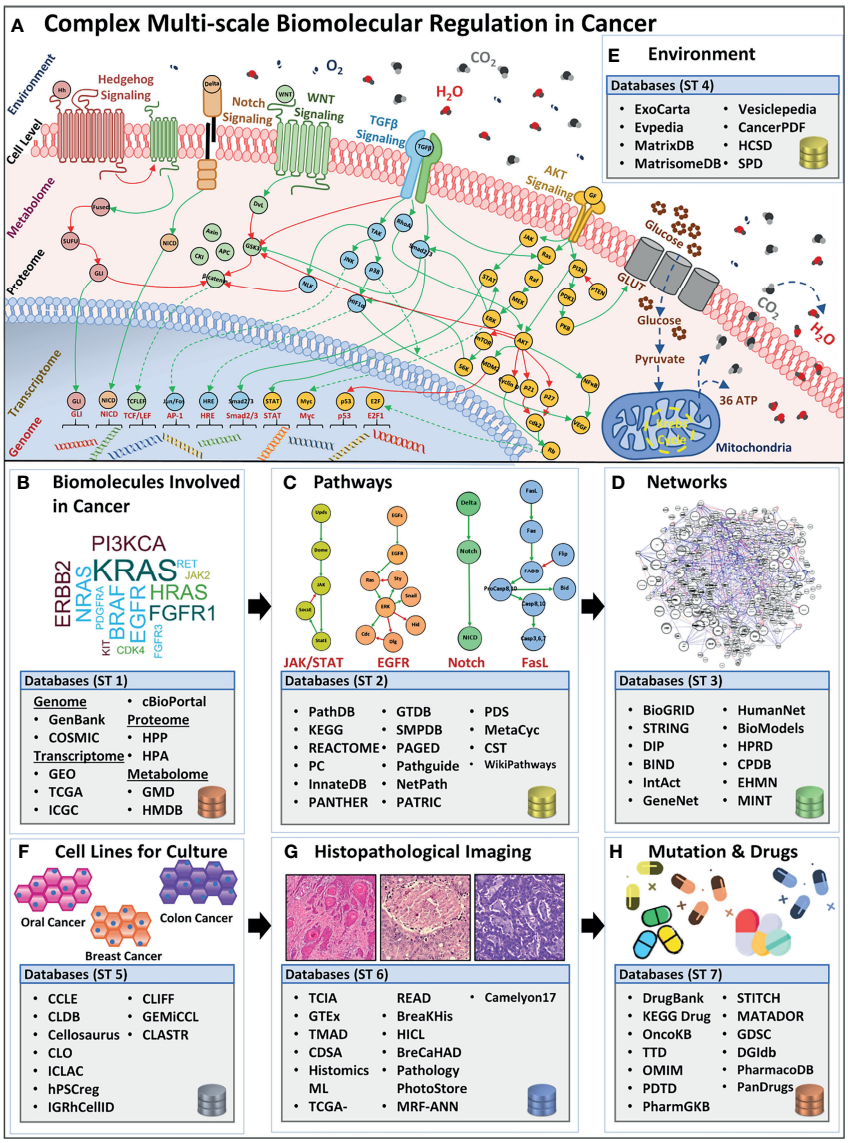


**FIGURE 1** | Overview of complex biomolecular regulation in cancer and scale-specific databases. **(A)** The complexity between genomic, transcriptomic, proteomic, metabolomic, cell-level, and environmental levels in a cancerous cell. Four examples of biomolecular signaling pathways are listed e.g., Hedgehog, Notch, (Wingless) Wnt, TGFβ, and AKT pathway. Stimuli from the extracellular environment signal the downstream pathway activation, in the cell, towards alternating the regulations in the proteomic, metabolomic, transcriptomic, and genomic scales, bringing out a system-level outcome in cancers. Lists **(B)** biomolecule (genes, transcripts, proteins, and metabolites) databases such as GenBank, GEO, TCGA, HPP, HMDB, etc. **(C)** Pathways databases such as PathDB, KEGG, STRING, etc. **(D)** Networks databases such as BioGRID, DIP, BIND, etc. **(E)** Environment databases e.g, ExoCarta, MatrixDB, MatrisomeDB, etc. **(F)** Cell lines databases such as CCLE, CLDB, Cellosaurus, etc. **(G)** Histopathological image database, for instance, TCIA, GTEx, TMAD, etc., and **(H)** Mutation and drug databases such as DrugBank, KEGG Drug, OncoKB, etc.

(64) (**Figure 1B** and **Table S1**). Towards developing such a transcriptional information resource, in 2000, Edgar et al. (31) launched the Gene Expression Omnibus (GEO) initiative. GEO acts as a tertiary resource providing coherent high-throughput transcriptomic and functional genomics data. The platform now hosts over 3800 datasets and is expanding exponentially. GEO was employed by Chakraborty et al. (65) for annotation of chemo-resistant cell line models which helped investigate chemoresistance and glycolysis in ovarian cancers. The study identified Mitochondrial Calcium Uptake 1 (MICU1) as an important component for cancer metabolism that influences aerobic glycolysis and chemoresistance and can have a potential role in cancer therapeutics. The curation of patient-specific gene and protein expression data led to the development of The Cancer Genome Atlas (TCGA) (66). TCGA also captures the copy number variations and DNA methylation profiles for different cancer subtypes. TCGA's potential (49, 67) is well exhibited by Leiserson et al.'s (68) pan-cancer analysis which

helped identify 14 significantly mutated subnetworks containing numerous genes with rare somatic mutations across many cancers types. Davis et al. (69) further evaluated the genomic landscape of chromophobe renal cell carcinomas (ChRCCs) to elicit molecular patterns as clues for determining the origin of cancer cells. To facilitate in data management across different cancer projects as well as to ensure data uniformity towards developing data-driven models, the International Cancer Genome Consortium (ICGC) was launched in 2010 (70). ICGC adopts a federated data storage architecture that enables it to host a collection of scale-specific data from TCGA and 24 other projects (71). Burn et al. (72) estimated the distribution of cytosine in liver tumor data using ICGC. The study reported APOBEC3B (A3B) catalyzed deamination as a chronic source of DNA damage in breast cancer which also explains tumor cell evolution and heterogeneity. Supek et al. (73) compared mutation rates between different human cancers and reported the influence of "silent" mutations as a frequent contributor to cancer. Numerous databases have been established to store large-scale genomic data, however, insights from an integrated analysis of genomic data across databases have the potential to provide precise biomolecular cues into complex processes and evolution in cancer cells. This was enabled by cBio Cancer Genomics Portal (cBioPortal) (74) in 2012, with multidimensional dataset retrieval, and exploration from multiple databases. The platform additionally provides data visualization tools, pathway exploration, statistical analysis, and selective data download features for seamless utilization of large-scale genomics data across genes, patient samples, projects, and databases (75). Numerous studies have effectively employed cBioPortal (76–78); in particular, Jiao et al. (79) evaluated the prognostic value of TP53 and its correlation with EGFR mutations in advanced non-small-cell lung cancer (NSCLC). The study established that TP53 coupled with EGFR mutation can lead to the more accurate prognosis of advanced NSCLC. Hou et al. (80) also used cBioPortal to deduce targetable genotypes which are present in young patients with lung adenocarcinomas and revealed that young patients with lung adenocarcinoma were more likely to harbor targetable genotype.

### 2.1.3 Proteome-Scale Databases

Transcriptomic data remains limited in providing a deterministic proteome profile (81–83). Particularly, transcripts produced in a cell can be degraded, translated inefficiently, or modified due to post-translational modification (84, 85) resulting in no or a very small amount of functional protein (64). This relatively low correlation between transcriptome and proteome data was highlighted in 2019, by Bathke et al. (86) where it was shown that an increase in transcript synthesis cannot be directly associated with an increase in functional response in a cell. To facilitate functional analysis, there is a need to utilize proteomic-level data, which can help to capture a more accurate quantitative assessment of complex biomolecular regulation for functional studies (**Figure 1B** and **Table S1**). Following the successful completion of the Human Genome Project (HGP) (1998), in 2003, a group of Swedish researchers reported the Human Protein Atlas (HPA) (87, 88) with an aim to map the entire set of human proteins in cells, tissues, and organs for normal as well as cancerous state (89). HPA employs large-scale omics-based technologies to localize and quantify protein expression patterns. The database has successfully managed to host comprehensive information on human proteins from cells, tissues, pathology, brain, and blood region-related studies. HPA data can be employed for various purposes such as investigating the spatial distribution of proteins in different tissue and comparing normal and cancerous protein expression patterns across samples, etc (87). In a salient study employing HPA, Gámez-Pozo et al. (90) studied the localized expression pattern of proteins to help profile human lung cancer subtypes. The study reported a combination of peptide-level expressions which can distinguish between non-small lung cancer samples and normal lung cancer in different histological subtypes. Imberg-Kazdan et al. (91) employed HPA to identify novel regulators of androgen receptor (AR) function in prostate cancer towards therapy. Another significant stride towards generation of proteome-level information came with the establishment of the Human Proteome Project (HPP) (92, 93) in 2008 (94) by the Human Proteome Organization (HUPO). HPP consolidated mass spectrometry-based proteomics data, and bioinformatics pipelines, with the aim to organize and map the entire human proteome. To date, numerous studies have utilized HPP towards identifying the complex protein machinery involved in cancer cell fate outcomes (95–100). Amongst the earliest attempts, in 2001, Sebastian et al. (101) employed the HPP platform to deduce the complex regulatory region of the human CYP19 gene ('*armatose*'), one of the contributors of breast cancer regulation. HPP project was later segmented into "biology and disease-oriented HPP" (B/D HPP) (102) and chromosome-centric HPP (C-HPP) (103). Specifically, Gupta et al. (104) carried out an extensive analysis of existing experimental and bioinformatics databases to annotate and decipher proteins associated with glioma on chromosome 12, while, Wang et al. (95) performed a qualitative and quantitative assessment of human chromosome 20 genes in cancer tissue and cells using C-HPP resources. The study revealed that several cancer-associated proteins on chromosome 20 were tissue or cell-type specific.

### 2.1.4 Metabolome-Scale Databases

Metabolic reprogramming is one of the earliest manifestations during tumorigenesis (105) and therefore, potentiates the usefulness of identifying metabolic biomarkers involved in cancer onset, its prognosis, as well as treatment. Large-scale efforts to collect metabolomics data have led to the development of several online databases (106–108) (**Figure 1B** and **Table S1**) including the Golm Metabolome Database (GMD) (106), in 2004. GMD provides a comprehensive resource on metabolic profiles, customized mass spectral libraries, along spectral information for use in metabolite identification. GMD was employed in 2011 by Wedge et al. (109) to identify and compare metabolic profiles in serum and plasma samples for small-cell lung cancer patients towards determining optimal agent for onwards analysis. The study showed that the discriminatory ability of both serum and plasma was

equivalent. In 2013, Pasikanti et al. (110) utilized GMD to identify biomarker metabolites present in bladder cancer. The study proposed a potential role of kynurenine in malignancy and therapeutic intervention in bladder cancer. To allow for large-scale metabolic data stratification and retrieval, in 2007, Wishart et al. published the Human Metabolome Database (HMDB) (107, 111). HMDB contains organism-specific information on metabolites across various biospecimens and their accompanying environments. It is now the world's largest metabolomics database with around 114,100 metabolites that have been characterized and annotated. HMDB was employed by Sugimoto et al. (112) to identify environmental compounds specific to oral, breast, and pancreatic cancer profiles. The study identified 57 principal metabolites to help predict disease susceptibility, besides being potential markers for medical screening. Agren et al. (113) employed metabolomic data from HMDB to construct metabolic network models for 69 human cells and 16 cancer types. The study's comprehensive metabolic network analysis between disease and normal cell types has the potential to provide avenues for the identification of cancer-specific metabolic targets for therapeutic interventions. The HMDB supports data deposition and dissemination, however, integrated exploratory analysis is not available. The Metabolomics Workbench (108), reported in 2016, provides information on metabolomics metadata and experimental data across species, along with an integrated set of exploratory analysis tools. The platform also acts as a resource to integrate, deposit, track, analyze, as well as disseminate large-scale heterogeneous metabolomics data from a variety of studies. In a case study built using this platform, Hattori et al. (114) studied the aberrant BCAA (branched-chain amino acids) metabolism activation by MSI2 (Musashi2)-BCAT1 axis which they reported to drive myeloid leukemia progression.

## 2.2 Biomolecular Pathway Databases

Investigations restricted to single biomolecular scales have limited translational potential as cancer dysregulation is driven by tightly coupled biomolecular pathways constituted by biomolecules from a variety of spatiotemporal scales (discussed above). Such biomolecular pathways represent organized cascades of interactions integrating different spatiotemporal scales towards reaching specific phenotypic cell fate outcomes. Numerous scale-specific and multi-omics biomolecular pathway databases now exist to help retrieve, store and analyze existing pathway information towards understanding cellular communication in light of complex cancer regulation (32, 34, 115). One of the earliest attempts at integrating genomics data for pathway construction came in 1995, with the establishment of the Kyoto Encyclopedia of Genes and Genomes (KEGG) database (32) (**Figure 1C** and **Table S2**). Over time, KEGG has significantly expanded to include high-throughput multi-omics data (116). As a result, the resource is divided into fifteen sub-groups including KEGG Genome (for genome-level pathways), KEGG Compound (for small molecules level pathways), KEGG Gene (for gene and protein pathways), KEGG Reaction (for biochemical reaction and metabolic pathways), etc. Li et al. (117) used the KEGG database to perform pathway enrichment analysis for predicting the function of circular RNA (circRNA) dysregulation in colorectal cancer (CRC). The study highlighted circDDX17 potential role as a tumor suppressor and biomarker for CRC. While employing KEGG, Feng et al. (118) identified four up-regulated differentially expressed genes associated with poor prognosis in ovarian cancer. Further, to furnish information on pathways for high-throughput functional analysis studies, PANTHER (protein annotation through evolutionary relationship) database was established in 2010 (34, 115). PANTHER hosts information on ontological gene and protein-protein interaction pathways by leveraging GenBank and Human Gene Mutation Database (HGMD) (119), etc. Turcan et al. (120) employed PANTHER to perform network pathway enrichment for biological processes in differentially expressed genes, especially to investigate IDH1 mutations in glioma hypermethylation phenotype. The study provided a framework for understanding gliomas and the interplay between genomic as well as epigenomic regulation in cancer. To store metabolic pathway information in a cell, Karp et al. (121) developed MetaCyc, a comprehensive reference database comprising of metabolic pathways. MetaCyc is currently available as a web-based resource with metabolic pathway information which can be employed to investigate metabolic reengineering in cancers, carry out biochemistry-based studies, and explore cancer cell metabolism, etc. Miller et al. (122) demonstrated the utility of MetaCyc database by evaluating plasma metabolomic profiles after limonene intervention in breast cancer patients. The study employed MetaCyc to perform pathway-based interpretations and revealed that such alterations were related with tissue-level cyclin D1 expression changes.

## 2.3 Biomolecular Network Databases

The regulatory complexity of cancer is compounded by the crosstalk between numerous multi-scale biomolecular pathways resulting in the formation of complex interaction networks (**Figure 1D** and **Table S3**). One of the earliest biomolecular network databases, the Biomolecular Interaction Network Database (BIND) (123) was established in 2001, with an aim to organize biomolecular interactions between genes, transcripts, proteins, metabolites, as well as small molecules. Chen et al. (124) employed BIND to construct a biological interaction network (BIN) towards investigating tyrosine kinase regulation in breast cancer development. The study identified SLC4A7 and TOLLIP as novel tyrosine kinase substrates which are also linked to tumorigenesis. BIND provides a comprehensive resource of predefined interacting pathways; however, it does not contain 'indirect' interaction information. In contrast, the Molecular INTeraction database (MINT) (37), developed in 2002, curates existing literature to develop networks with both direct as well as indirect interactions from large-scale projects with information from genes, transcripts, proteins, promoter regions, etc. MINT can store data on "functional" interaction such as enzymatic properties and modifications present in biomolecular regulatory networks. The database was employed by Vinayagam et al. (125) to construct a human immunodeficiency virus (HIV) network that helped identify novel cancer genes across genomic datasets. The Database of Interacting Proteins (DIP) (126) was developed

to mine existing literature and experimental studies on biomolecules and their pathways to construct protein interaction networks (127–129). Goh et al. (127) constructed a protein-protein interaction network for investigating liver cancer using DIP. The study revealed that hepatocellular carcinoma (HCC) at moderate stage is enriched in proteins that are involved in the immune response. Similarly, Zhao et al. (128) identified autophagic pathways in plants lectin-treated cancer cells which are regulated by microRNAs. The study showed that plant lectin has the potential to block sugar-containing receptor EGFR-mediated pathways thereby leading to autophagic cell death. To further consolidate and integrate protein interaction data across pathways as well as organisms, the Search Tool for the Retrieval of Interacting Genes/Proteins – STRING database was developed in 2005 (130). STRING provides a comprehensive text-mining and computational prediction platform which is accessible through an intuitive web interface (131). STRING database also provides information on interaction weights for edges between biomolecules to show an estimated likelihood for each interaction in the network (131). Mlecnik et al. (132) employed STRING database to study T-cells homing factors in colorectal cancer and demonstrated that specific chemokines and adhesion molecules had high densities of T-cell subsets in cancer.

## 2.4 Cellular Environment Databases

Each pathway within a biomolecular network requires input cues from the extracellular environment for onward downstream signal transduction (133–135). In the case of cancer, the biomolecular milieu constituting the tumor microenvironment (TME) acts as a niche for tumor development, metastasis, as well as therapy response (136) (**Figure 1E** and **Table S4**). Efforts to curate information from the environmental factors such as metabolites, matrisome, and other environmental compounds led to the development of MatrixDB (38) in 2011, which hosts matrix-based information on interactions between extracellular proteins and polysaccharides. MatrixDB additionally links databases with information on genes encoding extracellular proteins such as Human Protein Atlas (137) and UniGene (138) as well as host transcripts information. Celik et al. (139) employed MatrixDB data to evaluate epithelial-mesenchymal transition (EMT) inducers in the environment using nine ovarian cancer datasets and discovered a novel biomarker, HOPX, with the potential to drive tumor-associated stroma. To host studies on extracellular matrix (ECM) proteins from normal as well as disease-inflicted tissue samples, MatrisomeDB (39) was established in 2020. The database curates 17 studies on 15 physiologically healthy murine and human tissue as well as 6 cancer types from different stages (including breast, colon, ovarian, and lung cancer) along with other diseases. Levi-Galibov et al. (140) employed MatrisomeDB to investigate the progression of chronic intestinal inflammation in colon cancer. The study revealed the critical role of heat shock factor 1 (HSF1) during early changes in extracellular matrix structure as well as its composition.

## 2.5 Cell Line Databases

*In vitro* cell lines derived from cancer patients have become an essential tool for clinical and translational research (141). These cell lines are defined based on gene expression profiles and morphological features which have been cataloged in various databases such as the Cancer Cell Line Encyclopedia (CCLE) (42) (**Figure 1F** and **Table S5**). CCLE contains mutation data on 947 different human cancer cell lines coupled with pharmacological profiles of 24 anti-cancer drugs (42) for evaluating therapeutic effectiveness and sensitivity. Li et al. (142) employed CCLE data to investigate cancer cell line metabolism. The study showed that the mutated asparagine synthetase (ASNS) hypermethylation can cause gastric as well as hepatic cancers to sensitized asparaginase therapy. Hanniford et al. (143) demonstrated epigenetic silencing of RNA during invasion and metastasis in melanoma using the CCLE database. Other cell line databases include Cell Line Data Base (CLDB) (43), and The COSMIC Cell Lines Project (40), and CellMinerCDB (41). The CellMinerCDB (2018) curates data from National Cancer Institute (NCI) (144), BROAD institute (145), Sanger institute (146), and Massachusetts General Hospital (MGH) (147) and provides a platform for pharmacological and genomic analysis.

## 2.6 Histopathological Image Databases

Additionally, histopathological image datasets derived from the microscopic examination of tumor biopsy samples furnish information on cellular structure, function, chemistry, morphology, etc. Numerous histopathological image-based databases have been developed to store, manage, and retrieve such information (**Figure 1G** and **Table S6**). Amongst these databases, The Cancer Imaging Archive (TCIA) (46), reported in 2013, provides a multi-component architecture with various types of images including region-specific (e.g., Breast), cancer-type specific (e.g., TCGA-GBM, TCGA-BRCA), radiology, and anatomy images (e.g., Prostate-MRI). The cancer image collection in TCIA has been captured using a variety of modalities including radiation treatment, X-ray, mammography, and computed tomography (CT), etc (148). Li et al. (149) exploited TCIA by using radiomics data in predicting the risk for breast cancer recurrence, while Sun et al. (150) employed image data to perform a cohort study to validate a radiomics-based biomarker in cancer patients. The study developed a radiomic signature for CD8 cells using the TCGA dataset for predicting the immune phenotype of tumors and deduce clinical outcomes. In 2013, image data from TCIA was integrated with The Cancer Digital Slide Archive (CDSA) (44). The CDSA hosts imaging as well as histopathological data and provides more than 20,000 whole-slide images of 22 different cancer types. The whole-slide images of individual patients present in CDSA help in linking tumor morphology with the patient's genomic and clinical data. Khosravi et al. (151) performed a deep convolution study using CDSA, to distinguish heterogeneous digital pathology images across different types of cancers. To associate patient's genetic information and histology images, Genotype-Tissue Expression (GTEx) (45) was reported in 2014, and was curated using datasets from non-disease tissues of 1000 individuals. Patel et al. (152) employed GTEx to investigate intratumoral heterogeneity present in glioblastoma and concluded that glioblastoma subtype classifiers are variably expressed in individual cells.

## 2.7 Mutation and Drug Databases

Pharmacological investigations have elucidated the mechanism as well as efficacies of numerous cancer drugs, in clinical and preclinical studies (153, 154). Databases with drug-target information can be employed in precision oncology towards designing efficacious patient-centric therapeutic strategies (**Figure 1H**, **Table S7**). These databases include DrugBank (155), which was established in 2006 and contains information from over 4100 drug entries, 800 FDA-approved small molecules, and 14,000 protein or drug target sequences. DrugBank combines drug data with drug-target information thus enabling applications in cancer biology including *in silico* drug target discovery, drug design, drug interaction prediction, etc. In a study employing DrugBank, Augustyn et al. (156) evaluated potential therapeutic targets of achaete-scute homolog 1 (ASCL1) genes in lung cancers and reported unique molecular vulnerabilities for potential therapeutics, while Han et al. (157) determined synergistic combinations of drug targets in K562 chronic myeloid leukemia (CML) cells including BCL2L1 and MCL1 combination. Further to evaluate drugs in light of the patient's genomic signature, PanDrugs (52) database was established in 2019 and currently hosts data from 24 sources and 56297 drug-target pairs along with 9092 unique compounds and 4804 genes. Using PanDrugs, Fernández-Navarro et al. (158) prioritized personalized drug treatments using PanDrugs, for T-cell acute lymphoblastic (T-ALL) patients.

Altogether, the availability of voluminous high-resolution biomolecular data has enabled the development of a quantitative understanding of aberrant mechanisms underpinning hallmarks of cancer as well as create avenues for personalized therapeutic insights. Recently, Karimi et al. (159) systematically evaluated the current multi-omics data generation approaches, as well as their associated analysis pipelines for employment in cancer research.

# 3 DATA-DRIVEN INTEGRATIVE MODELING IN CANCER SYSTEMS BIOLOGY

The need to prognosticate system-level outcomes in light of oncogenic dysregulation (160, 161) has led researchers to develop integrative data-driven computational models (162–168). Such models can help decode emergent mechanisms underpinning tumorigenesis as well as aid in the development of patient-centered therapeutic strategies (162–168). These *in silico* models can be broadly grouped into four salient sub-scales as biomolecular (169–171), tumor environment (172–174), cell level (175, 176), and multi-scale integrative cancer models (177–179) (**Figure 2**).

## 3.1 Biomolecular-Scale Models

*In silico* biomolecular models of cancer can be classified into (i) genome-scale, (ii) transcriptome-scale, (iii) proteome-scale, (iv) metabolome-scale models.

### 3.1.1 Genome-Scale Models

Amongst initial attempts at developing cancer gene regulation models, in 1987, Leppert et al. (169) reported a computational model to study the genetic locus of familial polyposis coli and its involvement in colonic polyposis and colorectal cancer. The study was also validated by Mehl et al. (170) in 1991, which further elucidated the formation and development of familial

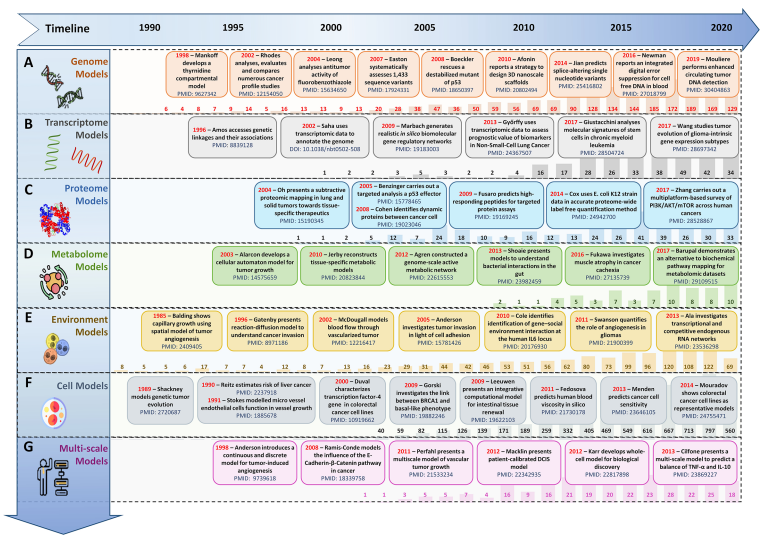


**FIGURE 2** | Evolution timeline of *in silico* scale-specific and multi-scale data-drive cancer models. Timeline of salient *in silico* scale-specific and multi-scale cancer models, along with PubMed yearly report (1990-2020) to display the evolutionary trends seen in the development of **(A)** genome-scale cancer models, **(B)** Transcript-level cancer models, **(C)** Proteome-scale models, **(D)** Metabolome scale models, **(E)** Environment-based models, **(F)** Cell-level models, and **(G)** Multi-scale cancer models.

polyposis coli genes in colorectal cancer patients. In 2014, Stratmann et al. (171) developed a personalized genome-scale 3D lung cancer model to study epithelial-mesenchymal transition (EMT) by TGFβ-based stimulation, while in 2016, Margolin et al. (180) developed a blood-based diagnostic model to help detect DNA hypermethylation of potential pan-cancer marker ZNF154. In 2017, Jahangiri et al. (181) employed an *in silico* pipeline to evaluate Staphylococcal Enterotoxin B for DNA-based vaccine for cancer therapy. A similar genome-scale model of DNA damage and repair was proposed by Smith et al. (182) to evaluate proton treatment in cancer (**Figure 2A**).

### 3.1.2 Transcriptome-Scale Models

*In silico* models developed using transcriptomic expression data can assist in comparing gene expression patterns in cancer for investigating genetic heterogeneity and cancer development as well as towards precision therapy (**Figure 2B**). In 2003, Huang et al. (183) presents a mathematical model using a large-scale transcriptional dataset of breast cancer patients to elucidate patterns of metagenes for nodal metastases and relapses. In another large-scale cancer transcriptomics study, 3,000 patient samples from nine different cancer types were used to decode the genomic evolution of cancer by Cheng et al. (184). In 2013, Chen et al. (185) employed an *in silico* pipeline which helped identify 183 new tumor-associated gene candidates with the potential to be involved in the development of hepatocellular carcinoma (HCC), while, in 2014, Agren et al. (186) developed a personalized transcriptomic data-based model to identify anticancer drugs for HCC. In 2019, Béal et al. (187) reported a logical network modeling pipeline for personalized cancer medicine using individual breast cancer patients' data. The pipeline was validated in 2021 (188), using *in silico* personalized logical models for melanomas and colorectal cancers samples in response to BRAF treatments. In a similar study conducted in 2019, Rodriguez et al. (189) developed a mathematical model for breast cancer using transcriptional regulation data to predict hypervariability in a large dynamic dataset which revealed the basis of expression heterogeneity in breast cancer.

### 3.1.3 Proteome-Scale Models

To capture the quantitative aspects of biomolecular regulations and functional studies (82, 83), data-driven proteomic-based cancer models are essential (**Figure 2C**). Such models can be particularly helpful in diagnostic as well as prognostic purposes as well as for monitoring response to treatment (82, 83). In a study employing proteome-level information, in 2011, Baloria et al. (190) carried out an *in silico* proteome-based characterization of the human epidermal growth factor receptor 2 (HER-2) to evaluate its immunogenicity in an *in silico* DNA vaccine. Akhoon et al. (191) simplified this approach with the development of a new prophylactic *in silico* DNA vaccine using IL-12 as an adjuvant. In 2017, Fang et al. (192) employed proteome level data towards predicting *in silico* drug-target interactions for applications in targeted cancer therapeutics, while in 2018, Azevedo et al. (193) designed novel glycobiomarkers in bladder cancer. Recently, in 2020, Lee et al. (194) reported an integrated proteome model of macrophage migration in a complex tumor microenvironment. However, proteome-level models are limited in their ability to provide a complete analysis of the biomolecules present in a cell since they lack information on low molecular weight biomolecular compounds such as metabolites (105).

### 3.1.4 Metabolome-Scale Models

Metabolic data-driven models can be especially useful in understanding cancer cell metabolism, mitochondrial dysfunction, metabolic pathway alteration, etc (**Figure 2D**). In 2007, Ma et al. (195) developed the Edinburgh Human Metabolic Network (EHMN) model with more than 3000 metabolic reactions alongside 2000 metabolic genes for employment in metabolite-related studies and functional analysis. In 2011, Folger et al.'s (196) employed the EHMN model to propose a large-scale flux balance analysis (FBA) model for investigating metabolic alterations in different cancer types and for predicting potential drug targets. In 2014, Aurich et al. (197) reported a workflow to characterize cellular metabolic traits using extracellular metabolic data from lymphoblastic leukemia cell lines (Molt-4) towards investigating cancer cell metabolism. Yurkovich et al. (198) augmented this workflow in 2017 and reported eight biomarkers for accurately predicting quantitative metabolite concentration in human red blood cells. Alakwaa et al. (199) employed a mathematical model to predict the status of Estrogen Receptor in breast cancer metabolomics dataset, while in 2018, Azadi et al. (200) used an integrative *in silico* pipeline to evaluate the anti-cancerous effects of *Syzygium aromaticum* employing data from the Human Metabolome Database (107).

## 3.2 Tumor Environment Models

Integrative mathematical models of environmental cues and extracellular matrix can help researchers abstract tumor microenvironments. Such data-driven models can be used to study angiogenesis (201), cell adhesion (202), and vasculature (203), etc (**Figure 2E**). Amongst initial attempts at developing cancer environment-based *in silico* models, in 1972, Greenpan et al. (172) designed a solid carcinoma *in silico* model to evaluate cancer cell behavior in limited diffusion settings. In 1976, the model was expanded (173) to investigate tumor growth in asymmetric conditions. In 1996, Chaplain developed a mathematical model to elucidate avascular growth, angiogenesis, and vascular growth in solid tumors (174). Anderson and Chaplain (204), in 1998, expanded this strategy and reported a continuous and discrete model for tumor-induced angiogenesis. This modeling approach was further augmented in 2005 by Anderson (202) to a hybrid mathematical model of a solid tumor to study cellular adhesion in tumor cell invasion. Organ-specific metastases and associated survival ratios in small cell lung cancer patients have been modeled and evaluated (205) using similar models.

## 3.3 Cell Models

To model cell population-level behavior in cancer, researchers are increasingly developing innovative cell lines *in silico* models which can complement *in vivo* wet-lab experiments, while overcoming wet-lab limitations (206) (**Figure 2F**). Such models

are employed to investigate cell-to-cell interactions as well as evaluate physical features of the synthetic extracellular matrix (ECM) (206), etc (175, 207). Amongst initial attempts at developing *in silico* cell line models, in 1989, Shackney et al. (175) proposed an *in silico* cancer cell model to study tumor evolution. Results showed an association between discrete aneuploidy peaks with the activation of growth-promoting genes. In 2007, Aubert et al. (207) developed an *in silico* glioma cell migration model and validated cell migration preferences for homotype and heterotypic gap junctions with experimental results. Gerlee and Nelander (176) expanded this work, in 2012, to investigate the effect of phenotype switching in glioblastoma growth. In conclusion, cell-based cancer models help provide scale-specific insights into cancer, however, they remain limited in investigating the spatiotemporal tissue diversity and heterogeneity in cancer patients.

## 3.4 Multi-Scale Models

Recently, data-driven multi-scale models are becoming increasingly popular in cancer (208) (**Figure 2G**). One of the earliest attempts at developing multi-scale cancer models was in 1985 when Balding developed a mathematical model to demonstrate tumor-induced capillary growth (201). In 2000, Swanson et al. (209) proposed a quantitative model to investigate glioma cells. In a similar study, Zhang et al. (210) generated a 3D, multi-scale agent-based model of the brain to study the role (EGFR)-mediated activation of signaling protein phospholipase role in a cell's decision to either proliferate or migrate. In 2010, Wang et al. (178) also took a multi-scale agent-based modeling approach to identify therapeutic targets in concurrent EGFR-TGFβ signaling pathway in non-small cell lung cancer (NSCLC). Later in 2011 (179), they employed the approach to identify critical molecular components in NSCLC. Similarly, Perfahl et al. (211) formulated a multi-scale vascular tumor growth model to investigate spatiotemporal regulations in cancer and response to therapy. In 2007, Anderson et al. (212) proposed a mathematical model for studying cancer growth, evolution, and invasion. This model was later built upon by Chaudhary et al. (165, 213) with a multi-scale modeling strategy to investigate tumorigenesis induced by mitochondrial incapacitation in cell death, in 2011. In 2017, Vavourakis et al. (214) developed a multi-scale model to investigate tumor angiogenesis and growth. In 2017, Norton et al. (215) used an agent-based computational model of triple-negative breast cancer to study the effects of migration in CCR5+ cancer cells, stem cell proliferation, and hypoxia on the system. They later (216) reported an agent-based and hybrid model to investigate tumor immune microenvironment, in 2019. In the same year, Karolak *et al.* (217) modeled *in silico* breast cancer organoid morphologies (218) to help elucidate efficacies amongst drug treatment based on the morphophenotypic classification. Similarly, Berrouet et al. (219) employed a multi-scale mathematical model to evaluate the effect of drug concentration on monolayers and spheroid cultures.

Summarily, data-integrative computational models have now assumed the forefront in decoding the complex biomolecular regulations involved in cancer and are increasingly been employed for the development of personalized preclinical models as well as therapeutics design (220).

# 4 SOFTWARE PLATFORMS FOR MODELING IN CANCER SYSTEMS BIOLOGY

Over the past decade, *in silico* modeling of cancer has gained significant popularity in systems biology research (162–168). In particular, data-drive computational models are now acting as an enabling technology for precision medicine and personalized treatment of cancer. To date, several single and multi-scale software platforms have been reported to model biomolecules (171, 221–228), cellular environments (229), as well as cell-level (230), and multi-scale (231) information into coherent *in silico* cancer models (**Figure 3**).

## 4.1 Biomolecular Modeling Platforms

Software platforms aimed at modeling biomolecular entities, abstract information from published literature as well as high-throughput technologies, and model them using a Boolean modeling approach or a differential equations modeling strategy.

### 4.1.1 Boolean Modeling Software

Boolean network modeling technique was first introduced by Kauffman (232, 233), in 1969. This approach has been widely adopted as a tool to model gene, transcript, protein, and metabolite regulatory networks. Numerous mathematical and computational cancer models have been developed using this representation (171, 221–225). To facilitate the Boolean model development and analysis process, several platforms have been devised (234–236) (**Table S8**). The applicability of these platforms can be further categorized into qualitative or quantitative Boolean network modeling.

#### *4.1.1.1 Qualitative Boolean Modeling*

Biomolecular qualitative Boolean models are a widely employed approach in cancer systems biology research to cater for cases where there is insufficient quantitative information, and/or lack of mechanistic understanding. Thus far, numerous platforms have been reported to help researchers develop qualitative Boolean network models. Amongst them, FluxAnalyzer (237), reported by Klamt et al. in 2003, was developed to undertake metabolic pathway construction, flux optimization, topological feature detection, flux analysis, etc. To expand the scope of the platform and include cell signaling, gene as well as protein regulatory networks, in 2007, Klamt et al. expanded FluxAnalyzer and reported CellNetAnalyzer (226). Tian et al. (238) employed CellNetAnalyzer to develop a p53 network model for evaluating DNA damage in cancer, while Hetmanski et al. (239) designed a MAPK-driven feedback loop in Rho-A-driven cancer cell invasion. Although CellNetAnalyzer remains a widely used logical modeling software, its programmability and MATLAB dependency hinders its clinical employment for developing personalized cancer models. Towards addressing this challenge, in 2008, Albert et al. published BooleanNet (235),

| Scales | | Network | | | | | | Environment | | | Cell Line | | | Multi-scale | | | | | |
|---|---|---|---|---|---|---|---|---|---|---|---|---|---|---|---|---|---|---|---|
| | Software | CellDesigner | Cytoscape | COPASI | CellNetAnalyzer | BoolNet | GIMsim | CellWare | Morpheus | BioFVM | E-Cell | Virtual Cell | ThinkCell | Compucell | CHASTE | ELECANS | PhysiCell | PhysiBoSS | TISON |
| | Year | 2003 | 2003 | 2006 | 2008 | 2010 | 2012 | 2003 | 2014 | 2015 | 1999 | 2008 | 2009 | 2004 | 2013 | 2013 | 2018 | 2019 | 2021 |
| Features List | Boolean/Qualitative Networks | | ● | | ● | ● | ● | | | | | | | | | | | ● | ● |
| | Boolean/Quantitative Networks | | ● | | | ● | | | | | | | | | | | | | ● |
| | Quantitative Networks | ● | ● | ● | | | | ● | ● | | ● | ● | | | | | | | |
| | Stochastic Semantics | | ● | ● | | ● | | | | | ● | ● | | ● | | | | ● | ● |
| | ODE | | | ● | | | | ● | ● | | | ● | ● | ● | ● | | | | ● |
| | Agent-based Modeling | | | | | | | | | | | | | ● | ● | ● | ● | ● | |
| | 2D Tissue | | | | | | | | ● | | ● | ● | | ● | ● | ● | ● | ● | ● |
| | 3D Tissue | | | | | | | | | ● | ● | ● | ● | ● | ● | ● | ● | ● | ● |
| | ***Biomolecular Diffusion** Continuous* | | | | | | | | | | ● | ● | | ● | ● | | | | ● |
| | ***Biomolecular Diffusion** Discrete* | | | | | | | | ● | ● | ● | ● | | | ● | ● | ● | ● | ● |
| | ***Biomolecular Diffusion** Hybrid* | | | | | | | ● | | | | ● | | | | | | | ● |
| | Parallelized | | ● | ● | ● | ● | | | ● | ● | | ● | | ● | | | | ● | ● |
| | GUI | ● | ● | ● | ● | | ● | ● | ● | ● | ● | ● | ● | ● | | ● | | ● | ● |
| | Web-based Platform | ● | | ● | | | ● | | ● | | ● | ● | ● | | | | | | ● |
| | Language | Java | Java | C++ | MATLAB | R | Java | Java | C++ | C++ | C++ | C++/Java | Python/C | C++ | C# | C++ | C++ | C++ | C# |
| | Reference PMID's | doi:10.1016/S1476-5586(03)02314-9 | 14597658 | 17032683 | 17408509 | 20378558 | 22144167 | 14871872 | 24443380 | 26656933 | 10068694 | 19045830 | 19874625 | 14764549 | 23516352 | 23380137 | 29474446 | 30169736 | doi:10.1101/2021.05.04.442539 |

**FIGURE 3** | Feature-by-feature comparison of networks, environments, cell lines, and multi-scale modeling software in chronological order.

an open-source, freely available Boolean modeling software for large-scale simulations of dynamic biological systems. Saadatpoort et al. (240) employed BooleanNet's general asynchronous (GA) method to deduce therapeutic targets for granular lymphocyte leukemia. Similarly, in 2008, Kachalo et al. presented NET-SYNTHESIS (227); a platform for undertaking network synthesis, inference, and simplification. Steinway et al. (241) employed both BooleanNet and NET-SYNTHESIS platforms to model epithelial-to-mesenchymal transition (EMT) in light of TFGβ cell signaling, in hepatocellular carcinoma patients towards elucidating potential therapeutic targets. BooleanNet was used to undertake model simulation and NET-SYNTHESIS for carrying out network interference and simplification. Another logical modeling platform, GIMsim (242), published by Naldi et al., in 2009, also employed asynchronous state transition graphs to perform qualitative logical modeling which is especially useful for networks with large state space. This platform was employed by Flobak et al. (243) to map cell fate decisions in gastric adenocarcinoma cell-line towards evaluating drug synergies for treatment purposes, while Remy et al. (244) studied mutually exclusive and co-occurring genetic alterations in bladder cancer. GIMsim also employed multi-valued logical functions, useful in simulating qualitative dynamical behavior in cancer research. However, the platform was unable to program automatic theoretical predictions, moreover, it only employed qualitative analysis approaches and could not be used to accurately map cell fates based on quantitative biomolecular expression data. Taken together, classical qualitative Boolean modeling approaches remain limited in developing predictive cancer models that could leverage quantitative biomolecular expression data generated from next-generation proteomics and related-sequencing projects.

#### *4.1.1.2 Quantitative Boolean Modeling*

Platforms aimed to integrate quantitative expression data from existing literature and databases towards carrying out network annotation and onwards analysis can be particularly useful in developing personalized cancer models. One such platform, the Markovian Boolean Stochastic Simulator (MaBoss), was established by Stoll et al. (245) in 2017, for stochastic and semi-quantitative Boolean network model development, mutations, and drug evaluation, sensitivity analysis based on experimental data, and eliciting model predictions. In 2019, Béal et al. (187) employed MaBoss to develop a logical model to evaluate breast cancer in light of individual patients' genomic signature for personalized cancer medicine. This model was later expanded, in 2021, to investigate BRAF treatments in melanomas and colorectal cancer patients (188). Similarly, Kondratova et al. (246) used MaBoss to model an immune checkpoint network to evaluate the synergistic effects of combined checkpoint inhibitors in different types of cancers. In a similar attempt at developing quantitative Boolean networks, BoolNet (247) was developed in 2010 by Müssel and Kestler. BoolNet allows its users to reconstruct networks from time-series data, perform robustness and perturbation analysis and visualize the resultant cell fates attractor. BoolNet was employed by Steinway et al. (248) to construct a metabolic network model towards evaluating gut microbiome in normal and disease conditions, whereas, Cohen et al. (249) studied tumor cell invasion and migration. BoolNet, however, lacks a graphical user interface, and results from the analysis cannot be

visualized interactively, which hindered its employment. To address this issue, Shah et al. (250), in 2018, developed an Attractor Landscape Analysis Toolbox for Cell Fate Discovery and Reprogramming (ATLANTIS). ATLANTIS has an intuitive graphical user interface and interactive result visualization feature, for ease in utilization. The platform can be employed to perform deterministic as well as probabilistic analysis and was validated through literature-based case studies on the yeast cell cycle (251), breast cancer (252), and colorectal cancer (253).

### 4.1.2 Differential Equations Modeling Software

Boolean models have proven to be a powerful tool in modeling complex biomolecular signaling networks, however, these models are unable to describe continuous concentration, and cannot be used to quantify the time-dependent behavior of biological systems, necessitating the need to switch to quantitative differential equations (254). As a result, numerous stand-alone and web-based tools have been developed to build continuous network models to help describe the temporal evolution of biomolecules towards elucidating more accurate cell fate outcomes from quantitative expression data (**Table S8**). Amongst initial attempts at developing such software, GEPASI (GEneral PAthway Simulator) was designed by Pedro Mendes et al. (228), in 1993. GEPASI is a stand-alone simulator that facilitates formulating mathematical models of biochemical reaction networks. GEPASI can also be used to perform parametric sensitivity analysis using an automatic pipeline that evaluates networks in light of exhaustive combinatorial input parameters. Ricci et al. (255) employed GEPASI to investigate the mechanism of action of anticancer drugs, while Marín-Hernández et al. (256) constructed kinetic models of glycolysis in cancer. In 2006, Hoops et al. reported a successor of GEPASI; COPASI (COmplex PAthway SImulator) (257), a user-friendly independent biochemical simulator that can handles larger networks for faster simulation results, through parallel computing. Orton et al. (258) employed COPASI to model cancerous mutations in EGFR/ERK pathway, while cellular senescence was evaluated by Pezze et al. (259) for targeted therapeutic interventions. Towards establishing a user-friendly software with an intuitive graphical user interface (GUI), another desktop application, CellDesigner was published by Funahashi et al. (260). CellDesigner application can be extended to include various simulation and analysis packages through integration with systems biology workbench (SBW) (261). In a case study using CellDesigner, Calzone et al. (262) developed a network of retinoblastoma protein (RB/RB1) and evaluated its influence in cell cycle, while Grieco et al. (263) investigated the impact of Mitogen-Activated Protein Kinase (MAPK) network on cancer cell fate outcomes.

## 4.2 Cell Environment Modeling Software

To facilitate the development of environmental models that can help investigate inter-, intra-, and extracellular interactions between cellular network models and their dynamic environment, several software and platforms have been reported (229, 264). These platforms employ discrete, continuous, and hybrid approaches to develop models of cellular microenvironments towards setting up specific biological contexts such as normoxia, hypoxia, Warburg effect, etc (**Table S9**). In 2014, Starruß et al. (229) published Morpheus, a platform for modeling complex tumor microenvironment. Morpheus leverages a cellular potts modeling approach to integrate and stimulate cell-based biomolecular systems for modeling intra- and extra cellular dynamics. In a case study using Morpheus, Felix et al. (265) evaluated pancreatic ductal adenocarcinoma's adaptive and innate immune response levels, while Meyer et al. (266) investigated the dynamics of biliary fluid in the liver lobule. Morpheus is a widely employed modeling software, however, its diffusion solver is limited in its capacity to model large 3D domains. Towards modeling fast simulations for larger cellular systems, the Finite Volume Method for biological problems (BioFVM) software (264) was reported by Ghaffarizadeh et al., in 2016. BioFVM is an efficient transport solver for single as well as multi-cell biological problems such as excretion, decomposition, diffusion, and consumption of substrates, etc (267). In a case study using BioFVM, Ozik et al. (268) evaluated tumor-immune interactions, while Wang et al. (269) elucidated the impact of tumor-parenchyma on the progression of liver metastasis. BioFVM, however, relies on its users to have programming-based knowledge to develop their models, which limits its translational potential. Towards minimizing programming requirements, SALSA (ScAffoLd SimulAtor) was developed by Cortesi et al. (206) in 2020. SALSA is general-purpose software that employs a minimum programming requirement, a significant advantage over its predecessors. The platform has been useful in studying cellular diffusion in 3D cultures. This recent tool was validated in 2021, with a case study that evaluated and predicted therapeutic agents in 3D cell cultures (270).

## 4.3 Cell-Level Modeling Software

Towards modeling cancer cell-specific behaviors such as cellular adhesion, membrane transport, loss of cell polarity, etc several software have been reported which can help develop *in silico* cancer cell models (**Table S10**). The foremost endeavor to develop software for cell-level modeling and simulation, led to the establishment of E-Cell (230), in 1999. E-Cell can be employed to model biochemical regulations and genetic processes using biomolecular regulatory networks in cells. Edwards et al. (271) employed E-cell to predict the metabolic capabilities of *Escherichia coli* and validated the results using existing literature, while Orton et al. (272) modeled the receptor-tyrosine-kinase-activated MAPK pathway. This software was expanded in 2001, with the development of Virtual Cell (V-Cell) (273), a web-based general-purpose modeling platform. V-Cell has an intuitive graphical and mathematical interface that allows ease in the design and simulation of whole cells, along with sub-cellular biomolecular networks and the external environment. Neves et al. (274) employed V-Cell to investigate the flow of spatial information in cAMP/PKA/B-Raf/MAPK1,2 networks, while Calebiro et al. (275) modeled cell signaling by internalized G-protein–coupled receptors. Similarly, to increase the efficiency in the design and modeling of synthetic regulatory networks in cells, in 2009, Chandran et al. reported TinkerCell

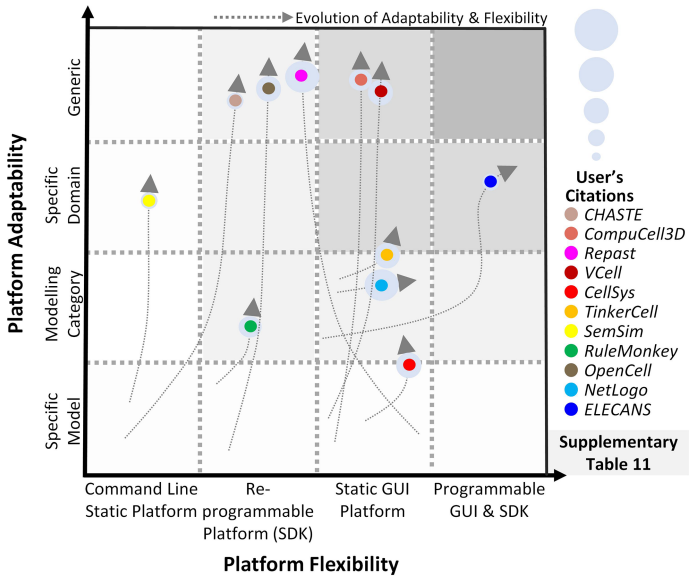


**FIGURE 4** | Evolution of scale-specific and multi-scale software. Evolution of multi-scale modeling software for abstracting and simulating the spatiotemporal biomolecular complexity. Highlighting the need for a generic, data-driven, zero-code software requirement.

(276) with computer-aided design (CAD) functionality which enabled faster simulation and associated analysis. The platform employed a modular approach for constructing networks and provides built-in features for ease in network construction, robustness analysis, and evaluating networks using existing databases. The evolutionary trend for TinkerCell's platform adaptability and flexibility is highlighted in **Figure 4**, which shows a gradual shift from being a model-specific platform to a domain modeling one. In a study employing TinkerCell, Renicke et al. (277) constructed a generic photosensitive degron (psd) model to investigate protein degradation and cellular function, while Chandran et al. (278) reported computer-aided biological circuits.

## 4.4 Multi-Scale Modeling Software

Multi-scale cancer modeling approaches bring together scale-specific information towards undertaking an integrative analysis of heterogeneous experimental data by building coherent and biologically plausible models (279–281). Several multi-scale modeling platforms have been reported to help develop multi-level cancer models (231) (**Table S11**). Amongst these, the REcursive Porous Agent Simulation Toolkit (Repast) (282) published in 2003, provides a free and open-source tool for modeling and simulating agent-based models, with high-performance computing (HPC) capability. Repast toolkit was employed in 2007, by Folcik et al. (283) to develop an agent-based model which was then used to study interactions between cells and the immune system. Similarly, Mehdizadeh et al. (284) used Repast to model angiogenesis in porous biomaterial scaffolds. Although Repast can be used for simulating several types of evolutionary trends between agents, there is no established guideline for selecting a mechanism to model such trends, hindering its use by naïve users. Moreover, Repast does not have a GUI or a software development kit (SDK) interface for implementing subcellular mechanisms e.g., gene, protein, and metabolic networks. In contrast, CompuCell (279), published in 2004 by Izaguirre et al., provides an elaborative GUI to model cell-scale or tissue-scale simulations by integrating biomolecular networks, intra- and extracellular environment, and cell to environment interactions. Mahoney et al. (285) employed CompuCell to develop an angiogenesis-based model in cancer for investigating novel cancer therapies. Although CompuCell provides an intuitive framework modeling paradigm, the platform core is not conducive to multi-scale cancer modeling. The focus of the software is primarily multi-agent simulations rather than multi-scale cancer modeling. This poses a significant challenge in the utilization of the software. In 2013, CHASTE (280) (Cancer Heart and Soft Tissue Environment) was launched, which provides a computational simulation pipeline for the mathematical modeling of complex multi-scale models. Users can employ CHASTE for a wide range of problems involving on and off-lattice modeling workflows. CHASTE has also previously been employed to model colorectal cancer crypts. Nonetheless, CHASTE does not have a GUI and can only be executed by command line text commands. Furthermore, it requires recompilation on part of the modeler to use the code updates performed by the group. To further improve the multi-scale modeling approach for investigating cancer, in 2013, Chaudhary et al. (281) published ELECANS (Electronic Cancer System). ELECANS had an intuitive but rigid GUI along with a programmable SDK besides the lack of a high-performance simulation engine (286, 287). ELECANS was employed to model the mitochondrial processes in cancer towards elucidating the hidden mechanisms involved in cell

death (165). ELECANS provided a feature-rich environment for constructing multi-scale models, however, the platform lacked a biomolecular network integration pipeline, and also placed a heavy programming requirement on its users. In contrast, in 2018, PhysiCell (288) was reported for 2D and 3D multi-cell off-lattice agent-based simulations. PhysiCell is coupled with BioFVM (264)'s finite volume method to model multi-scale cancer systems (268). In a salient example, Wang et al. (269) employed PhysiCell to model liver metastatic progression. In 2019, PhysiCell's agent-based modeling features and MaBoss's Boolean cell signaling network feature were coupled together to develop an integrated platform, PhysiBoss (289). As a result, PhysiBoss provided an agent-based modeling environment to study physical dimension and cell signaling networks in a cancer model. In 2020, Colin et al. (290) employed PhysiBoss's source code to model diffusion in oocytes during prophase 1 and meiosis 1, while Getz et al. (291) proposed a framework using PhysiBoss to develop a multi-scale model of SARS-CoV-2 dynamics in lung tissue. Recently, in 2021, Gondal et al. (292) reported Theatre for *in silico* Systems Oncology (TISON), a web-based multi-scale "zero-code" modeling and simulation platform for *in silico* oncology. TISON aims to develop single or multi-scale models for designing personalized cancer therapeutics. To exemplify the use case for TISON, Gondal et al. employed TISON to model colorectal tumorigenesis in *Drosophila melanogaster*'s midgut towards evaluating efficacious combinatorial therapies for individual colorectal cancer patients (225).

Summarily, multi-scale modeling software has enabled the development of biologically plausible cancer models to varying degrees. These platforms, however, fall short of providing a generic and high-throughput environment that could be conveniently translated into clinical settings.

# 5 PIPELINING PANOMICS DATA TOWARDS *IN SILICO* CLINICAL SYSTEMS ONCOLOGY

*In silico* multi-scale cancer models, annotated with patient-specific biomolecular and clinical data, can help decode complex mechanisms underpinning tumorigenesis and assist in clinical decision-making. Clinically driven *in silico* multi-scale cancer models simulate *in vivo* tumor growth and response to therapies across biocomplexity scales, within a clinical environment, towards evaluating efficacious treatment combinations. To facilitate the development of multi-scale cancer models, several large-scale program projects have been launched (**Table S12**) such as Advancing Clinico-Genomic Trials on Cancer (ACGT) (293), Clinically Oriented Translational Cancer Multilevel Modeling (ContraCancrum) (294), Personalized Medicine (p-medicine) (295), Transatlantic Tumor Model Repositories (TUMOR) (296), and Computational Horizons In Cancer (CHIC) (297), amongst others (**Figure 5**). Here, we review and evaluate five salient projects for multi-scale cancer modeling towards their clinical deployment.

## 5.1 ACGT Project

The ACGT project (293), launched in 2007, proposed to develop Clinico-Genomic infrastructure for organizing clinical and genomic data towards investigating personalized therapeutics regimens for an individual cancer patient. The ACGT platform provides an open-source and open-access infrastructure designed to support the development of "oncosimulators" to help clinicians accurately compare results from different clinical trials and enhance their efficiency towards optimizing cancer treatment. The ACGT framework employs molecular and clinical data generated from different sources including whole

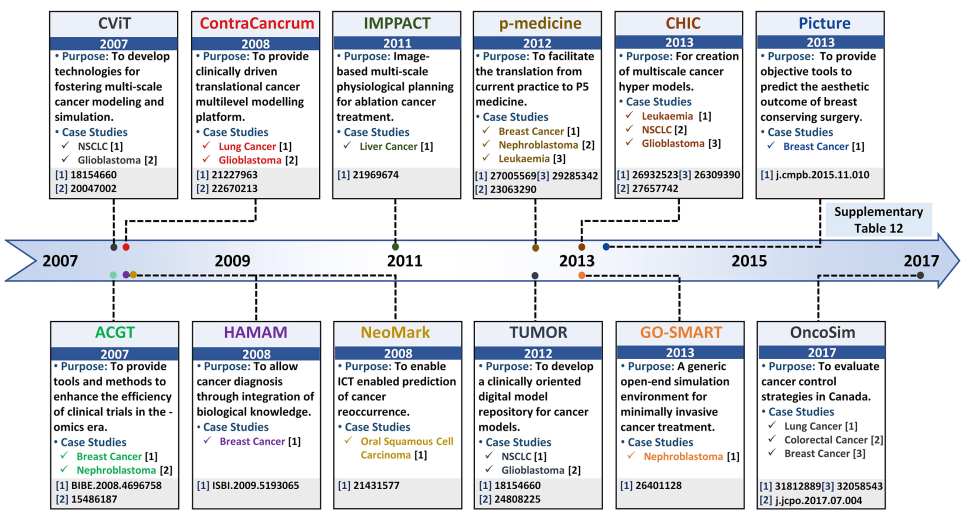


**FIGURE 5** | Salient projects pipelining multi-scale panomics data into clinical settings – a timeline. Timeline highlighting salient project platforms for developing realistic and clinically-driven multi-scale cancer models, along with their associated leading case studies.

genome sequencing, histopathological, imaging, molecular, and clinical data, etc. to develop simulators for mimicking clinical trials. Personalized panomics data employed to develop oncosimulators in ACGT is extracted from real patients which enables the oncosimulators to be clinically relevant for predictive purposes. Additionally, ACGT provides data retrieval, storage, integrative, anonymization, and analysis as well as results presentation capabilities. Using the platform, in 2004, a personalized, spatiotemporal oncosimulator model of breast cancer was developed to mimic a clinical trial based on protocols outlined in the Trial of Principle (TOP), towards evaluating the model response to chemotherapeutic treatment in neoadjuvant settings (298). Similarly, in 2009, Graf et al. (299) modeled nephroblastoma oncosimulator, a childhood cancer of the kidney, based on a clinical trial run by the International Society of Paediatric Oncology (SIOP) for simulating tumor response to therapeutic regimens in clinical trials. The results generated from the TOP and SIOP trials enabled the ACGT oncosimulators to adapt in light of real clinical conditions and the software to be validated against multi-scale patient data. The focus of ACGT oncosimulators, however, is limited to existing clinical trials for predicting efficacious treatment combinations.

## 5.2 The ContraCancrum Project

Towards establishing a platform for the development of composite multi-scale models for simulating malignant tumor models, in 2008, ContraCancrum project (294) was initiated. ContraCancrum aimed to construct a multi-scale computational framework for translating personalized cancer models into clinical settings towards simulating malignant tumor development and response to therapeutic regimens. For that, the Individualized MediciNe Simulation Environment (IMENSE) platform (300, 301) was established, to undertake the oncosimulator development process. The platform was employed for molecular and clinical data storage, retrieval, integration, and analysis. Oncosimulators, developed under the ContraCancrum project, employ patient data across biologically and clinically relevant scales including molecular, environmental, cell, and tissues level. These oncosimulators can be used to optimize personalized cancer therapeutics for assisting clinician decision-making process. To date, several oncosimulators have been reported, under the ContraCancrum project (27, 294, 299, 301–305). In particular, the initial validation of the ContraCancrum workflow was performed using two case studies; glioblastoma multiforme (GBM) (294, 305) and non-small cell lung cancer (NSCLC) (294, 304). In 2010, Folarin and Stamatakos (306) designed a glioblastoma oncosimulator using personalized molecular patient data to evaluate treatment response under the effect of a chemotherapeutic drug (temozolomide) (300). Similarly, Roniotis et al. (305) developed a multi-scale finite elements workflow to model glioblastoma growth, while Giatili et al. (307) outlined explicit boundary condition treatment in glioblastoma using an *in silico* tumor growth model. The results from the case studies were validated by comparing *in silico* prediction with pre- and post-operative imaging and clinical data (294, 302). Moreover, The ContraCancrum project hosts more than 100 lung patients' tumor and blood samples (294). This data is employed to develop clinically validated *in silico* multilevel cancer models for NSCLC using patient-specific data (304). In 2010, using a biochemical oncosimulator, Wan et al. (304) investigated the binding affinities for AEE788 and Gefitinib tyrosine kinase inhibitor against mutated epidermal growth factor receptor (EGFR) for NSCLC treatment. Similarly, Wang et al. (308) developed a 2D agent-based NSCLC model to investigate proliferation markers and evaluated ERK as a suitable target for targeted therapy. Although ContraCancrum's project has created numerous avenues for multilevel cancer model development, the platform is limited to only specific types of cancer for which data is internally available on the platform.

## 5.3 p-Medicine Project

Towards improving clinical deployment capabilities of oncosimulators, another pilot project: the personalized medicine (p-medicine) project was launched in 2011 (295). The main aim of p-medicine was to create biomedical tools facilitating translation of current medicine to P5 medicine (predictive, personalized, preventive, participatory, and psycho-cognitive) (309). For that, the p-medicine portal provides a web-based environment that hosts specifically-purpose tools for personalized panomics data integration, management, and model development. The portal has an intuitive graphical user interface (GUI) with an integrated workbench application for integrating information from clinical practices, histopathological imaging, treatment, and omics data, etc. Computational models developed under p-medicine workflow, are quantitatively adapted to clinical settings since they are derived using real multi-scale data. Several multi-scale cancer simulation models (oncosimulators) (295, 309) have been devised, using the p-medicine workflow. Amongst these, in 2012, Georgiadi et al. (310) developed a four-dimensional nephroblastoma treatment model and evaluated its employment in clinical decisions making. Towards evaluating personalized therapeutic combinations, in 2014, Blazewicz et al. (311) reported a p-medicine parallelized oncosimulator which evaluated nephroblastoma tumor response to therapy. The parallelization enhanced model usability and accuracy for eventual translation into clinical settings for supporting clinical decisions. In 2016, Argyri et al. (312) developed a breast cancer oncosimulator to evaluate vascular tumor growth in light of single-agent bevacizumab therapy (anti-angiogenic treatment), while in 2014, Stamatakos et al. (313) evaluated breast cancer treatment under an anthracycline drug for chemotherapy (epirubicin). In 2012, Ouzounoglou et al. (314) designed a personalized acute lymphoblastic leukemia (ALL) oncosimulator for evaluating the efficacy of prednisolone (a steroid medication). This study was further augmented, in 2015, by Kolokotroni et al. (315) to investigate the potential cytotoxic side effects of prednisolone. Later in 2017, Ouzounoglou et al. (316) expanded the ALL oncosimulator model to a hybrid oncosimulator for predicting pre-phase treatments for ALL patients. The validation of these models was undertaken using clinical trial data in pre and post-treatment (317). Although p-medicine presents a state-of-the-art *in silico* multi-scale cancer modeling environment, the project is limited in its application for determining individual biomarkers

for potential novel therapy identification. Moreover, the project is limited to its niche set of tools and models that cannot be integrated with other similar model repositories and platforms.

## 5.4 TUMOR Project

In 2012, a transatlantic USA-EU partnership was initiated with the launch of Transatlantic Tumor Model Repositories (TUMOR) (296). TUMOR provides an integrated, interoperable transatlantic research environment for developing a clinically driven cancer model repository. The repository aimed to integrate computational cancer models developed by different research groups. TUMOR's transatlantic aim was to couple models from ACGT and ContraCancrum projects with those at the Center for the Development of a Virtual Tumor (CViT) (318) as well as other relevant centers. TUMOR is predicted to serve as an international clinical translation, interoperable and validation platform for *in silico* oncology hosting multi-scale cancer models from different cancer model repositories and platforms such as E-Cell (230), CellML (319), FieldML (320), and BioModels (35, 321). To support model data interoperability between platforms, TumorML (Tumor model repositories Markup Language) (321) was developed towards facilitating inter-data operability in the TUMOR project. The TUMOR environment also offers a wide range of additional services supporting predictive oncology and individualized optimization of cancer treatment. For example, the platform allows remote access of predictive cancer models in hospitals and to clinicians for the development of quantitative cancer research and personalized cancer therapy model. TUMOR environment also incorporates deterministic as well as stochastic models through COPASI simulator (257). An automatic validation pipeline is also embedded for the execution and deployment of these models in clinical settings (296). TUMOR's ability to couple and integrate models from different scales, approaches, and repositories towards increasing model accuracy in predictive oncology was exemplified with Wang et al.'s (322) NSCLC model. In 2007, Wang et al. developed a 2D multi-scale NSCLC model for evaluating tumor expansion dynamics in NSCLC patients, in CViT. This model was exported in TumorML and made available in the TUMOR repository to help evaluate growth factor influence in aggressive cancer (321). Similarly, in 2014 Sakkalis et al. (323) employed the TUMOR platform to interlink and couple three independent glioblastoma-specific cancer models (EGFR signaling (324), cancer metabolism (325), Oncosimulator (323), reported by different research groups. The resultant model was used to investigate the impact of radiation and temozolomide (chemotherapy) on glioblastoma multiforme to evaluate treatment effectiveness.

## 5.5 CHIC Project

Another transatlantic project Computational Horizons In Cancer (CHIC) (297) launched in 2013, aimed to provide an oncosimulator modeling platform for *in silico* oncology. CHIC was initiated to develop and implement predictive oncology and individualized multi-scale cancer modeling tools towards assisting quantitative cancer research and personalized cancer therapy. The workflow and tools established under the ambient of the CHIC project allowed the development of robust, interoperable, and collaborative *in silico* models in cancer and normal conditions. The CHIC project also proposed a pipeline to translate the model towards supporting clinicians to make optimal personalized treatment plans for individual patients. To this end, several models are created using CHIC such as non-small cell lung cancer (326), glioblastoma (327), leukemia model (328), etc. These models furnish a quantitative understanding of tumorigenesis towards providing avenues for promoting individual cancer patient treatment combinations. One such model reported by Kolokotroni et al. (326) evaluated the efficacy of cisplatin-based therapy for NSCLC patients using *in silico* multi-scale cancer model. While, in 2015, Antonopoulos and Stamatakos (327) modeled the infiltration of glioblastoma cells in normal brain regions using a novel treatment. In 2017, Stamatakos and Giatili (329) extended glioblastoma oncosimulator for modeling tumor growth using reaction-diffusion numerical handling based on multi-scale panomics data. They further proposed a clinical pipeline to translate the model into clinical settings towards supporting clinicians to make optimal personalized treatment plans for individual patients. Ouzounoglou et al. (328) developed an *in silico* multi-scale leukemia oncosimulator model towards modeling deregulations in the G1/S pathway to investigate the altered function of retinoblastoma in ALL patients. However, a clinical translation of these models is currently in the works (297).

# 6 DISCUSSION

In this work, we have evaluated the use of data-driven multi-scale cancer models in deciphering complex biomolecular underpinnings in cancer research towards developing personalized therapeutics interventions for clinical decision-making. Specifically, we have discussed the chronological evolution of online cancer data repositories that host high-resolution datasets from multiple spatiotemporal scales. Next, we evaluate how this data drives single- and multi-scale systems biology models towards decoding complex cancer regulation in patients. We then track the development of various modeling software and associated applications in enhancing the translational role of cancer systems biology models in clinics.

We conclude that the contemporary multi-scale modeling software line-up remains limited in their clinical employment due to the lack of a generic, zero-code, panomic-based framework for translating research models into clinical settings. Such a framework would help annotate *in silico* cancer models developed using single and multi-scale databases (45, 61, 330–334). The framework should also provide an environment for developing the extra-cellular matrix of a cancer cell which can then be integrated into cellular models. Existing environment (38, 39) and cell line databases (41–43) need to be integrated to design environmental models along with biologically plausible cell line structures. These cell lines could then be assembled into three-dimensional geometries to create multi-scale *in silico* organoids. The pipeline should also furnish capabilities such as a convenient import workflow for clinical data integration through histopathological image data repositories (44–46) for designing biologically accurate organoid structures based on each cancer patient's underlying cellular morphology. Once the

personalized multi-scale model has been constructed, the pipeline would allow investigation into the temporal evolution of the multi-scale organoid under personalized inputs and user-designed biomolecular entities. Data generated from the multi-scale model simulation can be analyzed to elicit biomolecular cues for each cancer patient as well as determine its role. Due to the heterogeneity and complexity of biomolecular data a coherent panomics-based pipeline can be challenging to develop and will require a collaborative effort by various research groups, through close collaborations and data standardization.

Taken together, a translational *in silico* systems oncology pipeline is the need of the hour and will help develop and deliver personalized treatments of cancer as well as substantively inform clinical decision-making processes.

## AUTHOR CONTRIBUTIONS

SC and MG carried out the literature review and drafted the manuscript. All authors contributed to the article and approved the submitted version.

## FUNDING

This work was supported by the National ICT-R&D Fund (SRG-209), RF-NCBC-015, NGIRI-2020-4771, HEC (21-30SRGP/R&D/HEC/2014, 20-2269/NRPU/R&D/HEC/12/4792 and 20-3629/NRPU/R&D/HEC/14/585), TWAS (RG 14-319 RG/ITC/AS_C) and LUMS (STG-BIO-1008, FIF-BIO-2052, FIF-BIO-0255, SRP-185-BIO, SRP-058-BIO and FIF-477-1819-BIO) grants.

## ACKNOWLEDGMENTS

This manuscript has been released as a pre-print at bioRxiv (335).

## SUPPLEMENTARY MATERIAL

The Supplementary Material for this article can be found online at: https://www.frontiersin.org/articles/10.3389/fonc.2021.712505/full#supplementary-material

## REFERENCES

1. DeVita VT. The "War on Cancer" and its Impact. *Nat Clin Pract Oncol* (2004) 1(2):55. doi: 10.1038/ncponc0036
2. Wong AH-H, Deng C-X. Precision Medicine for Personalized Cancer Therapy. *Int J Biol Sci* (2015) 11(12):1410–2. doi: 10.7150/ijbs.14154
3. Giacomini KM, Yee SW, Ratain MJ, Weinshilboum RM, Kamatani N, Nakamura Y. Pharmacogenomics and Patient Care: One Size Does Not Fit All. *Sci Transl Med* (2012) 4(153):153ps18. doi: 10.1126/scitranslmed.3003471
4. Krzyszczyk P, Acevedo A, Davidoff EJ, Timmins LM, Marrero-Berrios I, Patel M, et al. The Growing Role of Precision and Personalized Medicine for Cancer Treatment. *Technol (Singap World Sci)* (2018) 6(3–4):79–100. doi: 10.1142/s2339547818300020
5. Binotto M, Reinert T, Werutsky G, Zaffaroni F, Schwartsmann G. Health-Related Quality of Life Before and During Chemotherapy in Patients With Early-Stage Breast Cancer. *Ecancermedicalscience* (2020) 14:1007. doi: 10.3332/ecancer.2020.1007
6. Adler AS, Lin M, Horlings H, Nuyten DSA, van de Vijver MJ, Chang HY. Genetic Regulators of Large-Scale Transcriptional Signatures in Cancer. *Nat Genet* (2006) 38(4):421–30. doi: 10.1038/ng1752
7. Shi Y, Wei J, Chen Z, Yuan Y, Li X, Zhang Y, et al. Integrative Analysis Reveals Comprehensive Altered Metabolic Genes Linking With Tumor Epigenetics Modification in Pan-Cancer. *BioMed Res Int* (2019) 2019:1–18. doi: 10.1155/2019/6706354
8. Chen Y, Ni J, Gao Y, Zhang J, Liu X, Chen Y, et al. Integrated Proteomics and Metabolomics Reveals the Comprehensive Characterization of Antitumor Mechanism Underlying Shikonin on Colon Cancer Patient-Derived Xenograft Model. *Sci Rep* (2020) 10(1):1–14. doi: 10.1038/s41598-020-71116-5
9. Angermueller C, Clark SJ, Lee HJ, Macaulay IC, Teng MJ, Hu TX, et al. Parallel Single-Cell Sequencing Links Transcriptional and Epigenetic Heterogeneity. *Nat Methods* (2016) 13(3):229–32. doi: 10.1038/nmeth.3728
10. Yoshida A, Kohyama S, Fujiwara K, Nishikawa S, Doi N. Regulation of Spatiotemporal Patterning in Artificial Cells by a Defined Protein Expression System. *Chem Sci* (2019) 10(48):11064–72. doi: 10.1039/c9sc02441g
11. Rejniak KA, Anderson ARA. Hybrid Models of Tumor Growth. *Wiley Interdiscip Rev Syst Biol Med* (2011) 3(1):115–25. doi: 10.1002/wsbm.102
12. Sanchez-Vega F, Mina M, Armenia J, Chatila WK, Luna A, La KC, et al. Oncogenic Signaling Pathways in The Cancer Genome Atlas. *Cell* (2018) 173(2):321–37. doi: 10.1016/j.cell.2018.03.035
13. Zehir A, Benayed R, Shah RH, Syed A, Middha S, Kim HR, et al. Mutational Landscape of Metastatic Cancer Revealed From Prospective Clinical Sequencing of 10,000 Patients. *Nat Med* (2017) 23(6):703–13. doi: 10.1038/nm.4333
14. Al Hajri Q, Dash S, Feng W, Garner HR, Anandakrishnan R. Identifying Multi-Hit Carcinogenic Gene Combinations: Scaling Up a Weighted Set Cover Algorithm Using Compressed Binary Matrix Representation on a GPU. *Sci Rep* (2020) 10(1):1–18. doi: 10.1038/s41598-020-58785-y
15. Roerink SF, Sasaki N, Lee-Six H, Young MD, Alexandrov LB, Behjati S, et al. Intra-Tumour Diversification in Colorectal Cancer at the Single-Cell Level. *Nature* (2018) 556(7702):457–62. doi: 10.1038/s41586-018-0024-3
16. Song Q, Merajver SD, Li JZ. Cancer Classification in the Genomic Era: Five Contemporary Problems. *Hum Genomics* (2015) 9(1):1–8. doi: 10.1186/s40246-015-0049-8
17. Hanahan D, Weinberg RA. The Hallmarks of Cancer. *Cell* (2000) 100(1):57–70. doi: 10.1016/s0092-8674(00)81683-9
18. Hanahan D, Weinberg RA. Hallmarks of Cancer: The Next Generation. *Cell* (2011) 144(5):646–74. doi: 10.1016/j.cell.2011.02.013
19. Saha R, Chowdhury A, Maranas CD. Recent Advances in the Reconstruction of Metabolic Models and Integration of Omics Data. *Curr Opin Biotechnol* (2014) 29:39–45. doi: 10.1016/j.copbio.2014.02.011
20. Deisboeck TS, Berens ME, Kansal AR, Torquato S, Stemmer-Rachamimov AO, Chiocca EA. Pattern of Self-Organization in Tumour Systems: Complex Growth Dynamics in a Novel Brain Tumour Spheroid Model. *Cell Prolif* (2001) 34(2):115–34. doi: 10.1046/j.1365-2184.2001.00202.x
21. Lorenzo G, Scott MA, Tew K, Hughes TJR, Zhang YJ, Liu L, et al. Tissue-Scale, Personalized Modeling and Simulation of Prostate Cancer Growth. *Proc Natl Acad Sci* (2016) 113(48):E7663–71. doi: 10.1073/pnas.1615791113
22. Pingle SC, Sultana Z, Pastorino S, Jiang P, Mukthavaram R, Chao Y, et al. *In Silico* Modeling Predicts Drug Sensitivity of Patient-Derived Cancer Cells. *J Transl Med* (2014) 12(1):1–13. doi: 10.1186/1479-5876-12-128
23. Zhang J, Chiodini R, Badr A, Zhang G. The Impact of Next-Generation Sequencing on Genomics. *J Genet Genomics* (2011) 38(3):95–109. doi: 10.1016/j.jgg.2011.02.003
24. Velculescu VE, Zhang L, Zhou W, Vogelstein J, Basrai MA, Bassett DEJ, et al. Characterization of the Yeast Transcriptome. *Cell* (1997) 88(2):243–51. doi: 10.1016/s0092-8674(00)81845-0
25. Anderson NL, Anderson NG. Proteome and Proteomics: New Technologies, New Concepts, and New Words. *Electrophoresis* (1998) 19(11):1853–61. doi: 10.1002/elps.1150191103

26. Manzoni C, Kia DA, Vandrovcova J, Hardy J, Wood NW, Lewis PA, et al. Genome, Transcriptome and Proteome: The Rise of Omics Data and Their Integration in Biomedical Sciences. *Brief Bioinform* (2016) 19(2):286–302. doi: 10.1093/bib/bbw114
27. Stamatakos GS, Dionysiou DD, Graf NM, Sofra NA, Desmedt C, Hoppe A, et al. The "Oncosimulator": A Multilevel, Clinically Oriented Simulation System of Tumor Growth and Organism Response to Therapeutic Schemes. Towards the Clinical Evaluation of *In Silico* Oncology. *Conf Proc IEEE Eng Med Biol Soc* (2007), 6629–32. doi: 10.1109/IEMBS.2007.4353879
28. Stephens ZD, Lee SY, Faghri F, Campbell RH, Zhai C, Efron MJ, et al. Big Data: Astronomical or Genomical? *PloS Biol* (2015) 13(7):e1002195. doi: 10.1371/journal.pbio.1002195
29. Krupp M, Marquardt JU, Sahin U, Galle PR, Castle J, Teufel A. RNA-Seq Atlas–a Reference Database for Gene Expression Profiling in Normal Tissue by Next-Generation Sequencing. *Bioinformatics* (2012) 28(8):1184–5. doi: 10.1093/bioinformatics/bts084
30. Park S-J, Yoon B-H, Kim S-K, Kim S-Y. GENT2: An Updated Gene Expression Database for Normal and Tumor Tissues. *BMC Med Genomics* (2019) 12(5):1–8. doi: 10.1186/s12920-019-0514-7
31. Edgar R, Domrachev M, Lash AE. Gene Expression Omnibus: NCBI Gene Expression and Hybridization Array Data Repository. *Nucleic Acids Res* (2002) 30(1):207–10. doi: 10.1093/nar/30.1.207
32. Ogata H, Goto S, Sato K, Fujibuchi W, Bono H, Kanehisa M. KEGG: Kyoto Encyclopedia of Genes and Genomes. *Nucleic Acids Res* (1999) 27(1):29–34. doi: 10.1093/nar/27.1.29
33. Nikitin A, Egorov S, Daraselia N, Mazo I. Pathway Studio–the Analysis and Navigation of Molecular Networks. *Bioinformatics* (2003) 19(16):2155–7. doi: 10.1093/bioinformatics/btg290
34. Thomas PD, Campbell MJ, Kejariwal A, Mi H, Karlak B, Daverman R, et al. PANTHER: A Library of Protein Families and Subfamilies Indexed by Function. *Genome Res* (2003) 13(9):2129–41. doi: 10.1101/gr.772403
35. Le Novère N, Bornstein B, Broicher A, Courtot M, Donizelli M, Dharuri H, et al. BioModels Database: A Free, Centralized Database of Curated, Published, Quantitative Kinetic Models of Biochemical and Cellular Systems. *Nucleic Acids Res* (2006) 34(suppl_1):D689–91. doi: 10.1093/nar/gkj092
36. Hermjakob H, Montecchi-Palazzi L, Lewington C, Mudali S, Kerrien S, Orchard S, et al. IntAct: An Open Source Molecular Interaction Database. *Nucleic Acids Res* (2004) 32(suppl_1):D452–5. doi: 10.1093/nar/gkh052
37. Zanzoni A, Montecchi-Palazzi L, Quondam M, Ausiello G, Helmer-Citterich M, Cesareni G. MINT: A Molecular INTeraction Database. *FEBS Lett* (2002) 513(1):135–40. doi: 10.1016/s0014-5793(01)03293-8
38. Chautard E, Fatoux-Ardore M, Ballut L, Thierry-Mieg N, Ricard-Blum S. MatrixDB, the Extracellular Matrix Interaction Database. *Nucleic Acids Res* (2011) 39(suppl_1):D235–40. doi: 10.1093/nar/gkq830
39. Shao X, Taha IN, Clauser KR, Gao YT, Naba A. MatrisomeDB: The ECM-Protein Knowledge Database. *Nucleic Acids Res* (2020) 48(D1):D1136–44. doi: 10.1093/nar/gkz849
40. Tate JG, Bamford S, Jubb HC, Sondka Z, Beare DM, Bindal N, et al. COSMIC: The Catalogue Of Somatic Mutations In Cancer. *Nucleic Acids Res* (2019) 47(D1):D941–7. doi: 10.1093/nar/gky1015
41. Rajapakse VN, Luna A, Yamade M, Loman L, Varma S, Sunshine M, et al. CellMinerCDB for Integrative Cross-Database Genomics and Pharmacogenomics Analyses of Cancer Cell Lines. *iScience* (2018) 10:247–64. doi: 10.1016/j.isci.2018.11.029
42. Barretina J, Caponigro G, Stransky N, Venkatesan K, Margolin AA, Kim S, et al. The Cancer Cell Line Encyclopedia Enables Predictive Modelling of Anticancer Drug Sensitivity. *Nature* (2012) 483(7391):603–7. doi: 10.1038/nature11003
43. Romano P, Manniello A, Aresu O, Armento M, Cesaro M, Parodi B. Cell Line Data Base: Structure and Recent Improvements Towards Molecular Authentication of Human Cell Lines. *Nucleic Acids Res* (2009) 37(suppl_1): D925–32. doi: 10.1093/nar/gkn730
44. Gutman DA, Cobb J, Somanna D, Park Y, Wang F, Kurc T, et al. Cancer Digital Slide Archive: An Informatics Resource to Support Integrated *In Silico* Analysis of TCGA Pathology Data. *J Am Med Inform Assoc* (2013) 20 (6):1091–8. doi: 10.1136/amiajnl-2012-001469
45. Lonsdale J, Thomas J, Salvatore M, Phillips R, Lo E, Shad S, et al. The Genotype-Tissue Expression (GTEx) Project. *Nat Genet* (2013) 45(6):580–5. doi: 10.1038/ng.2653
46. Clark K, Vendt B, Smith K, Freymann J, Kirby J, Koppel P, et al. The Cancer Imaging Archive (TCIA): Maintaining and Operating a Public Information Repository. *J Digit Imaging* (2013) 26(6):1045–57. doi: 10.1007/s10278-013-9622-7
47. Kanehisa M, Goto S, Furumichi M, Tanabe M, Hirakawa M. KEGG for Representation and Analysis of Molecular Networks Involving Diseases and Drugs. *Nucleic Acids Res* (2010) 38(suppl_1):D355–60. doi: 10.1093/nar/gkp896
48. Hamosh A, Scott AF, Amberger J, Bocchini C, Valle D, McKusick VA. Online Mendelian Inheritance in Man (OMIM), a Knowledgebase of Human Genes and Genetic Disorders. *Nucleic Acids Res* (2002) 30(1):52–5. doi: 10.1093/nar/30.1.52
49. Chakravarty D, Gao J, Phillips SM, Kundra R, Zhang H, Wang J, et al. OncoKB: A Precision Oncology Knowledge Base. *JCO Precis Oncol* (2017) 1:1–16. doi: 10.1200/PO.17.00011
50. Wishart DS, Knox C, Guo AC, Cheng D, Shrivastava S, Tzur D, et al. DrugBank: A Knowledgebase for Drugs, Drug Actions and Drug Targets. *Nucleic Acids Res* (2008) 36(suppl_1):D901–6. doi: 10.1093/nar/gkm958
51. Smirnov P, Kofia V, Maru A, Freeman M, Ho C, El-Hachem N, et al. PharmacoDB: An Integrative Database for Mining *In Vitro* Anticancer Drug Screening Studies. *Nucleic Acids Res* (2018) 46(D1):D994–1002. doi: 10.1093/nar/gkx911
52. Piñeiro-Yáñez E, Reboiro-Jato M, Gómez-López G, Perales-Patón J, Troulé K, Rodríguez JM, et al. PanDrugs: A Novel Method to Prioritize Anticancer Drug Treatments According to Individual Genomic Data. *Genome Med* (2018) 10(1):1–11. doi: 10.1186/s13073-018-0546-1
53. Pinu FR, Beale DJ, Paten AM, Kouremenos K, Swarup S, Schirra HJ, et al. Systems Biology and Multi-Omics Integration: Viewpoints From the Metabolomics Research Community. *Metabolites* (2019) 9(4):1–31. doi: 10.3390/metabo9040076
54. Bilofsky HS, Burks C, Fickett JW, Goad WB, Wayne FIL, Rindone P, et al. The GenBank Genetic Sequence Databank. *Nucleic Acids Res* (1986) 14(1):1–4. doi: 10.1093/nar/14.1.1
55. Benson DA, Cavanaugh M, Clark K, Karsch-Mizrachi I, Lipman DJ, Ostell J, et al. GenBank. *Nucleic Acids Res* (2012) 41(D1):D36–42. doi: 10.1093/nar/gks1195
56. Benson DA, Clark K, Karsch-Mizrachi I, Lipman DJ, Ostell J, Sayers EW. GenBank. *Nucleic Acids Res* (2015) 43(D1):D30–5. doi: 10.1093/nar/gku1216
57. Díez O, Osorio A, Durán M, Martinez-Ferrandis JI, de la Hoya M, Salazar R, et al. Analysis of BRCA1 and BRCA2 Genes in Spanish Breast/Ovarian Cancer Patients: A High Proportion of Mutations Unique to Spain and Evidence of Founder Effects. *Hum Mutat* (2003) 22(4):301–12. doi: 10.1002/humu.10260
58. Medrek C, Pontén F, Jirström K, Leandersson K. The Presence of Tumor Associated Macrophages in Tumor Stroma as a Prognostic Marker for Breast Cancer Patients. *BMC Cancer* (2012) 12(1):1–9. doi: 10.1186/1471-2407-12-306
59. Hubbard T, Barker D, Birney E, Cameron G, Chen Y, Clark L, et al. The Ensembl Genome Database Project. *Nucleic Acids Res* (2002) 30(1):38–41. doi: 10.1093/nar/30.1.38
60. Easton DF, Pooley KA, Dunning AM, Pharoah PDP, Thompson D, Ballinger DG, et al. Genome-Wide Association Study Identifies Novel Breast Cancer Susceptibility Loci. *Nature* (2007) 447(7148):1087–93. doi: 10.1038/nature05887
61. Bamford S, Dawson E, Forbes S, Clements J, Pettett R, Dogan A, et al. The COSMIC (Catalogue of Somatic Mutations in Cancer) Database and Website. *Br J Cancer* (2004) 91:355–8. doi: 10.1038/sj.bjc.6601894
62. Schubbert S, Shannon K, Bollag G. Hyperactive Ras in Developmental Disorders and Cancer. *Nat Rev Cancer* (2007) 7(4):295–308. doi: 10.1038/nrc2109
63. Weir BA, Woo MS, Getz G, Perner S, Ding L, Beroukhim R, et al. Characterizing the Cancer Genome in Lung Adenocarcinoma. *Nature* (2007) 450(7171):893–8. doi: 10.1038/nature06358
64. Zhao D, Tang Y, Xia X, Sun J, Meng J, Shang J, et al. Integration of Transcriptome, Proteome, and Metabolome Provides Insights Into How

Calcium Enhances the Mechanical Strength of Herbaceous Peony Inflorescence Stems. *Cells* (2019) 8(2):1–22. doi: 10.3390/cells8020102
65. Chakraborty PK, Mustafi SB, Xiong X, Dwivedi SKD, Nesin V, Saha S, et al. MICU1 Drives Glycolysis and Chemoresistance in Ovarian Cancer. *Nat Commun* (2017) 8(1):1–16. doi: 10.1038/ncomms14634
66. Tomczak K, Czerwińska P, Wiznerowicz M. The Cancer Genome Atlas (TCGA): An Immeasurable Source of Knowledge. *Contemp Oncol (Pozn)* (2015) 19(1A):A68–77. doi: 10.5114/wo.2014.47136
67. Tamborero D, Gonzalez-Perez A, Perez-Llamas C, Deu-Pons J, Kandoth C, Reimand J, et al. Comprehensive Identification of Mutational Cancer Driver Genes Across 12 Tumor Types. *Sci Rep* (2013) 3(1):1–10. doi: 10.1038/srep02650
68. Leiserson MDM, Vandin F, Wu H-T, Dobson JR, Eldridge JV, Thomas JL, et al. Pan-Cancer Network Analysis Identifies Combinations of Rare Somatic Mutations Across Pathways and Protein Complexes. *Nat Genet* (2015) 47 (2):106–14. doi: 10.1038/ng.3168
69. Davis CF, Ricketts CJ, Wang M, Yang L, Cherniack AD, Shen H, et al. The Somatic Genomic Landscape of Chromophobe Renal Cell Carcinoma. *Cancer Cell* (2014) 26(3):319–30. doi: 10.1016/j.ccr.2014.07.014
70. Zhang J, Baran J, Cros A, Guberman JM, Haider S, Hsu J, et al. International Cancer Genome Consortium Data Portal—a One-Stop Shop for Cancer Genomics Data. *Database* (2011) 2011:1–10. doi: 10.1093/database/bar026
71. Jones DTW, Jäger N, Kool M, Zichner T, Hutter B, Sultan M, et al. Dissecting the Genomic Complexity Underlying Medulloblastoma. *Nature* (2012) 488(7409):100–5. doi: 10.1038/nature11284
72. Burns MB, Lackey L, Carpenter MA, Rathore A, Land AM, Leonard B, et al. APOBEC3B Is an Enzymatic Source of Mutation in Breast Cancer. *Nature* (2013) 494(7437):366–70. doi: 10.1038/nature11881
73. Supek F, Miñana B, Valcárcel J, Gabaldón T, Lehner B. Synonymous Mutations Frequently Act as Driver Mutations in Human Cancers. *Cell* (2014) 156(6):1324–35. doi: 10.1016/j.cell.2014.01.051
74. Cerami E, Gao J, Dogrusoz U, Gross BE, Sumer SO, Aksoy BA, et al. The Cbio Cancer Genomics Portal: An Open Platform for Exploring Multidimensional Cancer Genomics Data. *Cancer Discovery* (2012) 2 (5):401–4. doi: 10.1158/2159-8290.CD-12-0095
75. Gao J, Aksoy BA, Dogrusoz U, Dresdner G, Gross B, Sumer SO, et al. Integrative Analysis of Complex Cancer Genomics and Clinical Profiles Using the Cbioportal. *Sci Signal* (2013) 6(269):pl1. doi: 10.1126/scisignal.2004088
76. Robinson D, Allen EMV, Wu Y-M, Schultz N, Lonigro RJ, Mosquera J-M, et al. Integrative Clinical Genomics of Advanced Prostate Cancer. *Cell* (2015) 161(5):1215–28. doi: 10.1016/j.cell.2015.05.001
77. Zaretsky JM, Garcia-Diaz A, Shin DS, Escuin-Ordinas H, Hugo W, Hu-Lieskovan S, et al. Mutations Associated With Acquired Resistance to PD-1 Blockade in Melanoma. *N Engl J Med* (2016) 375(9):819–29. doi: 10.1056/NEJMoa1604958
78. Bailey P, Chang DK, Nones K, Johns AL, Patch A-M, Gingras M-C, et al. Genomic Analyses Identify Molecular Subtypes of Pancreatic Cancer. *Nature* (2016) 531(7592):47–52. doi: 10.1038/nature16965
79. Jiao X-D, Qin B-D, You P, Cai J, Zang Y-S. The Prognostic Value of TP53 and its Correlation With EGFR Mutation in Advanced non-Small Cell Lung Cancer, an Analysis Based on Cbioportal Data Base. *Lung Cancer* (2018) 123:70–5. doi: 10.1016/j.lungcan.2018.07.003
80. Hou H, Zhang C, Qi X, Zhou L, Liu D, Lv H, et al. Distinctive Targetable Genotypes of Younger Patients With Lung Adenocarcinoma: A Cbioportal for Cancer Genomics Data Base Analysis. *Cancer Biol Ther* (2020) 21(1):26–33. doi: 10.1080/15384047.2019.1665392
81. Chen G, Gharib TG, Huang C-C, Taylor JMG, Misek DE, Kardia SLR, et al. Discordant Protein and mRNA Expression in Lung Adenocarcinomas. *Mol Cell Proteomics* (2002) 1(4):304–13. doi: 10.1074/mcp.m200008-mcp200
82. Cox J, Mann M. Is Proteomics the New Genomics? *Cell* (2007) 130(3):395–8. doi: 10.1016/j.cell.2007.07.032
83. Aslam B, Basit M, Nisar MA, Khurshid M, Rasool MH. Proteomics: Technologies and Their Applications. *J Chromatogr Sci* (2017) 55(2):182–96. doi: 10.1093/chromsci/bmw167
84. Williams CW, Elmendorf HG. Identification and Analysis of the RNA Degrading Complexes and Machinery of Giardia Lamblia Using an *In Silico* Approach. *BMC Genomics* (2011) 12(1):1–15. doi: 10.1186/1471-2164-12-586
85. Gill G. Post-Translational Modification by the Small Ubiquitin-Related Modifier SUMO has Big Effects on Transcription Factor Activity. *Curr Opin Genet Dev* (2003) 13(2):108–13. doi: 10.1016/S0959-437X(03)00021-2
86. Bathke J, Konzer A, Remes B, McIntosh M, Klug G. Comparative Analyses of the Variation of the Transcriptome and Proteome of Rhodobacter Sphaeroides Throughout Growth. *BMC Genomics* (2019) 20(1):1–3. doi: 10.1186/s12864-019-5749-3
87. Marx V. Proteomics: An Atlas of Expression. *Nature* (2014) 509(7502):645–9. doi: 10.1038/509645a
88. Persson A, Hober S, Uhlén M. A Human Protein Atlas Based on Antibody Proteomics. *Curr Opin Mol Ther* (2006) 8(3):185–90.
89. Uhlén M, Björling E, Agaton C, Szigyarto CAK, Amini B, Andersen E, et al. A Human Protein Atlas for Normal and Cancer Tissues Based on Antibody Proteomics. *Mol Cell Proteomics* (2005) 4(12):1920–32. doi: 10.1074/mcp.M500279-MCP200
90. Gámez-Pozo A, Sánchez-Navarro I, Nistal M, Calvo E, Madero R, Díaz E, et al. MALDI Profiling of Human Lung Cancer Subtypes. *PloS One* (2009) 4 (11):e7731. doi: 10.1371/journal.pone.0007731
91. Imberg-Kazdan K, Ha S, Greenfield A, Poultney CS, Bonneau R, Logan SK, et al. A Genome-Wide RNA Interference Screen Identifies New Regulators of Androgen Receptor Function in Prostate Cancer Cells. *Genome Res* (2013) 23(4):581–91. doi: 10.1101/gr.144774.112
92. Collins FS. New Goals for the U.S. Human Genome Project: 1998-2003. *Science* (1998) 282(5389):682–9. doi: 10.1126/science.282.5389.682
93. Legrain P, Aebersold R, Archakov A, Bairoch A, Bala K, Beretta L, et al. The Human Proteome Project: Current State and Future Direction. *Mol Cell Proteomics* (2011) 10(7):M111.009993. doi: 10.1074/mcp.M111.009993
94. Cottingham K. Hupo's Human Proteome Project: The Next Big Thing? *J Proteome Res* (2008) 7: (6):2192. doi: 10.1021/pr0837441
95. Wang Q, Wen B, Yan G, Wei J, Xie L, Xu S, et al. Qualitative and Quantitative Expression Status of the Human Chromosome 20 Genes in Cancer Tissues and the Representative Cell Lines. *J Proteome Res* (2013) 12 (1):151–61. doi: 10.1021/pr3008336
96. Hüttenhain R, Soste M, Selevsek N, Röst H, Sethi A, Carapito C, et al. Reproducible Quantification of Cancer-Associated Proteins in Body Fluids Using Targeted Proteomics. *Sci Transl Med* (2012) 4(142):142ra94–142ra94. doi: 10.1126/scitranslmed.3003989
97. Zhang B, Wang J, Wang X, Zhu J, Liu Q, Shi Z, et al. Proteogenomic Characterization of Human Colon and Rectal Cancer. *Nature* (2014) 513 (7518):382–7. doi: 10.1038/nature13438
98. Huang Z, Ma L, Huang C, Li Q, Nice EC. Proteomic Profiling of Human Plasma for Cancer Biomarker Discovery. *Proteomics* (2017) 17(6):1–13. doi: 10.1002/pmic.201600240
99. Mertins P, Mani DR, Ruggles KV, Gillette MA, Clauser KR, Wang P, et al. Proteogenomics Connects Somatic Mutations to Signalling in Breast Cancer. *Nature* (2016) 534(7605):55–62. doi: 10.1038/nature18003
100. Zhang H, Liu T, Zhang Z, Payne SH, Zhang B, McDermott JE, et al. Integrated Proteogenomic Characterization of Human High-Grade Serous Ovarian Cancer. *Cell* (2016) 166(3):755–65. doi: 10.1016/j.cell.2016.05.069
101. Sebastian S, Bulun SE. A Highly Complex Organization of the Regulatory Region of the Human CYP19 (Aromatase) Gene Revealed by the Human Genome Project. *J Clin Endocrinol Metab* (2001) 86(10):4600–2. doi: 10.1210/jcem.86.10.7947
102. Aebersold R, Bader GD, Edwards AM, Van Eyk JE, Kussmann M, Qin J, et al. The Biology/Disease-Driven Human Proteome Project (B/D-HPP): Enabling Protein Research for the Life Sciences Community. *J Proteome Res* (2013) 12 (1):23–7. doi: 10.1021/pr301151m
103. Paik Y-K, Jeong S-K, Omenn GS, Uhlen M, Hanash S, Cho SY, et al. The Chromosome-Centric Human Proteome Project for Cataloging Proteins Encoded in the Genome. *Nat Biotechnol* (2012) 30(3):221–3. doi: 10.1038/nbt.2152
104. Gupta MK, Jayaram S, Madugundu AK, Chavan S, Advani J, Pandey A, et al. Chromosome-Centric Human Proteome Project: Deciphering Proteins Associated With Glioma and Neurodegenerative Disorders on Chromosome 12. *J Proteome Res* (2014) 13(7):3178–90. doi: 10.1021/pr500023p

105. Fan W, Ge G, Liu Y, Wang W, Liu L, Jia Y. Proteomics Integrated With Metabolomics: Analysis of the Internal Causes of Nutrient Changes in Alfalfa at Different Growth Stages. *BMC Plant Biol* (2018) 18(1):1–15. doi: 10.1186/s12870-018-1291-8
106. Kopka J, Schauer N, Krueger S, Birkemeyer C, Usadel B, Bergmüller E, et al. GMD@CSB.DB: The Golm Metabolome Database. *Bioinformatics* (2005) 21 (8):1635–8. doi: 10.1093/bioinformatics/bti236
107. Wishart DS, Feunang YD, Marcu A, Guo AC, Liang K, Vázquez-Fresno R, et al. HMDB 4.0: The Human Metabolome Database for 2018. *Nucleic Acids Res* (2018) 46(D1):D608–17. doi: 10.1093/nar/gkx1089
108. Sud M, Fahy E, Cotter D, Azam K, Vadivelu I, Burant C, et al. Metabolomics Workbench: An International Repository for Metabolomics Data and Metadata, Metabolite Standards, Protocols, Tutorials and Training, and Analysis Tools. *Nucleic Acids Res* (2016) 44(D1):D463–70. doi: 10.1093/nar/gkv1042
109. Wedge DC, Allwood JW, Dunn W, Vaughan AA, Simpson K, Brown M, et al. Is Serum or Plasma More Appropriate for Intersubject Comparisons in Metabolomic Studies? An Assessment in Patients With Small-Cell Lung Cancer. *Anal Chem* (2011) 83(17):6689–97. doi: 10.1021/ac2012224
110. Pasikanti KK, Esuvaranathan K, Hong Y, Ho PC, Mahendran R, Raman Nee Mani L, et al. Urinary Metabotyping of Bladder Cancer Using Two-Dimensional Gas Chromatography Time-of-Flight Mass Spectrometry. *J Proteome Res* (2013) 12(9):3865–73. doi: 10.1021/pr4000448
111. Wishart DS, Tzur D, Knox C, Eisner R, Guo AC, Young N, et al. HMDB: The Human Metabolome Database. *Nucleic Acids Res* (2007) 35(suppl_1):D521–6. doi: 10.1093/nar/gkl923
112. Sugimoto M, Wong DT, Hirayama A, Soga T, Tomita M. Capillary Electrophoresis Mass Spectrometry-Based Saliva Metabolomics Identified Oral, Breast and Pancreatic Cancer-Specific Profiles. *Metabolomics* (2010) 6 (1):78–95. doi: 10.1007/s11306-009-0178-y
113. Agren R, Bordel S, Mardinoglu A, Pornputtapong N, Nookaew I, Nielsen J. Reconstruction of Genome-Scale Active Metabolic Networks for 69 Human Cell Types and 16 Cancer Types Using INIT. *PloS Comput Biol* (2012) 8(5): e1002518. doi: 10.1371/journal.pcbi.1002518
114. Hattori A, Tsunoda M, Konuma T, Kobayashi M, Nagy T, Glushka J, et al. Cancer Progression by Reprogrammed BCAA Metabolism in Myeloid Leukaemia. *Nature* (2017) 545(7655):500–4. doi: 10.1038/nature22314
115. Mi H, Muruganujan A, Casagrande JT, Thomas PD. Large-Scale Gene Function Analysis With the PANTHER Classification System. *Nat Protoc* (2013) 8(8):1551–66. doi: 10.1038/nprot.2013.092
116. Kanehisa M, Furumichi M, Tanabe M, Sato Y, Morishima K. KEGG: New Perspectives on Genomes, Pathways, Diseases and Drugs. *Nucleic Acids Res* (2017) 45(D1):D353–61. doi: 10.1093/nar/gkw1092
117. Li X-N, Wang Z-J, Ye C-X, Zhao B-C, Li Z-L, Yang Y. RNA Sequencing Reveals the Expression Profiles of circRNA and Indicates That Circddx17 Acts as a Tumor Suppressor in Colorectal Cancer. *J Exp Clin Cancer Res* (2018) 37(1):1–14. doi: 10.1186/s13046-018-1006-x
118. Feng H, Gu Z-Y, Li Q, Liu Q-H, Yang X-Y, Zhang J-J. Identification of Significant Genes With Poor Prognosis in Ovarian Cancer *via* Bioinformatical Analysis. *J Ovarian Res* (2019) 12(1):1–9. doi: 10.1186/s13048-019-0508-2
119. Stenson PD, Ball EV, Mort M, Phillips AD, Shaw K, Cooper DN. The Human Gene Mutation Database (HGMD) and its Exploitation in the Fields of Personalized Genomics and Molecular Evolution. *Curr Protoc Bioinforma* (2012) 39(1):1–13. doi: 10.1002/0471250953.bi0113s39
120. Turcan S, Rohle D, Goenka A, Walsh LA, Fang F, Yilmaz E, et al. IDH1 Mutation is Sufficient to Establish the Glioma Hypermethylator Phenotype. *Nature* (2012) 483(7390):479–83. doi: 10.1038/nature10866
121. Karp PD, Riley M, Paley SM, Pellegrini-Toole A. The MetaCyc Database. *Nucleic Acids Res* (2002) 30(1):59–61. doi: 10.1093/nar/30.1.59
122. Miller JA, Pappan K, Thompson PA, Want EJ, Siskos AP, Keun HC, et al. Plasma Metabolomic Profiles of Breast Cancer Patients After Short-Term Limonene Intervention. *Cancer Prev Res (Phila)* (2015) 8(1):86–93. doi: 10.1158/1940-6207.CAPR-14-0100
123. Bader GD, Donaldson I, Wolting C, Ouellette BF, Pawson T, Hogue CW. BIND–The Biomolecular Interaction Network Database. *Nucleic Acids Res* (2001) 29(1):242–5. doi: 10.1093/nar/29.1.242
124. Chen Y, Choong L-Y, Lin Q, Philp R, Wong C-H, Ang B-K, et al. Differential Expression of Novel Tyrosine Kinase Substrates During Breast Cancer Development. *Mol Cell Proteomics* (2007) 6(12):2072–87. doi: 10.1074/mcp.M700395-MCP200
125. Vinayagam A, Gibson TE, Lee HJ, Yilmazel B, Roesel C, Hu Y, et al. Controllability Analysis of the Directed Human Protein Interaction Network Identifies Disease Genes and Drug Targets. *Proc Natl Acad Sci USA* (2016) 113(18):4976–81. doi: 10.1073/pnas.1603992113
126. Xenarios I, Rice DW, Salwinski L, Baron MK, Marcotte EM, Eisenberg D. DIP: The Database of Interacting Proteins. *Nucleic Acids Res* (2000) 28 (1):289–91. doi: 10.1093/nar/28.1.289
127. Goh WWB, Lee YH, Zubaidah RM, Jin J, Dong D, Lin Q, et al. Network-Based Pipeline for Analyzing MS Data: An Application Toward Liver Cancer. *J Proteome Res* (2011) 10(5):2261–72. doi: 10.1021/pr1010845
128. Fu LL, Zhao X, Xu HL, Wen X, Wang SY, Liu B, et al. Identification of microRNA-Regulated Autophagic Pathways in Plant Lectin-Induced Cancer Cell Death. *Cell Prolif* (2012) 45(5):477–85. doi: 10.1111/j.1365-2184.2012.00840.x
129. Graeber TG, Eisenberg D. Bioinformatic Identification of Potential Autocrine Signaling Loops in Cancers From Gene Expression Profiles. *Nat Genet* (2001) 29(3):295–300. doi: 10.1038/ng755
130. Von Mering C, Jensen LJ, Snel B, Hooper SD, Krupp M, Foglierini M, et al. STRING: Known and Predicted Protein–Protein Associations, Integrated and Transferred Across Organisms. *Nucleic Acids Res* (2005) 33(suppl_1): D433–7. doi: 10.1093/nar/gki005
131. Szklarczyk D, Morris JH, Cook H, Kuhn M, Wyder S, Simonovic M, et al. The STRING Database in 2017: Quality-Controlled Protein-Protein Association Networks, Made Broadly Accessible. *Nucleic Acids Res* (2017) 45(D1):D362–8. doi: 10.1093/nar/gkw937
132. Mlecnik B, Tosolini M, Charoentong P, Kirilovsky A, Bindea G, Berger A, et al. Biomolecular Network Reconstruction Identifies T-Cell Homing Factors Associated With Survival in Colorectal Cancer. *Gastroenterology* (2010) 138(4):1429–40. doi: 10.1053/j.gastro.2009.10.057
133. Azpeitia E, Balanzario EP, Wagner A. Signaling Pathways Have an Inherent Need for Noise to Acquire Information. *BMC Bioinf* (2020) 21(1):1–21. doi: 10.1186/s12859-020-03778-x
134. Peng R, Xu L, Wang H, Lyu Y, Wang D, Bi C, et al. DNA-Based Artificial Molecular Signaling System That Mimics Basic Elements of Reception and Response. *Nat Commun* (2020) 11(1):1–10. doi: 10.1038/s41467-020-14739-6
135. Suderman R, Deeds EJ. Intrinsic Limits of Information Transmission in Biochemical Signalling Motifs. *Interface Focus* (2018) 8(6):1–15. doi: 10.1098/rsfs.2018.0039
136. Quail DF, Joyce JA. Microenvironmental Regulation of Tumor Progression and Metastasis. *Nat Med* (2013) 19(11):1423–37. doi: 10.1038/nm.3394
137. Thul PJ, Lindskog C. The Human Protein Atlas: A Spatial Map of the Human Proteome. *Protein Sci* (2018) 27(1):233–44. doi: 10.1002/pro.3307
138. Sehuler GD. Pieces of Use Puzzle: Expressed Sequence Tags and the Catalog of Human Genes. *J Mol Med* (1997) 75(10):694–8. doi: 10.1007/s001090050155
139. Celik S, Logsdon BA, Battle S, Drescher CW, Rendi M, Hawkins RD, et al. Extracting a Low-Dimensional Description of Multiple Gene Expression Datasets Reveals a Potential Driver for Tumor-Associated Stroma in Ovarian Cancer. *Genome Med* (2016) 8(1):1–31. doi: 10.1186/s13073-016-0319-7
140. Levi-Galibov O, Lavon H, Wassermann-Dozorets R, Pevsner-Fischer M, Mayer S, Wershof E, et al. Heat Shock Factor 1-Dependent Extracellular Matrix Remodeling Mediates the Transition From Chronic Intestinal Inflammation to Colon Cancer. *Nat Commun* (2020) 11(1):1–19. doi: 10.1038/s41467-020-20054-x
141. Mirabelli P, Coppola L, Salvatore M. Cancer Cell Lines Are Useful Model Systems for Medical Research. *Cancers (Basel)* (2019) 11(8):1–18. doi: 10.3390/cancers11081098
142. Li H, Ning S, Ghandi M, Kryukov GV, Gopal S, Deik A, et al. The Landscape of Cancer Cell Line Metabolism. *Nat Med* (2019) 25(5):850–60. doi: 10.1038/s41591-019-0404-8
143. Hanniford D, Ulloa-Morales A, Karz A, Berzoti-Coelho MG, Moubarak RS, Sánchez-Sendra B, et al. Epigenetic Silencing of CDR1as Drives IGF2BP3-

Mediated Melanoma Invasion and Metastasis. *Cancer Cell* (2020) 37(1):55–70.e15. doi: 10.1016/j.ccell.2019.12.007
144. Birkmeyer NJO, Goodney PP, Stukel TA, Hillner BE, Birkmeyer JD. Do Cancer Centers Designated by the National Cancer Institute Have Better Surgical Outcomes? *Cancer* (2005) 103(3):435–41. doi: 10.1002/cncr.20785
145. Deng M, Brägelmann J, Kryukov I, Saraiva-Agostinho N, Perner S. FirebrowseR: An R Client to the Broad Institute's Firehose Pipeline. *Database* (2017) 2017:1–6. doi: 10.1093/database/baw160
146. Holroyd N, Sanchez-Flores A. Producing Parasitic Helminth Reference and Draft Genomes at the Wellcome Trust Sanger Institute. *Parasit Immunol* (2012) 34(2–3):100–7. doi: 10.1111/j.1365-3024.2011.01311.x
147. O'Sullivan RL, Keuthen NJ, Hayday CF, Ricciardi JN, Buttolph ML, Jenike MA, et al. The Massachusetts General Hospital (MGH) Hairpulling Scale: 2. Reliability and Validity. *Psychother Psychosom* (1995) 64(3–4):146–8. doi: 10.1159/000289004
148. Prior F, Smith K, Sharma A, Kirby J, Tarbox L, Clark K, et al. The Public Cancer Radiology Imaging Collections of The Cancer Imaging Archive. *Sci Data* (2017) 4(1):1–7. doi: 10.1038/sdata.2017.124
149. Li H, Zhu Y, Burnside ES, Drukker K, Hoadley KA, Fan C, et al. MR Imaging Radiomics Signatures for Predicting the Risk of Breast Cancer Recurrence as Given by Research Versions of MammaPrint, Oncotype DX, and PAM50 Gene Assays. *Radiology* (2016) 281(2):382–91. doi: 10.1148/radiol.2016152110
150. Sun R, Limkin EJ, Vakalopoulou M, Dercle L, Champiat S, Han SR, et al. A Radiomics Approach to Assess Tumour-Infiltrating CD8 Cells and Response to Anti-PD-1 or Anti-PD-L1 Immunotherapy: An Imaging Biomarker, Retrospective Multicohort Study. *Lancet Oncol* (2018) 19(9):1180–91. doi: 10.1016/S1470-2045(18)30413-3
151. Khosravi P, Kazemi E, Imielinski M, Elemento O, Hajirasouliha I. Deep Convolutional Neural Networks Enable Discrimination of Heterogeneous Digital Pathology Images. *EBioMedicine* (2018) 27:317–28. doi: 10.1016/j.ebiom.2017.12.026
152. Nahed BV, Curry WT, Martuza RL. Single-Cell RNA-Seq Highlights Intratumoral Heterogeneity in Primary Glioblastoma. *Sci (80- )* (2014) 344 (6190):1396–401. doi: 10.1126/science.1254257
153. Guo S, Jiang X, Mao B, Li Q-X. The Design, Analysis and Application of Mouse Clinical Trials in Oncology Drug Development. *BMC Cancer* (2019) 19(1):1–14. doi: 10.1186/s12885-019-5907-7
154. Strickland JC, Lile JA, Rush CR, Stoops WW. Comparing Exponential and Exponentiated Models of Drug Demand in Cocaine Users. *Exp Clin Psychopharmacol* (2016) 24(6):447–55. doi: 10.1037/pha0000096
155. Wishart DS, Knox C, Guo AC, Shrivastava S, Hassanali M, Stothard P, et al. DrugBank: A Comprehensive Resource for *In Silico* Drug Discovery and Exploration. *Nucleic Acids Res* (2006) 34(suppl_1):D668–72. doi: 10.1093/nar/gkj067
156. Augustyn A, Borromeo M, Wang T, Fujimoto J, Shao C, Dospoy PD, et al. ASCL1 Is a Lineage Oncogene Providing Therapeutic Targets for High-Grade Neuroendocrine Lung Cancers. *Proc Natl Acad Sci USA* (2014) 111 (41):14788–93. doi: 10.1073/pnas.1410419111
157. Han K, Jeng EE, Hess GT, Morgens DW, Li A, Bassik MC. Synergistic Drug Combinations for Cancer Identified in a CRISPR Screen for Pairwise Genetic Interactions. *Nat Biotechnol* (2017) 35(5):463–74. doi: 10.1038/nbt.3834
158. Fernández-Navarro P, López-Nieva P, Piñeiro-Yañez E, Carreño-Tarragona G, Martinez-López J, Sánchez Pérez R, et al. The Use of PanDrugs to Prioritize Anticancer Drug Treatments in a Case of T-ALL Based on Individual Genomic Data. *BMC Cancer* (2019) 19(1):1–10. doi: 10.1186/s12885-019-6209-9
159. Karimi MR, Karimi AH, Abolmaali S, Sadeghi M, Schmitz U. Prospects and Challenges of Cancer Systems Medicine: From Genes to Disease Networks. *Brief Bioinform* (2021), 1–31. doi: 10.1093/bib/bbab343
160. Powathil GG, Swat M, Chaplain MAJ. Systems Oncology: Towards Patient-Specific Treatment Regimes Informed by Multiscale Mathematical Modelling. *Semin Cancer Biol* (2015) 30:13–20. doi: 10.1016/j.semcancer.2014.02.003
161. Valladares-Ayerbes M, Haz-Conde M, Blanco-Calvo M. Systems Oncology: Toward the Clinical Application of Cancer Systems Biology. *Futur Oncol* (2015) 11(4):553–5. doi: 10.2217/fon.14.255
162. Anderson ARA, Rejniak KA, Gerlee P, Quaranta V. Microenvironment Driven Invasion: A Multiscale Multimodel Investigation. *J Math Biol* (2009) 58(4–5):579–624. doi: 10.1007/s00285-008-0210-2
163. Stolarska MA, Yangjin KIM, Othmer HG. Multi-Scale Models of Cell and Tissue Dynamics. *Philos Trans R Soc A Math Phys Eng Sci* (2009) 367 (1902):3525–53. doi: 10.1098/rsta.2009.0095
164. Silva A, Anderson A, Gatenby R. A Multiscale Model of the Bone Marrow and Hematopoiesis. *Math Biosci Eng* (2011) 8(2):643–58. doi: 10.3934/mbe.2011.8.643
165. Chaudhary SU, Shin S, Won J, Cho K, Member S. Multiscale Modeling of Tumorigenesis Induced by Mitochondrial Incapacitation in Cell Death. *IEEE Trans BioMed Eng* (2011) 58(2):3028–32. doi: 10.1109/TBME.2011.2159713
166. Szabó A, Merks RMH. Blood Vessel Tortuosity Selects Against Evolution of Aggressive Tumor Cells in Confined Tissue Environments: A Modeling Approach. *PloS Comput Biol* (2017) 13(7):1–32. doi: 10.1371/journal.pcbi.1005635
167. Kumar S, Das A, Sen S. Multicompartment Cell-Based Modeling of Confined Migration: Regulation by Cell Intrinsic and Extrinsic Factors. *Mol Biol Cell* (2018) 29(13):1599–610. doi: 10.1091/mbc.E17-05-0313
168. Unni P, Seshaiyer P. Mathematical Modeling, Analysis, and Simulation of Tumor Dynamics With Drug Interventions. *Comput and Math Methods Med* (2019) 2019:1–14. doi: 10.1155/2019/4079298
169. Leppert M, Dobbs M, Scambler P, O'Connell P, Nakamura Y, Stauffer D, et al. The Gene for Familial Polyposis Coli Maps to the Long Arm of Chromosome 5. *Science* (1987) 238(4832):1411–3. doi: 10.1126/science.3479843
170. Mehl LE. A Mathematical Computer Simulation Model for the Development of Colonic Polyps and Colon Cancer. *J Surg Oncol* (1991) 47(4):243–52. doi: 10.1002/jso.2930470409
171. Stratmann AT, Fecher D, Wangorsch G, Göttlich C, Walles T, Walles H, et al. Establishment of a Human 3D Lung Cancer Model Based on a Biological Tissue Matrix Combined With a Boolean *In Silico* Model. *Mol Oncol* (2014) 8(2):351–65. doi: 10.1016/j.molonc.2013.11.009
172. Greenspan HP. Models for the Growth of a Solid Tumor by Diffusion. *Stud Appl Math* (1972) 51(4):317–40. doi: 10.1002/sapm1972514317
173. Greenspan HP. On the Growth and Stability of Cell Cultures and Solid Tumors. *J Theor Biol* (1976) 56(1):229–42. doi: 10.1016/S0022-5193(76)80054-9
174. Chaplain MAJ. Avascular Growth, Angiogenesis and Vascular Growth in Solid Tumours: The Mathematical Modelling of the Stages of Tumour Development. *Math Comput Model* (1996) 23(6):47–87. doi: 10.1016/0895-7177(96)00019-2
175. Shackney SE, Smith CA, Miller BW, Burholt DR, Murtha K, Pollice AA, et al. Model for the Genetic Evolution of Human Solid Tumors. *Cancer Res* (1989) 49(12):3344–54.
176. Gerlee P, Nelander S. The Impact of Phenotypic Switching on Glioblastoma Growth and Invasion. *PloS Comput Biol* (2012) 8(6):e1002556. doi: 10.1371/journal.pcbi.1002556
177. Setty Y. *In-Silico* Models of Stem Cell and Developmental Systems. *Theor Biol Med Model* (2014) 11:1–12. doi: 10.1186/1742-4682-11-1
178. Wang Z, Bordas V, Sagotsky J, Deisboeck TS. Identifying Therapeutic Targets in a Combined EGFR–Tgfβr Signalling Cascade Using a Multiscale Agent-Based Cancer Model. *Math Med Biol J IMA* (2012) 29 (1):95–108. doi: 10.1093/imammb/dqq023
179. Wang Z, Bordas V, Deisboeck T. Identification of Critical Molecular Components in a Multiscale Cancer Model Based on the Integration of Monte Carlo, Resampling, and ANOVA. *Front Physiol* (2011) 2:35. doi: 10.3389/fphys.2011.00035
180. Margolin G, Petrykowska HM, Jameel N, Bell DW, Young AC, Elnitski L. Robust Detection of DNA Hypermethylation of ZNF154 as a Pan-Cancer Locus With *In Silico* Modeling for Blood-Based Diagnostic Development. *J Mol Diagn* (2016) 18(2):283–98. doi: 10.1016/j.jmoldx.2015.11.004
181. Jahangiri A, Amani J, Halabian R, Imani fooladi AA. *In Silico* Analyses of Staphylococcal Enterotoxin B as a DNA Vaccine for Cancer Therapy. *Int J Pept Res Ther* (2018) 24(1):131–42. doi: 10.1007/s10989-017-9595-3
182. Smith EAK, Henthorn NT, Warmenhoven JW, Ingram SP, Aitkenhead AH, Richardson JC, et al. *In Silico* Models of DNA Damage and Repair in Proton Treatment Planning: A Proof of Concept. *Sci Rep* (2019) 9(1):1–10. doi: 10.1038/s41598-019-56258-5

183. Huang E, Cheng SH, Dressman H, Pittman J, Tsou MH, Horng CF, et al. Gene Expression Predictors of Breast Cancer Outcomes. *Lancet* (2003) 361 (9369):1590–6. doi: 10.1016/S0140-6736(03)13308-9
184. Cheng F, Liu C, Lin CC, Zhao J, Jia P, Li WH, et al. A Gene Gravity Model for the Evolution of Cancer Genomes: A Study of 3,000 Cancer Genomes Across 9 Cancer Types. *PloS Comput Biol* (2015) 11(9):1–25. doi: 10.1371/journal.pcbi.1004497
185. Chen J-S, Hung W-S, Chan H-H, Tsai S-J, Sun HS. *In Silico* Identification of Oncogenic Potential of Fyn-Related Kinase in Hepatocellular Carcinoma. *Bioinformatics* (2013) 29(4):420–7. doi: 10.1093/bioinformatics/bts715
186. Agren R, Mardinoglu A, Asplund A, Kampf C, Uhlen M, Nielsen J. Identification of Anticancer Drugs for Hepatocellular Carcinoma Through Personalized Genome-Scale Metabolic Modeling. *Mol Syst Biol* (2014) 10 (3):721. doi: 10.1002/msb.145122
187. Béal J, Montagud A, Traynard P, Barillot E, Calzone L. Personalization of Logical Models With Multi-Omics Data Allows Clinical Stratification of Patients. *Front Physiol* (2019) 9:1965. doi: 10.3389/fphys.2018.01965
188. Béal J, Pantolini L, Noël V, Barillot E, Calzone L. Personalized Logical Models to Investigate Cancer Response to BRAF Treatments in Melanomas and Colorectal Cancers. *PloS Comput Biol* (2021) 17(1):e1007900. doi: 10.1371/journal.pcbi.1007900
189. Rodriguez J, Ren G, Day CR, Zhao K, Chow CC, Larson DR. Intrinsic Dynamics of a Human Gene Reveal the Basis of Expression Heterogeneity. *Cell* (2019) 176(1–2):213–226.e18. doi: 10.1016/j.cell.2018.11.026
190. Baloria U, Akhoon BA, Gupta SK, Sharma S, Verma V. *In Silico* Proteomic Characterization of Human Epidermal Growth Factor Receptor 2 (HER-2) for the Mapping of High Affinity Antigenic Determinants Against Breast Cancer. *Amino Acids* (2012) 42(4):1349–60. doi: 10.1007/s00726-010-0830-x
191. Akhoon BA, Slathia PS, Sharma P, Gupta SK, Verma V. *In Silico* Identification of Novel Protective VSG Antigens Expressed by Trypanosoma Brucei and an Effort for Designing a Highly Immunogenic DNA Vaccine Using IL-12 as Adjuvant. *Microb Pathog* (2011) 51(1–2):77–87. doi: 10.1016/j.micpath.2011.01.011
192. Fang J, Wu Z, Cai C, Wang Q, Tang Y, Cheng F. Quantitative and Systems Pharmacology. 1. *In Silico* Prediction of Drug–Target Interactions of Natural Products Enables New Targeted Cancer Therapy. *J Chem Inf Model* (2017) 57(11):2657–71. doi: 10.1021/acs.jcim.7b00216
193. Azevedo R, Silva AMN, Reis CA, Santos LL, Ferreira JA. *In Silico* Approaches for Unveiling Novel Glycobiomarkers in Cancer. *J Proteomics* (2018) 171:95–106. doi: 10.1016/j.jprot.2017.08.004
194. Lee SWL, Seager RJ, Litvak F, Spill F, Sieow JL, Leong PH, et al. Integrated *In Silico* and 3D *In Vitro* Model of Macrophage Migration in Response to Physical and Chemical Factors in the Tumor Microenvironment. *Integr Biol* (2020) 12(4):90–108. doi: 10.1093/intbio/zyaa007
195. Ma H, Sorokin A, Mazein A, Selkov A, Selkov E, Demin O, et al. The Edinburgh Human Metabolic Network Reconstruction and its Functional Analysis. *Mol Syst Biol* (2007) 3(1):135. doi: 10.1038/msb4100177
196. Folger O, Jerby L, Frezza C, Gottlieb E, Ruppin E, Shlomi T. Predicting Selective Drug Targets in Cancer Through Metabolic Networks. *Mol Syst Biol* (2011) 7(1):501. doi: 10.1038/msb.2011.35
197. Aurich MK, Paglia G, Rolfsson Ó, Hrafnsdóttir S, Magnúsdóttir M, Stefaniak MM, et al. Prediction of Intracellular Metabolic States From Extracellular Metabolomic Data. *Metabolomics* (2015) 11(3):603–19. doi: 10.1007/s11306-014-0721-3
198. Yurkovich JT, Yang L, Palsson BO. Biomarkers Are Used to Predict Quantitative Metabolite Concentration Profiles in Human Red Blood Cells. *PloS Comput Biol* (2017) 13(3):e1005424. doi: 10.1371/journal.pcbi.1005424
199. Alakwaa FM, Chaudhary K, Garmire LX. Deep Learning Accurately Predicts Estrogen Receptor Status in Breast Cancer Metabolomics Data. *J Proteome Res* (2018) 17(1):337–47. doi: 10.1021/acs.jproteome.7b00595
200. Azadi M, Alemi F, Sadeghi S, Mohammadi M, Rahimi NA, Mirzaie S, et al. An Integrative *In Silico* Mathematical Modelling Study of the Anti-Cancer Effect of Clove Extract (Syzygium Aromaticum) Combined With *In Vitro* Metabolomics Study Using 1HNMR Spectroscopy. *Iran J Biotechnol* (2020) 18(3):45–54. doi: 10.30498/ijb.2020.141102.2336
201. Balding D, McElwain DL. A Mathematical Model of Tumour-Induced Capillary Growth. *J Theor Biol* (1985) 114(1):53–73. doi: 10.1016/s0022-5193(85)80255-1
202. Anderson ARA. A Hybrid Mathematical Model of Solid Tumour Invasion: The Importance of Cell Adhesion. *Math Med Biol A J IMA* (2005) 22(2):163–86. doi: 10.1093/imammb/dqi005
203. McDougall SR, Anderson ARA, Chaplain MAJ, Sherratt JA. Mathematical Modelling of Flow Through Vascular Networks: Implications for Tumour-Induced Angiogenesis and Chemotherapy Strategies. *Bull Math Biol* (2002) 64(4):673–702. doi: 10.1006/bulm.2002.0293
204. Anderson ARA, Chaplain MAJ. Continuous and Discrete Mathematical Models of Tumor-Induced Angiogenesis. *Bull Math Biol* (1998) 60(5):857–99. doi: 10.1006/bulm.1998.0042
205. Nakazawa K, Kurishima K, Tamura T, Kagohashi K, Ishikawa H, Satoh H, et al. Specific Organ Metastases and Survival in Small Cell Lung Cancer. *Oncol Lett* (2012) 4(4):617–20. doi: 10.3892/ol.2012.792
206. Cortesi M, Liverani C, Mercatali L, Ibrahim T, Giordano E. An *In-Silico* Study of Cancer Cell Survival and Spatial Distribution Within a 3D Microenvironment. *Sci Rep* (2020) 10(1):1–14. doi: 10.1038/s41598-020-69862-7
207. Aubert M, Badoual M, Christov C, Grammaticos B. A Model for Glioma Cell Migration on Collagen and Astrocytes. *J R Soc Interface* (2008) 5(18):75–83. doi: 10.1098/rsif.2007.1070
208. Harris LA, Beik S, Ozawa PMM, Jimenez L, Weaver AM. Modeling Heterogeneous Tumor Growth Dynamics and Cell–Cell Interactions at Single-Cell and Cell-Population Resolution. *Curr Opin Syst Biol* (2019) 17:24–34. doi: 10.1016/j.coisb.2019.09.005
209. Swanson KR, Alvord ECJ, Murray JD. A Quantitative Model for Differential Motility of Gliomas in Grey and White Matter. *Cell Prolif* (2000) 33(5):317–29. doi: 10.1046/j.1365-2184.2000.00177.x
210. Zhang L, Athale CA, Deisboeck TS. Development of a Three-Dimensional Multiscale Agent-Based Tumor Model: Simulating Gene-Protein Interaction Profiles, Cell Phenotypes and Multicellular Patterns in Brain Cancer. *J Theor Biol* (2007) 244(1):96–107. doi: 10.1016/j.jtbi.2006.06.034
211. Perfahl H, Byrne HM, Chen T, Estrella V, Alarcón T, Lapin A, et al. Multiscale Modelling of Vascular Tumour Growth in 3D: The Roles of Domain Size and Boundary Conditions. *PloS One* (2011) 6(4):e14790. doi: 10.1371/journal.pone.0014790
212. Anderson ARA, Rejniak KA, Gerlee P, Quaranta V. Modelling of Cancer Growth, Evolution and Invasion: Bridging Scales and Models. *Math Model Nat Phenom* (2007) 2(3):1–29. doi: 10.1051/mmnp:2007001
213. Chaudhary SU, Sormark JE, Won J-K, Shin SY, Cho K-H. Multi-Scale Modeling and Game-Theoretic Analysis of Mitochondrial Process Elucidates the Hidden Mechanism of Warburg Effect in Tumorigenesis. In: *11th International Conference on Systems Biology (Icsb2010)* (2010).
214. Vavourakis V, Wijeratne PA, Shipley R, Loizidou M, Stylianopoulos T, Hawkes DJ. A Validated Multiscale *in-Silico* Model for Mechano-Sensitive Tumour Angiogenesis and Growth. *PloS Comput Biol* (2017) 13(1): e1005259. doi: 10.1371/journal.pcbi.1005259
215. Norton K-A, Wallace T, Pandey NB, Popel AS. An Agent-Based Model of Triple-Negative Breast Cancer: The Interplay Between Chemokine Receptor CCR5 Expression, Cancer Stem Cells, and Hypoxia. *BMC Syst Biol* (2017) 11 (1):1–15. doi: 10.1186/s12918-017-0445-x
216. Norton KA, Gong C, Jamalian S, Popel AS. Multiscale Agent-Based and Hybrid Modeling of the Tumor Immune Microenvironment. *Processes* (2019) 7(1):1–23. doi: 10.3390/pr7010037
217. Karolak A, Poonja S, Rejniak KA. Morphophenotypic Classification of Tumor Organoids as an Indicator of Drug Exposure and Penetration Potential. *PloS Comput Biol* (2019) 15(7):e1007214. doi: 10.1371/journal.pcbi.1007214
218. Kenny PA, Lee GY, Myers CA, Neve RM, Semeiks JR, Spellman PT, et al. The Morphologies of Breast Cancer Cell Lines in Three-Dimensional Assays Correlate With Their Profiles of Gene Expression. *Mol Oncol* (2007) 1(1):84–96. doi: 10.1016/j.molonc.2007.02.004
219. Berrouet C, Dorilas N, Rejniak KA, Tuncer N. Comparison of Drug Inhibitory Effects (IC50) in Monolayer and Spheroid Cultures. *Bull Math Biol* (2020) 82(6):68. doi: 10.1007/s11538-020-00746-7
220. Stamatakos GS, Graf N, Radhakrishnan R. Multiscale Cancer Modeling and *In Silico* Oncology: Emerging Computational Frontiers in Basic and

Translational Cancer Research. *J Bioeng BioMed Sci* (2013) 3(2):1–6. doi: 10.4172/2155-9538.1000e114
221. Nagaraj SH. Reverter A. A Boolean-Based Systems Biology Approach to Predict Novel Genes Associated With Cancer: Application to Colorectal Cancer. *BMC Syst Biol* (2011) 5(1):1–15. doi: 10.1186/1752-0509-5-35
222. Fumiã HF, Martins ML. Boolean Network Model for Cancer Pathways: Predicting Carcinogenesis and Targeted Therapy Outcomes. *PloS One* (2013) 8(7):e69008. doi: 10.1371/journal.pone.0069008
223. Yang L, Meng Y, Bao C, Liu W, Ma C, Li A, et al. Robustness and Backbone Motif of a Cancer Network Regulated by miR-17-92 Cluster During the G1/S Transition. *PloS One* (2013) 8(3):e57009. doi: 10.1371/journal.pone.0057009
224. der Heyde SV, Bender C, Henjes F, Sonntag J, Korf U, Beißbarth T. Boolean ErbB Network Reconstructions and Perturbation Simulations Reveal Individual Drug Response in Different Breast Cancer Cell Lines. *BMC Syst Biol* (2014) 8(1):1–22. doi: 10.1186/1752-0509-8-75
225. Gondal MN, Butt RN, Shah OS, Sultan MU, Mustafa G, Nasir Z, et al. A Personalized Therapeutics Approach Using an *In Silico* Drosophila Patient Model Reveals Optimal Chemo- and Targeted Therapy Combinations for Colorectal Cancer. *Front Oncol* (2021) 11:692592. doi: 10.3389/fonc.2021.692592
226. Klamt S, Saez-Rodriguez J, Gilles ED. Structural and Functional Analysis of Cellular Networks With CellNetAnalyzer. *BMC Syst Biol* (2007) 1(1):1–3. doi: 10.1186/1752-0509-1-2
227. Kachalo S, Zhang R, Sontag E, Albert R, DasGupta B. NET-SYNTHESIS: A Software for Synthesis, Inference and Simplification of Signal Transduction Networks. *Bioinformatics* (2008) 24(2):293–5. doi: 10.1093/bioinformatics/btm571
228. Mendes P. GEPASI: A Software Package for Modelling the Dynamics, Steady States and Control of Biochemical and Other Systems. *Bioinformatics* (1993) 9(5):563–71. doi: 10.1093/bioinformatics/9.5.563
229. Starruß J, De Back W, Brusch L, Deutsch A. Morpheus: A User-Friendly Modeling Environment for Multiscale and Multicellular Systems Biology. *Bioinformatics* (2014) 30(9):1331–2. doi: 10.1093/bioinformatics/btt772
230. Tomita M, Hashimoto K, Takahashi K, Shimizu TS, Matsuzaki Y, Miyoshi F, et al. E-CELL: Software Environment for Whole-Cell Simulation. *Bioinformatics* (1999) 15(1):72–84. doi: 10.1093/bioinformatics/15.1.72
231. Eissing T. A Computational Systems Biology Software Platform for Multiscale Modeling and Simulation: Integrating Whole-Body Physiology, Disease Biology, and Molecular Reaction Networks. *Front Physiol* (2011) 2:4. doi: 10.3389/fphys.2011.00004
232. Kauffman SA. Metabolic Stability and Epigenesis in Randomly Constructed Genetic Nets. *J Theor Biol* (1969) 22(3):437–67. doi: 10.1016/0022-5193(69)90015-0
233. Glass L, Kauffman SA. The Logical Analysis of Continuous, non-Linear Biochemical Control Networks. *J Theor Biol* (1973) 39(1):103–29. doi: 10.1016/0022-5193(73)90208-7
234. Wegner K, Knabe J, Robinson M, Egri-Nagy A, Schilstra M. The Netbuilder' Project: Development of a Tool for Constructing, Simulating, Evolving, and Analysing Complex Regulatory Networks. *BMC Syst Biol* (2007) 1(1):1–2. doi: 10.1186/1752-0509-1-S1-P72
235. Albert I, Thakar J, Li S, Zhang R, Albert R. Boolean Network Simulations for Life Scientists. *Source Code Biol Med* (2008) 3(1):1–8. doi: 10.1186/1751-0473-3-16
236. Zheng J, Zhang D, Przytycki PF, Zielinski R, Capala J, Przytycka TM. Simboolnet-A Cytoscape Plugin for Dynamic Simulation of Signaling Networks. *Bioinformatics* (2009) 26(1):141–2. doi: 10.1093/bioinformatics/btp617
237. Klamt S, Stelling J, Ginkel M, Gilles ED. FluxAnalyzer: Exploring Structure, Pathways, and Flux Distributions in Metabolic Networks on Interactive Flux Maps. *Bioinformatics* (2003) 19(2):261–9. doi: 10.1093/bioinformatics/19.2.261
238. Tian K, Rajendran R, Doddananjaiah M, Krstic-Demonacos M, Schwartz J-M. Dynamics of DNA Damage Induced Pathways to Cancer. *PloS One* (2013) 8(9):e72303. doi: 10.1371/journal.pone.0072303
239. Hetmanski JHR, Zindy E, Schwartz J-M. Caswell PT. A MAPK-Driven Feedback Loop Suppresses Rac Activity to Promote RhoA-Driven Cancer Cell Invasion. *PloS Comput Biol* (2016) 12(5):e1004909. doi: 10.1371/journal.pcbi.1004909
240. Saadatpour A, Wang R-S, Liao A, Liu X, Loughran TP, Albert I, et al. Dynamical and Structural Analysis of a T Cell Survival Network Identifies Novel Candidate Therapeutic Targets for Large Granular Lymphocyte Leukemia. *PloS Comput Biol* (2011) 7(11):e1002267. doi: 10.1371/journal.pcbi.1002267
241. Steinway SN, Zañudo JGT, Ding W, Rountree CB, Feith DJ, Loughran TPJ, et al. Network Modeling of Tgfβ Signaling in Hepatocellular Carcinoma Epithelial-to-Mesenchymal Transition Reveals Joint Sonic Hedgehog and Wnt Pathway Activation. *Cancer Res* (2014) 74(21):5963–77. doi: 10.1158/0008-5472.CAN-14-0225
242. Naldi A, Berenguier D, Fauré A, Lopez F, Thieffry D, Chaouiya C. Logical Modelling of Regulatory Networks With GINsim 2.3. *Biosystems* (2009) 97(2):134–9. doi: 10.1016/j.biosystems.2009.04.008
243. Flobak Å, Baudot A, Remy E, Thommesen L, Thieffry D, Kuiper M, et al. Discovery of Drug Synergies in Gastric Cancer Cells Predicted by Logical Modeling. *PloS Comput Biol* (2015) 11(8):e1004426. doi: 10.1371/journal.pcbi.1004426
244. Remy E, Rebouissou S, Chaouiya C, Zinovyev A, Radvanyi F, Calzone L. A Modeling Approach to Explain Mutually Exclusive and Co-Occurring Genetic Alterations in Bladder Tumorigenesis. *Cancer Res* (2015) 75(19):4042–52. doi: 10.1158/0008-5472.CAN-15-0602
245. Stoll G, Caron B, Viara E, Dugourd A, Zinovyev A, Naldi A, et al. MaBoSS 2.0: An Environment for Stochastic Boolean Modeling. *Bioinformatics* (2017) 33(14):2226–8. doi: 10.1093/bioinformatics/btx123
246. Kondratova M, Barillot E, Zinovyev A, Calzone L. Modelling of Immune Checkpoint Network Explains Synergistic Effects of Combined Immune Checkpoint Inhibitor Therapy and the Impact of Cytokines in Patient Response. *Cancers (Basel)* (2020) 12(12):1–19. doi: 10.3390/cancers12123600
247. Müssel C, Hopfensitz M, Kestler HA. BoolNet—an R Package for Generation, Reconstruction and Analysis of Boolean Networks. *Bioinformatics* (2010) 26(10):1378–80. doi: 10.1093/bioinformatics/btq124
248. Steinway SN, Biggs MB, Loughran TPJr., Papin JA, Albert R. Inference of Network Dynamics and Metabolic Interactions in the Gut Microbiome. *PloS Comput Biol* (2015) 11(6):e1004338. doi: 10.1371/journal.pcbi.1004338
249. Cohen DPA, Martignetti L, Robine S, Barillot E, Zinovyev A, Calzone L. Mathematical Modelling of Molecular Pathways Enabling Tumour Cell Invasion and Migration. *PloS Comput Biol* (2015) 11(11):e1004571. doi: 10.1371/journal.pcbi.1004571
250. Shah OS, Chaudhary MFA, Awan HA, Fatima F, Arshad Z, Amina B, et al. ATLANTIS - Attractor Landscape Analysis Toolbox for Cell Fate Discovery and Reprogramming. *Sci Rep* (2018) 8(1):3554. doi: 10.1038/s41598-018-22031-3
251. Han B, Wang J. Quantifying Robustness and Dissipation Cost of Yeast Cell Cycle Network: The Funneled Energy Landscape Perspectives. *Biophys J* (2007) 92(11):3755–63. doi: 10.1529/biophysj.106.094821
252. Choi M, Shi J, Jung SH, Chen X, Cho K-H. Attractor Landscape Analysis Reveals Feedback Loops in the P53 Network That Control the Cellular Response to DNA Damage. *Sci Signal* (2012) 5(251):1–14. doi: 10.1126/scisignal.2003363
253. Cho S-H, Park S-M, Lee H-S, Lee H-Y, Cho K-H. Attractor Landscape Analysis of Colorectal Tumorigenesis and its Reversion. *BMC Syst Biol* (2016) 10(1):1–13. doi: 10.1186/s12918-016-0341-9
254. Wittmann DM, Krumsiek J, Saez-Rodriguez J, Lauffenburger DA, Klamt S, Theis FJ. Transforming Boolean Models to Continuous Models: Methodology and Application to T-Cell Receptor Signaling. *BMC Syst Biol* (2009) 3(1):1–21. doi: 10.1186/1752-0509-3-98
255. Ricci G, De Maria F, Antonini G, Turella P, Bullo A, Stella L, et al. 7-Nitro-2,1,3-Benzoxadiazole Derivatives, a New Class of Suicide Inhibitors for Glutathione S-Transferases: Mechanism of Action of Potential Anticancer Drugs. *J Biol Chem* (2005) 280(28):26397–405. doi: 10.1074/jbc.M503295200
256. Marín-Hernández A, Gallardo-Pérez JC, Rodríguez-Enríquez S, Encalada R, Moreno-Sánchez R, Saavedra E. Modeling Cancer Glycolysis. *Biochim Biophys Acta - Bioenerg* (2011) 1807(6):755–67. doi: 10.1016/j.bbabio.2010.11.006

257. Hoops S, Sahle S, Gauges R, Lee C, Pahle J, Simus N, et al. COPASI—A COmplex PAthway SImulator. *Bioinformatics* (2006) 22(24):3067–74. doi: 10.1093/bioinformatics/btl485
258. Orton RJ, Adriaens ME, Gormand A, Sturm OE, Kolch W, Gilbert DR. Computational Modelling of Cancerous Mutations in the EGFR/ERK Signalling Pathway. *BMC Syst Biol* (2009) 3(1):1–17. doi: 10.1186/1752-0509-3-100
259. Dalle Pezze P, Nelson G, Otten EG, Korolchuk VI, Kirkwood TBL, von Zglinicki T, et al. Dynamic Modelling of Pathways to Cellular Senescence Reveals Strategies for Targeted Interventions. *PloS Comput Biol* (2014) 10(8): e1003728. doi: 10.1371/journal.pcbi.1003728
260. Funahashi A, Morohashi M, Kitano H, Tanimura N. CellDesigner: A Process Diagram Editor for Gene-Regulatory and Biochemical Networks. *Biosilico* (2003) 1(5):159–62. doi: 10.1016/S1478-5382(03)02370-9
261. Sauro HM, Hucka M, Finney A, Wellock C, Bolouri H, Doyle J, et al. Next Generation Simulation Tools: The Systems Biology Workbench and BioSPICE Integration. *OMICS* (2003) 7(4):355–72. doi: 10.1089/153623103322637670
262. Calzone L, Gelay A, Zinovyev A, Radvanyi F, Barillot E. A Comprehensive Modular Map of Molecular Interactions in RB/E2F Pathway. *Mol Syst Biol* (2008) 4(1):0174. doi: 10.1038/msb.2008.7
263. Grieco L, Calzone L, Bernard-Pierrot I, Radvanyi F, Kahn-Perlès B, Thieffry D. Integrative Modelling of the Influence of MAPK Network on Cancer Cell Fate Decision. *PloS Comput Biol* (2013) 9(10):e1003286. doi: 10.1371/journal.pcbi.1003286
264. Ghaffarizadeh A, Friedman SH, MacKlin P. BioFVM: An Efficient, Parallelized Diffusive Transport Solver for 3-D Biological Simulations. *Bioinformatics* (2016) 32(8):1256–8. doi: 10.1093/bioinformatics/btv730
265. Felix TF, Lopez Lapa RM, de Carvalho M, Bertoni N, Tokar T, Oliveira RA, et al. MicroRNA Modulated Networks of Adaptive and Innate Immune Response in Pancreatic Ductal Adenocarcinoma. *PloS One* (2019) 14(5): e0217421. doi: 10.1371/journal.pone.0217421
266. Meyer K, Ostrenko O, Bourantas G, Morales-Navarrete H, Porat-Shliom N, Segovia-Miranda F, et al. A Predictive 3D Multi-Scale Model of Biliary Fluid Dynamics in the Liver Lobule. *Cell Syst* (2017) 4(3):277–290.e9. doi: 10.1016/j.cels.2017.02.008
267. Ozik J, Collier N, Heiland R, An G, Macklin P. Learning-Accelerated Discovery of Immune-Tumour Interactions. *Mol Syst Des Eng* (2019) 4 (4):747–60. doi: 10.1039/c9me00036d
268. Ozik J, Collier N, Wozniak JM, Macal C, Cockrell C, Friedman SH, et al. High-Throughput Cancer Hypothesis Testing With an Integrated PhysiCell-EMEWS Workflow. *BMC Bioinf* (2018) 19(18):81–97. doi: 10.1186/s12859-018-2510-x
269. Wang Y, Brodin E, Nishii K, Frieboes HB, Mumenthaler SM, Sparks JL, et al. Impact of Tumor-Parenchyma Biomechanics on Liver Metastatic Progression: A Multi-Model Approach. *Sci Rep* (2021) 11(1):1–20. doi: 10.1038/s41598-020-78780-7
270. Cortesi M, Liverani C, Mercatali L, Ibrahim T, Giordano E. Development and Validation of an *In-Silico* Tool for the Study of Therapeutic Agents in 3D Cell Cultures. *Comput Biol Med* (2021) 130:1–9. doi: 10.1016/j.compbiomed.2021.104211
271. Edwards JS, Ibarra RU, Palsson BO. *In Silico* Predictions of Escherichia Coli Metabolic Capabilities Are Consistent With Experimental Data. *Nat Biotechnol* (2001) 19(2):125–30. doi: 10.1038/84379
272. Orton RJ, Sturm OE, Vyshemirsky V, Calder M, Gilbert DR, Kolch W. Computational Modelling of the Receptor-Tyrosine-Kinase-Activated MAPK Pathway. *Biochem J* (2005) 392(2):249–61. doi: 10.1042/BJ20050908
273. Loew LM, Schaff JC. The Virtual Cell: A Software Environment for Computational Cell Biology. *Trends Biotechnol* (2001) 19(10):401–6. doi: 10.1016/S0167-7799(01)01740-1
274. Neves SR, Tsokas P, Sarkar A, Grace EA, Rangamani P, Taubenfeld SM, et al. Cell Shape and Negative Links in Regulatory Motifs Together Control Spatial Information Flow in Signaling Networks. *Cell* (2008) 133(4):666–80. doi: 10.1016/j.cell.2008.04.025
275. Calebiro D, Nikolaev VO, Gagliani MC, de Filippis T, Dees C, Tacchetti C, et al. Persistent cAMP-Signals Triggered by Internalized G-Protein–Coupled Receptors. *PloS Biol* (2009) 7(8):e1000172. doi: 10.1371/journal.pbio.1000172
276. Chandran D, Bergmann FT, Sauro HM. TinkerCell: Modular CAD Tool for Synthetic Biology. *J Biol Eng* (2009) 3(1):1–17. doi: 10.1186/1754-1611-3-19
277. Renicke C, Schuster D, Usherenko S, Essen L-O, Taxis C. A LOV2 Domain-Based Optogenetic Tool to Control Protein Degradation and Cellular Function. *Chem Biol* (2013) 20(4):619–26. doi: 10.1016/j.chembiol.2013.03.005
278. Chandran D, Bergmann FT, Sauro HM. Computer-Aided Design of Biological Circuits Using TinkerCell. *Bioeng Bugs* (2010) 1(4):276–83. doi: 10.4161/bbug.1.4.12506
279. Izaguirre JA, Chaturvedi R, Huang C, Cickovski T, Coffland J, Thomas G, et al. CompuCell, a Multi-Model Framework for Simulation of Morphogenesis. *Bioinformatics* (2004) 20(7):1129–37. doi: 10.1093/bioinformatics/bth050
280. Mirams GR, Arthurs CJ, Bernabeu MO, Bordas R, Cooper J, Corrias A, et al. Chaste: An Open Source C++ Library for Computational Physiology and Biology. *PloS Comput Biol* (2013) 9(3):1–8. doi: 10.1371/journal.pcbi.1002970
281. Chaudhary SU, Shin S-Y, Lee D, Song J-H, Cho K-H. ELECANS–an Integrated Model Development Environment for Multiscale Cancer Systems Biology. *Bioinformatics* (2013) 29(7):957–9. doi: 10.1093/bioinformatics/btt063
282. North MJ, Collier NT, Ozik J, Tatara ER, Macal CM, Bragen M, et al. Complex Adaptive Systems Modeling With Repast Simphony. *Complex Adapt Syst Model* (2013) 1(1):1–26. doi: 10.1186/2194-3206-1-3
283. Folcik VA, An GC, Orosz CG. The Basic Immune Simulator: An Agent-Based Model to Study the Interactions Between Innate and Adaptive Immunity. *Theor Biol Med Model* (2007) 4(1):1–18. doi: 10.1186/1742-4682-4-39
284. Mehdizadeh H, Sumo S, Bayrak ES, Brey EM, Cinar A. Three-Dimensional Modeling of Angiogenesis in Porous Biomaterial Scaffolds. *Biomaterials* (2013) 34(12):2875–87. doi: 10.1016/j.biomaterials.2012.12.047
285. Mahoney AW, Podgorski GJ, Flann NS. Multiobjective Optimization Based-Approach for Discovering Novel Cancer Therapies. *IEEE/ACM Trans Comput Biol Bioinforma* (2012) 9(1):169–84. doi: 10.1109/TCBB.2010.39
286. Cho K-H, Chaudhary SU, Lee D *Biosimulation Method and Computing Device With High Expandability*. Korea Patent No. 10-2013-0033839. Korea: Korea Patent Office (2013).
287. Cho KH, Chaudhary SU, Lee D *Biosimulation Method and Computing Device Using Compiler Embedded There Within*. Korea Patent Office; 10-2013–0033837. South Korea: Korea Patent Office (2013).
288. Ghaffarizadeh A, Heiland R, Friedman SH, Mumenthaler SM, Macklin P. PhysiCell: An Open Source Physics-Based Cell Simulator for 3-D Multicellular Systems. *PloS Comput Biol* (2018) 14(2):e1005991. doi: 10.1371/journal.pcbi.1005991
289. Letort G, Montagud A, Stoll G, Heiland R, Barillot E, MacKlin P, et al. PhysiBoSS: A Multi-Scale Agent-Based Modelling Framework Integrating Physical Dimension and Cell Signalling. *Bioinformatics* (2019) 35(7):1188–96. doi: 10.1093/bioinformatics/bty766
290. Colin A, Letort G, Razin N, Almonacid M, Ahmed W, Betz T, et al. Active Diffusion in Oocytes Nonspecifically Centers Large Objects During Prophase I and Meiosis I. *J Cell Biol* (2020) 219(3):1–21. doi: 10.1083/jcb.201908195
291. Getz M, Wang Y, An G, Becker A, Cockrell C, Collier N. Rapid Community-Driven Development of a SARS- CoV-2 Tissue Simulator. *bioRxiv* (2020), 1–55. doi: 10.1101/2020.04.02.019075
292. Gondal MN, Sultan MU, Arif A, Rehman A, Awan HA, Arshad Z, et al. TISON: A Next-Generation Multi-Scale Modeling Theatre for *In Silico* Systems Oncology. *bioRxiv* (2021). doi: 10.1101/2021.05.04.442539
293. Martin L, Anguita A, Graf N, Tsiknakis M, Brochhausen M, Rüping S, et al. ACGT: Advancing Clinico-Genomic Trials on Cancer–Four Years of Experience. *Stud Heal Technol Inf* (2011) 169:734–8. doi: 10.3233/978-1-60750-806-9-734
294. Marias K, Sakkalis V, Roniotis A, Farmaki C, Stamatakos G, Dionysiou D, et al. Clinically Oriented Translational Cancer Multilevel Modeling: The ContraCancrum Project. *World Congress Medical Physics Biomed Eng* (2009) 2124–7. doi: 10.1007/978-3-642-03882-2_564

295. Rossi S, Christ-Neumann M, Rüping S, Buffa F, Wegener D, McVie G, et al. P-Medicine: From Data Sharing and Integration *via* VPH Models to Personalized Medicine. *Ecancermedicalscience* (2011) 5:1–6. doi: 10.3332/ecancer.2011.218
296. Johnson D, McKeever S, Stamatakos G, Dionysiou D, Graf N, Sakkalis V, et al. Dealing With Diversity in Computational Cancer Modeling. *Cancer Inform* (2013) 12:1–10. doi: 10.4137/CIN.S11583
297. Stamatakos G, Graf N. Computational Horizons in Cancer (CHIC). *Clin Ther* (2017) 39(8):e107–8. doi: 10.1016/j.clinthera.2017.05.333
298. Durbecq V, Paesmans M, Cardoso F, Desmedt C, Di Leo A, Chan S, et al. Topoisomerase-Iiα Expression as a Predictive Marker in a Population of Advanced Breast Cancer Patients Randomly Treated Either With Single-Agent Doxorubicin or Single-Agent Docetaxel. *Mol Cancer Ther* (2004) 3 (10):1207–14.
299. Graf N, Hoppe A, Georgiadi E, Belleman R, Desmedt C, Dionysiou D, et al. '*In Silico*' Oncology for Clinical Decision Making in the Context of Nephroblastoma. *Klin Paediatr* (2009) 221(03):141–9. doi: 10.1055/s-0029-1216368
300. Zasada SJ, Wang T, Haidar A, Liu E, Graf N, Clapworthy G, et al. IMENSE: An E-Infrastructure Environment for Patient Specific Multiscale Data Integration, Modelling and Clinical Treatment. *J Comput Sci* (2012) 3 (5):314–27. doi: 10.1016/j.jocs.2011.07.001
301. Marias K, Dionysiou D, Sakkalis V, Graf N, Bohle RM, Coveney PV, et al. Clinically Driven Design of Multi-Scale Cancer Models: The ContraCancrum Project Paradigm. *Interface Focus* (2011) 1(3):450–61. doi: 10.1098/rsfs.2010.0037
302. Li XL, Oduola WO, Qian L, Dougherty ER. Integrating Multiscale Modeling With Drug Effects for Cancer Treatment. *Cancer Inform* (2015) 14(Suppl 5):21–31. doi: 10.4137/CIN.S30797
303. Stamatakos GS, Georgiadi EC, Graf N, Kolokotroni EA, Dionysiou DD. Exploiting Clinical Trial Data Drastically Narrows the Window of Possible Solutions to the Problem of Clinical Adaptation of a Multiscale Cancer Model. *PloS One* (2011) 6(3):e17594. doi: 10.1371/journal.pone.0017594
304. Wan S, Coveney PV. Rapid and Accurate Ranking of Binding Affinities of Epidermal Growth Factor Receptor Sequences With Selected Lung Cancer Drugs. *J R Soc Interface* (2011) 8(61):1114–27. doi: 10.1098/rsif.2010.0609
305. Roniotis A, Panourgias K, Ekaterinaris J, Marias K, Sakkalis V. Approximating the Diffusion–Reaction Equation for Developing Glioma Models for the ContraCancrum Project: A Showcase. In: *4th Int Adv Res Work Silico Oncol Cancer Investig (4th IARWISOCI) – ContraCancrum Work*. p. 80–2.
306. Folarin AA, Stamatakos GS. Molecular Personalization of Cancer Treatment *via* a Multiscale Simulation Model of Tumor Response to Therapy. The Paradigm of Glioblastoma Treated With Temozolomide. In: *4th Int Adv Res Work Silico Oncol Cancer Investig* (2010). p. 23–5.
307. Giatili SG, Uzunoglu NK, Stamatakos GS. An Explicit Boundary Condition Treatment of a Diffusion–Based Glioblastoma Tumor Growth Model. *4th Int Adv Res Work Silico Oncol Cancer Investig (4th IARWISOCI) – ContraCancrum Work* (2010), 86–8.
308. Wang Z, Deisboeck TS. Application of ANOVA-Based Global Sensitivity Analysis to a Multiscale Cancer Model. In: *4th Int Adv Res Work Silico Oncol Cancer Investig (4th IARWISOCI) – ContraCancrum Work*. p. 27–9.
309. Schera F, Weiler G, Neri E, Kiefer S, Graf N. The P-Medicine Portal—A Collaboration Platform for Research in Personalised Medicine. *Ecancermedicalscience* (2014) 8:1–18. doi: 10.3332/ecancer.2014.398
310. Georgiadi EC, Dionysiou DD, Graf N, Stamatakos GS. Towards *In Silico* Oncology: Adapting a Four Dimensional Nephroblastoma Treatment Model to a Clinical Trial Case Based on Multi-Method Sensitivity Analysis. *Comput Biol Med* (2012) 42(11):1064–78. doi: 10.1016/j.compbiomed.2012.08.008
311. Blazewicz M, Georgiadi EC, Pukacki J, Stamatakos GS. Development of the P-Medicine Oncosimulator as a Parallel Treatment Support System. In: *6th Int Adv Res Work Silico Oncol Cancer Investig - CHIC Proj Work*. Athens, Greece: Proceedings of the 2014 6th International Advanced Research Workshop on *In Silico* Oncology and Cancer Investigation - The CHIC Project Workshop (IARWISOCI) (2014). p. 1–5. doi: 10.1109/IARWISOCI.2014.7034641
312. Argyri KD, Dionysiou DD, Misichroni FD, Stamatakos GS. Numerical Simulation of Vascular Tumour Growth Under Antiangiogenic Treatment: Addressing the Paradigm of Single-Agent Bevacizumab Therapy With the Use of Experimental Data. *Biol Direct* (2016) 11(1):1–31. doi: 10.1186/s13062-016-0114-9
313. Stamatakos G, Dionysiou D, Lunzer A, Belleman R, Kolokotroni E, Georgiadi E, et al. The Technologically Integrated Oncosimulator: Combining Multiscale Cancer Modeling With Information Technology in the *In Silico* Oncology Context. *IEEE J BioMed Heal Informatics*. Athens, Greece: The TUMOR Project Workshop (IARWISOCI) (2014) 18(3):840–54. doi: 10.1109/JBHI.2013.2284276
314. Ouzounoglou EN, Dionysiou DD, Stanulla M, Stamatakos GS. Towards Patient Personalization of an Acute Lymphoblastic Leukemia Model During the Oral Administration of Prednisone in Children: Initiating the ALL Oncosimulator. In: *5th Int Adv Res Work Silico Oncol Cancer Investig* (2012). p. 1–4.
315. Kolokotroni E, Ouzounoglou E, Systems C, Stanulla M, Dionysiou DD, Systems C. *In Silico* Oncology: Developing and Clinically Adapting the Acute Lymphoblastic Leukemia (ALL) Oncosimulator by Exploiting Pathway Based Gene Expression Analysis in the Context of the ALL-BFM 2000 Clinical Study. *Virtual Physiol Hum Conf* (2015). doi: 10.13140/RG.2.1.1430.3123
316. Ouzounoglou E, Kolokotroni E, Stanulla M, Stamatakos GS. A Study on the Predictability of Acute Lymphoblastic Leukaemia Response to Treatment Using a Hybrid Oncosimulator. *Interface Focus* (2018) 8(1):1–14. doi: 10.1098/rsfs.2016.0163
317. Bucur A, van Leeuwen J, Christodoulou N, Sigdel K, Argyri K, Koumakis L, et al. Workflow-Driven Clinical Decision Support for Personalized Oncology. *BMC Med Inform Decis Mak* (2016) 16(2):151–62. doi: 10.1186/s12911-016-0314-3
318. Deisboeck TS, Zhang L, Martin S. Advancing Cancer Systems Biology: Introducing the Center for the Development of a Virtual Tumor, CViT. *Cancer Inform* (2007) 5:1–8. doi: 10.1177/117693510700500001
319. Hedley WJ, Nelson MR, Bellivant DP, Nielsen PF. A Short Introduction to CellML. *Philos Trans R Soc London Ser A Math Phys Eng Sci* (2001) 359 (1783):1073–89. doi: 10.1098/rsta.2001.0817
320. Christie GR, Nielsen PMF, Blackett SA, Bradley CP, Hunter PJ. FieldML: Concepts and Implementation. *Philos Trans R Soc A Math Phys Eng Sci* (2009) 367(1895):1869–84. doi: 10.1098/rsta.2009.0025
321. Johnson D, McKeever S, Deisboeck TS, Wang Z. Connecting Digital Cancer Model Repositories With Markup: Introducing TumorML Version 1.0. *ACM SIGBioinform Rec* (2013) 3(3):5–11. doi: 10.1145/2544063.2544064
322. Wang Z, Zhang L, Sagotsky J, Deisboeck TS. Simulating non-Small Cell Lung Cancer With a Multiscale Agent-Based Model. *Theor Biol Med Model* (2007) 4(1):1–14. doi: 10.1186/1742-4682-4-50
323. Sakkalis V, Sfakianakis S, Tzamali E, Marias K, Stamatakos G, Misichroni F, et al. Web-Based Workflow Planning Platform Supporting the Design and Execution of Complex Multiscale Cancer Models. *IEEE J BioMed Heal Informatics* (2014) 18(3):824–31. doi: 10.1109/JBHI.2013.2297167
324. Athale C, Mansury Y, Deisboeck TS. Simulating the Impact of a Molecular 'Decision-Process' on Cellular Phenotype and Multicellular Patterns in Brain Tumors. *J Theor Biol* (2005) 233(4):469–81. doi: 10.1016/j.jtbi.2004.10.019
325. Shlomi T, Benyamini T, Gottlieb E, Sharan R, Ruppin E. Genome-Scale Metabolic Modeling Elucidates the Role of Proliferative Adaptation in Causing the Warburg Effect. *PloS Comput Biol* (2011) 7(3):e1002018. doi: 10.1371/journal.pcbi.1002018
326. Kolokotroni E, Dionysiou D, Veith C, Kim Y-J, Sabczynski J, Franz A, et al. *In Silico* Oncology: Quantification of the *In Vivo* Antitumor Efficacy of Cisplatin-Based Doublet Therapy in non-Small Cell Lung Cancer (NSCLC) Through a Multiscale Mechanistic Model. *PloS Comput Biol* (2016) 12(9): e1005093. doi: 10.1371/journal.pcbi.1005093
327. Antonopoulos M, Stamatakos G. *In Silico* Neuro-Oncology: Brownian Motion-Based Mathematical Treatment as a Potential Platform for Modeling the Infiltration of Glioma Cells Into Normal Brain Tissue. *Cancer Inform* (2015) 14:33–40. doi: 10.4137/CIN.S19341
328. Ouzounoglou E, Dionysiou D, Stamatakos GS. Differentiation Resistance Through Altered Retinoblastoma Protein Function in Acute Lymphoblastic Leukemia: *In Silico* Modeling of the Deregulations in the G1/S Restriction Point Pathway. *BMC Syst Biol* (2016) 10(1):1–22. doi: 10.1186/s12918-016-0264-5

329. Stamatakos GS, Giatili SG. A Numerical Handling of the Boundary Conditions Imposed by the Skull on an Inhomogeneous Diffusion-Reaction Model of Glioblastoma Invasion Into the Brain: Clinical Validation Aspects. *Cancer Inform* (2017) 16:1–16. doi: 10.1177/1176935116684824
330. Lee HJ, Palm J, Grimes SM, Ji HP. The Cancer Genome Atlas Clinical Explorer: A Web and Mobile Interface for Identifying Clinical-Genomic Driver Associations. *Genome Med* (2015) 7(1):1–14. doi: 10.1186/s13073-015-0226-3
331. Shaul YD, Yuan B, Thiru P, Nutter-Upham A, McCallum S, Lanzkron C, et al. MERAV: A Tool for Comparing Gene Expression Across Human Tissues and Cell Types. *Nucleic Acids Res* (2016) 44(D1):D560–6. doi: 10.1093/nar/gkv1337
332. Jensen MA, Ferretti V, Grossman RL, Staudt LM. The NCI Genomic Data Commons as an Engine for Precision Medicine. *Blood* (2017) 130(4):453–9. doi: 10.1182/blood-2017-03-735654
333. Li J, Lu Y, Akbani R, Ju Z, Roebuck PL, Liu W, et al. TCPA: A Resource for Cancer Functional Proteomics Data. *Nat Methods* (2013) 10(11):1046–7. doi: 10.1038/nmeth.2650
334. Pontén F, Jirström K, Uhlen M. The Human Protein Atlas—a Tool for Pathology. *J Pathol* (2008) 216(4):387–93. doi: 10.1002/path.2440
335. Gondal MN, Chaudhary SU. Navigating Multi-Scale Cancer Systems Biology Towards Model-Driven Personalized Therapeutics. *bioRxiv* (2021) 7. doi: 10.1101/2021.05.17.444410

**Conflict of Interest:** The authors declare that the research was conducted in the absence of any commercial or financial relationships that could be construed as a potential conflict of interest.

**Publisher's Note:** All claims expressed in this article are solely those of the authors and do not necessarily represent those of their affiliated organizations, or those of the publisher, the editors and the reviewers. Any product that may be evaluated in this article, or claim that may be made by its manufacturer, is not guaranteed or endorsed by the publisher.

frontiers in Oncology

MINI REVIEW
published: 09 December 2021
doi: 10.3389/fonc.2021.705634

# MiRNAs as Anti-Angiogenic Adjuvant Therapy in Cancer: Synopsis and Potential

*Behnaz Lahooti*[1], *Sagun Poudel*[2], *Constantinos M. Mikelis*[1,3]* *and George Mattheolabakis*[2]*

[1] Department of Pharmaceutical Sciences, School of Pharmacy, Texas Tech University Health Sciences Center, Amarillo, TX, United States, [2] School of Basic Pharmaceutical and Toxicological Sciences, College of Pharmacy, University of Louisiana Monroe, Monroe, LA, United States, [3] Department of Pharmacy, University of Patras, Patras, Greece

Angiogenesis is a key mechanism for tumor growth and metastasis and has been a therapeutic target for anti-cancer treatments. Intensive vascular growth is concomitant with the rapidly proliferating tumor cell population and tumor outgrowth. Current angiogenesis inhibitors targeting either one or a few pro-angiogenic factors or a range of downstream signaling molecules provide clinical benefit, but not without significant side effects. miRNAs are important post-transcriptional regulators of gene expression, and their dysregulation has been associated with tumor progression, metastasis, resistance, and the promotion of tumor-induced angiogenesis. In this mini-review, we provide a brief overview of the current anti-angiogenic approaches, their molecular targets, and side effects, as well as discuss existing literature on the role of miRNAs in angiogenesis. As we highlight specific miRNAs, based on their activity on endothelial or cancer cells, we discuss their potential for anti-angiogenic targeting in cancer as adjuvant therapy and the importance of angiogenesis being evaluated in such combinatorial approaches.

**Keywords: angiogenesis, adjuvant therapy, miRNAs, drugs, combinatorial**

OPEN ACCESS

***Edited by:***
*Ulf Schmitz,*
*James Cook University, Australia*

***Reviewed by:***
*Khuloud Bajbouj,*
*University of Sharjah, United Arab Emirates*
*Xin Lai,*
*University Hospital Erlangen, Germany*

***Correspondence:**
*Constantinos M. Mikelis*
*constantinos.mikelis@ttuhsc.edu*
*George Mattheolabakis*
*matthaiolampakis@ulm.edu*

***Specialty section:***
*This article was submitted to Pharmacology of Anti-Cancer Drugs, a section of the journal Frontiers in Oncology*

***Received:*** *05 May 2021*
***Accepted:*** *22 November 2021*
***Published:*** *09 December 2021*

***Citation:***
*Lahooti B, Poudel S, Mikelis CM and Mattheolabakis G (2021) MiRNAs as Anti-Angiogenic Adjuvant Therapy in Cancer: Synopsis and Potential. Front. Oncol. 11:705634. doi: 10.3389/fonc.2021.705634*

## INTRODUCTION

Angiogenesis is the physiological process for new blood vessel development from pre-existing ones. It is a highly coordinated, multistage process that occurs in physiological conditions, such as wound healing, the female reproductive cycle, and embryonic development, and many pathological conditions, including cancer. The angiogenic outcome highly depends on the balance of growth factors and angiogenesis inhibitors. Dysregulation of this balance leads to the increased or limited vascular network identified in a series of pathologies, such as retinopathies, inflammatory disorders, cardiovascular disorders, and tumors (1–3).

The rapid growth of tumor cells requires the continuous supply of oxygen and nutrients, the diffusion of which *in vivo* is significantly limited at 100-500 microns from the nearest capillary. Solid tumors cannot grow more than 2-3 mm in diameter and thus become dormant without vascular support (4, 5). The rapid proliferation of the tumor cells leads to their distant localization from the nearest capillary and the induction of hypoxia, a major driver of angiogenesis. Hypoxia leads to the secretion of many growth factors, such as vascular endothelial growth factor (VEGF) and basic fibroblast growth factor (bFGF), cytokines, such as interleukin 8 (IL-8), and other pro-angiogenic

mediators, such as sphingosine-1 phosphate (S1P), leading to the proliferation, migration and tumor-like formation of the nearby endothelial cells (5–8). The newly formed tumor vessels are markedly distinct from the normal capillaries due to their chaotic structure characterized by the absence of proper orientation, the limited pericyte and smooth muscle cell coverage, blunt capillary ends, increased leakiness, and limited perfusion. The increased leakiness provides fertile ground for tumor cell dissemination and metastasis, while the limited mural support often leads to their collapse due to the higher interstitial pressure of the tumoral area, increasing further the hypoxic conditions (3, 5, 9).

Targeting the tumor vascular network with anti-angiogenic therapy, despite the excellent preclinical results and the high potential these provided, did not meet the expectations in the clinic, with ephemeral results and not significant benefit in overall survival in most tumors. A prominent reason for this is considered the induction of compensatory mechanisms due to increased hypoxia upon anti-angiogenic treatment, which drives the overexpression of other pro-angiogenic factors, blocks immune functionality, and limits the perfusion of cytotoxic therapies (10, 11). During the last decade, the notion of vascular normalization as an outcome of anti-angiogenic therapy has risen, which can be achieved within a short therapeutic window during anti-angiogenic therapy. Tumor vascular normalization is expected to induce the integrity of the tumor vessels providing increased mural cell support, limited leakiness, inhibition of trans-endothelial cancer cell migration and metastatic incidence, and higher perfusion, which would limit the hypoxic areas and accommodate improved anti-cancer drug delivery in the tumoral area (12–14). The majority of the studies have focused on VEGF inhibition, the main target of anti-angiogenic therapies. A precise dosage of VEGF inhibitors has been demonstrated to inhibit vascular permeability by tightening cell-to-cell contacts and recruiting pericytes. VEGF is not the sole mediator of vascular permeability, as an increasing volume of data has highlighted the involvement of other molecular players and pathways, such as Angiopoietin-2, Semaphorin 3A, nitric oxide, superoxide dismutase-3, Notch, WNT, platelet-derived growth factor-B (PDGF-B) and bone morphogenetic protein (MBP) signaling in this process (10, 11, 13, 15, 16).

Nucleic acid-based therapeutics have attracted attention for the treatment of several diseases, including cancer (17, 18), inflammation (19), or the development of vaccines, such as against SARS-CoV-2 (i.e. COVID-19) (20–22). Among the different types of nucleic acids currently under research, miRNAs, natural molecules produced by the cells frequently transcribed along with protein-expressing genes (23, 24), are commonly dysregulated in diseases, such as cancer, inflammation, and others. Not surprisingly, miRNAs were recognized as potential prognostic and diagnostic markers in cancer (23–26). More importantly, as miRNAs are small, non-coding RNAs that utilize the cell's RNA interference mechanism to regulate multiple gene expressions, miRNAs are evaluated as therapeutic tools against cancer (23). An increasing body of literature focuses on dysregulated miRNAs for their properties as tumor suppressors or oncogenes, and on their action to either suppress or activate tumor-promoting pathways (23). Exogenous delivery of miRNA constructs, similarly to the exogenous delivery of siRNAs, aims to replace or correct observed miRNA dysregulations. Unlike siRNAs though, miRNA replacement therapies induce the expression or increase the levels of nucleic acid sequences naturally occurring in the cells, which should have an indistinguishable effect on the endogenous miRNAs (23, 24). Though this approach has limitations, the exogenous delivery of miRNAs should induce a strong beneficial effect on cells associated with the disease (i.e., cancer cells or cells of the tumor microenvironment with dysregulated miRNA expression) while having minimal effects on normal cells (i.e., absence of dysregulation) (27).

Representatively, miR-34a is characterized as a master tumor suppressor against multiple cancer types, capable of regulating proliferation, migration (28), apoptosis (29), metastasis, senescence, differentiation, and immune responses (30). Similarly, the clinical potential and translation of other miRNAs are currently undergoing. We are not outlining these studies, as several review publications focus on the current and past clinical trials [indicatively, refer to: (31–33)]. As miRNAs are expressed in all types of cells, miRNAs regulate vascular development and angiogenesis in endothelial cells (EC). Landskroner-Eiger et al. (34) summarized the importance of miRNAs in angiogenesis from the perspective of the Dicer enzyme. Dicer enzyme is a key component in the biogenesis of miRNAs, and several studies evaluated the effect of Dicer deletion/inactivation in normal vascular development. Dicer activity affected angiogenesis, attributed to defective miRNA expression, dysregulating the expression of VEGF and its receptors. As miRNA dysregulation in cancer has been well documented (35) either through cell-to-cell communication between cancer cells and EC or EC intracellular miRNA dysregulation, utilization of miRNAs as targets or regiments can benefit cancer treatments through regulation of EC function and formation of blood vessels (36, 37). There is an increasing interest in the combination of anti-angiogenic agents with traditional chemotherapeutics and several clinical trials pursued that approach (2, 38). We sought to explore the use of miRNAs for cancer treatment due to their ability to regulate angiogenesis and focus on their potential and utilization as adjuvant therapies with chemotherapeutics because of their anti-angiogenic properties. Although there is a substantial body of literature focusing on miRNAs and angiogenesis, limited work exists on their combination with chemotherapeutics predominately due to their anti-angiogenic properties. Here, we present miRNAs that are frequently studied due to their angiogenesis-inhibiting capacity and have been combined with traditional chemotherapeutics, even when the utilization of these miRNAs was not because of their anti-angiogenic properties.

## CURRENT ANTI-ANGIOGENIC THERAPIES

Not long after its discovery, VEGF was characterized as a principal vascular regulator (39, 40). VEGF haploinsufficiency led to embryonic lethality due to impaired angiogenesis and

blood vessel formation (41, 42). The striking impact on angiogenesis, vascular morphology, and functions upon VEGF inhibition or deficiency, along with its overexpression in most solid tumors, including lung, breast, liver, and ovarian cancers, brought it to the frontline of anti-angiogenic targets, where it remains till today. The first FDA-approved anti-angiogenic drug was bevacizumab, a monoclonal antibody against VEGF (43, 44). Bevacizumab, combined with chemotherapy, improved overall survival in colorectal cancer (45) and soon provided encouraging results when tested in ovarian, cervical, non-small cell lung cancers, and mesothelioma. Today, bevacizumab is FDA-approved for colorectal cancer, non-small cell lung cancer, renal cell carcinoma, cervical, fallopian tube cancer, peritoneal cancer, and glioblastoma, whereas it failed to provide clinical benefit in the majority of the other cancer types, including breast cancer, for which the FDA approval lasted for a short period (2). Apart from bevacizumab, other antibody-based anti-angiogenic inhibitors are ramucirumab and aflibercept, which target VEGF receptor 2 (VEGFR2) or VEGF-A, VEGF-B and placental growth factor (PlGF), respectively. The rest of the angiogenesis inhibitors include small molecule or tyrosine kinase inhibitors that target one or more signaling pathways. Some of these tyrosine kinase inhibitors, such as sunitinib and regorafenib, inhibit a wide range of molecular targets and downstream mediators. The current, clinically administered anti-angiogenic inhibitors, their molecular targets, and the approved cancer types are presented below (2, 46–54):

- Bevacizumab, targeting VEGF-A, for glioblastoma, colorectal, cervical, fallopian tube, peritoneal, non-small cell lung cancers and renal cell carcinoma.
- Ramucirumab, targeting VEGFR2, for gastric, gastroesophageal junction, non-small cell lung and colorectal cancers.
- Aflibercept, targeting VEGF-A,-B and PlGF, for colorectal cancer.
- Axitinib, targeting VEGFR1-3, for renal cell carcinoma.
- Cabozantinib, targeting VEGFR1-3, receptor tyrosine kinase (KIT), tropomyosin receptor kinase B (TRKB), anexelekto receptor tyrosine kinase (AXL), Rearranged during transfection (RET), tyrosine kinase MET, Fms-like tyrosine kinase-3 (FLT-3), TEK receptor tyrosine kinase (TIE2), for hepatocellular and renal cell carcinomas, and Medullary thyroid cancer.
- Everolimus, targeting mammalian target of rapamycin (mTOR), for breast, pancreatic, gastrointestinal, and lung cancers, Renal cell and subependymal giant cell carcinomas.
- Lenalidomide, targeting Ikaros family zinc finger protein 1,3 (IKZF1,3), E3 ubiquitin ligase, for follicular, mantle cell and marginal zone lymphomas, and multiple myeloma.
- Lenvatinib, targeting VEGFR1-3, for endometrial, hepatocellular and renal cell carcinomas and Thyroid cancer.
- Pazopanib, targeting VEGFR1-3, PDGF receptor-α/β (PDGFR-α/β), fibroblast growth factor receptor 1,2 (FGFR1,2), c-KIT, for renal cell and soft tissue carcinomas.
- Sorafenib, targeting VEGFR1-3, PDGFR-β, FLT-3, c-KIT, RAF kinases, for hepatocellular and renal cell carcinomas and thyroid cancer.
- Sunitinib, targeting VEGFR1-3, PDGFR-α/β, KIT, FLT-3, colony-stimulating factor receptor Type 1 (CSF-1R), RET, for gastrointestinal stromal and pancreatic cancers and renal cell carcinoma.
- Regorafenib, targeting VEGFR1-3, KIT, PDGFR-α/β, FGFR1,2, TIE2, discoidin domain receptor tyrosine kinase 2 (DDR2), tropomyosin receptor kinase A (TRKA), Eph2A, RAF-1, BRAF, BRAFV600E, SAPK2, PTK5, Abelson tyrosine kinase 1 (ABL), for gastrointestinal stromal and colorectal cancers and hepatocellular carcinoma.
- Thalidomide, targeting tumor necrosis factor-α (TNF-α), for multiple myeloma.
- Vandetanib, targeting VEGFR, epidermal growth factor receptor (EGFR), RET, for medullary thyroid cancer.

## LIMITATIONS AND SIDE EFFECTS OF ANTI-ANGIOGENIC THERAPIES

As seen above, most anti-angiogenic drugs are targeting VEGF or VEGFR, either solely or in combination with other growth factor receptors or downstream kinases. Their administration provides encouraging clinical benefit; however, their application is not without side effects. The two most critical side effects of anti-angiogenic therapy are the induction of tumor aggressiveness along with metastatic potential and the tumor angiogenesis relapse due to the development of resistance mechanisms. The induction of tumor aggressiveness and metastatic potential upon anti-angiogenic therapy is still under debate, as it has been reported in preclinical models, but not always verified in other studies, demonstrating the variability of this phenomenon (55–57).

One of the limiting factors of anti-angiogenic therapy in cancer is that since cancer cells are not eradicated, as they do not consist the target of anti-angiogenic therapy, anti-angiogenic drugs have to be administered over long periods. The ephemeral outcome of anti-angiogenic therapy and the need for prolonged treatment eventually lead to the development of resistance upon anti-angiogenic inhibition. Resistance can be driven by the tumor cells, the stroma, immune cells, or endothelial progenitors, is mediated by the upregulation of alternative pro-angiogenic mediators, and presents cancer type- and patient-specific variability (8, 58).

Systemic anti-angiogenic drug administration, both in the case of antibody-specific VEGF inhibition and a wide range of tyrosine kinase inhibitors, can lead to organ- or tissue-specific side effects (59). A meta-analysis of five randomized clinical trials of metastatic colorectal, breast, and non-small cell lung cancers highlighted the risk of a thromboembolic event as another side effect of bevacizumab treatment in combination with chemotherapy (60). Cardiomyopathy and congestive heart failure have also been reported as side effects of anti-angiogenic inhibitors (61). Although the exact mechanism for cardiomyopathy and congestive heart failure upon VEGF signaling blockade has not yet been fully delineated, the current notion is that existing conditions depleting the vascular

reserve, such as hypertension and coronary artery disease, may be considered risk factors for cardiotoxicity with VEGF signaling inhibitors, while reduced nitric oxide production, mitochondrial dysfunction and pericyte population depletion have been attributed as potential mechanisms (62, 63). It has been further preclinically demonstrated that abrogation of the physiological VEGF activity can result in increased systemic (and coronary) vascular resistance and decreased cardiac output *per se*, which is the typical reason for cardiomyopathy development. Moreover, the roles of chemotherapy or radiation therapy as concomitant factors in VEGF blockade-induced cardiotoxicity have been further reported (63, 64).

Two well-known side effects of anti-angiogenic therapy that go hand in hand are the increased rate of hemorrhage and the inhibited wound healing process, both of which are determining factors for the timing of surgical procedures (65). Pulmonary hemorrhage with fatal outcome has been reported for non-small cell lung cancer patients with different anti-angiogenesis inhibitors, such as bevacizumab, ramucirumab, sunitinib, axitinib, and motesanib. A small percentage of gastrointestinal tumor patients developed bleeding at the tumor sites, while central nervous bleeding has also been reported (61, 65). Impaired wound healing is a common issue. Angiogenesis is a pivotal part of the wound healing process, mediated by VEGF and other growth factors, thus is expected that VEGF inhibition hampers the inflammatory and granulation wound healing phases, pivotal for the wound healing process. As an alternative, milder anti-angiogenic treatments have been proposed to overcome this issue (66).To avoid wound healing deficiency of the surgical area anti-angiogenic treatment has to be terminated for at least four weeks before the surgical procedure so that the body will "wash out" the drug's effects (61, 65).

The above demonstrate the impact and role of angiogenic factors in physiological vascular functions, the interdependence of the primary tumor and the tumor microenvironment, the need for highly targeted, vascular-specific anti-angiogenic approaches, and the consideration of anti-angiogenic therapies specifically targeting aberrant angiogenesis, without affecting regular angiogenic functions.

## MiRNA THERAPEUTICS AND THEIR ADJUVANT POTENTIAL AGAINST ANGIOGENESIS

As research on miRNAs rapidly proliferates, miRNAs' contribution in tumor suppression *via* anti-angiogenic function presented multifaceted therapeutic potentials for these molecules. miRNAs have primarily been studied for their activity as single molecules against cancer (17, 35, 67). With numerous miRNAs being able to regulate cell functions and pathways, the number of potential mechanisms of action of miRNAs in angiogenesis correlates to the potential pathways associated with angiogenesis. Nonetheless, similarly to traditional anti-angiogenic approaches, studies on miRNAs and angiogenesis have primarily focused in known, more traditional angiogenic pathways. Thus, miRNAs studies focus on angiogenic factor receptors or signaling molecules in ECs to inhibit tumor angiogenesis (68), among them more prominently being VEGF, VEGFR and PDGFR (69–71). As numerous dysregulated miRNAs have been identified in tumor samples, here, we will present a few of the miRNAs with explicit action on angiogenesis and their identified molecular targets.

miR-34a, a master tumor suppressor, is one of the best-studied miRNAs, and, hence, its activity on tumor cells and cells of the tumor microenvironment has been thoroughly evaluated. Several studies have reported on miR-34a's ability to inhibit tumor angiogenesis. This activity takes place *via* multiple approaches, including the inhibition of the Silent Information Regulator 1 (*Sirt1*) expression, increase of the expression of acetylated Forkhead Box O1 (*FoxO1*) transcription factor, Notch1 targeting, and the *p53* protein in endothelial progenitor cells and human cancer cells (72–75). miR-34a downregulation in EC induced BCL-2-overexpression and inhibition of apoptosis, while miR-34a upregulation suppresses tumor angiogenesis, EC proliferation, migration, and tube formation (76, 77). miR-34a has also extensively been studied in combination with several chemotherapeutics, such as cisplatin (78, 79), doxorubicin (80), sorafenib (81), and paclitaxel (82), among others. Despite the well-studied anti-angiogenic properties of the miRNA, we did not find research on its combination with a chemotherapeutic agent based solely due to its anti-angiogenic properties, rather than miR-34a's activity on the tumor cells.

Similarly, the miR-29 family, miR-29a, miR-29b, and miR-29c, are downregulated in various cancers, such as endometrial carcinoma, hepatocellular carcinoma, gastric cancer, and breast cancer (83–86). miR-29b overexpression inhibits angiogenesis and tumorigenesis *in vivo* and weakens tube formation, cell proliferation, and migration *in vitro* (83). miR-29b prevented tumor angiogenesis by targeting *AKT3* and inhibited Akt3-mediated VEGF and C-myc activations (86). In a gastric cancer mouse model, miR-29a/c prevented tumor growth, tube formation, and suppressed angiogenesis by suppressing VEGF-A expression (87). Similar to miR-34a, members of the miR-29 family have been attributed with tumor-suppressive properties and evaluated with several chemotherapeutic agents, such as cisplatin (88), and paclitaxel (89), among others. Of interest, miR-29a has been reported to contribute to doxorubicin resistance in breast cancer cells (90) and inhibit doxorubicin resistance in colon cancer cells (91). Li et al. (92) reported that cisplatin treatment induces upregulation of miR-29b, which suppressed invasion and angiogenesis of the cancer cells *in vitro* and inhibited tumor growth and neovascularization *in vivo*. The authors demonstrated that ectopic expression of miR-29b *via* intravenous administration in a subcutaneous xenograft mouse model of cervical cancer (HeLa cells) inhibited tumor growth and VEGF expression, corresponding to a decrease in vessel formation, although the authors did not evaluate this activity with the co-administration with cisplatin.

miR-221 and miR-222 modulated the angiogenic behavior of human umbilical vein endothelial cells (HUVECs) through the

regulation of c-Kit expression (93). As these miRNAs were among the most abundantly expressed miRNAs in ECs (94), Nicoli et al. reported that miR-221 is essential for angiogenesis, in the zebrafish model (95). In human venous or lymphatic endothelial cells, miR-221 has been shown to inhibit angiogenesis (93, 96–98). miR-221 has been identified as oncogenic in pancreatic cancer cells (99), glioblastoma (100), breast cancer (101), and lung cancer (102), among others. miR-221/222 have also been associated with increased chemoresistance to cisplatin in ovarian (103) and breast cancer cells (104). Similar results have been reported with Adriamycin (doxorubicin) (105, 106), 5-fluorouracil (107), and paclitaxel (108). Representatively, *in vivo* analysis of downregulation of miR-221/222 through local injection in a breast cancer mouse model enhanced the cisplatin's tumor growth inhibition capacity, but no analysis on tumor vasculature took place (104). In fact, in the *in vivo* studies of the miRNA-drug combinations, angiogenesis was not evaluated. This complex behavior is a representative example of the multi-faceted activity of miRNAs, which can be cancer- or cell-type-specific, and their combination with drugs can extend outside of the tumor cells, to the tumor microenvironment.

The expression of the most potent angiogenesis modulators in different tumors in terms of downstream targets of miRNAs has been extensively studied. Multiple miRNAs have been found to target VEGF since it is the most potent trigger for angiogenesis. miR-20 (109), miR-29b (110), miR-93 (111, 112), miR-126 (113, 114) target the 3'-UTR region of VEGF-A mRNA. Following, we provide representative examples of miRNAs with anti-angiogenic properties that also demonstrated anti-tumoral activity. miR-27b (115, 116) and miR-128 (69) suppress tumor progression and angiogenesis by targeting VEGF-C. miR-125b suppressed EC tube formation by inhibiting E-cadherin (117). miR-192 targets EGR1 and HOXB9, leading to anti-tumor and anti-angiogenic activity in human ovarian epithelial tumors (118). miR-200 family inhibited angiogenesis through direct and indirect mechanisms by targeting interleukin-8 (IL8) and CXCL1 secreted by the tumor endothelial and cancer cells (119). Overexpression of miR-190 inhibited EMT and angiogenesis by inactivating AKT-ERK signaling (120). miR-206 inhibited HGF-induced epithelial-mesenchymal transition (EMT) and angiogenesis in lung cancer, by suppressing Met/PI3k/Akt/mTOR signaling (121). miR-135a promoted cell apoptosis and inhibited cell proliferation, migration, invasion, and tumor angiogenesis by targeting the IGF-1 gene through the IGF-1/PI3K/Akt signaling pathway in non-small cell lung cancer (NSCLC) (122). Finally, miR-143 and miR-506, alone and in combination have been reported to affect angiogenesis, by inhibiting tube formation in HUVEC cells, while causing apoptosis to lung cancer cells (123).

As the VEGF family and its downregulation have been implicated in drug resistance in tumor cells (124–126), it is reasonable to predict that miRNAs with the capacity to target members of the VEGF family will become part of a cell-sensitization goal for specific chemotherapeutics. Due to this reason alone, studies of miRNA-chemotherapeutic drugs combinatorial use for cancer treatment have the potential to proliferate in the future (**Figure 1**). One representative example would be miR-126, where Zhu et al., (127) demonstrated that miR-126 decreased the minimum inhibitory concentration of Adriamycin and Vincristine by targeting VEGF-A. In **Table 1**, we present a short list of studies with miRNAs with known anti-angiogenic activity in combination with chemotherapeutics.

Illustratively, Wang et al. (155) studied the combination of miR-30a-5p with gefitinib to overcome drug resistance *via* regulation of the insulin-like growth factor receptor-1 (IGF1R) and hepatocyte growth factor receptor signaling pathways in NSCLC both *in vitro* and *in vivo*. Liang et al. (156) formulated exosomes to simultaneously deliver the anticancer drug 5-FU and a miR-21 inhibitor oligonucleotide (miR-21i) to 5-FU-resistant colon cancer cells. This approach reversed drug resistance and significantly enhanced the drug's cytotoxicity in 5-FU-resistant colon cancer cells, compared to the single treatment with either miR-21i or 5-FU in an *in vivo* mouse model. Similarly. miR-375-3p, which has been reported to suppress tumorigenesis and reverse chemoresistance in colon cancer, along with 5-FU co-delivered in lipid-coated calcium carbonate nanoparticles were used to study the role of miR-375-3p in 5-FU-resistance in colorectal cancer (157, 158).

## DISCUSSION

It is evident that miRNAs can have a significant impact on angiogenesis and cancer treatment. As our knowledge on miRNA activity expands, the highly complex interaction between miRNA and angiogenesis due to autocrine or paracrine interactions will dictate the future potential of the miRNAs as therapeutic tools. One major hurdle of anti-cancer therapies, including the anti-angiogenic therapies described above, is the off-target effects due to non-specific tissue- or cell-targeting. This hurdle is further exacerbated with the miRNAs, as the tumor type and the multifaceted activity of the miRNAs can have synergistic or antagonistic therapeutic outcomes through the tumor microenvironment. Thus, the *in vivo* evaluation of the miRNAs needs to expand outside the tumor cell growth and incorporate aspects, such as angiogenesis. Another parameter to be taken into account for miRNA-based therapies is the promiscuous binding of high miRNA dose, causing multiple off-target effects. This significant hurdle of miRNA-based treatments can be resolved by miRNA cooperativity and lower miRNA doses, while it is noteworthy that the final outcome of the targets of the cooperating genes strongly depends on the cellular environment (159).

miRNA delivery has been challenging by itself, due to the nucleic acids' rapid elimination from the circulation, the abundance of nucleases *in vivo*, and the need for a carrier for the large hydrophilic nucleic acid constructs to enter the cells (23, 24). The added complexity of the required cell type drug delivery specificity presents an additional challenge, which needs to be potentially overcome in the presence of an already impaired tumor vascular system (26). Several novel delivery carriers have been developed and studied for the delivery of miRNAs. These

**TABLE 1** | Representative examples of combinatorial miRNA-chemotherapeutics treatments.

| miRNA | Drug | Cancer | References |
|---|---|---|---|
| miR-34a | Doxorubicin | Hepatocellular carcinoma | (80) |
| | | Osteosarcoma | (128) |
| | Paclitaxel | Cervical cancer | (129) |
| | | Melanoma cancer | (130) |
| | | Colorectal Cancer | (131) |
| | Docetaxel | Breast cancer | (132) |
| | 5- Fluorouracil | Colorectal cancer | (133, 134) |
| Let-7c-5p | 5-Flurouracil | Hepatocellular carcinoma | (135) |
| Anti-miR-21 | Sunitinib | Glioblastoma | (136) |
| | | Pancreatic ductal adenocarcinoma | (137) |
| miR-145 | Sunitinib | Glioblastoma | (138) |
| | 5-Fluorouracil | Breast cancer | (139) |
| miR-205 | Gemcitabine | Pancreatic cancer | (140) |
| miR-129 | 5-Fluorouracil | Colorectal cancer | (141) |
| miR-497 | 5-Fluorouracil | Colorectal cancer | (142) |
| miR-34a and miR-27b | Docetaxel | Prostate cancer | (143) |
| miR-29b | Dihydroartemisinin | Cholangiocarcinoma | (144) |
| miR-221 | Doxorubicin | Glioma | (145) |
| miR-192-5p | Doxorubicin | Breast cancer | (146) |
| miR-378a | Sorafenib | Liver cancer | (147) |
| miR-122, miR-338-3p | Sorafenib | Hepatocellular carcinoma | (148) |
| miR-193a | Taxol | Colorectal cancer | (149) |
| miR-143 | Cisplatin | Cervical cancer | (150) |
| miR-29 | Cisplatin | Ovarian cancer | (151) |
| miR-7 | Doxorubicin and Temozolomide | Glioma, Cervical carcinoma, Papillary thyroid | (152) |
| miR-506-3p | Cisplatin | Ovarian cancer | (153) |
| miR-135 and miR-138 | 5- Fluorouracil | Colon cancer, pancreatic cancer, cervical cancer | (154) |

*All miRNAs listed have tumor-inhibiting properties.*

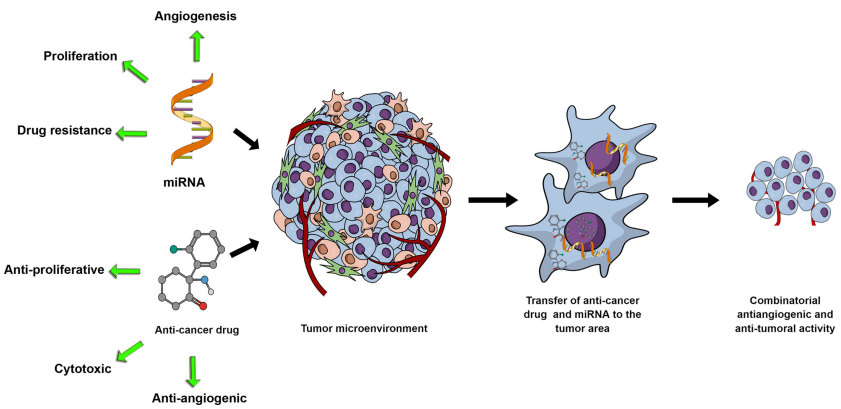


**FIGURE 1** | miRNA and anti-cancer drug combinations can potentially synergistically affect tumor growth through their respective activities and potential synergistic effects on the tumor cells and the tumor microenvironment. With miRNAs mediating cell proliferation, drug resistance or angiogenesis, exogenous upregulation or inhibition of miRNAs in combination with anti-proliferative, cytotoxic or anti-angiogenic drugs represents a rationally designed and promising research development.

include micelles, polymeric nanocarriers, lipid-based carriers, viruses, inorganic carriers, and systems with long-circulating properties and/or active targeting to receptors over-expressed in cancer cells (23). Although the goal of a single organ and single-cell type targeting maybe be understandably impractical, these methodologies have provided significant benefits for minimizing off-target effects, increasing accumulation in the tumor, and preferentially increasing drug/nucleic acid concentration in specific cell types. Nonetheless, off-target effects will persist, even due to cell-to-cell communication.

This perspective has a significant impact when studying miRNA-drug combinations. Although *in vitro* analysis is fundamental to evaluate the synergistic/antagonistic behavior of a miRNA and a drug, the effect of the co-delivery of the miRNA-drug combination *in vivo* should take into consideration the anti-angiogenic properties of the miRNAs. Of course, this

easily expands to other aspects of the tumor microenvironment, such as macrophages, though immunosuppressed animal models will present challenges for such evaluation.

Though we recognize that there might be published research on miRNA-drug combination focusing on angiogenesis we overlooked, it is apparent from our analysis that currently the anti-angiogenic aspect of miRNAs co-delivered with drugs is not the primary focus, or is not studied in detail or at all, even for miRNAs with known anti-angiogenic properties. Simply stated, the question arises on how much of the enhanced anti-tumoral activity of miRNA-drug combinations can be attributed to the alteration of tumor cell behavior, angiogenesis, or both. Finally, another important aspect is the toxicity potential from the miRNAs. We described above the side effects attributed to the clinically used anti-angiogenic therapies, which have a clinical history with well-defined side effects. In contrast, miRNAs have not achieved clinical translation to the same extent, and, thus, similar or other side effects may not yet have become apparent. Nonetheless, the utilization of dysregulated miRNAs, their property of being natural cell products, and the development of novel nanocarriers provide significant advantages to overcome side-effects, commonly present in traditional anti-angiogenic therapies (160). In conclusion, miRNAs are fundamentally important targets and tools for cancer therapy. They have significant potential, based alone on their multifaceted activities on the tumor cells and tumor vascular microenvironment. Identification of miRNAs with combined anti-angiogenic and anti-tumoral effects can provide significant advantages in cancer treatment, alone or in combination with clinically used chemotherapeutics.

## AUTHOR CONTRIBUTIONS

BL, SP, CM, and GM contributed to the conception of the article, wrote and revised the final manuscript and agreed on its submission to this journal. All authors contributed to the article and approved the submitted version.

## FUNDING

This work was supported for GM by the College of Pharmacy, University of Louisiana Monroe start-up funding and the National Institutes of Health (NIH) through the National Institute of General Medical Science Grants 5 P20 GM103424-15, 3 P20 GM103424-15S1 and for CM in part by National Institutes of Health Grant (NCI) R15CA231339 and Texas Tech University Health Sciences Center (TTUHSC) School of Pharmacy Office of Sciences grant. The funders had no role in study design, decision to write and preparation of the manuscript.

## REFERENCES

1. Sajib S, Zahra FT, Lionakis MS, German NA, Mikelis CM. Mechanisms of Angiogenesis in Microbe-Regulated Inflammatory and Neoplastic Conditions. *Angiogenesis* (2018) 21:1–14. doi: 10.1007/s10456-017-9583-4
2. Zirlik K, Duyster J. Anti-Angiogenics: Current Situation and Future Perspectives. *Oncol Res Treat* (2018) 41:166–71. doi: 10.1159/000488087
3. Teleanu RI, Chircov C, Grumezescu AM, Teleanu DM. Tumor Angiogenesis and Anti-Angiogenic Strategies for Cancer Treatment. *J Clin Med* (2019) 9:84. doi: 10.3390/jcm9010084
4. Folkman J. Tumor Angiogenesis: Therapeutic Implications. *N Engl J Med* (1971) 285:1182–6. doi: 10.1056/NEJM197111182852108
5. Bielenberg DR, Zetter BR. The Contribution of Angiogenesis to the Process of Metastasis. *Cancer J* (2015) 21:267–73. doi: 10.1097/PPO.0000000000000138
6. Ramjiawan RR, Griffioen AW, Duda DG. Anti-Angiogenesis for Cancer Revisited: Is There a Role for Combinations With Immunotherapy? *Angiogenesis* (2017) 20:185–204. doi: 10.1007/s10456-017-9552-y
7. Zahra FT, Sajib MS, Ichiyama Y, Akwii RG, Tullar PE, Cobos C, et al. Endothelial RhoA GTPase Is Essential for In Vitro Endothelial Functions But Dispensable for Physiological In Vivo Angiogenesis. *Sci Rep* (2019) 9:11666. doi: 10.1038/s41598-019-48053-z
8. Zahra FT, Sajib MS, Mikelis CM. Role of bFGF in Acquired Resistance Upon Anti-VEGF Therapy in Cancer. *Cancers* (2021) 13:1422. doi: 10.3390/cancers13061422
9. Schaaf MB, Garg AD, Agostinis P. Defining the Role of the Tumor Vasculature in Antitumor Immunity and Immunotherapy. *Cell Death Dis* (2018) 9:115. doi: 10.1038/s41419-017-0061-0
10. Carmeliet P, Jain RK. Principles and Mechanisms of Vessel Normalization for Cancer and Other Angiogenic Diseases. *Nat Rev Drug Discov* (2011) 10:417–27. doi: 10.1038/nrd3455
11. Jain RK. Antiangiogenesis Strategies Revisited: From Starving Tumors to Alleviating Hypoxia. *Cancer Cell* (2014) 26:605–22. doi: 10.1016/j.ccell.2014.10.006
12. Huang Y, Goel S, Duda DG, Fukumura D, Jain RK. Vascular Normalization as an Emerging Strategy to Enhance Cancer Immunotherapy. *Cancer Res* (2013) 73:2943–8. doi: 10.1158/0008-5472.CAN-12-4354
13. Peterson TE, Kirkpatrick ND, Huang Y, Farrar CT, Marijt KA, Kloepper J, et al. Dual Inhibition of Ang-2 and VEGF Receptors Normalizes Tumor Vasculature and Prolongs Survival in Glioblastoma by Altering Macrophages. *Proc Natl Acad Sci USA* (2016) 113:4470–5. doi: 10.1073/pnas.1525349113
14. Mpekris F, Panagi M, Voutouri C, Martin JD, Samuel R, Takahashi S, et al. Normalizing the Microenvironment Overcomes Vessel Compression and Resistance to Nano-Immunotherapy in Breast Cancer Lung Metastasis. *Adv Sci (Weinh)* (2021) 8:2001917. doi: 10.1002/advs.202001917
15. Viallard C, Larrivee B. Tumor Angiogenesis and Vascular Normalization: Alternative Therapeutic Targets. *Angiogenesis* (2017) 20:409–26. doi: 10.1007/s10456-017-9562-9
16. Martinez-Rey D, Carmona-Rodriguez L, Fernandez-Acenero MJ, Mira E, Manes S. Extracellular Superoxide Dismutase, the Endothelial Basement Membrane, and the WNT Pathway: New Players in Vascular Normalization and Tumor Infiltration by T-Cells. *Front Immunol* (2020) 11:579552. doi: 10.3389/fimmu.2020.579552
17. Si W, Shen J, Zheng H, Fan W. The Role and Mechanisms of Action of microRNAs in Cancer Drug Resistance. *Clin Epigenet* (2019) 11:25. doi: 10.1186/s13148-018-0587-8
18. Hossian AKMN, Mackenzie GG, Mattheolabakis G. Combination of Mir −143 and Mir−506 Reduces Lung and Pancreatic Cancer Cell Growth Through the Downregulation of Cyclin−Dependent Kinases. *Oncol Rep* (2021) 45:2. doi: 10.3892/or.2021.7953
19. Tahamtan A, Teymoori-Rad M, Nakstad B, Salimi V. Anti-Inflammatory MicroRNAs and Their Potential for Inflammatory Diseases Treatment. *Front Immunol* (2018) 9:1377. doi: 10.3389/fimmu.2018.01377
20. Chung JY, Thone MN, Kwon YJ. COVID-19 Vaccines: The Status and Perspectives in Delivery Points of View. *Adv Drug Delivery Rev* (2020) 170:1–25. doi: 10.1016/j.addr.2020.12.011
21. Chung YH, Beiss V, Fiering SN, Steinmetz NF. COVID-19 Vaccine Frontrunners and Their Nanotechnology Design. *ACS Nano* (2020) 14:12522–37. doi: 10.1021/acsnano.0c07197
22. Pushparajah D, Jimenez S, Wong S, Alattas H, Nafissi N, Slavcev RA. Advances in Gene-Based Vaccine Platforms to Address the COVID-19

Pandemic. *Adv Drug Delivery Rev* (2021) 170:113–41. doi: 10.1016/j.addr.2021.01.003
23. Labatut AE, Mattheolabakis G. Non-Viral Based miR Delivery and Recent Developments. *Eur J Pharm Biopharm* (2018) 128:82–90. doi: 10.1016/j.ejpb.2018.04.018
24. Hossian A, Mackenzie GG, Mattheolabakis G. miRNAs in Gastrointestinal Diseases: Can We Effectively Deliver RNA-Based Therapeutics Orally? *Nanomed (Lond)* (2019) 14:2873–89. doi: 10.2217/nnm-2019-0180
25. Macha MA, Seshacharyulu P, Krishn SR, Pai P, Rachagani S, Jain M, et al. MicroRNAs (miRNAs) as Biomarker(s) for Prognosis and Diagnosis of Gastrointestinal (GI) Cancers. *Curr Pharm Des* (2014) 20:5287–97. doi: 10.2174/1381612820666140128213117
26. Mattheolabakis G, Mikelis CM. Nanoparticle Delivery and Tumor Vascular Normalization: The Chicken or The Egg? *Front Oncol* (2019) 9:1227. doi: 10.3389/fonc.2019.01227
27. Bader AG, Brown D, Winkler M. The Promise of microRNA Replacement Therapy. *Cancer Res* (2010) 70:7027–30. doi: 10.1158/0008-5472.CAN-10-2010
28. Li L, Yuan L, Luo J, Gao J, Guo J, Xie X. MiR-34a Inhibits Proliferation and Migration of Breast Cancer Through Down-Regulation of Bcl-2 and SIRT1. *Clin Exp Med* (2013) 13:109–17. doi: 10.1007/s10238-012-0186-5
29. Wang JX, Zhang QJ, Pei SG, Yang BL. Effect and Mechanism of miR-34a on Proliferation, Apoptosis and Invasion of Laryngeal Carcinoma Cells. *Asian Pac J Trop Med* (2016) 9:494–8. doi: 10.1016/j.apjtm.2016.03.018
30. Zhang L, Liao Y, Tang L. MicroRNA-34 Family: A Potential Tumor Suppressor and Therapeutic Candidate in Cancer. *J Exp Clin Cancer Res* (2019) 38:53. doi: 10.1186/s13046-019-1059-5
31. Bonneau E, Neveu B, Kostantin E, Tsongalis GJ, De Guire V. How Close Are miRNAs From Clinical Practice? A Perspective on the Diagnostic and Therapeutic Market. *EJIFCC* (2019) 30:114–27. doi: 10.3389/fgene.2019.00478
32. Hanna J, Hossain GS, Kocerha J. The Potential for microRNA Therapeutics and Clinical Research. *Front Genet* (2019) 10:478. doi: 10.3389/fgene.2019.00478
33. Chakraborty C, Sharma AR, Sharma G, Lee SS. Therapeutic Advances of miRNAs: A Preclinical and Clinical Update. *J Adv Res* (2021) 28:127–38. doi: 10.1016/j.jare.2020.08.012
34. Landskroner-Eiger S, Moneke I, Sessa WC. miRNAs as Modulators of Angiogenesis. *Cold Spring Harb Perspect Med* (2013) 3:a006643. doi: 10.1101/cshperspect.a006643
35. Peng Y, Croce CM. The Role of MicroRNAs in Human Cancer. *Signal Transduct Target Ther* (2016) 1:15004. doi: 10.1038/sigtrans.2015.4
36. Fish JE, Srivastava D. MicroRNAs: Opening a New Vein in Angiogenesis Research. *Sci Signal* (2009) 2:pe1. doi: 10.1126/scisignal.252pe1
37. Finn NA, Searles CD. Intracellular and Extracellular miRNAs in Regulation of Angiogenesis Signaling. *Curr Angiogenes* (2012) 4:299–307. doi: 10.2174/2211552811201040299
38. Ma J, Waxman DJ. Combination of Antiangiogenesis With Chemotherapy for More Effective Cancer Treatment. *Mol Cancer Ther* (2008) 7:3670–84. doi: 10.1158/1535-7163.MCT-08-0715
39. Senger DR, Galli SJ, Dvorak AM, Perruzzi CA, Harvey VS, Dvorak HF. Tumor Cells Secrete a Vascular Permeability Factor That Promotes Accumulation of Ascites Fluid. *Science* (1983) 219:983–5. doi: 10.1126/science.6823562
40. Leung DW, Cachianes G, Kuang WJ, Goeddel DV, Ferrara N. Vascular Endothelial Growth Factor Is a Secreted Angiogenic Mitogen. *Science* (1989) 246:1306–9. doi: 10.1126/science.2479986
41. Carmeliet P, Ferreira V, Breier G, Pollefeyt S, Kieckens L, Gertsenstein M, et al. Abnormal Blood Vessel Development and Lethality in Embryos Lacking a Single VEGF Allele. *Nature* (1996) 380:435–9. doi: 10.1038/380435a0
42. Ferrara N, Carver-Moore K, Chen H, Dowd M, Lu L, O'shea KS, et al. Heterozygous Embryonic Lethality Induced by Targeted Inactivation of the VEGF Gene. *Nature* (1996) 380:439–42. doi: 10.1038/380439a0
43. Ferrara N, Hillan KJ, Novotny W. Bevacizumab (Avastin), a Humanized Anti-VEGF Monoclonal Antibody for Cancer Therapy. *Biochem Biophys Res Commun* (2005) 333:328–35. doi: 10.1016/j.bbrc.2005.05.132
44. Ferrara N, Kerbel RS. Angiogenesis as a Therapeutic Target. *Nature* (2005) 438:967–74. doi: 10.1038/nature04483
45. Hurwitz H, Fehrenbacher L, Novotny W, Cartwright T, Hainsworth J, Heim W, et al. Bevacizumab Plus Irinotecan, Fluorouracil, and Leucovorin for Metastatic Colorectal Cancer. *N Engl J Med* (2004) 350:2335–42. doi: 10.1056/NEJMoa032691
46. Herbst RS, Heymach JV, O'reilly MS, Onn A, Ryan AJ. Vandetanib (ZD6474): An Orally Available Receptor Tyrosine Kinase Inhibitor That Selectively Targets Pathways Critical for Tumor Growth and Angiogenesis. *Expert Opin Investig Drugs* (2007) 16:239–49. doi: 10.1517/13543784.16.2.239
47. Houghton PJ. Everolimus. *Clin Cancer Res* (2010) 16:1368–72. doi: 10.1158/1078-0432.CCR-09-1314
48. Govindaraj C, Madondo M, Kong YY, Tan P, Wei A, Plebanski M. Lenalidomide-Based Maintenance Therapy Reduces TNF Receptor 2 on CD4 T Cells and Enhances Immune Effector Function in Acute Myeloid Leukemia Patients. *Am J Hematol* (2014) 89:795–802. doi: 10.1002/ajh.23746
49. Fink EC, Ebert BL. The Novel Mechanism of Lenalidomide Activity. *Blood* (2015) 126:2366–9. doi: 10.1182/blood-2015-07-567958
50. Hsieh JJ, Purdue MP, Signoretti S, Swanton C, Albiges L, Schmidinger M, et al. Renal Cell Carcinoma. *Nat Rev Dis Primers* (2017) 3:17009. doi: 10.1038/nrdp.2017.9
51. Zhu YJ, Zheng B, Wang HY, Chen L. New Knowledge of the Mechanisms of Sorafenib Resistance in Liver Cancer. *Acta Pharmacol Sin* (2017) 38:614–22. doi: 10.1038/aps.2017.5
52. Abou-Alfa GK, Meyer T, Cheng AL, El-Khoueiry AB, Rimassa L, Ryoo BY, et al. Cabozantinib in Patients With Advanced and Progressing Hepatocellular Carcinoma. *N Engl J Med* (2018) 379:54–63. doi: 10.1056/NEJMoa1717002
53. Nci. *Angiogenesis Inhibitors* (2018). Available at: https://www.cancer.gov/about-cancer/treatment/types/immunotherapy/angiogenesis-inhibitors-fact-sheet (Accessed 3.24 2021).
54. Fondevila F, Mendez-Blanco C, Fernandez-Palanca P, Gonzalez-Gallego J, Mauriz JL. Anti-Tumoral Activity of Single and Combined Regorafenib Treatments in Preclinical Models of Liver and Gastrointestinal Cancers. *Exp Mol Med* (2019) 51:1–15. doi: 10.1038/s12276-019-0308-1
55. Ebos JM, Lee CR, Cruz-Munoz W, Bjarnason GA, Christensen JG, Kerbel RS. Accelerated Metastasis After Short-Term Treatment With a Potent Inhibitor of Tumor Angiogenesis. *Cancer Cell* (2009) 15:232–9. doi: 10.1016/j.ccr.2009.01.021
56. Paez-Ribes M, Allen E, Hudock J, Takeda T, Okuyama H, Vinals F, et al. Antiangiogenic Therapy Elicits Malignant Progression of Tumors to Increased Local Invasion and Distant Metastasis. *Cancer Cell* (2009) 15:220–31. doi: 10.1016/j.ccr.2009.01.027
57. Wang D, Tan C, Xiao F, Zou L, Wang L, Wei Y, et al. The "Inherent Vice" in the Anti-Angiogenic Theory may Cause the Highly Metastatic Cancer to Spread More Aggressively. *Sci Rep* (2017) 7:2365. doi: 10.1038/s41598-017-02534-1
58. Lugano R, Ramachandran M, Dimberg A. Tumor Angiogenesis: Causes, Consequences, Challenges and Opportunities. *Cell Mol Life Sci* (2020) 77:1745–70. doi: 10.1007/s00018-019-03351-7
59. Rust R, Gantner C, Schwab ME. Pro- and Antiangiogenic Therapies: Current Status and Clinical Implications. *FASEB J* (2019) 33:34–48. doi: 10.1096/fj.201800640RR
60. Scappaticci FA, Skillings JR, Holden SN, Gerber HP, Miller K, Kabbinavar F, et al. Arterial Thromboembolic Events in Patients With Metastatic Carcinoma Treated With Chemotherapy and Bevacizumab. *J Natl Cancer Inst* (2007) 99:1232–9. doi: 10.1093/jnci/djm086
61. Chen HX, Cleck JN. Adverse Effects of Anticancer Agents That Target the VEGF Pathway. *Nat Rev Clin Oncol* (2009) 6:465–77. doi: 10.1038/nrclinonc.2009.94
62. Touyz RM, Lang NN, Herrmann J, Van Den Meiracker AH, Danser AHJ. Recent Advances in Hypertension and Cardiovascular Toxicities With Vascular Endothelial Growth Factor Inhibition. *Hypertension* (2017) 70:220–6. doi: 10.1161/HYPERTENSIONAHA.117.08856
63. Touyz RM, Herrmann J. Cardiotoxicity With Vascular Endothelial Growth Factor Inhibitor Therapy. *NPJ Precis Oncol* (2018) 2:13. doi: 10.1038/s41698-018-0056-z
64. Seymour JF, Pfreundschuh M, Trneny M, Sehn LH, Catalano J, Csinady E, et al. R-CHOP With or Without Bevacizumab in Patients With Previously

Untreated Diffuse Large B-Cell Lymphoma: Final MAIN Study Outcomes. *Haematologica* (2014) 99:1343–9. doi: 10.3324/haematol.2013.100818
65. Bailey CE, Parikh AA. Assessment of the Risk of Antiangiogenic Agents Before and After Surgery. *Cancer Treat Rev* (2018) 68:38–46. doi: 10.1016/j.ctrv.2018.05.002
66. Bodnar RJ. Anti-Angiogenic Drugs: Involvement in Cutaneous Side Effects and Wound-Healing Complication. *Adv Wound Care (New Rochelle)* (2014) 3:635–46. doi: 10.1089/wound.2013.0496
67. Davis-Dusenbery BN, Hata A. MicroRNA in Cancer: The Involvement of Aberrant MicroRNA Biogenesis Regulatory Pathways. *Genes Cancer* (2010) 1:1100–14. doi: 10.1177/1947601910396213
68. Wang Y, Wang L, Chen C, Chu X. New Insights Into the Regulatory Role of microRNA in Tumor Angiogenesis and Clinical Implications. *Mol Cancer* (2018) 17:22. doi: 10.1186/s12943-018-0766-4
69. Hu J, Cheng Y, Li Y, Jin Z, Pan Y, Liu G, et al. microRNA-128 Plays a Critical Role in Human Non-Small Cell Lung Cancer Tumourigenesis, Angiogenesis and Lymphangiogenesis by Directly Targeting Vascular Endothelial Growth Factor-C. *Eur J Cancer* (2014) 50:2336–50. doi: 10.1016/j.ejca.2014.06.005
70. Yang L, Dong C, Yang J, Yang L, Chang N, Qi C, et al. MicroRNA-26b-5p Inhibits Mouse Liver Fibrogenesis and Angiogenesis by Targeting PDGF Receptor-Beta. *Mol Ther Nucleic Acids* (2019) 16:206–17. doi: 10.1016/j.omtn.2019.02.014
71. Sun T, Yin L, Kuang H. miR-181a/B-5p Regulates Human Umbilical Vein Endothelial Cell Angiogenesis by Targeting PDGFRA. *Cell Biochem Funct* (2020) 38:222–30. doi: 10.1002/cbf.3472
72. Yamakuchi M, Ferlito M, Lowenstein CJ. miR-34a Repression of SIRT1 Regulates Apoptosis. *Proc Natl Acad Sci USA* (2008) 105:13421–6. doi: 10.1073/pnas.0801613105
73. Zhao T, Li J, Chen AF. MicroRNA-34a Induces Endothelial Progenitor Cell Senescence and Impedes Its Angiogenesis via Suppressing Silent Information Regulator 1. *Am J Physiol Endocrinol Metab* (2010) 299:E110–116. doi: 10.1152/ajpendo.00192.2010
74. Tabuchi T, Satoh M, Itoh T, Nakamura M. MicroRNA-34a Regulates the Longevity-Associated Protein SIRT1 in Coronary Artery Disease: Effect of Statins on SIRT1 and microRNA-34a Expression. *Clin Sci (Lond)* (2012) 123:161–71. doi: 10.1042/CS20110563
75. Shi S, Jin Y, Song H, Chen X. MicroRNA-34a Attenuates VEGF-Mediated Retinal Angiogenesis via Targeting Notch1. *Biochem Cell Biol* (2019) 97:423–30. doi: 10.1139/bcb-2018-0304
76. Yu G, Yao W, Xiao W, Li H, Xu H, Lang B. MicroRNA-34a Functions as an Anti-Metastatic microRNA and Suppresses Angiogenesis in Bladder Cancer by Directly Targeting CD44. *J Exp Clin Cancer Res* (2014) 33:779. doi: 10.1186/s13046-014-0115-4
77. Su G, Sun G, Liu H, Shu L, Liang Z. Downregulation of miR-34a Promotes Endothelial Cell Growth and Suppresses Apoptosis in Atherosclerosis by Regulating Bcl-2. *Heart Vessels* (2018) 33:1185–94. doi: 10.1007/s00380-018-1169-6
78. Vinall RL, Ripoll AZ, Wang S, Pan CX, Devere White RW. MiR-34a Chemosensitizes Bladder Cancer Cells to Cisplatin Treatment Regardless of P53-Rb Pathway Status. *Int J Cancer* (2012) 130:2526–38. doi: 10.1002/ijc.26256
79. Song C, Lu P, Sun G, Yang L, Wang Z, Wang Z. miR-34a Sensitizes Lung Cancer Cells to Cisplatin via P53/miR-34a/MYCN Axis. *Biochem Biophys Res Commun* (2017) 482:22–7. doi: 10.1016/j.bbrc.2016.11.037
80. Zheng SZ, Sun P, Wang JP, Liu Y, Gong W, Liu J. MiR-34a Overexpression Enhances the Inhibitory Effect of Doxorubicin on HepG2 Cells. *World J Gastroenterol* (2019) 25:2752–62. doi: 10.3748/wjg.v25.i22.2752
81. Jian C, Tu MJ, Ho PY, Duan Z, Zhang Q, Qiu JX, et al. Co-Targeting of DNA, RNA, and Protein Molecules Provides Optimal Outcomes for Treating Osteosarcoma and Pulmonary Metastasis in Spontaneous and Experimental Metastasis Mouse Models. *Oncotarget* (2017) 8:30742–55. doi: 10.18632/oncotarget.16372
82. Wen D, Peng Y, Lin F, Singh RK, Mahato RI. Micellar Delivery of miR-34a Modulator Rubone and Paclitaxel in Resistant Prostate Cancer. *Cancer Res* (2017) 77:3244–54. doi: 10.1158/0008-5472.CAN-16-2355
83. Fang JH, Zhou HC, Zeng C, Yang J, Liu Y, Huang X, et al. MicroRNA-29b Suppresses Tumor Angiogenesis, Invasion, and Metastasis by Regulating Matrix Metalloproteinase 2 Expression. *Hepatology* (2011) 54:1729–40. doi: 10.1002/hep.24577
84. Kriegel AJ, Liu Y, Fang Y, Ding X, Liang M. The miR-29 Family: Genomics, Cell Biology, and Relevance to Renal and Cardiovascular Injury. *Physiol Genomics* (2012) 44:237–44. doi: 10.1152/physiolgenomics.00141.2011
85. Chen HX, Xu XX, Tan BZ, Zhang Z, Zhou XD. MicroRNA-29b Inhibits Angiogenesis by Targeting VEGFA Through the MAPK/ERK and PI3K/Akt Signaling Pathways in Endometrial Carcinoma. *Cell Physiol Biochem* (2017) 41:933–46. doi: 10.1159/000460510
86. Li Y, Cai B, Shen L, Dong Y, Lu Q, Sun S, et al. MiRNA-29b Suppresses Tumor Growth Through Simultaneously Inhibiting Angiogenesis and Tumorigenesis by Targeting Akt3. *Cancer Lett* (2017) 397:111–9. doi: 10.1016/j.canlet.2017.03.032
87. Zhang H, Bai M, Deng T, Liu R, Wang X, Qu Y, et al. Cell-Derived Microvesicles Mediate the Delivery of miR-29a/C to Suppress Angiogenesis in Gastric Carcinoma. *Cancer Lett* (2016) 375:331–9. doi: 10.1016/j.canlet.2016.03.026
88. Sun DM, Tang BF, Li ZX, Guo HB, Cheng JL, Song PP, et al. MiR-29c Reduces the Cisplatin Resistance of Non-Small Cell Lung Cancer Cells by Negatively Regulating the PI3K/Akt Pathway. *Sci Rep* (2018) 8:8007. doi: 10.1038/s41598-018-26381-w
89. Huang L, Hu C, Chao H, Wang R, Lu H, Li H, et al. miR-29c Regulates Resistance to Paclitaxel in Nasopharyngeal Cancer by Targeting ITGB1. *Exp Cell Res* (2019) 378:1–10. doi: 10.1016/j.yexcr.2019.02.012
90. Shen H, Li L, Yang S, Wang D, Zhong S, Zhao J, et al. MicroRNA-29a Contributes to Drug-Resistance of Breast Cancer Cells to Adriamycin Through PTEN/AKT/GSK3beta Signaling Pathway. *Gene* (2016) 593:84–90. doi: 10.1016/j.gene.2016.08.016
91. Shi X, Valizadeh A, Mir SM, Asemi Z, Karimian A, Majidina M, et al. miRNA-29a Reverses P-Glycoprotein-Mediated Drug Resistance and Inhibits Proliferation via Up-Regulation of PTEN in Colon Cancer Cells. *Eur J Pharmacol* (2020) 880:173138. doi: 10.1016/j.ejphar.2020.173138
92. Li Y, Zhang Z, Xiao Z, Lin Y, Luo T, Zhou Q, et al. Chemotherapy-Mediated miR-29b Expression Inhibits the Invasion and Angiogenesis of Cervical Cancer. *Oncotarget* (2017) 8:14655–65. doi: 10.18632/oncotarget.14738
93. Poliseno L, Tuccoli A, Mariani L, Evangelista M, Citti L, Woods K, et al. MicroRNAs Modulate the Angiogenic Properties of HUVECs. *Blood* (2006) 108:3068–71. doi: 10.1182/blood-2006-01-012369
94. Bartel DP. MicroRNAs: Target Recognition and Regulatory Functions. *Cell* (2009) 136:215–33. doi: 10.1016/j.cell.2009.01.002
95. Nicoli S, Knyphausen CP, Zhu LJ, Lakshmanan A, Lawson ND. miR-221 Is Required for Endothelial Tip Cell Behaviors During Vascular Development. *Dev Cell* (2012) 22:418–29. doi: 10.1016/j.devcel.2012.01.008
96. Chen Y, Banda M, Speyer CL, Smith JS, Rabson AB, Gorski DH. Regulation of the Expression and Activity of the Antiangiogenic Homeobox Gene GAX/MEOX2 by ZEB2 and microRNA-221. *Mol Cell Biol* (2010) 30:3902–13. doi: 10.1128/MCB.01237-09
97. Wu YH, Hu TF, Chen YC, Tsai YN, Tsai YH, Cheng CC, et al. The Manipulation of miRNA-Gene Regulatory Networks by KSHV Induces Endothelial Cell Motility. *Blood* (2011) 118:2896–905. doi: 10.1182/blood-2011-01-330589
98. Li Y, Yan C, Fan J, Hou Z, Han Y. MiR-221-3p Targets Hif-1alpha to Inhibit Angiogenesis in Heart Failure. *Lab Invest* (2021) 101:104–15. doi: 10.1038/s41374-020-0450-3
99. Mercatelli N, Coppola V, Bonci D, Miele F, Costantini A, Guadagnoli M, et al. The Inhibition of the Highly Expressed miR-221 and miR-222 Impairs the Growth of Prostate Carcinoma Xenografts in Mice. *PloS One* (2008) 3:e4029. doi: 10.1371/journal.pone.0004029
100. Le Sage C, Nagel R, Egan DA, Schrier M, Mesman E, Mangiola A, et al. Regulation of the P27(Kip1) Tumor Suppressor by miR-221 and miR-222 Promotes Cancer Cell Proliferation. *EMBO J* (2007) 26:3699–708. doi: 10.1038/sj.emboj.7601790
101. Miller TE, Ghoshal K, Ramaswamy B, Roy S, Datta J, Shapiro CL, et al. MicroRNA-221/222 Confers Tamoxifen Resistance in Breast Cancer by Targeting p27Kip1. *J Biol Chem* (2008) 283:29897–903. doi: 10.1074/jbc.M804612200
102. Garofalo M, Quintavalle C, Di Leva G, Zanca C, Romano G, Taccioli C, et al. MicroRNA Signatures of TRAIL Resistance in Human Non-Small Cell Lung Cancer. *Oncogene* (2008) 27:3845–55. doi: 10.1038/onc.2008.6

103. Amini-Farsani Z, Sangtarash MH, Shamsara M, Teimori H. MiR-221/222 Promote Chemoresistance to Cisplatin in Ovarian Cancer Cells by Targeting PTEN/PI3K/AKT Signaling Pathway. *Cytotechnology* (2018) 70:203–13. doi: 10.1007/s10616-017-0134-z
104. Li S, Li Q, Lu J, Zhao Q, Li D, Shen L, et al. Targeted Inhibition of miR-221/222 Promotes Cell Sensitivity to Cisplatin in Triple-Negative Breast Cancer MDA-MB-231 Cells. *Front Genet* (2019) 10:1278. doi: 10.3389/fgene.2019.01278
105. Chen D, Yan W, Liu Z, Zhang Z, Zhu L, Liu W, et al. Downregulation of miR-221 Enhances the Sensitivity of Human Oral Squamous Cell Carcinoma Cells to Adriamycin Through Upregulation of TIMP3 Expression. *BioMed Pharmacother* (2016) 77:72–8. doi: 10.1016/j.biopha.2015.12.002
106. Du L, Ma S, Wen X, Chai J, Zhou D. Oral Squamous Cell Carcinoma Cells Are Resistant to Doxorubicin Through Upregulation of Mir221. *Mol Med Rep* (2017) 16:2659–67. doi: 10.3892/mmr.2017.6915
107. Wang Y, Zhao Y, Herbst A, Kalinski T, Qin J, Wang X, et al. miR-221 Mediates Chemoresistance of Esophageal Adenocarcinoma by Direct Targeting of DKK2 Expression. *Ann Surg* (2016) 264:804–14. doi: 10.1097/SLA.0000000000001928
108. Ni L, Xu J, Zhao F, Dai X, Tao J, Pan J, et al. MiR-221-3p-Mediated Downregulation of MDM2 Reverses the Paclitaxel Resistance of Non-Small Cell Lung Cancer In Vitro and In Vivo. *Eur J Pharmacol* (2021) 899:174054. doi: 10.1016/j.ejphar.2021.174054
109. Lei Z, Li B, Yang Z, Fang H, Zhang GM, Feng ZH, et al. Regulation of HIF-1alpha and VEGF by miR-20b Tunes Tumor Cells to Adapt to the Alteration of Oxygen Concentration. *PloS One* (2009) 4:e7629. doi: 10.1371/journal.pone.0007629
110. Chou J, Lin JH, Brenot A, Kim JW, Provot S, Werb Z. GATA3 Suppresses Metastasis and Modulates the Tumour Microenvironment by Regulating microRNA-29b Expression. *Nat Cell Biol* (2013) 15:201–13. doi: 10.1038/ncb2672
111. Long J, Wang Y, Wang W, Chang BH, Danesh FR. Identification of microRNA-93 as a Novel Regulator of Vascular Endothelial Growth Factor in Hyperglycemic Conditions. *J Biol Chem* (2010) 285:23457–65. doi: 10.1074/jbc.M110.136168
112. Li F, Liang X, Chen Y, Li S, Liu J. Role of microRNA-93 in Regulation of Angiogenesis. *Tumour Biol* (2014) 35:10609–13. doi: 10.1007/s13277-014-2605-6
113. Tirpe A, Gulei D, Tirpe GR, Nutu A, Irimie A, Campomenosi P, et al. Beyond Conventional: The New Horizon of Anti-Angiogenic microRNAs in Non-Small Cell Lung Cancer Therapy. *Int J Mol Sci* (2020) 21:8002. doi: 10.3390/ijms21218002
114. Chen Q, Chen S, Zhao J, Zhou Y, Xu L. MicroRNA-126: A New and Promising Player in Lung Cancer. *Oncol Lett* (2021) 21:35. doi: 10.3892/ol.2020.12296
115. Ye J, Wu X, Wu D, Wu P, Ni C, Zhang Z, et al. miRNA-27b Targets Vascular Endothelial Growth Factor C to Inhibit Tumor Progression and Angiogenesis in Colorectal Cancer. *PloS One* (2013) 8:e60687. doi: 10.1371/journal.pone.0060687
116. Liu HT, Xing AY, Chen X, Ma RR, Wang YW, Shi DB, et al. MicroRNA-27b, microRNA-101 and microRNA-128 Inhibit Angiogenesis by Down-Regulating Vascular Endothelial Growth Factor C Expression in Gastric Cancers. *Oncotarget* (2015) 6:37458–70. doi: 10.18632/oncotarget.6059
117. Muramatsu F, Kidoya H, Naito H, Sakimoto S, Takakura N. microRNA-125b Inhibits Tube Formation of Blood Vessels Through Translational Suppression of VE-Cadherin. *Oncogene* (2013) 32:414–21. doi: 10.1038/onc.2012.68
118. Wu SY, Rupaimoole R, Shen F, Pradeep S, Pecot CV, Ivan C, et al. A miR-192-EGR1-HOXB9 Regulatory Network Controls the Angiogenic Switch in Cancer. *Nat Commun* (2016) 7:11169. doi: 10.1038/ncomms11169
119. Pecot CV, Rupaimoole R, Yang D, Akbani R, Ivan C, Lu C, et al. Tumour Angiogenesis Regulation by the miR-200 Family. *Nat Commun* (2013) 4:2427. doi: 10.1038/ncomms3427
120. Sun G, Liu M, Han H. Overexpression of microRNA-190 Inhibits Migration, Invasion, Epithelial-Mesenchymal Transition, and Angiogenesis Through Suppression of Protein Kinase B-Extracellular Signal-Regulated Kinase Signaling Pathway via Binding to Stanniocalicin 2 in Breast Cancer. *J Cell Physiol* (2019) 234:17824–38. doi: 10.1002/jcp.28409
121. Chen QY, Jiao DM, Wu YQ, Chen J, Wang J, Tang XL, et al. MiR-206 Inhibits HGF-Induced Epithelial-Mesenchymal Transition and Angiogenesis in Non-Small Cell Lung Cancer via C-Met /PI3k/Akt/mTOR Pathway. *Oncotarget* (2016) 7:18247–61. doi: 10.18632/oncotarget.7570
122. Zhou Y, Li S, Li J, Wang D, Li Q. Effect of microRNA-135a on Cell Proliferation, Migration, Invasion, Apoptosis and Tumor Angiogenesis Through the IGF-1/PI3K/Akt Signaling Pathway in Non-Small Cell Lung Cancer. *Cell Physiol Biochem* (2017) 42:1431–46. doi: 10.1159/000479207
123. Hossian A, Sajib MS, Tullar PE, Mikelis CM, Mattheolabakis G. Multipronged Activity of Combinatorial miR-143 and miR-506 Inhibits Lung Cancer Cell Cycle Progression and Angiogenesis. *Vitro Sci Rep* (2018) 8:10495. doi: 10.1038/s41598-018-28872-2
124. Belcheva A, Wey JS, Fan F, Ellis LM. Expression of Vascular Endothelial Growth Factor Receptors (VEGF-Rs) on Human Breast Cancer Cells Confers Chemoresistance. *Cancer Res* (2004) 64:1000.
125. Stanton MJ, Dutta S, Zhang H, Polavaram NS, Leontovich AA, Honscheid P, et al. Autophagy Control by the VEGF-C/NRP-2 Axis in Cancer and Its Implication for Treatment Resistance. *Cancer Res* (2013) 73:160–71. doi: 10.1158/0008-5472.CAN-11-3635
126. Wang CA, Harrell JC, Iwanaga R, Jedlicka P, Ford HL. Vascular Endothelial Growth Factor C Promotes Breast Cancer Progression via a Novel Antioxidant Mechanism That Involves Regulation of Superoxide Dismutase 3. *Breast Cancer Res* (2014) 16:462. doi: 10.1186/s13058-014-0462-2
127. Zhu X, Li H, Long L, Hui L, Chen H, Wang X, et al. miR-126 Enhances the Sensitivity of Non-Small Cell Lung Cancer Cells to Anticancer Agents by Targeting Vascular Endothelial Growth Factor A. *Acta Biochim Biophys Sin (Shanghai)* (2012) 44:519–26. doi: 10.1093/abbs/gms026
128. Zhao Y, Tu MJ, Yu YF, Wang WP, Chen QX, Qiu JX, et al. Combination Therapy With Bioengineered miR-34a Prodrug and Doxorubicin Synergistically Suppresses Osteosarcoma Growth. *Biochem Pharmacol* (2015) 98:602–13. doi: 10.1016/j.bcp.2015.10.015
129. Yu J, Zhao Y, Liu C, Hu B, Zhao M, Ma Y, et al. Synergistic Anti-Tumor Effect of Paclitaxel and miR-34a Combined With Ultrasound Microbubbles on Cervical Cancer In Vivo and In Vitro. *Clin Transl Oncol* (2020) 22:60–9. doi: 10.1007/s12094-019-02131-w
130. Shi S, Han L, Deng L, Zhang Y, Shen H, Gong T, et al. Dual Drugs (microRNA-34a and Paclitaxel)-Loaded Functional Solid Lipid Nanoparticles for Synergistic Cancer Cell Suppression. *J Control Release* (2014) 194:228–37. doi: 10.1016/j.jconrel.2014.09.005
131. Soltani-Sedeh H, Irani S, Mirfakhraie R, Soleimani M. Potential Using of microRNA-34A in Combination With Paclitaxel in Colorectal Cancer Cells. *J Cancer Res Ther* (2019) 15:32–7. doi: 10.4103/jcrt.JCRT_267_17
132. Zhang L, Yang X, Lv Y, Xin X, Qin C, Han X, et al. Cytosolic Co-Delivery of miRNA-34a and Docetaxel With Core-Shell Nanocarriers via Caveolae-Mediated Pathway for the Treatment of Metastatic Breast Cancer. *Sci Rep* (2017) 7:46186. doi: 10.1038/srep46186
133. Zhang Q, Wang J, Li N, Liu Z, Chen Z, Li Z, et al. miR-34a Increases the Sensitivity of Colorectal Cancer Cells to 5-Fluorouracil In Vitro and In Vivo. *Am J Cancer Res* (2018) 8:280–90.
134. Xu J, Zhang G, Luo X, Wang D, Zhou W, Zhang Y, et al. Co-Delivery of 5-Fluorouracil and miRNA-34a Mimics by Host-Guest Self-Assembly Nanocarriers for Efficacious Targeted Therapy in Colorectal Cancer Patient-Derived Tumor Xenografts. *Theranostics* (2021) 11:2475–89. doi: 10.7150/thno.52076
135. Jilek JL, Tu MJ, Zhang C, Yu AM. Pharmacokinetic and Pharmacodynamic Factors Contribute to Synergism Between Let-7c-5p and 5-Fluorouracil in Inhibiting Hepatocellular Carcinoma Cell Viability. *Drug Metab Dispos* (2020) 48:1257–63. doi: 10.1124/dmd.120.000207
136. Costa PM, Cardoso AL, Custodia C, Cunha P, Pereira De Almeida L, Pedroso De Lima MC. MiRNA-21 Silencing Mediated by Tumor-Targeted Nanoparticles Combined With Sunitinib: A New Multimodal Gene Therapy Approach for Glioblastoma. *J Control Release* (2015) 207:31–9. doi: 10.1016/j.jconrel.2015.04.002
137. Passadouro M, Pedroso De Lima MC, Faneca H. MicroRNA Modulation Combined With Sunitinib as a Novel Therapeutic Strategy for Pancreatic Cancer. *Int J Nanomed* (2014) 9:3203–17. doi: 10.2147/IJN.S64456

138. Liu H, Liu Z, Jiang B, Huo L, Liu J, Lu J. Synthetic miR-145 Mimic Enhances the Cytotoxic Effect of the Antiangiogenic Drug Sunitinib in Glioblastoma. *Cell Biochem Biophys* (2015) 72:551–7. doi: 10.1007/s12013-014-0501-8
139. Kim SJ, Oh JS, Shin JY, Lee KD, Sung KW, Nam SJ, et al. Development of microRNA-145 for Therapeutic Application in Breast Cancer. *J Control Release* (2011) 155:427–34. doi: 10.1016/j.jconrel.2011.06.026
140. Mittal A, Chitkara D, Behrman SW, Mahato RI. Efficacy of Gemcitabine Conjugated and miRNA-205 Complexed Micelles for Treatment of Advanced Pancreatic Cancer. *Biomaterials* (2014) 35:7077–87. doi: 10.1016/j.biomaterials.2014.04.053
141. Karaayvaz M, Zhai H, Ju J. miR-129 Promotes Apoptosis and Enhances Chemosensitivity to 5-Fluorouracil in Colorectal Cancer. *Cell Death Dis* (2013) 4:e659. doi: 10.1038/cddis.2013.193
142. Liu L, Zheng W, Song Y, Du X, Tang Y, Nie J, et al. miRNA-497 Enhances the Sensitivity of Colorectal Cancer Cells to Neoadjuvant Chemotherapeutic Drug. *Curr Protein Pept Sci* (2015) 16:310–5. doi: 10.2174/1389203716041 50429154142
143. Zhang G, Tian X, Li Y, Wang Z, Li X, Zhu C. miR-27b and miR-34a Enhance Docetaxel Sensitivity of Prostate Cancer Cells Through Inhibiting Epithelial-to-Mesenchymal Transition by Targeting ZEB1. *BioMed Pharmacother* (2018) 97:736–44. doi: 10.1016/j.biopha.2017.10.163
144. Hu H, Wang Z, Tan C, Liu X, Zhang H, Li K. Dihydroartemisinin/miR-29b Combination Therapy Increases the Pro-Apoptotic Effect of Dihydroartemisinin on Cholangiocarcinoma Cell Lines by Regulating Mcl-1 Expression. *Adv Clin Exp Med* (2020) 29:911–9. doi: 10.17219/acem/121919
145. Lee J, Choi KJ, Moon SU, Kim S. Theragnosis-Based Combined Cancer Therapy Using Doxorubicin-Conjugated microRNA-221 Molecular Beacon. *Biomaterials* (2016) 74:109–18. doi: 10.1016/j.biomaterials.2015.09.036
146. Zhang Y, He Y, Lu LL, Zhou ZY, Wan NB, Li GP, et al. miRNA-192-5p Impacts the Sensitivity of Breast Cancer Cells to Doxorubicin via Targeting Peptidylprolyl Isomerase A. *Kaohsiung J Med Sci* (2019) 35:17–23. doi: 10.1002/kjm2.12004
147. Fu H, Zhang J, Pan T, Ai S, Tang L, Wang F. Mir378a Enhances the Sensitivity of Liver Cancer to Sorafenib by Targeting VEGFR, PDGFRbeta and Craf. *Mol Med Rep* (2018) 17:4581–8. doi: 10.3892/mmr.2018.8390
148. Xu H, Zhao L, Fang Q, Sun J, Zhang S, Zhan C, et al. MiR-338-3p Inhibits Hepatocarcinoma Cells and Sensitizes These Cells to Sorafenib by Targeting Hypoxia-Induced Factor 1alpha. *PloS One* (2014) 9:e115565. doi: 10.1371/journal.pone.0115565
149. Hejazi M, Baghbani E, Amini M, Rezaei T, Aghanejad A, Mosafer J, et al. MicroRNA-193a and Taxol Combination: A New Strategy for Treatment of Colorectal Cancer. *J Cell Biochem* (2020) 121:1388–99. doi: 10.1002/jcb.29374
150. Esfandyari YB, Doustvandi MA, Amini M, Baradaran B, Zaer SJ, Mozammel N, et al. MicroRNA-143 Sensitizes Cervical Cancer Cells to Cisplatin: A Promising Anticancer Combination Therapy. *Reprod Sci* (2021) 28:2036–49. doi: 10.1007/s43032-021-00479-5
151. Yu PN, Yan MD, Lai HC, Huang RL, Chou YC, Lin WC, et al. Downregulation of miR-29 Contributes to Cisplatin Resistance of Ovarian Cancer Cells. *Int J Cancer* (2014) 134:542–51. doi: 10.1002/ijc.28399
152. Gajda E, Godlewska M, Mariak Z, Nazaruk E, Gawel D. Combinatory Treatment With miR-7-5p and Drug-Loaded Cubosomes Effectively Impairs Cancer Cells. *Int J Mol Sci* (2020) 21:5039. doi: 10.3390/ijms21145039
153. Sun Y, Wu J, Dong X, Zhang J, Meng C, Liu G. MicroRNA-506-3p Increases the Response to PARP Inhibitors and Cisplatin by Targeting EZH2/beta-Catenin in Serous Ovarian Cancers. *Transl Oncol* (2021) 14:100987. doi: 10.1016/j.tranon.2020.100987
154. Golubovskaya VM, Sumbler B, Ho B, Yemma M, Cance WG. MiR-138 and MiR-135 Directly Target Focal Adhesion Kinase, Inhibit Cell Invasion, and Increase Sensitivity to Chemotherapy in Cancer Cells. *Anticancer Agents Med Chem* (2014) 14:18–28. doi: 10.2174/1871520614011401081134 35
155. Wang F, Meng F, Wong SCC, Cho WCS, Yang S, Chan LWC. Combination Therapy of Gefitinib and miR-30a-5p may Overcome Acquired Drug Resistance Through Regulating the PI3K/AKT Pathway in Non-Small Cell Lung Cancer. *Ther Adv Respir Dis* (2020) 14:1753466620915156. doi: 10.1177/1753466620915156
156. Liang G, Zhu Y, Ali DJ, Tian T, Xu H, Si K, et al. Engineered Exosomes for Targeted Co-Delivery of miR-21 Inhibitor and Chemotherapeutics to Reverse Drug Resistance in Colon Cancer. *J Nanobiotechnol* (2020) 18:10. doi: 10.1186/s12951-019-0563-2
157. Xu X, Chen X, Xu M, Liu X, Pan B, Qin J, et al. miR-375-3p Suppresses Tumorigenesis and Partially Reverses Chemoresistance by Targeting YAP1 and SP1 in Colorectal Cancer Cells. *Aging (Albany NY)* (2019) 11:7357–85. doi: 10.18632/aging.102214
158. Xu F, Ye ML, Zhang YP, Li WJ, Li MT, Wang HZ, et al. MicroRNA-375-3p Enhances Chemosensitivity to 5-Fluorouracil by Targeting Thymidylate Synthase in Colorectal Cancer. *Cancer Sci* (2020) 111:1528–41. doi: 10.1111/cas.14356
159. Lai X, Eberhardt M, Schmitz U, Vera J. Systems Biology-Based Investigation of Cooperating microRNAs as Monotherapy or Adjuvant Therapy in Cancer. *Nucleic Acids Res* (2019) 47:7753–66. doi: 10.1093/nar/gkz638
160. Rupaimoole R, Han HD, Lopez-Berestein G, Sood AK. MicroRNA Therapeutics: Principles, Expectations, and Challenges. *Chin J Cancer* (2011) 30:368–70. doi: 10.5732/cjc.011.10186


**Conflict of Interest:** The authors declare that the research was conducted in the absence of any commercial or financial relationships that could be construed as a potential conflict of interest.

**Publisher's Note:** All claims expressed in this article are solely those of the authors and do not necessarily represent those of their affiliated organizations, or those of the publisher, the editors and the reviewers. Any product that may be evaluated in this article, or claim that may be made by its manufacturer, is not guaranteed or endorsed by the publisher.

# Advantages of publishing in Frontiers

**OPEN ACCESS**
Articles are free to read for greatest visibility and readership

**FAST PUBLICATION**
Around 90 days from submission to decision

**HIGH QUALITY PEER-REVIEW**
Rigorous, collaborative, and constructive peer-review

**TRANSPARENT PEER-REVIEW**
Editors and reviewers acknowledged by name on published articles

**Frontiers**
Avenue du Tribunal-Fédéral 34
1005 Lausanne | Switzerland

**Visit us:** www.frontiersin.org
**Contact us:** frontiersin.org/about/contact

**REPRODUCIBILITY OF RESEARCH**
Support open data and methods to enhance research reproducibility

**DIGITAL PUBLISHING**
Articles designed for optimal readership across devices

**FOLLOW US**
@frontiersin

**IMPACT METRICS**
Advanced article metrics track visibility across digital media

**EXTENSIVE PROMOTION**
Marketing and promotion of impactful research

**LOOP RESEARCH NETWORK**
Our network increases your article's readership